

Coordination chemistry

2017

Lecture: Tue 11:00 a.m. – 1:30 p.m., B21

Irena Hoskovcová, hoskovci@vscht.cz, A207

Seminar 1(CZ): Tue 2:15 p.m., BX04

Petr Holzhauser, holzhausp@vscht.cz

Seminar 2 (EN): Fri 8:30-9.45 a.m., A211



EUROPEAN UNION
European Structural and Investing Funds
Operational Programme Research,
Development and Education



Dílo podléhá licenci Creative Commons 4.0 Česko
Uvedte původ - Zachovějte licenci

Syllabus 2017

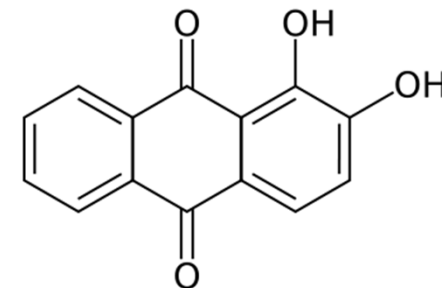
1. History
2. Structure, description, nomenclature
3. How to stabilize them – HSAB, chelate effect, isolobality
4. Electron count – ligand types X, L; 18e rule
5. Central metal atom – spectroscopic terms, splitting
6. Bonding theories, explanation of properties (colour, magnetism):
 1. Crystal Field Theory (CFT)
 2. Molecular orbitals
7. Ligand properties changed by coordination
8. Reactivity
 1. ligand substitution
 2. Redox reactions
9. More centres – metal-metal bond, clusters
10. Applications

Early history – once upon a time...

Compound known from ancient times (Persia, Egypt, 1500 B.C.):

alizarin dye (red) (1,2-dihydroxyanthraquinone)

a vegetable red dye used for leather, wool, cotton, silk (Turkey red), “redcoats”



The red dye was isolated from the roots of plants of the madder genus (*mořena barvířská*, *garance des teinturiers*, *Rubia tinctorum*) and treated with alum ($KAl(SO_4)_2 \cdot 12H_2O$) => formation of a more stable Al(III) complex of alizarin



The alizarin component became the first natural dye to be synthetically duplicated, in 1868 by German chemists Carl Gräbe and Carl Liebermann, from BASF



Rubia tinctorum



Johannes Vermeer, Christ in the House of Martha and Mary, 1654-56. The red blouse of Mary is painted in madder lake

https://upload.wikimedia.org/wikipedia/commons/thumb/b/b1/Rubia_tinctorum_002.JPG/330px-Rubia_tinctorum_002.JPG



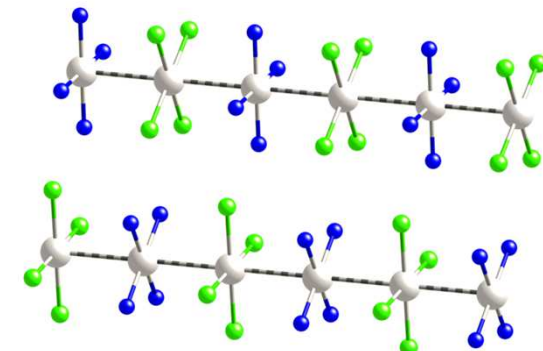
Early history – once upon a time...

- 1597 $[\text{Cu}(\text{NH}_3)_4]^{2+}$, Andreas Libavius, 1st documented observation:
bronze (Cu, Sn alloy) + $\text{Ca}(\text{OH})_2$ + NH_4Cl = blue solution
the colour caused by $[\text{Cu}(\text{NH}_3)_4]^{2+}$ ions; analytical proof
- 1704 Prussian blue $\text{Fe}_4[\text{Fe}(\text{CN})_6]_3$ Johann Conrad Dippel
1st isolated coordination compound, use: pigment
berlínská modř, bleu de Prusse (bleu de Berlin)
prepared from potassium hydrogen tartarate, potassium nitrate, charcoal, dried bovine blood, calcinated FeSO_4 , HCl.
- 1760 use of sparingly soluble $\text{K}_2[\text{PtCl}_6]$ to refine platinum
- 1798 B.M.Tassaert - ammoniacal solutions of cobalt chloride or nitrate develop a brownish mahogany colour. Without isolation.
 $[\text{Co}(\text{NH}_3)_6]_2(\text{C}_2\text{O}_4)_3$ was isolated by Leopold Gmelin in 1822, also cyanido complexes $\text{K}_3[\text{Fe}(\text{CN})_6]$, $\text{M}_3[\text{Co}(\text{CN})_6]$, $\text{M}_2[\text{Pt}(\text{CN})_4]$.

History – compounds with names

Early 19th century

- Vauquelin's salt $[\text{Pd}(\text{NH}_3)_4][\text{PdCl}_4]$
- Magnus' green salt $[\text{Pt}(\text{NH}_3)_4][\text{PtCl}_4]$,
tetraammineplatinum(II) tetrachloroplatinate(II)
(! isolated cation: colourless; anion: red)



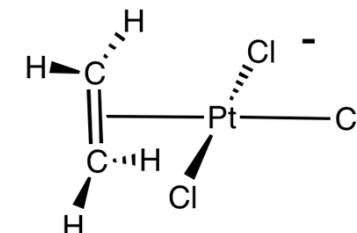
- Zeise's salt, 1825, $\text{K}[\text{Pt}(\eta^2\text{-C}_2\text{H}_4)\text{Cl}_3]\cdot\text{H}_2\text{O}$

1st organometallic compound,

potassium trichloro(ethene)platinate(II)

original synthesis: $\text{PtCl}_2 + \text{PtCl}_4$ refluxed in EtOH, resulting black product extracted by a water soln. of KCl + HCl => pale yellow product

later synthesis: $\text{C}_2\text{H}_4 + \text{K}_2[\text{PtCl}_4]$ in diluted HCl



- 1844 *cis*- and *trans*- $[\text{PtCl}_2(\text{NH}_3)_2]$

Coordination compounds in context

1743 *Lavoisier; 13 elements known

1774 law of conservation of mass

1799 law fo definite proportions
(Proust)

1808 Dalton – atomic theory

1830 radical theory of organic
molecules (Liebig, Wöhler, Berzelius)

1852 fixed valence concept

1854 C is always tetravalent, Kekulé

1859 spectroscope (Bunsen, Kirchhoff)

1860 Congress in Karlsruhe – symbols
of elements, branches of chemistry

1869 periodic table, 60 elements

1884 Arrhenius –dissociation of
electrolytes in solution

1798 Tassaert observed Co + ammonia

1822 solid $[\text{Co}(\text{NH}_3)_6]_2(\text{C}_2\text{O}_4)_3$; Gmelin

1851 more complexes of Co with NH_3

1896 atoms are composed from protons and
electrons

1902 experimental proof of electron
(Thompson)

1913 Bohr's model of atom

1862 Blomsted-Jørgensen chain theory
applied to Co ammine complexes

1884 Jørgensen – further improvement

1892 Werner (age 26) proposed his
coordination theory (NP 1913)

Early coordination compounds – properties to explain

- unusual stoichiometry – exceeding the valence number typical for the given metal
- variety of colours (green and violet $[\text{Co}(\text{en})_2\text{Cl}_2]\text{Cl}$)
- chirality
- strange magnetic behaviour (paramagnetic $[\text{CoF}_6]^{3-}$ and diamagnetic $[\text{Co}(\text{CN})_6]^{3-}$)

Complex compounds = 2 stable compounds with saturated valences form a new stable compound

Evaluated properties – indirect data (first crystallographic confirmation in 1921):

- ✓ colour
- ✓ molar conductivity
- ✓ precipitation of the chloride anion (gravimetry, AgCl)

Hypotheses:

1. Blomstrand, Jørgensen – chains (like carbon)
2. Werner – violation of the fixed valence rule

Cobalt ammine complexes

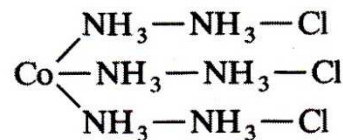
1852 – Edmond Frémy invented a colour-based naming scheme

1856 – O. W. Gibbs and F. A. Genth published data about 35 cobalt-ammine cations

Composition	Colour	Original name	Modern formula
$\text{Co}(\text{NO}_2)_3 \cdot 4\text{NH}_3$	brown	<i>flavo</i> complex	<i>cis</i> - $[\text{Co}(\text{NH}_3)_4(\text{NO}_2)_2]\text{NO}_2$
$\text{Co}(\text{NO}_2)_3 \cdot 4\text{NH}_3$	yellow	<i>croceo</i> complex	<i>trans</i> - $[\text{Co}(\text{NH}_3)_4(\text{NO}_2)_2]\text{NO}_2$
$\text{CoCl}_3 \cdot 6\text{NH}_3$	yellow	<i>luteo</i> complex	$[\text{Co}(\text{NH}_3)_6]\text{Cl}_3$
$\text{CoCl}(\text{H}_2\text{O}) \cdot 5\text{NH}_3$	rose-red	<i>roseo</i> complex	$[\text{Co}(\text{NH}_3)_5(\text{H}_2\text{O})]\text{Cl}_3$
$\text{CoCl}_3 \cdot 5\text{NH}_3$	purple	<i>purpureo</i> complex	$[\text{Co}(\text{NH}_3)_5\text{Cl}]\text{Cl}_2$
$\text{CoCl}_3 \cdot 4\text{NH}_3$	green	<i>praseo</i> complex	<i>trans</i> - $[\text{Co}(\text{NH}_3)_4\text{Cl}_2]\text{Cl}$
$\text{CoCl}_3 \cdot 4\text{NH}_3$	violet	<i>violeo</i> complex	<i>cis</i> - $[\text{Co}(\text{NH}_3)_4\text{Cl}_2]\text{Cl}$

Chain representations

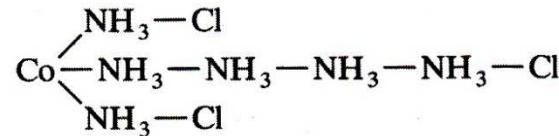
(a) $\text{CoCl}_3 \cdot 6\text{NH}_3$



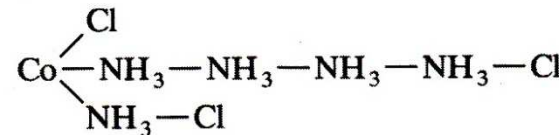
Blomstrand - upper

Jorgensen - lower

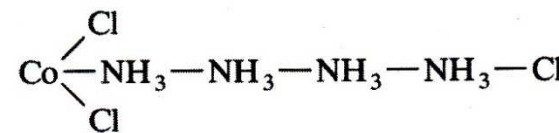
(1) $\text{CoCl}_3 \cdot 6\text{NH}_3$



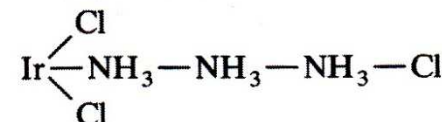
(2) $\text{CoCl}_3 \cdot 5\text{NH}_3$



(3) $\text{CoCl}_3 \cdot 4\text{NH}_3$

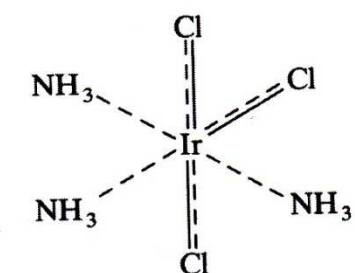
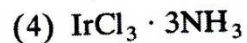
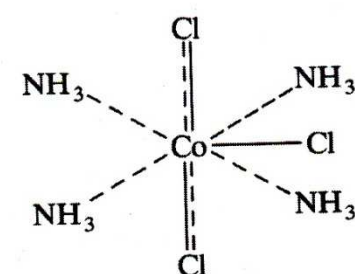
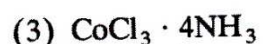
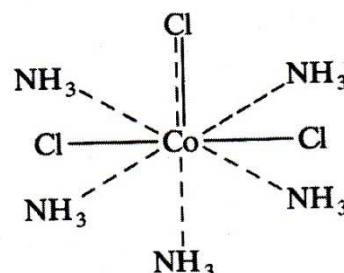
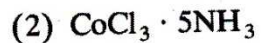
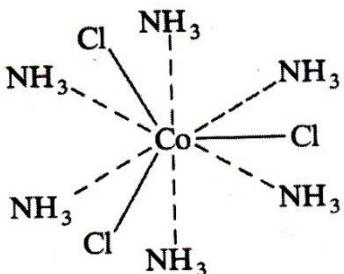


(4) $\text{IrCl}_3 \cdot 3\text{NH}_3$



colour	conductivity	precip.Cl
luteo	high	3
purpureo	medium	2
praseo	low	1

Werner – higher valence



Two type of valences:

- Haupvalenz – primary valence (oxid. state compensation), full line
 - ionizable
- Nebenvalenz – secondary valence (coordination number), dashed line
 - fixed in space

Both valences must be saturated

Orientation in space - isomers

- Coordination number 4

Two possible geometries – tetrahedron or square

Number of predicted isomers:

stoichiometry	TETRAHEDRON	SQUARE	
$[MAB_3]$			
$[MA_2B_2]$			

Experimental example: *cis*- and *trans*- $[PtCl_2(NH_3)_2]$ => square geometry

Orientation in space - isomers

- Coord. number 6 - theoretical number of isomers:

The Number of Actual versus Predicted Isomers for Three Different Geometries of Coordination Number 6 (Ref. 2)

	Hexagonal planar	Trigonal prism	Octahedral	
Formula	No. of predicted isomers (numbers in parentheses indicate position of the B ligands)			No. of actual isomers
MA_5B	One	One	One	One
MA_4B_2	Three (1, 2) (1, 3) (1, 4)	Three (1, 2) (1, 4) (1, 6)	Two (1, 2) (1, 6)	Two
MA_3B_3	Three (1, 2, 3) (1, 2, 4) (1, 3, 5)	Three (1, 2, 3) (1, 2, 4) (1, 2, 6)	Two (1, 2, 3) (1, 2, 6)	Two

X

NEGATIVE EVIDENCE

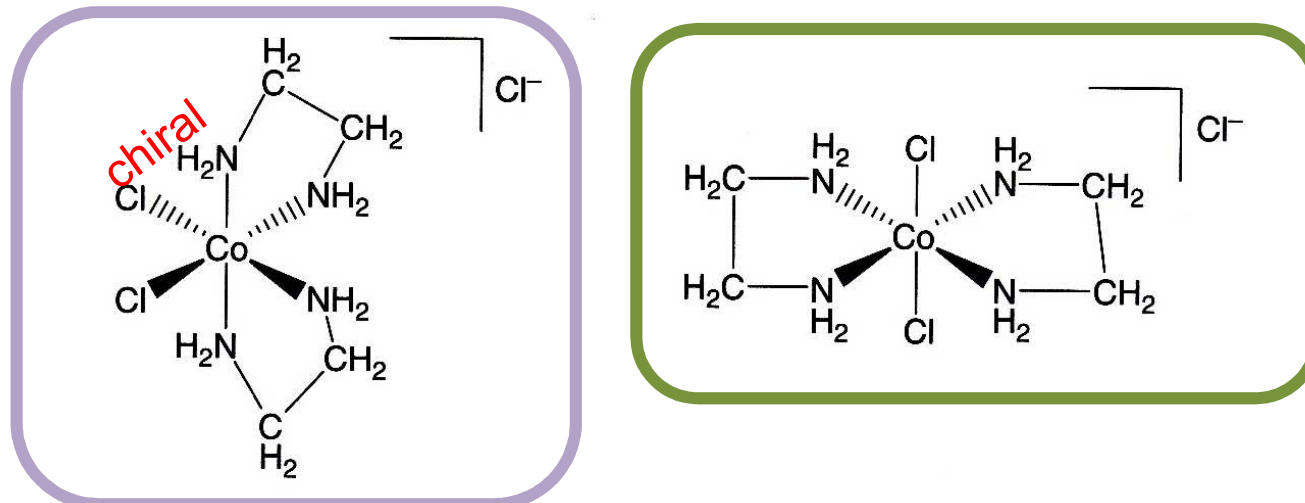
Source: Rodgers, G. E.: Descriptive Inorganic, Coordination, and Solid-State Chemistry, Brooks/Cole



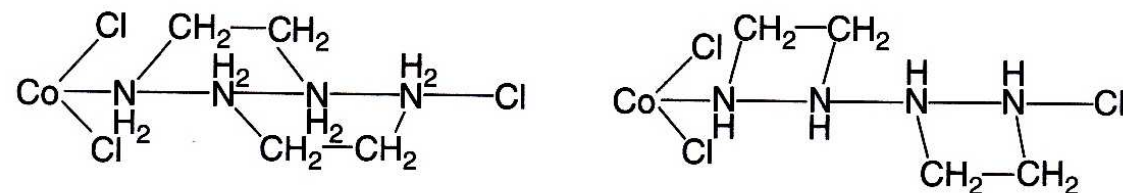
Chelates

Experimental result: 2 isomers of $[\text{CoCl}_2(\text{en})_2]\text{Cl}$ – **violet (*cis*)** and **green (*trans*)**

Werner's solution



Jørgensen's solution



“... chirality is due to the presence of carbon..“

Figure 2.2 Isomeric structures of $\text{CoCl}_3 \cdot (\text{en})_2$ as predicted by Werner's Coordination Theory (VII,VIII) and Jorgensen's Chain Theory (IX,X).

1st chiral compound without C

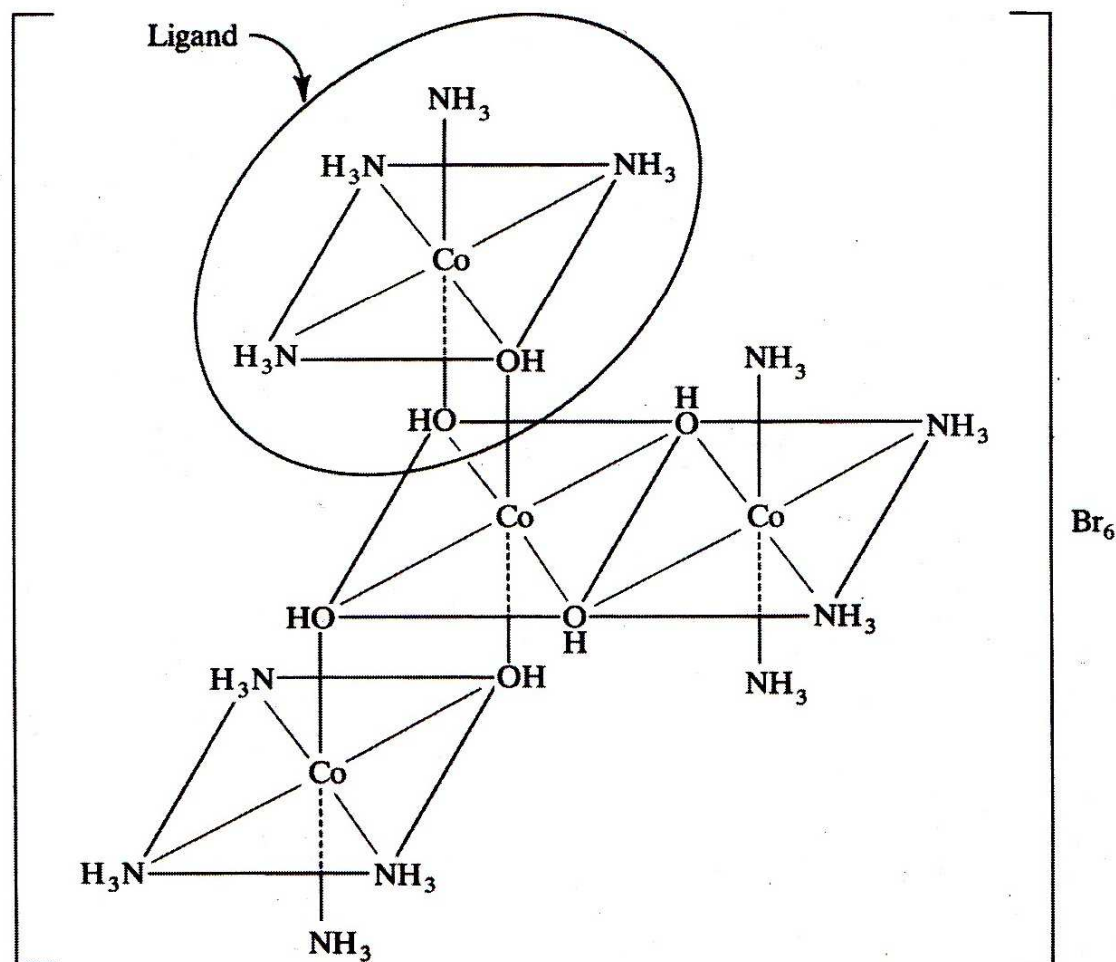
- Alfred Werner, Sophie Matissen,
1914

FIGURE 3.13

$\{\text{Co}[\text{Co}(\text{OH})_2(\text{NH}_3)_4]_3\}\text{Br}_6$, a chiral coordination compound containing no carbon, resolved by Werner and Matissen.

Chirality (optical activity) is not conditioned by the presence of carbon.

A positive proof for octahedral arrangement of the hexacoordinated species.



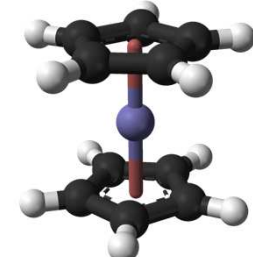
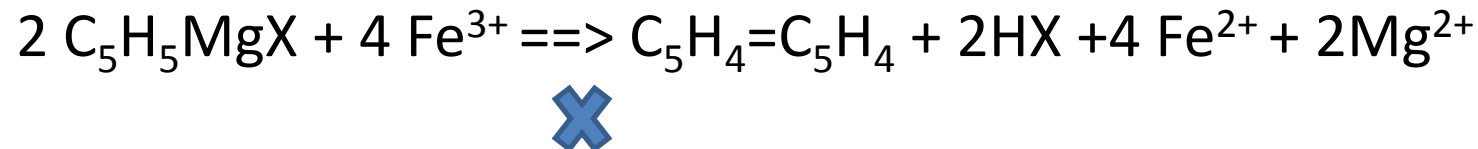
Further steps to understanding

- ❖ 1916: G. N. Lewis – general theory of the covalent bond
 - metal – ligand interaction described in terms of Lewis acid – base interaction
- ❖ 1926: I. I. Chernyaev (Čerňajev) – formulation of *trans*-effect in ligand substitution
- ❖ 1931: L. Pauling – valence bond theory
 - based on hybrid orbitals
- ❖ 1929: Hans Albert Bethe – crystal field model for ionic solids
- 1930 – 1940: J. H. Van Vleck – Theory of the Crystal Field
- since 1950 – the CFT used also for coordination compounds
- ❖ 1937: Ryutaro Tsuchida published the „spectrochemical series“
- ❖ since 1960: compounds with M–M bond, up to quadruple



Important milestones

- 1888 Ludwig Mond synthesized $[\text{Ni}(\text{CO})_4]$
Production of pure Ni
- 1952 ferrocene, $[\text{Fe}(\eta^5\text{-C}_5\text{H}_5)]$, 1st sandwich complex (abbrev. fc)
(Pauson, Kealy; Wilkinson)
discovered accidentally, thanks to an unsuccessful synthesis of fulvalene:



- 1955 Ziegler – Natta catalyst (Ti based; alkene polymerization)
- Biocoordination chemistry
 - crystal structure of myoglobin and haemoglobin – M. Perutz, J. Kendrew
 - *cis*- $[\text{PtCl}_2(\text{NH}_3)_2]$, cisplatin, cytotoxicity discovered by B. Rosenberg, 1965
- after 1970 – photochemistry of coordination compounds aimed to water splitting and H_2 production – Ru(II) compounds

Uveřejněné materiály jsou určeny studentům Vysoké školy chemicko-technologické v Praze jako studijní materiál. Některá textová i obrazová data v nich obsažená jsou převzata z veřejných zdrojů. V případě nedostatečných citací nebylo cílem autorky záměrně poškodit autora/y původního díla.

S případnými výhradami se prosím obracejte na autorku tohoto výukového materiálu, aby bylo možno zjednat nápravu.



The published materials are intended for students of the University of Chemistry and Technology, Prague as a study material. Some text and image data contained therein are taken from public sources. In the case of insufficient quotations, the author's intention was not to intentionally infringe the possible author(s) rights to the original work.

If you have any reservations, please contact the author(s) of the specific teaching material in order to remedy the situation.

Nomenclature of coordination compounds

IUPAC Red Book, *Nomenclature of Inorganic Chemistry –IUPAC Recommendations 2005*, N. G. Connelly, T. Damhus, R. M. Hartshorn, A. T. Hutton (Eds.), Royal Society of Chemistry, Cambridge, U.K., ISBN 0-85404-438-8

https://www.iupac.org/fileadmin/user_upload/databases/Red_Book_2005.pdf

<http://www.chem.qmul.ac.uk/iupac/>

Brief Guide to the Nomenclature of Inorganic Chemistry, IUPAC, *Pure Appl. Chem.* **87**, 1039–1049 (2015)



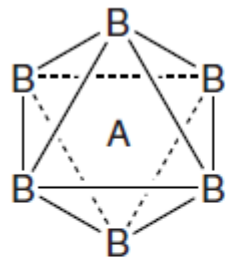
EUROPEAN UNION
European Structural and Investing Funds
Operational Programme Research,
Development and Education

ME
MT
MINISTRY OF EDUCATION,
YOUTH AND SPORTS

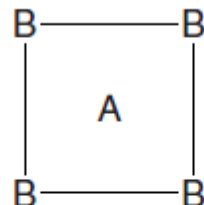


Key terms

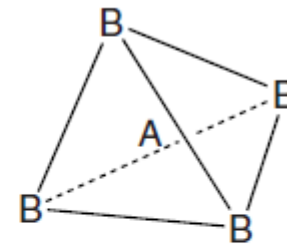
- coordination entity – square brackets; central atom first
examples: $[\text{Co}(\text{NH}_3)_6]^{3+}$, $[\text{PtCl}_4]^{2-}$, $[\text{Fe}_3(\text{CO})_{12}]$
- central atom
- ligand
- coordination polyhedron



1. octahedral
coordination
polyhedron



2. square planar
coordination
polygon

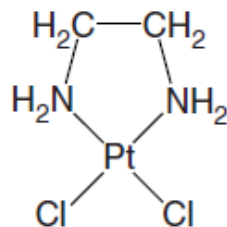


3. tetrahedral
coordination
polyhedron

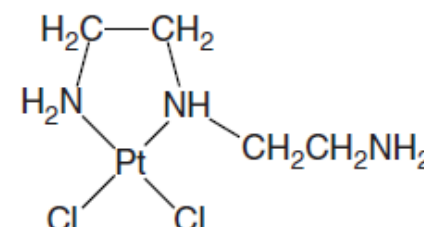
Key terms – cont.

- coordination number – number of σ -bonds between ligands and the central atom (Zeise's salt – C.N. 4, not 5)
- chelation

1.



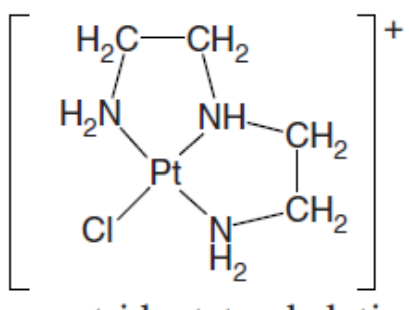
2.



bidentate chelation

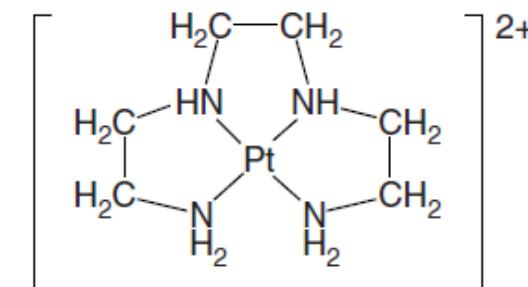
bidentate chelation

3.



tridentate chelation

4.



tetradeятate chelation

Key terms – cont.

- oxidation state

	<i>Formula</i>	<i>Ligands</i>	<i>Central atom oxidation state</i>
1.	$[\text{Co}(\text{NH}_3)_6]^{3+}$	6 NH ₃	III
2.	$[\text{CoCl}_4]^{2-}$	4 Cl ⁻	II
3.	$[\text{MnO}_4]^-$	4 O ²⁻	VII
4.	$[\text{MnFO}_3]$	3 O ²⁻ +1 F ⁻	VII
5.	$[\text{Co}(\text{CN})_5\text{H}]^{3-}$	5 CN ⁻ +1 H ⁻	III
6.	$[\text{Fe}(\text{CO})_4]^{2-}$	4 CO	-II

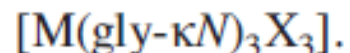
Notice: ligand = donor of 1 electron pair

Do not confuse oxidation number (Roman numeral) and overall charge (Arabic numerals)
ex: pentaammine(nitrito)cobalt(2+) contains Co(III) central metal

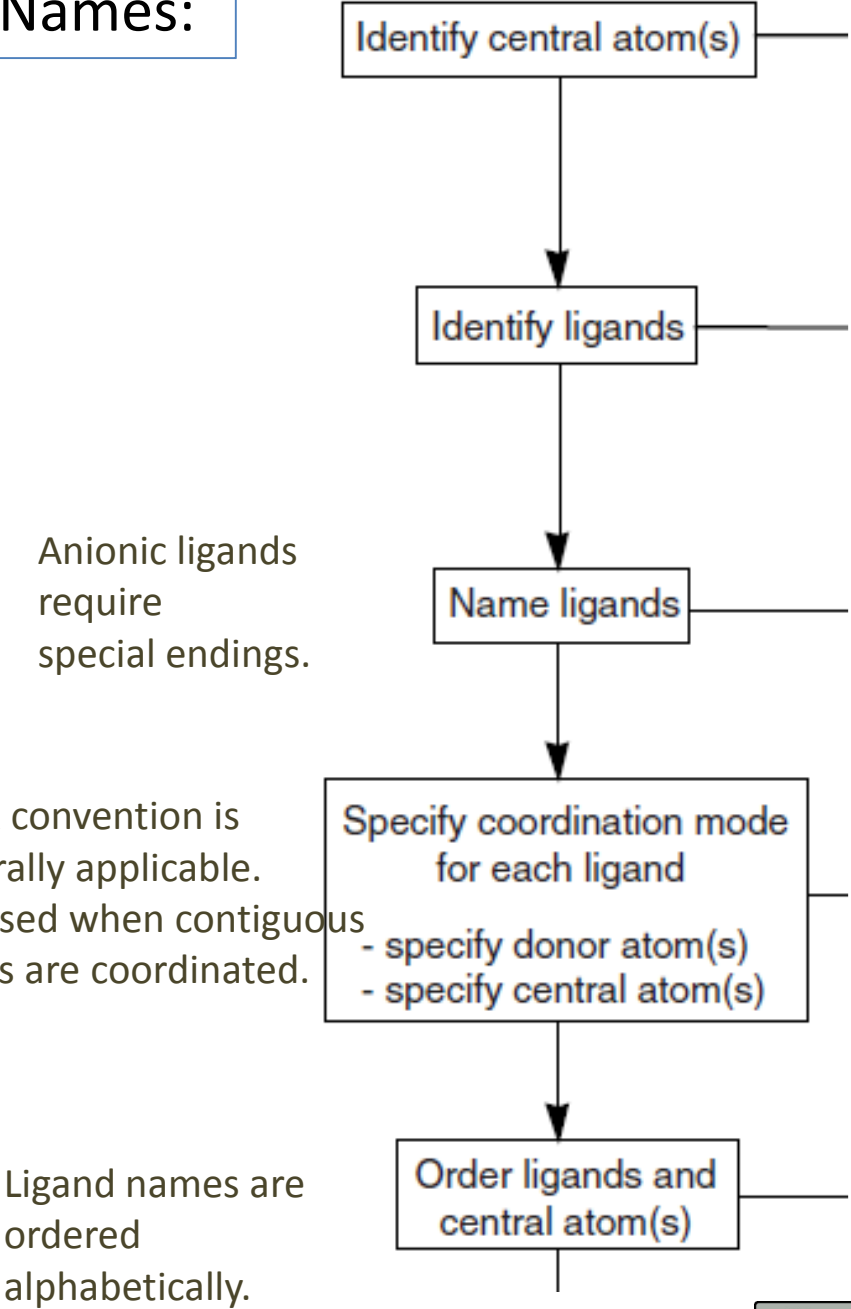
Describing the constitution of coordination compounds – from drawing structure to writing names and formulae

Formulae:

- [coordination entity]
- (polyatomic ligand)
- central atom first
- ligand sequence: alphabetical order, regardless their charge
(different position of CH₃CN and MeCN)
- ionic charge, oxidation numbers – superscripts
- abbreviations, further details with symbols of atom

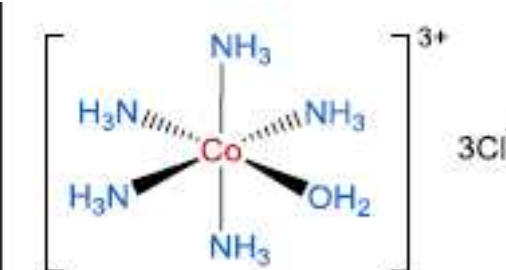
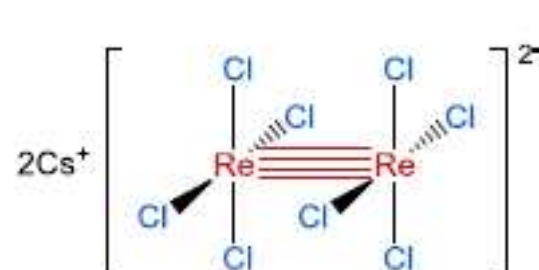


Names:



Producing names – simple ligands

- ligands are listed in alphabetical order
- anionic ligands need special endings, -o.
 - ide => ido, -ate => -ato, -ite => ito
- small molecules: aqua, ammine, carbonyl, nitrosyl (+ simple numbering prefixes di-, tri-...), no brackets in names
- overall name of a complex anion: **-ate** (...ferrate (*latin!*), cobaltate)

Structure to be named		
Central atom(s)	cobalt(III)	2 × rhenium
Identify and name ligands	ammonia → ammine water → aqua	chloride → chlorido
Assemble name	pentaammineaqua= cobalt(III) chloride	caesium bis(tetrachlorido= rhenate)(Re—Re)(2-)

Synonyms are possible, BUT each of them must be unambiguous

Ex.: $K_4[Fe(CN)_6]$

- potassium hexacyanidoferate(II), or
- potassium hexacyanidoferrate(4-), or
- tetrapotassium hexacyanidoferrate

Compare:

$[Pt(NH_3)_4]^{2+}$ tetraammineplatinum(II) or tetraammineplatinum(2+) ion

$[PtCl_4]^{2-}$ tetrachloridoplatinate(II) or tetrachloridoplatinate(2-) ion

$[PtCl_2(NH_3)_2]$ diamminedichloridoplatinum(II)

Oxidation state and charge needs to be distinguished:

$[PtCl_6]^{2-}$

$[Cr(OH_2)_6]^{3+}$

$[Cr^{III}(NCS)_4(NH_3)_2]^-$

$[Cr^{III}Cl_3(OH_2)_3]$

$[Fe^{-II}(CO)_4]^{2-}$

Connectivity – μ , η , κ

- μ - symbol of a bridging ligand,
- η – contiguous ligatin atoms, donation from bonding electron systém
- κ – specifying of a coordination mode
thiocyanato- κS vs. thiocyanato- κN

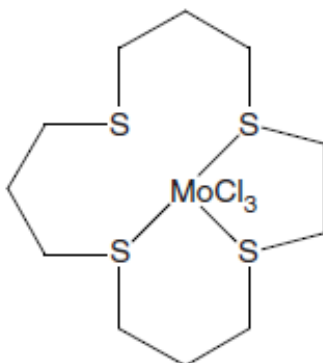
Specification of the donor atom is not required:

- monodentate O-bound carboxylate groups
- monodentate C-bound cyanide (ligand name ‘cyanido’)
- monodentate C-bound carbon monoxide (ligand name ‘carbonyl’)
- monodentate N-bound nitrogen monoxide (ligand name ‘nitrosyl’)

The kappa convention

- The κ -term comprises the Greek letter κ followed by the *italicised* element symbol of the ligating atom. For more complicated ligands the κ - term is often placed within the ligand name following the group to which the κ - term refers. Multiple identical links to a central atom can be indicated by addition of the appropriate numeral as a superscript between the κ and element symbols
- Multiplicative prefixes which apply to a ligand or portions of a ligand also apply to the donor atom symbols. In some cases this may require the use of an alternative ligand name.
- When the kappa descriptor is used for describing bridges, it counts all donor atom-to-central atom bonds

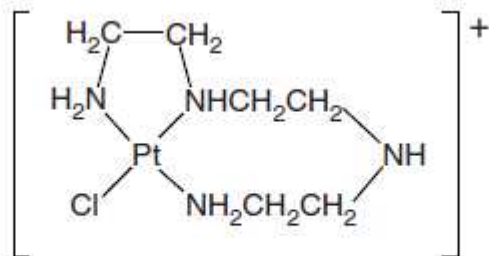
Example:



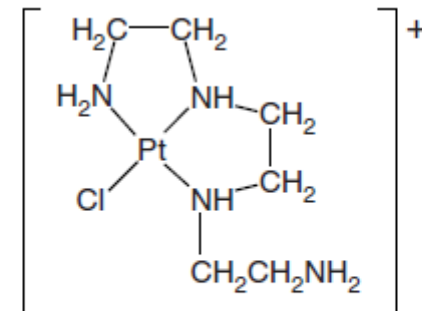
trichlorido(1,4,8,12-tetrathiacyclopentadecane- κ^3 S^{1,4,8})molybdenum, or
trichlorido(1,4,8,12-tetrathiacyclopentadecane- κ^3 S¹,S⁴,S⁸)molybdenum

Compare names of the following compounds:

ligand = *N,N'*-bis(2-aminoethyl)ethane-1,2-diamine



[*N,N'*-bis(2-amino- κN -ethyl)ethane-1,2-diamine- κN]chloridoplatinum(II)



[*N*-(2-amino- κN -ethyl)-*N'*-(2-aminoethyl)ethane-1,2-diamine- $\kappa^2 N,N'$] chloridoplatinum(II)

Another example:

Structure to be named	
Central atom	cobalt(III)
Identify and name ligands	ethane-1,2-diamine peroxide → peroxido
Specify ligating atoms	ethane-1,2-diamine- $\kappa^2 N$ η^2 -peroxido
Assemble name	bis(ethane-1,2-diamine- $\kappa^2 N$)= (η^2 -peroxido)cobalt(III)

Table 6: Producing names for complexes: complicated ligands

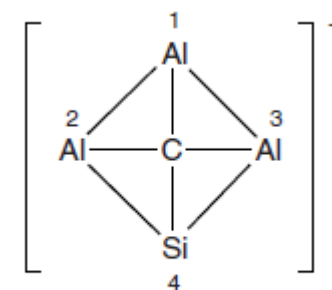
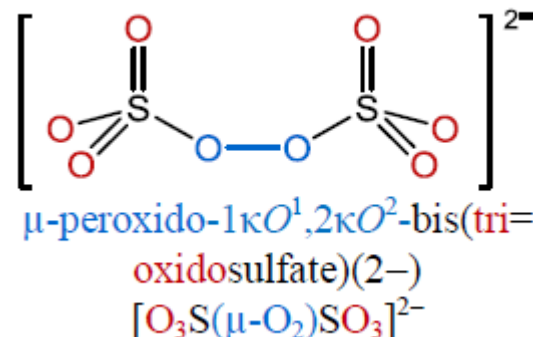
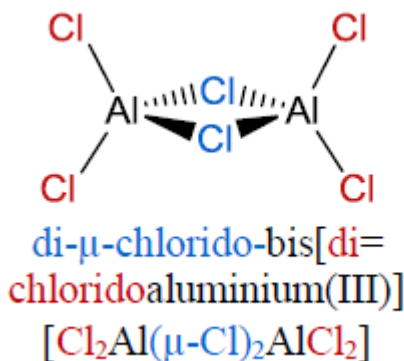
Structure to be named	$\text{Ba}^{2+} \quad 2$	
Central atom	cobalt(III) → cobaltate(III)	platinum(II)
Identify and name ligands	$2,2',2'',2'''$ - $(\text{ethane}-1,2\text{-diyl})$ dinitriolo)tetraacetate → $2,2',2'',2'''$ - $(\text{ethane}-1,2\text{-diyl})$ dinitriolo)tetraacetato	chloride → chlorido triphenylphosphane
Specify ligating atoms	$2,2',2'',2'''$ - $(\text{ethane}-1,2\text{-diyl})$ dinitriolo- κ^2N)tetraacetato- κ^4O	<i>not required for chloride</i> triphenylphosphane- κP
Assemble name	barium [$2,2',2'',2'''$ - $(\text{ethane}-1,2\text{-diyl})$ dinitriolo- κ^2N)tetraacetato- κ^4O]cobaltate(III)	dichloridobis(triphenylphosphane- κP)platinum(II)

Bridging ligands

Bridging ligands are indicated by the Greek letter μ appearing before the ligand name and separated from it by a hyphen. e.g. ammine- μ -chlorido-chlorido.

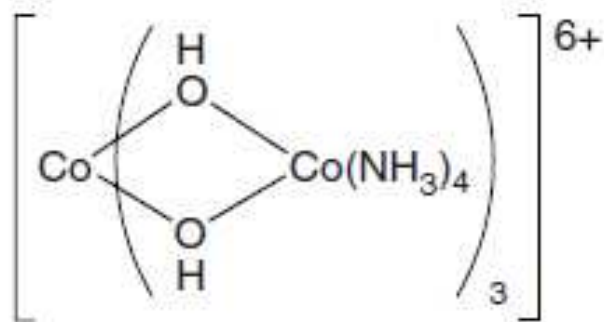
In names, a bridging ligand is cited before a corresponding non-bridging ligand,

In formulae, it is placed after terminal ligands of the same kind. Thus, in both names and formulae bridging ligands are placed further away from the central atoms than are terminal ligands of the same kind.



The bridging index n is placed as a right subscript, it indicates the number of coordination centres connected by a bridge (number 2 is not used).

Modern name of the first fully „inorganic“ chiral coordination compound (see History)

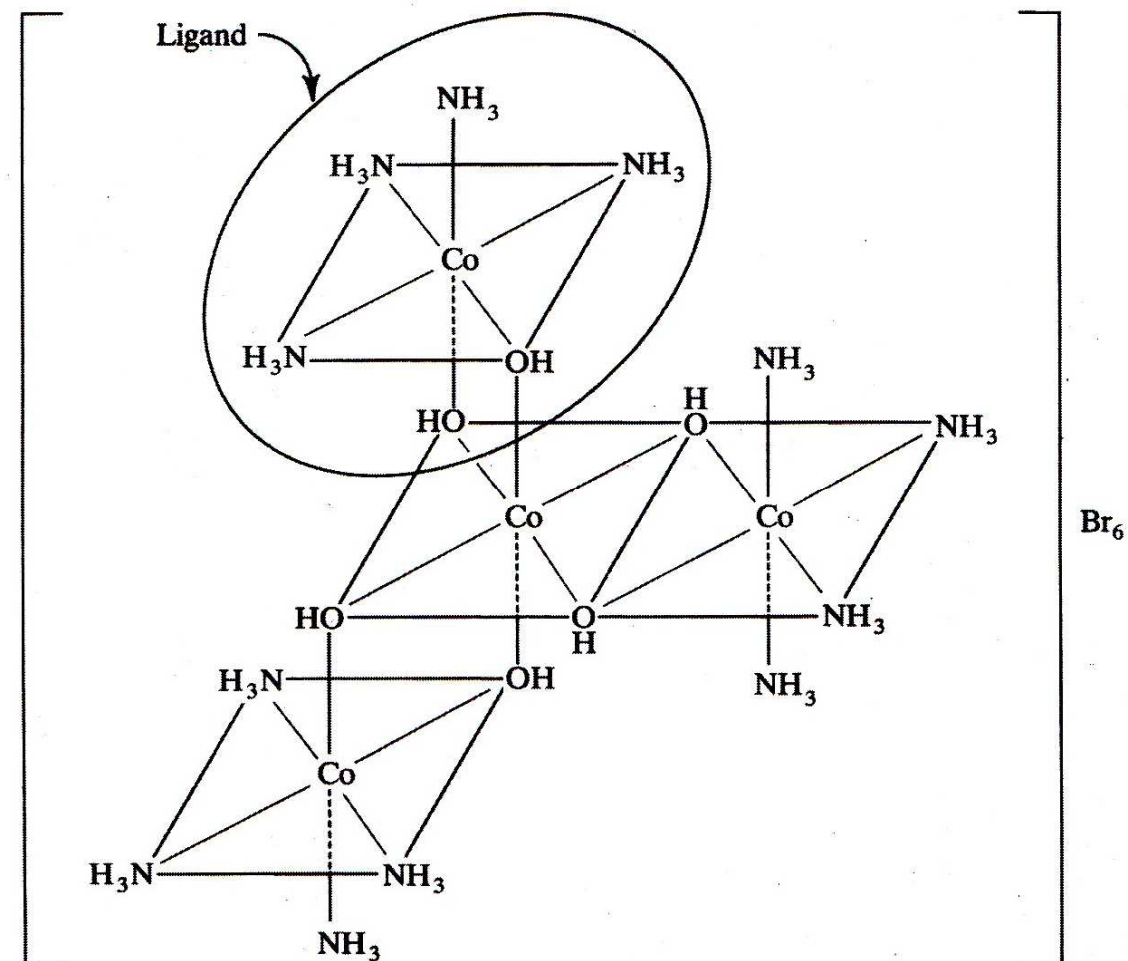


Cobalt atoms:

- 1,2,3 identical;
- 4 central

Name:

dodecaammine-1 κ^4 N,2 κ^4 N,3 κ^4 N-hexa- μ -hydroxido-1:4 κ^4 O;2:4 κ^4 O;3:4 κ^4 O-tetracobalt(6+)



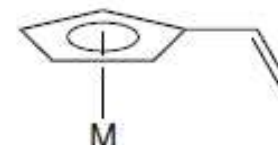
Notice: The kappa descriptor used for bridges counts all donor atom-to-central atom bonds (here: 2 bridges, but 4 bonds)

Eta convention

A complementary notation, the eta (η) convention, is used to specify the number ('hapticity') of *contiguous* ligating atoms that are involved in bonding to one or more metals. The need for this convention arises from the special nature of the bonding of unsaturated hydrocarbons to metals *via* their π -electrons, and it is used only when there are several contiguous atoms involved in the bond to the metal. The contiguous atoms of the π -coordinated ligand are often the same element, but they need not be, and they may also be atoms other than carbon.



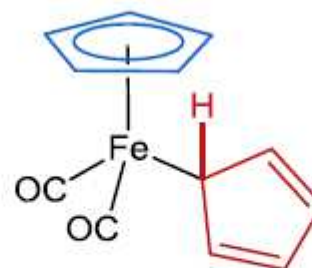
cyclopenta-2,4-dien-1-yl- η^2 -ethene



vinyl- η^5 -cyclopentadienyl

The ligand name η^5 -cyclopentadienyl, although strictly speaking ambiguous, is acceptable as a short form of η^5 -cyclopenta-2,4-dien-1-yl, due to common usage.

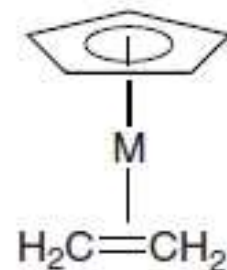
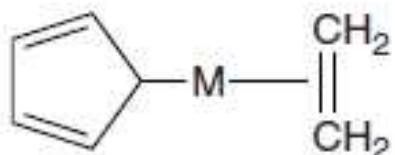
The symbol η^1 should not be used, as the eta convention applies only to the bonding of contiguous atoms in a ligand.



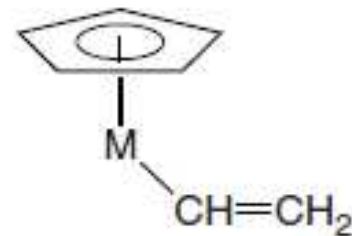
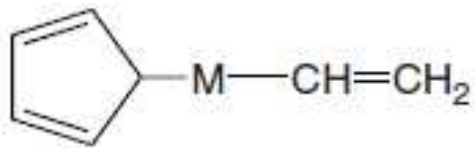
dicarbonyl(η^5 -cyclopentadienido)(cyclopenta-2,4-dien-1-ido- κC^1)iron
or dicarbonyl(η^5 -cyclopentadienyl)(cyclopenta-2,4-dien-1-yl- κC^1)iron

Eta convention

Compare the following examples:



(cyclopenta-2,4-dien-1-yl-κC¹)(η²-ethene) (η⁵-cyclopentadienyl)(η²-ethene)



(cyclopenta-2,4-dien-1-yl-κC¹)(vinyl)

(η⁵-cyclopentadienyl)(vinyl)

Part II: Describing the configuration of coordination compounds – from drawing structure to writing names and formulae

Once the constitution of a coordination entity has been defined, it remains to describe the spatial relationships between the structural components of the molecule or ion.

Stereoisomers: differ only in the spatial distribution of the components

1. enantiomers - mirror images; identical properties (except in the presence of other chiral entities)
2. diastereoisomers (= geometrical isomers) are not mirror images; exhibit different physical, chemical and spectroscopic properties

Most structures will deviate from ideal polyhedra. The closest should be chosen.

Order ligands and central atom(s)

Identify coordination geometry and select polyhedral symbol

Describe relative configuration

CIP priority is used.

Determine absolute configuration

Constitution:

1. central atom(s)
2. ligands
3. bonding modes

Configuration:

1. coordination geometry - the overall shape of the molecule, e.g. octahedron
2. relative configuration - relative positions of the components of the molecule (mutual position)
3. absolute configuration - identification of which enantiomer is being specified (if the mirror images are non-superimposable).

1. COORDINATION GEOMETRY

Polyhedral symbol = an affix, before any other spatial features, enclosed in parentheses and separated from the name by a hyphen

Constitution: one or more capital italic letters (denoting the idealized geometry of the ligands around the coordination centre), and an arabic numeral = coordination number

Ex.: (*SP-4*)-tetrachloroplatinate(II)

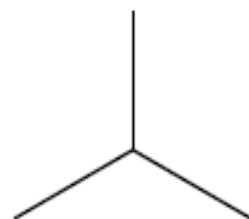
<i>Coordination polyhedron</i>	Polyhedra:	<i>Coordination number</i>	<i>Polyhedral symbol</i>
linear		2	<i>L</i> -2
angular		2	<i>A</i> -2
trigonal plane		3	<i>TP</i> -3
trigonal pyramid		3	<i>TPY</i> -3
T-shape		3	<i>TS</i> -3
tetrahedron		4	<i>T</i> -4
square plane		4	<i>SP</i> -4
square pyramid		4	<i>SPY</i> -4
see-saw		4	<i>SS</i> -4
trigonal bipyramid		5	<i>TBPY</i> -5
square pyramid		5	<i>SPY</i> -5
octahedron		6	<i>OC</i> -6
trigonal prism		6	<i>TPR</i> -6
pentagonal bipyramid		7	<i>PBPY</i> -7
octahedron, face monocapped		7	<i>OCF</i> -7
trigonal prism, square-face monocapped		7	<i>TPRS</i> -7
cube		8	<i>CU</i> -8

cube	Polyhedra:	8	<i>CU</i> -8
square antiprism		8	<i>SAPR</i> -8
dodecahedron		8	<i>DD</i> -8
hexagonal bipyramid		8	<i>HBPY</i> -8
octahedron, <i>trans</i> -bicapped		8	<i>OCT</i> -8
trigonal prism, triangular-face bicapped		8	<i>TPRT</i> -8
trigonal prism, square-face bicapped		8	<i>TPRS</i> -8
trigonal prism, square-face tricapped		9	<i>TPRS</i> -9
heptagonal bipyramid		9	<i>HBPY</i> -9

^a Strictly, not all geometries can be represented by polyhedra.

Three-coordination

trigonal plane



TP-3

trigonal pyramid



TPY-3

T-shape

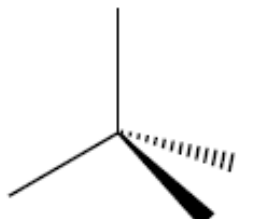


TS-3

Four-coordination

CN 4

tetrahedron



T-4

square plane



SP-4

square pyramid



SPY-4

see-saw

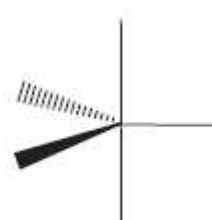


SS-4

Five-coordination

CN 5

trigonal bipyramidal



TBPY-5

square pyramid

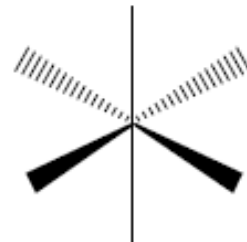


SPY-5

CN 6

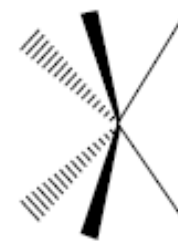
Six-coordination

octahedron



OC-6

trigonal prism

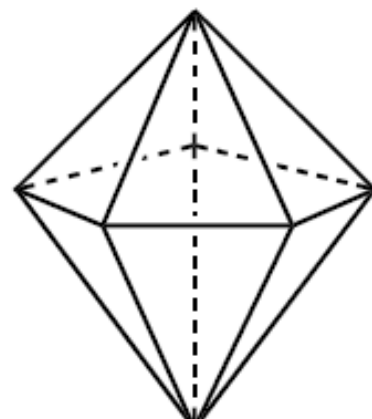


TPR-6

Seven-coordination

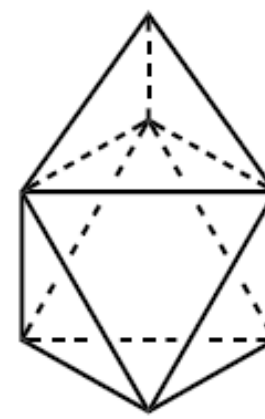
CN 7

pentagonal bipyramid



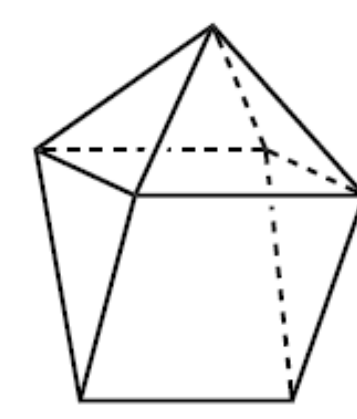
PBPY-7

octahedron, face monocapped



OCF-7

trigonal prism,
square-face monocapped



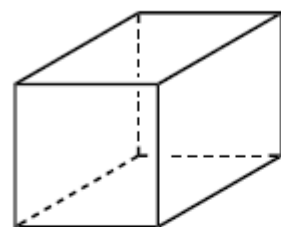
TPRS-7

monocapped = + 1 apex

CN 8

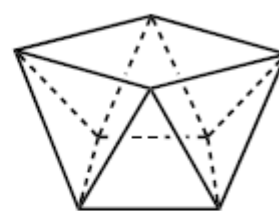
Eight-coordination

cube



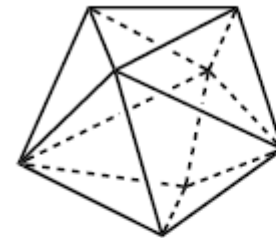
CU-8

square
antiprism



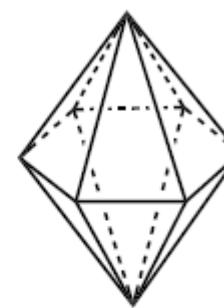
SAPR-8

dodecahedron



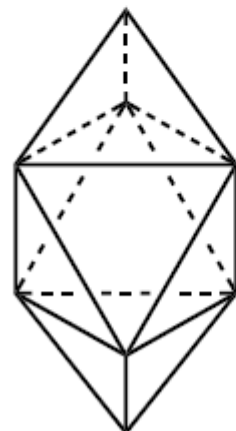
DD-8

hexagonal
bipyramid



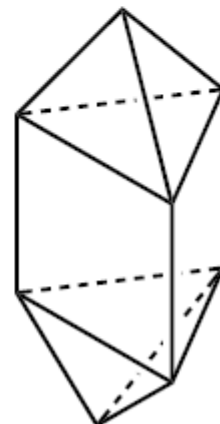
HBPY-8

octahedron,
trans-bicapped



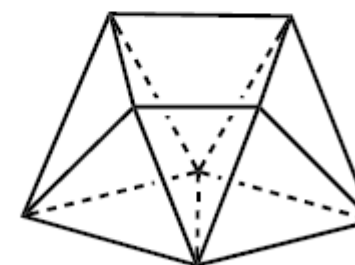
OCT-8

trigonal prism,
triangular-face bicapped



TPRT-8

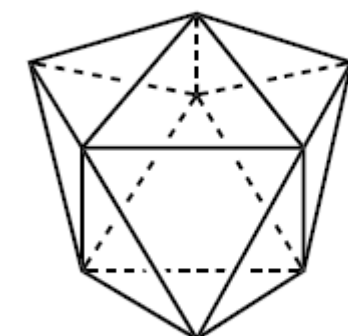
trigonal prism,
square-face bicapped



TPRS-8

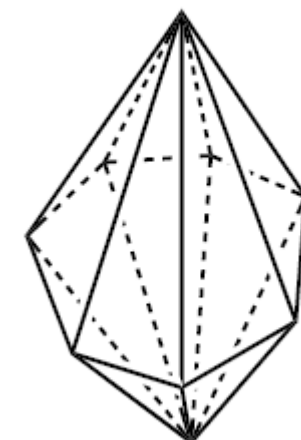
CN 9

trigonal prism,
square-face tricapped



TPRS-9

heptagonal
bipyramid



HBPY-9

2. DIASTEREOISOMERES

Common terms ***cis, trans; mer, fac***

- when a particular geometry is present (*OCT, SP*)
- only 2 kinds of donor atom

General method – CONFIGURATION INDEX

- a series of digits identifying the positions of the ligating atoms on the vertices of the coordination polyhedron
- distinguishes between diastereoisomers.
- appears within the parentheses enclosing the polyhedral symbol.

Use of a priority number for each donor

based on the Cahn, Ingold and Prelog rules (the CIP rules). These priority numbers are then used to form the configuration index for the compound.

Donor atoms that have a higher atomic number have higher priority than those that have a lower atomic number.

The presence of polydentate ligands may require the use of primes on some of the numbers in the configuration index.

Square planar systems (SP-4):

cis and trans are used commonly as prefixes to distinguish between stereoisomers of the form $[M a_2 b_2]$

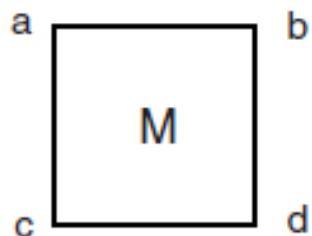
The configuration index : 1 digit after the polyhedral symbol (SP-4).

the priority number for the ligating atom trans to the ligating atom of priority number 1

If there are two possibilities, the configuration index is the priority number with the higher numerical value (the principle of trans maximum difference).

Priority sequence: a > b > c > d

Priority number sequence: 1 < 2 < 3 < 4



SP-4-4

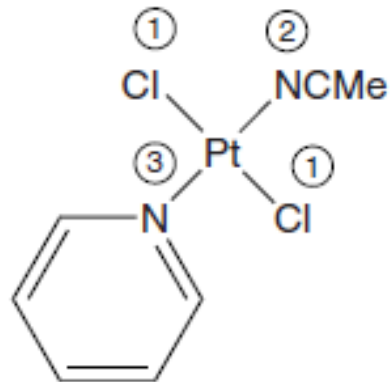


SP-4-2

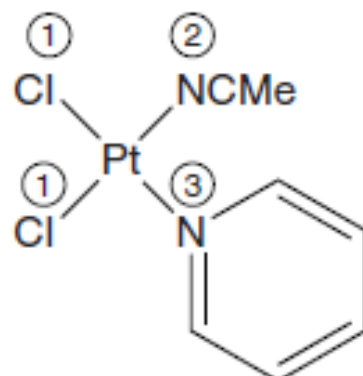


SP-4-3

Examples



(*SP*-4-1)-(acetonitrile)dichlorido(pyridine)platinum(II)



2 possibilities
trans maximum difference

(*SP*-4-3)-(acetonitrile)dichlorido(pyridine)platinum(II)

Octahedral systems (OC-6):

cis and trans are used commonly as prefixes to distinguish between stereoisomers of the form $[M a_2 b_4]$

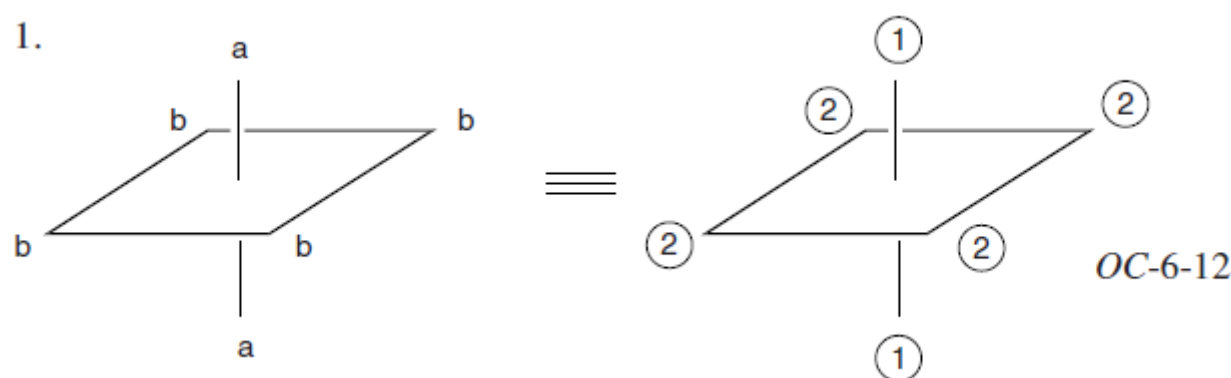
The terms mer (meridional) and fac (facial) are used commonly to distinguish between stereoisomers of complexes of the form $[M a_3 b_3]$.

The configuration index : 2 digits after the polyhedral symbol (OC-6).

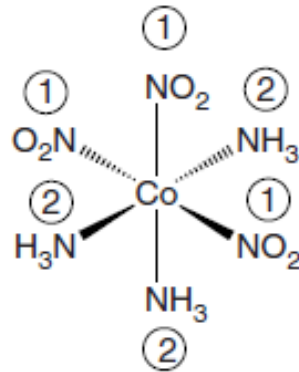
- The first digit is the priority number of the ligating atom trans to the ligating atom of priority number 1

These two ligating atoms, the priority 1 atom and the (lowest priority) atom trans to it, define the reference axis of the octahedron. Without these axial ligands, we have a square => we continue like in *SP-4 systems*,

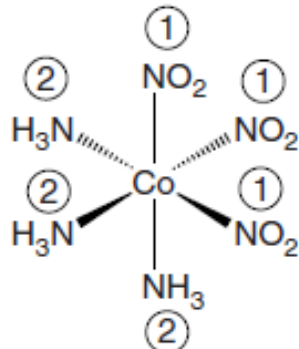
- the second digit of the configuration index is the priority number of the ligating atom trans to the most preferred ligating atom in the plane that is perpendicular to the reference axis.



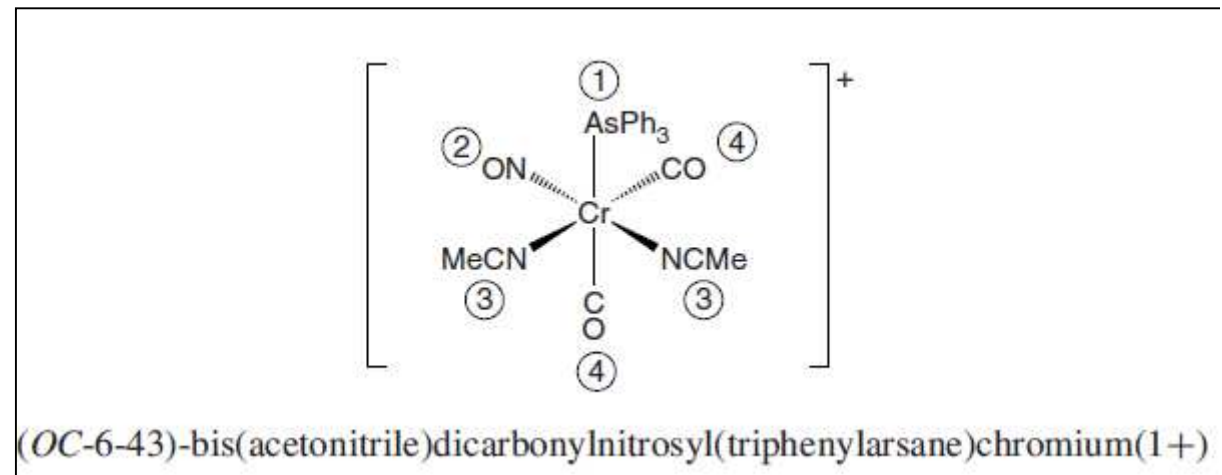
Octahedral coordination systems (OC-6)



mer-[Co(NH₃)₃(NO₂)₃]
(OC-6-21)-triamminetrinitrito-κ³N-cobalt(III)



fac-[Co(NH₃)₃(NO₂)₃]
(OC-6-22)-triamminetrinitrito-κ³N-cobalt(III)



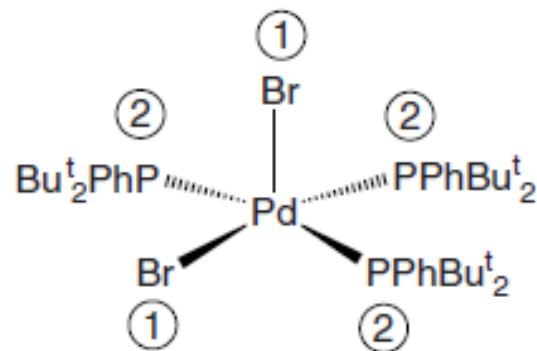
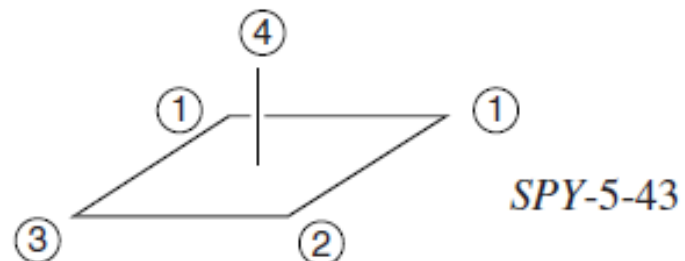
(OC-6-43)-bis(acetonitrile)dicarbonylnitrosyl(triphenylarsane)chromium(1+)

Square pyramidal coordination systems (SPY-4, SPY-5)

The configuration index of an SPY-5 system consists of two digits.

The first digit is the priority number of the ligating atom on the C4 symmetry axis (the reference axis)

The second digit is the priority number of the ligating atom trans to the ligating atom with the lowest priority number in the plane perpendicular to the C4 symmetry axis (= in the square).



(SPY-5-12)-dibromidotris[di-*tert*-butyl(phenyl)phosphane]palladium

Describing absolute configuration – distinguishing between enantiomers

A chiral molecule lacks an improper axis of symmetry S_n .
Notice that S_1 = mirror plane; S_2 = centre of inversion.

Two well-established systems for distinguishing between two enantiomers exist:

1. the R/S convention used for describing tetrahedral centres and the closely related C/A convention used for other polyhedra. The R/S and C/A conventions use the priority sequence.
2. based on the geometry of the molecule; this system makes use of the skew-lines convention; it is usually applied only to octahedral complexes. The two enantiomers are identified by the symbols Δ and Λ in this system.

The R/S convention for tetrahedral centres

R = the cyclic sequence of priority numbers, proceeding **from highest** priority, is **clockwise** when the viewer is looking **down** the vector from the tetrahedral centre **to the least preferred** substituent (the substituent having the priority number with the highest numerical value, i.e. 4).

S = **anticlockwise**

The C/A convention for other polyhedral centres

The same principles extended to geometries other than tetrahedral.

Trigonal bipyramidal centres:

the viewer looks down the reference axis

the more preferred donor atom is closer to the viewer

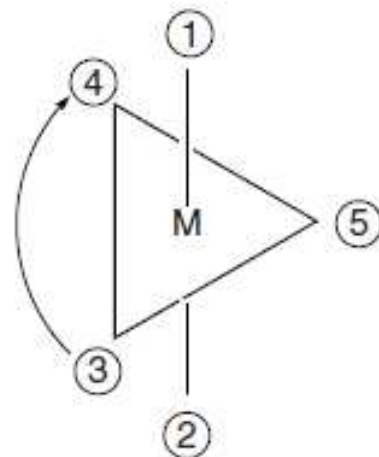
If the priority sequence of the three ligating atoms proceeds from the

highest priority to the lowest priority in a **clockwise** fashion => C

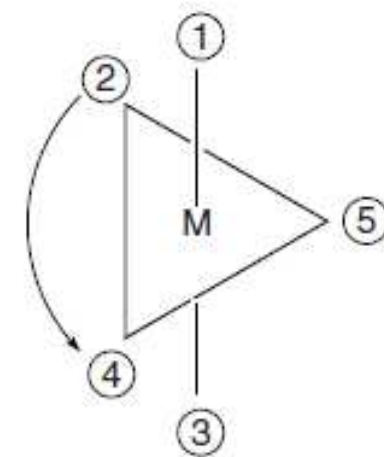
anticlockwise = A

1.

TB PY-5



2.

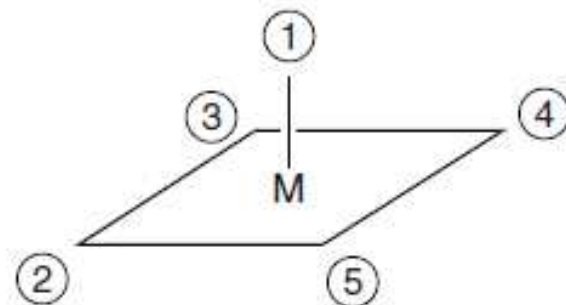


Chirality symbol = C

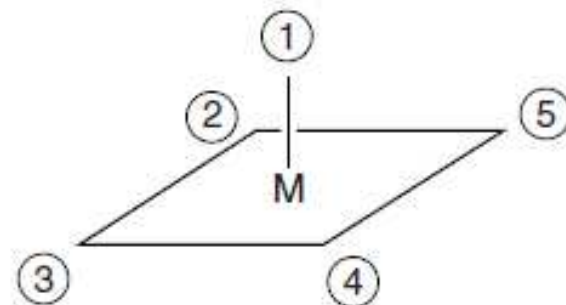
Chirality symbol = A

SP PY-5

1.



2.

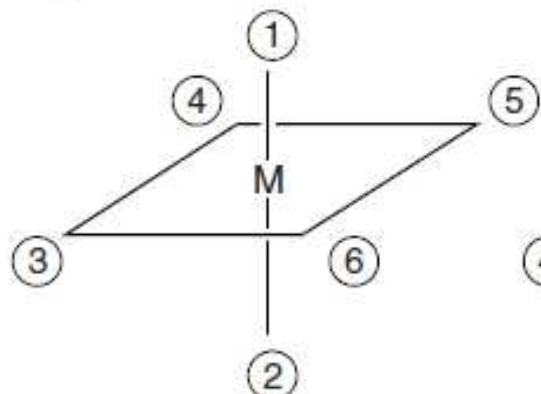


Chirality symbol = C

Chirality symbol = A

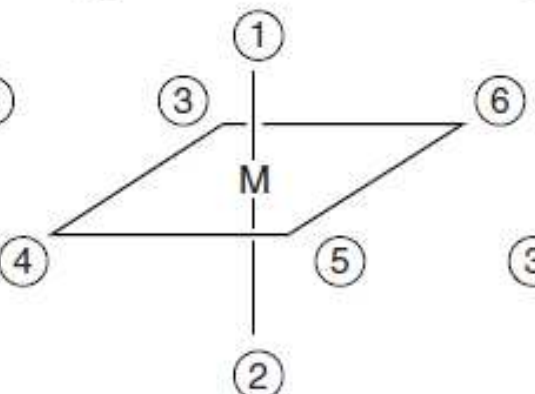
OC-6

1.



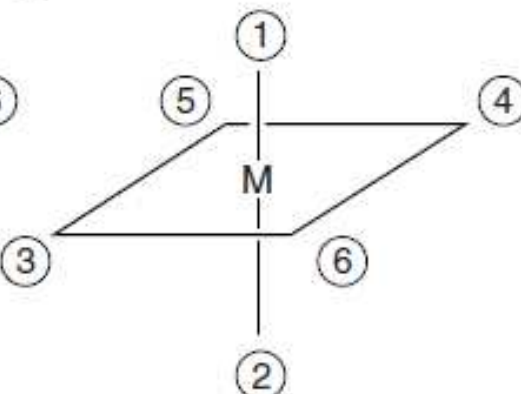
Chirality symbol = C

2.

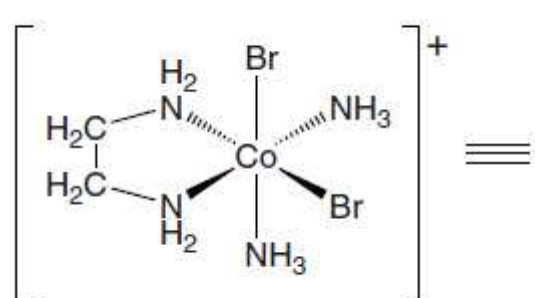


Chirality symbol = A

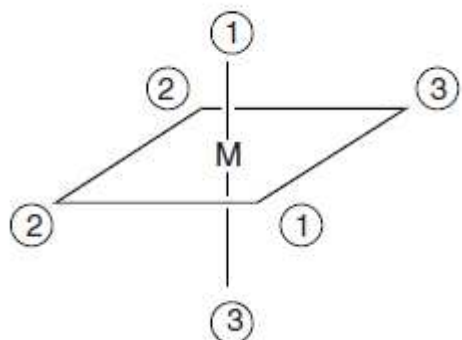
3.



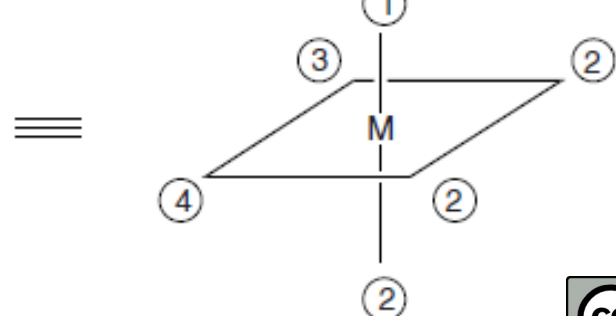
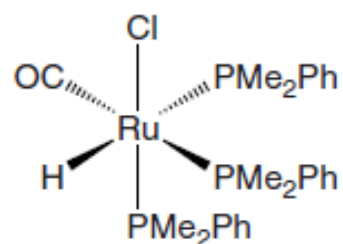
Chirality symbol = C



OC-6-32-C



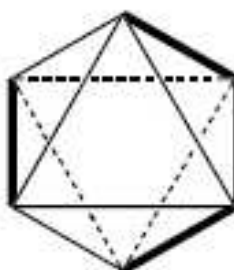
OC-6-24-A



The skew-lines convention

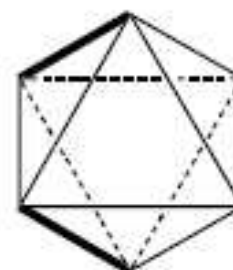
The skew-lines convention applies for tris(bidentate) complexes, the cis-bis(bidentate) octahedral structures and the conformations of certain chelate rings.

1.



delta (Δ)

2.



lambda (Λ)

Two **skew-lines** which are not orthogonal possess the property of having one, and only one, **normal** in common. **They define a helical system**, as illustrated in Figures IR-9.1 (next slide). In Figure IR-9.1, one of the skew-lines, AA, determines the axis of a helix upon a cylinder whose radius is equal to the length of the common normal, NN, to the two skew-lines, AA and BB. The other of the skew-lines, BB, is a tangent to the helix at N and determines the pitch of the helix. In Figure IR-9.2, the two skew-lines AA and BB are seen in projection onto a plane orthogonal to their common normal.

AA horizontal, at the back
BB in the front

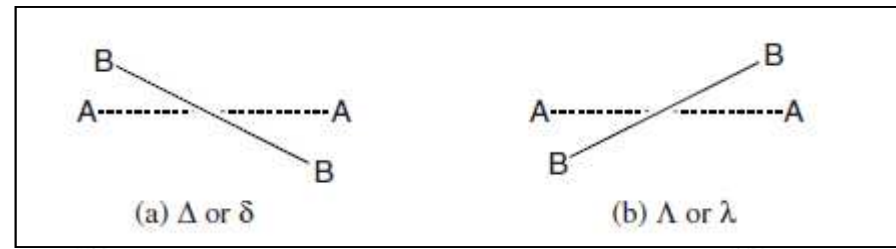


Figure IR-9.2

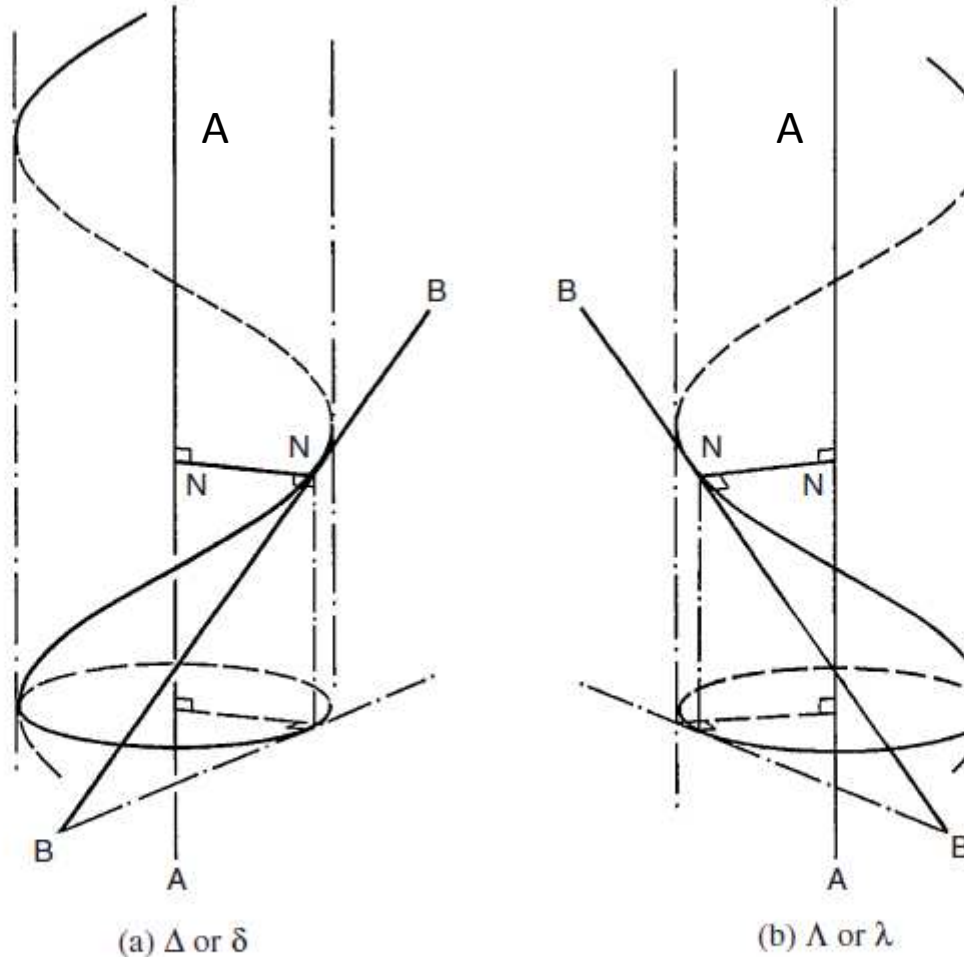


Figure IR-9.1. Two skew lines AA and BB which are not orthogonal define a helical system. In the Figure, AA is taken as the axis of a cylinder whose radius is determined by the common normal NN of the two skew-lines. The line BB is a tangent to the above cylinder at its crossing point with NN and defines a helix upon this cylinder. Cases (a) and (b) illustrate a right- and left-handed helix, respectively.

Application of the skew-lines convention to bis(bidentate) octahedral complexes

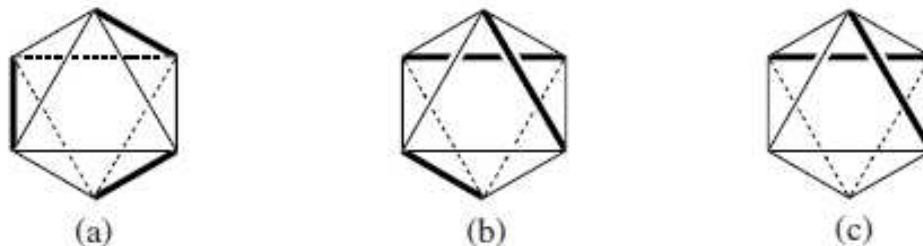


Figure IR-9.3. Two orientations of a tris(bidentate) structure, (a) and (b), to show the chiral relationship between these two species and the bis(bidentate) structure (c).

The skew-lines convention – chelate rings conformation

The line AA is defined as that line joining the 2 ligating atoms of the chelate ring.
The BB line is joining the two atoms which are neighbours to each of the ligating atom.
The Greek letters δ and λ are used for the right- and left-handed helices, respectively.

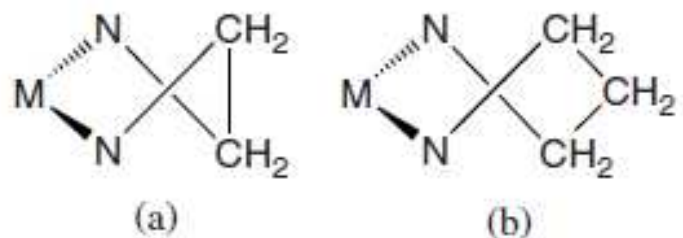
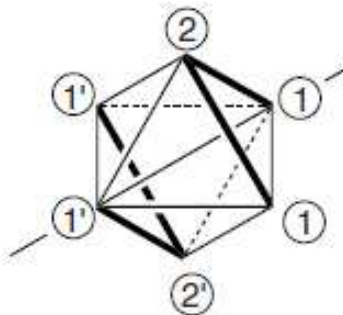


Figure IR-9.4. δ -Conformation of chelate rings: (a) five-membered; (b) six-membered.

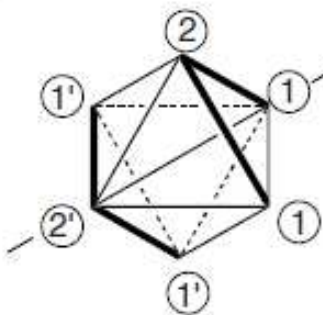
Priming convention

Bis(tridentate) complexes (i.e. octahedral complexes containing two identical linear tridentate ligands) may exist in three stereoisomeric forms, and there will be more if the tridentate ligands do not themselves contain some symmetry elements. The three isomers of the simplest case are represented below (Examples 1, 2 and 3), along with their polyhedral symbols and configuration indexes.

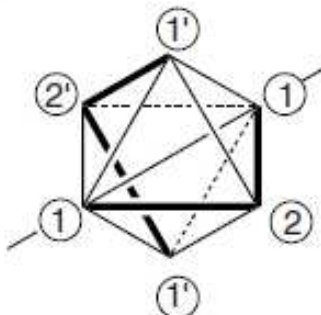
1.



2.



3.



The need for the priming convention can be seen by considering what the configuration indexes of Examples 1 and 3 would be in the absence of the priming convention. The two ligands are identical and consist of two similar fragments fused together. If the primes are ignored, the two complexes have the same distributions of ligating atoms. One way to highlight the difference between these two examples is to note that, in Example 1, all the donor atoms are *trans* to donors that are part of the other ligand. This is not true in Example 3. Using primes to indicate the groupings of donor atoms in particular ligands allows these two stereoisomers to be distinguished from one another by their configuration indexes.

Uveřejněné materiály jsou určeny studentům Vysoké školy chemicko-technologické v Praze jako studijní materiál. Některá textová i obrazová data v nich obsažená jsou převzata z veřejných zdrojů. V případě nedostatečných citací nebylo cílem autorky záměrně poškodit autora/y původního díla.

S případnými výhradami se prosím obracejte na autorku tohoto výukového materiálu, aby bylo možno zjednat nápravu.



The published materials are intended for students of the University of Chemistry and Technology, Prague as a study material. Some text and image data contained therein are taken from public sources. In the case of insufficient quotations, the author's intention was not to intentionally infringe the possible author(s) rights to the original work.

If you have any reservations, please contact the author(s) of the specific teaching material in order to remedy the situation.

Stabilization factors

- Lewis theory – HSAB principle
- Chelate and macrocyclic effects
- Electronic stabilization – 18 electron rule



EUROPEAN UNION
European Structural and Investing Funds
Operational Programme Research,
Development and Education



Acid Base Theories

- Brønsted theory – PRESENCE OF A PROTON is necessary
 - acid = proton donor
 - base = proton acceptor

Acidity (basicity) can be quantified, K_a , K_b , acids and bases sorted to strong, moderate, fable
- Lewis theory – also for aprotic environment
 - acid = electron pair acceptor
 - base = electron pair donor

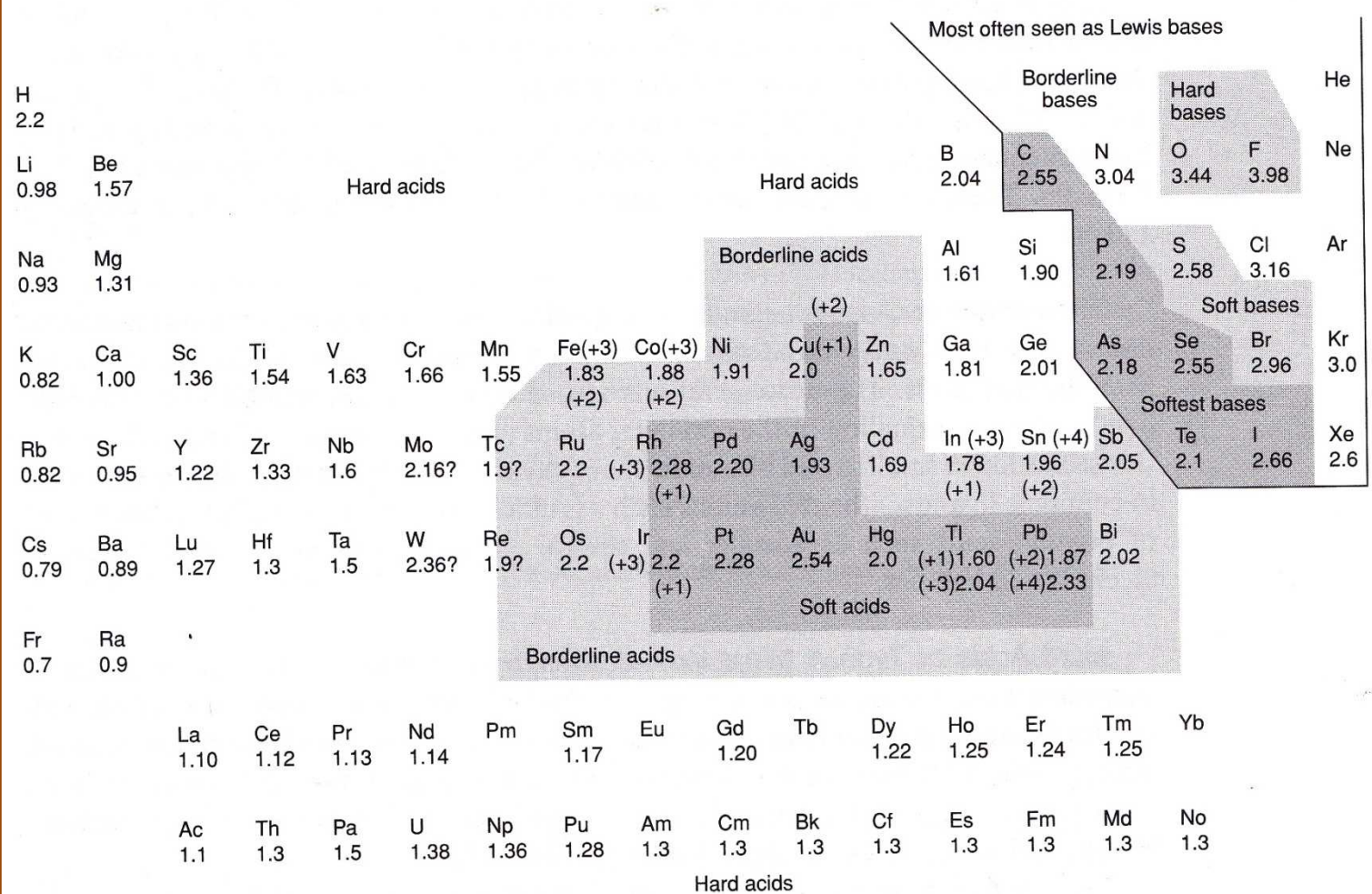
Acidity (basicity) is difficult to describe quantitatively; (Pearson, Drago), most commonly a relative softness / hardness are compared
- (Usanovich theory – combines acidobazicity and redox)
 - acid – electron acceptor (= oxidation agent)
 - base – electron donor

HSAB principle:

A hard acid tends to combine with a hard base – HA:HB

A soft acid tends to combine with a soft base – SA:SB

Hard and Soft Acids and Bases^a



Numbers below symbols: Pauling electronegativities
Numbers in (): oxidation numbers

Ex: G. Wulfsberg,
Inorganic Chemistry,
University Science
Books, Sausalito, CA,
2000



Characteristic properties of hard and soft Lewis acids and bases

property	hard acids	soft acids	soft bases	hard bases
electronegativity	0,7 – 1,6	1,9 – 2,5	2,1 – 3,0	3,4 – 4,0
ionic radius [pm]	< 90	> 90	> 170	~ 120
charge	≥ +3	≤ +2		

Soft AB are better **polarizable** than hard AB; anion H⁻ behaves like a soft base.

		Examples	
	HARD	INTERMEDIATE	SOFT
ACID	H ⁺ , alkali (1+), alkaline earths(2+), lanthanides(3+), Ce ⁴⁺ , Th ⁴⁺ , U ⁴⁺ , UO ₂ ²⁺ , Ti ⁴⁺ , Zr ⁴⁺ , Hf ⁴⁺ , Sn ⁴⁺ , VO ²⁺ , Cr ³⁺ , Mn ²⁺ , Fe ³⁺ , Co ³⁺ , In ³⁺ ; B ³⁺ , C ⁴⁺	Fe ²⁺ , Co ²⁺ , In ⁺ , Sn ²⁺ , Zn ²⁺ , Ni ²⁺ , Cu ²⁺ , Ru, Os, Ir ³⁺ , Rh ³⁺ , Bi	Cu ⁺ , Ir ⁺ , Rh ⁺ , Pd, Pt, Ag, Au, Hg, Tl, Pb
BASE	F ⁻ , O-donors (oxoanions, OH ⁻ , carboxylates, ethers, R-C=O etc.)	Amines, NO ₂ ⁻ , SO ₃ ²⁻ , Cl ⁻ , Br ⁻	H ⁻ , R ⁻ , CN ⁻ , I ⁻ , SCN ⁻ , S-donors, C-donors, PR ₃ , AsR ₃ , CO, C ₂ H ₄ , C ₆ H ₆ ,

Relative softness

Hard particles (both A and B) are only **slightly polarizable**.
Soft particles are better polarizable.

- influence of charge: oxidation state increases => hardness
- influence of size: smaller ions are harder

Symbiosis effect

Presence of a hard substituent or of a hard ligand increases hardness of the respective centre (and *vice versa*)

Ex.:

- PF_3 is harder than PPh_3
- fragment $[\text{Co}(\text{NH}_3)_5]^{3+}$ is harder than $[\text{Co}(\text{CN})_5]^{2-}$: $[\text{CoX}(\text{NH}_3)_5]^{2+}$ is more stable for $\text{X} = \text{F}^-$ than I^- ; $[\text{CoI}(\text{CN})_5]^{3-}$ is the most stable.
Bonding isomers: $[\text{Co}(\text{NH}_3)_5(\text{NCS})]^{2+}$ but $[\text{Co}(\text{CN})_5(\text{SCN})]^{3-}$

Attempts to quantify hardness / softness

Pearson, Parr – absolute hardness η ,

difference in ionisation energy and electron affinity

$$\eta = \frac{1}{2} (\text{IE} - \text{EA}) = \frac{1}{2} (\text{orbital energy of LUMO} - \text{orbital energy of HOMO})$$

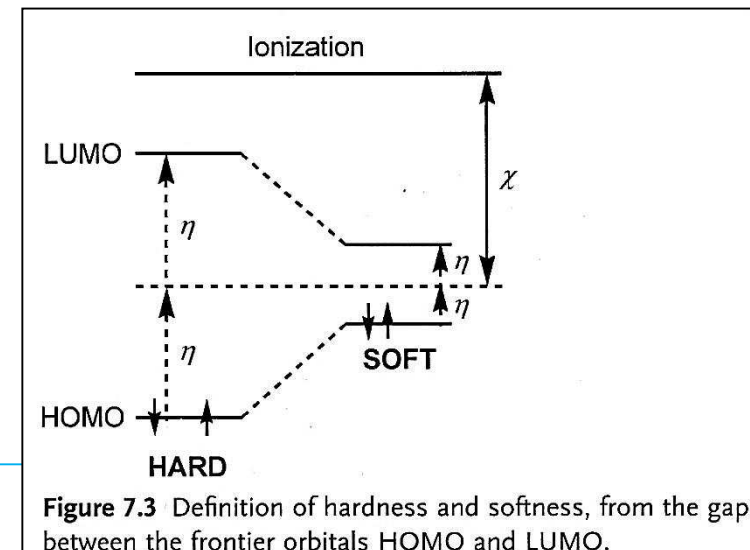
softness $\sigma = 1/\eta$ (inverse of hardness)

Hard acids, bases:

frontier orbitals are far apart

Soft acids, bases:

frontier orbitals are close in energy

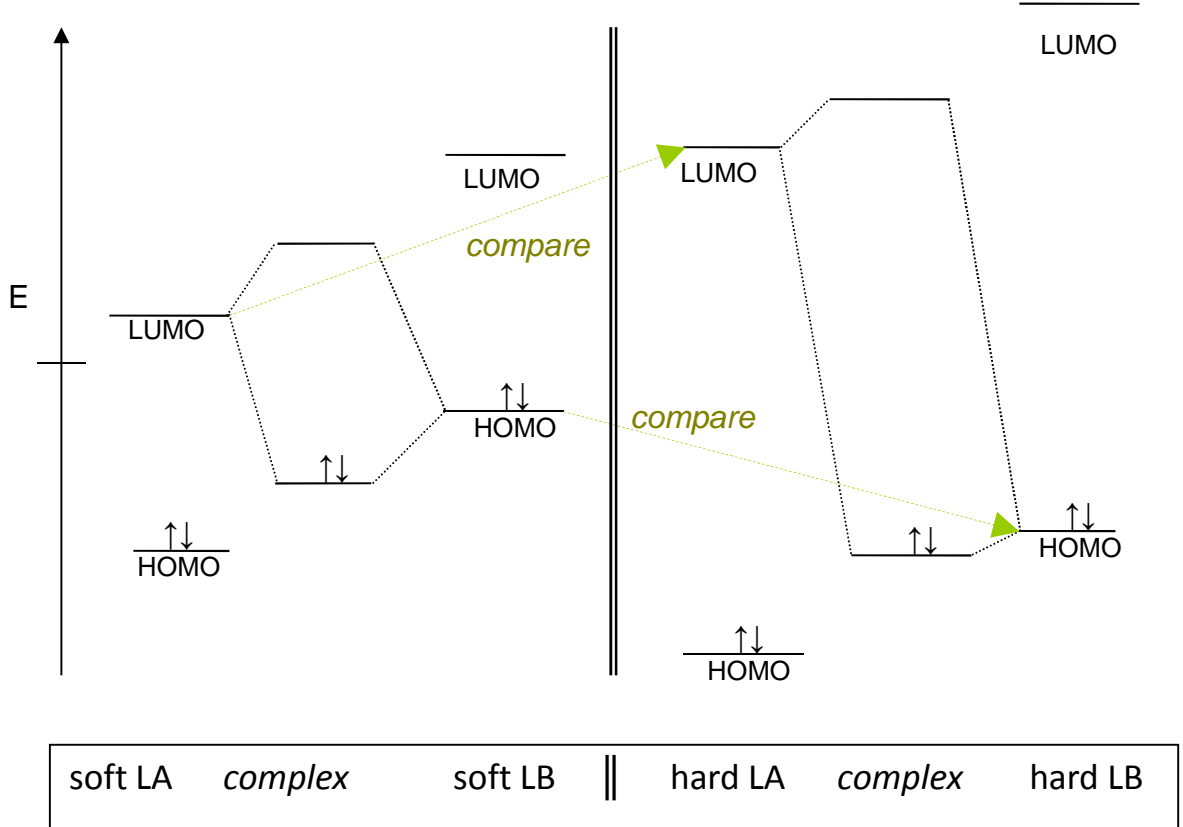


Drago's equation – empirical

series of tabulated parameters E (electrostatic) and C (covalent)
for both acids (E_A, C_A) and bases (E_B, C_B)

$$-\Delta H_{AB} = E_A E_B + C_A C_B$$

Interaction between SA:SB, and HA:HB



SA:SB => NEARLY
COVALENT BOND

HA:HB => VERY
POLAR BOND

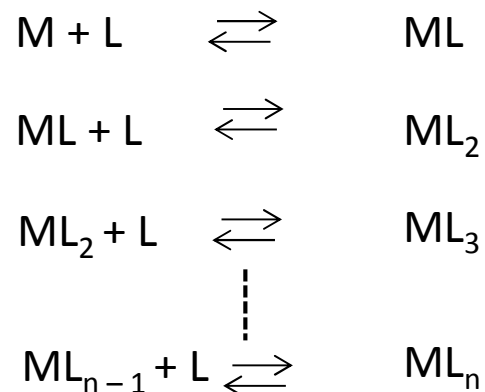
Application of HSAB approach

- metal – ligand preferences
- geochemistry: differentiation of elements; lithophiles (HA:HA; limestone CaCO_3 , bauxite AlO(OH)), chalcophiles (SA:SB; galena PbS , cinnabar HgS)
- solubility of halides, chalcogenides – those of softer cations are less soluble (cf. solubility of Hg_2Cl_2 and HgCl_2)
- colours: SA:SB are coloured due to charge transfer band
- analytical chemistry – the qualitative analysis scheme for metal ions (*hydrogen sulphide method; sirovodíkový způsob*)
- biochemistry – bonding environment for a given metal ion, siderophores, metallothionein
- medicinal chemistry – treatment of (heavy)metal poisoning, diagnostic kits (Gd)

Chelate and macrocyclic effects

Formation of a complex ML_n
stepwise process

Equilibrium constant for each step



$$K_1 = \frac{[ML]}{[M][L]}$$

|

$$K_n = \frac{[ML_n]}{[ML_{n-1}][L]}$$

$$K_1 > K_2 > K_3 \dots K_n$$

K_n – individual stability constant (individual formation constant, step formation constant)
Higher K implies more stable complex.

β_n – global stability constant (global formation constant)

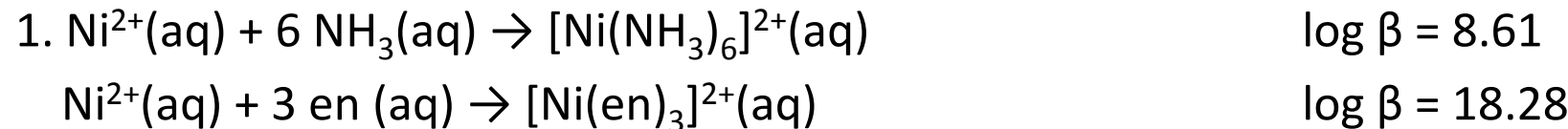
$$\beta_n = \frac{[ML_n]}{[M][L]^n}$$

$$\beta_i = \prod_1^i K_i$$

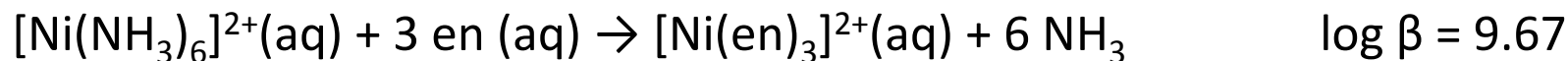
$$\begin{aligned}\Delta G^\circ &= -RT \ln \beta \\ \Delta G^\circ &= \Delta H^\circ - T\Delta S^\circ\end{aligned}$$

Chelate rings form much more stable complexes.

Examples:

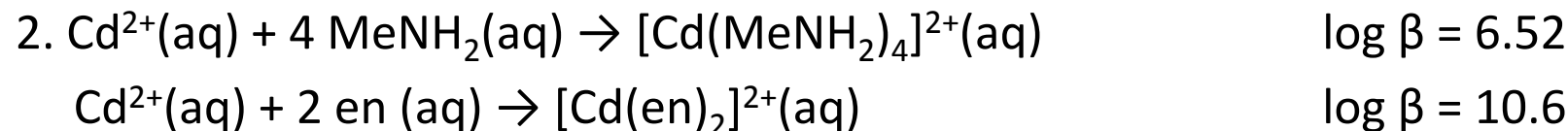


the system with 3 chelate rings is 10^{10} more stable



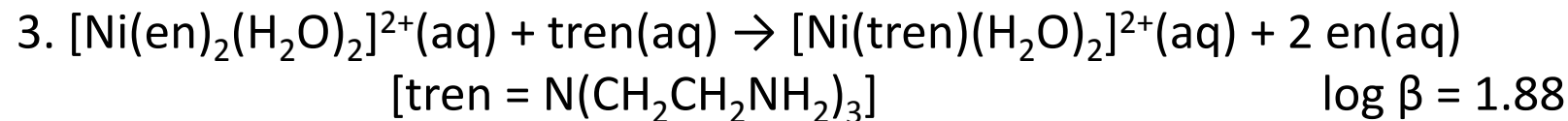
For this system, $\Delta H^\circ = -12.1 \text{ kJ/mol}$, $-T\Delta S^\circ = -43.0 \text{ kJ/mol}$

Both enthalpic and entropic (growing number of particles) reason



ligands	$\Delta H^\circ \text{ kJ/mol}$	$\Delta S^\circ \text{ kJ/mol.deg}$	$-T\Delta S^\circ \text{ kJ/mol}$	$\Delta G^\circ \text{ kJ/mol}$
4 MeNH ₂	-57.3	-67.3	+20.1	-37.2
2 en	-56.5	+14.1	-4.2	-60.7

Purely entropy-based chelate effect



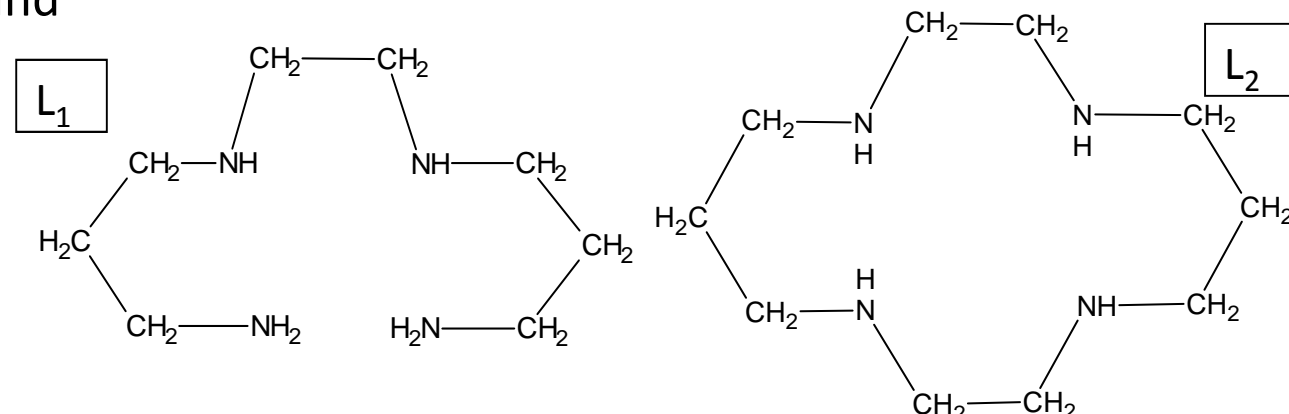
$$\Delta H^\circ = + 13.0 \text{ kJ/mol}, - T\Delta S^\circ = - 23.7 \text{ kJ/mol}, \Delta G^\circ = - 10.7 \text{ kJ/mol}$$

Chelate effect overcomes a positive enthalpy change (higher number of rings)

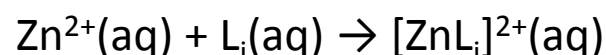
SIZE OF THE RING IS IMPORTANT: 5 or 6 membered rings are the most favorable.

Macrocyclic effect

Cyclic vs. noncyclic ligand



Reaction with zinc(II):



	L ₁	L ₂
log K	11,25	15,34
$\Delta H^\circ \text{ [kJ/mol]}$	-44,4	-61,9
$\Delta S^\circ \text{ [J/deg mol]}$	66,5	85,8

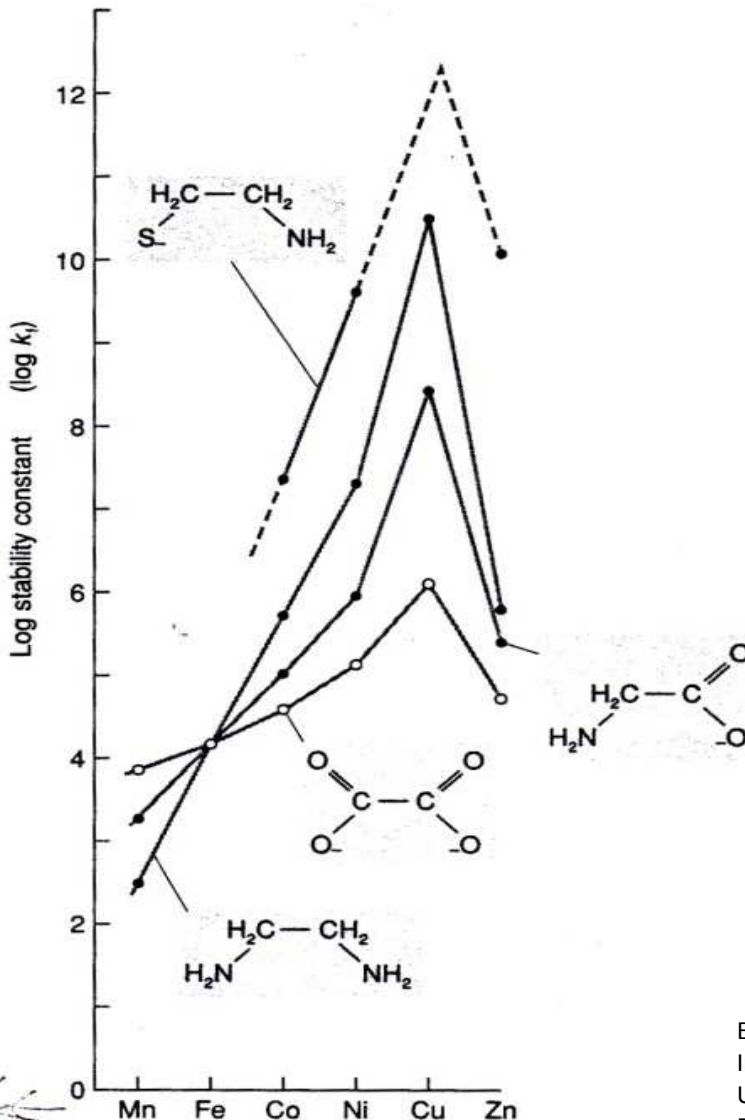
Irving – Williams series

A given ligand:

stability constants follow the size of the central metal ion = electrostatic effect
(polarizing effect of the ion)

Different ligands:

relative stability for a given ion and ligands with different donor atoms **does not** depend only on the polarizability of the ligand (electrostatics) but also on the relative softness/hardness of the reaction partners.



Ex: G. Wulfsberg,
Inorganic Chemistry,
University Science
Books, Sausalito, CA,
2000



HSAB principle and chelate effect in medicine

Treatment of metal poisoning:

chelates; donor atoms according to the metal hardness/softness; soluble complex

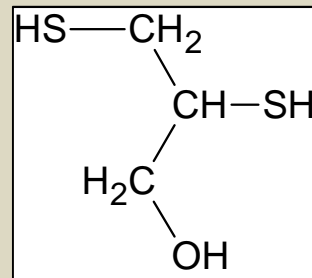
Heavy metals:

soft acids

Hg^{2+} , TI^+

British Anti-Lewisite

S-donor ligand



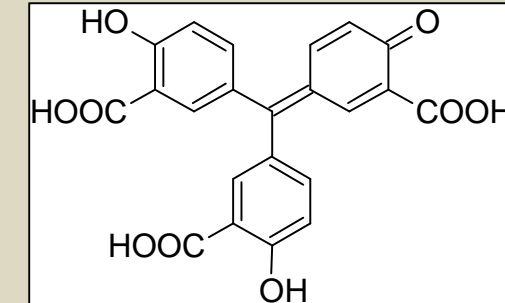
Light metals:

hard acids

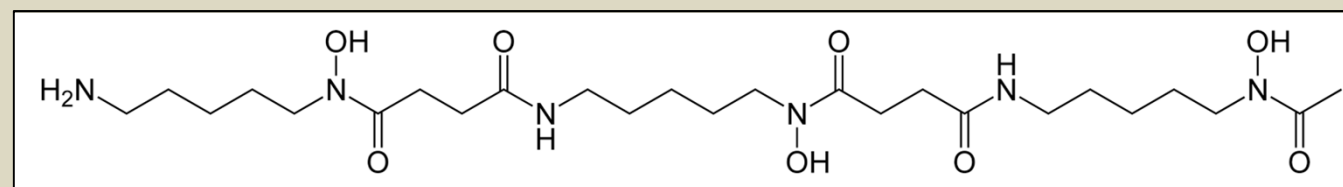
Be^{2+} , Al^{3+}

Aurinetricarboxylic acid

O-donor ligand



Iron (congenital metabolic disorder):
Desferrioxamine
combined N, O-donor



Medical diagnostics:

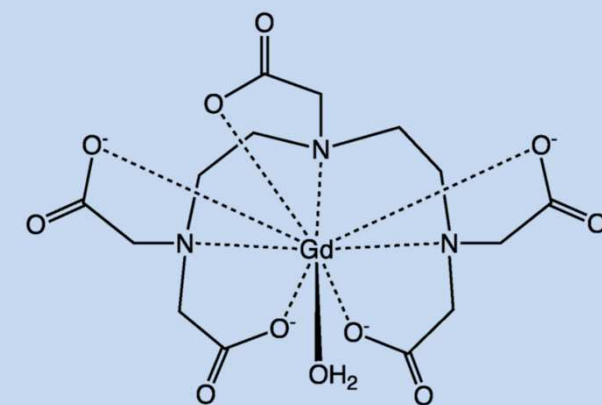
Gadolinium(+III) complexes for magnetic resonance

imaging (MRI) – contrast agent

Requirements: stable complex ($\text{Gd}^{3+}(\text{aq})$ is toxic), soluble in water, water molecule in the inner coordination sphere

Ligand: DTPA⁵⁻, poly(carboxylic) acids

DTPA = diethylenetriaminepentaacetate



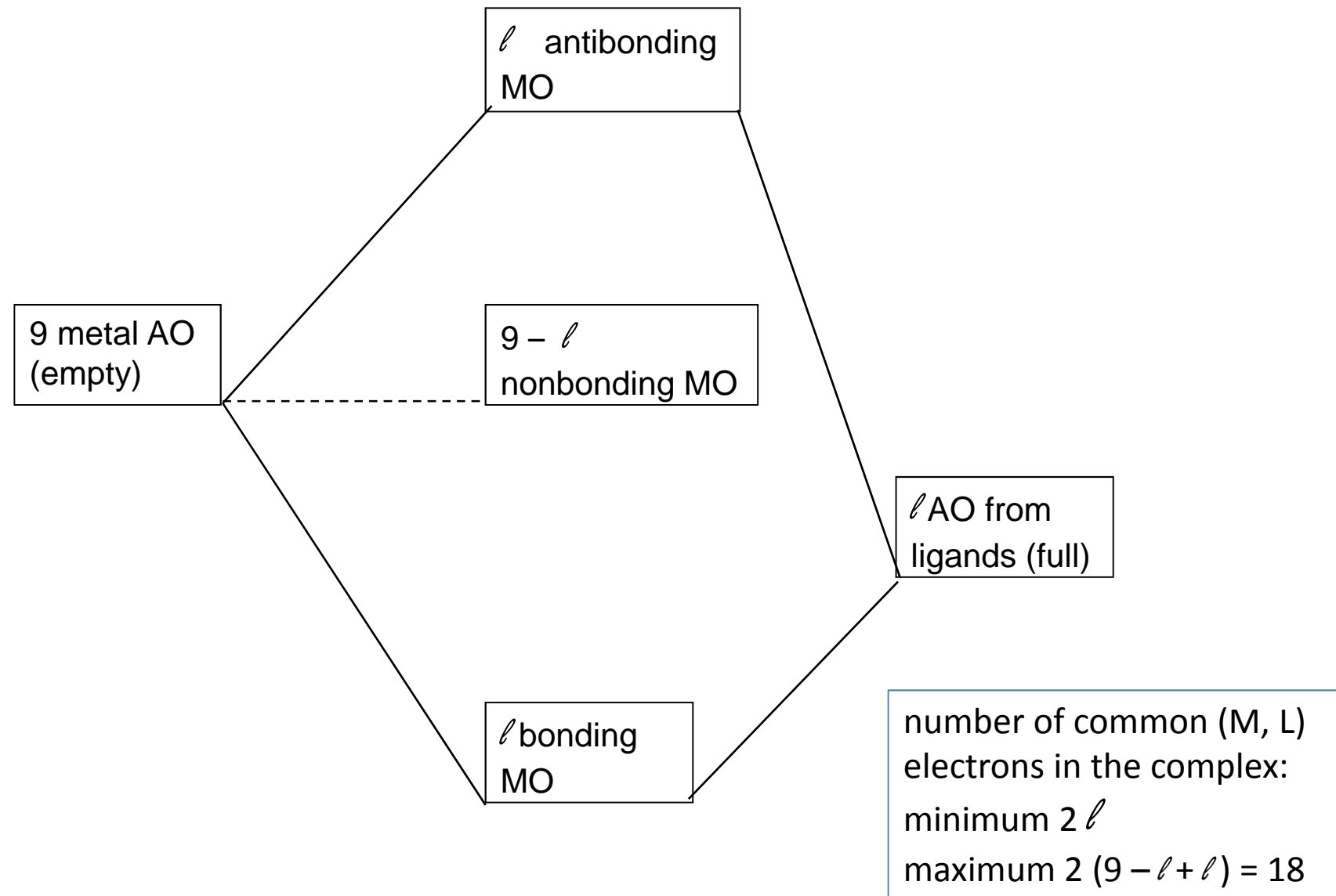
Electronic stabilization – 18 electron rule

- empirical rule
- organometallic compounds = the most covalent bond = SA:SB
- stoichiometry of carbonyls:
 - $[\text{Co}(\text{CO})_6]$, $[\text{Fe}(\text{CO})_5]$, $[\text{Ni}(\text{CO})_4]$
 - $[\text{Mn}_2(\text{CO})_{10}]$, $[\text{Mn}(\text{CO})_6]^+$, $[\text{Mn}(\text{CO})_5]^-$

electronic reason,

problem of electron count – ionic or covalent model?

Basic bonding scheme – 1 transition metal M, ℓ ligands L, $[ML_\ell]$



Electron count in a complex: the covalent model

Total amount of electrons:

electrons from metal(s) + electrons from ligands + charge of the particle

Covalent model:

both M, L, are not charged (odd number of electrons may be present)

Ionic model:

charged M, L (electron pairs)

Electrons from the metal:

- (COV) valence electrons, transition metals: orbitals $(nd + (n+1)s)$, d^m
- (ION) oxidation state

Electrons from the ligands:

- (COV) L- or X-type ligands
- (ION) 2 electrons from each donor

Covalent model: L- and X-type ligands (M.L.H.Green)

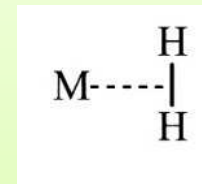
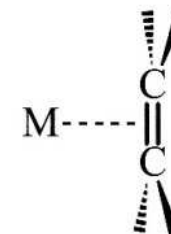
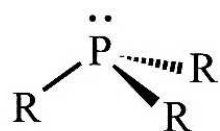
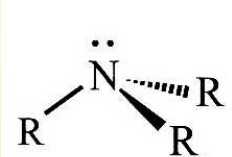
- L supplies $2e$
- X supplies $1e$
- total ligand electrons: LX_x

Total number of electrons N_t :

- m electrons of the central metal
- ℓ number of L-type ligands
- x number of X-type ligands
- q charge of the particle

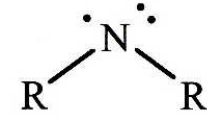
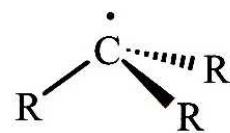
$$N_t = m + 2\ell + x - q$$

L-type ligands



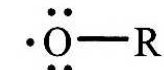
2-electron donors, free electron pair

X-type ligands



1-electron donors, single electron.

2nd step: subsequent donation from an electron pair
is possible.



Ligands of L_xX_x type

X_2 type



X_3 type



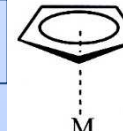
according to the ground electronic state

Conjugated polyenes

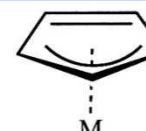
cyclopentadienyl



$\eta^5,\text{L}_2\text{X}$



$\eta^3,\text{L}_2\text{X}$

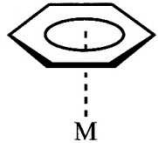


$\kappa\text{-N}(\eta^5),\text{L}_2\text{X}$

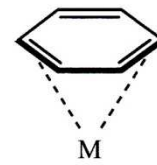


benzene

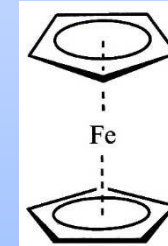
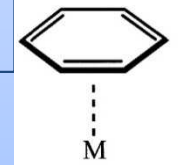
η^6,L_3



η^4,L_2



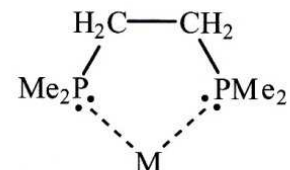
η^2,L



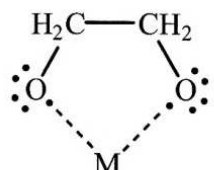
ferrocene,
bis(cyclopenta-dienyl)iron(II)

Ligands of $L_x X$ type – cont.

Chelating ligands

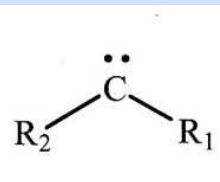


L_2

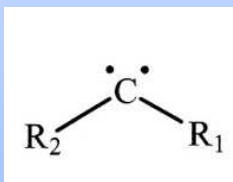


X_2

Carbenes

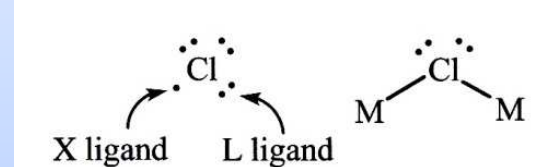


L_2 , Fischer
type



X_2 , Schrock
type

Bridging ligands



X ligand L ligand



Ionic model – different distribution of the same number of electrons

Ligands – always act as Lewis bases, supplying *pairs* of electrons. X-type ligands – anions X^-

Metal – number of electrons depends on its oxidation state.

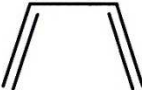
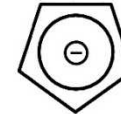
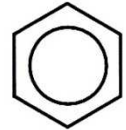
uncharged particle: $[ML_x X_x]$ (covalent model) $\rightarrow [M^{x+}(L)(X^-)_x]$ (ionic model)

charged particle: $[ML_x X_x]^q$ (covalent model) $\rightarrow [M^{(x+q)+}(L)(X^-)_x]$ (ionic model)

Ex: Y. Jean, Les orbitales moléculaires dans les complexes, Éditions de l'École polytechnique, Palaiseau, 2003



Covalent and ionic model – comparison of the electron count of ligands

Covalent model		Ionic model	
Ligand (<i>type</i>)	Number of electrons	Ligand	Number of electrons
H, Cl, OR, NR ₂ , CR ₃ , CN (<i>ligands X</i>)	1 e	H ⁻ , Cl ⁻ , OR ⁻ , NR ₂ ⁻ , CR ₃ ⁻ , CN ⁻	2 e
CO, NR ₃ , PR ₃ , H ₂ , R ₂ C=CR ₂ (<i>ligands L</i>)	2 e	CO, NR ₃ , PR ₃ , H ₂ , R ₂ C=CR ₂	2 e
O, S, NR (<i>ligands X₂</i>)	2 e	O ²⁻ , S ²⁻ , NR ²⁻	4 e
	4 e		4 e
$\eta^4\text{-diène}$ (<i>ligand L₂</i>)		$\eta^4\text{-diène}$	
	5 e		6 e
$\eta^5\text{-Cp}$ (<i>ligand L₂X</i>)		$\eta^5\text{-Cp}^-$	
	6 e		6 e
$\eta^6\text{-arène}$ (<i>ligand L₃</i>)		$\eta^6\text{-arène}$	
$\mu\text{-Cl}$ (<i>ligand LX</i>)	3 e	$\mu\text{-Cl}^-$	4 e
$\mu\text{-O}$ (<i>ligand X₂</i>)	2 e	$\mu\text{-O}^{2-}$	4

Covalent and ionic model – identical results, DO NOT MIX THEM TOGETHER



covalent model

[Ir(L)₃(X)] type

Ir

3L

1X

total

Ir oxid. number +I, configuration d⁸

ionic model

[Ir⁺(CO)(Cl⁻)(PPh₃)₂]

Ir⁺

4 ligands

8e

total

16e



covalent model

[Fe(L₂X)₂] type

Fe

2 cp

total

Fe oxidation number +II, configuration d⁶

ionic model

[(Fe²⁺)(cp⁻)₂]

Fe²⁺

2 cp⁻

total

18e



covalent model

[Ni(X)₅]³⁻

Ni

5 CN

charge

total

Ni oxid. number +II, configuration d⁸

ionic model

[(Ni²⁺)(CN⁻)₅]³⁻

Ni²⁺

5 CN⁻

XXXXXX

total

18e

Oxidation number of the central metal ion:
from the covalent model

general formula [ML_xX_y]^q

$$\text{ox.n.} = x + q$$

Uveřejněné materiály jsou určeny studentům Vysoké školy chemicko-technologické v Praze jako studijní materiál. Některá textová i obrazová data v nich obsažená jsou převzata z veřejných zdrojů. V případě nedostatečných citací nebylo cílem autorky záměrně poškodit autora/y původního díla.

S případnými výhradami se prosím obracejte na autorku tohoto výukového materiálu, aby bylo možno zjednat nápravu.



The published materials are intended for students of the University of Chemistry and Technology, Prague as a study material. Some text and image data contained therein are taken from public sources. In the case of insufficient quotations, the author's intention was not to intentionally infringe the possible author(s) rights to the original work.

If you have any reservations, please contact the author(s) of the specific teaching material in order to remedy the situation.

Bonding theories

Valence bond theory

Crystal field theory

Ligand field theory

Molecular orbitals



EUROPEAN UNION
European Structural and Investing Funds
Operational Programme Research,
Development and Education



MINISTRY OF EDUCATION,
YOUTH AND SPORTS



Valence bond theory (VB)

- used also for main groups' elements
- AO hybridisation on the central atom; overlap with AO's of the bonding partner
- localised pairs of bonding electrons

Coord. Numb.	Geometry	Hybridized AO	Hybrid orbital	Example
2	L-2	s, p _z	sp	[Ag(NH ₃) ₂] ⁺
3	TP-3	s, p _x , p _y	sp ²	[HgI ₃] ⁻
4	T-4	s, p _x , p _y , p _z	sp ³	[FeBr ₄] ²⁻
4	SP-4	s, p _x , p _y , d _{x²-y²}	sp ² d	[Ni(CN) ₄] ²⁻
5	TBPY-5	s, p _x , p _y , p _z , d _{z²}	sp ³ d	[CuCl ₅] ³⁻
5	SPY-5	s, p _x , p _y , p _z , d _{x²-y²}	sp ³ d	[Ni(CN) ₅] ³⁻
6	OC-6	s, p _x , p _y , p _z , d _{x²-y²} , d _{z²}	sp ³ d ²	[Co(NH ₃) ₆] ³⁺

Valence bond theory (VB)

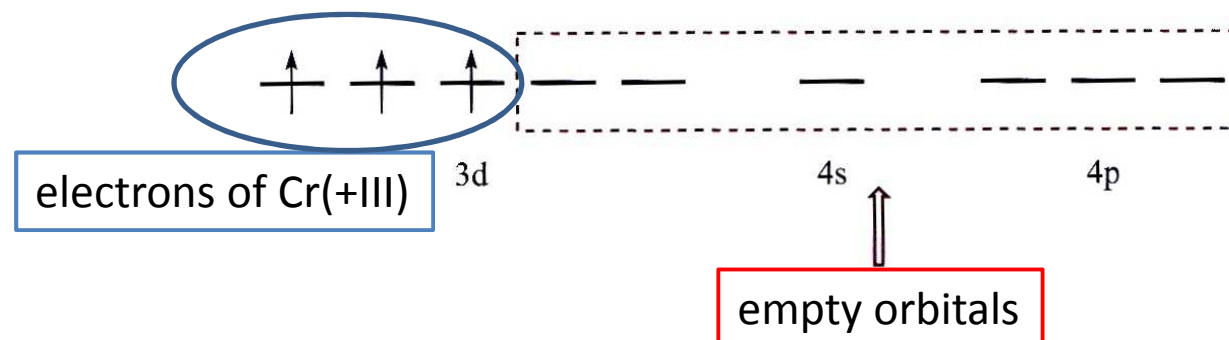
higher hybrids

Coord. Numb.	Geometry	Hybridized AO	Hybrid orbital	Example
6	<i>TPR</i> -6	$s, d_{xy}, d_{xz}, d_{yz}, d_{x^2-y^2}, d_{z^2}$ <i>or</i> $s, p_x, p_y, p_z, d_{xz}, d_{yz}$	sd^5 <i>or</i> sp^3d^2	$[ZrMe_4]^{2-}$
7	<i>PBPY</i> -7	$s, p_x, p_y, p_z, , d_{x^2-y^2}, d_{z^2}$	sp^3d^3	$[V(CN)_7]^{4-}$
7	<i>TPRS</i> -7	$s, p_x, p_y, p_z, d_{xy}, d_{xz}, d_{z^2}$	sp^3d^3	$[NbF_7]^{2-}$
8	<i>CU</i> -8	$s, p_x, p_y, p_z, d_{xy}, d_{xz}, d_{yz}, f_{xyz}$	sp^3d^3f	$[PaF_8]^{3-}$
8	<i>DD</i> -8	$s, p_x, p_y, p_z, d_{z^2}, d_{xy}, d_{xz}, d_{yz},$	sp^3d^4	$\underline{[Mo(CN)_8]}^4$
8	<i>SAPR</i> -8	$s, p_x, p_y, p_z, d_{xy}, d_{xz}, d_{yz}, d_{x^2-y^2}$	sp^3d^4	$[TaF_8]^{3-}$
9	<i>TPRS</i> -9	$s, p_x, p_y, p_z, d_{xy}, d_{xz}, d_{yz},$ $d_{x^2-y^2}, d_{z^2}$	sp^3d^5	$[ReH_9]^-$

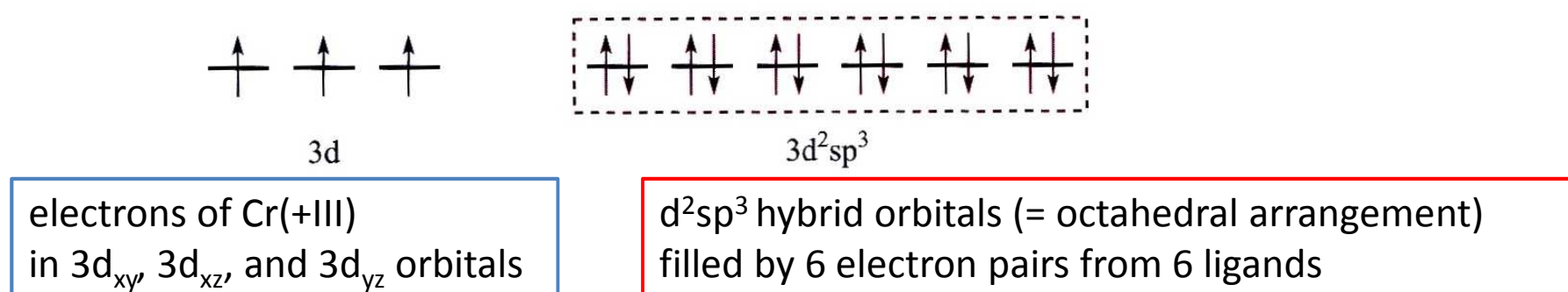
Valence bond theory (VB)

Description of the bonding in a Cr^{3+} (d^3) octahedral complex:

Free ion:



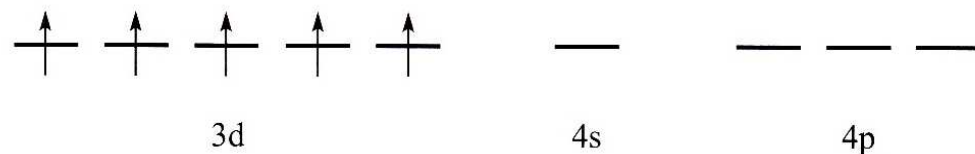
Complex:



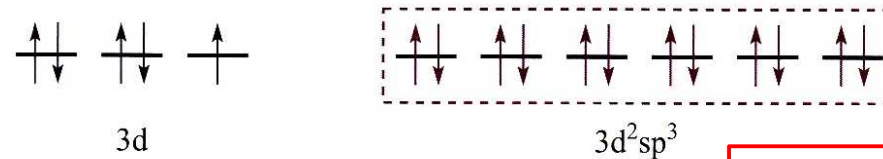
Valence bond theory (VB)

Description of the bonding in a Fe^{3+} (d^5) octahedral complexes:
both high spin and low spin possibilities exist

Free ion:

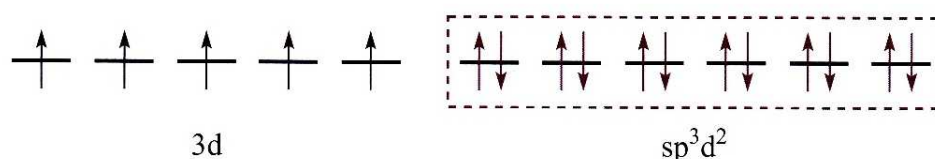


Low-spin complex:
e.g. $[\text{Fe}(\text{CN})_6]^{3-}$



d²sp³ hybrid orbitals

High-spin complex:
e.g. $[\text{FeF}_6]^{3-}$



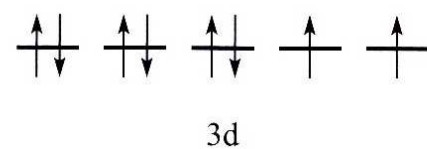
**sp³d² hybrid orbitals
4d AO have to be used**

The 4d orbitals are used to form the high-spin arrangement => LOW PROBABILITY

Valence bond theory (VB)

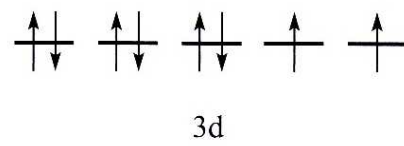
Description of the bonding in a Ni^{2+} (d^8) complexes:
tetrahedral, octahedral, and square planar geometries, different spin states

Tetrahedral:



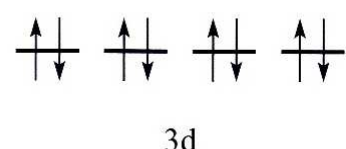
sp^3 hybrid orbitals

Octahedral:



sp^3d^2 hybrid orbitals
4d AOs have to be used

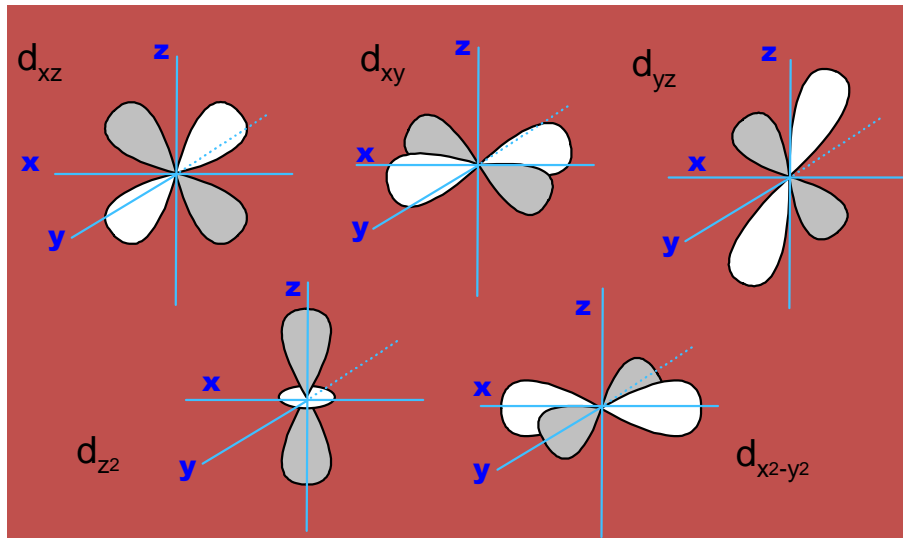
Square planar:



dsp^2 hybrid orbitals

The valence bond theory is able to explain, in a rather simplified way, stereochemistry and magnetic properties of the complexes. It has no explanation for the kinetic inertness typical for the low-spin d^6 ions, for electronic spectra, for existence of the high-spin – low-spin duality. Furthermore, it uses both nd and $(n+1)d$ -orbitals which is not justified experimentally.

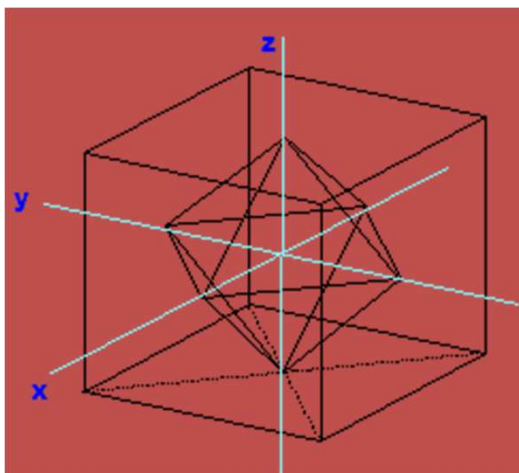
Crystal field theory (CFT)



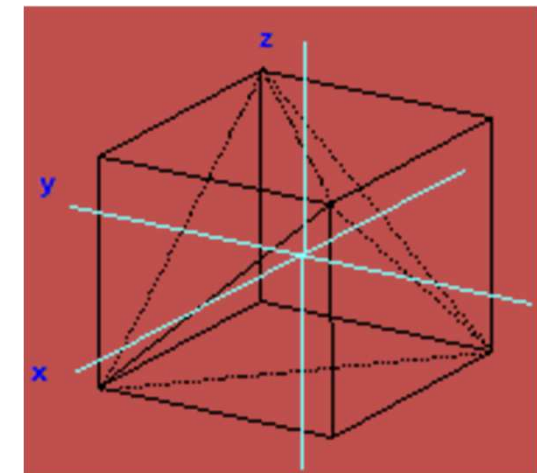
All interactions are **purely electrostatic** in nature.

Central metal, ligands – point charges, given geometry (symmetry).

Splitting of 5 degenerated d -orbitals by effect of the surrounding ligands.



Common arrangement of an octahedral (*left*) and tetrahedral (*right*) set of ligands

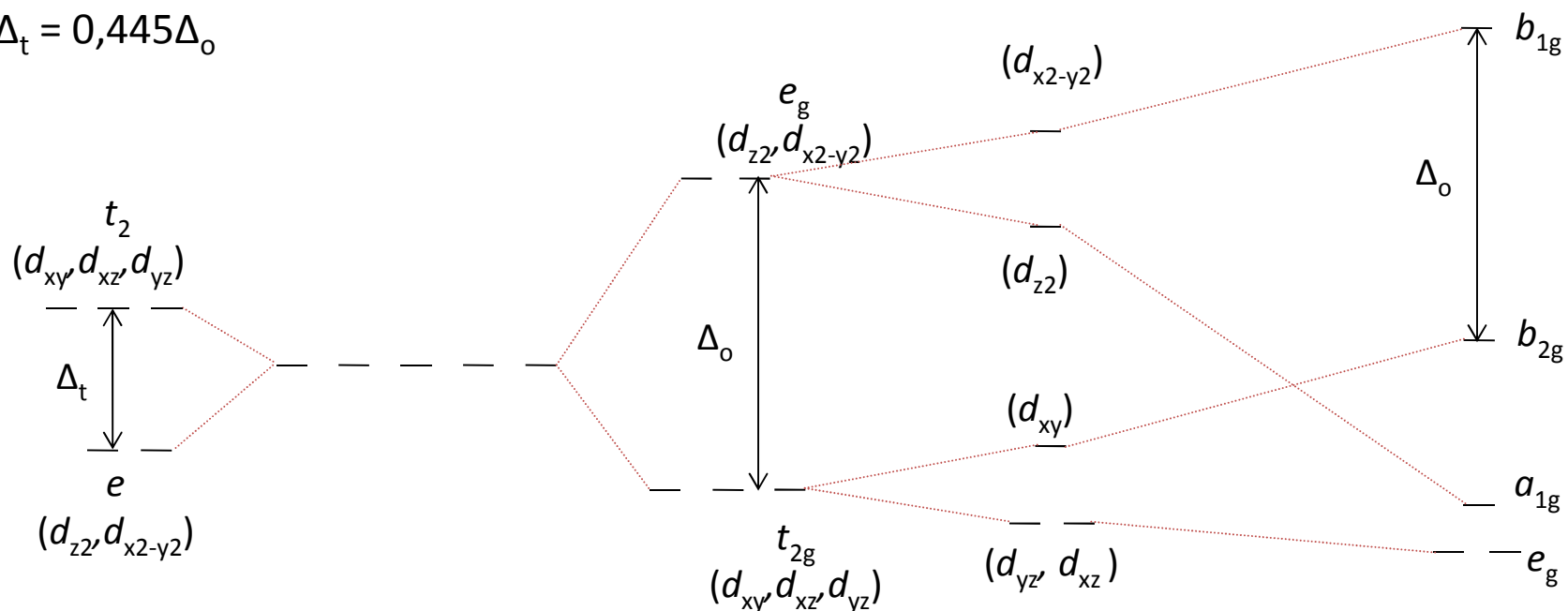


Crystal field theory

Splitting of d -orbitals: tetrahedron, octahedron, from octahedron to square

$$\Delta_t = 4/9 \Delta_o$$

$$\Delta_t = 0,445 \Delta_o$$



tetrahedron

degenerated d orbitals

octahedron

tetragonal bipyramidal,
elongated, z-axis

square

Mulliken symbols

Mulliken Symbol	Interpretation
a	Non-degenerate orbital; symmetric to principal C_n
b	Non-degenerate orbital; unsymmetric to principal C_n
e	Doubly degenerate orbital
t	Triply degenerate orbital
(subscript) g	Symmetric with respect to center of inversion
(subscript) u	Unsymmetric with respect to center of inversion
(subscript) 1	Symmetric with respect to C_2 perp. to principal C_n
(subscript) 2	Unsymmetric with respect to C_2 perp. to principal C_n
(superscript) '	Symmetric with respect to σ_h
(superscript) "	Unsymmetric with respect to σ_h

Splitting of *d*-orbitals in an octahedral crystal field - CFT

The potential created by 6 point charges (O_h symmetry) at a point x, y, z is:

$$V_{(x,y,z)} = \sum_{i=1}^6 \frac{ez_i}{r_{ij}}$$

r_{ij} distance from the charge i to the point $[x,y,z]$
 ze charge of the anion

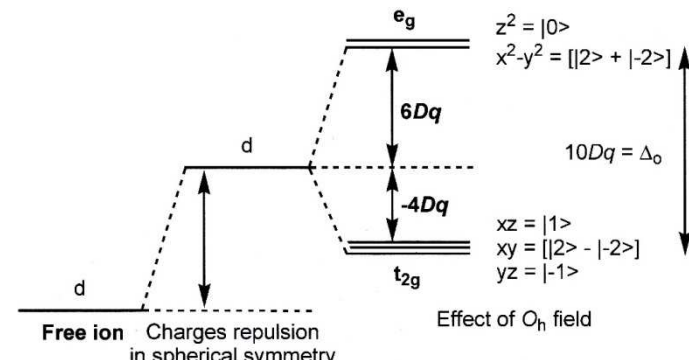


Figure 1.4 Splitting of the *d* orbitals in a crystal field of O_h symmetry.

From this, energy difference of the split *d*-orbitals (octahedral field) is $10 D \cdot q$

where $D = \frac{35ze}{4a^5}$ and $q = \frac{2e<r>^4}{105}$

$$\text{therefore } Dq = \frac{1}{6} \left(\frac{ze^2 <r>^4}{a^5} \right)$$

where a internuclear distance between the metal and the anion
 $<r>$ average distance of the *d*-electron from its nucleus

CRYSTAL FIELD THEORY:

The splitting energy of *d*-orbitals is **proportional** to the size of the central atom ($<r>$) and **inversely proportional** to the M – L distance (a), which depends on the metal charge.

Geometries

Energy Levels of d Orbitals in Complexes of Various Geometries^a

CN ^b	Geometry	d_{z^2}	$d_{x^2-y^2}$	d_{xy}	d_{xz}	d_{yz}	Largest Splitting
2	Linear ^c	1.028	-0.628	-0.628	0.114	0.114	0.914
3	Trigonal ^d	-0.321	0.546	0.546	-0.386	-0.386	0.867
4	Tetrahedral	-0.267	-0.267	0.178	0.178	0.178	0.445
4	Square planar ^d	-0.428	1.228	0.228	-0.514	-0.514	1.000
5	Trigonal bipyramide ^e	0.707	-0.082	-0.082	-0.272	-0.272	0.789
5	Square pyramid ^e	0.086	0.914	-0.086	-0.457	-0.457	0.828
6	Octahedron	0.600	0.600	-0.400	-0.400	-0.400	1.000
6	Trigonal prism	0.096	-0.584	-0.584	0.536	0.536	0.680
7	Pentagonal bipyramide ^e	0.493	0.282	0.282	-0.528	-0.528	0.810
8	Cube	-0.534	-0.534	0.356	0.356	0.356	0.890
8	Square antiprism	-0.534	-0.089	-0.089	0.356	0.356	0.445
9	Tricapped trigonal prism	-0.225	-0.038	-0.038	0.151	0.151	0.189
12	Icosahedron	0.000	0.000	0.000	0.000	0.000	0.000

^a Units of Δ_o , the octahedral crystal field splitting, assuming the same overall charge density and distance. [Adapted from J. E. Huheey, E. A. Keiter, and R. L. Keiter, *Inorganic Chemistry: Principles of Structure and Reactivity*, 4th ed., Harper-Collins, New York, 1993, p. 405.]

^b Coordination number = CN.

^c Ligands lie along z axis.

^d Ligands lie in xy plane.

^e Pyramid base in xy plane.

Ex: G. Wulfsberg, Inorganic Chemistry, University Science Books, 2000

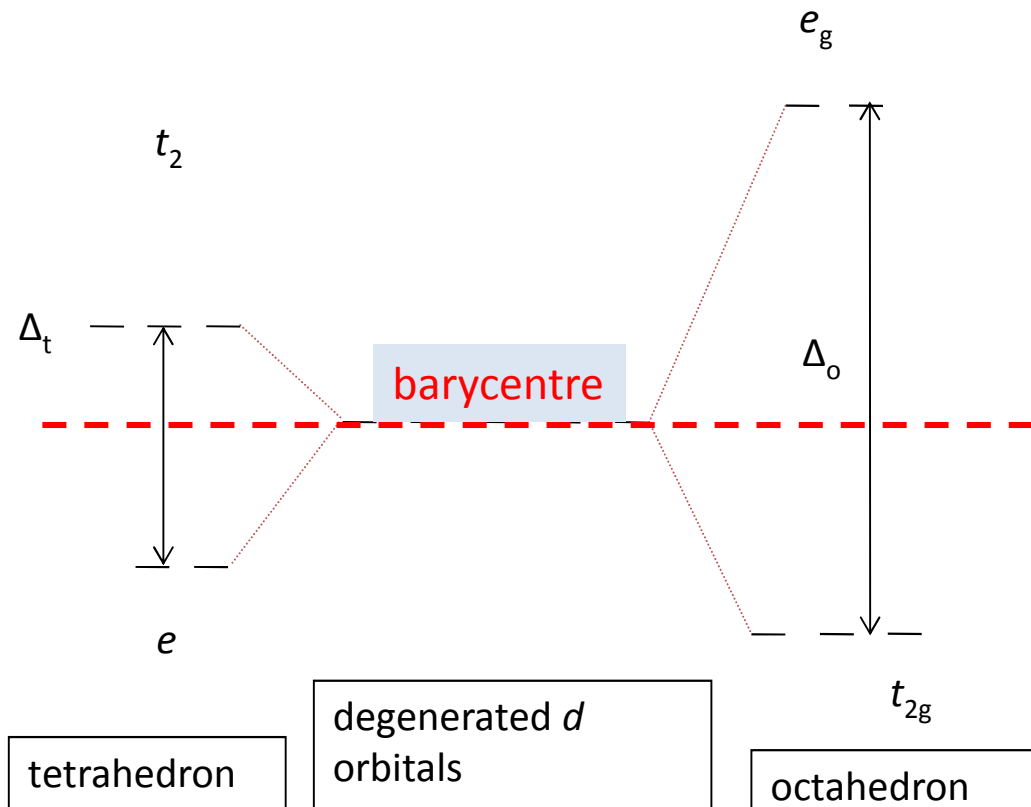


Crystal field stabilisation energy, CFSE

Partly filled split d -orbitals often gain energy relative to the unsplit state => Crystal Field Stabilisation Energy, CFSE

CFSE = 0 for d^0 , d^{10} , and HS d^5 configurations, e.g. for empty, filled and half-filled orbitals.

Position of the barycentre remains unchanged



Δ_o experimental value; $10Dq$ from computation.

NEW LEVELS

octahedron:

level t_{2g} $-2/5 \Delta_o$, stabilisation

level e_g $+3/5 \Delta_o$, labilisation

$$\text{difference: } +3/5 \Delta_o - (-2/5 \Delta_o) = \Delta_o$$

Overall energy of the splitted orbitals:

$$3 \cdot (-2/5 \Delta_o) + 2 \cdot (3/5 \Delta_o) = 0$$

configuration t_{2g}^1

gains CFSE = $-2/5 \Delta_o$

configuration t_{2g}^3

gains CFSE = $3 \cdot (-2/5 \Delta_o) = -6/5 \Delta_o$

tetrahedron:

level e_g $-3/5 \Delta_t$, stabilisation

level t_2 $+2/5 \Delta_t$, labilisation

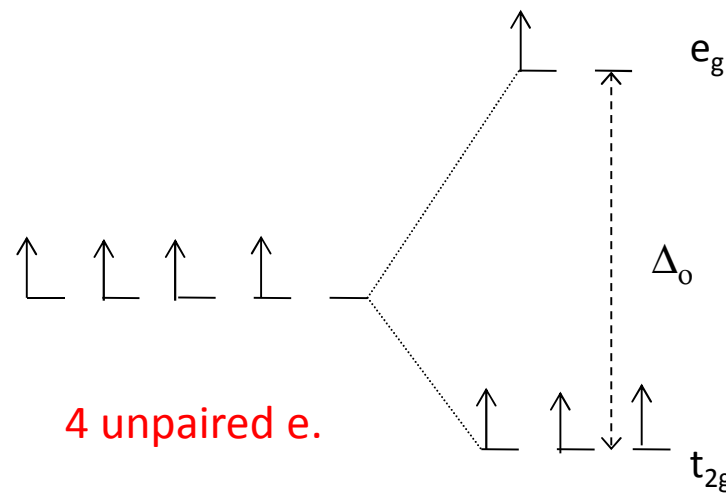
$$\text{total: } 3 \cdot (-2/5 \Delta_t) + 2 \cdot (3/5 \Delta_t) = 0$$

Crystal field stabilisation energy, CFSE

High-spin (HS) and low-spin (LS) arrangement - octahedron

Key parameter: difference between Δ_o and pairing energy P

High-spin, $P > \Delta_o$, electron fills e_g orbitals



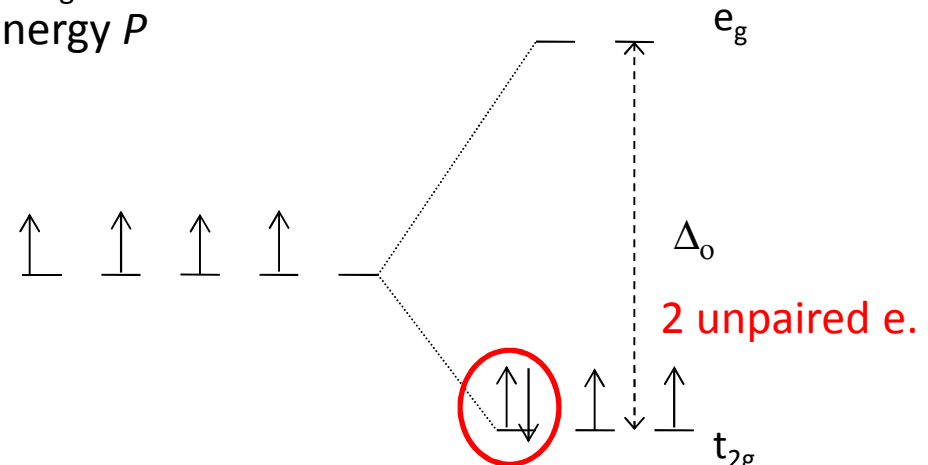
$$d^4: t_{2g}^3 e_g^1 \text{ CFSE} = -3/5 \Delta_o$$

$$d^5: t_{2g}^3 e_g^2 \text{ CFSE} = 0$$

$$d^6: t_{2g}^4 e_g^2 \text{ CFSE} = -2/5 \Delta_o \quad 4 \text{ unpaired e.}$$

$$d^7: t_{2g}^5 e_g^2 \text{ CFSE} = -4/5 \Delta_o \quad 3 \text{ unpaired e.}$$

Low-spin, $P < \Delta_o$, electron forms a new pair at t_{2g} level, the pair formation needs pairing energy P



$$d^4: t_{2g}^4 e_g^0 \text{ CFSE} = -8/5 \Delta_o + P$$

$$d^5: t_{2g}^5 e_g^0 \text{ CFSE} = -10/5 \Delta_o + 2P \quad 1 \text{ unpaired e.}$$

$$d^6: t_{2g}^6 e_g^0 \text{ CFSE} = -12/5 \Delta_o + 2P \quad 0 \text{ unpaired e.}$$

$$d^7: t_{2g}^7 e_g^0 \text{ CFSE} = -9/5 \Delta_o + P \quad 1 \text{ unpaired e.}$$

Most of tetrahedral complexes are high-spin – Δ_t is small compared to P .

Crystal field stabilisation energy

Changes in Crystal Field Stabilization Energies^a

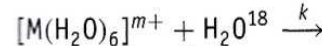
d^n	CFSE ML_6 (oct)	CFSE ML_5 (sp)	ΔCFSE	
d^1	0.40	0.46	+ 0.06	
d^2	0.80	0.91	+ 0.11	
d^3	1.20	1.00	- 0.20	
<hr/>				
Low-spin-strong field		High-spin-weak field		
CFSE ML_6 (oct)	CFSE ML_5 (sp)	ΔCFSE	CFSE ML_6 (oct)	
d^4	1.60 - P	1.46 - P	- 0.14	0.60
d^5	2.00 - 2 P	1.91 - 2 P	- 0.09	0
d^6	2.40 - 2 P	2.00 - 2 P	- 0.40	0.40
d^7	1.80 - P	1.91 - P	+ 0.11	0.80
<hr/>				
CFSE ML_6 (oct)	CFSE ML_5 (sp)	ΔCFSE		
d^8	1.20	1.00	- 0.20	
d^9	0.60	0.91	+ 0.31	
d^{10}	0	0	0	

^aThe CFSEs (in units of Δ_o) for octahedral (oct) and square pyramidal (sp) fields are shown followed by the change in CFSE for the process ML_6 (octahedral) \rightarrow ML_5 (square pyramidal). A + indicates a gain in CFSE during the process, and a - indicates a loss in CFSE.

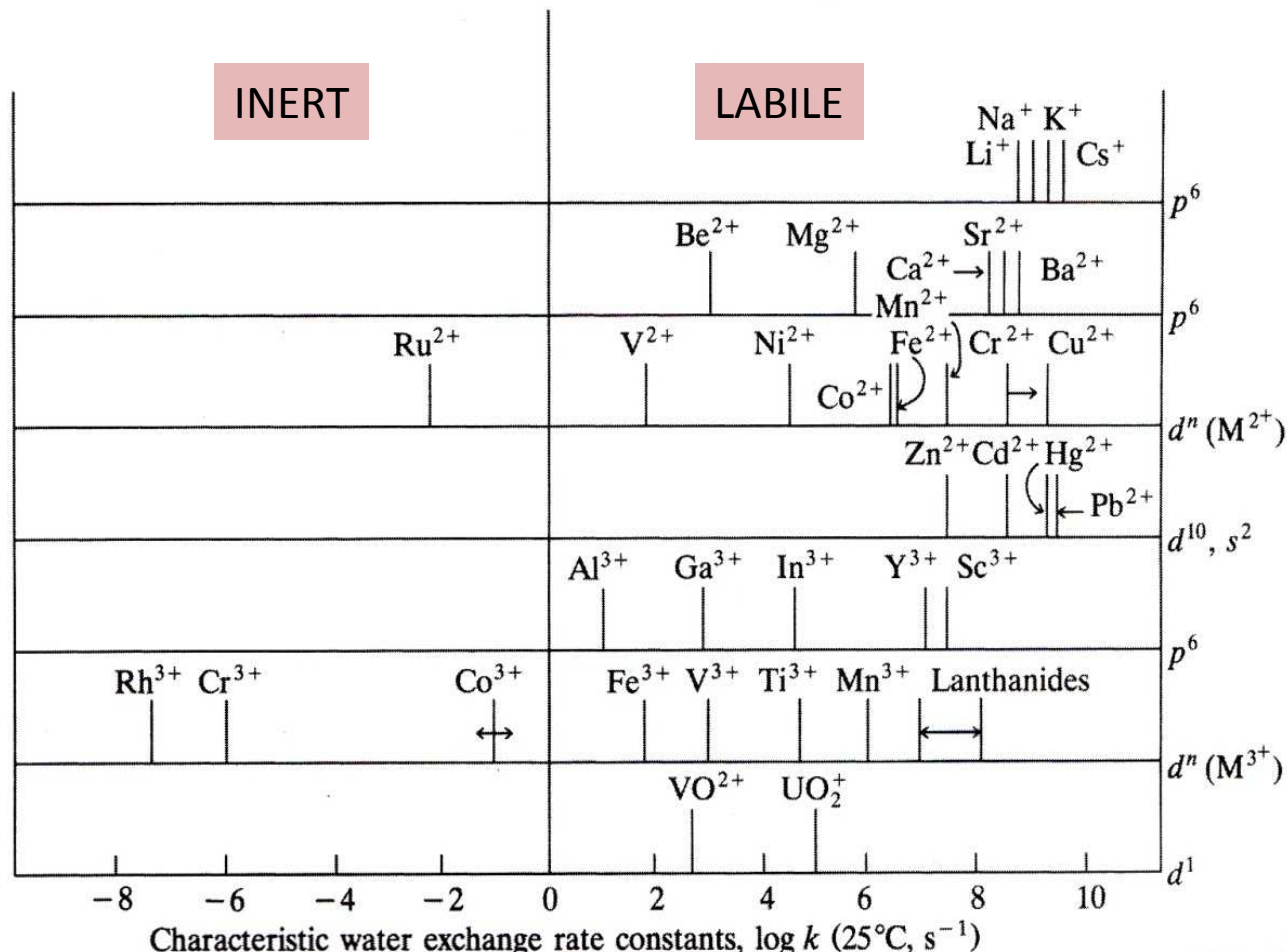
Experimental data – ligand exchange rate

FIGURE 5.5

Rate constants for water exchange for various ions:

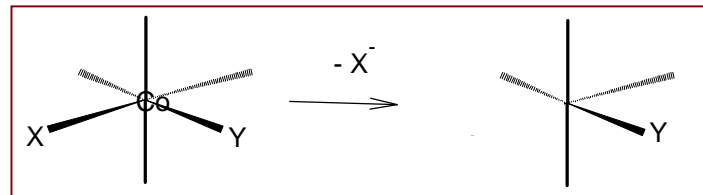


Data are tabulated as the log of the rate constant at 25°C. Inert hydrated ions, those that only slowly exchange water molecules between the hydration sphere and bulk water structure, are given on the left, and labile hydrated ions are on the right. (Ref. 7.)

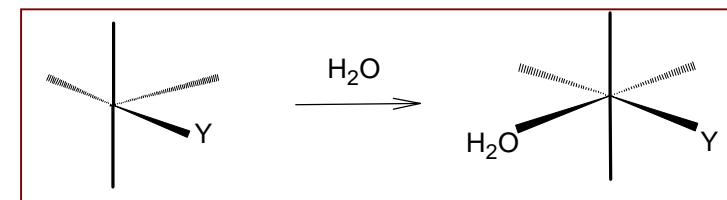


Substitution mechanism:

step 1:

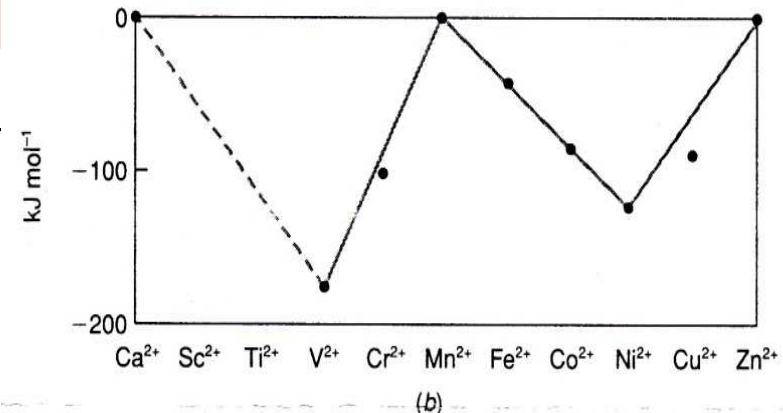
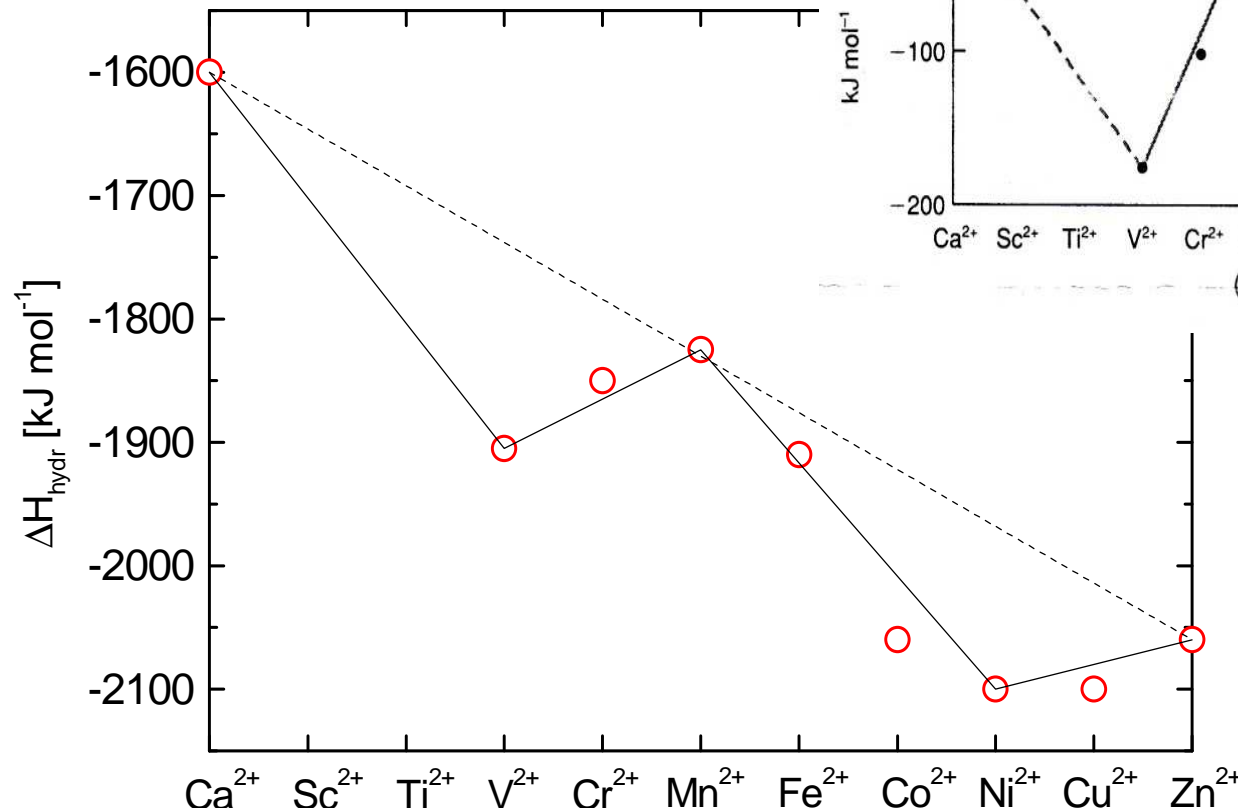


step 2:



CFSE in practice

Hydration energies in ionic crystals, ions M^{2+}

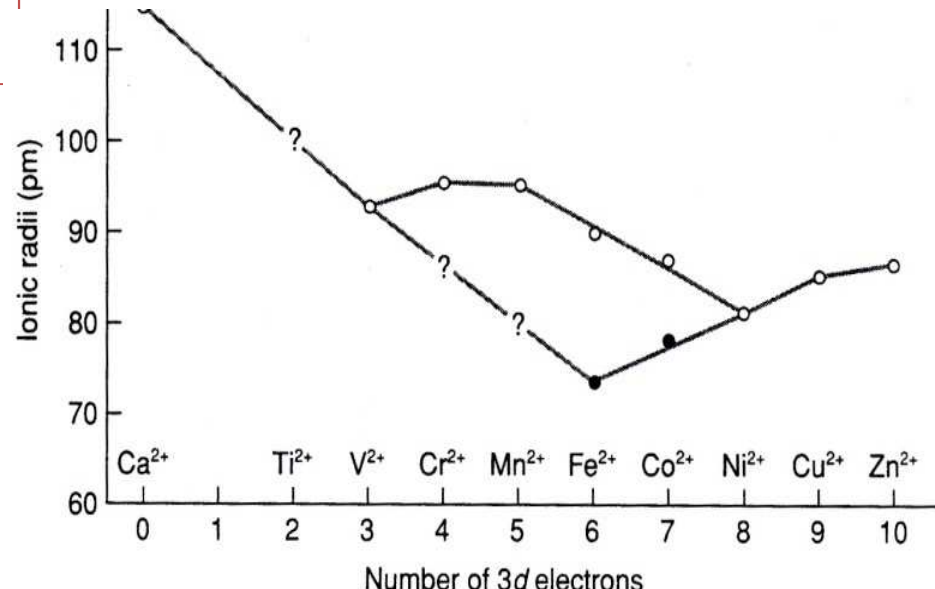


(b)

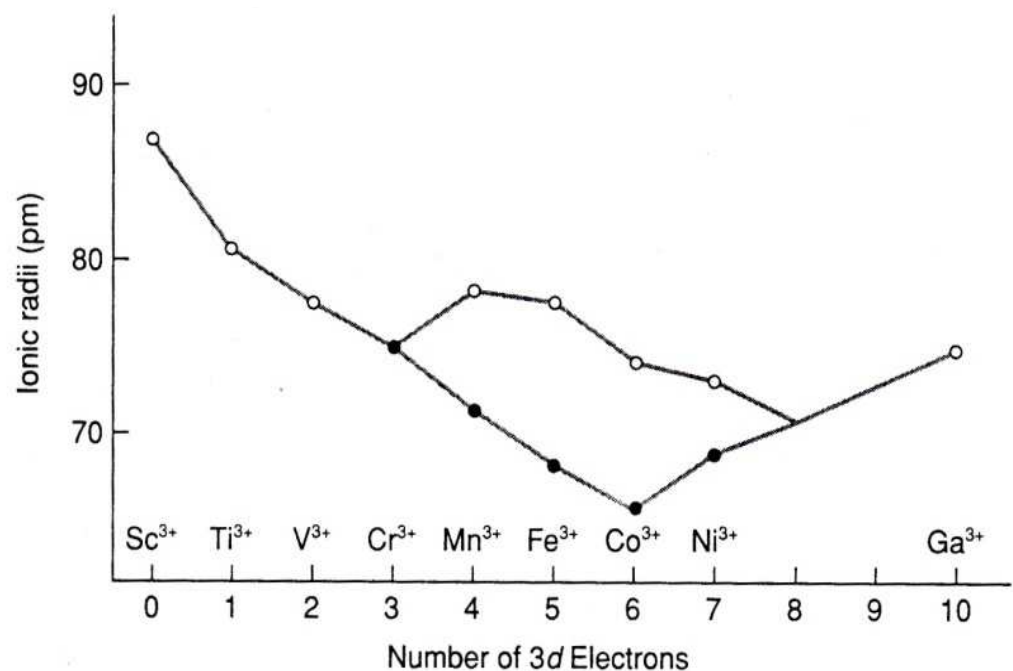
configuration: $d^3, d^4, d^5\text{HS}, d^6, d^7, d^8, d^9, d^{10}.$

CFSE = 0 in d^0, d^5 HS and d^{10} (Ca²⁺, Mn²⁺, Zn²⁺)

Ionic radii – LS HS



(a)



(b)

Change of the spin state =
change of the ionic radius
important in BIOCHEMISTRY

Experimental data - colours

Violet, 13000

TABLE 4.2

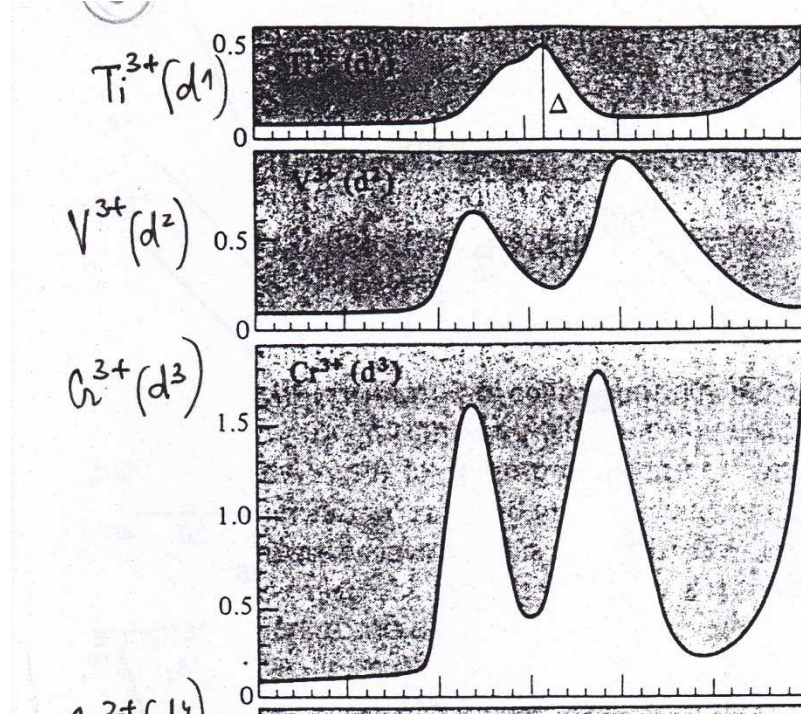
Octahedral Crystal Field Splitting Energies Δ_o , cm^{-1}

$(M')^{2+}$	$(M')^{3+}$	$(M'')^{3+}$	$(M''')^{3+}$
$\text{Cr}^{2+}, \text{Cr}^{3+}, \text{Mo}^{3+}$			
$[\text{CrCl}_6]^{4-}$	13,000	$[\text{CrCl}_6]^{3-}$	13,200
$[\text{Cr}(\text{H}_2\text{O})_6]^{2+}$	14,000	$[\text{Cr}(\text{H}_2\text{O})_6]^{3+}$	17,400
		$[\text{Cr}(\text{NH}_3)_6]^{3+}$	21,500
$[\text{Cr}(\text{en})_3]^{2+}$	18,000	$[\text{Cr}(\text{en})_3]^{3+}$	21,900
		$[\text{Cr}(\text{CN})_6]^{3-}$	26,600
$\text{Co}^{2+}, \text{Co}^{3+}, \text{Rh}^{3+}, \text{Ir}^{3+}$			
$[\text{Co}(\text{H}_2\text{O})_6]^{2+}$	9,300	$[\text{Co}(\text{H}_2\text{O})_6]^{3+}$	18,200
$[\text{Co}(\text{NH}_3)_6]^{2+}$	10,100	$[\text{Co}(\text{NH}_3)_6]^{3+}$	22,900
$[\text{Co}(\text{en})_3]^{2+}$	11,000	$[\text{Co}(\text{en})_3]^{3+}$	23,200
		$[\text{Co}(\text{CN})_6]^{3-}$	33,500
$\text{Mn}^{2+}, \text{Mn}^{3+}$			
$[\text{MnCl}_6]^{4-}$	7,500	$[\text{MnCl}_6]^{3-}$	20,000
$[\text{Mn}(\text{H}_2\text{O})_6]^{2+}$	8,500	$[\text{Mn}(\text{H}_2\text{O})_6]^{3+}$	21,000
$[\text{Mn}(\text{en})_3]^{2+}$	10,100		
$\text{Fe}^{2+}, \text{Fe}^{3+}$			
$[\text{Fe}(\text{H}_2\text{O})_6]^{2+}$	8,500	$[\text{FeCl}_6]^{3-}$	11,000
$[\text{Fe}(\text{CN})_6]^{4-}$	32,800	$[\text{Fe}(\text{H}_2\text{O})_6]^{3+}$	14,300
		$[\text{Fe}(\text{CN})_6]^{3-}$	35,000

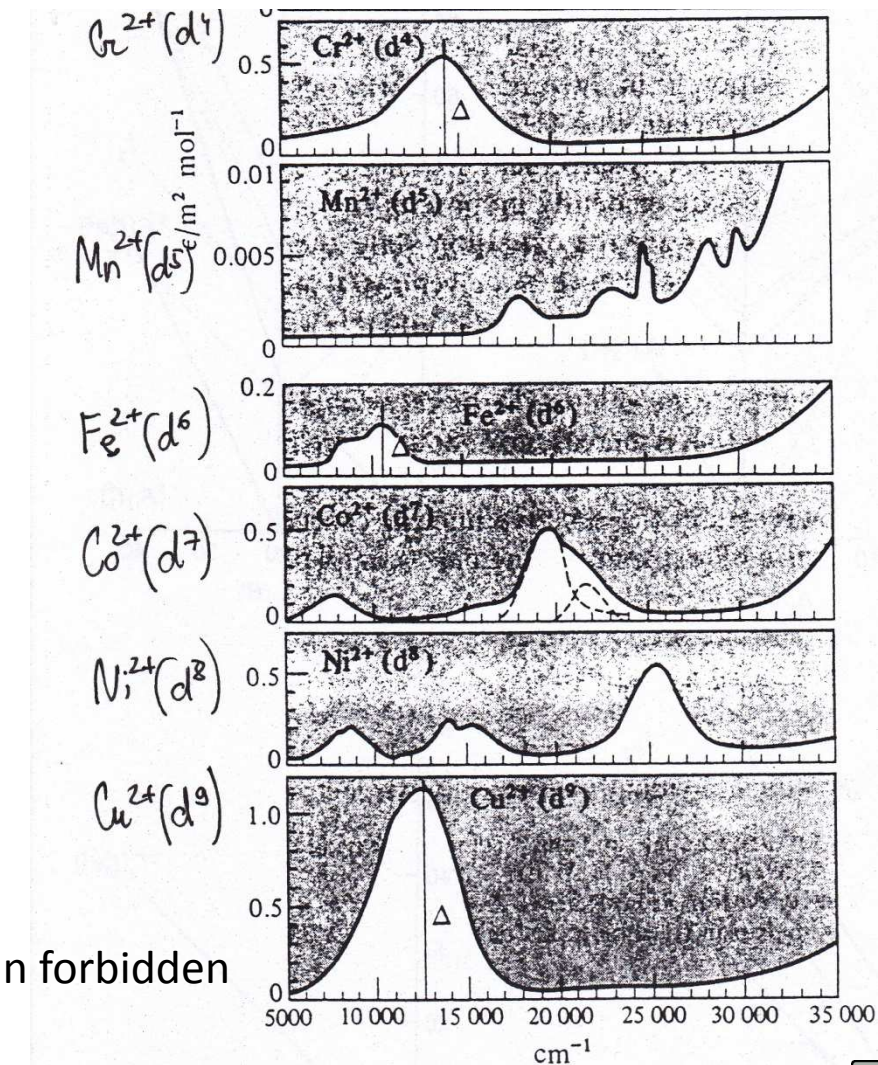
Spectrochemical series of ligands – growing Δ : I^- , Br^- , S^{2-} , SCN^- , Cl^- , NO_3^- , F^- , OH^- , $\text{C}_2\text{O}_4^{2-}$, H_2O , gly^- , NH_3 , $\text{C}_5\text{H}_5\text{N}$, en, phen, NO_2^- , PH_3 , CO, CN^-

Problem not solved by CFT

Electron transfer: more than 1 band in octahedral complexes => more than 2 energy levels
Multielectronic systems involve intra-electron interaction => (spectroscopic) TERMS



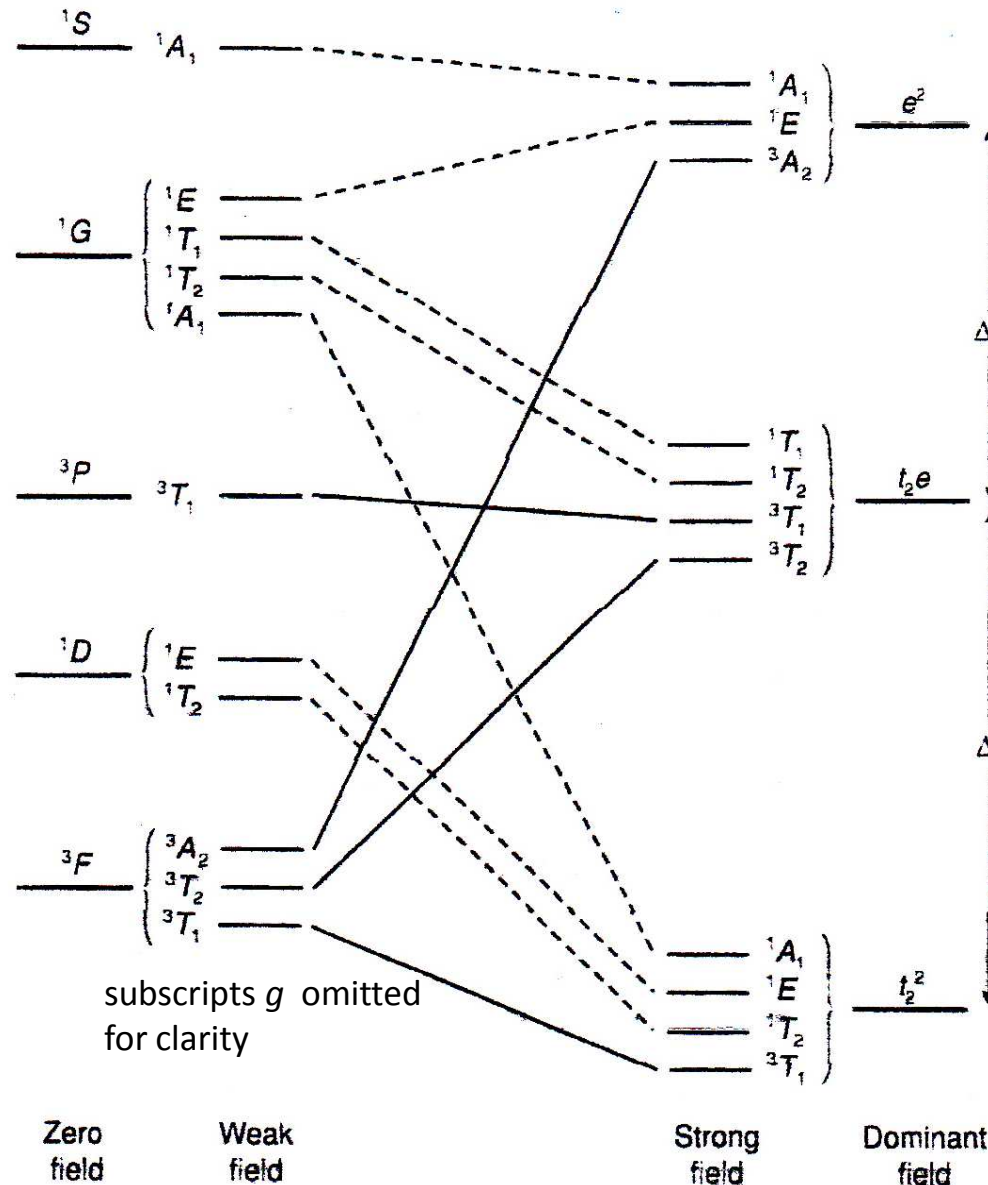
Spectra of various aqua complexes
Notice low intensity of the Mn^{2+} spectrum – spin forbidden



Comparison of the weak field and strong field approach, configuration d^2 in an octahedral field

Weak field:

- d^2 config.: 2 e^- in 5 orbitals = 45 microstates
- 45 microstates constitute 5 terms of different energies
- some of these **terms** (orbital degeneracy!) are **split by the crystal field**
- Ground state: ${}^3T_{1g}$ all triplet states: ${}^3T_{1g}, {}^3T_{2g}, {}^3A_{2g}, {}^3T_{1g}(P)$



Strong field:

- **d orbitals split by the crystal field** to t_{2g} and e_g levels
- ground state configuration $t_{2g}^2 = 2 e^-$ in 3 orbitals = 15 microstates (excited states $t_{2g}{}^1e_g{}^1$ and $e_g{}^2$)
- 15 microstates of the ground term constitute 4 terms of different energies
- Ground state: ${}^3T_{1g}$; 3 other triplet states from $t_{2g}{}^1e_g{}^1$ and $e_g{}^2$

Term energy depends on the crystal field strength

Ligand field theory (LFT)

LFT is an extension of CFT. It uses a set of parameters derived from experimental data (e.g. Racah parameters) to explain the existing covalency of the metal – ligand bonds.

The localized field arising from point charge ligands is changed for rather delocalized variety (see “nephelauxetic effect”).

Uveřejněné materiály jsou určeny studentům Vysoké školy chemicko-technologické v Praze jako studijní materiál. Některá textová i obrazová data v nich obsažená jsou převzata z veřejných zdrojů. V případě nedostatečných citací nebylo cílem autorky záměrně poškodit autora/y původního díla.

S případnými výhradami se prosím obracejte na autorku tohoto výukového materiálu, aby bylo možno zjednat nápravu.



The published materials are intended for students of the University of Chemistry and Technology, Prague as a study material. Some text and image data contained therein are taken from public sources. In the case of insufficient quotations, the author's intention was not to intentionally infringe the possible author(s) rights to the original work.

If you have any reservations, please contact the author(s) of the specific teaching material in order to remedy the situation.

Colours and structure of coordination compounds



EUROPEAN UNION
European Structural and Investing Funds
Operational Programme Research,
Development and Education



Colours - general

Absorption of light (electromagnetic radiation) = electron excitation to a higher level
(e.g. from HOMO to LUMO)

Colour of a compound – energy of the absorbed light (difference in orbital energies)
Intensity of the colour: frequency, type of electronic transition (forbidden, allowed)

Colour wheel

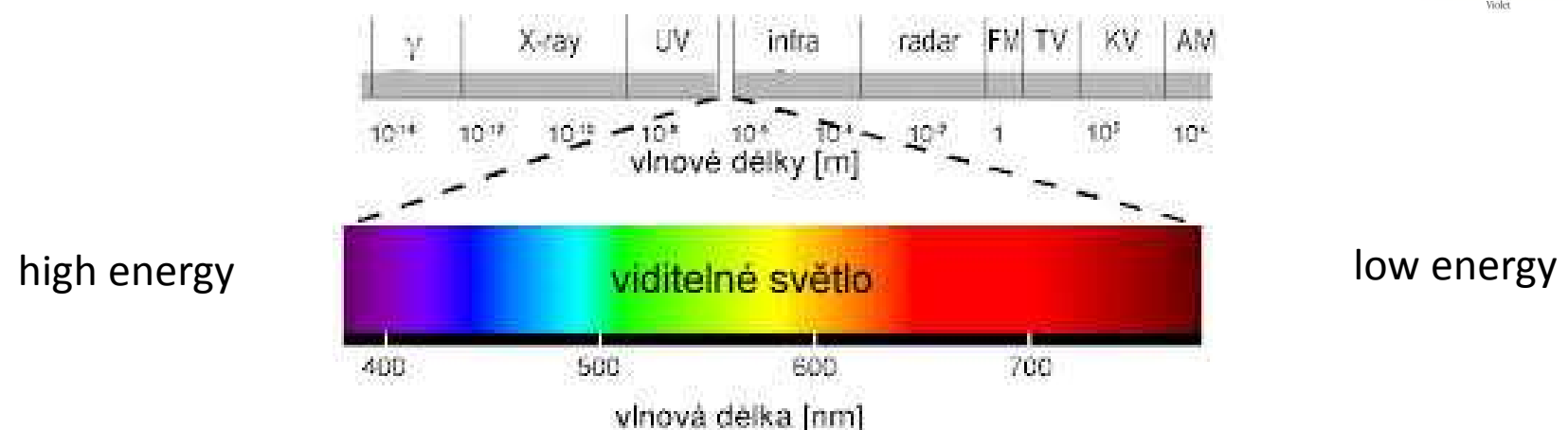
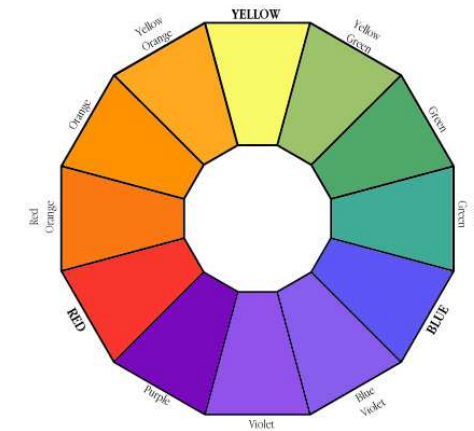
Complementary colours – opposite

red – green

violet – yellow

blue – orange

absorption of light of certain colour = appearance of the
complementary colour



Optical properties

Light absorption (of electromagnetic radiation) in $\lambda = 200 - 1000 \text{ nm}$ region

visible light:
from 400 nm (violet) to 750 nm (red)

Energy: $\Delta E = h\nu$

wavelength λ [nm]

wavenumber $\tilde{\nu}$ [cm^{-1}]

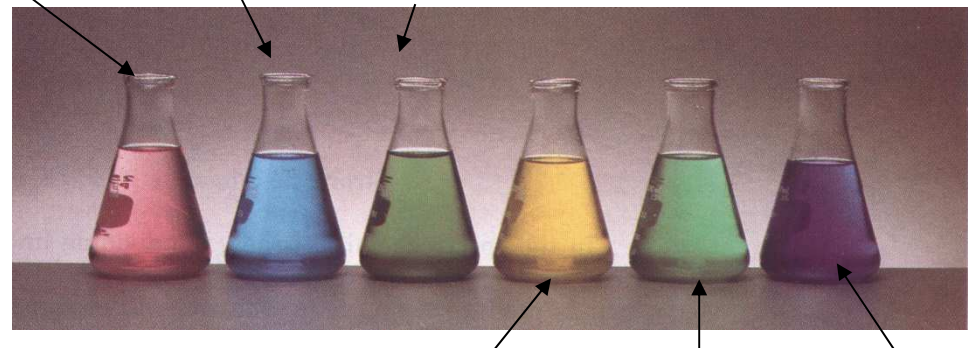
$$\tilde{\nu} = 1/\lambda = \nu/c$$

c speed of light, ν frequency

Intensity:

absorbance $A = \log(I_0/I)$

molar absorption coefficient ϵ
usual unit ϵ [$\text{L cm}^{-1} \text{ mol}^{-1}$]



	λ/nm	$\tilde{\nu}/\text{cm}^{-1}$
Red	700	14 300
Orange	620	16 130
Yellow	580	17 240
Green	530	18 870
Cyan	500	20 000
Blue	470	21 280
Violet	420	23 810

Types of electronic transitions in coordination compounds

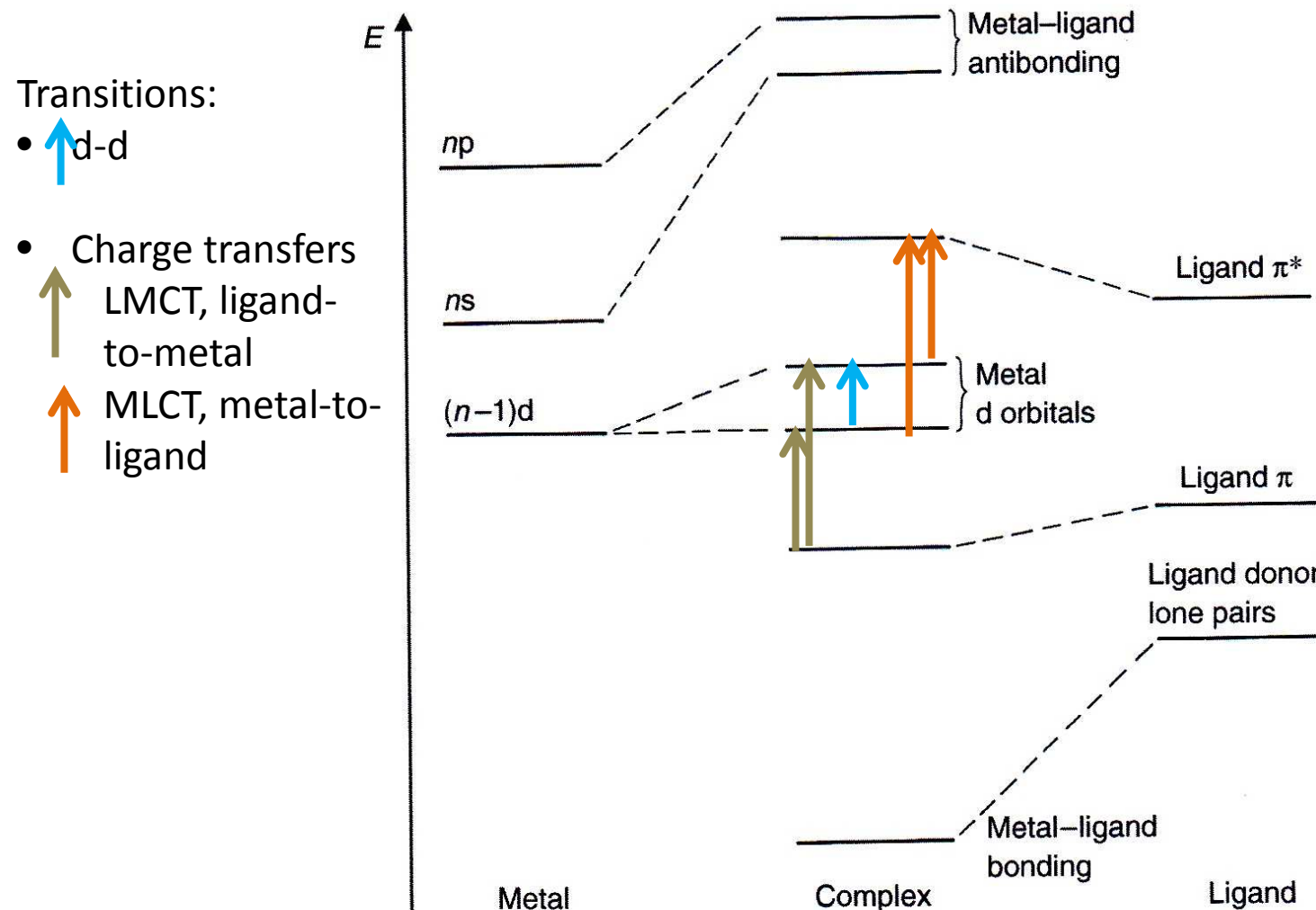


Figure 9.11

Generic energy-level diagram showing levels in a transition-metal complex derived from metal, ligand and metal-ligand bonding orbitals.

Selection rules - Intensity of the transition

Spin selection rules:

1. Only 1 electron is involved in any transition
2. There must be no net change of spin, i.e. $\Delta S = 0$

Spin forbidden

Laporte forbidden

d^5 ions, e.g. $[\text{Mn}(\text{OH}_2)_6]^{2+}$

Spin allowed

Laporte forbidden

e.g. $[\text{Ni}(\text{OH}_2)_6]^{2+}$

Orbital selection rules (Laporte):

3. a) Allowed transitions must involve an overall change in orbital angular momentum $\Delta L = \pm 1$ ($d-d$ and $p-p$ transitions are forbidden)
- b) Transitions from g to g and from u to u states are forbidden.

vibronic coupling

Spin allowed; Laporte forbidden

tetrahedral complexes

e.g. $[\text{NiCl}_4]^{2-}$

Charge transfer

spin allowed; Laporte allowed

e.g. $[\text{MnO}_4]^-$

$\pi-\pi^*$ transitions,

e.g. $\text{Zn}(\text{phthalocyanine})^{2-}$

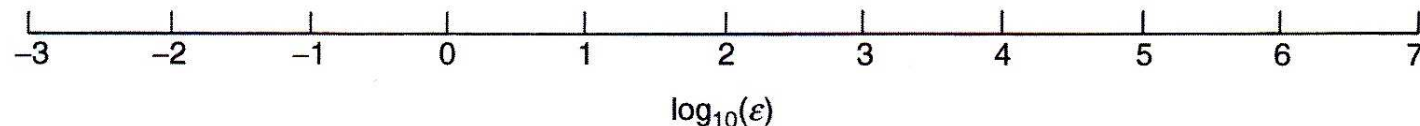


Figure 9.13

Some typical molar extinction coefficients, ϵ , for d-d and charge-transfer transitions.

Laporte forbidden bands in symmetries with *g* or *u* symmetry

- octahedron – higher energy, lower intensity

- tetrahedron

cf. energy and intensity of the transitions

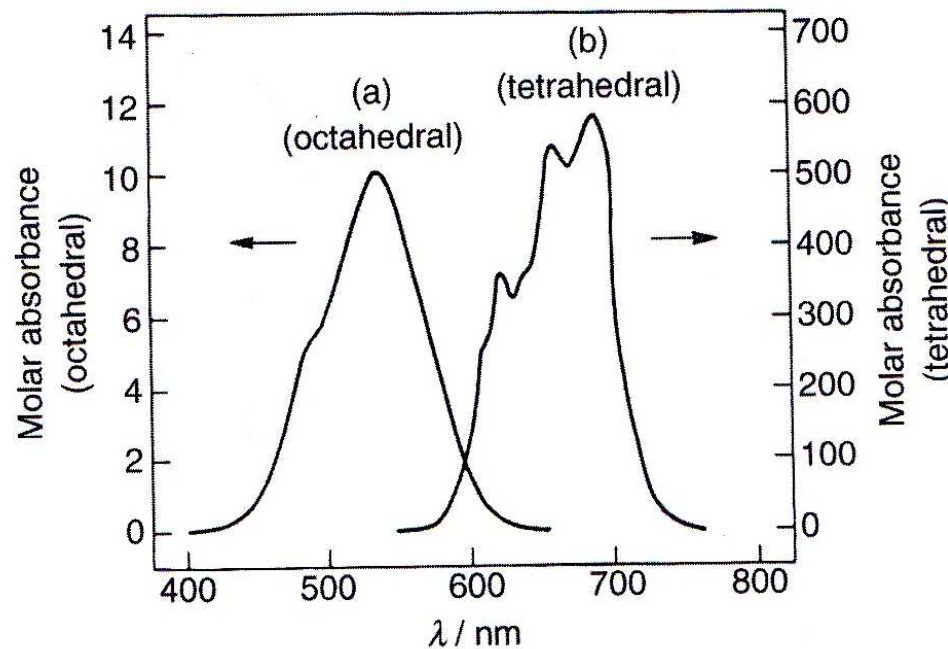


Figure 9.12

Visible spectra of (a) $[\text{Co}(\text{OH}_2)_6]^{2+}$ and (b) $[\text{CoCl}_4]^{2-}$. Note that the intensity scales differ by a factor of 50, the tetrahedral complex giving a much more intense band. The energy of the transition is smaller for the tetrahedral complex, reflecting the smaller crystal-field splitting in this case. Redrawn with permission from [12]. Copyright 1999 John Wiley & Sons.

Charge transfer (CT) bands

Fully allowed bands, very intense; colorimetry, dyes.

Types of CT bands

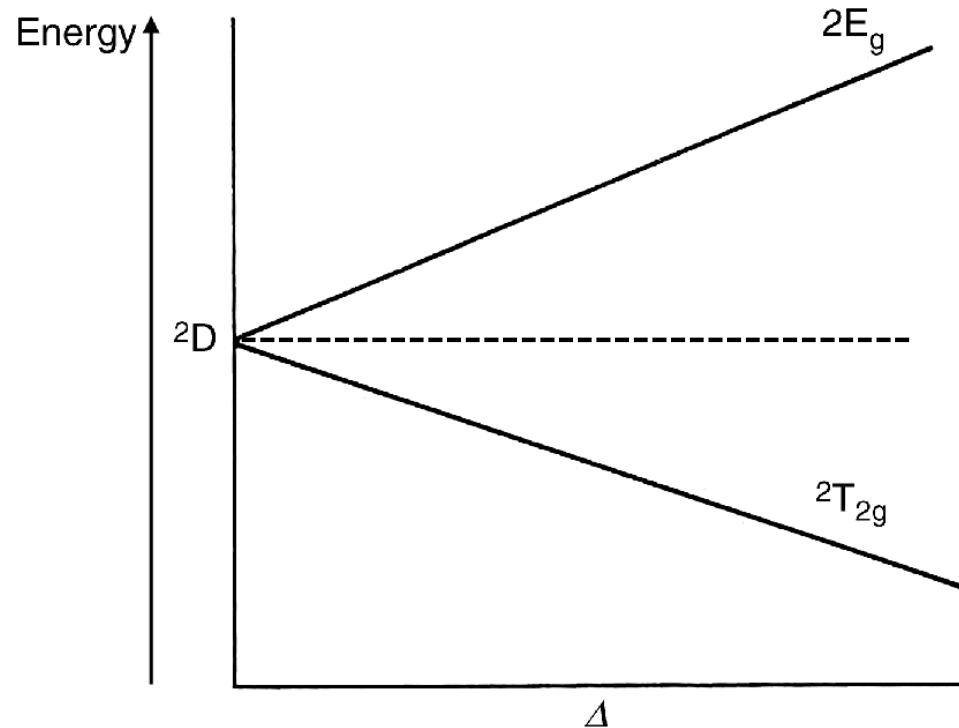
1. LMCT – ligand-to-metal, „reduction“ of the metal, ligand rich in electrons, metal in a higher oxidation state. Ex.: MnO_4^-
2. MLCT – metal-to-ligand, „oxidation“ of the metal, ligand with low energy LUMO orbitals, metal in low (oxidizable) oxidation state. Ex.: $[\text{Fe}(\text{phen})_3]^{2+}$ for colorimetric determination of Fe(II).
3. MMCT or IVCT – metal-metal, intervalence transfers in multinuclear species
4. LLCT – ligand-to-ligand transitions

Energy of CT bands and its relation to the redox nature of M and L

complex	$\pi(L) \rightarrow t_{2g}(M)$ [cm ⁻¹]	complex	$\pi(L) \rightarrow t_2(M)$ [cm ⁻¹]
$[\text{OsCl}_6]^{3-}$	35 450	TiCl_4	35 400
$[\text{OsCl}_6]^{2-}$	27 000	TiBr_4	29 500
$[\text{OsI}_6]^{3-}$	19 100	TiI_4	19 600
$[\text{OsI}_6]^{2-}$	12 300	$[\text{NiCl}_4]^{2-}$	35 500
		$[\text{NiBr}_4]^{2-}$	28 300
		$[\text{NiI}_4]^{2-}$	12 300

d-d bands, origin

Splittered term levels (low field approximation). Dependence on Δ (for all geometries)



For a given geometry, Δ depends on

1. nature of the metal ion – heavier atoms exhibit higher Δ values
2. charge of the metal ion – the higher is the charge, the higher is Δ

Data see in „Crystal field theory“

3. ligand - see Spectrochemical series of the ligands

Energy levels for a d^1 octahedral ion as a function of the ligand-field splitting, Δ .

Colours - examples

Cation Ni^{2+} in various environment



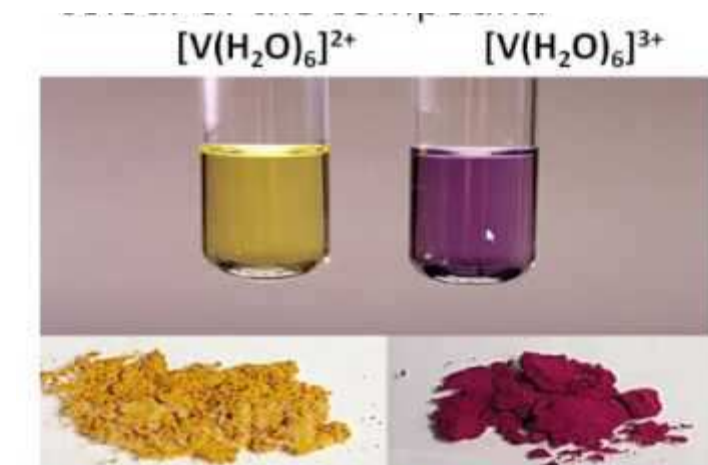
Different ions in the same environment (water): Co^{2+} , Ni^{2+} , Cu^{2+}



Empirical factors: $\Delta = f_L \cdot g_M$

Metal ion	$g_M [\text{cm}^{-1}]$	ligand	f_L
Fe^{2+}	10000	Br^-	0.72
Ru^{2+}	19800	SCN^-	0.73
Co^{2+}	9000	Cl^-	0.78
Ni^{2+}	8700	F^-	0.9
Cu^{2+}	13000	H_2O	1
Cr^{3+}	17400	NH_3	1.25
Mo^{3+}	24600	phen	1.34
Co^{3+}	18200	CN^-	~ 1.7

The same metal in different oxidation states (water): V^{2+} , V^{3+}



Colours - examples

Termochromism: ligand field geometry changes => colour change

Data from: Mechanochemical synthesis
and characterization
of a nickel(II) complex as a reversible
thermochromic nanostructure

Seyed Abolghasem Kahani* and Fatemeh
Abdevali

RSC Adv., 2016, 6, 5116

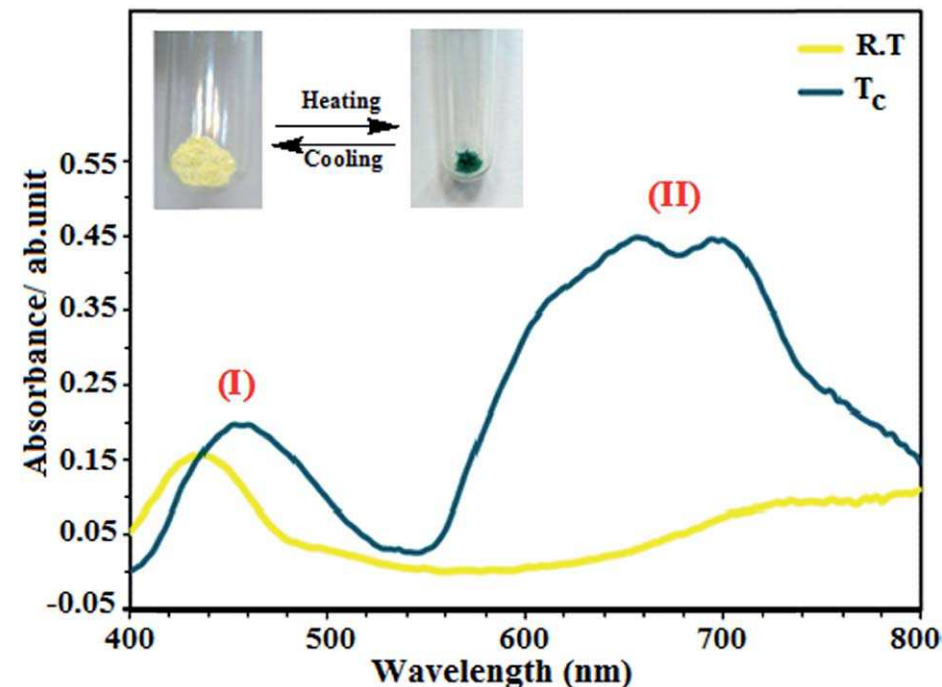
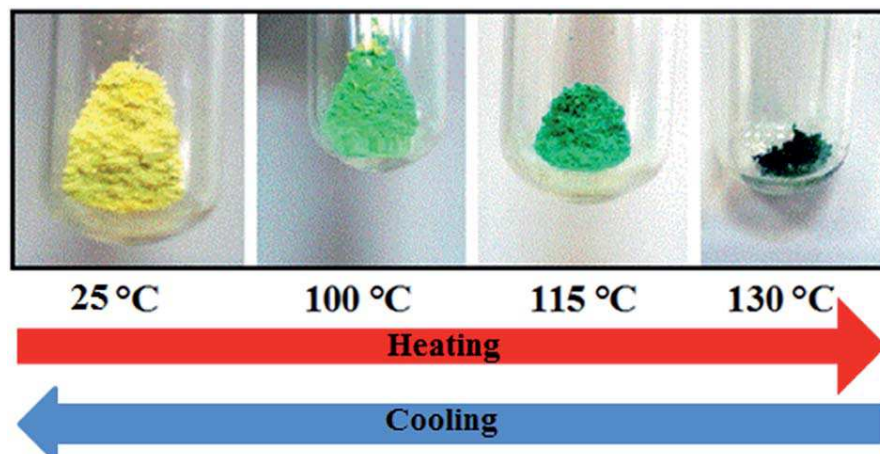


Fig. 3 UV-Vis spectra changes for the complex at room temperature (yellow line) and thermochromic temperature (blue line). The up left inset shows the photographs of the corresponding sample.



Spectrochemical series of the ligands

Different ligands split degenerated d - orbitals by different strength.

- reflects covalency in metal – ligand bond
- influence of π interaction (highest Δ : σ donors + π acceptors)

spectrochemical series – list of ligands ordered on strength

Ni(+II) complexes:

ligand H_2O ,
lower Δ_0 ,
absorbs red light



ligand en,
higher Δ_0 ,
absorbs yellow light



increasing impact of ligand on the central atom – growing Δ_0



different position of bonding isomers



ligands with more
electron pairs – both σ -
donors + π -donors

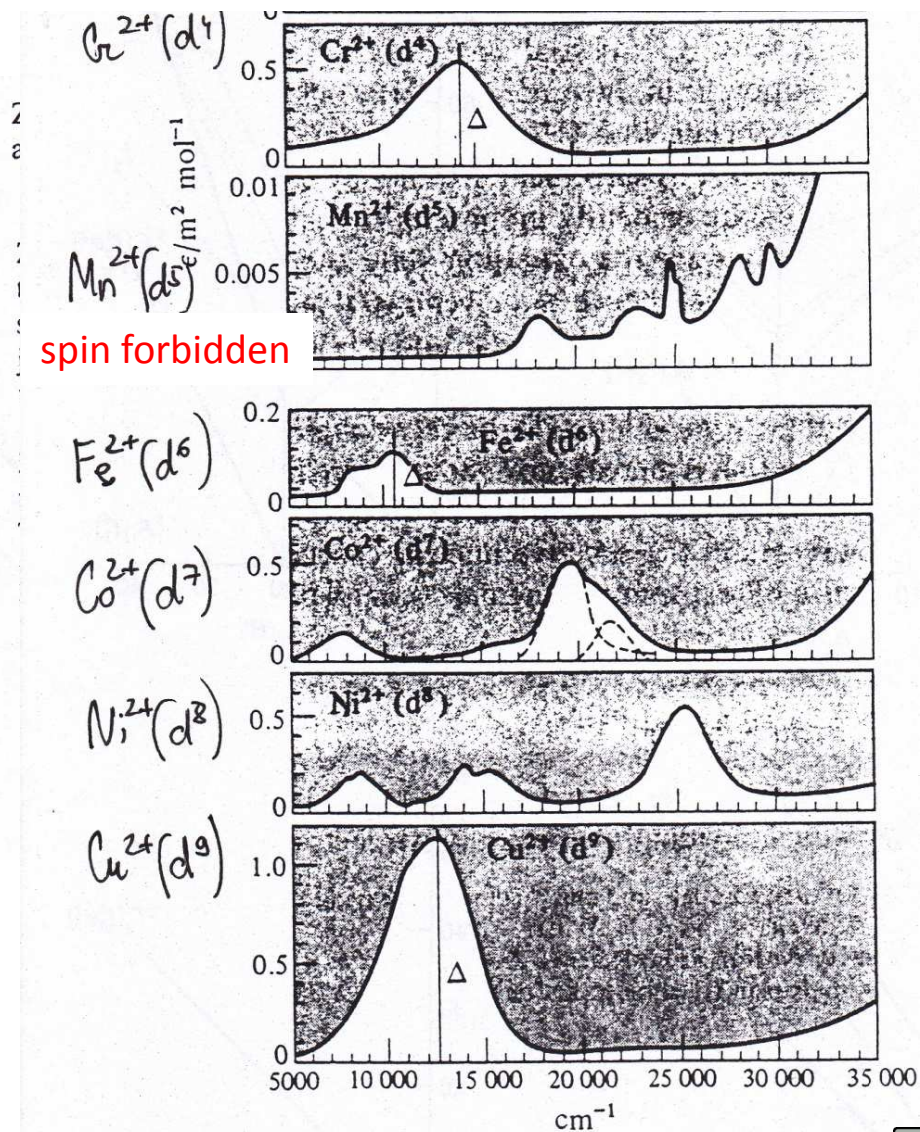
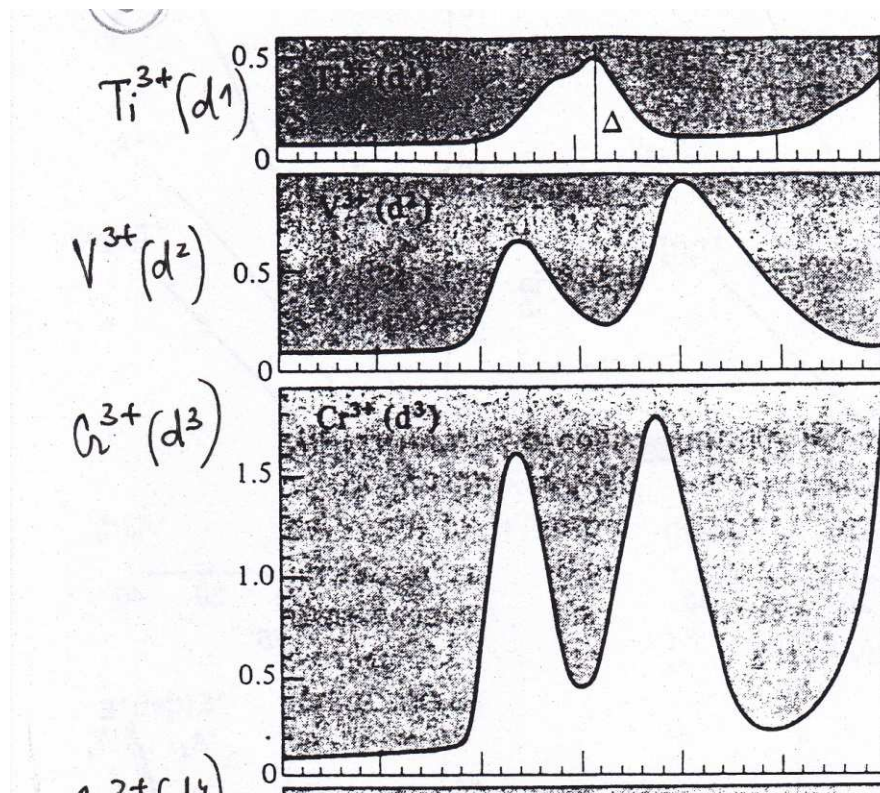
oxygen donors

nitrogen donors
- only σ -donors
of 1 electron pair

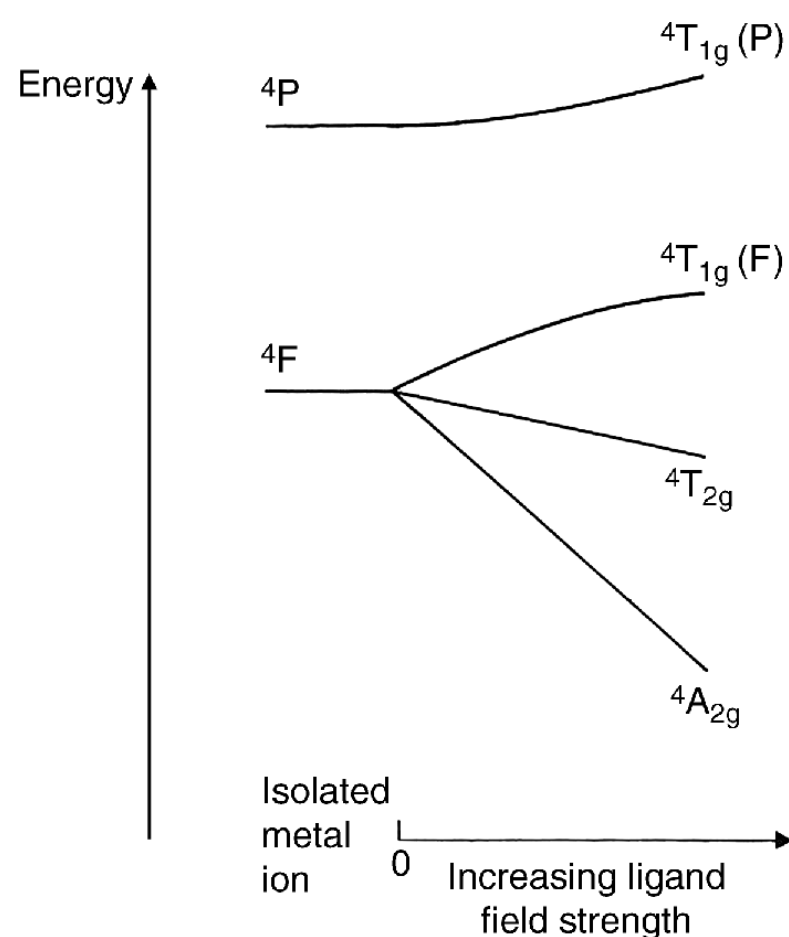
σ -donors +
 π -acceptors

Experimental spectra of some aqueous cations

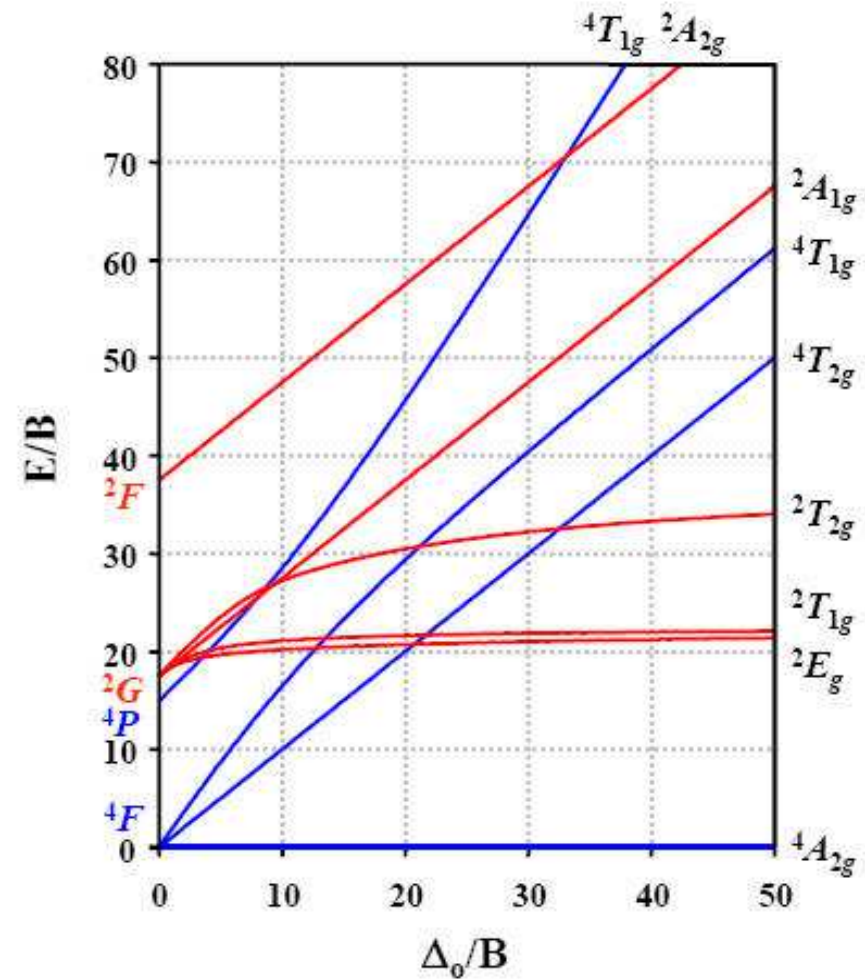
Octahedral aqueous complexes of 3d metal ions exhibit more than 1 band:



Energy diagrams (E vs. Δ_o) for d^3 system in an octahedral environment



Orgel diagram



Tanabe-Sugano diagram
Racah parameter B

Interpreting the electronic spectrum of aqueous Cr³⁺

d^3

band at $E_1 = 17\ 000\ \text{cm}^{-1}$

band at $E_2 = 24\ 000\ \text{cm}^{-1}$

shoulder of a CT band $E_3 = 37\ 000\ \text{cm}^{-1}$

$$\Delta_o = E_1 = 17\ 000\ \text{cm}^{-1}$$

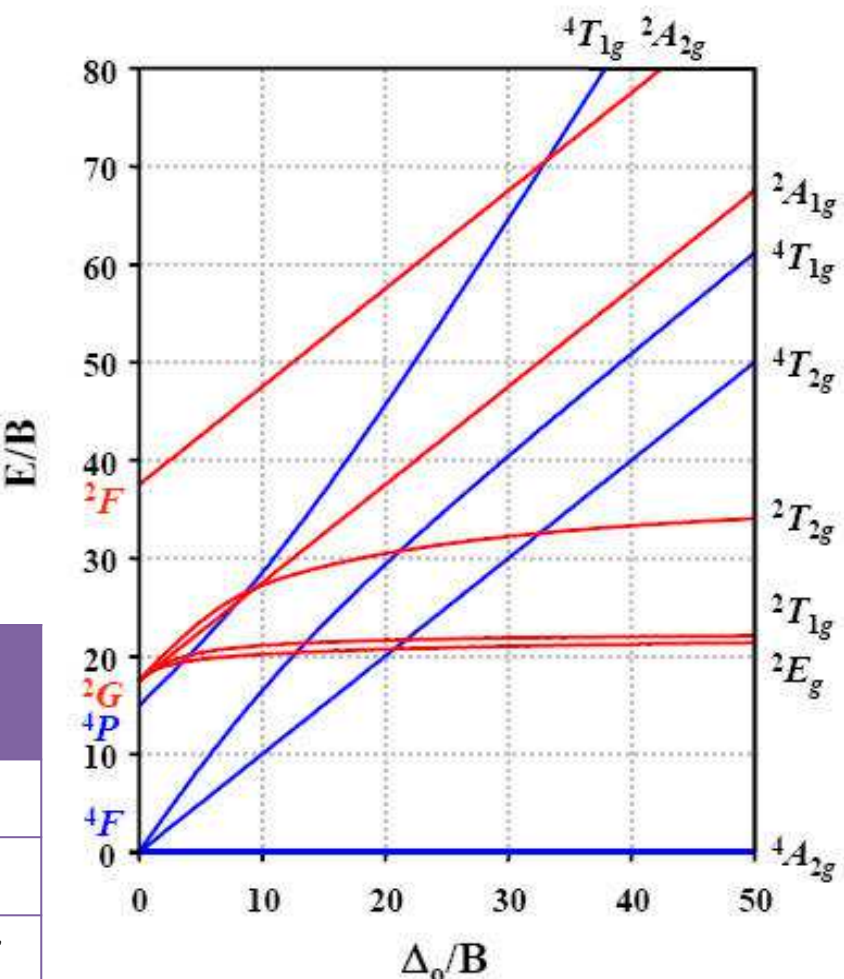
B

$$E_2 + E_3 = 15B + 30 Dq = 15B + 3 \Delta_o$$

$B = 670$, in free ion $B = 918$ - covalency

d^3 or d^8	Energy	Energy difference (ground state = 0)
A_{2g}	$-12 Dq$	0
T_{2g}	$-2 Dq$	$10 Dq$
$T_{1g}(F)$	$7.5B + 3 Dq - 0.5 G$	$7.5B + 15 Dq - 0.5 G$
$T_{1g}(P)$	$7.5B + 3 Dq + 0.5 G$	$7.5B + 15 Dq + 0.5 G$

d^3 Tanabe-Sugano Diagram



Interpreting the electronic spectrum of aqueous Ti^{3+}

d^1

Broad band at $20\ 030\ \text{cm}^{-1}$

shoulder at $18\ 300\ \text{cm}^{-1}$

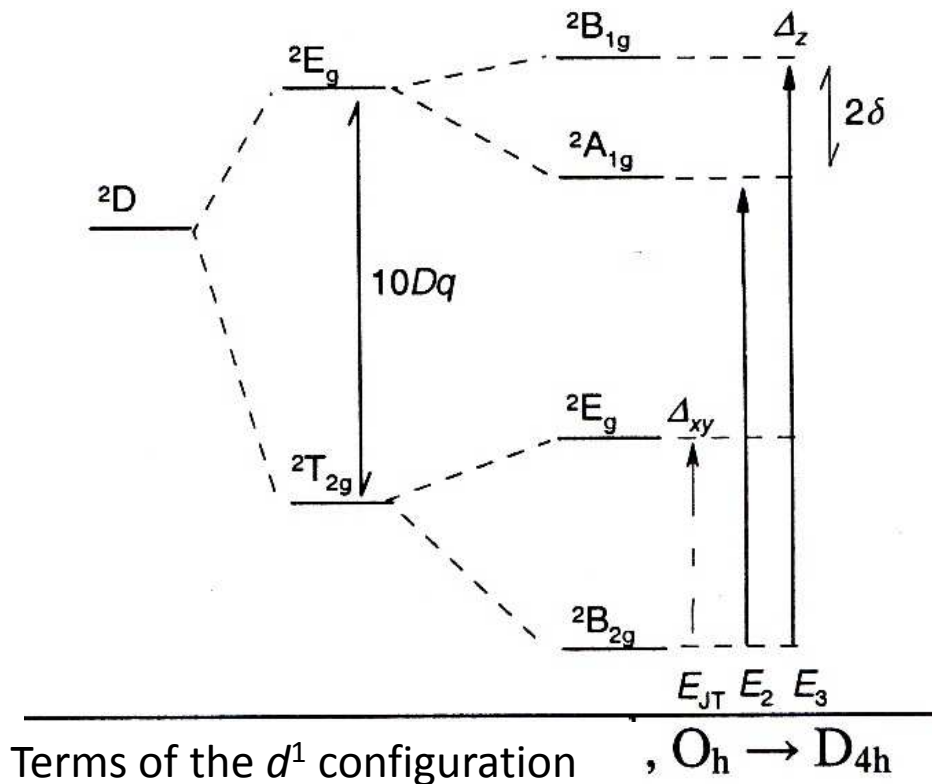
difference $2\delta = 2000\ \text{cm}^{-1}$

Ground term splitting is negligible
($E_{\text{JT}}=0$); small influence of ligands
(geometry!)

$$\Delta_0 = E_3 - \delta = 19\ 300\ \text{cm}^{-1}$$

B cannot be determined

Tetragonal distortion of the
octahedron, Jahn-Teller effect



Terms of the d^1 configuration

, $O_h \rightarrow D_{4h}$

Jahn – Teller effect

Splitting of degenerated orbitals occupied by non-equivalent number of electrons

Deformation, lower symmetry – orbital degeneracy disappears

Examples:

octahedron (O_h) → tetragonal bipyramidal (D_{4h})

tetrahedron (T_d) → trigonal pyramidal (C_{3v})

equilateral triangle (D_{3h}) → isosceles triangle (C_{2v})

Jahn–Teller theorem:

A nonlinear molecule cannot be stable in a degenerated electronic state, but must become distorted in such a way as to break down the degeneracy.

Reasons for a band splitting:

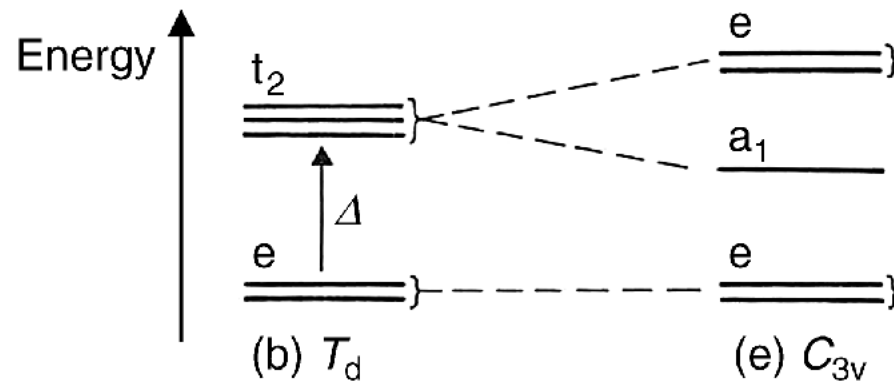
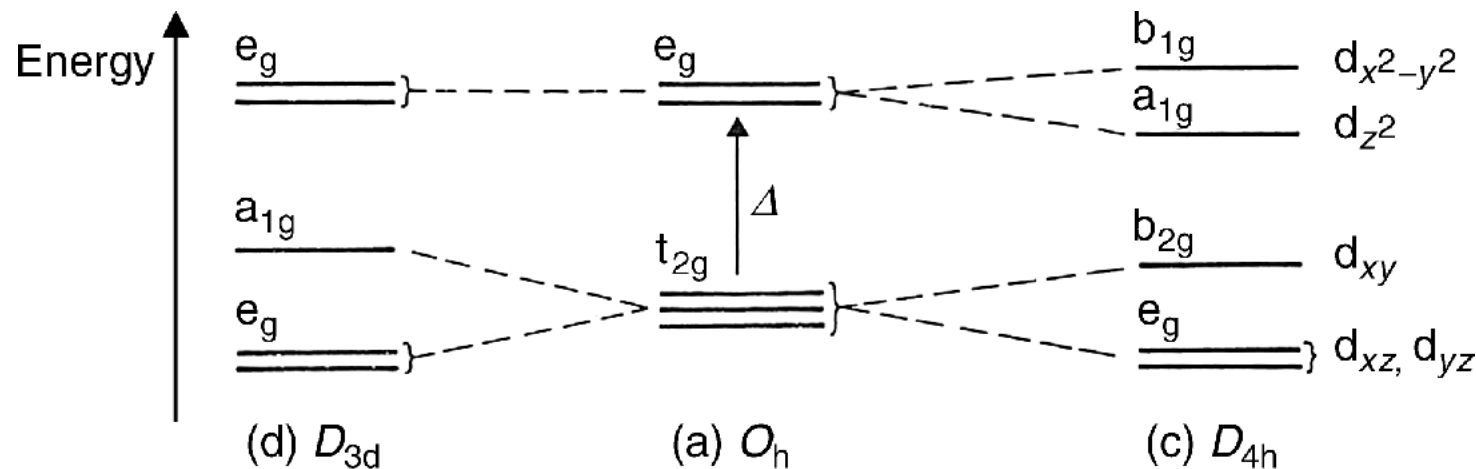
- Symmetry
 - Jahn-Teller effect

– assymetrical chromophore (donor atoms)

- Properties of electrons

spin-orbital coupling, when comparable with Δ (tetrahedron; heavier atoms)

Orbitals in some common distorted geometries

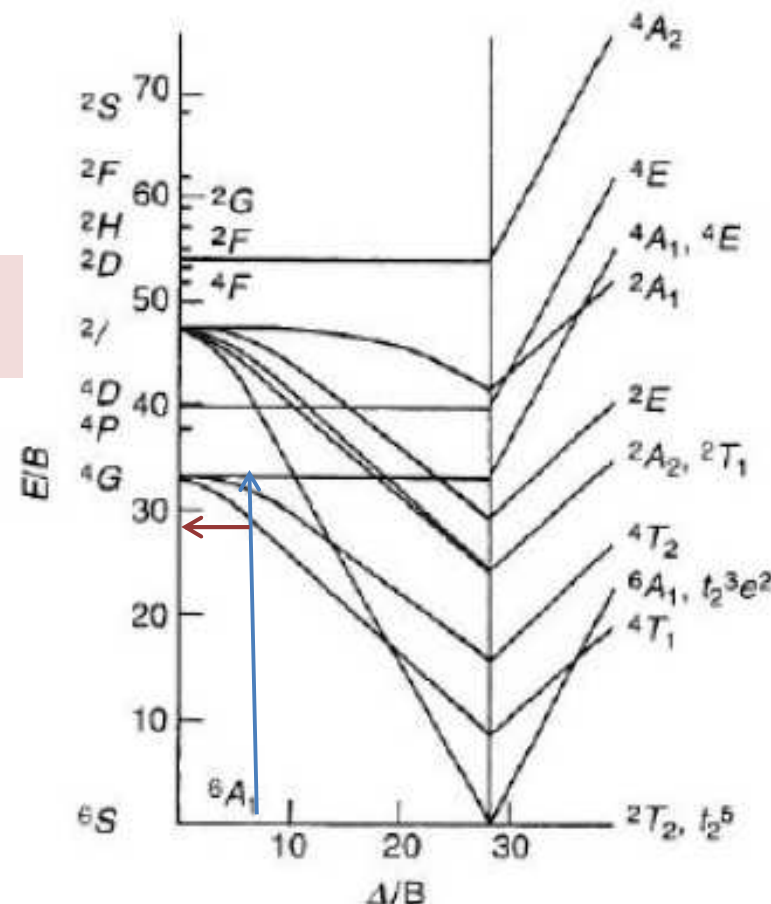
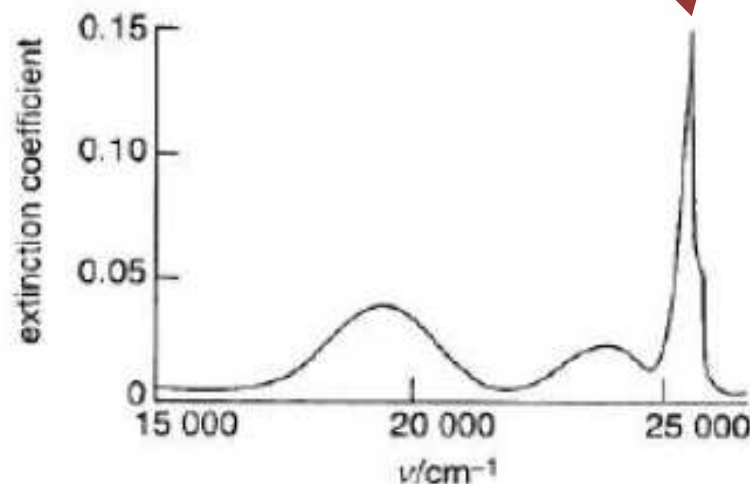


One-electron energy levels associated with metal d orbitals in complexes of various symmetries:
 (a) octahedral; (b) tetrahedral; (c) tetragonal distortion of an octahedron;
 (d) trigonal distortion of an octahedron; (e) trigonal distortion of a tetrahedron.

Interpreting the electronic spectrum of MnF_2

Assign the first 3 bands
Approx. value of Δ and B

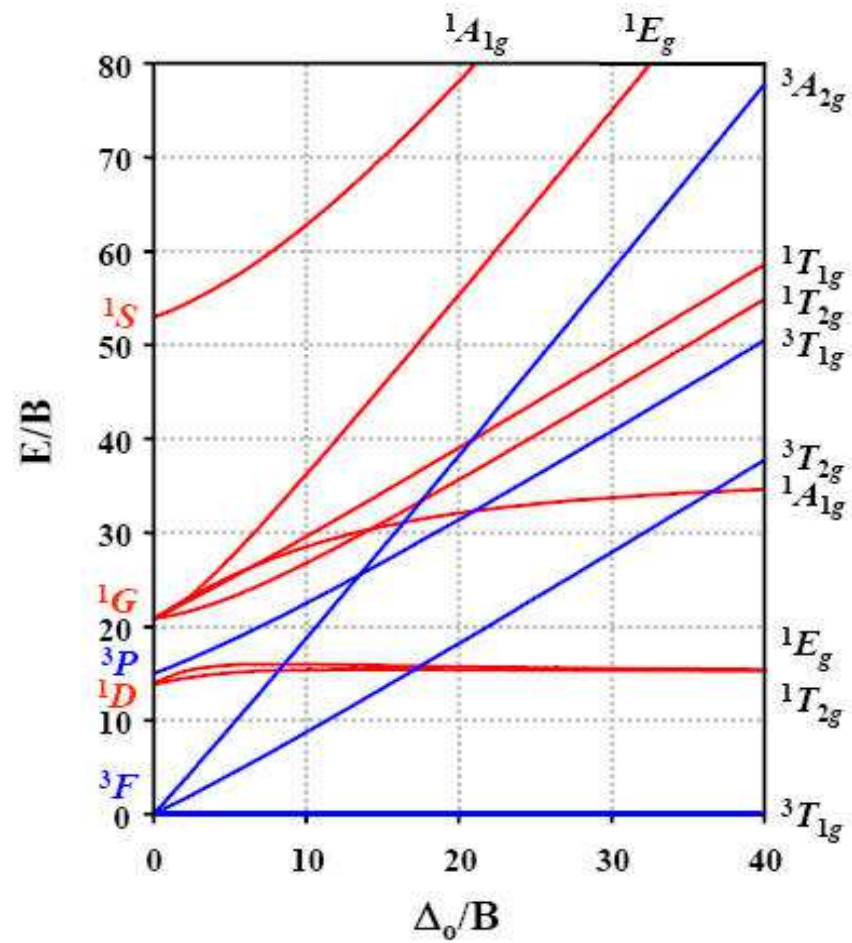
Sharp band: transition to a level parallel with the ground one



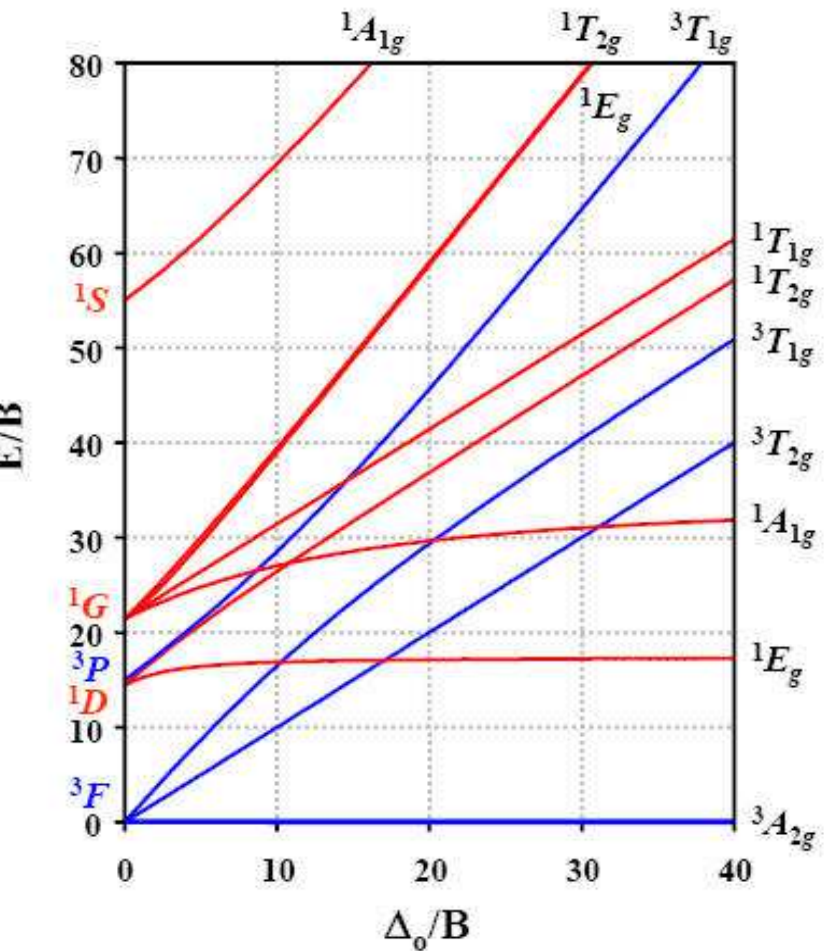
No spin-allowed transitions possible
Ratio of the transition (peak) energies 19:24:25
less forbidden: to a quadruplet state
found: Δ/B about 6 (blue arrow)
 E/B of the 1st transition = 28 (brown arrow)

Experimental E value $19\ 000\ \text{cm}^{-1}$
 $B = 19\ 000 / 28 \approx 680\ \text{cm}^{-1}$
 B° for a free ion: $960\ \text{cm}^{-1}$
 $\Delta = 6 B \approx 4000\ \text{cm}^{-1}$

d^2 Tanabe-Sugano Diagram

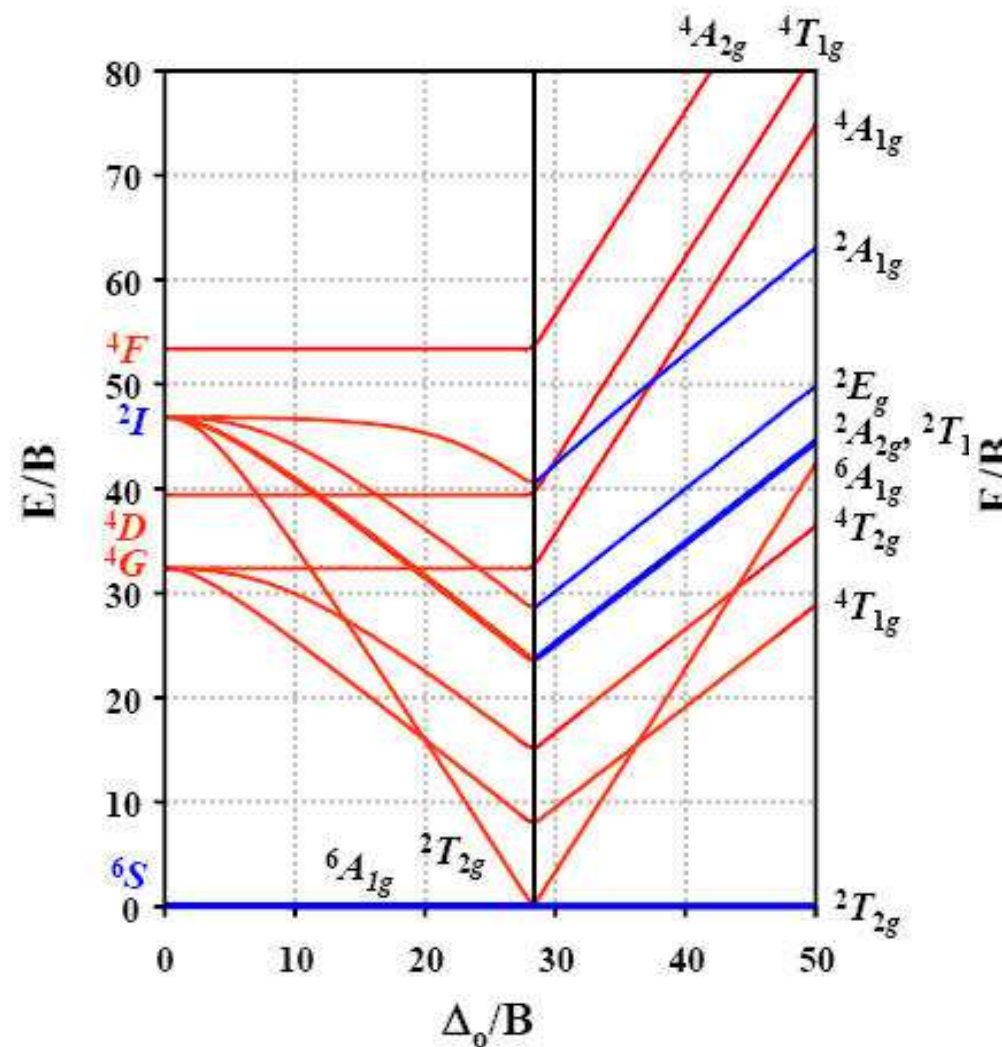


d^8 Tanabe-Sugano Diagram

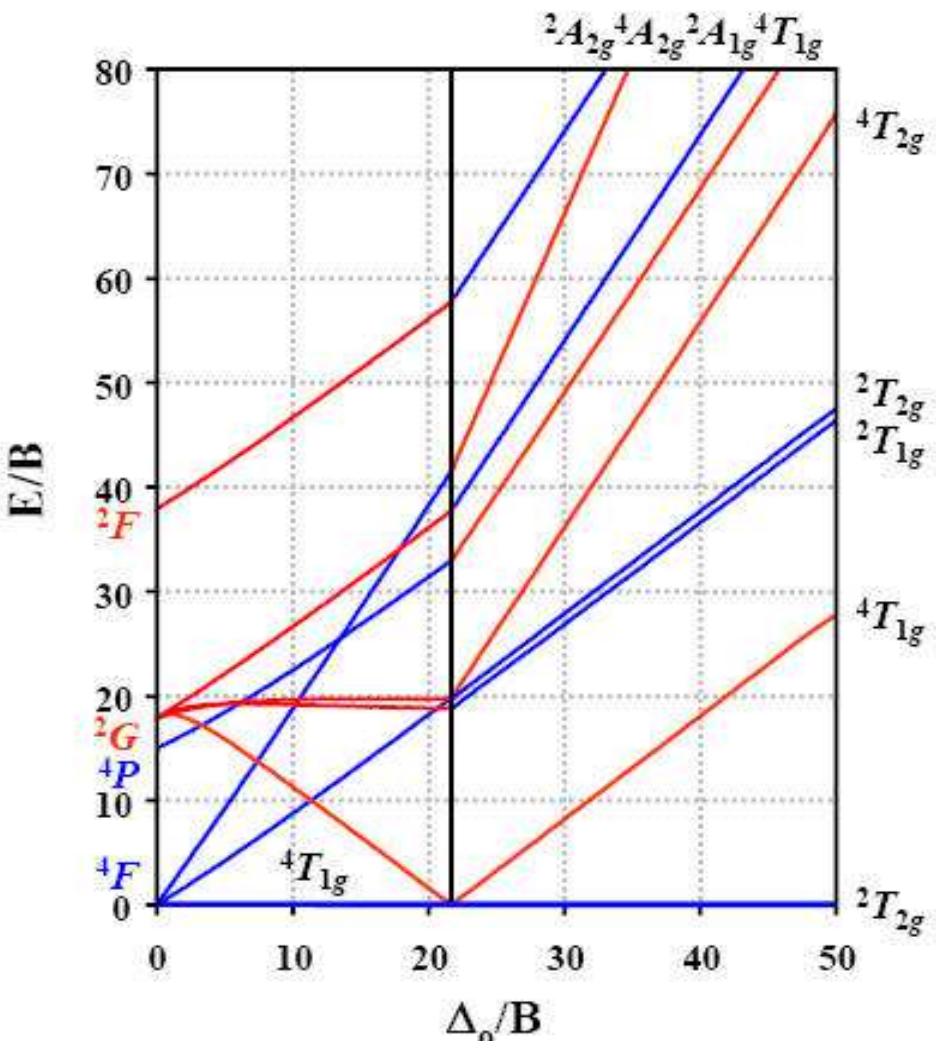


Electron – hole formalism; same terms, reverse splitting

d^5 Tanabe-Sugano Diagram

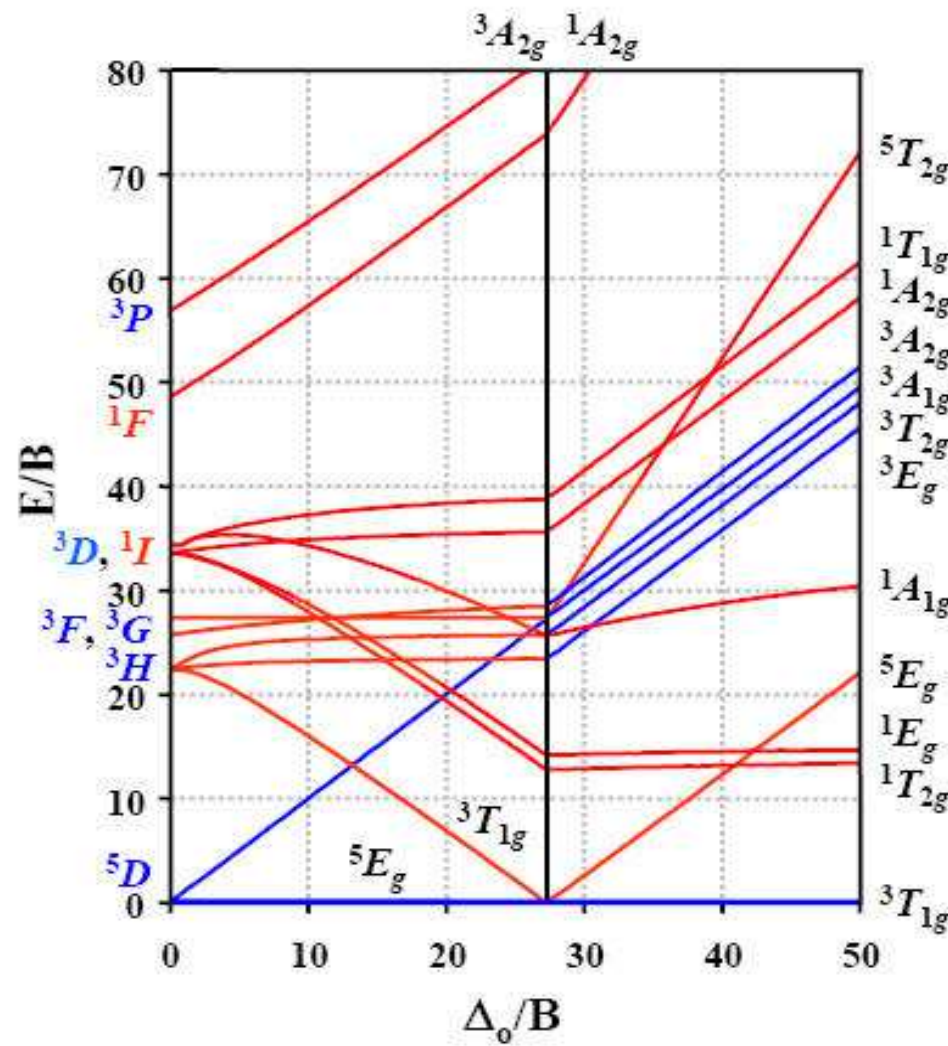


d^7 Tanabe-Sugano Diagram

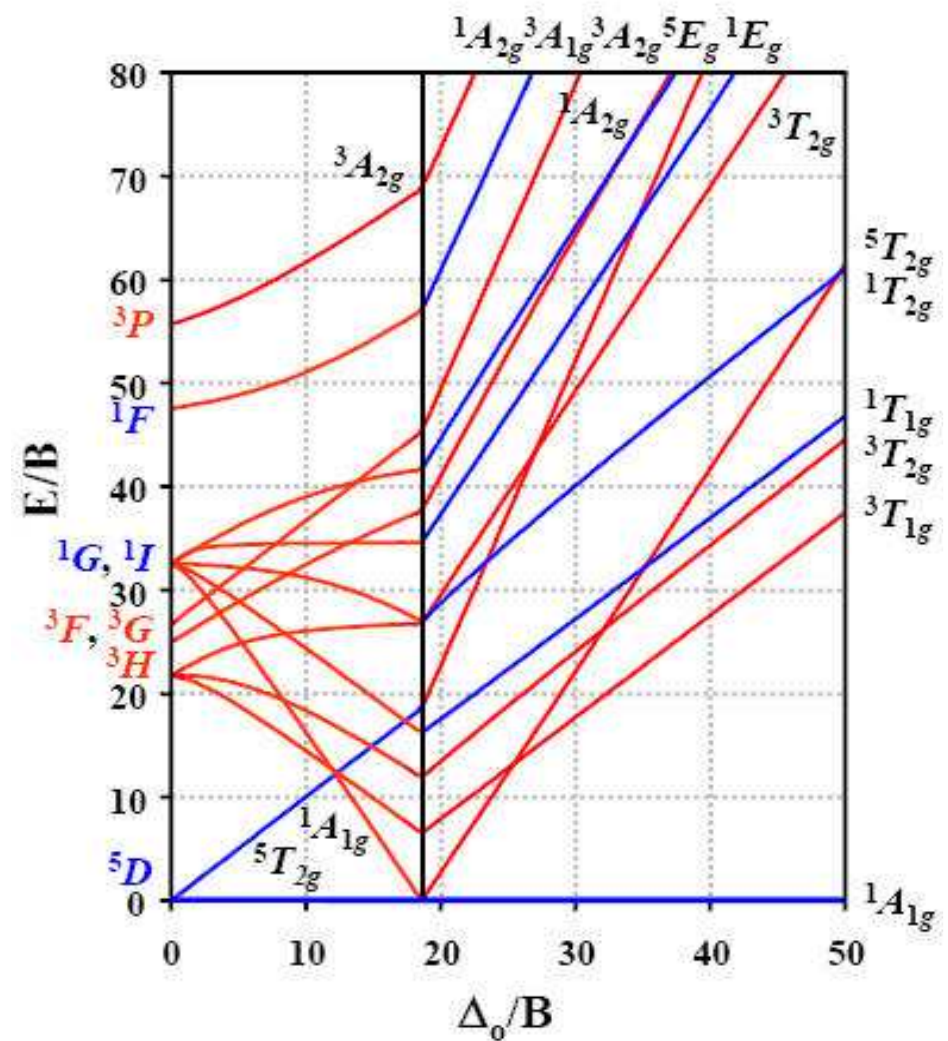


Change from the high spin to the low spin arrangement; Δ/B values of the spin transition are different for each configuration

d^4 Tanabe-Sugano Diagram



d^6 Tanabe-Sugano Diagram



Uveřejněné materiály jsou určeny studentům Vysoké školy chemicko-technologické v Praze jako studijní materiál. Některá textová i obrazová data v nich obsažená jsou převzata z veřejných zdrojů. V případě nedostatečných citací nebylo cílem autorky záměrně poškodit autora/y původního díla.

S případnými výhradami se prosím obracejte na autorku tohoto výukového materiálu, aby bylo možno zjednat nápravu.



The published materials are intended for students of the University of Chemistry and Technology, Prague as a study material. Some text and image data contained therein are taken from public sources. In the case of insufficient quotations, the author's intention was not to intentionally infringe the possible author(s) rights to the original work.

If you have any reservations, please contact the author(s) of the specific teaching material in order to remedy the situation.

Multielectronic Systems: Origin and Use of Energy Terms and Multiplets

Sources:

- J. Ribas Gispert, Coordination Chemistry, chapter 8, WILEY-VCH, 2008
- G. Wulfsberg, Inorganic Chemistry, University Science Books, 2000, chapter 17.1.
- E. I. Solomon, A. B. P. Lever, Inorganic Electronic Structure and Spectroscopy, 2. ed., WILEY 2006, Vol.1, p.35
- C. Housecroft, A Sharpe, Inorganic Chemistry, 4th ed., Pearson 2012, chapter 20
- A. A. Vlček



EUROPEAN UNION
European Structural and Investing Funds
Operational Programme Research,
Development and Education

ME
MINISTRY OF EDUCATION,
YOUTH AND SPORTS



Microstates

A given electronic configuration (d^2 , p^3 etc.) can be arranged in orbitals by several different unique ways – **microstates**.

Pauli exclusion principle is valid!

Example: Possible arrangement of 2 electrons in 2 orbitals gives 6 possibilities - microstates:

$[(\uparrow\downarrow)(\)]$ $[(\)(\uparrow\downarrow)]$ $[(\uparrow)(\uparrow)]$ $[(\downarrow)(\downarrow)]$ $[(\uparrow)(\downarrow)]$ $[(\downarrow)(\uparrow)]$

x electrons in y degenerated orbitals

$$N = \frac{(2y)!}{x!(2y-x)!} \quad \text{possibilities - microstates}$$

Each electron is described by

- magnetic quantum number m_l
- spin quantum number m_s

Each microstate is described by

- $M_L = \sum m_l$
- $M_s = \sum m_s$

Microstates of the same energy form an **electronic state**. The electronic state of the lowest energy – **ground state**. Each electronic state is designated by a **term symbol**.

Ground state (**Hund's rules**):

- maximal spin multiplicity
- maximal orbital multiplicity

Term symbols

General term symbol ^{2S+1}L

S total spin quantum number, the maximum M_s value

L total orbital angular momentum q.n., the maximum M_L value

$2S+1$	spin multiplicity	$2S+1$	Unpaired e ⁻	is named
		1	0	Singlet
		2	1	Doublet
		3	2	Triplet
		4	3	Quadruplet
		5	4	Quintuplet
		6	5	Sextuplet

$2L+1$ orbital multiplicity, equal to the degeneracy of L ; letters instead of numbers

Value of L	0	1	2	3	4	5	6	7
Letter	S	P	D	F	G	H	I	K
Degeneracy of L	1	3	5	7	9	11	13	15

Any filled set of orbitals by itself gives a non-degenerate 1S electronic state.

A given term ^{2S+1}L involves $(2S+1)(2L+1)$ microstates.

configuration	Terms (the ground term in bold letters)	Total degeneracy
p, p^5	2P	6
p^2, p^4	$^3P, ^1D, ^1S$	15
p^3	$^4S, ^2D, ^2P,$	20
d^1, d^9	2D	10
d^2, d^8	$^3F, ^3P, ^1G, ^1D, ^1S$	45
d^3, d^7	$^4F, ^4P, ^2H, ^2G, ^2F, 2\ ^2D, ^2P$	120
d^4, d^6	$^5D, ^3H, ^3G, 2^3F, ^3D, 2^3P, ^1I, 2^1G, ^1F, 2^1D, 2^1S$	210
d^5	$^6S, ^4G, ^4F, ^4D, ^4P, ^2I, ^2H, 2^2G, 2^2F, 3^2D, ^2P, ^2S$	252
d^{10}, s^2, p^6	1S	1

Electron – positive hole formalism

The terms of interest are the ground term and those with the same spin multiplicity.

Splitting (and re-naming) of degenerated electronic states in O_h symmetry

Term	Orbital degeneracy	Terms in O_h symmetry	Terms in T_d symmetry	Terms in D_{4h} symmetry
S	1	A_{1g}	A_1	A_{1g}
P	3	T_{1g}	T_1	$A_{2g} + E_g$
D	5	$T_{2g} + E_g$	$T_2 + E$	$A_{1g} + B_{1g} + B_{2g} + E_g$
F	7	$T_{1g} + T_{2g} + A_{2g}$	$T_1 + T_2 + A_2$	$A_{2g} + B_{1g} + B_{2g} + 2E_g$

GROUND STATE TERMS IN OCTAHEDRAL SYMMETRY

Weak field = high-spin arrangement

$d^1 = {}^2T_{2g}$	$d^2 = {}^3T_{1g}$	$d^3 = {}^4A_{2g}$	$d^4 = {}^5E_g$	$d^5 = {}^6A_{1g}$
$d^6 = {}^5T_{2g}$	$d^7 = {}^4T_{1g}$	$d^8 = {}^3A_{2g}$	$d^9 = {}^2E_g$	$d^{10} = {}^1A_{1g}$

Reminder – ground terms of non-split states

d^1, d^9	2D
d^2, d^8	3F
d^3, d^7	4F
d^4, d^6	5D
d^5	6S

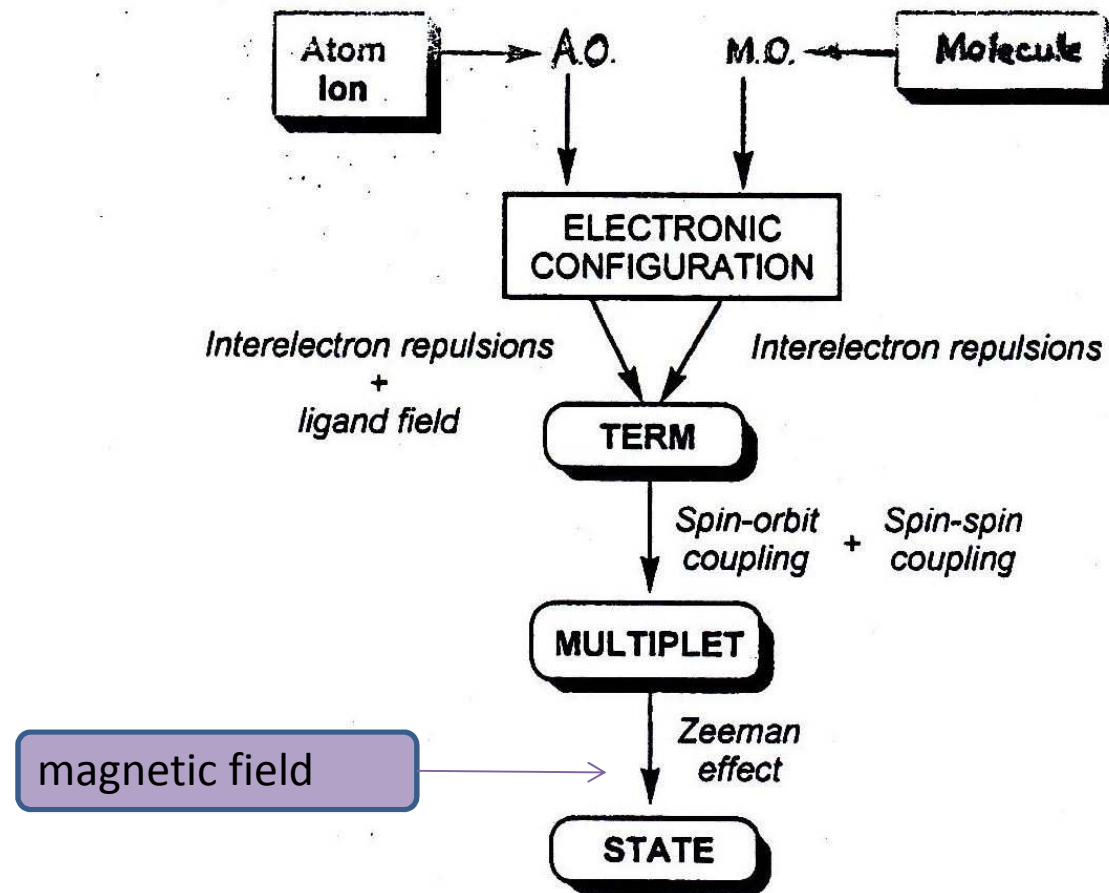


Figure 8.1 Scheme showing the concept of term, multiplet and state from the electron configuration.

Spin-orbit coupling

1. Russell-Sounders coupling

Total spin angular momentum S and total atomic orbital angular momentum L combine giving the total atomic angular momentum J .

$$J = L + S, L + S - 1, \dots, |L - S|$$

Term symbol: $2S+1L_J$

Ground state:

- less than half-full subshell => lowest J
- more than half-full subshell => highest J

2. $j-j$ coupling

The individual electronic orbital and spin angular momenta combine to give a total angular momentum for each electron, denoted j . The j values couple to J .

Energy: $E_J = \frac{1}{2} \lambda [J(J + 1) - L(L + 1) - S(S + 1)]$;

multiplet interval $E_{J+1} - E_J = (J + 1)\lambda$

λ spin-orbit splitting parameter; measures the strength of the spin-orbit interaction

Importance of J – heavier elements ground states

Ln^{3+}	Electronic Configuration	Ground level	Colour	$\mu_{\text{eff}}/\text{Bohr Magnets}$ Calculated (Eqn 3.5)	Observed
Ce ³⁺	[Xe]4f ¹	² F _{5/2}	Colourless	2.54	2.3–2.5
Pr ³⁺	[Xe]4f ²	³ H ₄	Green	3.58	3.4–3.6
Nd ³⁺	[Xe]4f ³	⁴ I _{9/2}	Lilac	3.62	3.5–3.6
Pm ³⁺	[Xe]4f ⁴	⁵ I ₄	Pink	2.68	—
Sm ³⁺	[Xe]4f ⁵	⁶ H _{5/2}	Yellow	0.85	1.4–1.7
Eu ³⁺	[Xe]4f ⁶	⁷ F ₀	Pale pink	0	3.3–3.5
Gd ³⁺	[Xe]4f ⁷	⁸ S _{7/2}	Colourless	7.94	7.9–8.0
Tb ³⁺	[Xe]4f ⁸	⁷ F ₆	Pale pink	9.72	9.5–9.8
Dy ³⁺	[Xe]4f ⁹	⁶ H _{15/2}	Yellow	10.65	10.4–10.6
Ho ³⁺	[Xe]4f ¹⁰	⁵ I ₈	Yellow	10.60	10.4–10.7
Er ³⁺	[Xe]4f ¹¹	⁴ H _{15/2}	Rose-pink	9.58	9.4–9.6
Tm ³⁺	[Xe]4f ¹²	³ H ₆	Pale green	7.56	7.1–7.5
Yb ³⁺	[Xe]4f ¹³	² F _{7/2}	Colourless	4.54	4.3–4.9
Lu ³⁺	[Xe]4f ¹⁴	¹ S ₀	Colourless	0	0

Table 3.1 Spectroscopic and magnetic properties of Ln^{3+} ions in hydrated salts.

$$\text{Eqn. 3.5: } \mu_{\text{eff}} = g_J \sqrt{J(J + 1)}$$

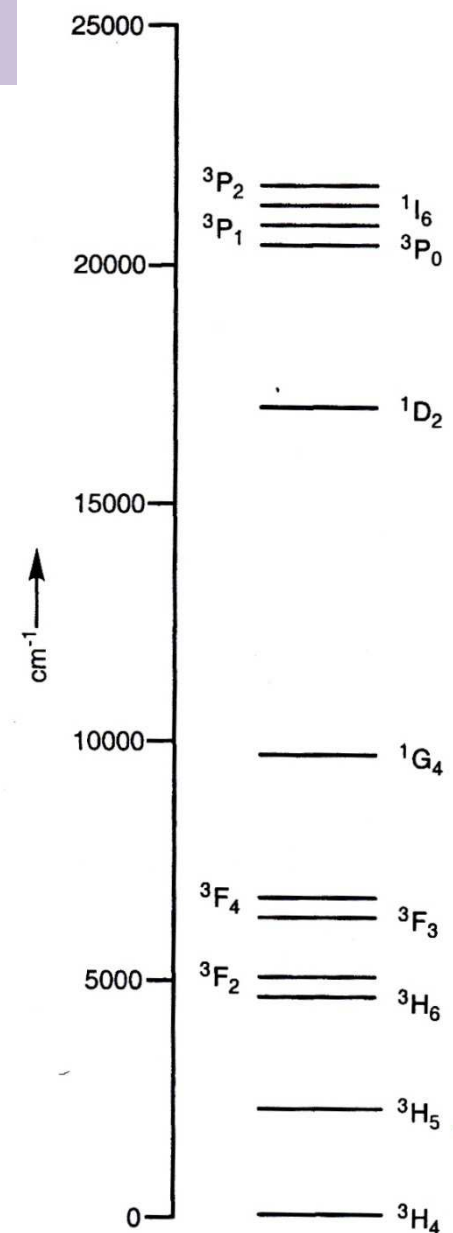


Fig. 3.3 Electronic energy level diagram for Pr^{3+} ($[\text{Xe}]4f^2$).

The ground term - summary

Hund's rules applied, in the following order.

Rule 1:

The ground term always has the largest value of S

rule of maximum multiplicity

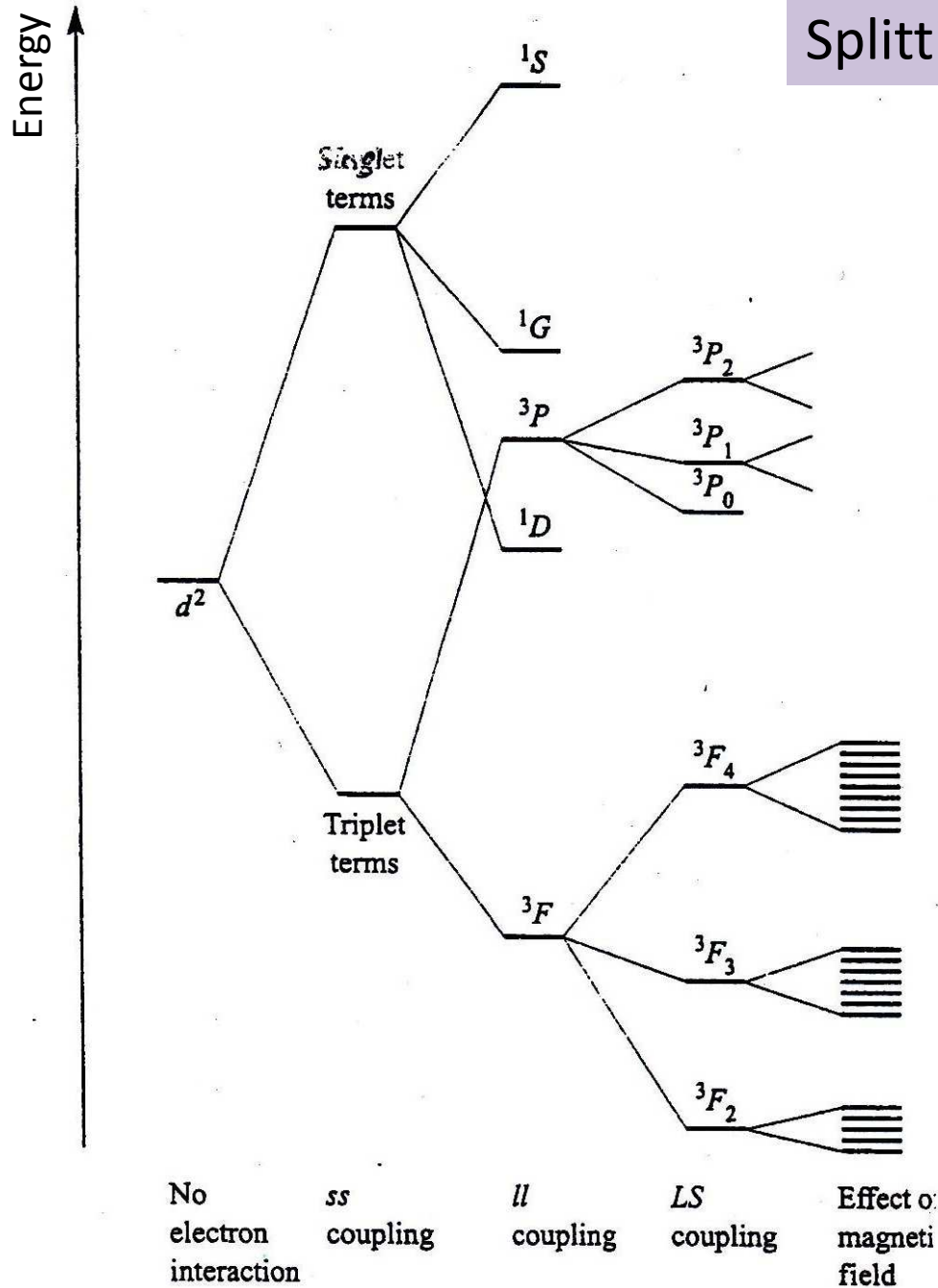
Rule 2:

If two terms have the same multiplicity, the one with the highest value of L lies lowest in energy

Rule 3:

For electronic subshells that are less than half full, the level with the lowest value of J lies lowest in energy.

For greater than half-filled subshells, the level with the highest value of J lies lowest in energy.



Splitting of the terms of a d^2 ion

All possible terms:
 $^3F, ^3P, ^1G, ^1D, ^1S$

Two triplet terms, 3F and 3P

Determination of J

- $^3F: S = 1, L = 3$

$$J = L + S = 4$$

$$J = L + S - 1 = 3$$

$$J = |L - S| = 2$$

$$^3F_4, ^3F_3, ^3F_2$$

Ground state – lowest J

(less than $\frac{1}{2}$ filled) – 3F_2

- $^3P: S = 1, L = 1$

$$J = L + S = 2$$

$$J = L + S - 1 = 1$$

$$J = |L - S| = 0$$

$$^3P_0, ^3P_1, ^3P_2$$

Spin-orbit coupling parameters, λ , for some free ions in the ground state

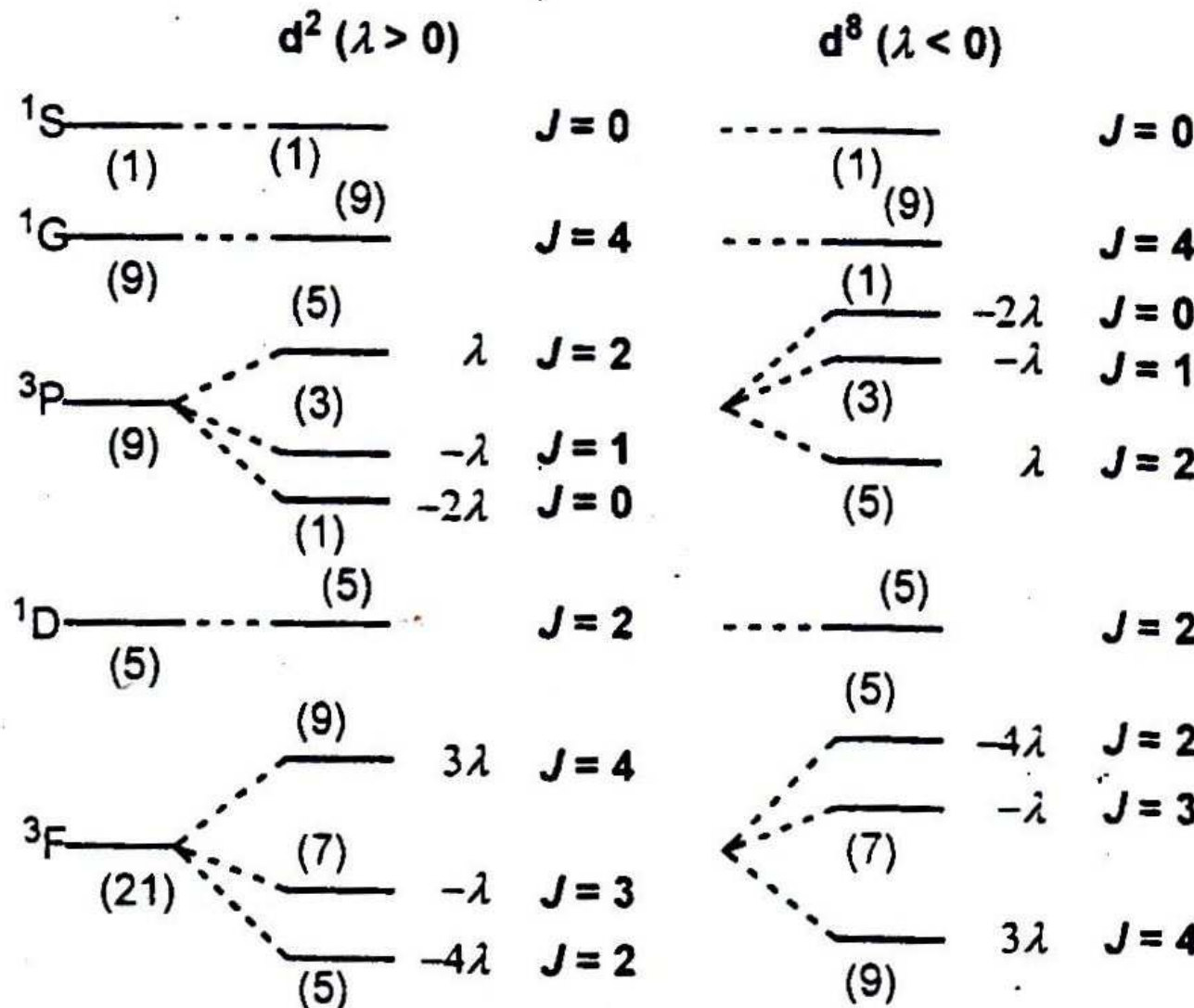
<i>Ion</i>	<i>dⁿ</i>	<i>Ground state</i>	λ (cm^{-1})	<i>Ion</i>	<i>dⁿ</i>	<i>Ground state</i>	λ (cm^{-1})
Ti ³⁺	d ¹	² D	154	Mn ³⁺	d ⁴	⁵ D	85
V ³⁺	d ²	³ F	104	Fe ²⁺	d ⁶	⁵ D	-100
V ²⁺	d ³	⁴ F	55	Co ²⁺	d ⁷	⁴ F	-180
Cr ³⁺	d ³	⁴ F	87	Ni ²⁺	d ⁸	³ F	-335
Cr ²⁺	d ⁴	⁵ D	57	Cu ²⁺	d ⁹	² D	-852

Notice:

- less than $\frac{1}{2}$ filled – positive values; more than $\frac{1}{2}$ filled – negative values
- no data for an A term (d^5 , d^{10}) – there is no orbital moment to couple with the spin moment

Splitting of the terms from d^2 and d^8 configurations by spin-orbit coupling (multiplicities in parentheses)

Free ion terms



Reminder: multiplet interval $E_{J+1} - E_J = (J + 1)\lambda$

12

Free ion term energies

Racah parameters A,B,C

Slater-Condon parameters F

THE FREE ION TERM ENERGIES FOR d^2 AND d^3 CONFIGURATIONS¹

(See Table 7.2 for values of B and C . Data for other d^n configurations may be obtained from ref. 1, p. 86)

d^2	3F	$A - 8B$	$F_0 - 8F_2 - 9F_4$
	3P	$A + 7B$	$F_0 + 7F_2 - 84F_4$
	1G	$A + 4B + 2C$	$F_0 + 4F_2 + F_4$
	1D	$A - 3B + 2C$	$F_0 - 3F_2 + 36F_4$
	1S	$A + 14B + 7C$	$F_0 + 14F_2 + 224F_4$
d^3	4F	$3A - 15B$	$3F_0 - 15F_2 - 72F_4$
	4P	$3A$	$3F_0 - 147F_4$
	$^2H, ^2P$	$3A - 6B + 3C$	$3F_0 - 6F_2 - 12F_4$
	2G	$3A - 11B + 3C$	$3F_0 - 11F_2 + 13F_4$
	2F	$3A + 9B + 3C$	$3F_0 + 9F_2 - 87F_4$
	2D	$3A + 5B + 5C \pm (193B^2 + 8BC + 4C^2)^{\frac{1}{2}}$	$3F_0 + 5F_2 + 3F_4 \pm (193F_2^2 + 8325F_4^2 - 1650F_2F_4)^{\frac{1}{2}}$

Racah parameter B : measure of the interelectronic repulsion;
differs in free (highest value) and in bonded ions (lower value)

Free ion values of B – influence of size, charge

FREE ION VALUES OF B AND C , ACCORDING TO ELECTRON CONFIGURATION,
FOR GASEOUS IONS^{1,6}

	<i>Ion</i>	<i>B</i>	<i>C</i>		<i>Ion</i>	<i>B</i>	<i>C</i>
$3d^2$	Ti ²⁺	718	2629	$4d^3$	Mo ³⁺	610	
	V ³⁺	861	4165 3814		Rh ³⁺	720	
	Cr ⁴⁺	1039	4238		Rh ²⁺	620	4002
$3d^3$	Sc ⁺	480		$4d^8$	Pd ²⁺	683	2620
	V ²⁺	766	2855	$5d^2$	Os ⁶⁺	780	
	Cr ³⁺	918	3850	$5d^3$	Re ⁴⁺	650	
	Mn ⁴⁺	1064			Ir ⁶⁺	810	
$3d^4$	Cr ²⁺	830	3430	$5d^4$	Os ⁴⁺	700	
	Mn ³⁺	1140	3675	$5d^6$	Ir ³⁺	660	
$3d^5$	Mn ²⁺	960	3325		Pt ⁴⁺	720	
$3d^6$	Fe ²⁺	1058	3901	$5d^8$	Pt ²⁺	600	
	Co ³⁺	1100					
$3d^7$	Co ²⁺	971	4366				
$3d^8$	Ni ²⁺	1041	4831				

Gaseous state: $C \sim 4B$

Interelectronic repulsion is higher in smaller ions (cf. Ni²⁺ and Pt²⁺)
and in less charged ions (cf. Mn²⁺, Mn³⁺ and Mn⁴⁺)



Splitting by O_h field: D terms

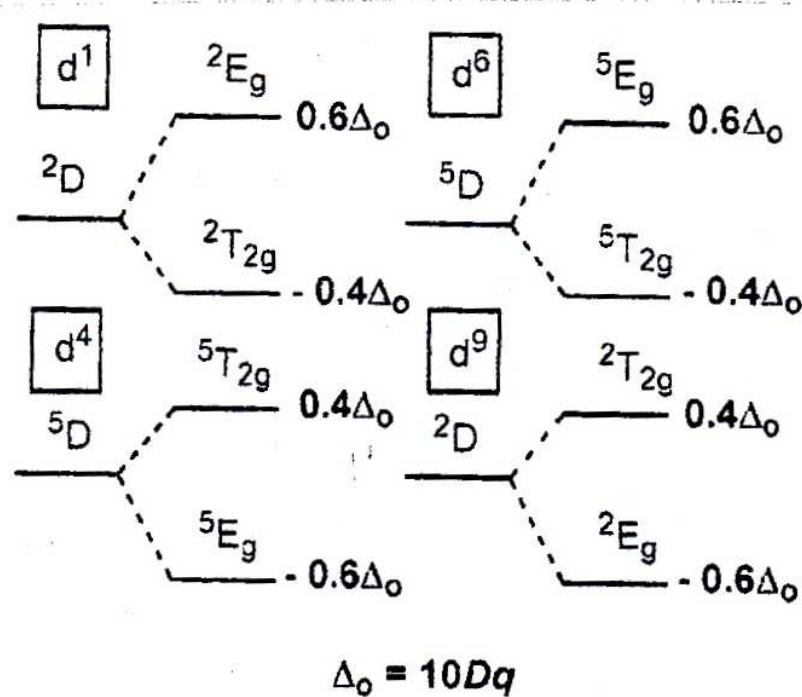
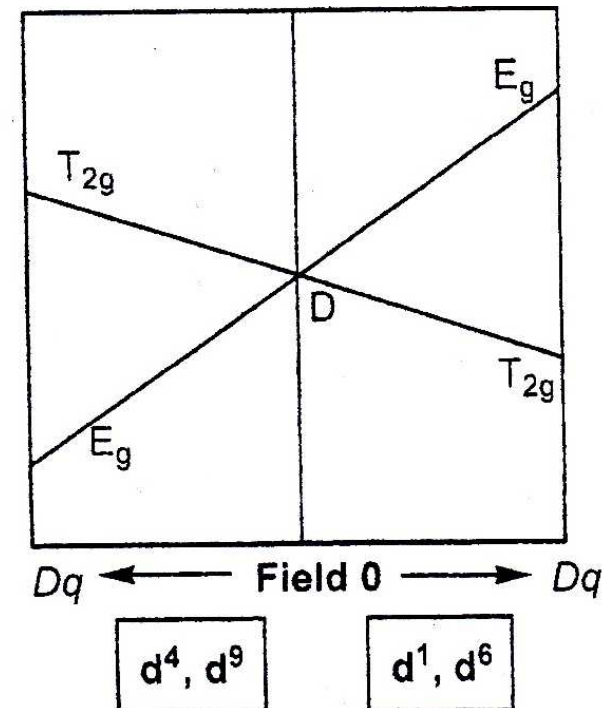


Figure 8.5 The effect of an octahedral crystal field on the D terms of d^1 , d^5 , d^4 and d^9 configurations. The energy of each term is given on the right-hand side.

Reminder – ground terms of the non-split states

d^1, d^9	2D
d^2, d^8	3F
d^3, d^7	4F
d^4, d^6	5D
d^5	6S



Orgel diagram

Splitting by O_h field: F terms

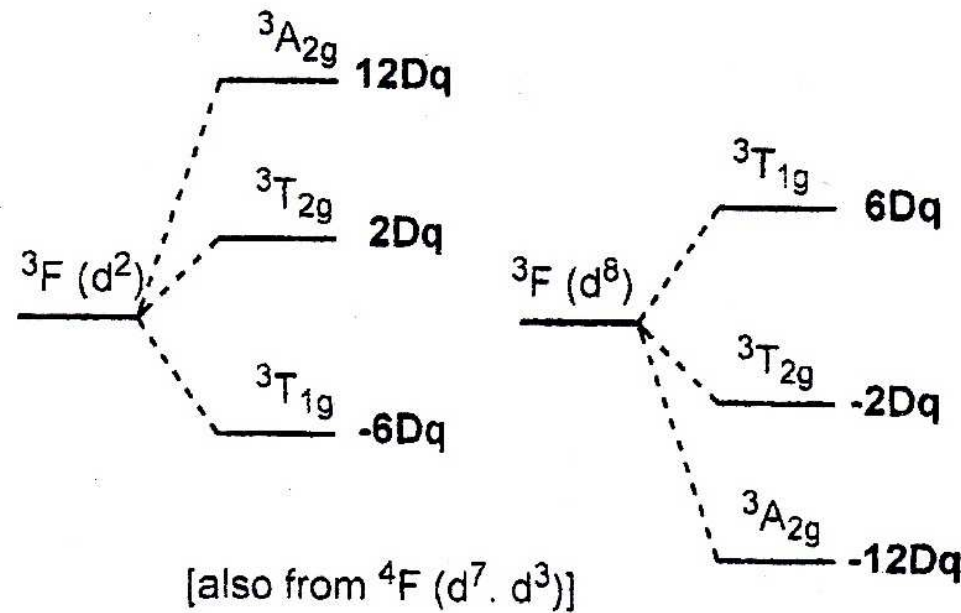


Figure 8.6 The effect of an octahedral crystal field on the 3F term of d^2 and d^8 configuration. The energy of each term is given on the right-hand side.

Differences between the energy levels: 10 Dq, 8 Dq.

Reminder – ground terms of non-split states	
d^1, d^9	2D
d^2, d^8	3F
d^3, d^7	4F
d^4, d^6	5D
d^5	6S

For these configurations, one more energy level of the same spin multiplicity is present: 3P (or 4P).

This needs to be taken into account (next slide).

Two energy states of the same symmetry: T_{1g} (*F*) and T_{1g} (*P*)

T_{1g} states perturbation: repulsion. Non-linear dependence on Dq (field strength)

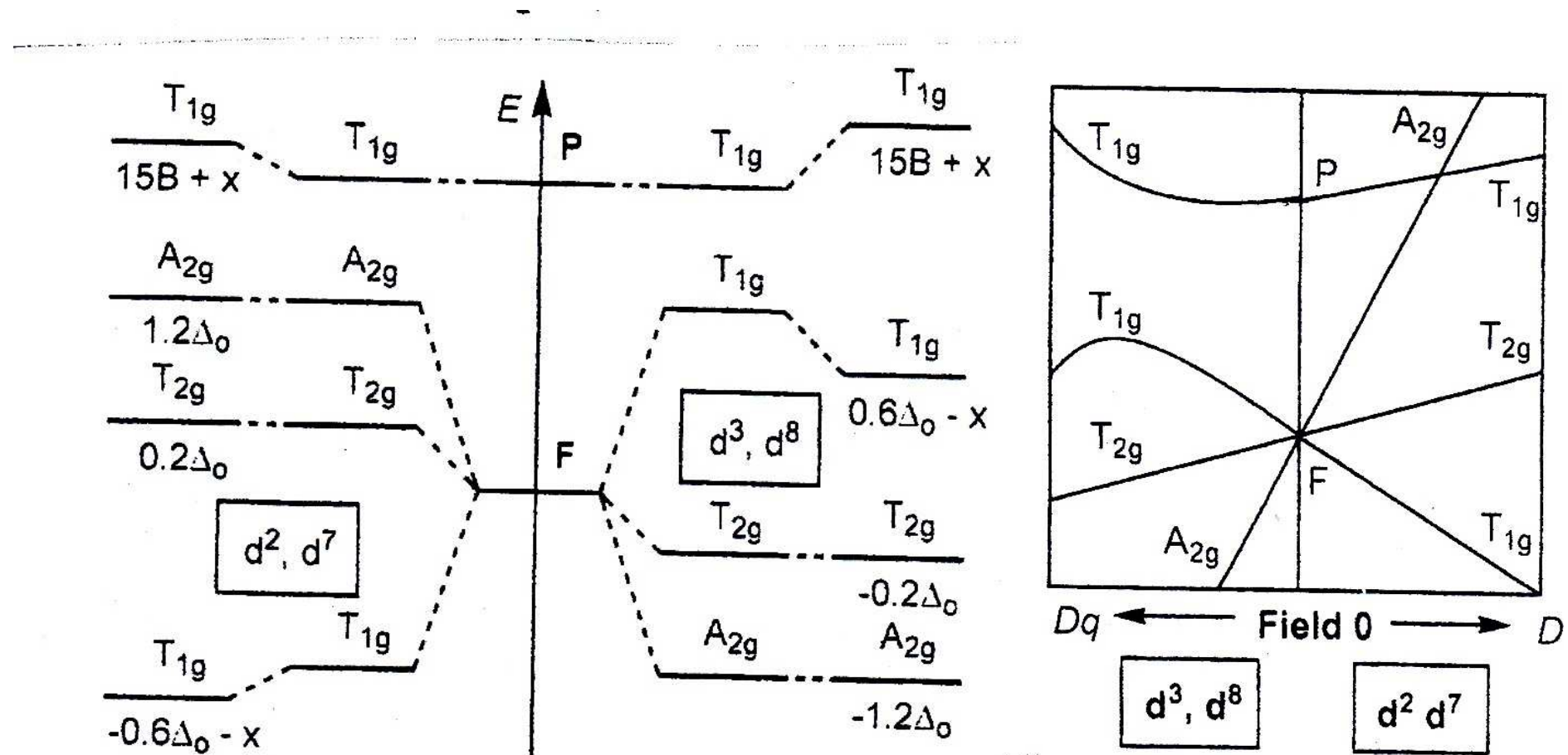


Figure 8.7 Energy diagram for the d^2 , d^7 , d^3 and d^8 configurations, assuming a weak field. Note the interaction between the T_{1g} terms derived from *F* and *P* free-ion terms.

Orgel diagram

Energy of the terms arising from d^2 (d^7) and d^3 (d^8) configuration

d^2 or d^7	Energy	Energy difference (ground state = 0)
$T_{1g}(F)$	$7.5B - 3Dq - 0.5F$	0
T_{2g}	$2Dq$	$-7.5B + 5Dq + 0.5F$
$T_{1g}(P)$	$7.5B - 3Dq + 0.5F$	F
A_{2g}	$12Dq$	$-7.5B + 15Dq + 0.5F$

10 Dq from energy difference between the 1st and the 3rd band energies:

$$T_{1g}(F) \rightarrow T_{2g}$$

$$T_{1g}(F) \rightarrow A_{2g}$$

$$F = [225B^2 + 180BDq + Dq^2]^{1/2}$$

d^3 or d^8	Energy	Energy difference (ground state = 0)
A_{2g}	$-12Dq$	0
T_{2g}	$-2Dq$	$10Dq$
$T_{1g}(F)$	$7.5B + 3Dq - 0.5G$	$7.5B + 15Dq - 0.5G$
$T_{1g}(P)$	$7.5B + 3Dq + 0.5G$	$7.5B + 15Dq + 0.5G$

10 Dq directly from the 1st band energy:
 $A_{2g} \rightarrow T_{2g}$

$$G = [225B^2 - 180BDq + Dq^2]^{1/2}$$

Racah parameter B values – experimental determination

From electronic spectra (more bands needed, e.g. F ground terms)

Values B' in complexes are always smaller than B in free ions = reduced interelectronic repulsion = metal d electrons become in some extent delocalized from the metal atom out onto the ligands = covalency => NEPHELAUXETIC EFFECT (“nephelauxetic” means “cloud expanding” in Greek)

$$\text{Nephelauxetic parameter } \beta = \frac{B'}{B} \quad \beta < 1$$

Practical importance:

Tanabe Sugano diagrams, plots E/B , vs. Δ/B ,

Nephelauxetic series of ligands, decreasing β (increasing metal – ligand covalency)
 $F^- > H_2O > NH_3 > C_2O_4^{2-}, NH_2CH_2CH_2NH_2 > Cl^- > CN^- > Br^- > I^-$

Example: Determination of Δ_{oct} and B' from spectroscopic data

The octahedrally hydrated Ni^{2+} ions has a near-IR absorption at 8700 cm^{-1} and two absorption in the visible region at $14\ 500 \text{ cm}^{-1}$ and at $25\ 300 \text{ cm}^{-1}$. Calculate Δ_{oct} , B' and β for this complex.

Solution:

Ni^{2+} ion has d^8 configuration, ground term ${}^3A_{2g}$, excited terms of the same multiplicity ${}^3T_{2g}$, ${}^3T_{1g}(F)$, ${}^3T_{1g}(P)$

Energy of the bands (slide 18):

$$\text{1st transition} \quad \Delta_{\text{oct}} \quad (\text{eq.1})$$

$$\text{2nd transition} \quad 7.5B' + 1.5 \Delta_{\text{oct}} - 0.5 G \quad (\text{eq.2})$$

$$\text{3rd transition} \quad 7.5B' + 1.5 \Delta_{\text{oct}} + 0.5 G \quad (\text{eq.3})$$

$$\Delta_{\text{oct}} = 8700 \text{ cm}^{-1} \text{ (from eq.1)}$$

$$B' = 900 \text{ (combined eq.2 and eq.3)}$$

$$B = 1041 \text{ (for the free ion, slide 14)}$$

$$\beta = \frac{B'}{B} = 0.86$$

For exam:

- explain origin of the terms
- derive the ground term for a given configuration
- explain splitting of the terms (not to draw the graphs!) and origin of the perturbation
- use energy equations for determination of Dq (Δ), Racah parameter B
- explain meaning of the Racah parameter B

Uveřejněné materiály jsou určeny studentům Vysoké školy chemicko-technologické v Praze jako studijní materiál. Některá textová i obrazová data v nich obsažená jsou převzata z veřejných zdrojů. V případě nedostatečných citací nebylo cílem autorky záměrně poškodit autora/y původního díla.

S případnými výhradami se prosím obracejte na autorku tohoto výukového materiálu, aby bylo možno zjednat nápravu.



The published materials are intended for students of the University of Chemistry and Technology, Prague as a study material. Some text and image data contained therein are taken from public sources. In the case of insufficient quotations, the author's intention was not to intentionally infringe the possible author(s) rights to the original work.

If you have any reservations, please contact the author(s) of the specific teaching material in order to remedy the situation.

Magnetic properties

Spin-only magnetism

Spin-orbital interaction

Molecular magnets

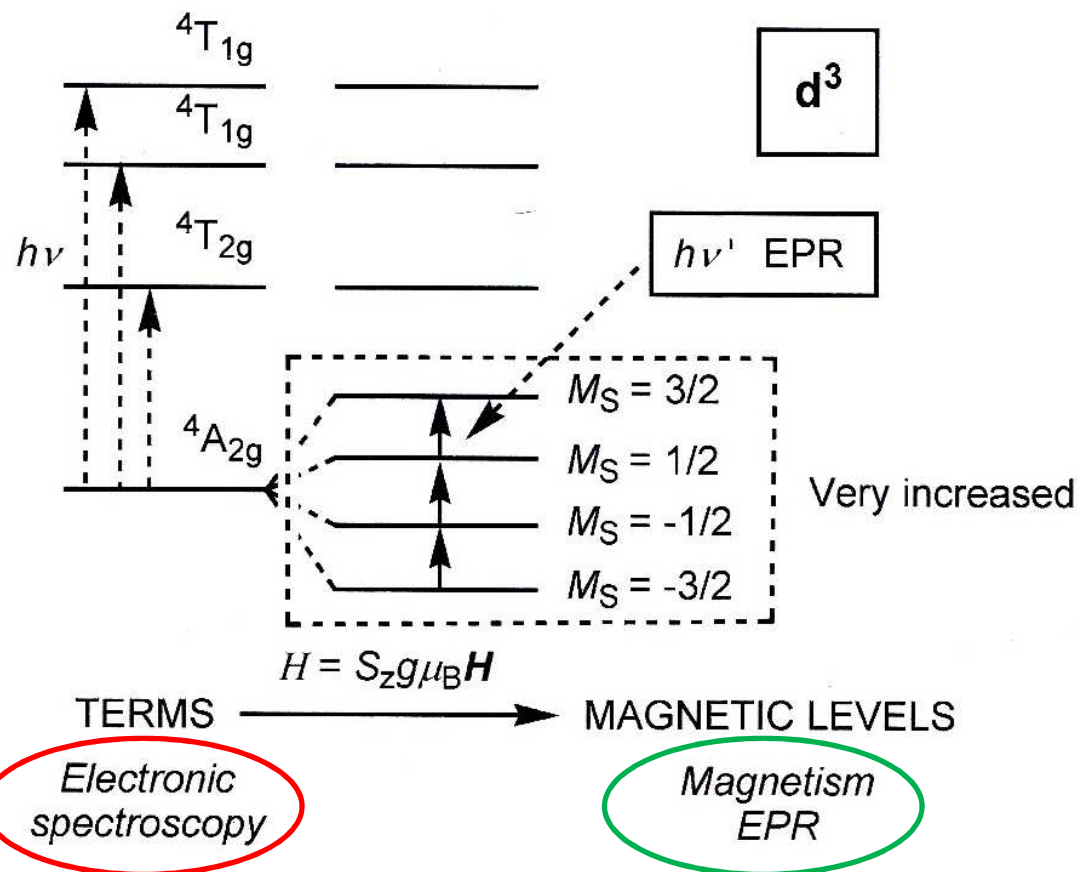
EPR spectroscopy



EUROPEAN UNION
European Structural and Investing Funds
Operational Programme Research,
Development and Education

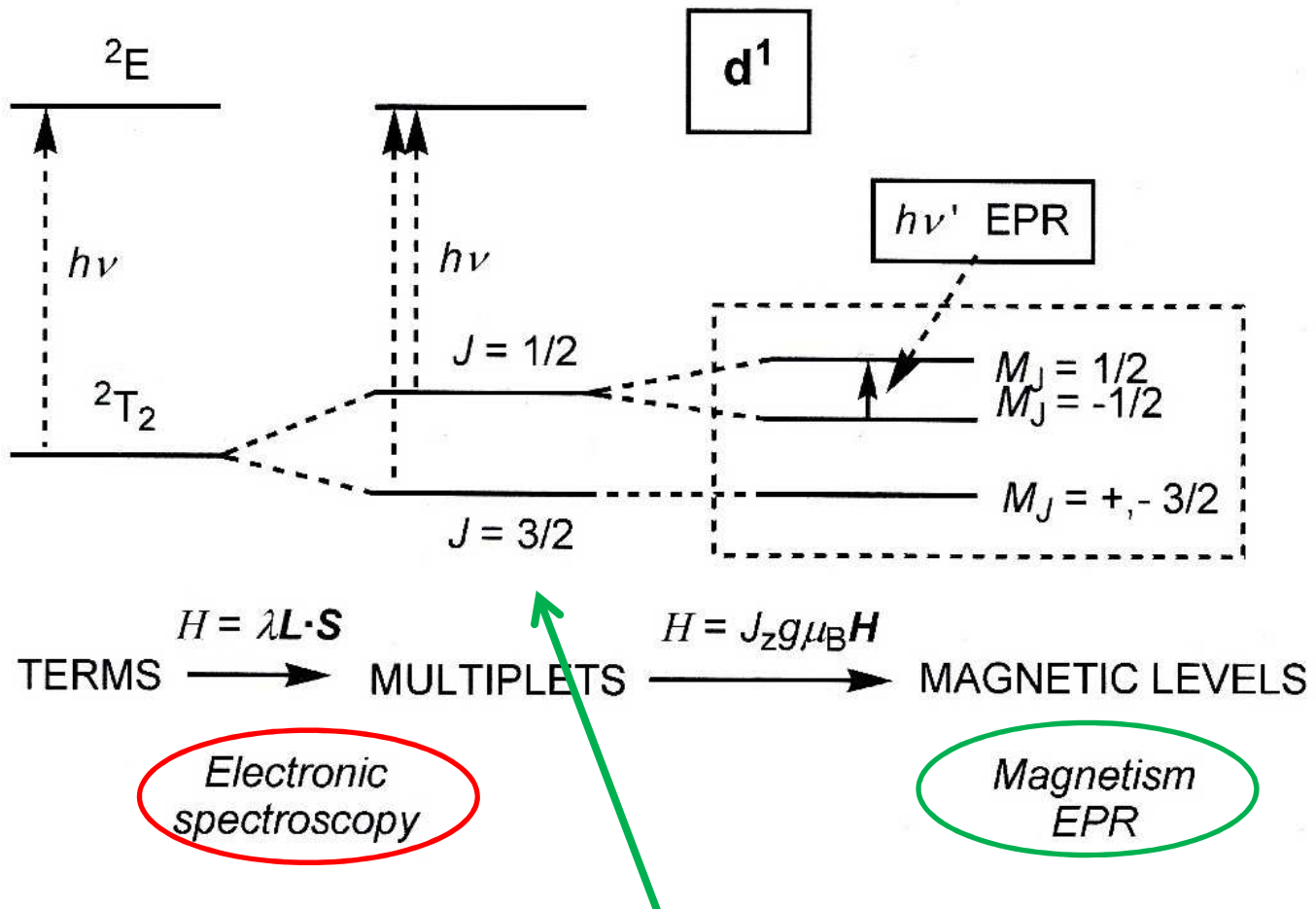


Splitting of selected ground terms: ${}^4A_{2g}$



cubic symmetry

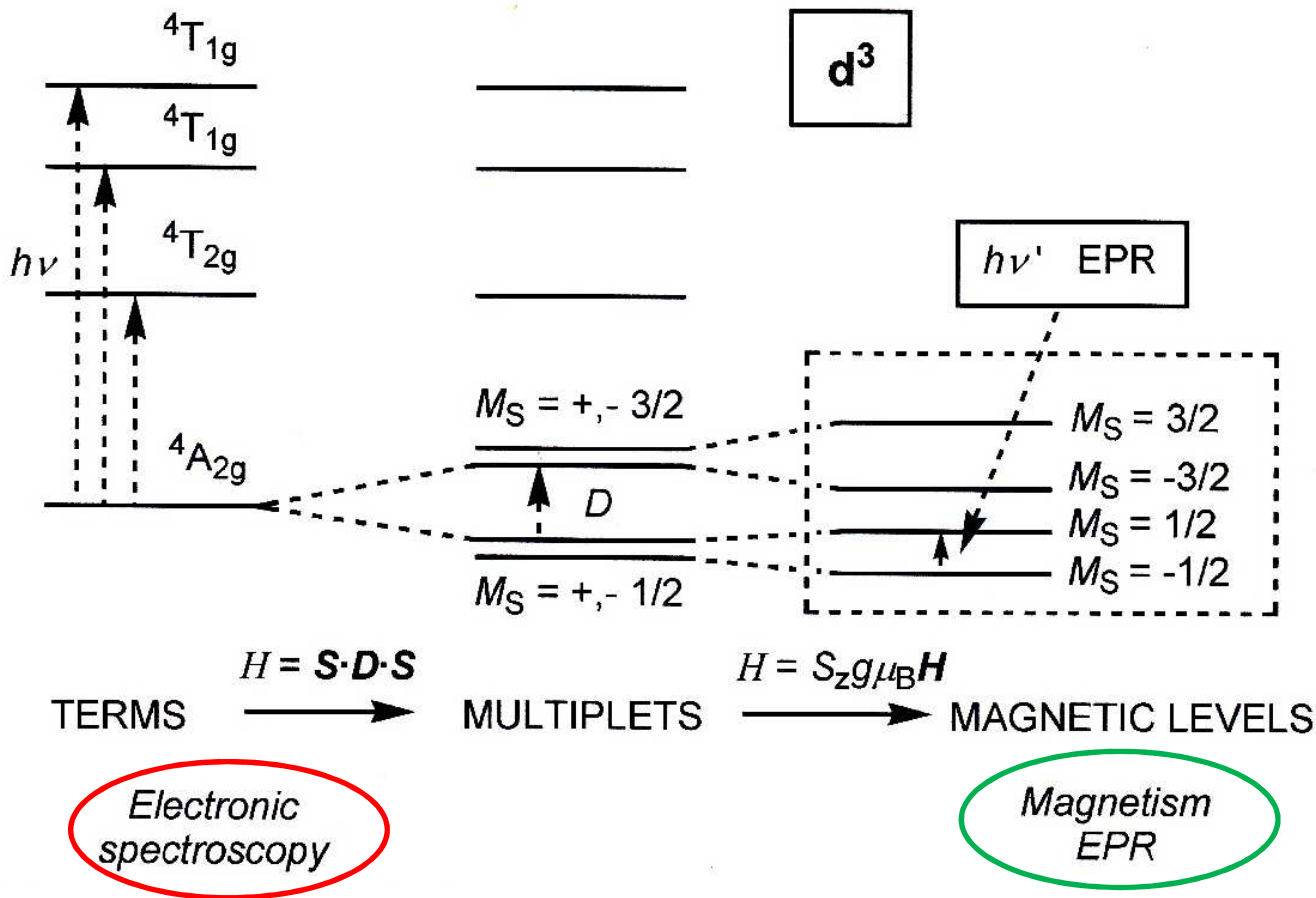
Splitting of selected ground terms: 2T_2



The first-order spin – orbit coupling is present

The multiplet with $J = 3/2$ is not split by the magnetic field in this case

Splitting of selected ground terms: ${}^4A_{2g}$ with both distortion and second – order spin – orbit coupling



Splitting of a ${}^4A_{2g}$ term with both distortion and second-order spin–orbit coupling

Magnetic properties

Magnetic moment - given by number of unpaired electrons n , spin number S :

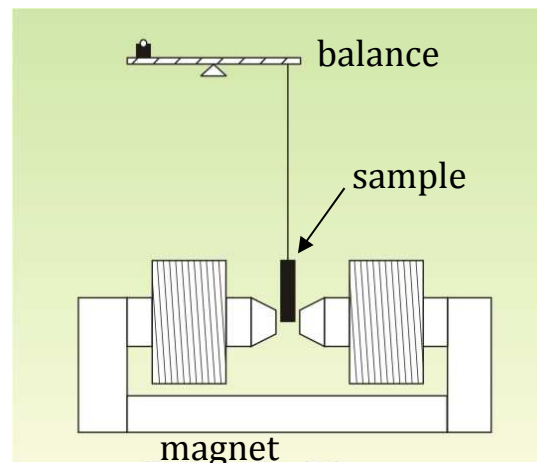
Spin-only value: $\mu_s = 2\sqrt{S(S+1)} = \sqrt{n(n+2)}$

unit: B.M.
(Bohr magneton)

- Experimental : attraction of the sample into magnetic field (Gouy balance) paramagnetic sample repulsion – diamagnetic sample
- Spin state determination:

highspin Co^{2+} : $n = 3$, $\mu_s \sim 3,9 \text{ BM}$

lowspin Co^{2+} : $n = 1$, $\mu_s \sim 1,7 \text{ BM}$



Mn^{2+}	Fe^{2+}	Co^{2+}	Ni^{2+}	Cu^{2+}	Zn^{2+}
$\mu_s \text{ [B.M.]}$	5,92	4,90	3,88	2,83	1,73
					0

Magnetic properties

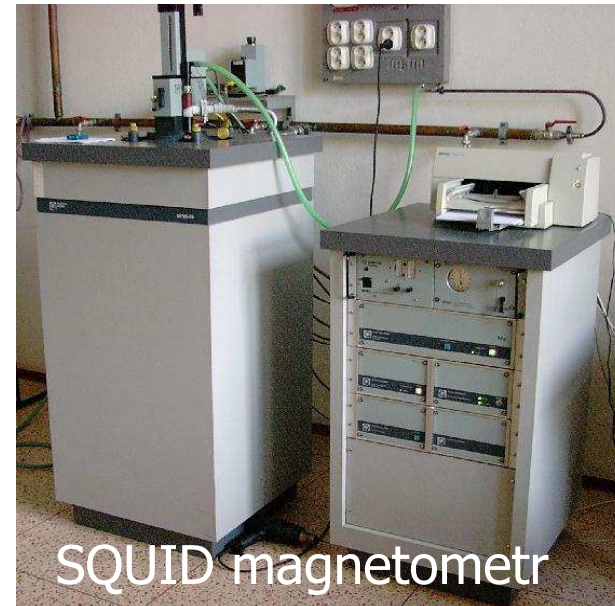
magnetisation

magnetic susceptibility χ ,

magnetic moment μ at given temperature

$$\chi_M = \frac{N_A \cdot \mu^2}{3kT} = \frac{C}{T}$$

$$\chi = \frac{M}{H} \quad \chi_M = \frac{\chi \cdot M_w}{\rho}$$



SQUID magnetometr

Magnetic moment μ at a given temperature is compared with a theoretical value. Result:

- number of unpaired electrons
oxidation state, HS or LS configuration, geometry

Theoretical value of the spin-only magnetic moment:

$$\mu = 2\sqrt{S(S+1)} = \sqrt{n(n+2)}$$

Heavier metals (4d, 5d, lanthanoids, actinoids) complicated magnetic behaviour due to spin-orbital coupling

$$\mu = \sqrt{4S(S+1) + L(L+1)}$$

or

$$\mu = g_J \sqrt{J(J+1)}$$

Magnetic properties

Spin-only magnetic moment, $3d$ ions; deviation: spin-orbital coupling (terms $L \neq 0$)

μ_s [B.M.]		Unpaired electrons	Calculated μ_s [B.M.]	Experimental	
Ti ³⁺	1		1.73	1.73	
V ⁴⁺	1			1.68–1.78	
Cu ²⁺	1			1.70–2.20	d ⁹ , Jahn-Teller
V ³⁺	2		2.83	2.75–2.85	
Ni ²⁺	2			2.8–3.5	
V ²⁺	3		3.87	3.80–3.90	⁴ A
Cr ³⁺	3			3.70–3.90	⁴ A
Co ²⁺	3			4.3–5.0	⁴ T, orbital moment
Mn ⁴⁺	3			3.80–4.0	⁴ A
Cr ²⁺	4		4.90	4.75–4.90	
Fe ²⁺	4			5.1–5.7	
Mn ²⁺	5		5.92	5.65–6.10	⁶ A
Fe ³⁺	5			5.7–6.0	⁶ A

Problems

Magnetism – deviation from the spin-only behaviour

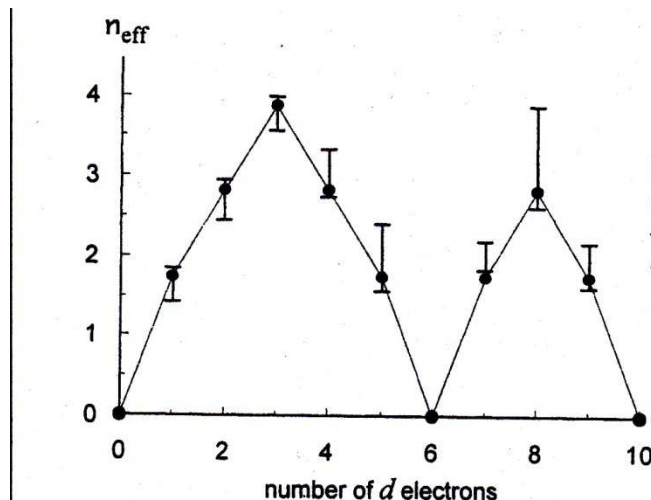
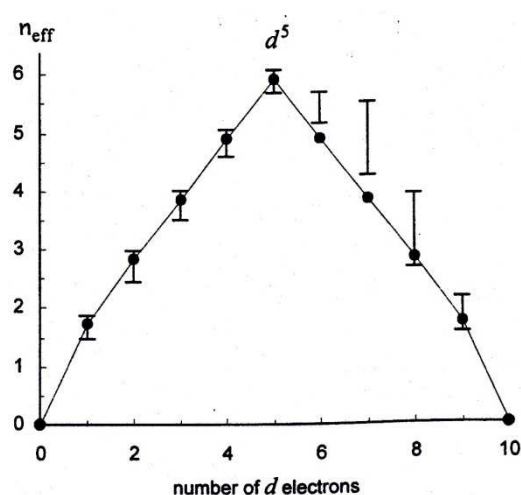
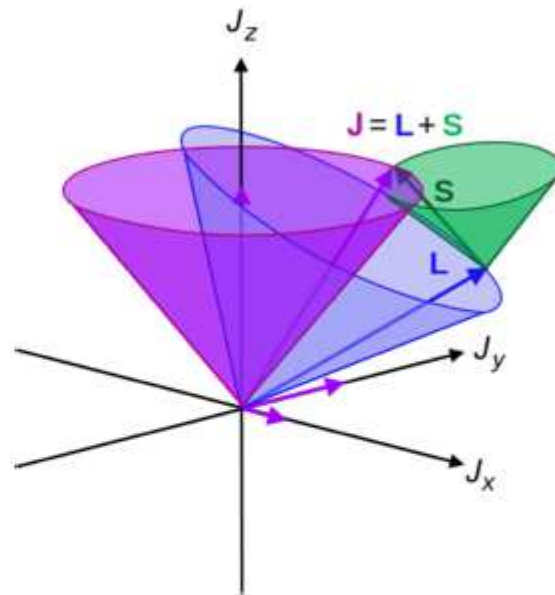
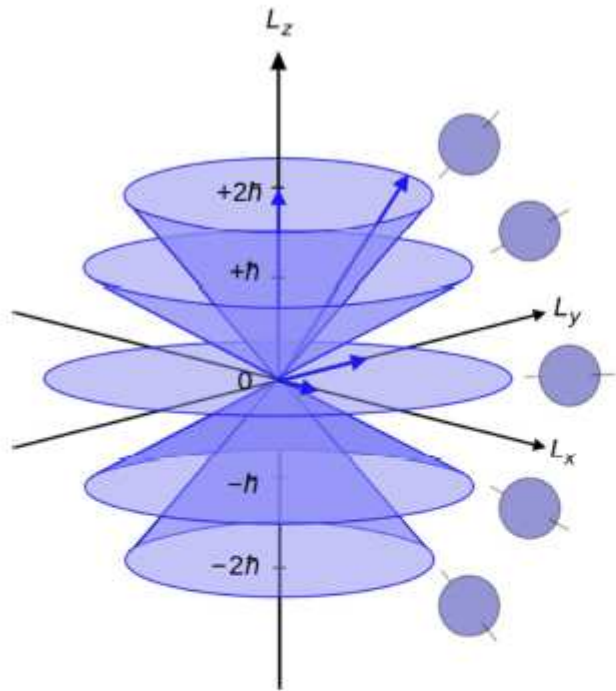


Fig. 5.10 n_{eff} data (300 K) for octahedral complexes of the first transition series, low spin in the case of d^4 – d^7 , compared with the predictions (●) of the spin-only formula. (Compare Fig. 5.1.)

Solution of the observed experimental behaviour:

- multielectronic system
- spin-orbital interaction

Spin – orbital coupling of the magnetic moments

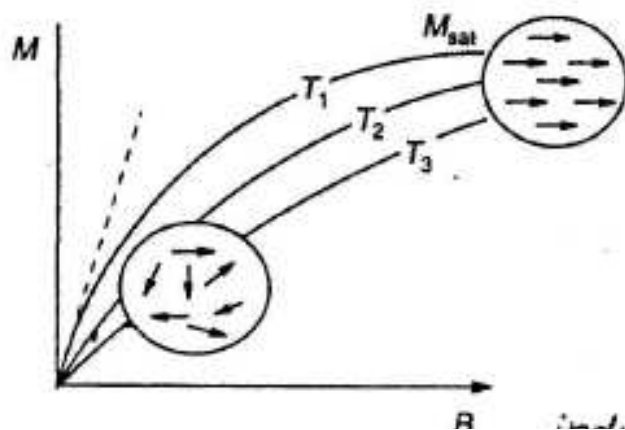


Orbital angular momentum (denoted **L** or \mathbf{L}).

Illustration of L-S coupling. Total angular momentum \mathbf{J} is purple, orbital \mathbf{L} is blue, and spin \mathbf{S} is green.

Magnetization M

„What happens inside the sample when a homogeneous magnetic field is applied.“



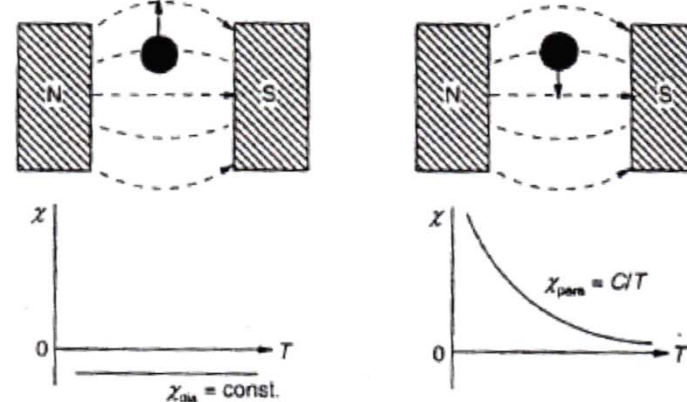
Magnetization curves for different temperatures, $T_1 < T_2 < T_3$; zone of the saturated magnetization

1. volume magnetization M [G] gauss
2. mass magnetization M_p : $M/\text{density}$ = [G cm³ g⁻¹]
3. molar magnetization M_m : [G cm³ mol⁻¹]

Magnetic susceptibility χ

$$\chi = \frac{\partial M}{\partial H} \quad H \text{ magnetic field}$$

under certain condition $\chi = M / H$



Basic behaviour in magnetic field:
diamagnetism paramagnetism

Experimental:

1. volume susceptibility χ : G/G (dimensionless)
2. mass susceptibility χ_ρ : [cm³ g⁻¹]
3. molar susceptibility χ_m : [cm³ mol⁻¹]

diamagnetism - core electrons, always present; positive, 1.10⁻⁶

paramagnetism – angular moment + electron spin, negative, 0 – 10⁻⁴

Molecular magnets

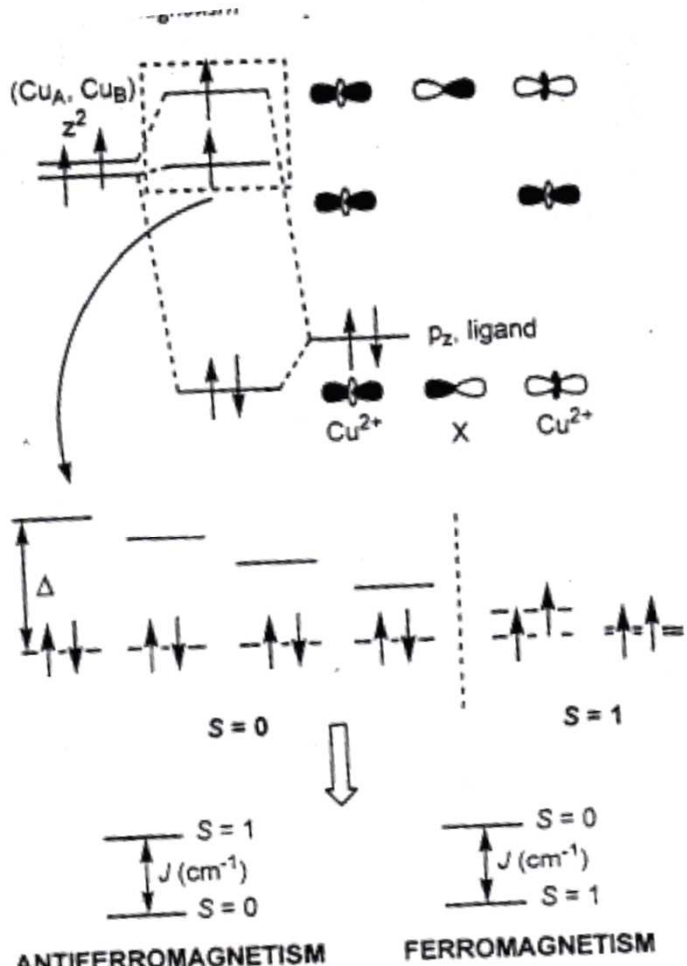


Figure 10.11 Relationship between the MOs of a $\text{Cu}^{2+}-\text{X}-\text{Cu}^{2+}$ system and the concepts of antiferro- and ferromagnetism (see text).

2 Cu ions cooperating magnetically,
antiferromagnetic or ferromagnetic possibility

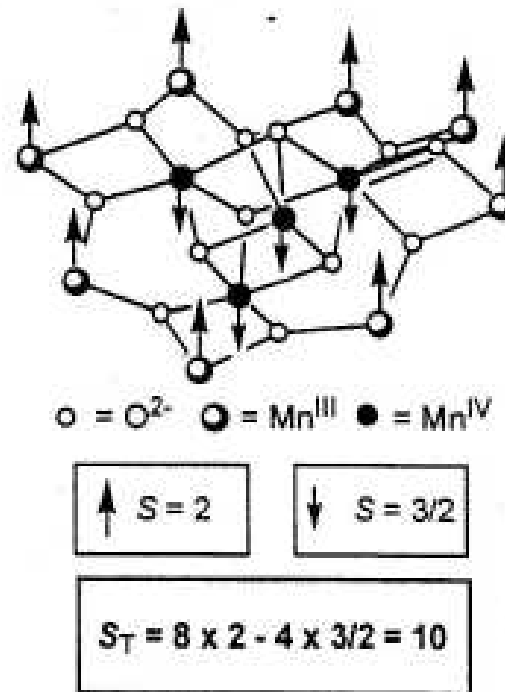


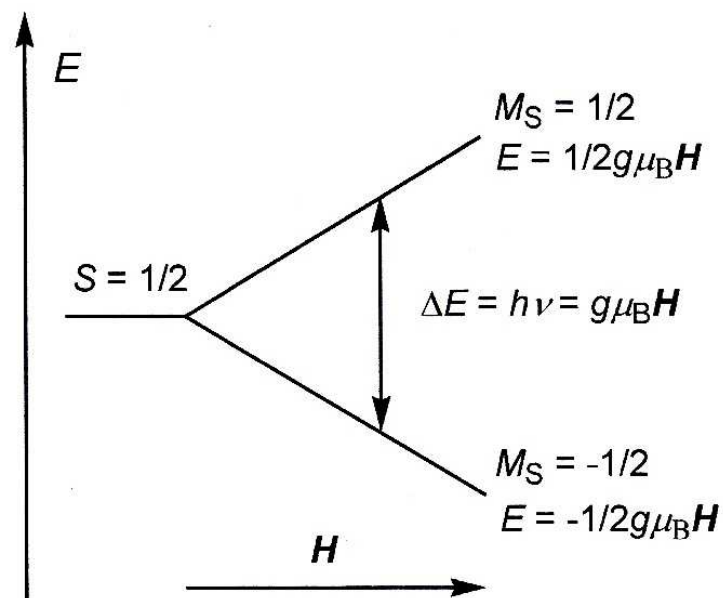
Figure 10.27 Schematic representation of $[\text{Mn}_{12}\text{Ac}]$ with the calculation of its S_T ground state.

12 Mn ions in two oxidation state:
ferrimagnetic arrangement

Electron paramagnetic resonance (EPR) in coordination compounds

Zeeman effect – when an external magnetic field (H) is applied to an isolated electron, the two M_S components of the $S = \frac{1}{2}$ are split and their population is not the same.

Boltzmann distribution: population is proportional to $e^{-E/kT}$, enhanced at low temperature

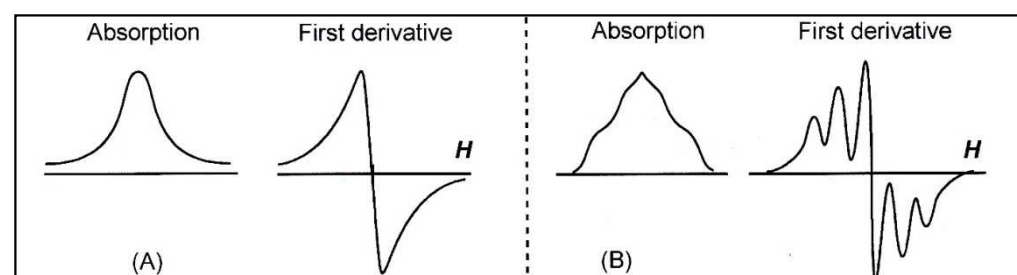


Splitting of the levels in magnetic field

EPR spectra measurement:
fixed frequency, varying magnetic field, resonance
Characteristic:
resonant field (and g)
number, relative intensity, spacing of the lines

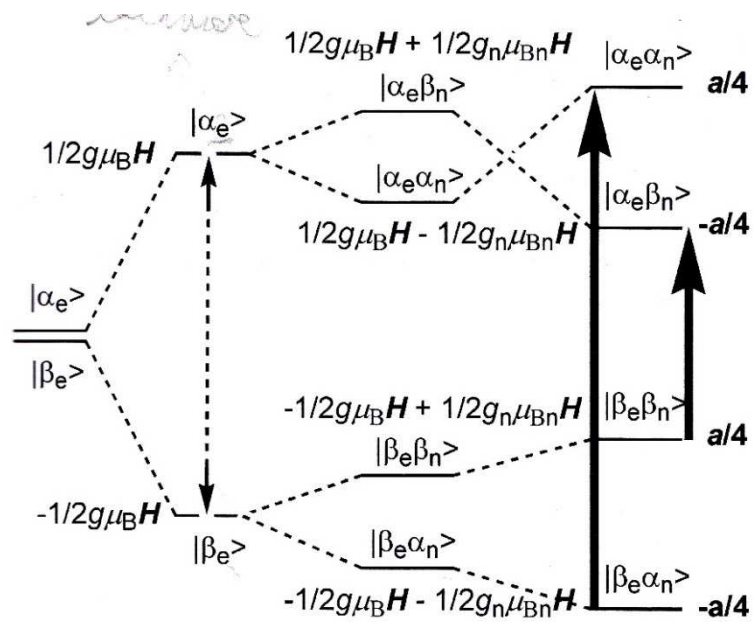
Free electron g value: $g_e = 2.0023193$
Experimental values show some deviation

1st derivative of the lines is recorded



Electron paramagnetic resonance – hydrogen atom

Origin of the hyperfine splitting
in a hydrogen atom:

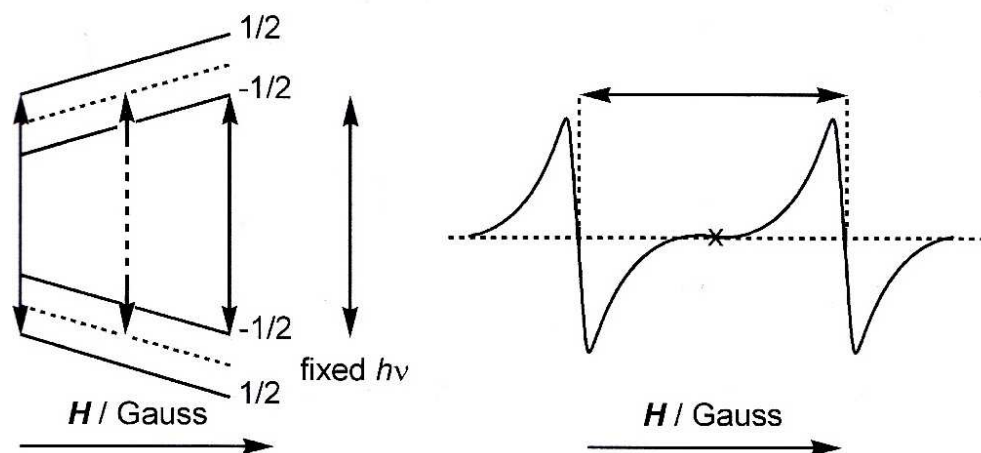


Spin: $\alpha = + \frac{1}{2}$; $\beta = - \frac{1}{2}$

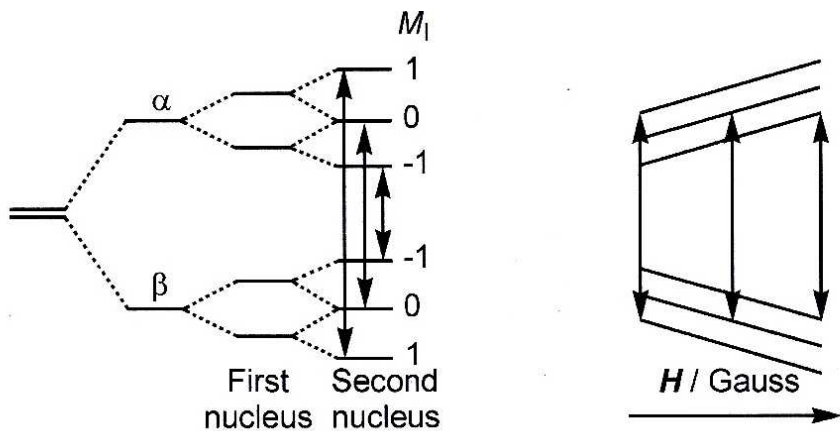
$S = \frac{1}{2}$; $I = \frac{1}{2}$

SELECTION RULES:
 $\Delta M_I = 0$; $\Delta M_S = \pm 1$

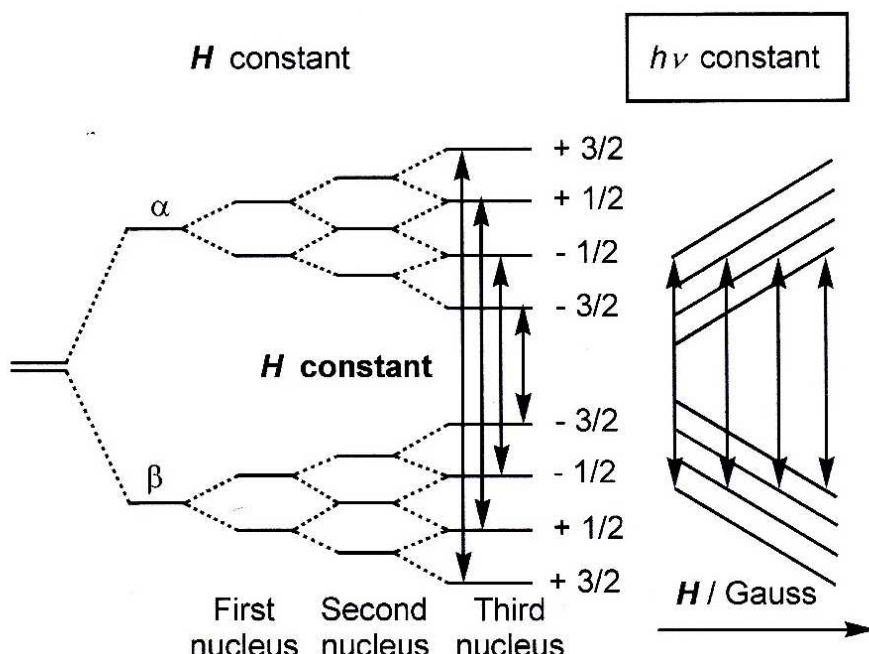
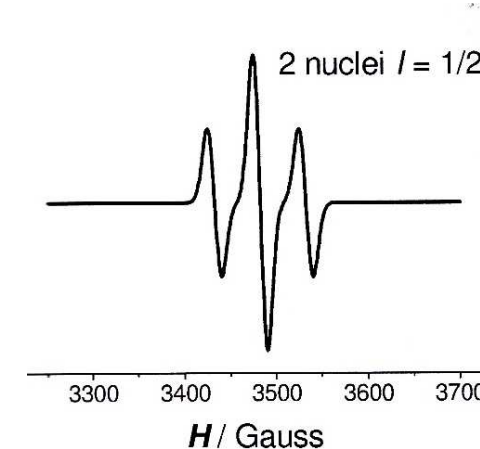
Energy scheme (at fixed frequency)
and simulated EPR spectrum for a
hydrogen atom



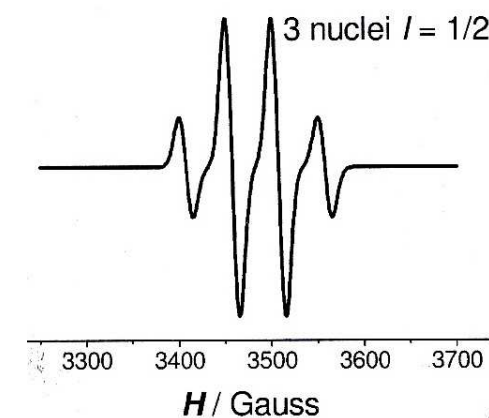
EPR – hyperfine coupling created by equivalent $I = \frac{1}{2}$ nuclei



2 nuclei
1:2:1



3 nuclei
1:3:3:1



Simulated spectra

EPR – hyperfine coupling by non-equivalent $I = \frac{1}{2}$ nuclei

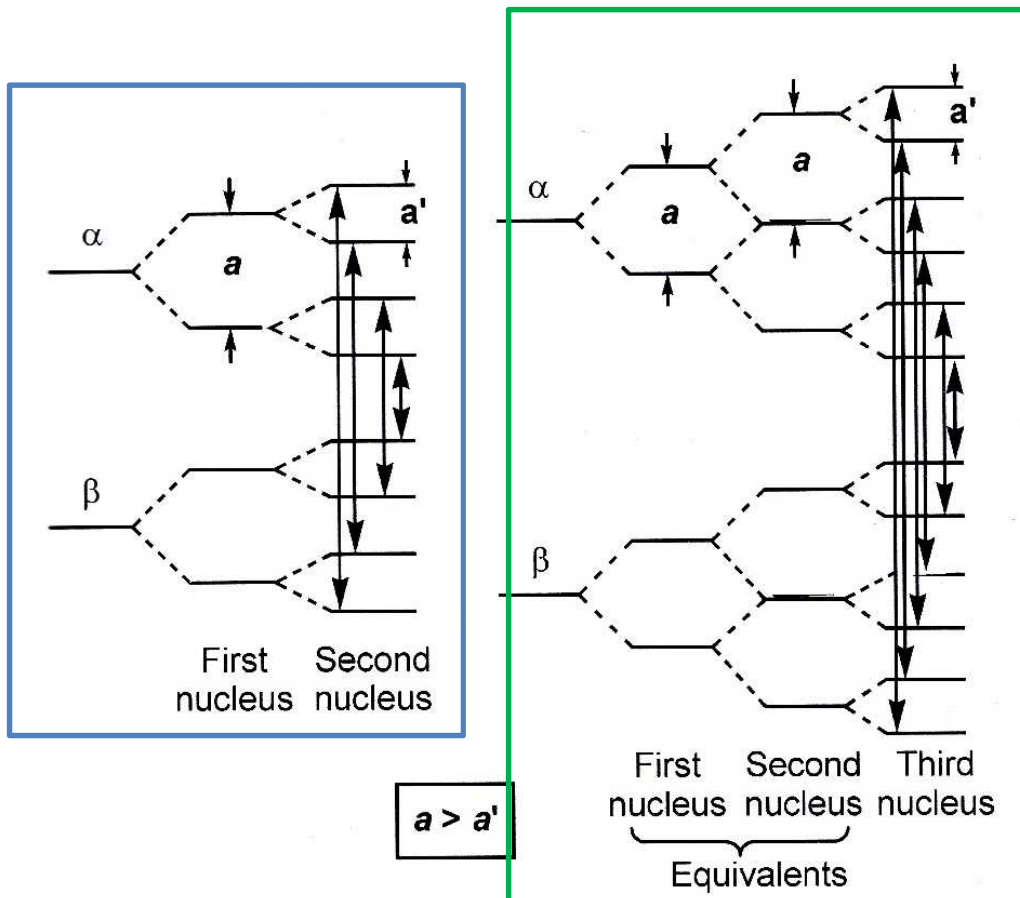
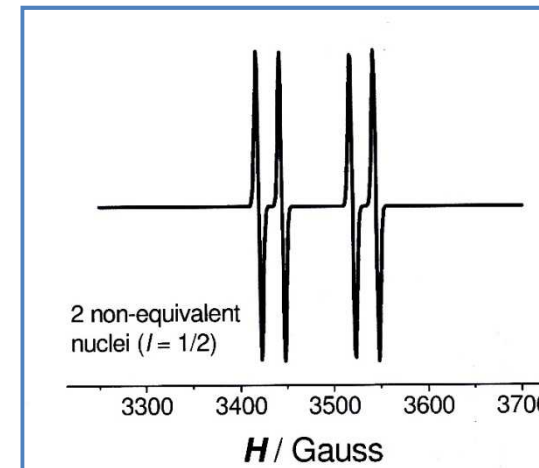
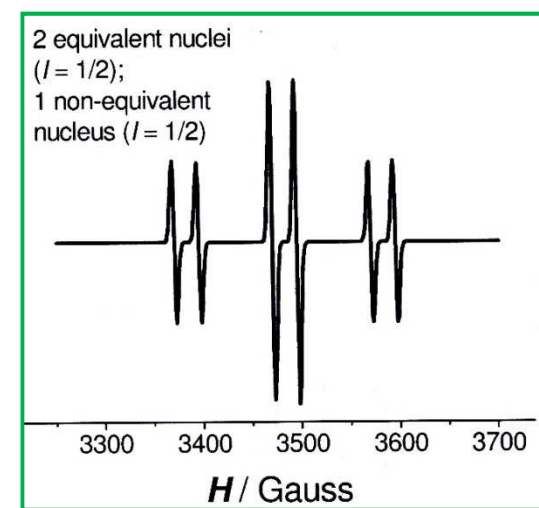


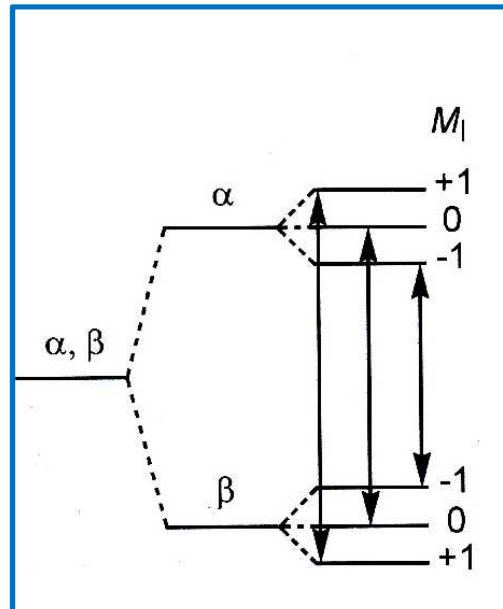
Figure 11.7 (A) Energy scheme for an electron coupled to 2 non-equivalent nuclei with $I = 1/2$, (B) energy scheme for an electron coupled to 2 equivalent and one non-equivalent nuclei with $I = 1/2$.



Simulated EPR spectra

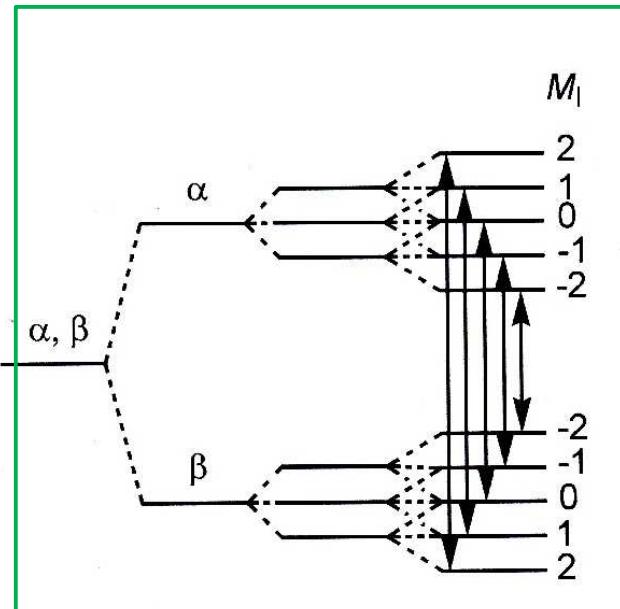


EPR – hyperfine coupling originated by nuclei with $I > \frac{1}{2}$



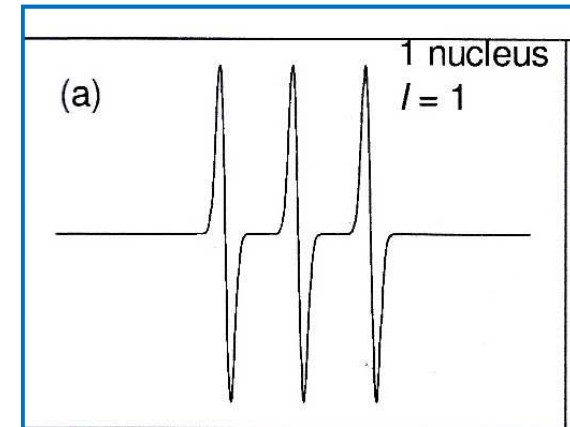
1:1:1

1 electron coupled to 1 nucleus,
 $I = 1$; intensities 1 : 1 : 1

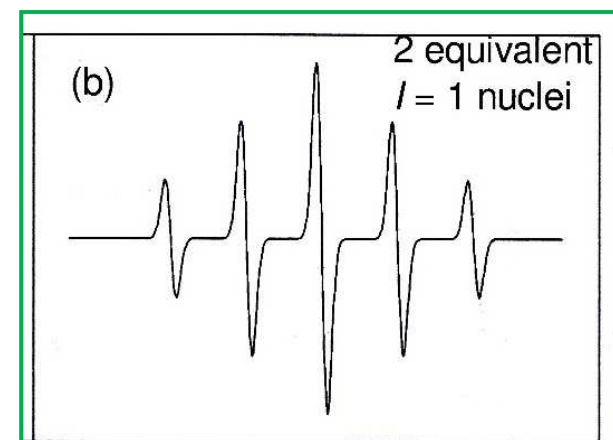


Intensities =
1 : 2 : 3 : 2 : 1

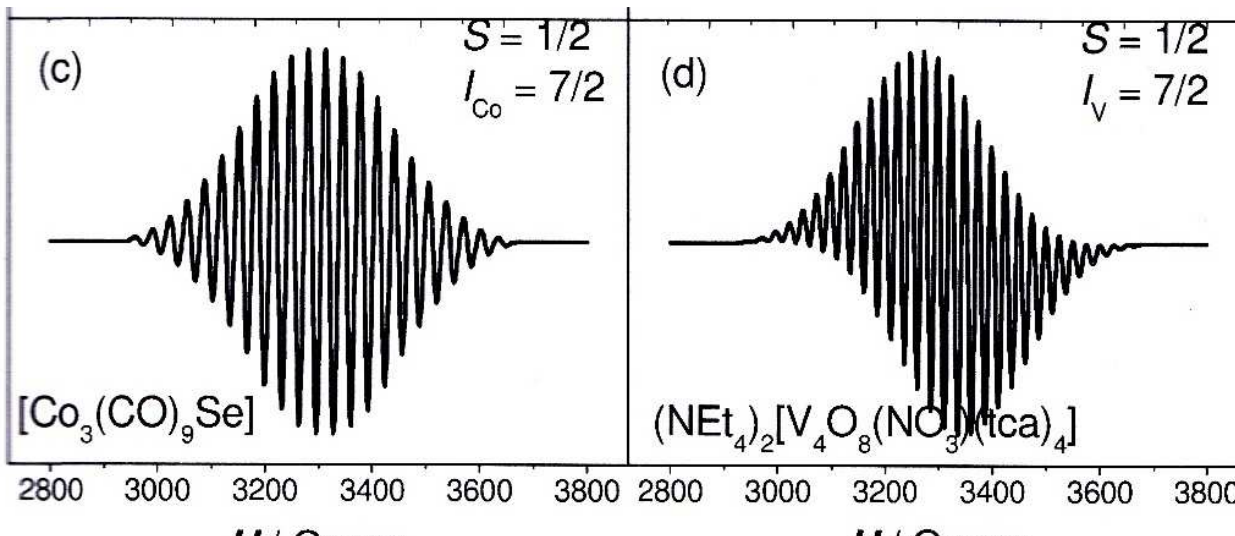
1 electron coupled to 2
equivalent nuclei, $I = 1$;
intensities 1 : 2 : 3 : 2 : 1



Simulated EPR spectra



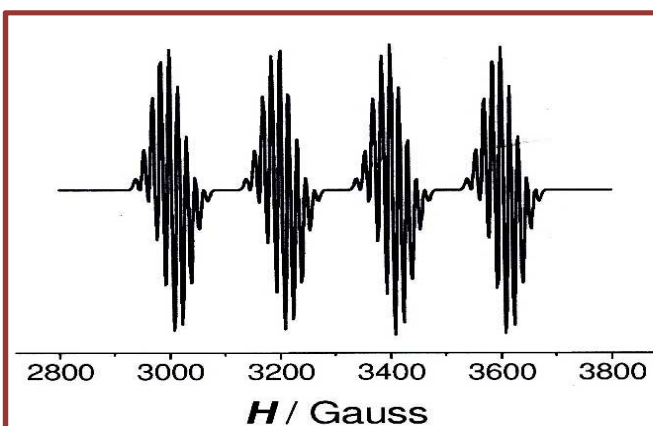
EPR – hyperfine coupling originated by nuclei with $I > \frac{1}{2}$



H / Gauss
Tetrahedron of 3 Co and 1 Se;
3 equivalent Co, $I = 7/2$;
 $2nl + 1 = 2 * 3 * 7/2 + 1 = 22$ signals

H / Gauss
Cluster from 3 V⁵⁺ (d^0) and 1 V⁴⁺ (d^1); 1 delocalized electron
 $2nl + 1 = 2 * 4 * 7/2 + 1 = 29$ signals

Hyperfine coupling = electron coupled to its own nucleus
Superhyperfine coupling = delocalization of the unpaired electron on the ligand nuclei



Cu²⁺ atom bonded to 4 equivalent nitrogens
quadruplet due to Cu (*hyperfine coupling*)
splitted into 9 signals due to 4 N (*superhyperfine coupling*)

EPR - isotropic polyelectronic system

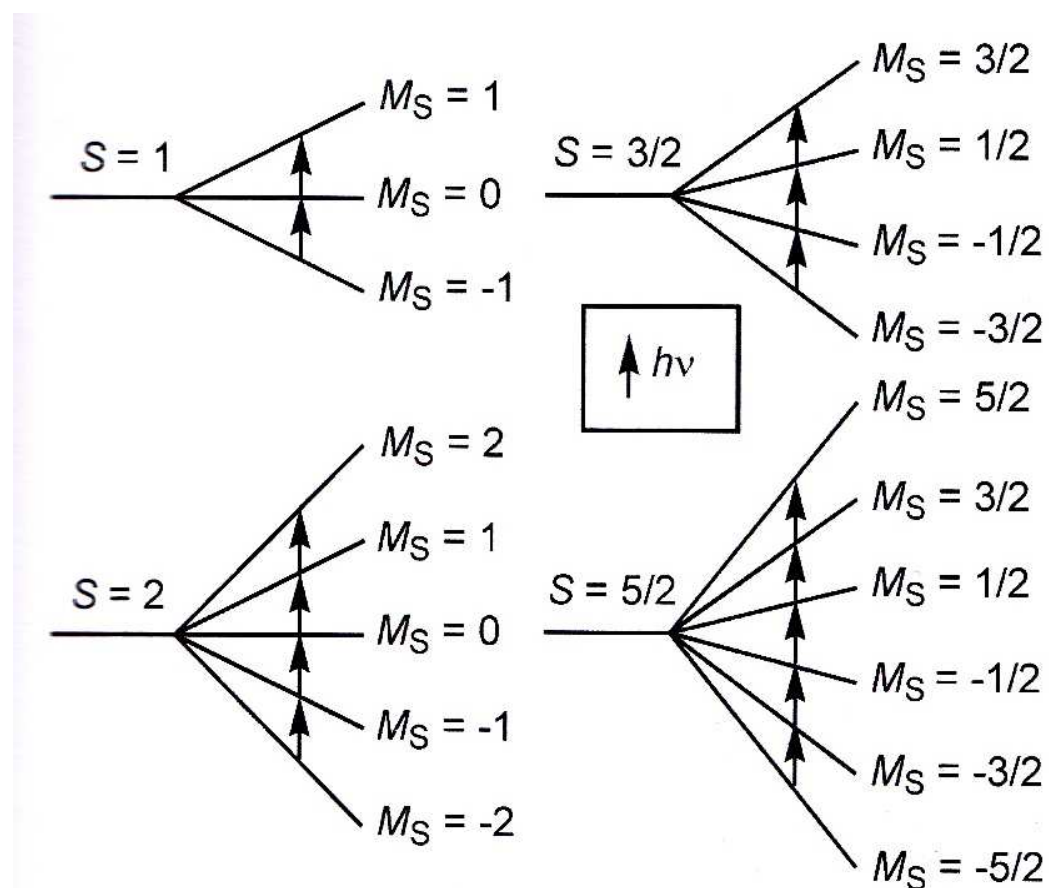
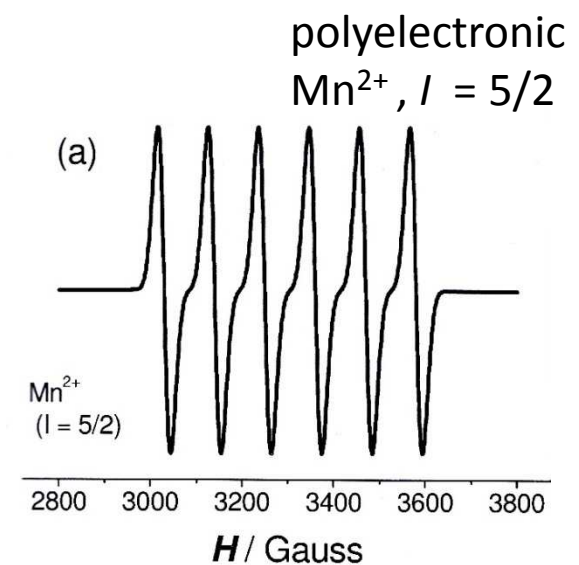
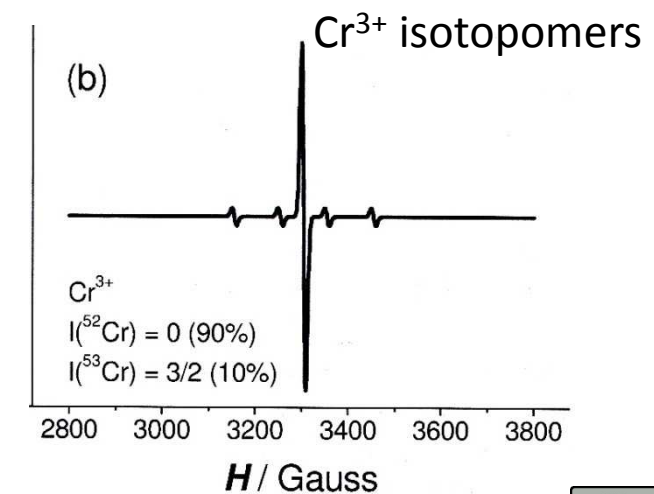


Figure 11.12 Splitting of the energy terms corresponding to $S = 1, 3/2, 2$, and $5/2$, assuming isotropic behavior.



Simulated EPR spectra



EPR - Anisotropic monoelectronic ions

g factor anisotropy can be observed under certain conditions
monocrystals; dilute frozen solutions; microcrystalline solids

Generally $g_x \neq g_y \neq g_z$

Axial anisotropy: $g_x = g_y \neq g_z$;

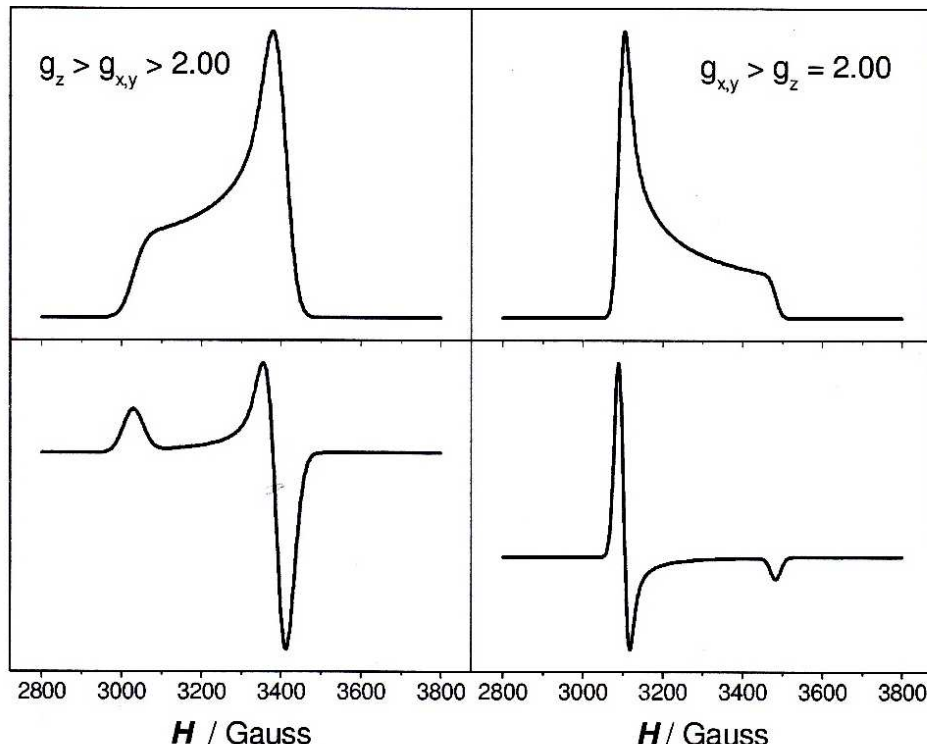


Figure 11.15 Absorption and first derivative plots for anisotropic monoelectronic systems with axial distortion.

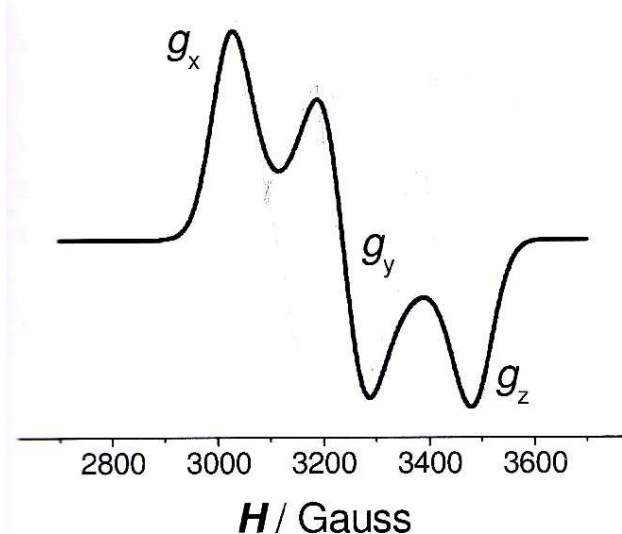


Figure 11.16 Simulated EPR spectrum for a totally an

EPR method in biology – high sensitivity

Blue copper protein

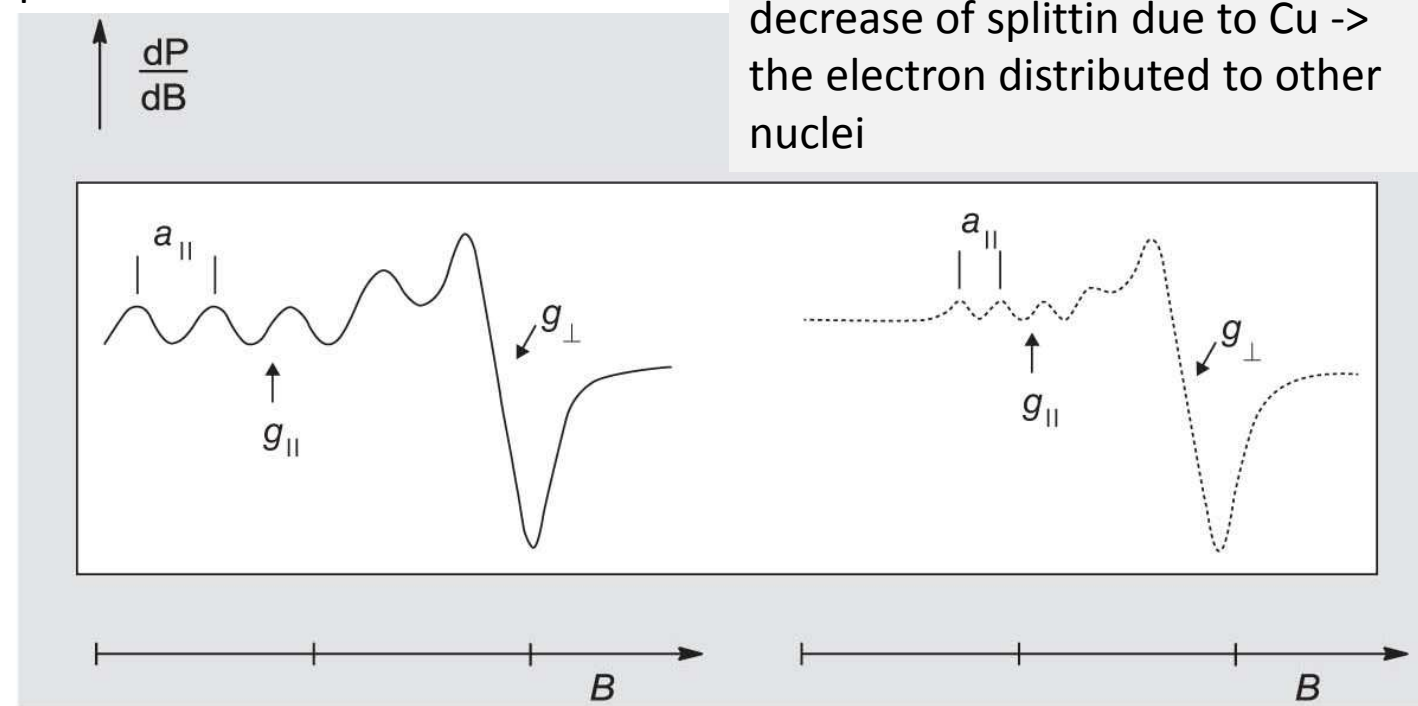


Figure 10.1

Typical anisotropic EPR signals of a normal Cu^{II} complex (—) and of a “blue” copper(II) protein (...); (first derivative spectra).

Uveřejněné materiály jsou určeny studentům Vysoké školy chemicko-technologické v Praze jako studijní materiál. Některá textová i obrazová data v nich obsažená jsou převzata z veřejných zdrojů. V případě nedostatečných citací nebylo cílem autorky záměrně poškodit autora/y původního díla.

S případnými výhradami se prosím obracejte na autorku tohoto výukového materiálu, aby bylo možno zjednat nápravu.



The published materials are intended for students of the University of Chemistry and Technology, Prague as a study material. Some text and image data contained therein are taken from public sources. In the case of insufficient quotations, the author's intention was not to intentionally infringe the possible author(s) rights to the original work.

If you have any reservations, please contact the author(s) of the specific teaching material in order to remedy the situation.

Molecular orbitals

Constructed from AO
number of AO = number of MO

- Symmetry
- Energy
- Overlapping



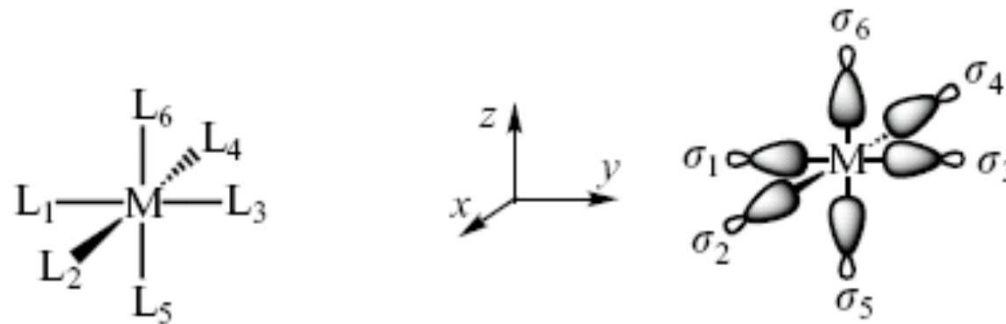
EUROPEAN UNION
European Structural and Investing Funds
Operational Programme Research,
Development and Education

MŠMT
MINISTRY OF EDUCATION,
YOUTH AND SPORTS



Octahedral ML_6 complex

The metal is placed at the origin, the ligands on the axes x (L_2, L_4), y (L_1, L_3), and z (L_5, L_6). Each ligand possesses an orbital σ directed towards the metal.



Orbital “bookkeeping”:

6 ligands surrounding the centre = 6 donor orbitals

9 AO of the central metal ($s + 3 \times p + 5 \times d$)

total 15 MO of the complex

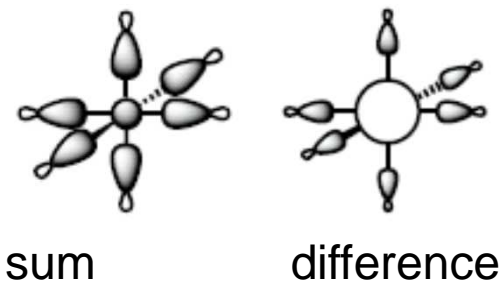
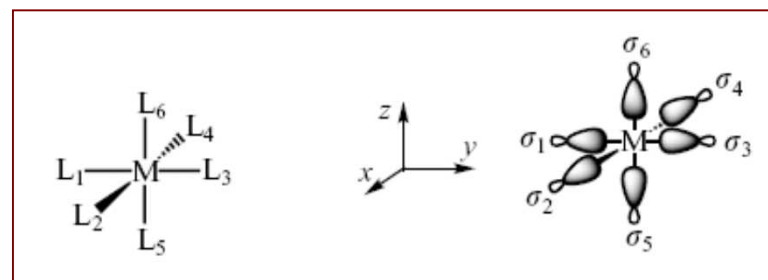
We have to

- choose **symmetrically suitable** subsets from the 6 donor orbitals (*symmetry-adapted ligand orbitals*),
- follow the symmetry of the metal orbitals
- make always both the sum and the difference

Pictures: Y. Jean, Les orbitales moléculaires dans les complexes, Éditions de l’École polytechnique, Palaiseau, 2003;

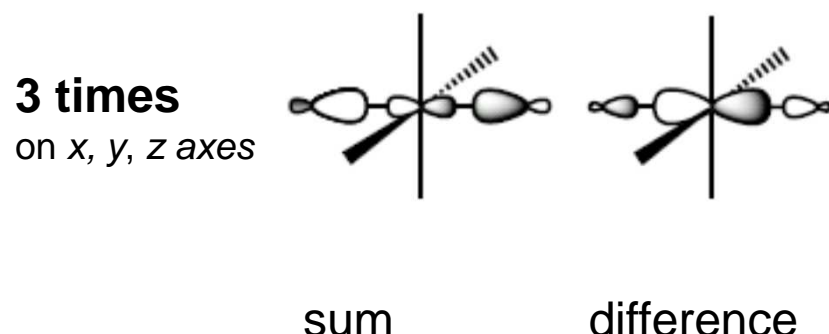
Octahedron - continuation

What will fit to the s orbital?
All six σ orbitals.



2 MO result:
One bonding (sum), one antibonding (difference)
Different electronegativities of M and L

What will fit to p orbitals ?
Three pairs, combining + and – on opposite sides.



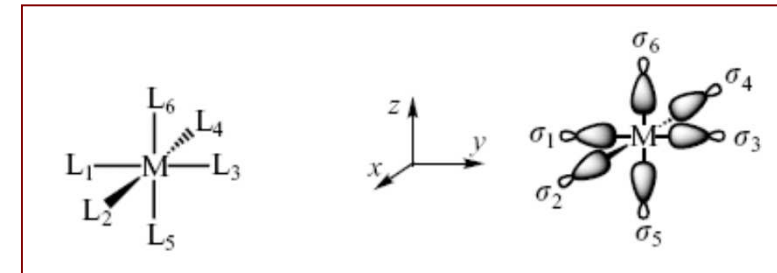
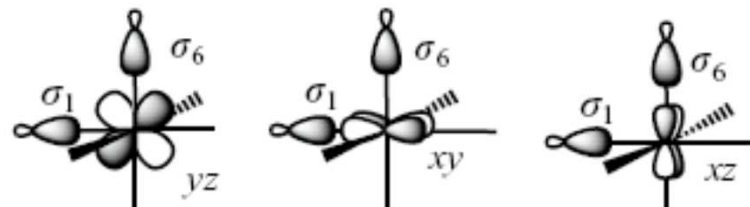
RESULT: 3 pairs of MO = 6 MO ,
Three bonding (sum),
Three antibonding (difference)

**Subtotal: we have produced 8 MO,
having material for 15 MO,
Let's continue to d orbitals**

Octahedron - continuation

What will fit to d orbitals?
It depends (on symmetry).

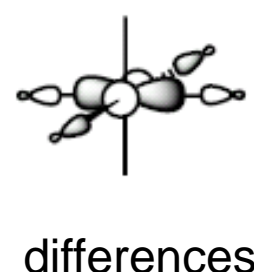
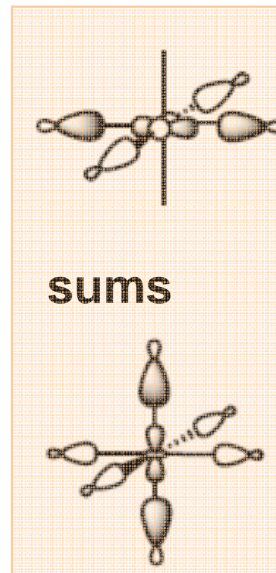
Three of them are not able to overlap with any of the σ ligand orbitals – unsuitable symmetry



RESULT: 3 nonbonding MO
which are exactly the same as the AO of the metal
Now we have 11 MO

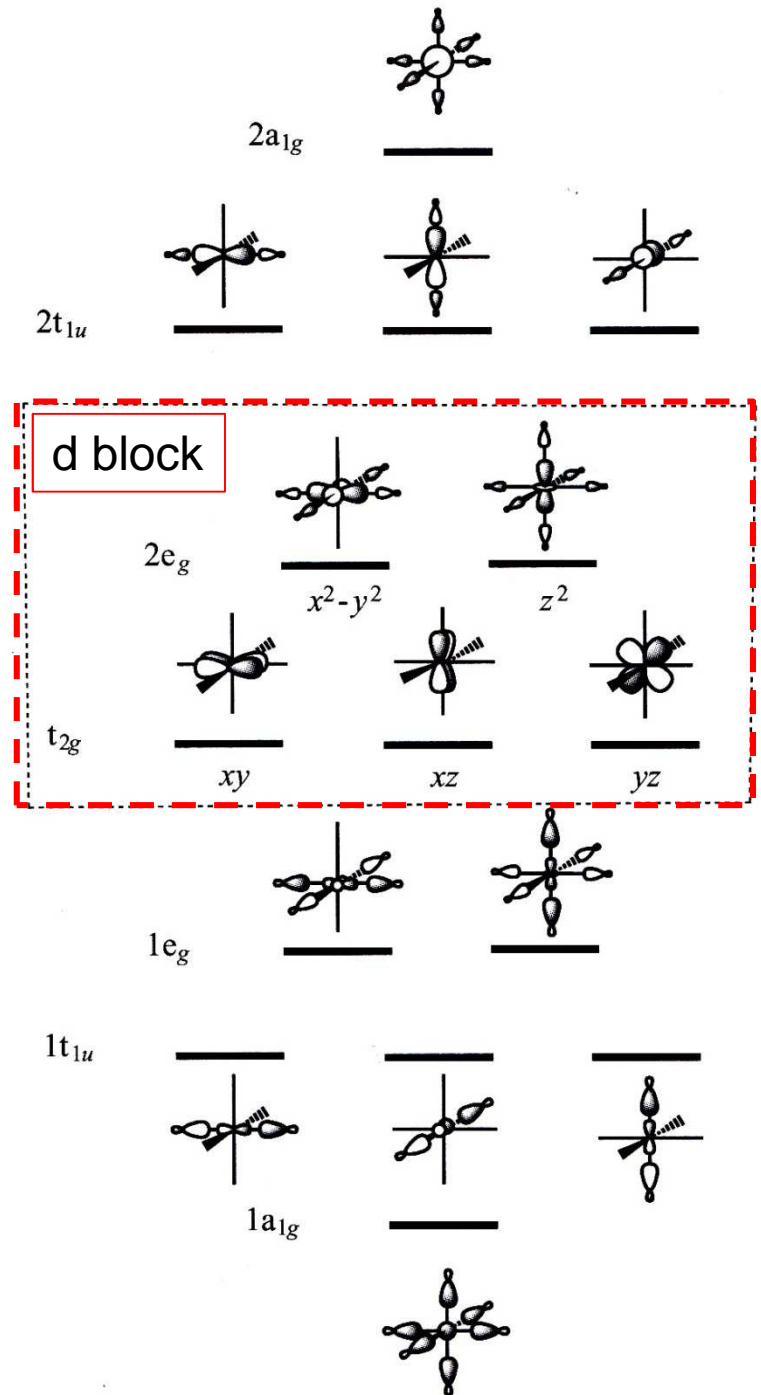
The last two can find suitable partners:

- four σ orbitals, in plane, two opposite pairs + and – (g)
- all six σ orbitals, but now combining + and –.

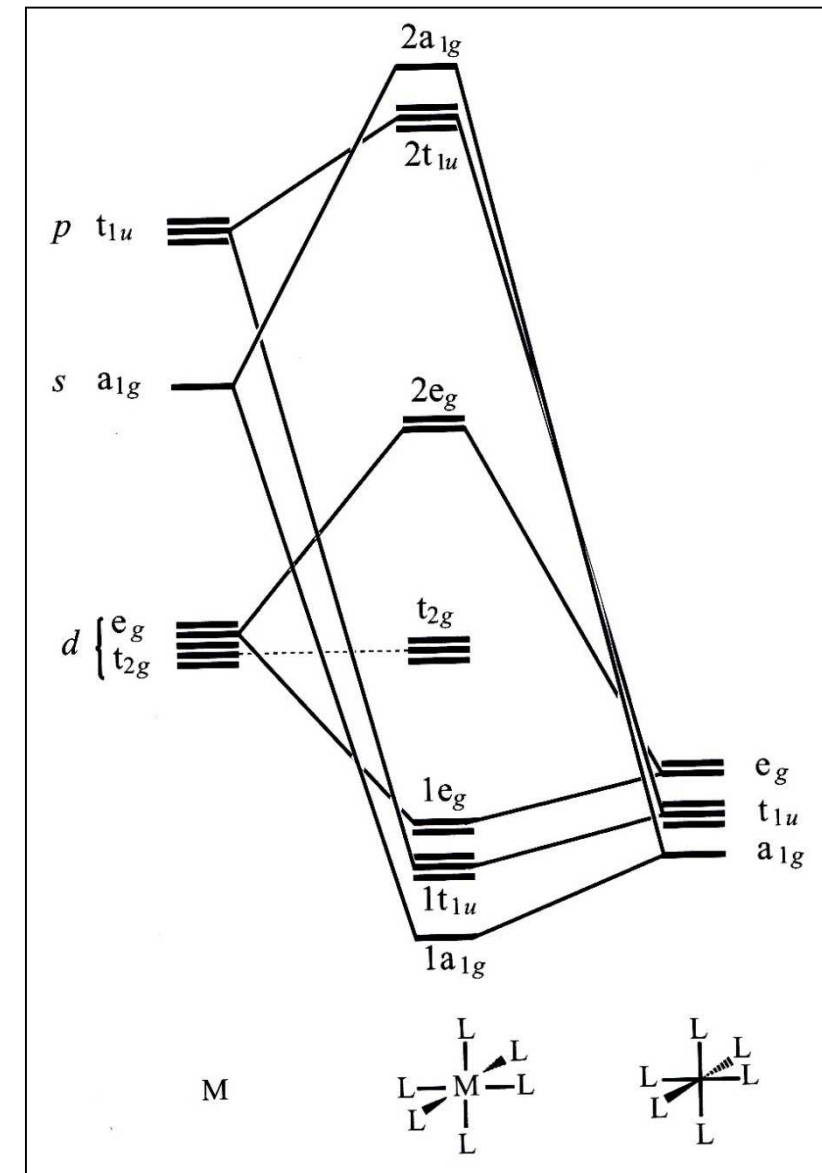


FORMING
2 pairs of MO = 4 MO ,
two bonding (sum),
two antibonding
(difference)

THE WORK IS READY:
we have 15 MO



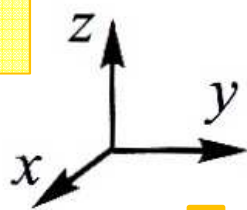
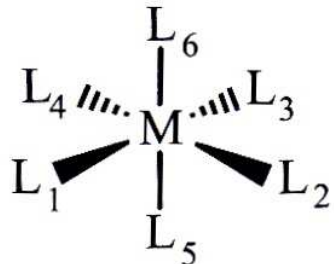
Octahedron – complete view



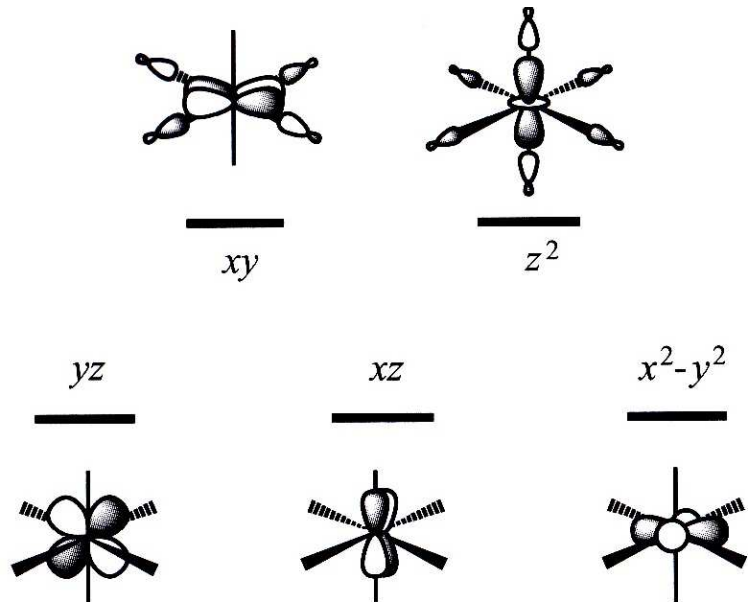
Interaction diagram for an octahedral complex ML_6 ; metal orbitals – left; symmetry-adapted ligand orb. - right

Octahedron – other representations

A. 4 metal – ligand bonds bisect the x- and y- axes

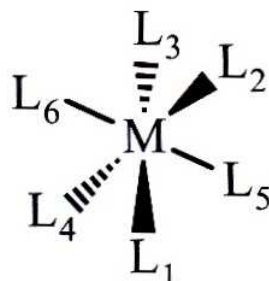


Result:



B. z-axis is a threefold symmetry axis C_3 of the octahedron

Redefinition of d orbitals:

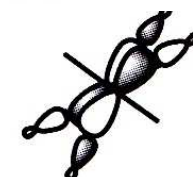
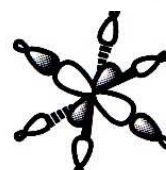


$$\phi_1 = \sqrt{\frac{2}{3}}(x^2 - y^2) - \sqrt{\frac{1}{3}}yz$$

$$\phi_2 = \sqrt{\frac{2}{3}}xy - \sqrt{\frac{1}{3}}xz$$

$$\phi_3 = \sqrt{\frac{1}{3}}(x^2 - y^2) + \sqrt{\frac{2}{3}}yz$$

$$\phi_4 = \sqrt{\frac{1}{3}}xy + \sqrt{\frac{2}{3}}xz$$



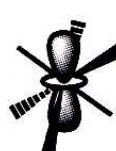
ϕ_3

ϕ_4

z^2

ϕ_1

ϕ_2

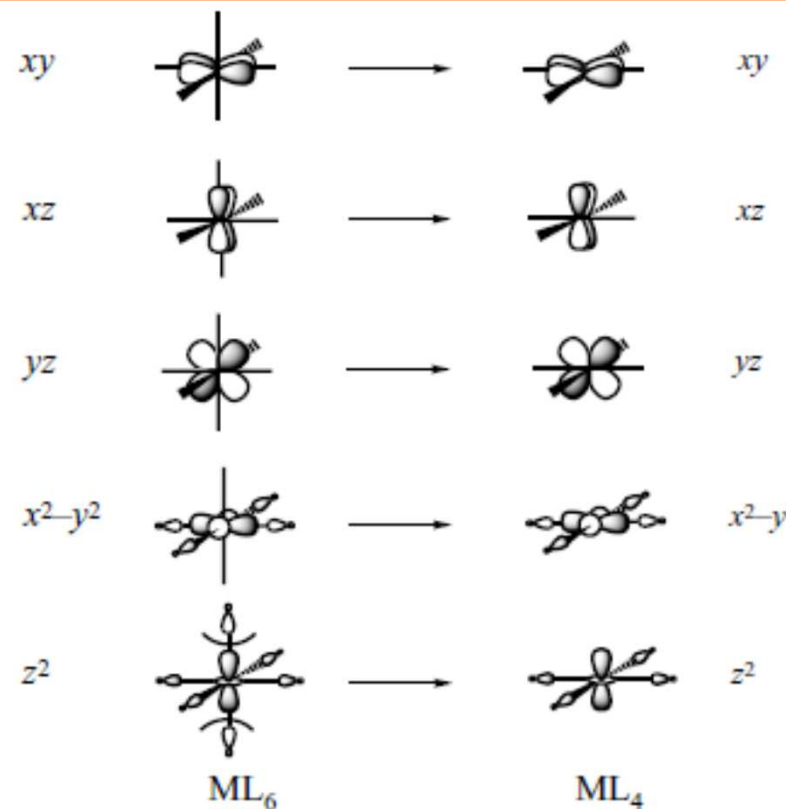
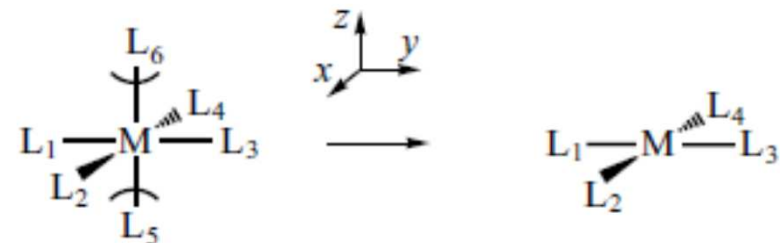


General result:
3 stabilized and 2 labilized orbitals

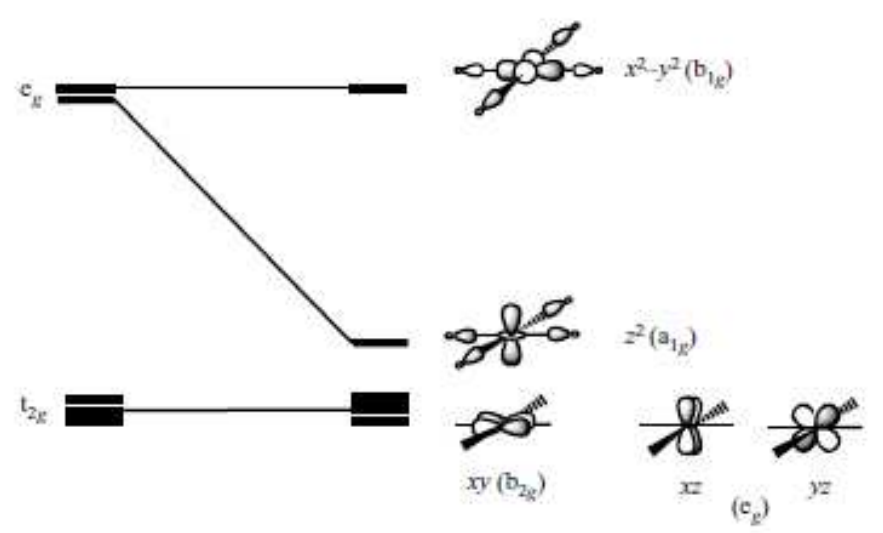
SQUARE PLANAR GEOMETRY, ML_4

Symmetry adapted orbitals - from octahedron to square:

- d-orbitals which are non-bonding in octahedron remain non-bonding
- $d_{x^2-y^2}$ is strongly antibonding
- d_{z^2} is stabilized

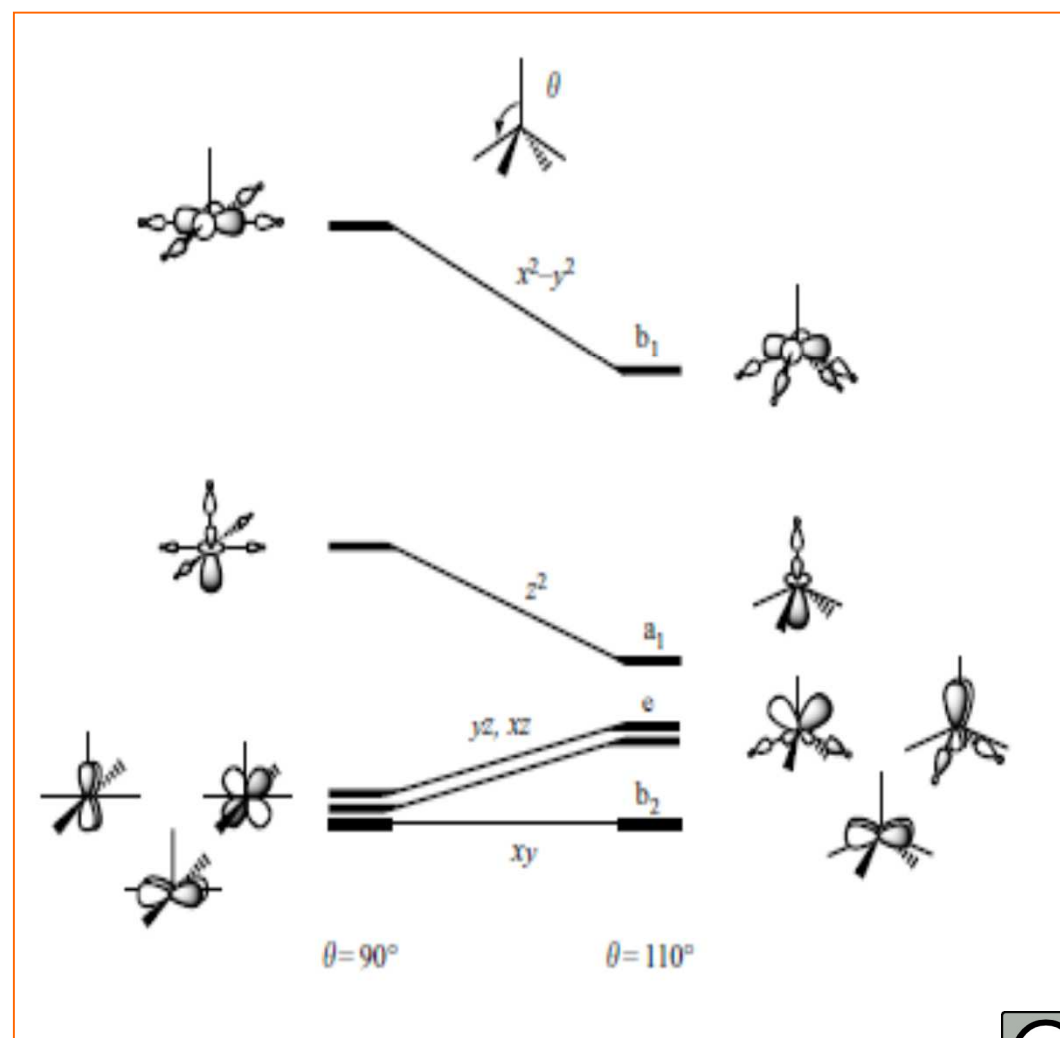
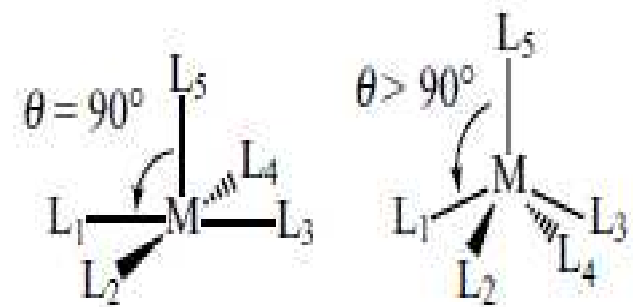
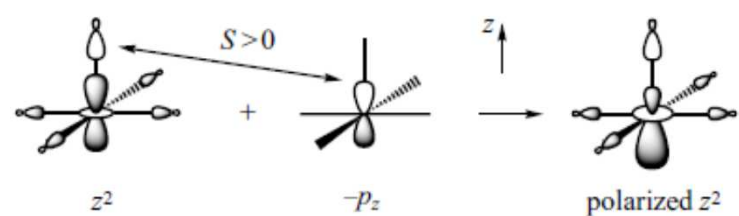
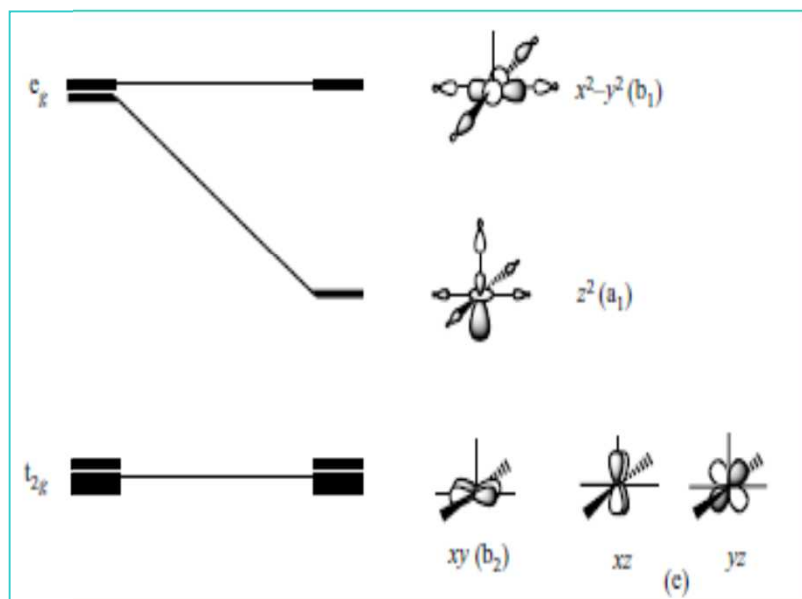
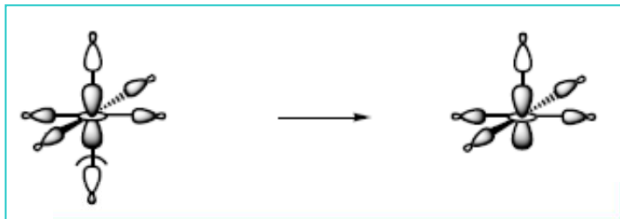


Detailed comparison :



the three t_{2g} orbitals lose their degeneration (symmetry!)
NEW only 1 orbital really high in energy

ML₅ TETRAHEDRAL PYRAMID



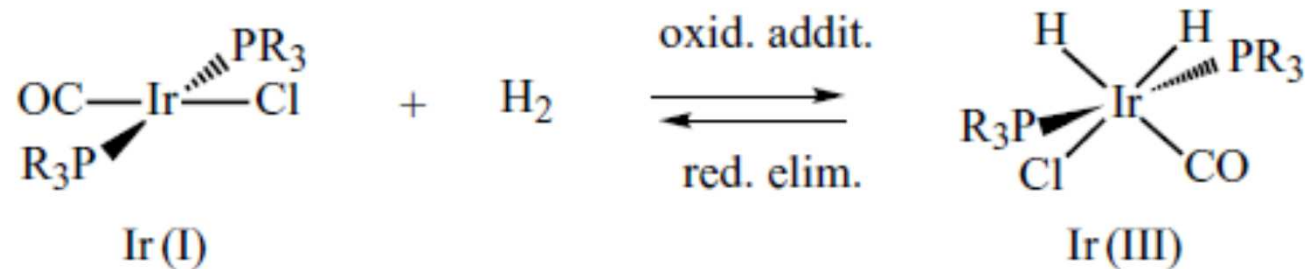
SQUARE PLANAR COMPLEXES d^8 – 16 electron complexes

Vaska complex $[\text{Ir}(\text{CO})(\text{Cl})(\text{PPh}_3)]$

Wilkinson hydrogenation catalyst $[\text{Rh}(\text{Cl})(\text{PPh}_3)_3]$

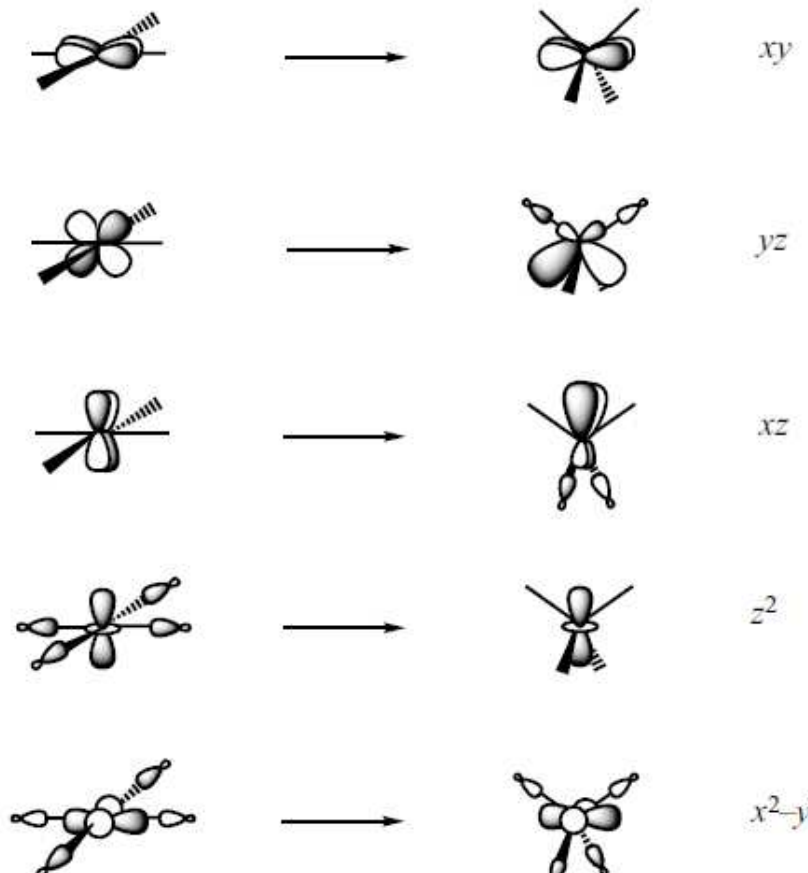
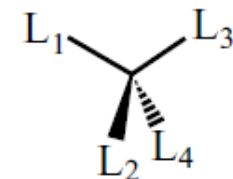
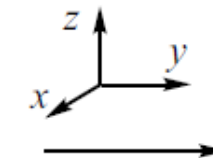
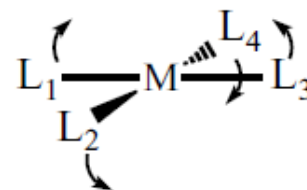
a NON-BONDING orbital remains on the central metal atom

Common reactivity: oxidative addition, to a 18 e intermediate

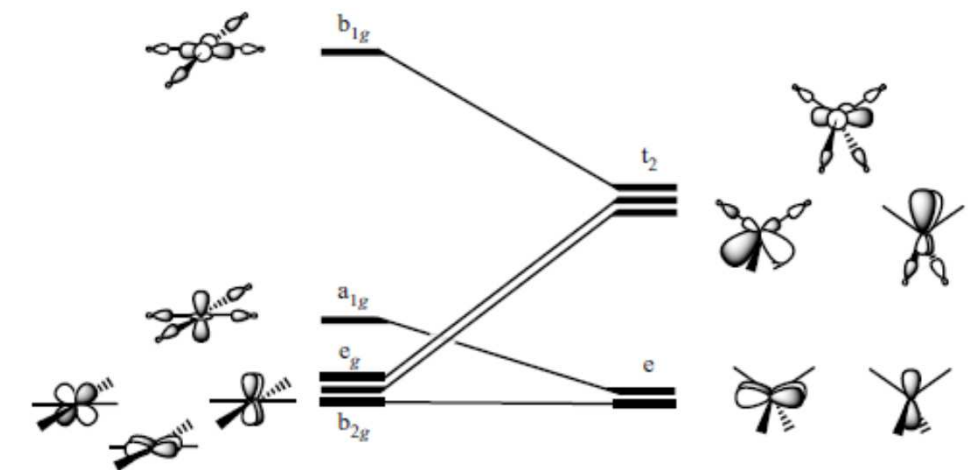


FROM SQUARE TO TETRAHEDRON :

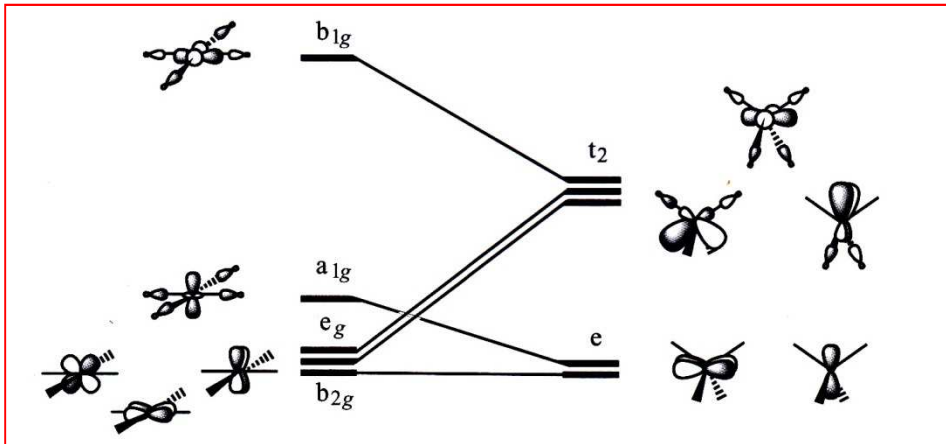
d-block of the square changes when distorted :



Relationship between square and tetrahedron:



COMPLEXES ML_4 – TETRAHEDRON, SQUARE or something in between?



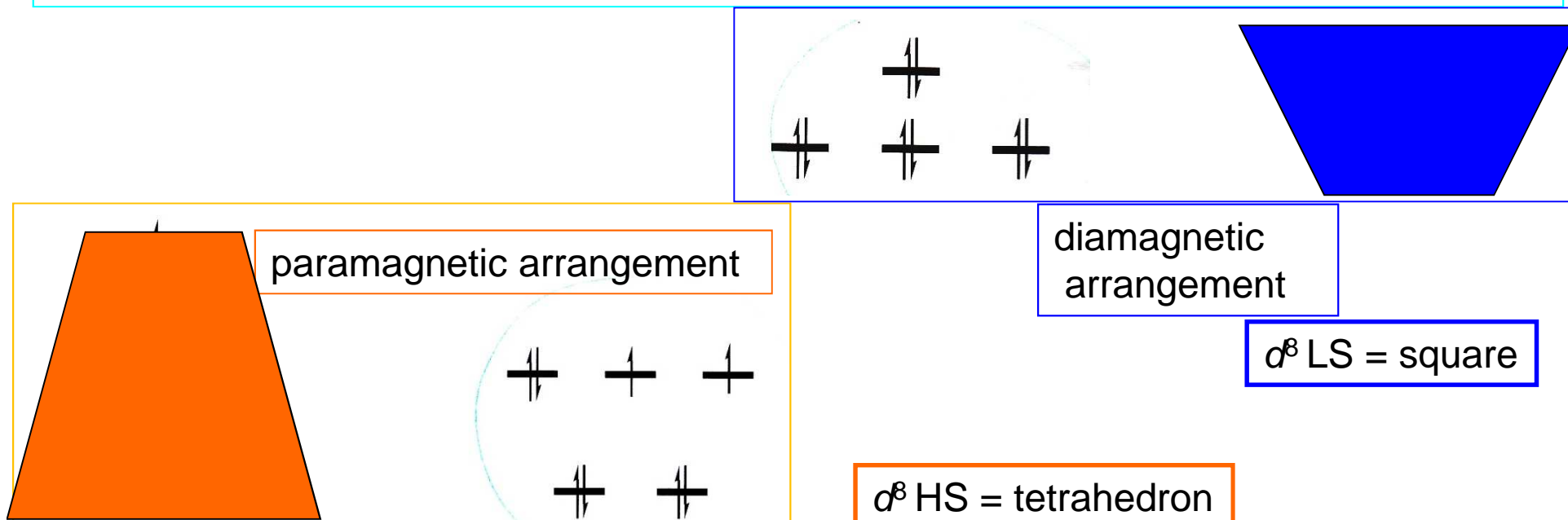
Steric reasons – tetrahedron
Electrons – sometimes square

Tetrahedrons:

d^{10} : 18 e, no labilized orbital
 d^0 : with π -donor ligands

and steric reasons (small size of the central cation); MnO_4^- , $TiCl_4$

Squares: d^8 , if the centre is not too small (Ni^{2+}) due to a stable electronic configuration



Ligands capable of π interaction

Typically:

1. with a non-bonding p orbital, full or empty
2. possessing π bond on the donor atom, hence a full π or an empty π^* orbital

π donors

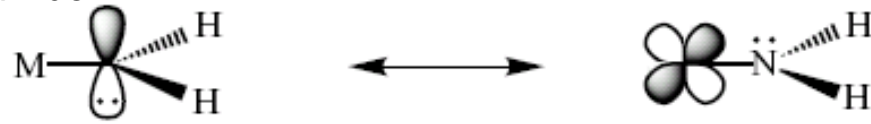
- ad 1) the non-bonding p orbital is full
ad 2) π bonding orbital is near to the donor atom (polarized)

π acceptors

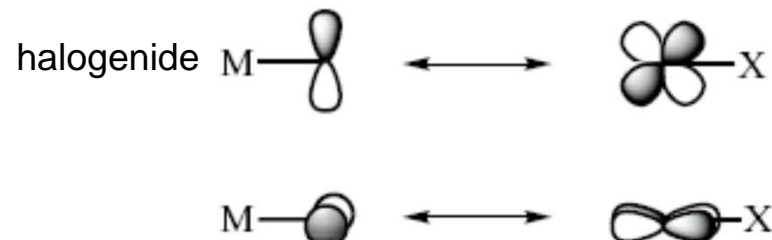
- ad 1) empty non-bonding p orbital
ad 2) π antibonding orbital is near to the donor atom

examples of π donors

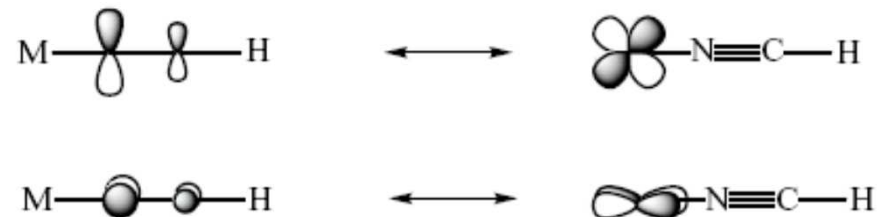
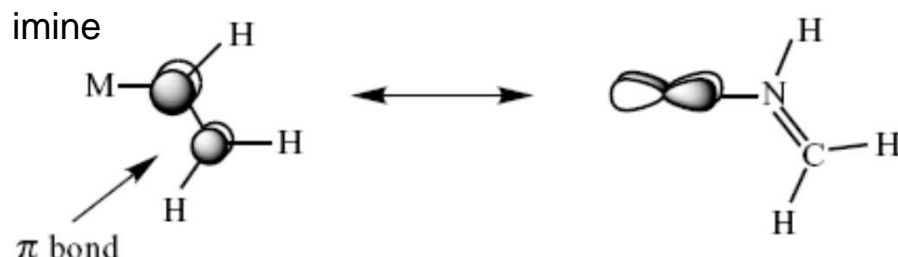
amide



double-face:



imine

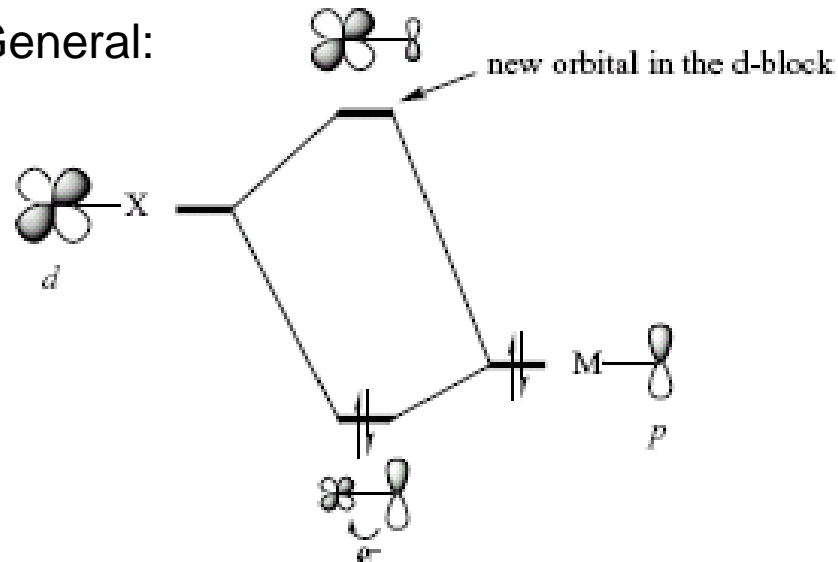


? multiple polar bonds:

always capable of a simultaneous π acceptance to the π^* orbitals

Perturbation of the d orbitals by influence of π donors

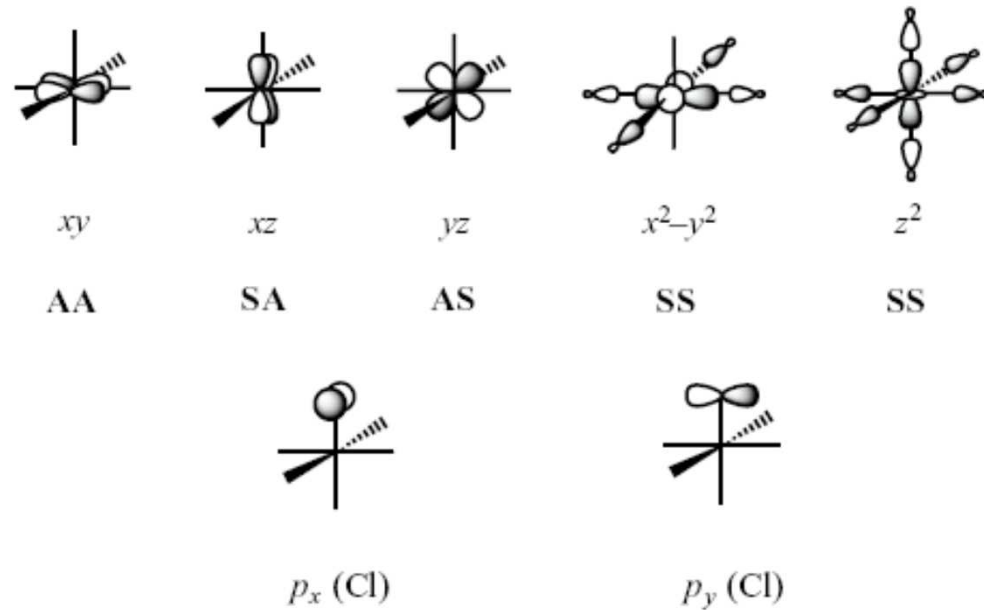
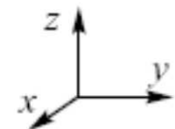
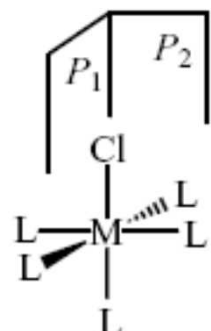
General:



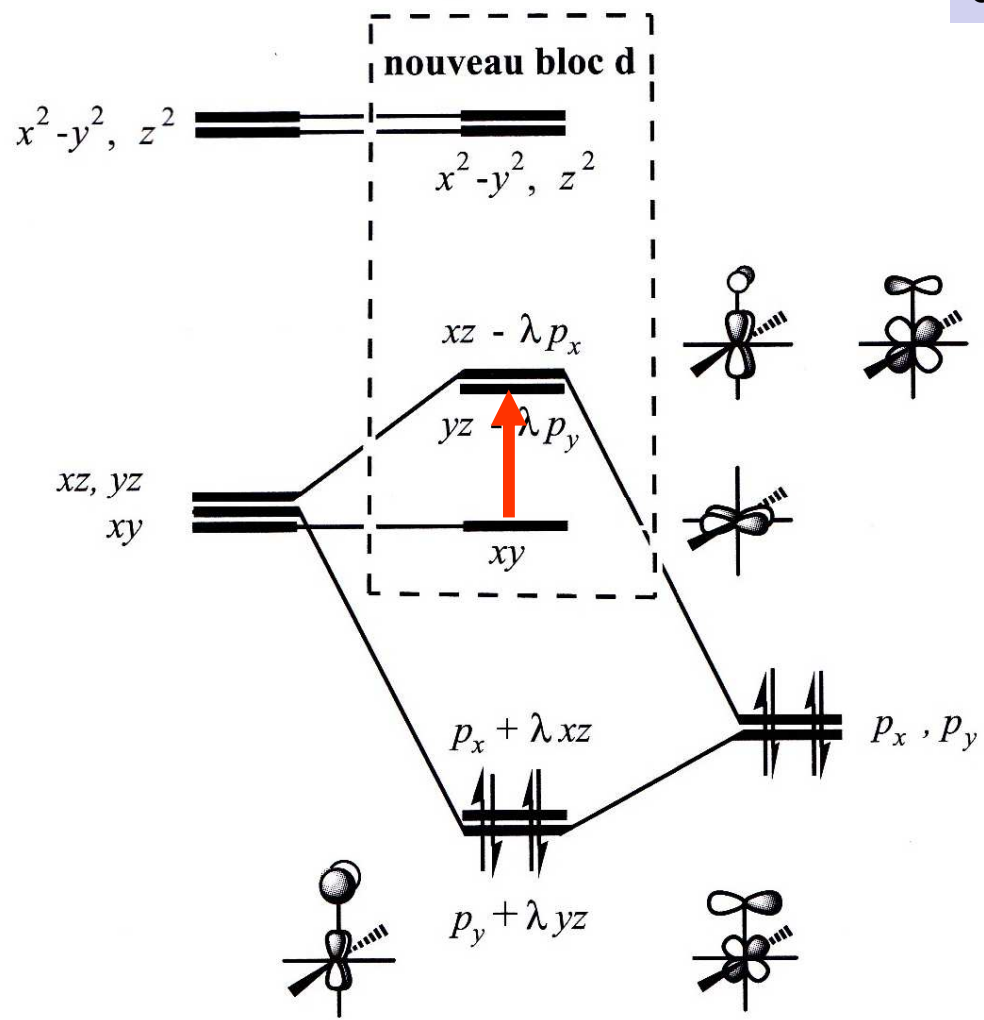
d orbital (neat) and a π donor:

- energy of the basic levels
- 2 new MO
- the MO which is prevalently formed from d is **destabilized**

Example - molecule ML_5Cl
situation:
2 symmetry planes



RESULT for ML_5Cl



destabilization of the *d*-block orbitals

Rule:

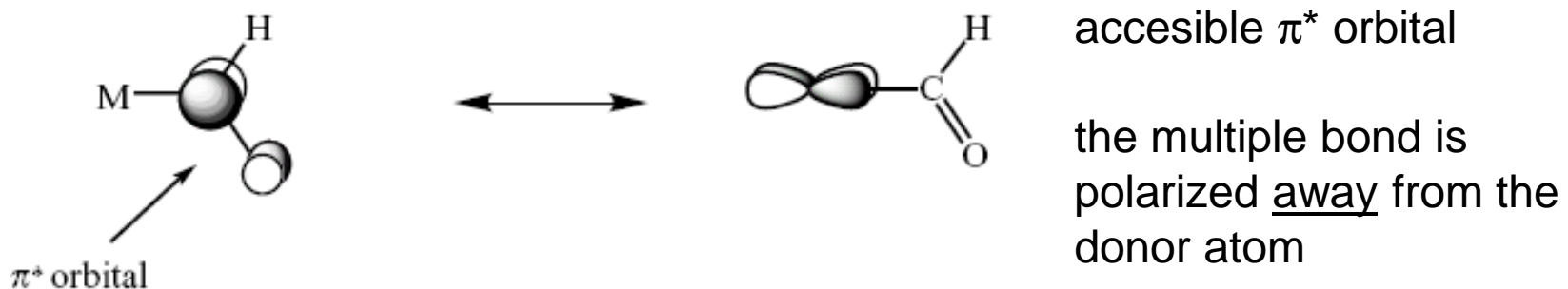
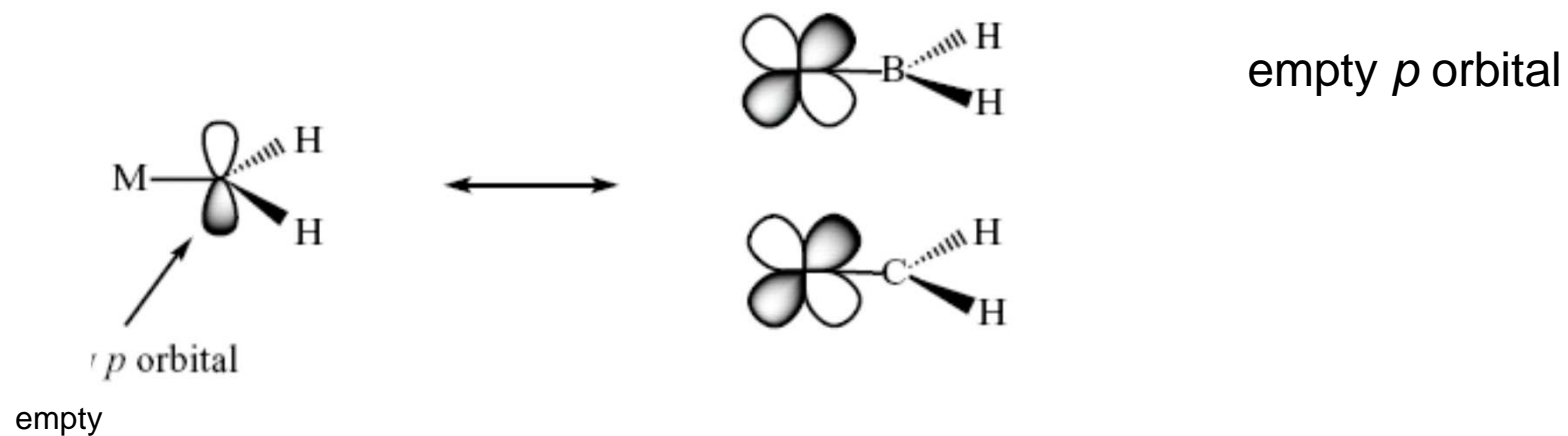
the π interaction between a d-block orbital and the orbital of a π -donor ligand leads to a *destabilization* of the d-block orbital, by mixing with the ligand orbital *in an antibonding sense*.

RESULT for MCl_6



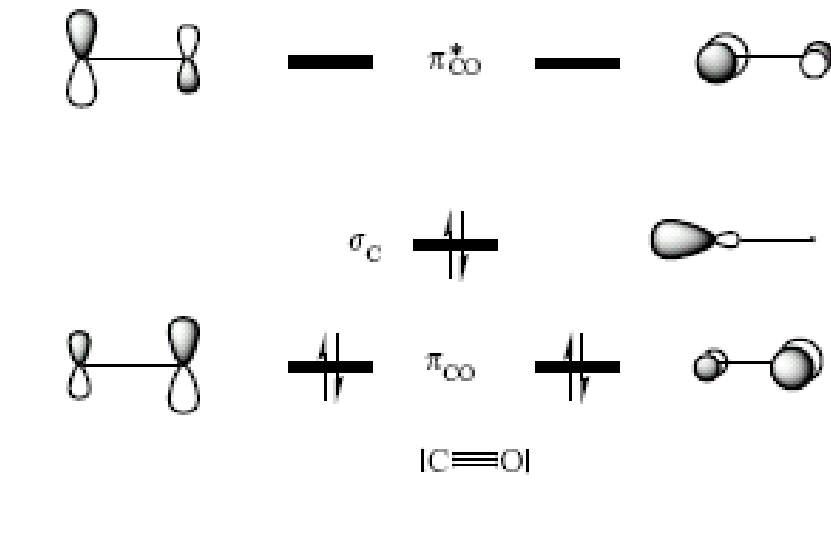
Perturbation of the d orbitals by influence of π acceptor

Examples of π acceptors

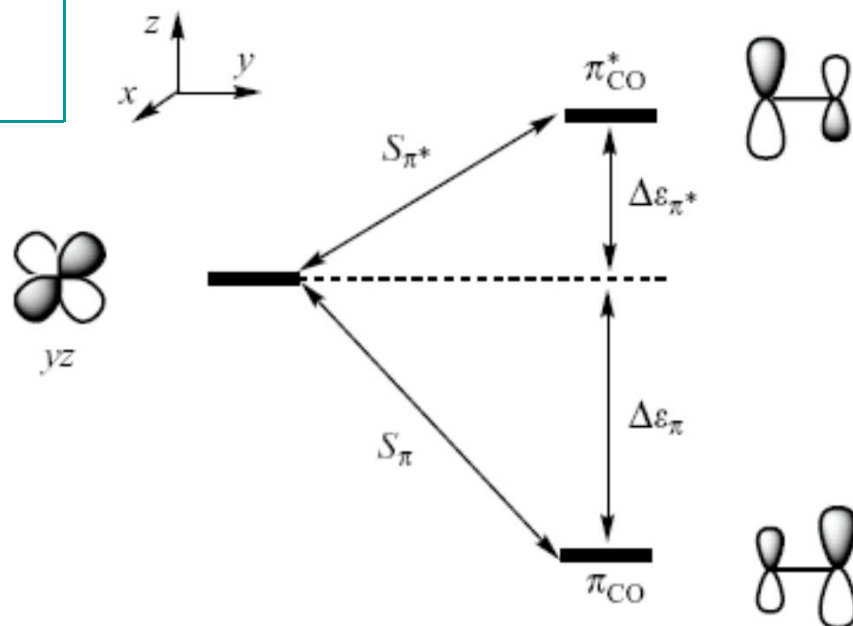


Structure

CARBONYL – a DOUBLE-FACE π acceptor

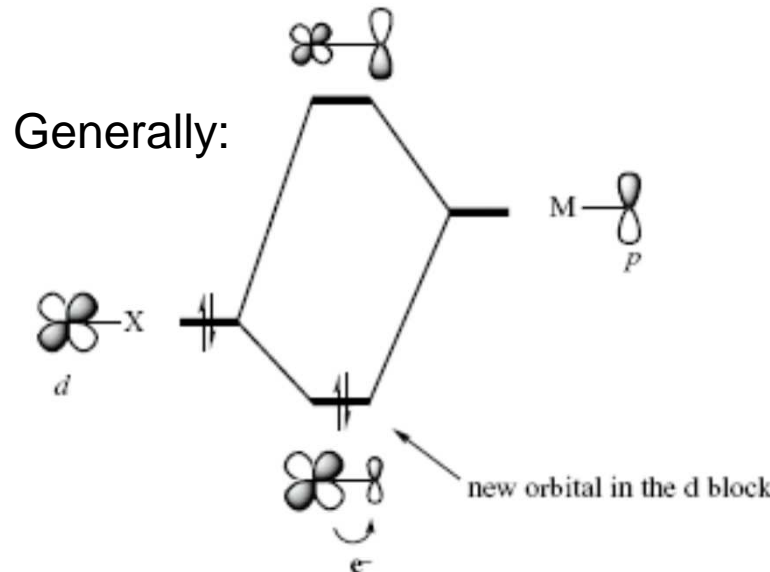


Interaction with a metal



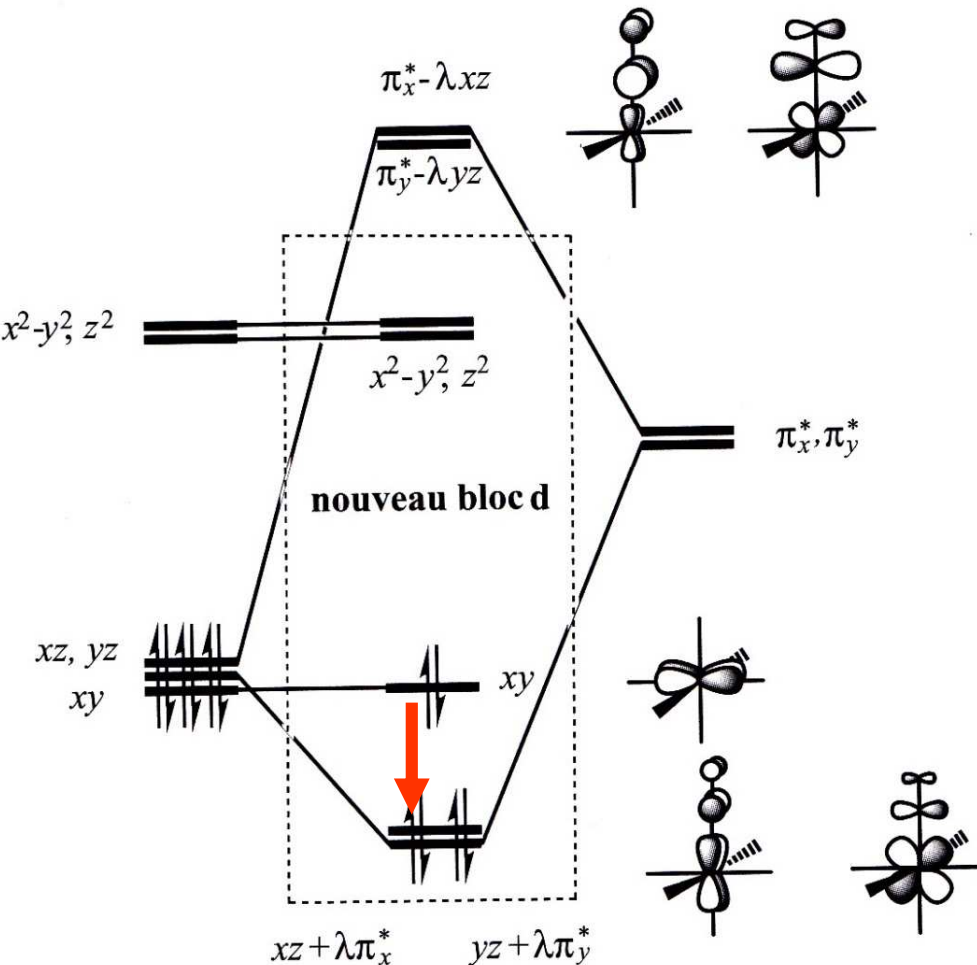
$M-C \equiv O$

Perturbation of the d orbitals by influence of π acceptor

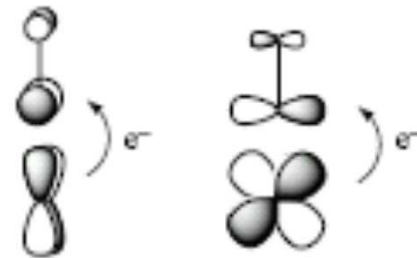
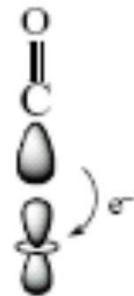


d orbital (neat) and a π acceptor:
 • energy of the basic levels !
 • 2 new MO
 • the MO which is prevalently formed from d is **stabilized**

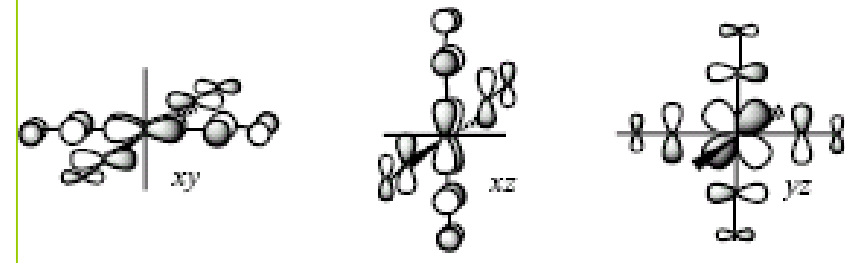
Rule:
 the π interaction between a d-block orbital and the orbital of a π -acceptor ligands leads to *stabilization* of the d-block orbital, by mixing with the ligand orbital *in a bonding sense*.



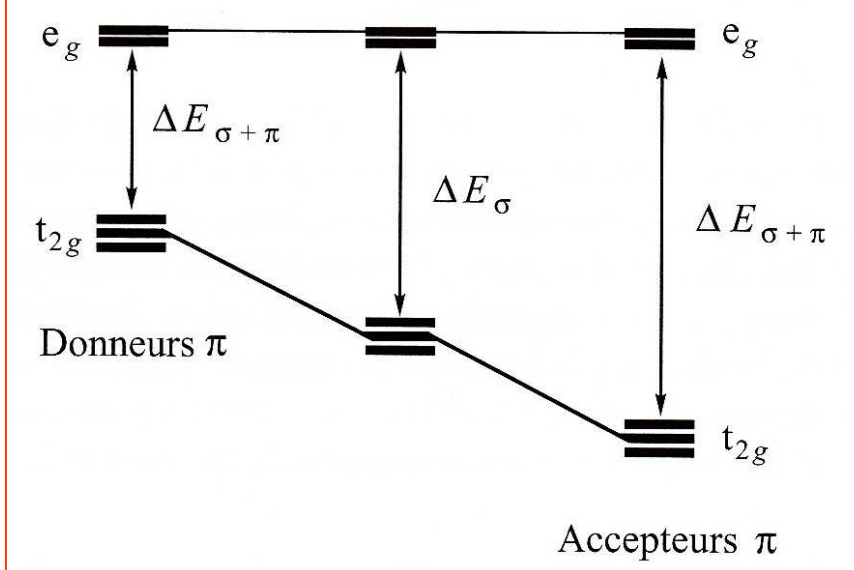
Carbonyl: σ -donation and π -back donation



Six CO's at the same time— $[M(CO)_6]$



Energetic consequences of the π -interaction for the d-block orbitals

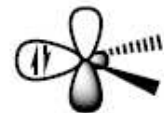


Explanation of the spectrochemical series of the ligands:

$I^- < Br^- < S^{2-} < SCN^- < Cl^- < NO_3^- < N_3^-$, $F^- < OH^- < C_2O_4^{2-} < H_2O < NCS^- < \text{gly}^- < CH_3CN < NH_3 \approx \text{py} < \text{en} < \text{bpy} < \text{phen} < NO_2^- < PR_3 < CN^- < CO$

CARBENE COMPLEXES

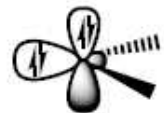
The simplest ligand: CH_2



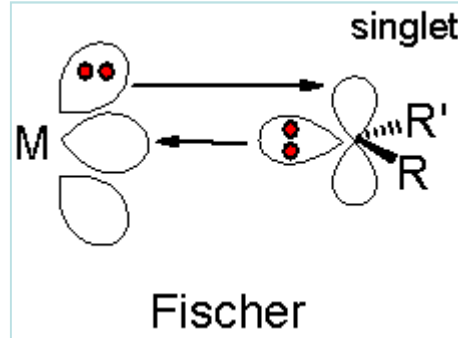
4-36a (L)



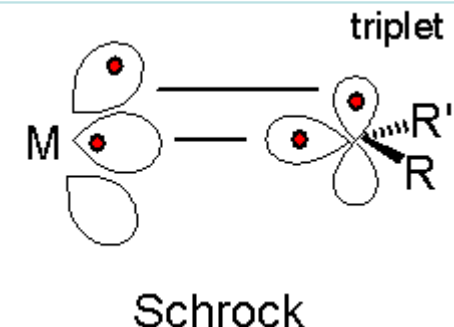
4-36b (X_2)



4-36c (dianion)



Fischer

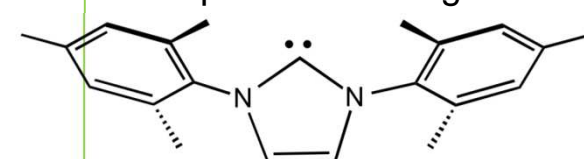


Schrock

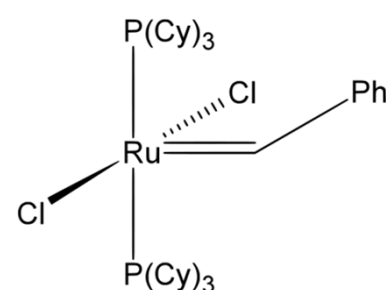
3 basic types of carbene complexes:

1. Fischer
2. Schrock
3. NHC (N-heterocyclic carbenes) – only small π -interaction

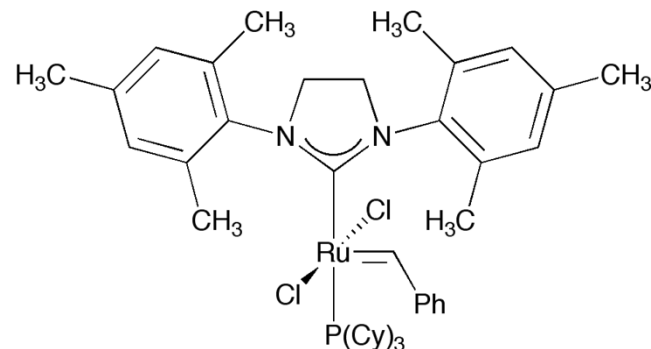
example of a NHC ligand



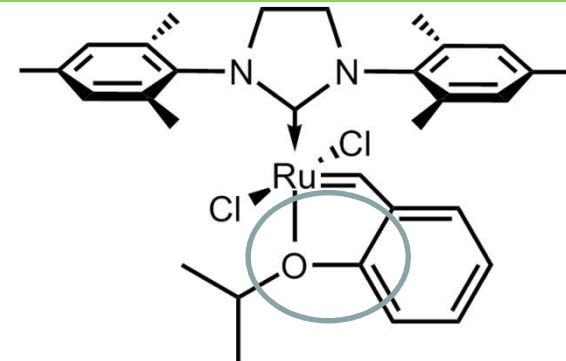
Grubbs catalysts, 1. a 2. generation



olefin metathesis



Hoveyda-Grubbs catalyst, 2. generation



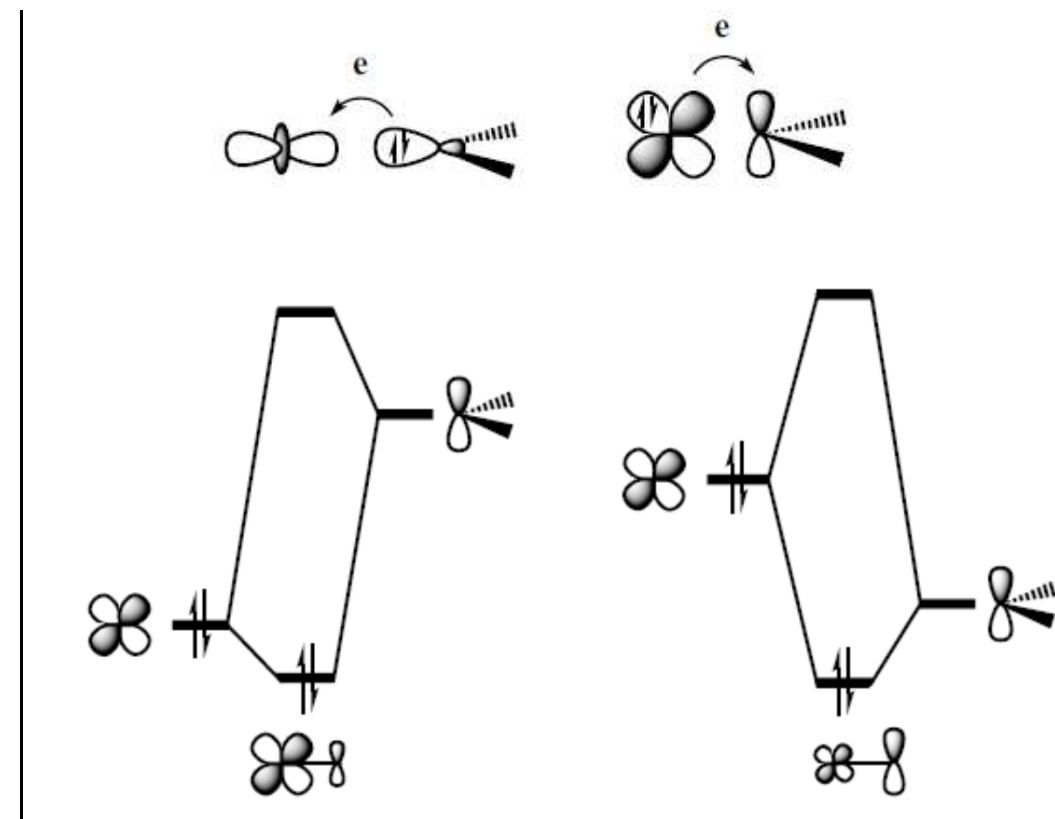
CARBENE COMPLEXES

Fischer carbenes:

M from the right part of the transition row,
 π -acceptor ligands (low ox.number)
 π -donor substituents on =C (carbene carbon)

Schrock carbenes:

M from the left part of the transition row,
 π -donor ligands
alkyls on =C, "alkylidene"



Fischer carbenes

$M(\delta-) = C(\delta+)$

=C reacts with nucleophiles



Schrock carbenes

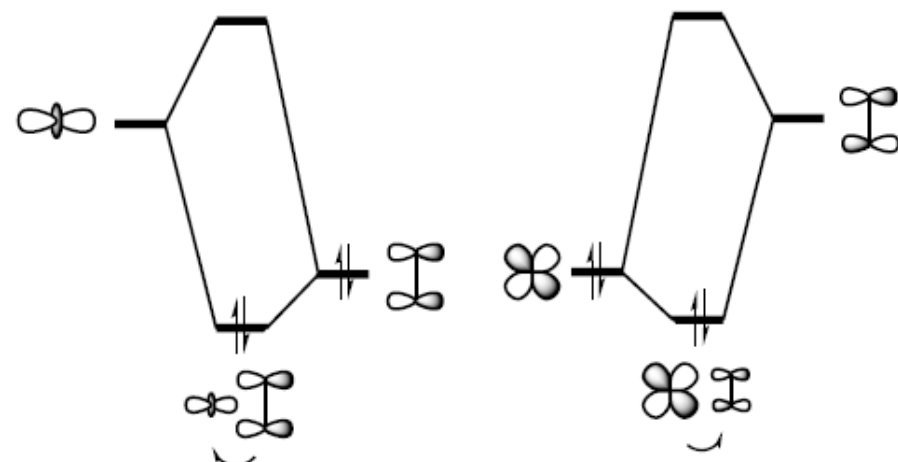
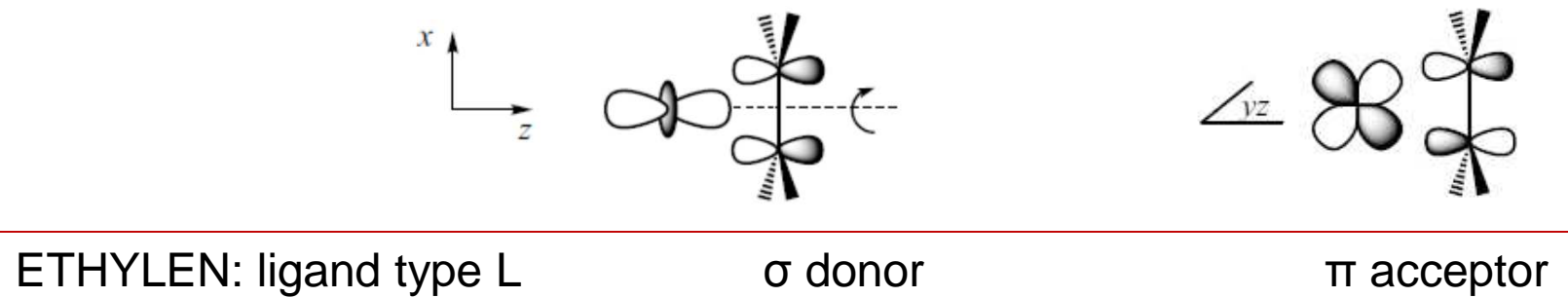
$M(\delta+) = C(\delta-)$

=C react as a Lewis Base

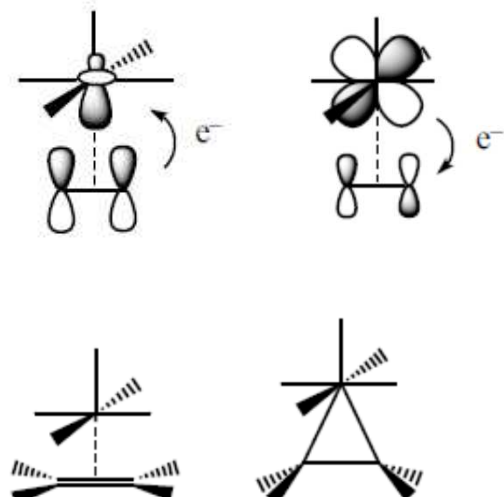


η -BONDING LIGANDS

ethylene: the Dewar–Chatt–Duncanson model

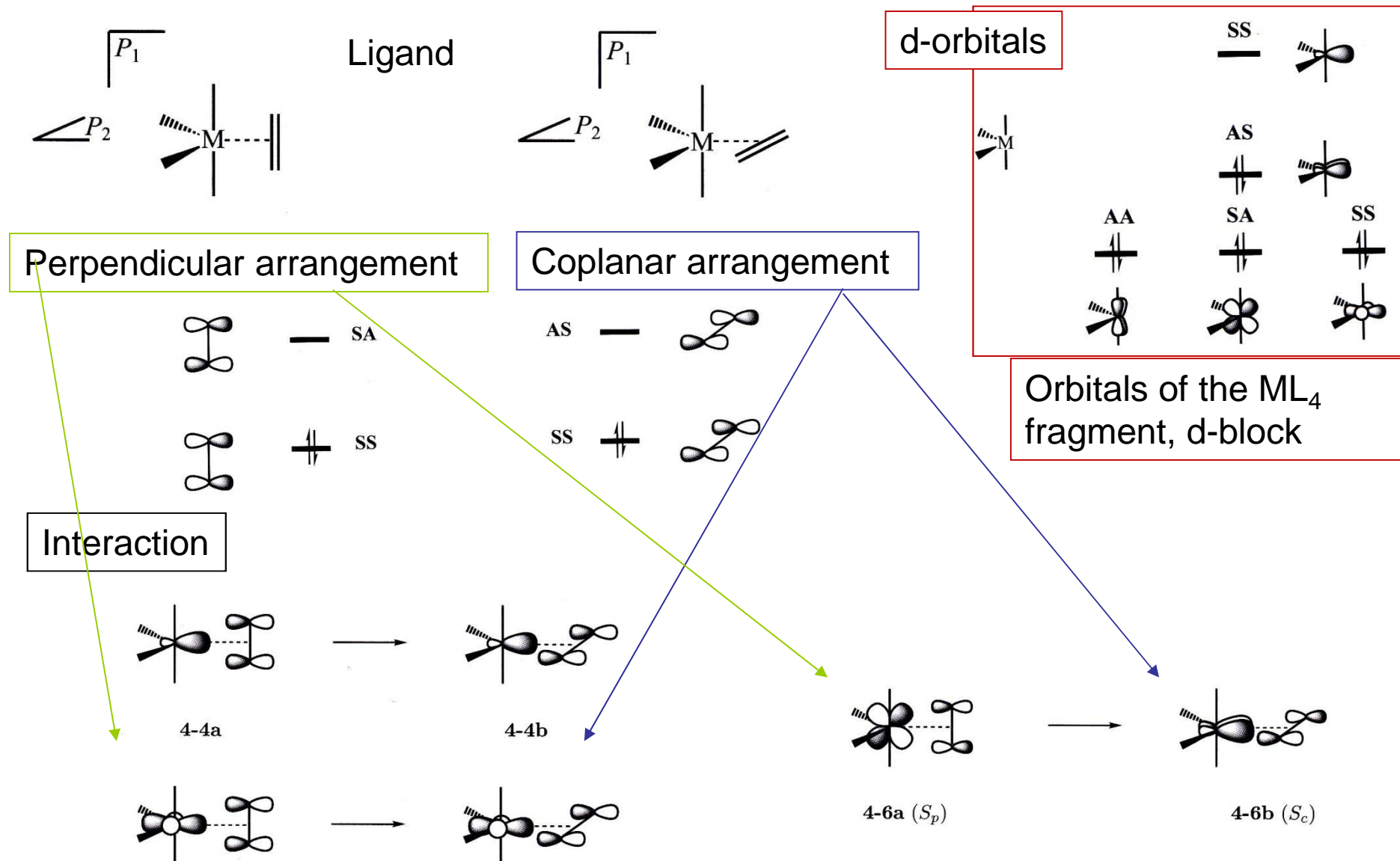


Ethylene ligand or
metallacyclopropane?

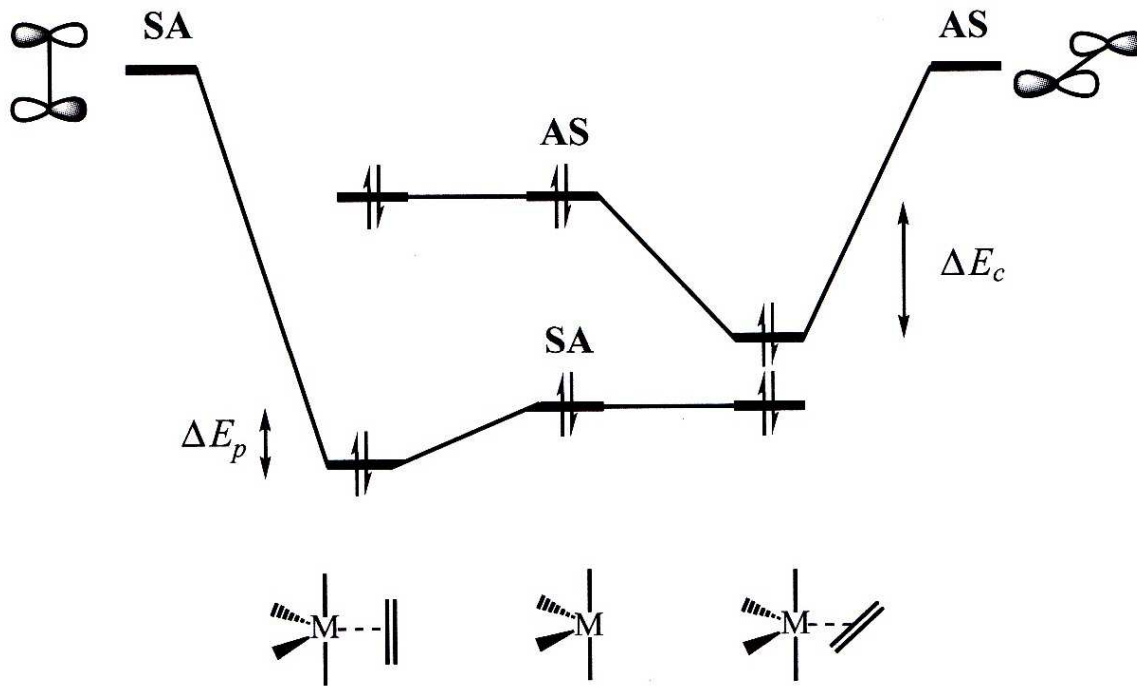


ELECTRONIC STRUCTURE OF d⁸- [ML₄(η²-C₂H₄)]

Symmetry to P₁ plane (yz;) and P₂ plane(xz;) :



ELECTRONIC STRUCTURE OF d⁸- [ML₄(η²-C₂H₄)] - detail



Coplanar conformation (right) is better

ELECTRONIC STRUCTURE OF d⁶- [ML₅(η²-C₂H₄)]

Symmetry to P_1 plane (yz) and P_2 plane(xz) :

Ligand



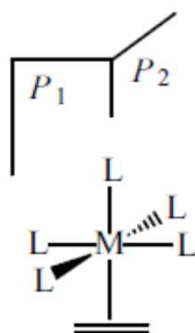
— SA

Orbitals of the ML₅ fragment, d-block



+ SS

Eclipsed arrangement



d-orbitals

z^2 — SS



AA

AS

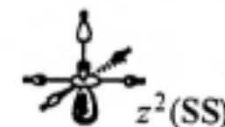
SA



xy

xz

yz



z^2 (SS)



xz (AS)



xy (AA)



yz (SA)



z^2

— SS



SS

AS

SA



$x^2 - y^2$



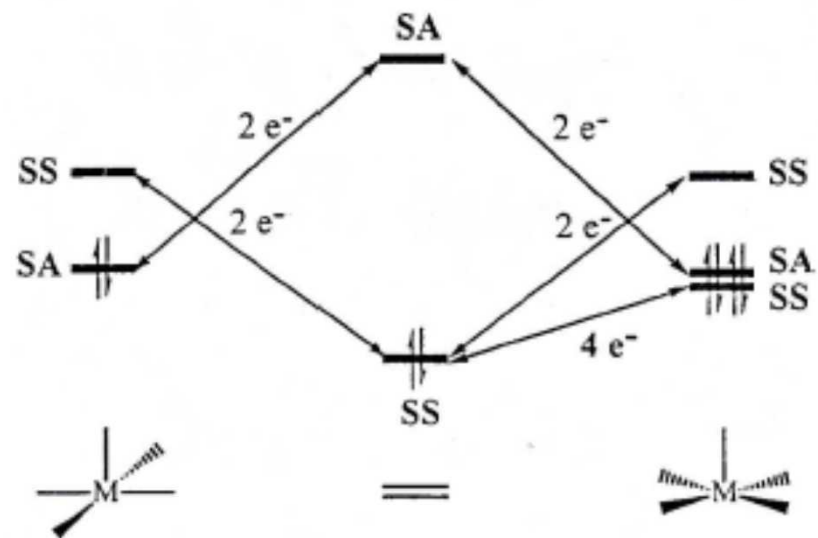
xz



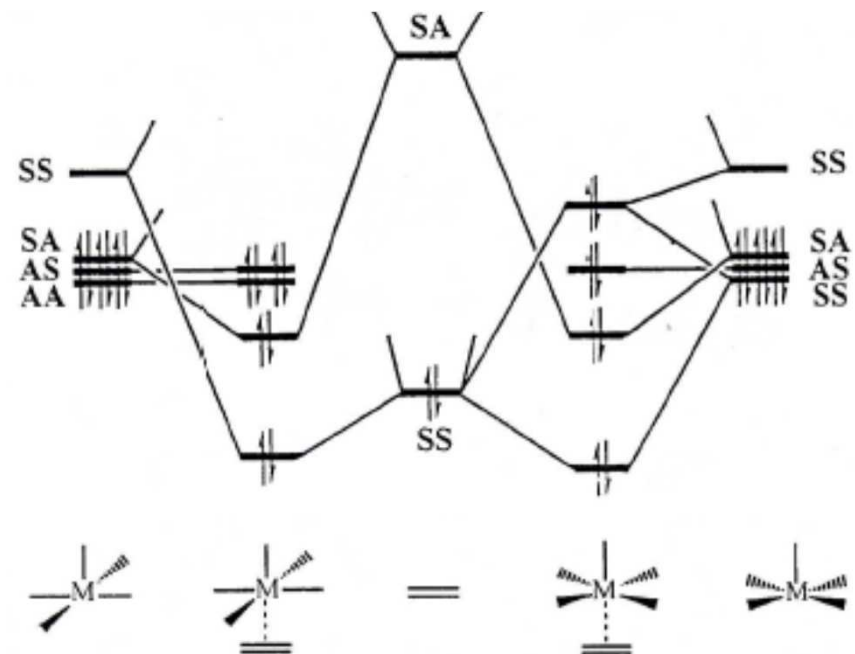
yz

ELECTRONIC STRUCTURE OF d⁶- [ML₅(η²-C₂H₄)]

only MO symmetrically allowed

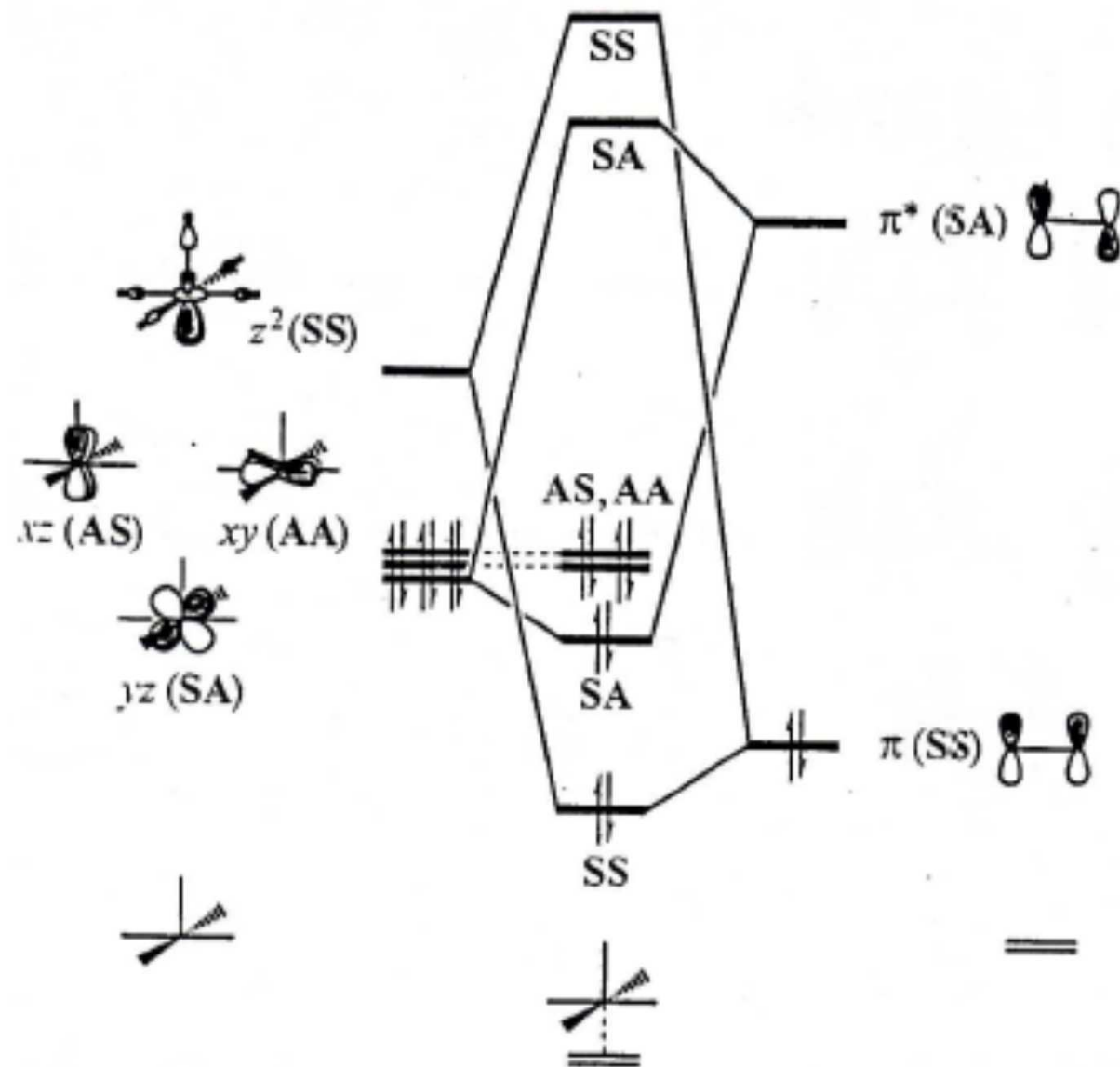


whole picture



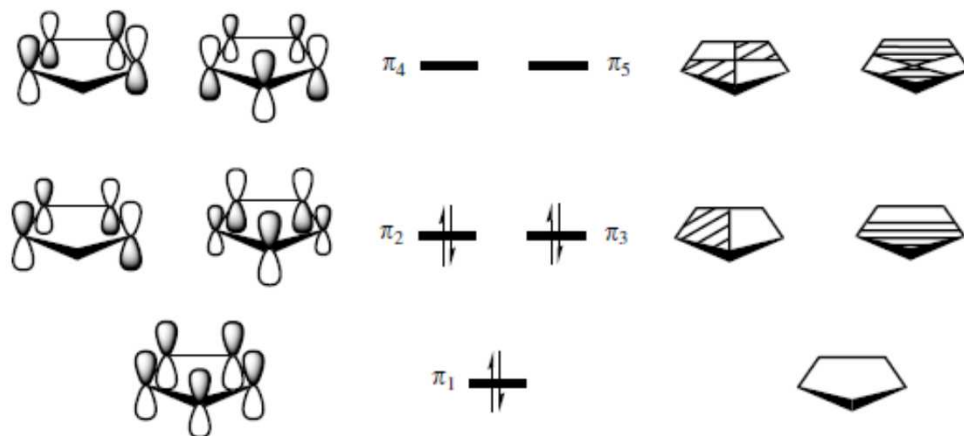
Eclipsed conformation (left) is better

ELECTRONIC STRUCTURE OF d⁶- [ML₅(η²-C₂H₄)] – eclipsed conformation, full picture

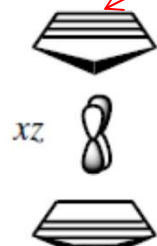
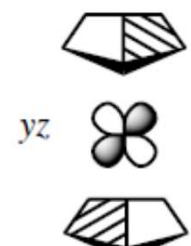
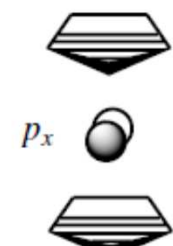
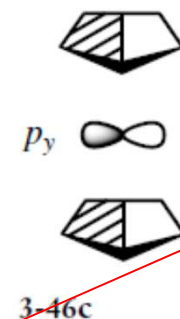
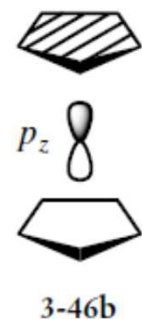
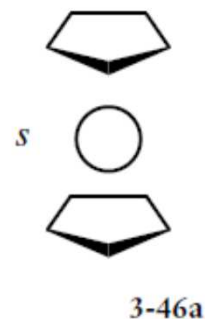


FERROCENE

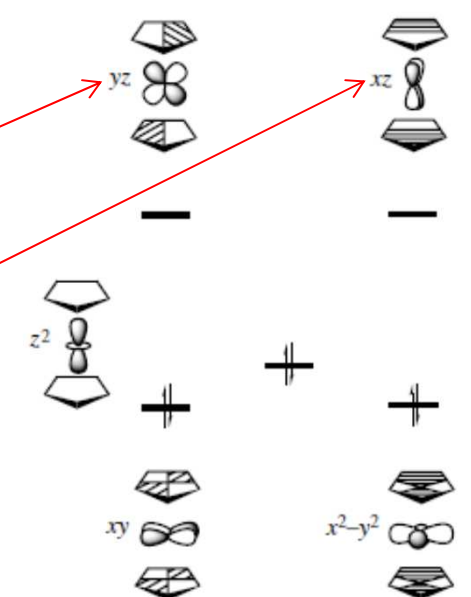
MO of the cyclopentadienyl



Ligand donor

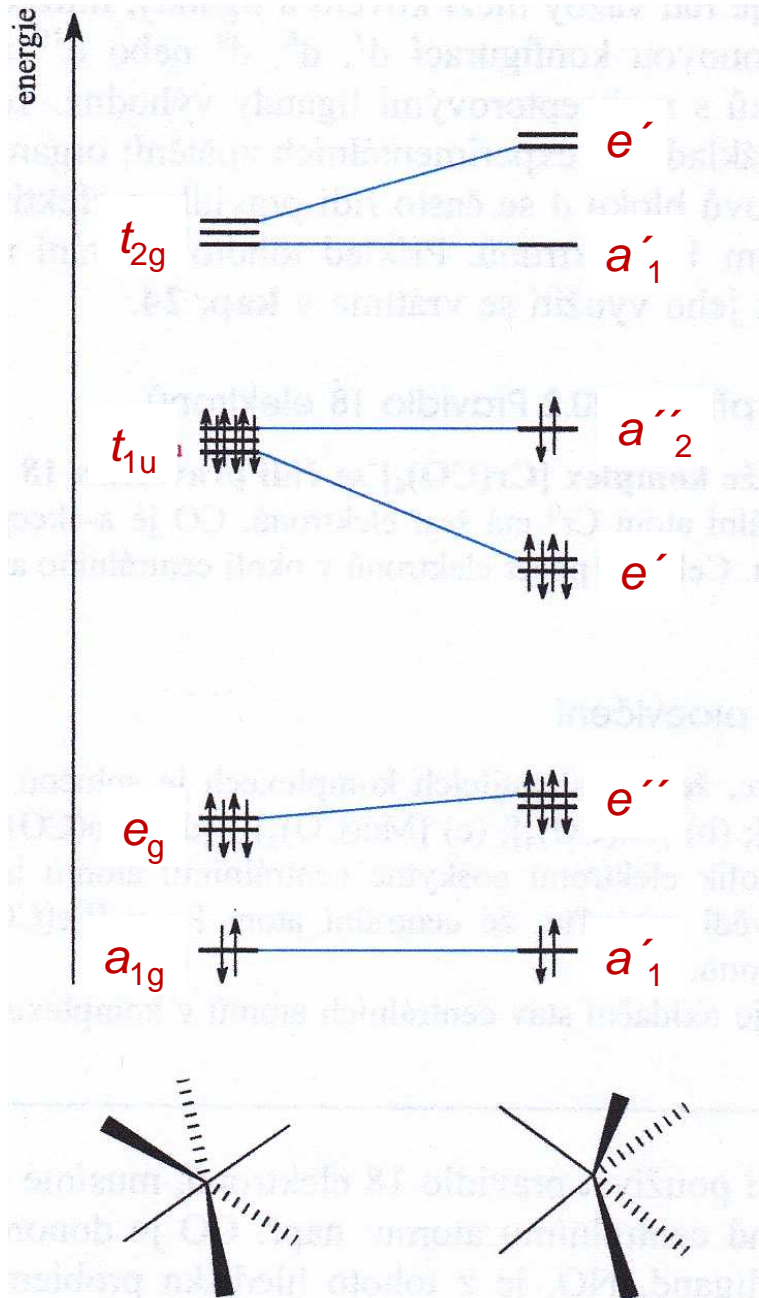


d-block of the metal, 6 electrons



2 weakly
antibonding
orbitals

3 nearly
nonbonding
orbitals



octahedron, O_h

trigonal prism, D_{3h}

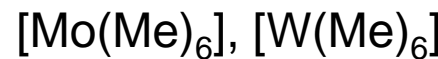
Trigonal prism or octahedron ?

Trigonal prismatic complexes with d^0 or d^1 configuration:



only 12 electrons

Distorted trigonal prism:



Net gain of energy for the trigonal prismatic arrangement

Uveřejněné materiály jsou určeny studentům Vysoké školy chemicko-technologické v Praze jako studijní materiál. Některá textová i obrazová data v nich obsažená jsou převzata z veřejných zdrojů. V případě nedostatečných citací nebylo cílem autorky záměrně poškodit autora/y původního díla.

S případnými výhradami se prosím obracejte na autorku tohoto výukového materiálu, aby bylo možno zjednat nápravu.



The published materials are intended for students of the University of Chemistry and Technology, Prague as a study material. Some text and image data contained therein are taken from public sources. In the case of insufficient quotations, the author's intention was not to intentionally infringe the possible author(s) rights to the original work.

If you have any reservations, please contact the author(s) of the specific teaching material in order to remedy the situation.

Properties and reactivity of coordinated ligands

Small aprotic molecules

Small protonizable molecules

Polar molecules

Covalent molecules

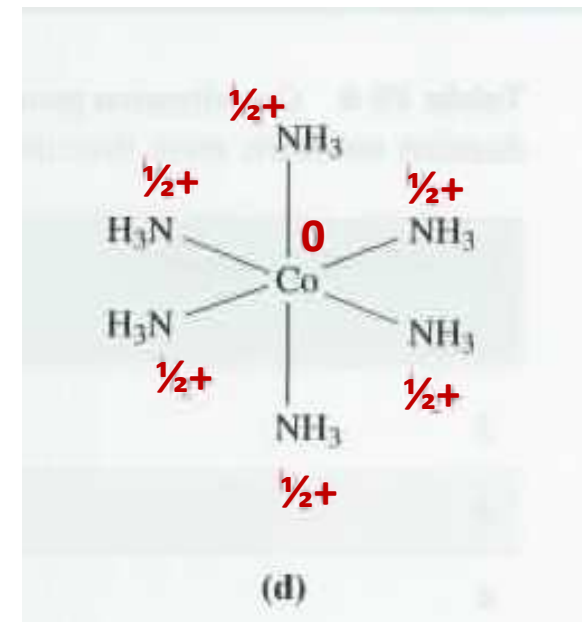
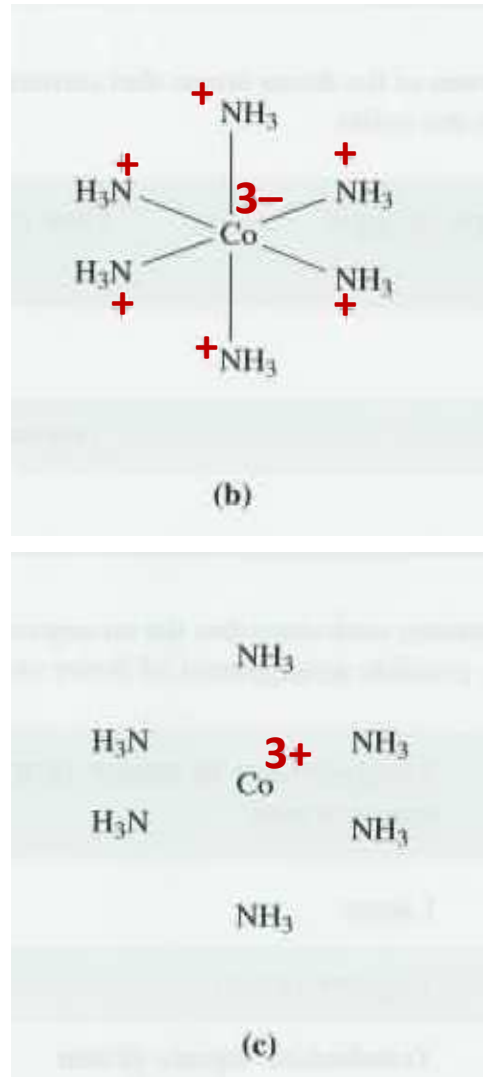
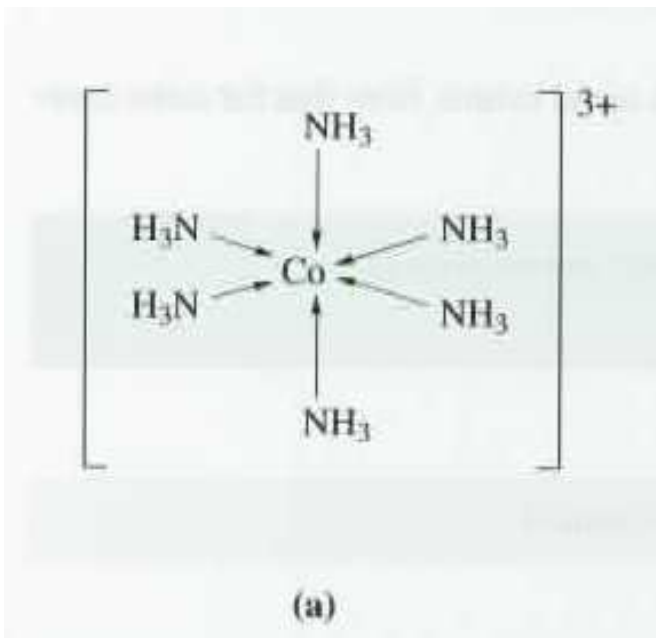


EUROPEAN UNION
European Structural and Investing Funds
Operational Programme Research,
Development and Education

MŠMT
MINISTRY OF EDUCATION,
YOUTH AND SPORTS

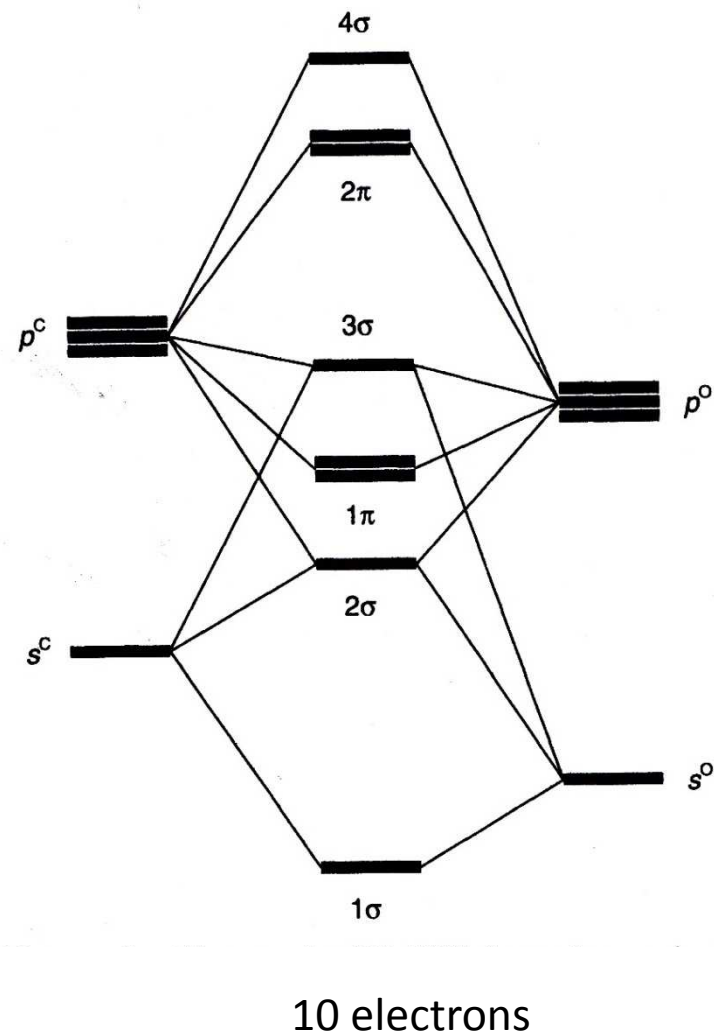
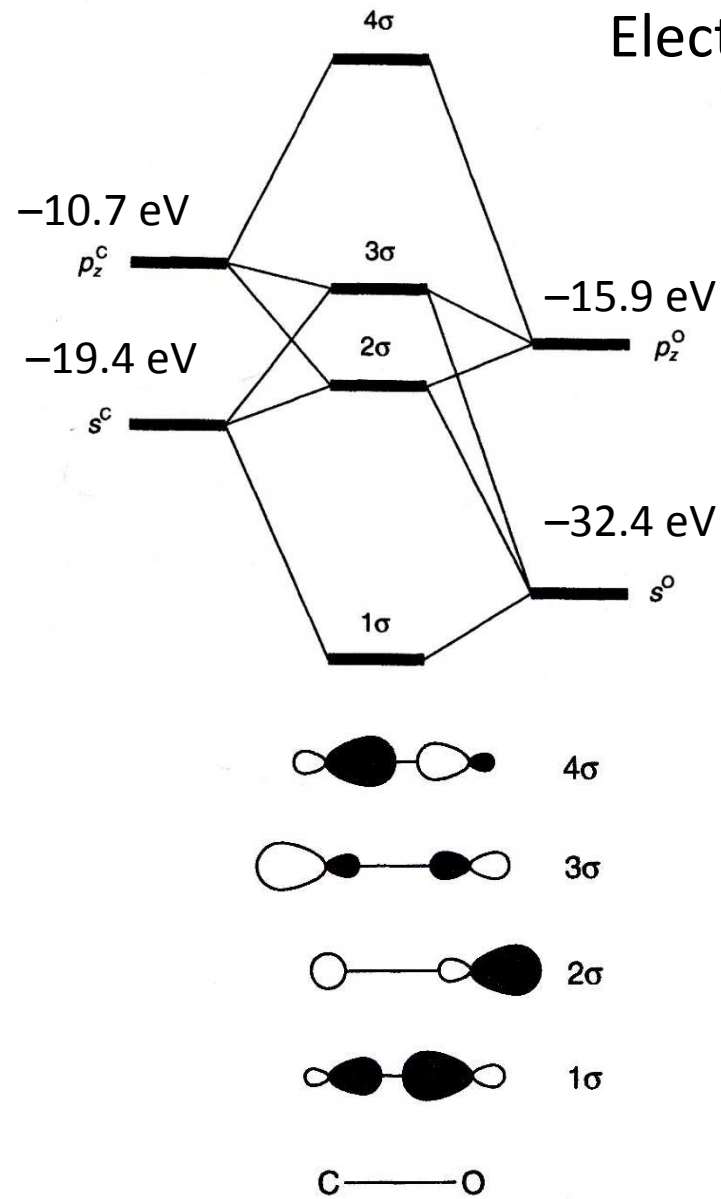


Pauling's electroneutrality principle

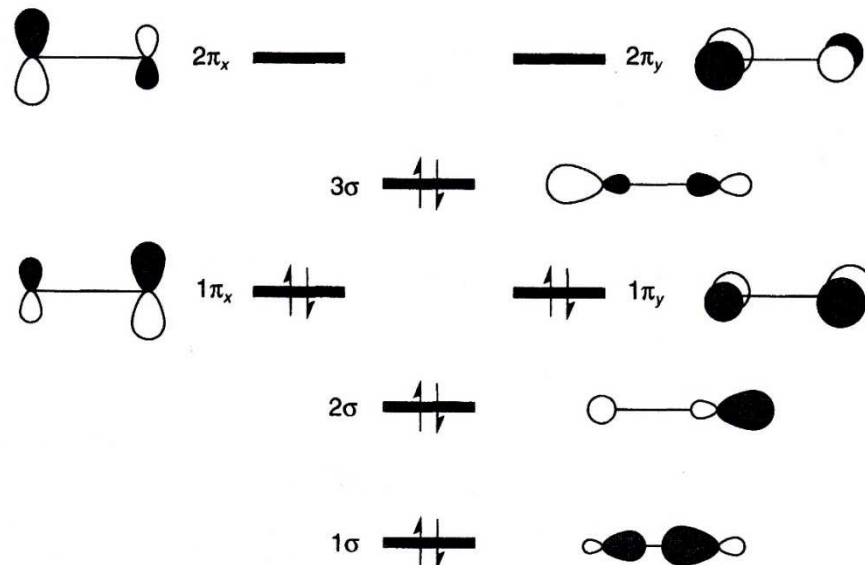


Re-distribution of charge, max. $|1|$ on any single atom, ideally close to 0

Small molecules: CO, CN⁻, N₂, NO; π-acceptors

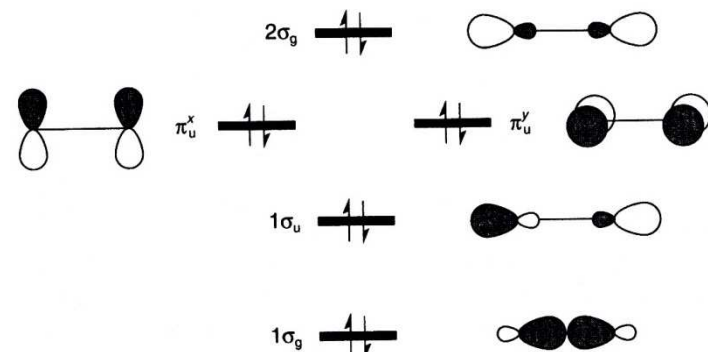


Electronic structure of CO



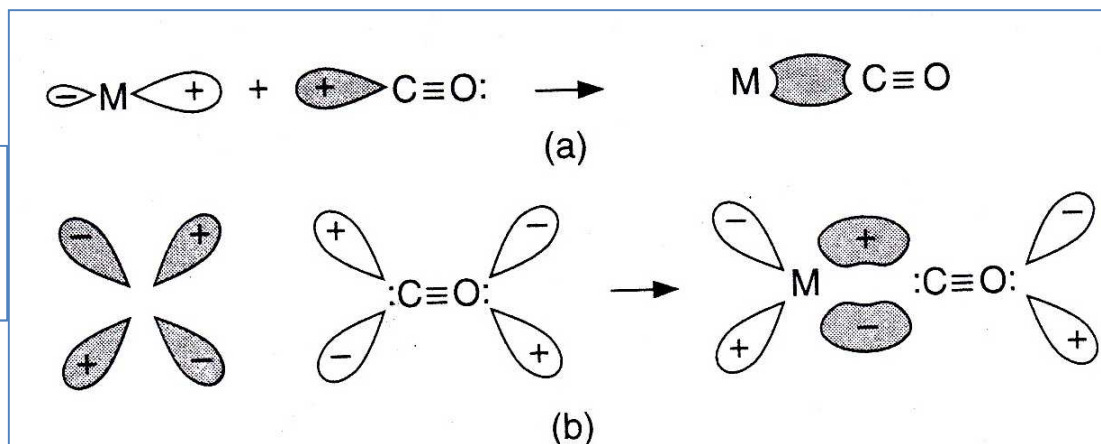
Electronic structure of nitrogen

no polarization
less accessible frontier orbitals



Polarity of the frontier orbitals

Bonding properties:



single – triple and
double – double
bond resonance

Properties of coordinated CO

Measure of the π -back donation

- C–O distance: only small changes
- M–C distance
- CO stretching frequencies

free CO vibration frequency: 2143 cm^{-1}

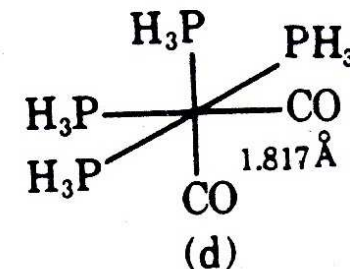
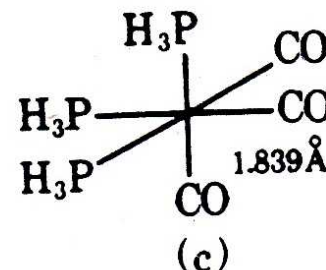
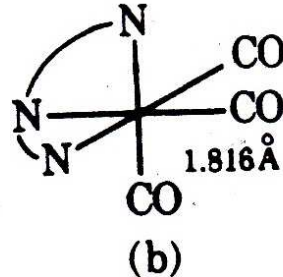
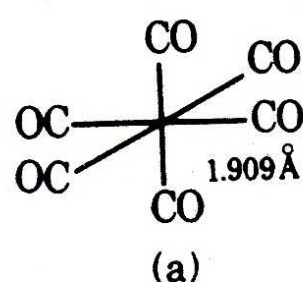


Figure 16-3 Cr–C bond distances in (a) $\text{Cr}(\text{CO})_6$, (b) $\text{fac}-[\text{H}_2\text{N}(\text{CH}_2)_2\text{NH}(\text{CH}_2)_2\text{NH}_2]\text{-Cr}(\text{CO})_3$, (c) $\text{fac}-(\text{PH}_3)_3\text{Cr}(\text{CO})_3$, and (d) $\text{cis}-(\text{PH}_3)_4\text{Cr}(\text{CO})_2$.

$\nu(\text{CO}) \sim 2000\text{ cm}^{-1}$ $\nu(\text{CO}) \sim 1900, \sim 1760\text{ cm}^{-1}$

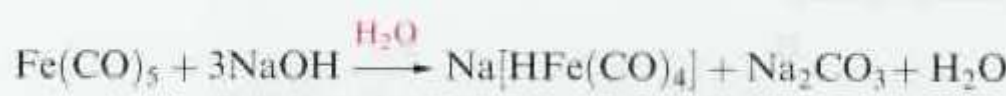
Influence of the central atom

$[\text{Mn}(\text{CO})_6]^+$	~ 2090	$[\text{Mn}(\text{dien})(\text{CO})_3]^+$	$\sim 2020, \sim 1900$	$[\text{Ni}(\text{CO})_4]$	~ 2060
$[\text{Cr}(\text{CO})_6]$	~ 2000	$[\text{Cr}(\text{dien})(\text{CO})_3]$	$\sim 1900, \sim 1760$	$[\text{Co}(\text{CO})_4]^-$	~ 1890
$[\text{V}(\text{CO})_6]^-$	~ 1860			$[\text{Fe}(\text{CO})_4]^{2-}$	~ 1790
$[\text{W}(\text{CO})_6]$	2115, 1998, 1977				

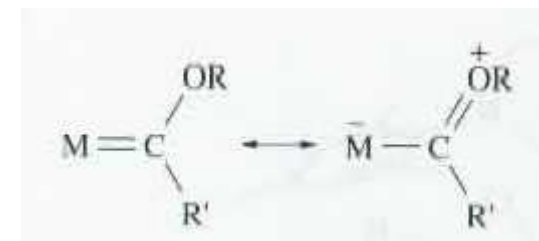
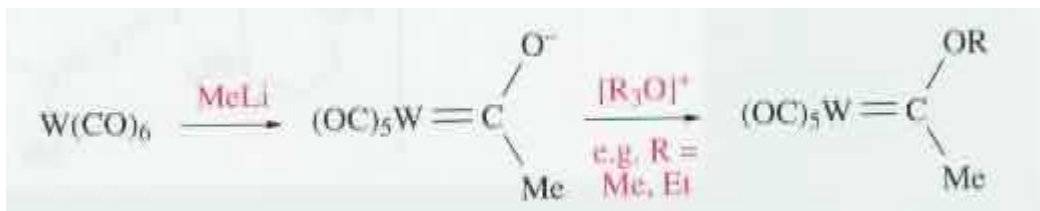
Reaction of the coordinated CO

with nucleophile:

- OH⁻ hydrido complexes + carbonate



- LiMe – Fischer carbenes



Isoelectronic with CO

- Cyanide
 - worse π -acceptor capacity
- Isocyanides
 - comparable π -acceptor capacity, similar evidence (M-L bond length, vibration)
difference: better Lewis base, can act as a pure σ -donor (no need of a metal rich in electrons)
- Dinitrogen

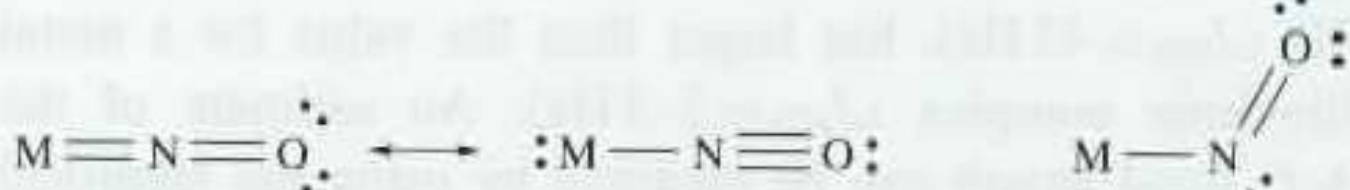
$[\text{Ru}(\text{NH}_3)_5](\text{N}_2)]^{2+}$, discovered in 1965
linear bond, quantitative difference
free 2331 cm^{-1}
coordinated $1930 - 2230 \text{ cm}^{-1}$

NO – nitrogen monoxide

Biological importance

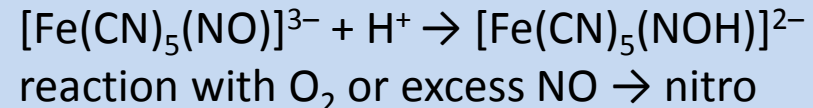
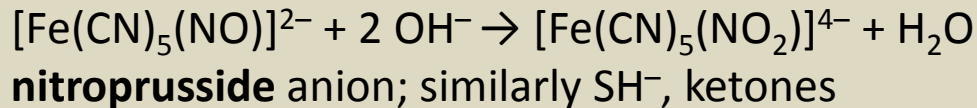
MO scheme similar to CO. 1 electron more in an antibonding MO; radical.

2 bonding
modes:



Linear – XL donor (3 electrons)
approx. NO^+ , electrophilic character

Bent – X donor (1 electron)
approx. NO^- , nucleophile



Sodium nitroprusside is intravenously infused in cases of acute hypertensive crises. Its effects are usually seen within a few minutes. Signalling function of released NO.

3 electron donor – stoichiometrical relationship:

$[(\text{cp})\text{Cu}(\text{CO})]$ and $[(\text{cp})\text{Ni}(\text{NO})]$ are isoelectronic

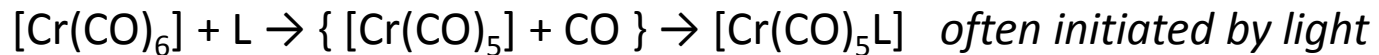
$3 \text{CO} = 2 \text{NO}$:

$[\text{Fe}(\text{CO})_5]$, $[\text{Fe}(\text{CO})_2(\text{NO})_2]$; $[\text{Co}(\text{CO})_3(\text{NO})]$; $[\text{Mn}(\text{CO})_4(\text{NO})]$, $[\text{Mn}(\text{CO})(\text{NO})_3]$; $[\text{Cr}(\text{CO})_6]$, $[\text{Cr}(\text{NO})_4]$.

NO – nitrogen monoxide

CO and NO – overall reactivity

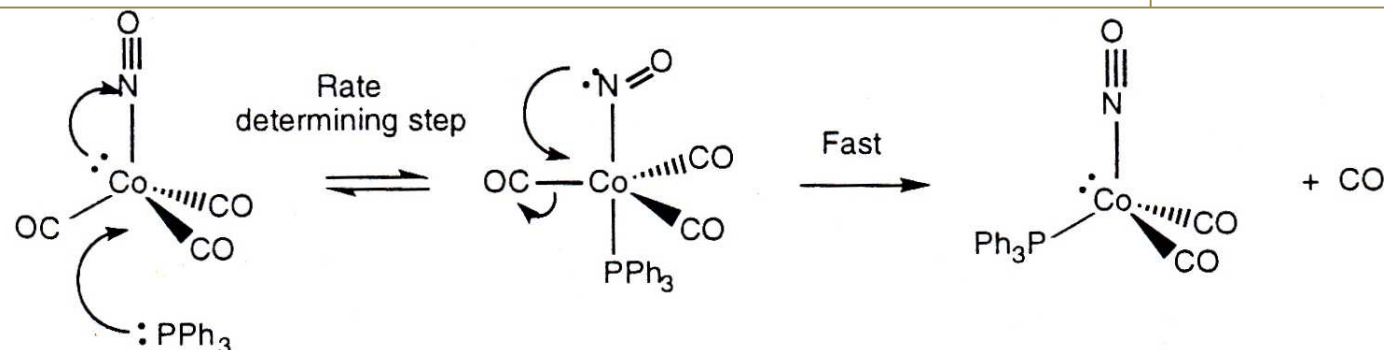
Carbonyl complexes: dissociative mechanism



Nitrosyl complexes: associative mechanism



NO: Reaction mechanism with interchange of bonding modes:



Distinguishing between the NO bonding modes:

IR v (cm ⁻¹)	free NO	1876	bonded NO ⁺ (linear)	1600 – 2000
	free NO ⁺	2200	bonded NO ⁻ (bent)	1400 – 1650

¹⁵N NMR – ¹⁵N labeled NO

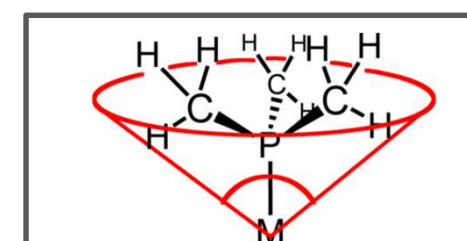
linear $-50 \text{ ppm} \leq \delta \leq 50 \text{ ppm}$

bent $\delta \geq 350 \text{ ppm}$

Phosphanes, PR_3

Comparison with CO: better σ donors, π - acidity to ?? orbitals (d AO of P or σ^* MO of PR_3)
remarkable variation of steric demand (Tollman cone angle)
electronic influence of R; PF_3 comparable with CO

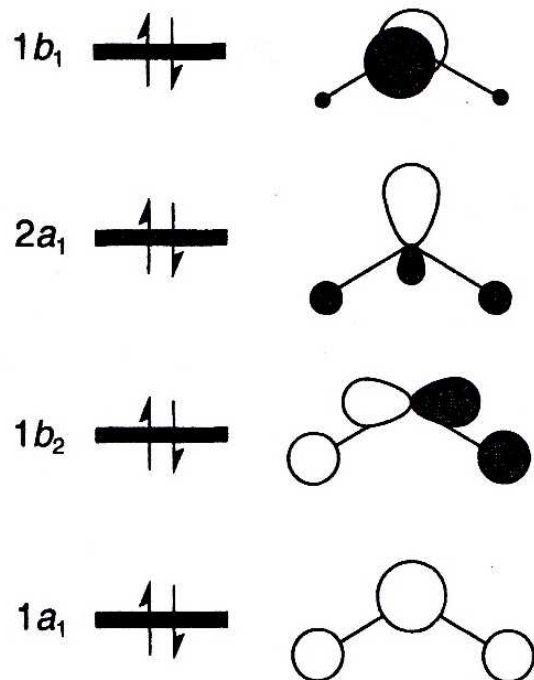
		CO vibration frequencies (cm^{-1})
$[\text{Et}_3\text{P}]$	$\text{Mo}(\text{CO})_3]$	1937, 1841
$[(\text{PhO})_3\text{P}]$	$\text{Mo}(\text{CO})_3]$	1994, 1922
$[\text{Cl}_2(\text{PhO})\text{P}]$	$\text{Mo}(\text{CO})_3]$	2027, 1969
$[\text{Cl}_3\text{P}]$	$\text{Mo}(\text{CO})_3]$	2024, 1991
$[\text{F}_3\text{P}]$	$\text{Mo}(\text{CO})_3]$	2090, 2055
$[(\text{dien})]$	$\text{Mo}(\text{CO})_3]$	1898, 1758



Steric demands of a ligand describes Tollman's cone angle
 PMe_3 118°
 P(t-Bu)_3 182°

Deprotoinizable ligands: water, ammonia (amines)

water MO's



General:

If any group attached to the donor atom is capable of leaving as a cation, then this leaving ability will be enhanced by coordination.

pK_a values of some aqua complexes and hydrated ions

K ⁺ (aq)	14.5	[Zn(H ₂ O) ₆] ²⁺	9.0
[Al(H ₂ O) ₆] ³⁺	5.0	[Cu(H ₂ O) ₆] ²⁺	8.0
[Fe(H ₂ O) ₆] ³⁺	2.2	[Co(H ₂ O) ₆] ²⁺	9.7
[Ni(H ₂ O) ₆] ²⁺	9.9	[Mn(H ₂ O) ₆] ²⁺	10.6

pK_a values of some metal-amine complexes

[Ru(NH ₃) ₆] ³⁺	12.4	[Pt(NH ₃) ₅ (NH ₂)] ³⁺	10.1
[Ru(NH ₃) ₆] ²⁺	7.9	[Pt(NH ₃) ₆] ⁴⁺	7.2
[Co(NH ₃) ₆] ³⁺	> 14	cis-[Pt(NH ₃) ₄ Cl ₂] ²⁺	9.8
		[Pt(en) ₃] ⁴⁺	5.5

Carbonate dehydratase, carboanhydrase (CA)



Key reaction in:

1. photosynthesis
2. breathing
3. calcification
4. pH regulation

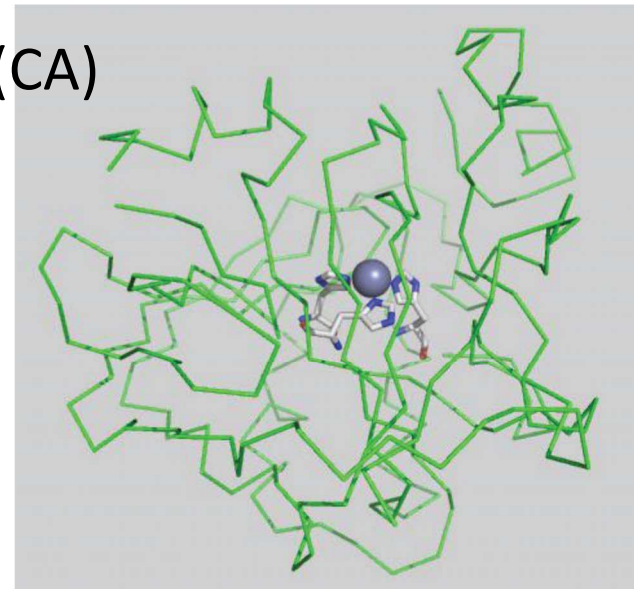
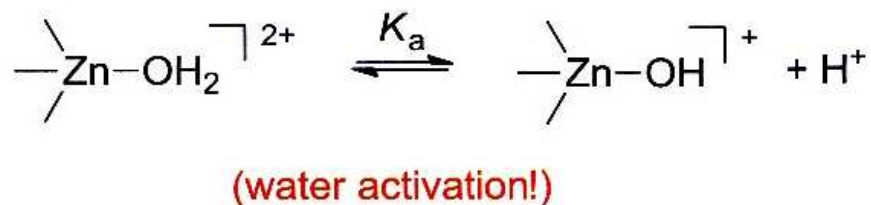
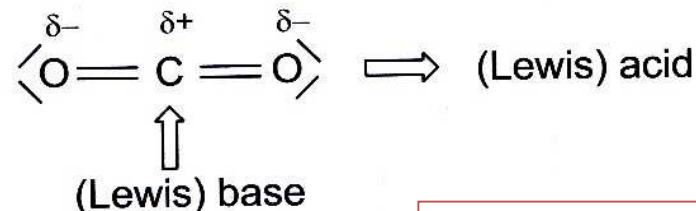


Figure 12.1

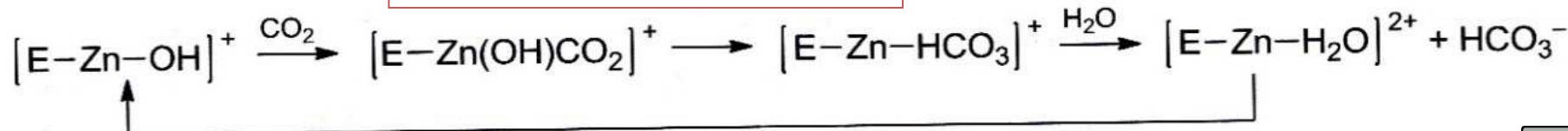
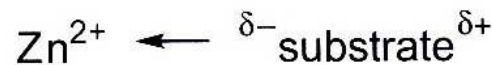
Structural representation of human CA II, showing the protein folding and the Zn^{2+} coordination to three imidazole rings of histidine side chains (PDB code 4CAC) [8].

Non-enzymatic catalysis: combine both LK and LB (*push-pull* effect)

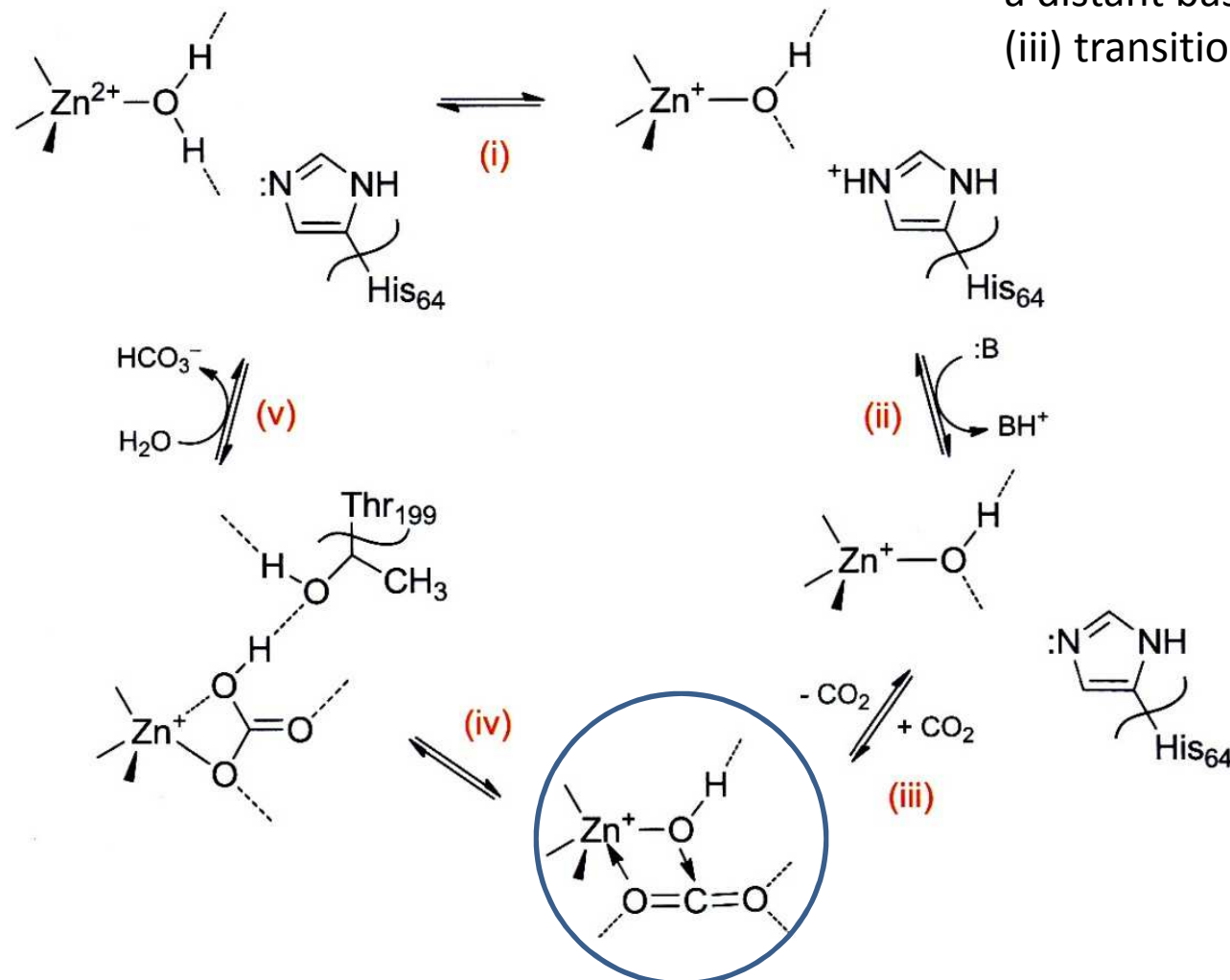


Enzymatic catalysis

sulfite, HBrO , $[\text{M-OH}]^+$



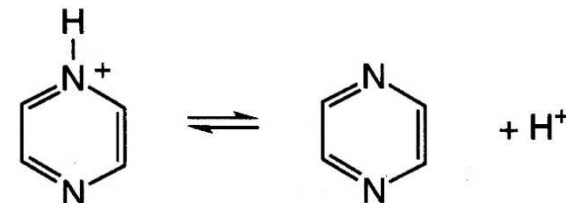
Carbonate dehydratase, (CA), hypothetical reaction mechanism



steps (i) and (ii) proton to a distant base (buffer)
 (iii) transition state

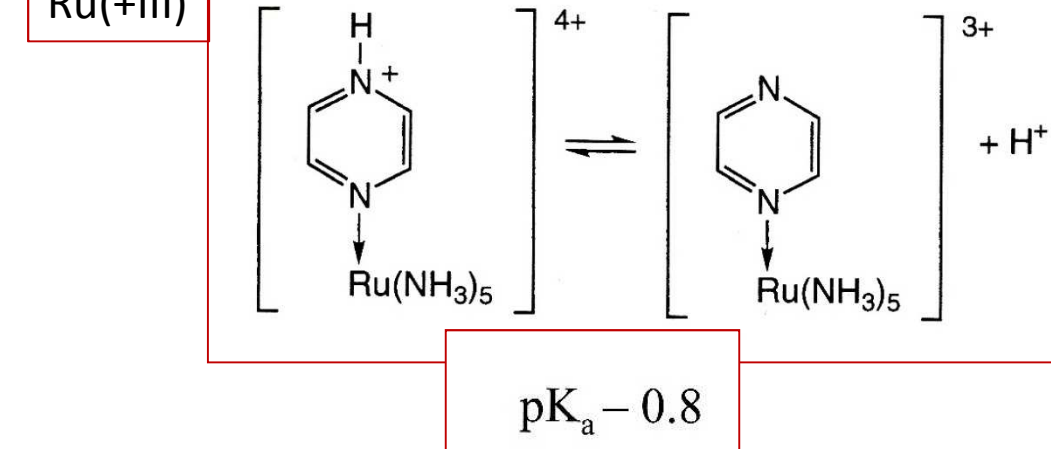
Inhibitors of CA: similar substrates formate, HSO_3^- , sulfonamides form more stable intermediate

Pyrazine / pyrazinium



pK_a 0.6

Ru(+III)



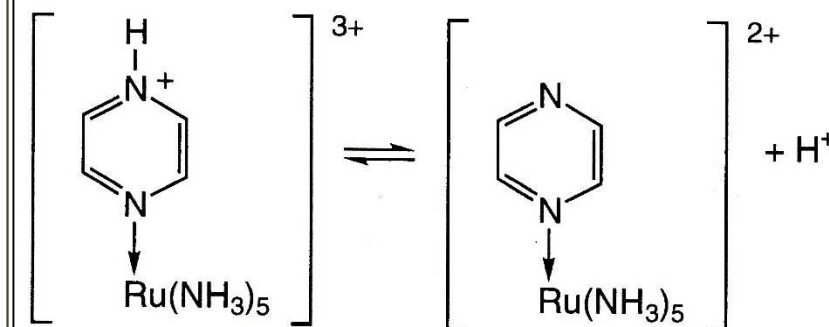
$pK_a - 0.8$

Stronger acid due to the electron-withdrawing metal centre (= ligand polarization)

But

after coordination to Ru(+II)
decrease of acidity was observed:

Competition between polarization
and π -back bonding .

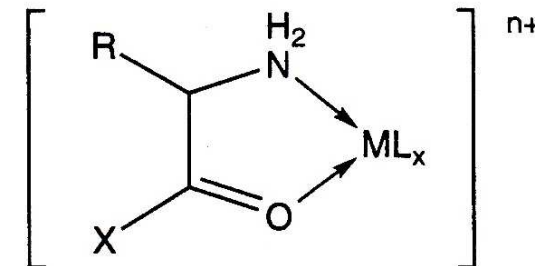


Hydrolysis of aminoacids esters (amides)

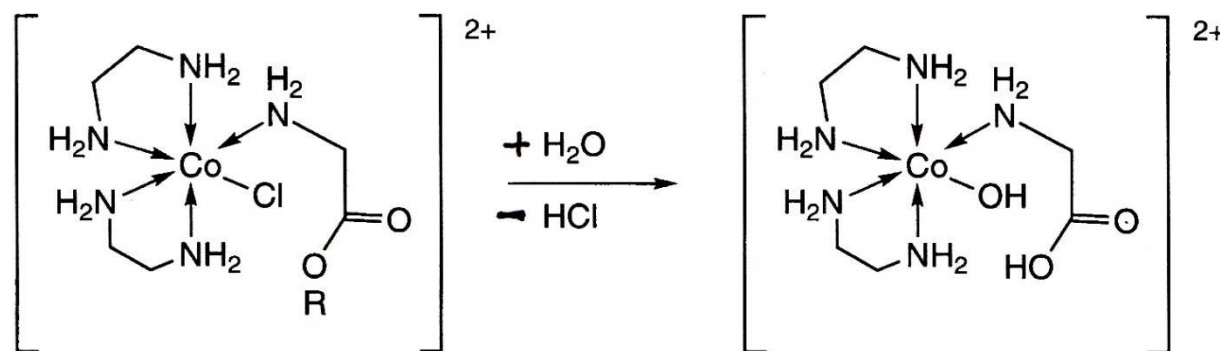
Hydrolysis of methyl glycinate

	rate/ M ⁻¹ s ⁻¹
k_{uncat}	1.28
k_{H^+}	28.3
$k_{\text{Cu}^{2+}}$	7.6×10^4

With Cu – chelate formation: rate enhancement

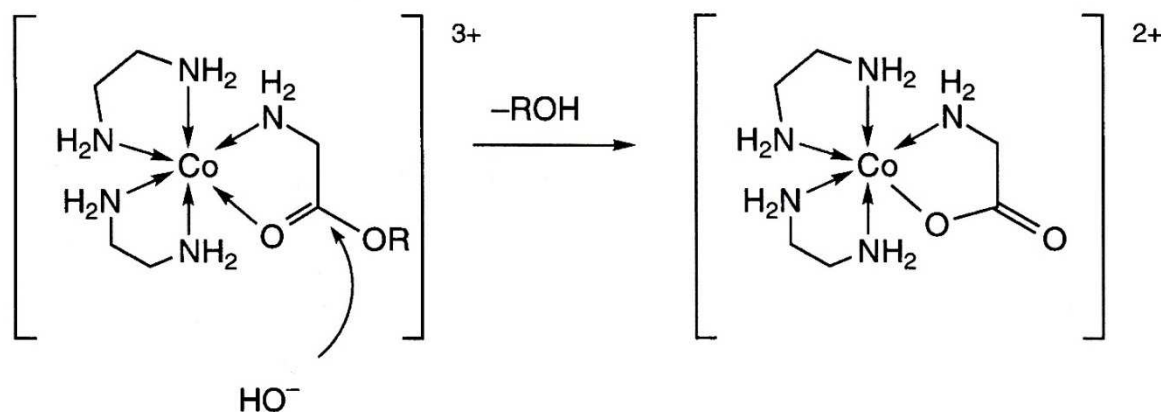
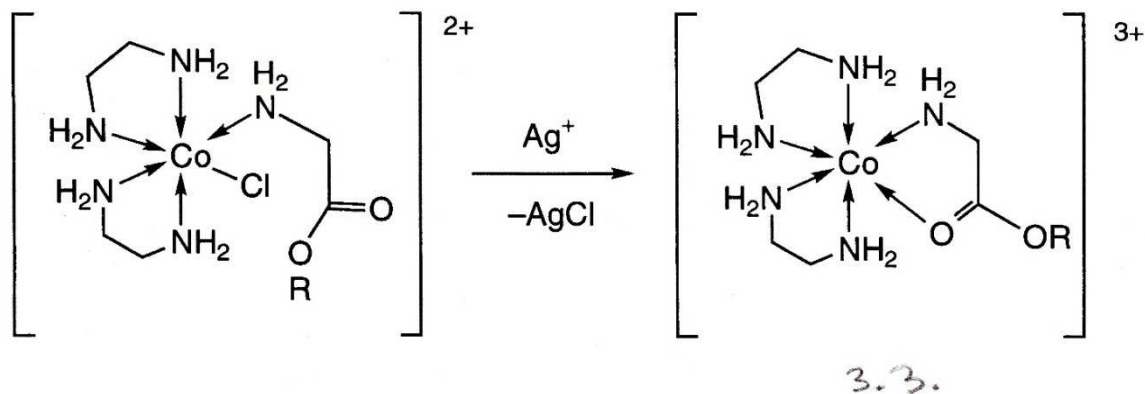


With kinetically inert Co(+III) – monodentate bonding, hydrolysis rate like in H⁺

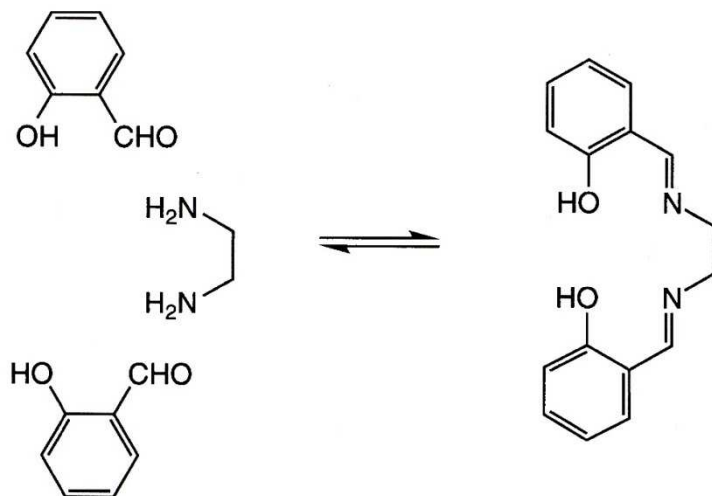


Hydrolysis of aminoacids esters (amides)

Chelate formation with Co(+III)



Imines

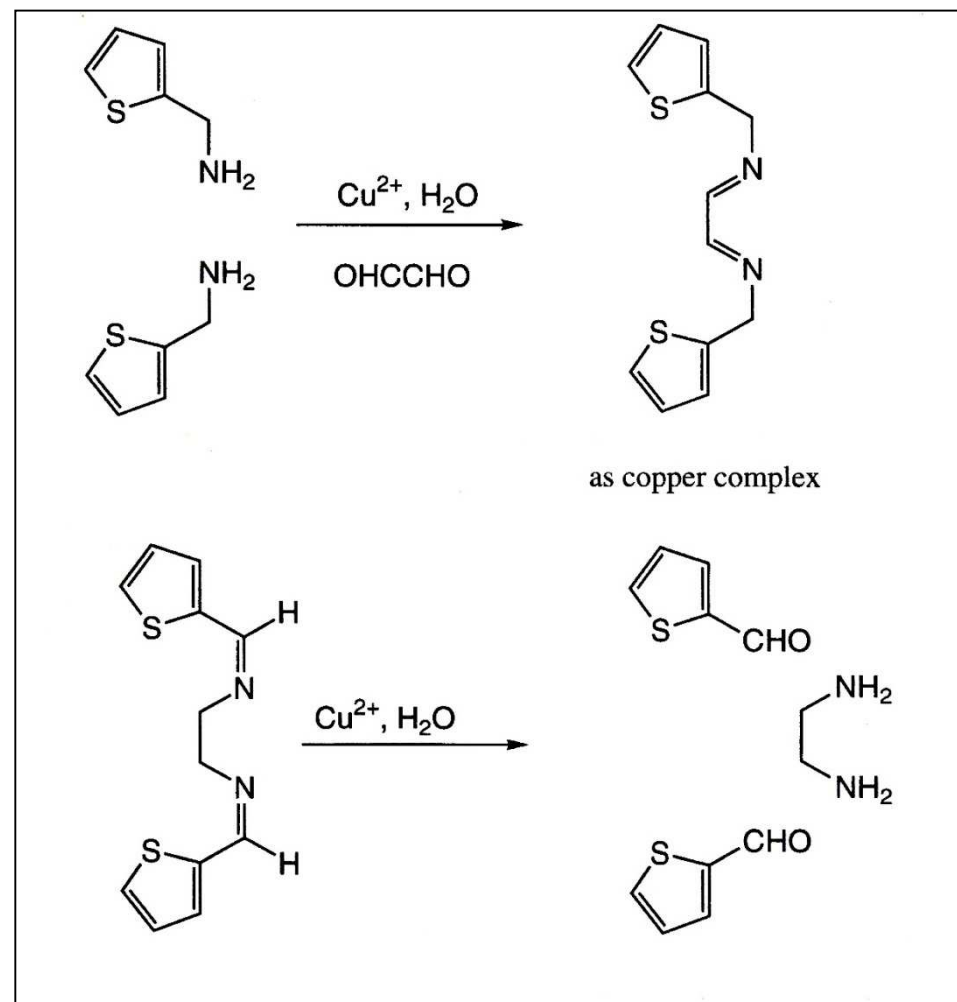


Schiff base, abbrev. salen or sal₂en

Factors:

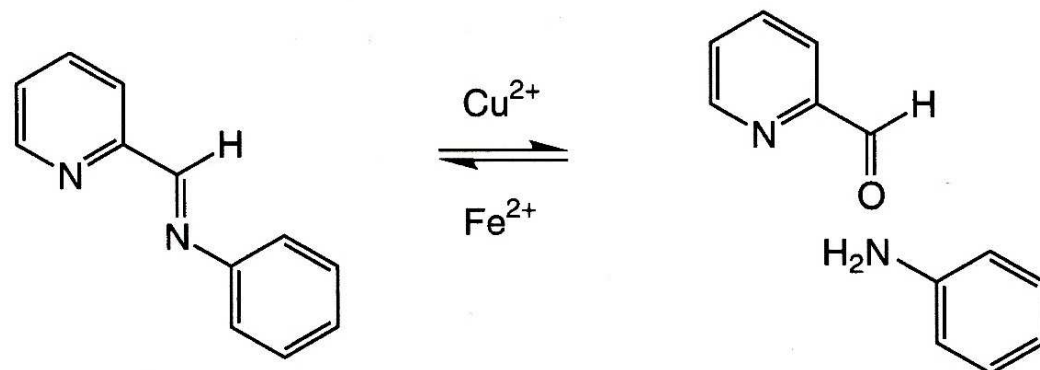
- d-orbitals, possible bonding interactions
- metal ion charge
- ligand charge
- ligand configuration

ligand variation – imine formation / hydrolysis,
Cu(+II)

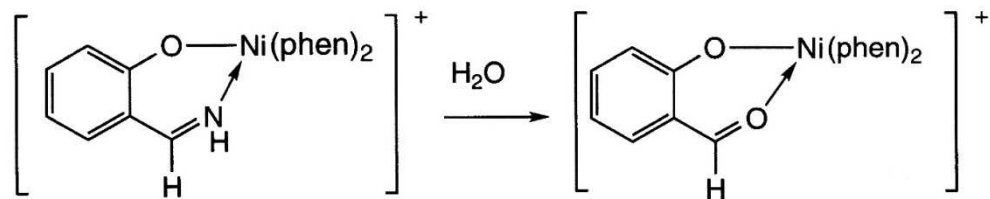
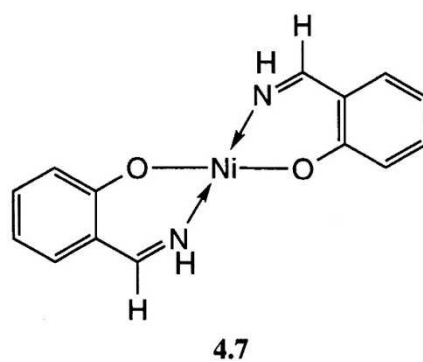


Imines

Metal nature,
hydrolysis Cu(+II) 10⁵ faster

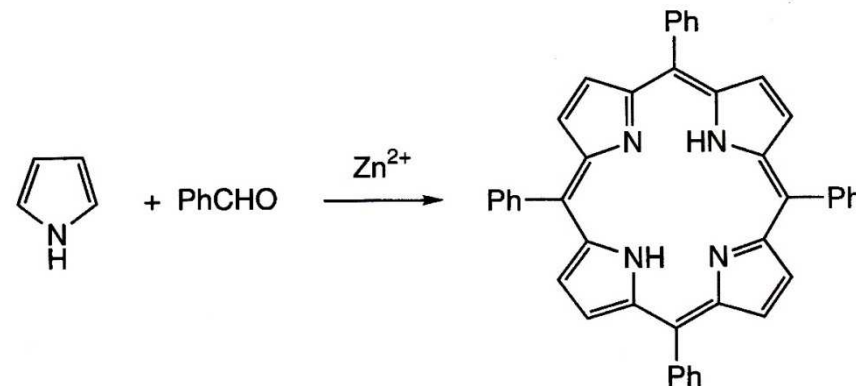


Charge of the complex:



Template syntheses

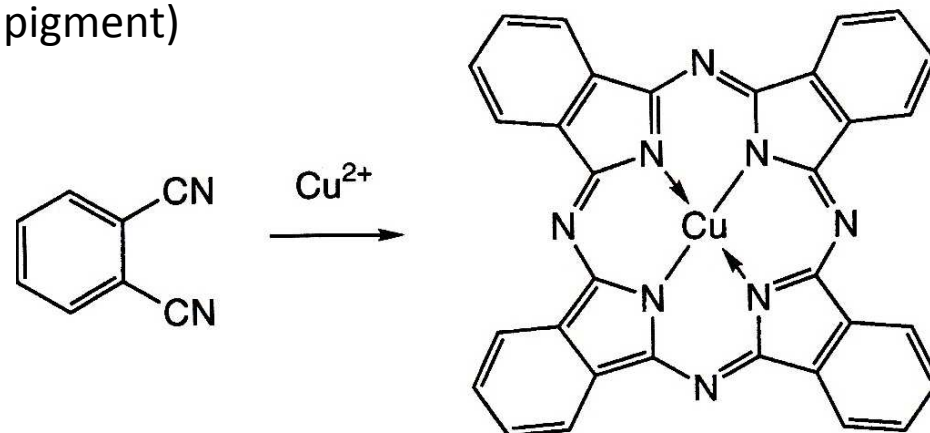
Macrocycles



6.21

Figure 6-20. The [4+4] condensation of benzaldehyde and pyrrole in the presence of Lewis acids yields *meso*-tetraphenylporphyrin.

copper phthalocyanine (blue pigment)



chlorated (8 Cl) – green pigment

Template syntheses

Encapsulatin ligand

kinetically inert metal ion

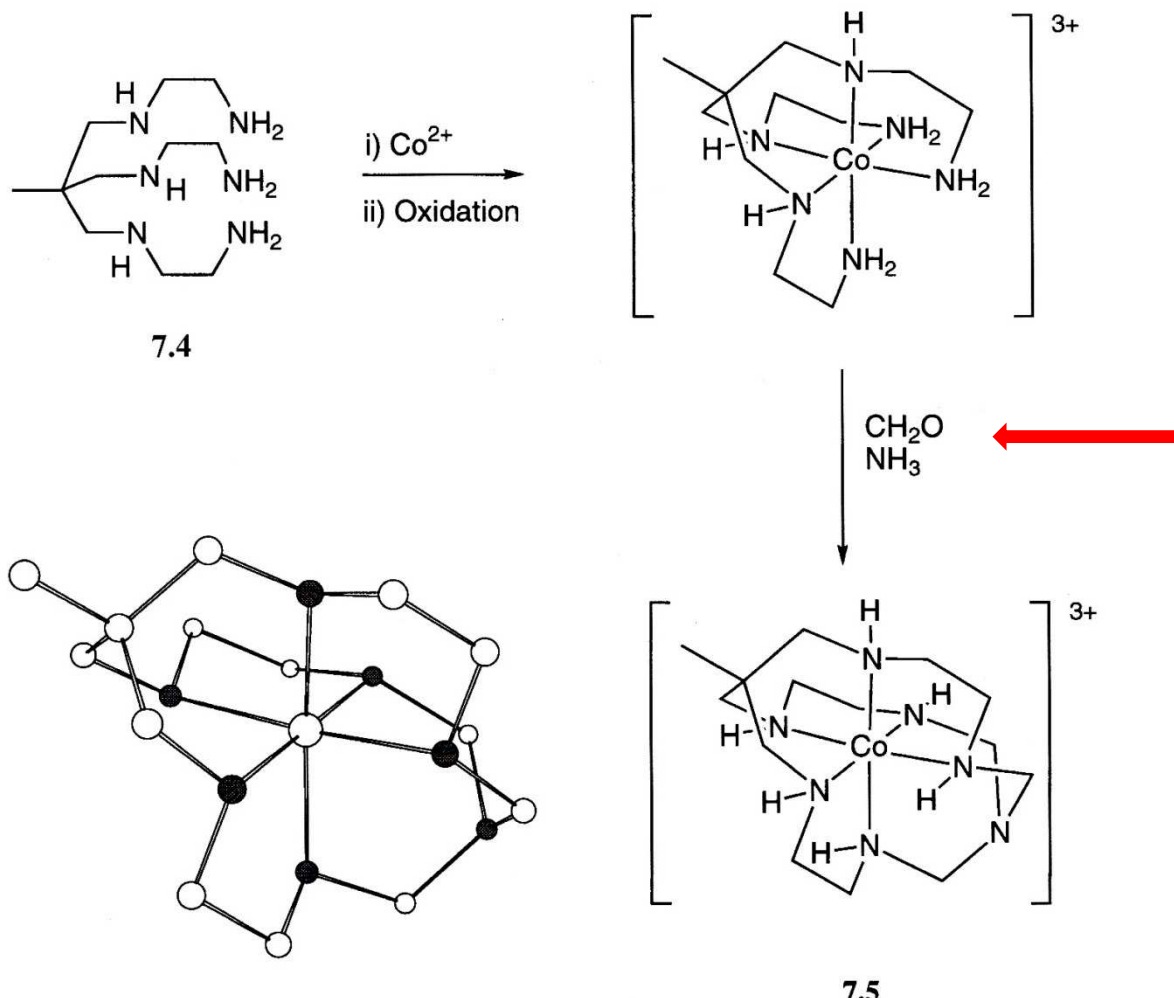


Figure 7-9. The condensation of the cobalt(III) complex of the hexadentate ligand **7.4**, which contains three primary amino groups, with formaldehyde and ammonia, gives the encapsulated complex **7.5**. A view of the cation **7.5** as found in the solid state structure of its perchlorate salt is also presented.

Template syntheses

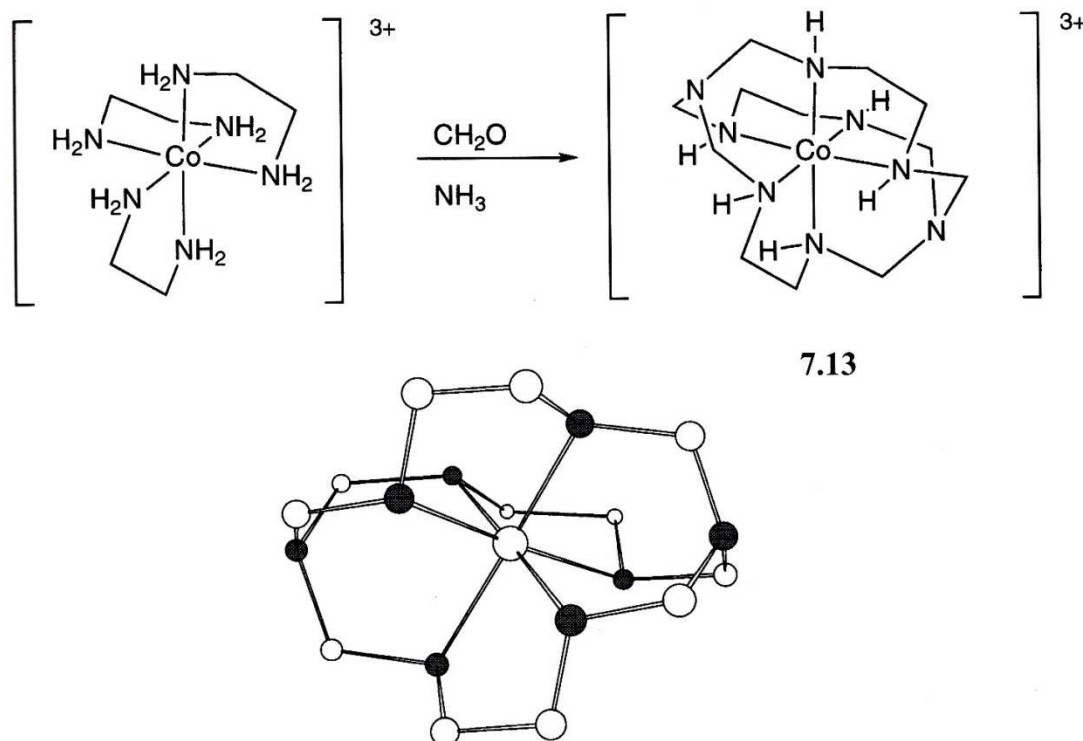
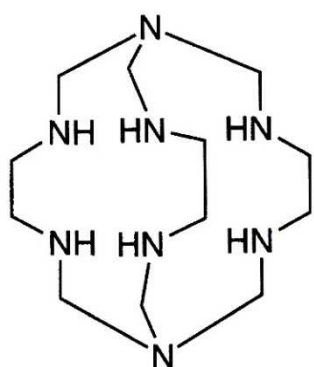


Figure 7-12. The reaction of $[\text{Co}(\text{en})_3]^{3+}$ with formaldehyde and ammonia gives cobalt(II) sepulchrate 7.13. A representation of the complex ion in the solid state is also presented.



Uveřejněné materiály jsou určeny studentům Vysoké školy chemicko-technologické v Praze jako studijní materiál. Některá textová i obrazová data v nich obsažená jsou převzata z veřejných zdrojů. V případě nedostatečných citací nebylo cílem autorky záměrně poškodit autora/y původního díla.

S případnými výhradami se prosím obracejte na autorku tohoto výukového materiálu, aby bylo možno zjednat nápravu.



The published materials are intended for students of the University of Chemistry and Technology, Prague as a study material. Some text and image data contained therein are taken from public sources. In the case of insufficient quotations, the author's intention was not to intentionally infringe the possible author(s) rights to the original work.

If you have any reservations, please contact the author(s) of the specific teaching material in order to remedy the situation.

Ligand substitution

Rate laws and stoichiometric mechanism

Intimate mechanism

Isomerisation

- pentacoordinated intermediate
- octahedral tris-chelates

Entering group, leaving group, and metal effects

Spectator ligand effects

- base-assisted hydrolysis
- trans-effect

No mechanism can be taken as absolute. Currently, it is only possible to propose the most probable mechanism.



EUROPEAN UNION
European Structural and Investing Funds
Operational Programme Research,
Development and Education

MS
MT
MINISTRY OF EDUCATION,
YOUTH AND SPORTS



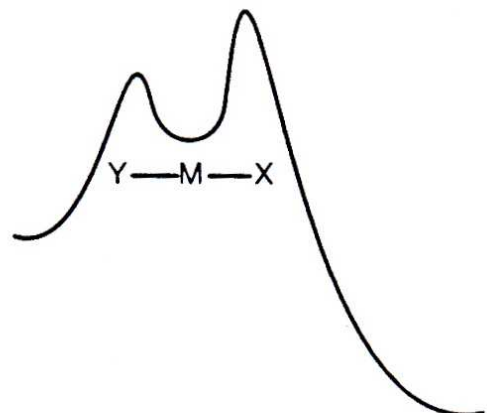
Mechanisms

associative, A

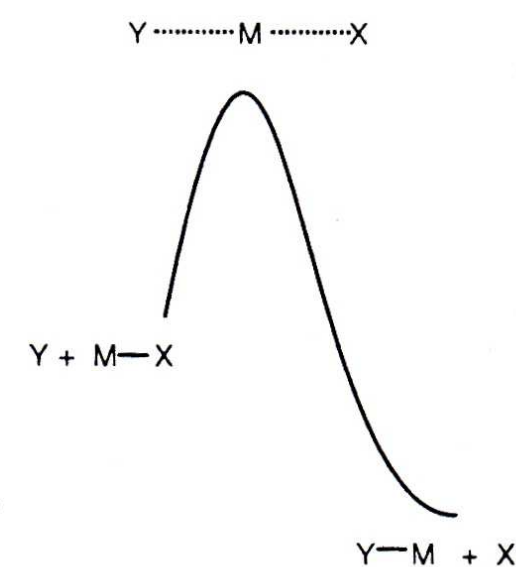
intermediate, I

dissociative, D

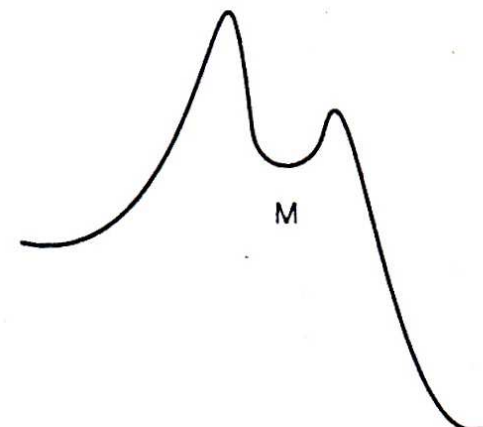
(a)



(b)



(c)



A

I_a

I

I_d

D



Transition state, intermediate?

Rate laws

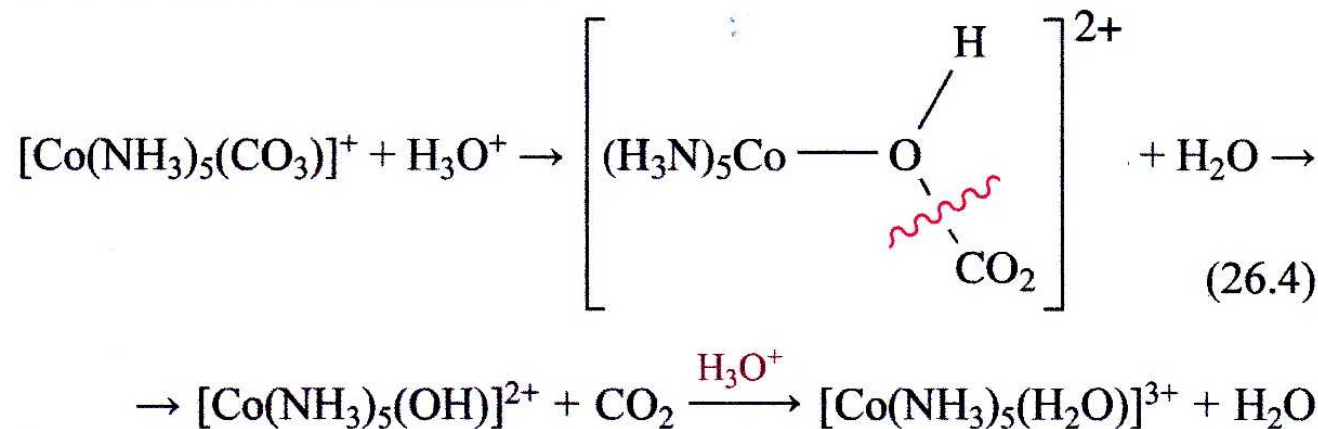
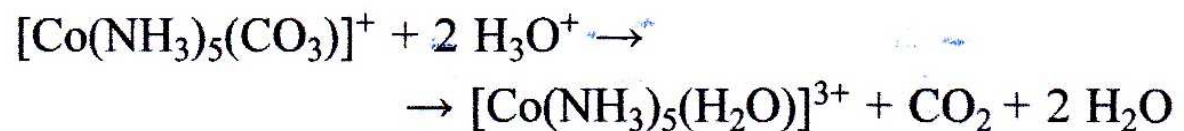
Limiting Forms of Rate Laws Depending on Magnitude of Denominator Term in [Y]^{a,b}

Stoichiometric Mechanism	Very Large [Y] Term	Very Small [Y] Term
D	$k_1[L_5MX]$	$\frac{k_1k_2[L_5MX][Y]}{k_{-1}[X]}$
A	$\frac{k_1[L_5MX][Y]}{k_{-1} + k_2}$	$\frac{k_1[L_5MX][Y]}{k_{-1} + k_2}$
I	$k[L_5MX]$	$kK[L_5MX][Y]$

^aFor example, $k_2[Y]$, $K[Y]$, $[Y]$.

Intermediate : Eigen-Wilkins mechanism
low conc. of Y – first order; high conc. of Y – second order

Experimental data



Overall view: carbonate substitution by water
Mechanism: carbonate hydrolysis

Water exchange



Table L.2 Rate constants, k , for exchange of OH_2 at 25°C

I_a M = Ti^{II}, V^{III}, Cr^{III}, V^{II}; I/I_a Mn^{II}, Fe^{II}, and Fe^{III}; I_d M = Co^{II} and Ni^{II}

$d^0 \quad d^2 \quad d^3 \quad d^4 \quad d^5 \quad d^6 \quad d^7 \quad d^8$

Metal ion	d^n	k/s^{-1}
$[\text{Na}(\text{OH}_2)_6]^+$	0	8×10^9
$[\text{Mg}(\text{OH}_2)_6]^{2+}$	0	1×10^5
$[\text{Ca}(\text{OH}_2)_6]^{2+}$	0	2×10^8
$[\text{Sr}(\text{OH}_2)_6]^{2+}$	0	4×10^8
$[\text{Al}(\text{OH}_2)_6]^{3+}$	0	1.8
$[\text{Ga}(\text{OH}_2)_6]^{3+}$	0	1×10^3
$[\text{In}(\text{OH}_2)_6]^{3+}$	0	2×10^5
<u>$[\text{Cr}(\text{OH}_2)_6]^{3+}$</u>	3	3×10^{-6}
$[\text{Cr}(\text{OH}_2)_6]^{2+}$	4	7×10^9 m
$[\text{Mn}(\text{OH}_2)_6]^{2+}$	5	3×10^7
$[\text{Fe}(\text{OH}_2)_6]^{3+}$	5	3×10^3
$[\text{Fe}(\text{OH}_2)_6]^{2+}$	6	3×10^6
$[\text{Co}(\text{OH}_2)_6]^{2+}$	7	1×10^6
$[\text{Ni}(\text{OH}_2)_6]^{2+}$	8	3×10^4
$[\text{Cu}(\text{OH}_2)_6]^{2+}$	9	8×10^9 m
$[\text{Zn}(\text{OH}_2)_6]^{2+}$	10	2×10^7

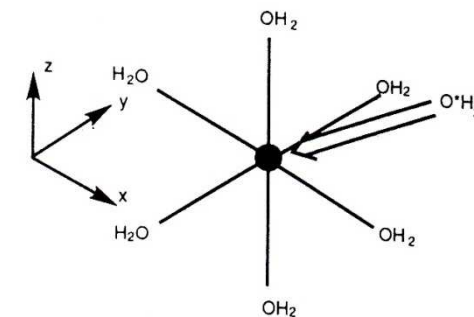


Fig. L.2 The nucleophilic substitution by the labelled water molecule is favoured along the three-fold axis of the octahedron for steric reasons. The metal d_{z^2} and $d_{x^2-y^2}$ orbitals point directly towards the ligands and the d_{xy} , d_{xz} , and d_{yz} orbitals have their maxima in between the axes. If one or more of these orbitals are empty the lone pair on the incoming water molecule can enter into a favourable two-orbital two-electron stabilizing interaction. This encourages an I_a mechanism. However, if they are fully occupied then there is a repulsive interaction between the lone pair and the filled d orbital and an I_a mechanism is less favoured

Rate Constants for Acid Aquation of Some Octahedral Complexes of Co(III) at 25 °C^a

Complex	k (s ⁻¹)	Complex	k (s ⁻¹)
$\{\text{Co}(\text{NH}_3)_5[\text{OP}(\text{OMe})_3]\}^{3+}$	2.5×10^{-4}	$[\text{Co}(\text{NH}_3)_5\text{Cl}]^{2+}$	1.8×10^{-6}
$[\text{Co}(\text{NH}_3)_5(\text{NO}_3)]^{2+}$	2.4×10^{-5}	$[\text{Co}(\text{NH}_3)_5(\text{SO}_4)]^+$	8.9×10^{-7}
$[\text{Co}(\text{NH}_3)_5\text{I}]^{2+}$	8.3×10^{-6}	$[\text{Co}(\text{NH}_3)_5\text{F}]^{2+}$	8.6×10^{-8}
$[\text{Co}(\text{NH}_3)_5(\text{H}_2\text{O})]^{3+}$	5.8×10^{-6}	$[\text{Co}(\text{NH}_3)_5\text{N}_3]^{2+}$	2.1×10^{-9}
		$[\text{Co}(\text{NH}_3)_5(\text{NCS})]^{2+}$	3.7×10^{-10}

A

different X
reaction rates
ranging from 10^{-4}
to 10^{-10} ,
dissociation

Rate Constants for Substitution Reactions of $[\text{Co}(\text{NH}_3)_5(\text{H}_2\text{O})]^{3+}$ with Y^{n-} at 45 °C

Y^{n-}	k (s ⁻¹)
H_2O	10.0×10^{-5}
N_3^-	10.0×10^{-5}
SO_4^{2-}	2.4×10^{-5}
Cl^-	2.1×10^{-5}
NCS^-	1.6×10^{-5}

B

different Y
similar reaction rates
dissociation

X – leaving group
Y – entering group

Rates of Substitution of $[\text{Ti}(\text{H}_2\text{O})_6]^{3+}$ by Y^{n-} at 13 °C

Y^{n-} ($n = 0$)	k ($M^{-1}\text{s}^{-1}$)	Y^{n-} ($n = 1$)	k ($M^{-1}\text{s}^{-1}$)
$\text{ClCH}_2\text{CO}_2\text{H}$	6.7×10^2	NCS^- (8–9 °C)	8.0×10^3
MeCO_2H	9.7×10^2	$\text{ClCH}_2\text{CO}_2^-$	2.1×10^5
H_2O	8.6×10^3	MeCO_2^-	1.8×10^6

C

different Y
reaction rates ranging
from 10^2 to 10^6 ,
association

Activation parameters: entropy , volume

Eyring equation

$$k = \frac{k_B T}{h} e^{\frac{\Delta S^\ddagger}{R}} e^{-\frac{\Delta H^\ddagger}{RT}}$$

Entropy of activation term Enthalpy of activation term

k	rate constant
k_B	Boltzmann constant
h	Planck constant
R	molar gas constant
T	temperature [K]
S	entropy of activation
H	enthalpy of activation

Entropy of activation

large, negative values of $\Delta S^\ddagger \Rightarrow$ association

Volume of activation

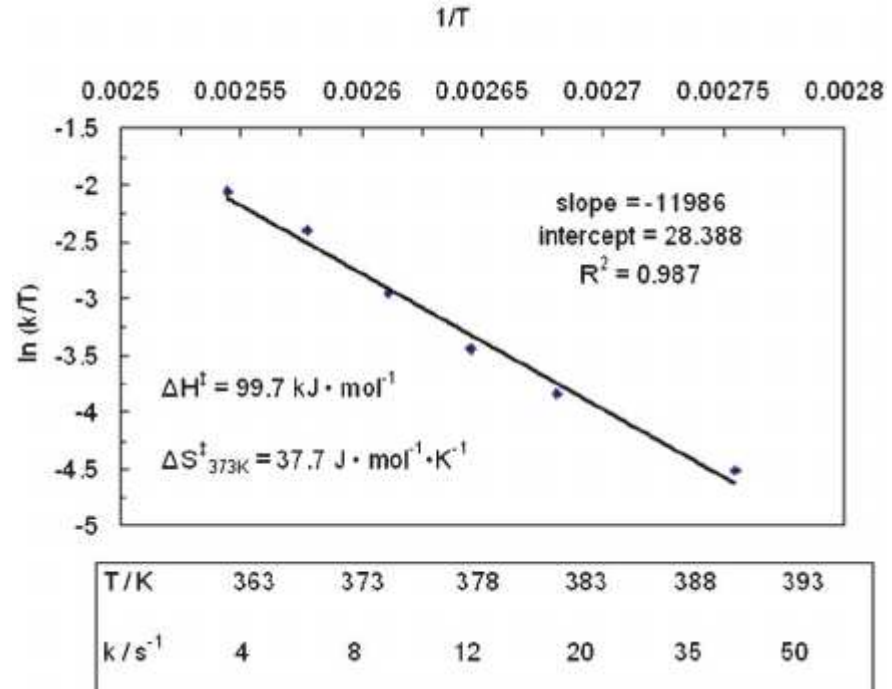
from the pressure dependence of rate constant
large, negative values of $\Delta V^\ddagger \Rightarrow$ association

Caution: solvent reorganisation!

<https://image.slidesharecdn.com/lecture6-150330025135-conversion-gate01/95/lecture6-46-638.jpg?cb=1427702038>

Eyring plot

determination of ΔS^\ddagger from $\ln(k/T)$ vs. $1/T$



$$\ln\left(\frac{k}{T}\right) = \frac{\Delta H^\ddagger}{RT} + \ln\left(\frac{k_B}{h}\right) + \frac{\Delta S^\ddagger}{R}$$

$$\text{intercept: } \ln\left(\frac{k_B}{h}\right) + \frac{\Delta S^\ddagger}{R}$$

$$\text{slope: } -\frac{\Delta H^\ddagger}{R}$$

$$\text{Volume of activation: } \frac{d(\ln k)}{dp} = \frac{-\Delta V^\ddagger}{RT}$$

https://www.researchgate.net/profile/Meyer_Tern/publication/255772611/figure/fig3/AS:2978747567_@1448030284882/Fig-4-Eyring-plot-analysis-and-rate-constant-data-for-the-enantiomerization-of-2g-i

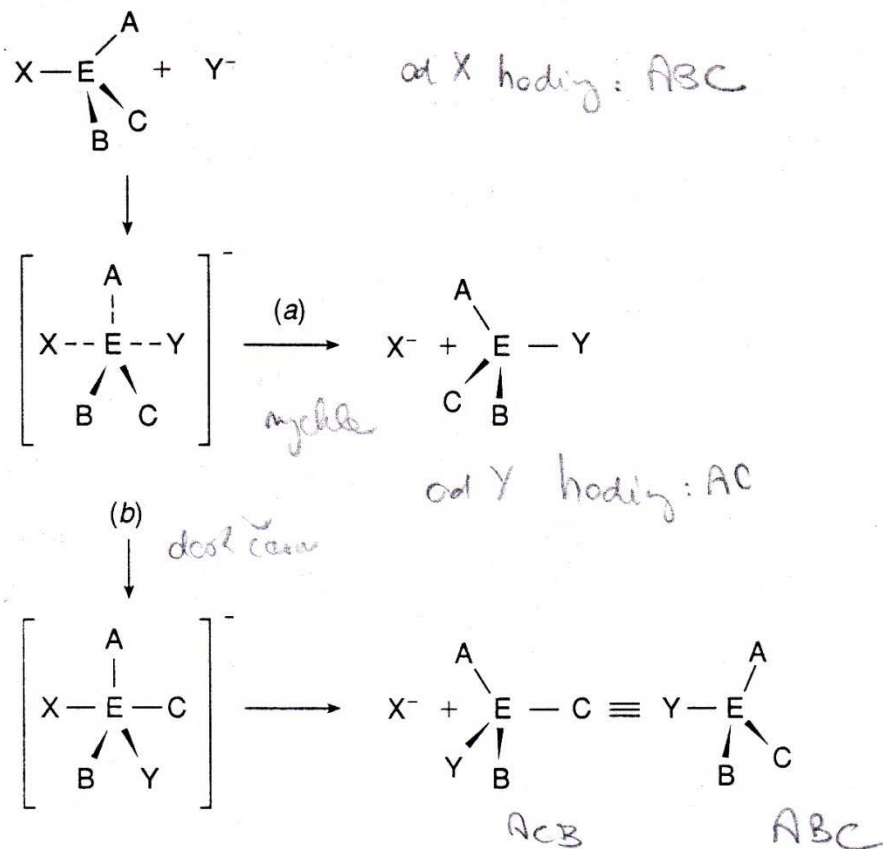


Table L.1 Some entropies ($\text{J K}^{-1} \text{mol}^{-1}$) and volumes ($\text{cm}^3 \text{mol}^{-1}$) of activation for the exchange of dimethylformamide (dmf) in octahedral high-spin complexes

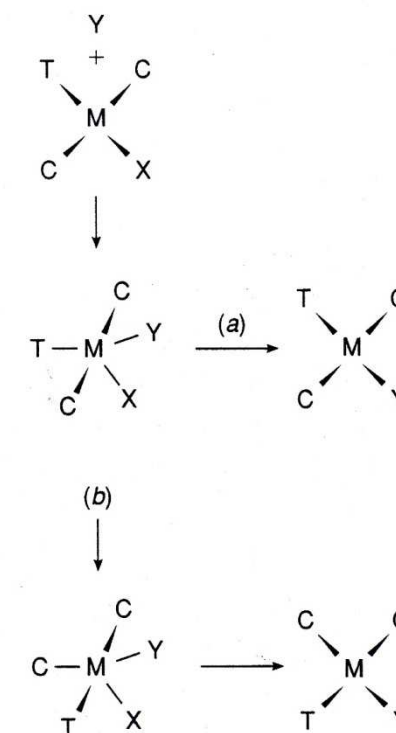
	ΔS^\ddagger	ΔV^\ddagger
$[\text{Al}(\text{dmf})_6]^{3+}$	28	+13.7
$[\text{Cr}(\text{dmf})_6]^{3+}$	-43	-6.3
$[\text{Fe}(\text{dmf})_6]^{3+}$	-69	-0.9
$[\text{Fe}(\text{dmf})_6]^{2+}$	+14	+8.5
$[\text{Ni}(\text{dmf})_6]^{2+}$	+34	+9.1

Isomerisation , CN 5 intermediate

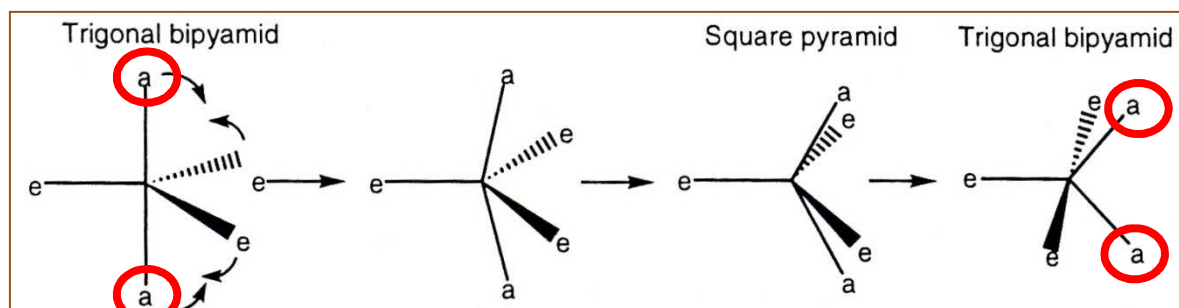
Tetrahedron



Square,
retention of geometry or isomerization

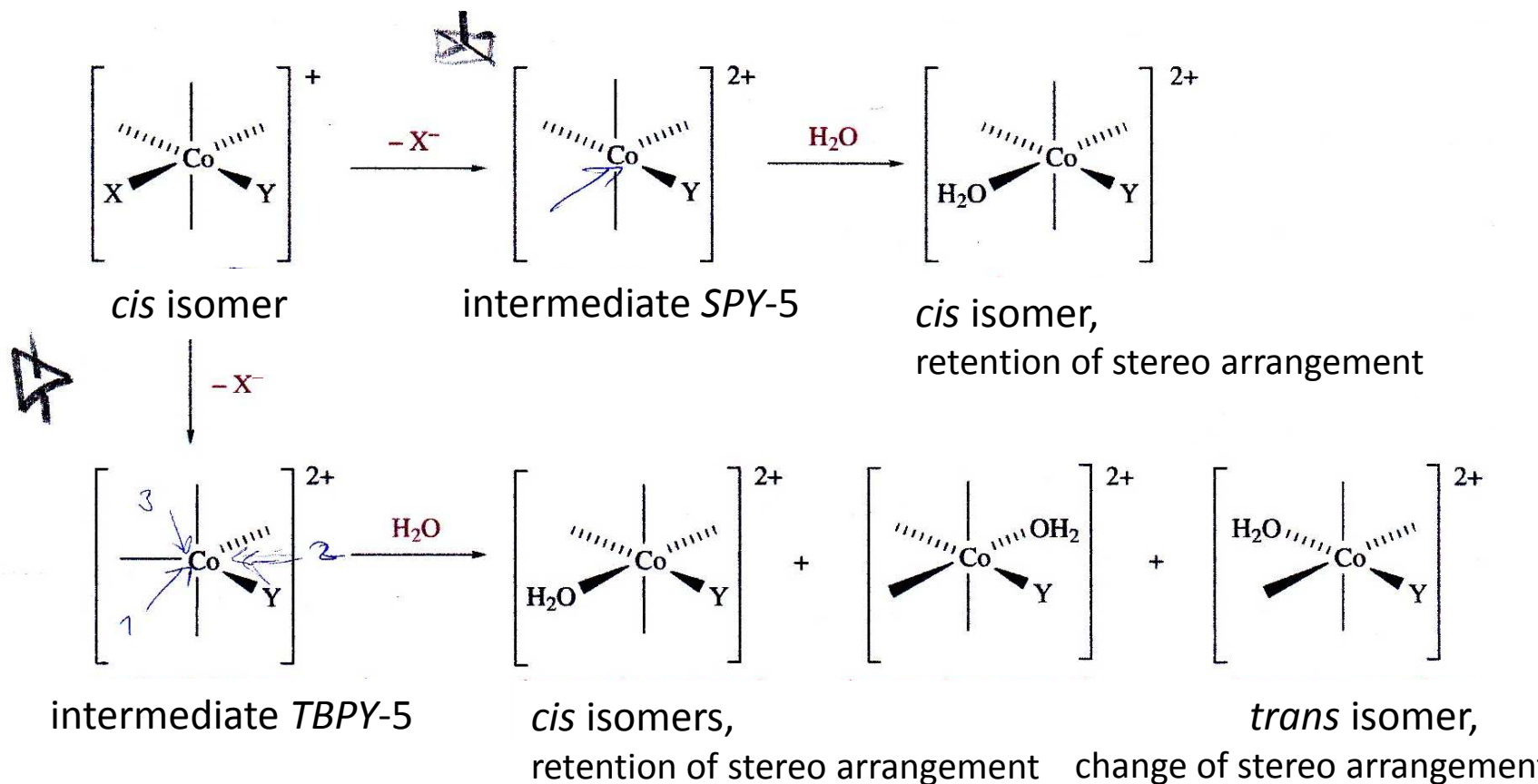


Berry pseudorotation



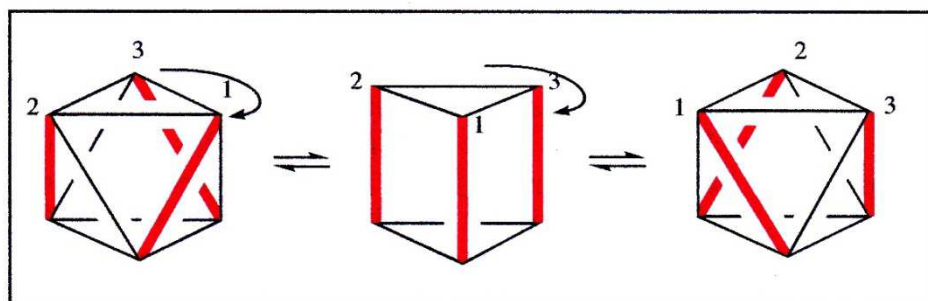
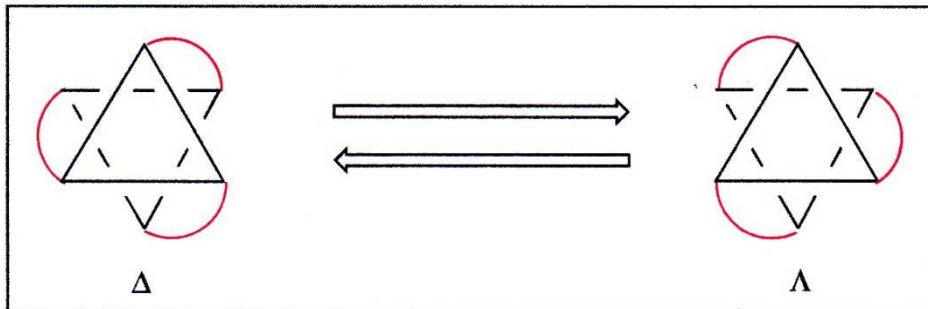
Possible pathways for a ligand substitution in an OC-6 complex

5-coordinated intermediate, the leaving group X, the entering group H₂O

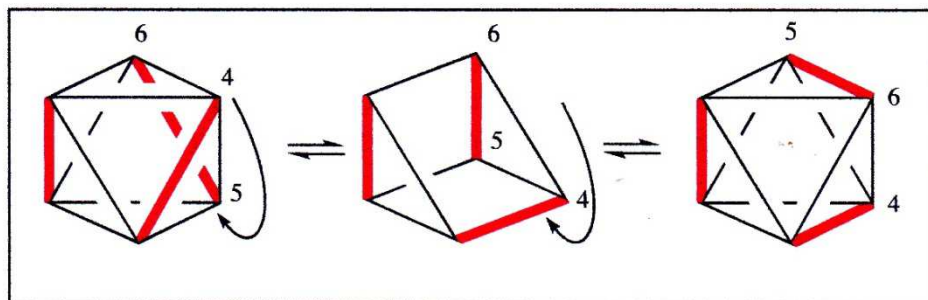


Racemisation of a tris(chelate) octahedral complex in solution

Re-arrangement without a band interruption

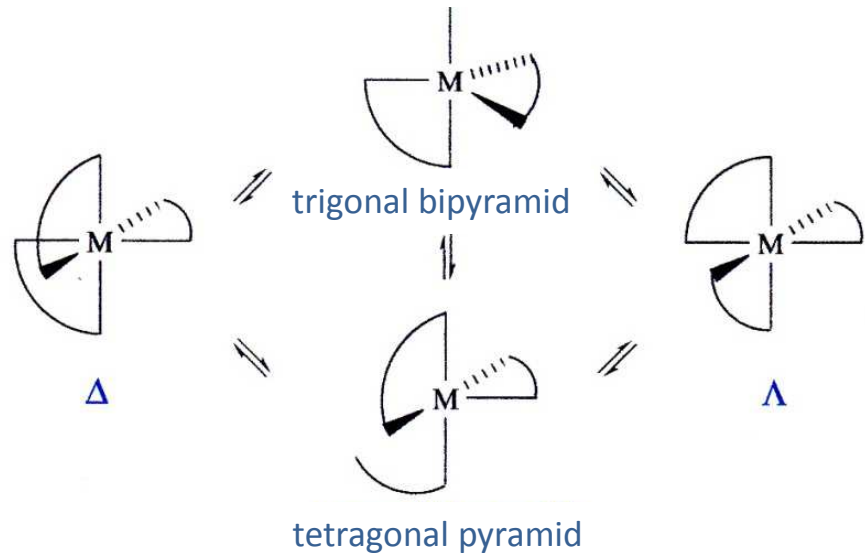


(a) Bailar twist (trigonal)



(b) Ray -Dutt twist (rhombic)

Re-arrangements with a band interruption



Entering group, leaving group, and metal effects

Entering group effect

in associative (I_a or A type) reactions;

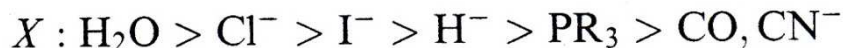
substitution reaction rate, Pt(II) SP-4



nucleophilicity parameters n_{Pt} , follows HSAB principle

Leaving group effect

in dissociative (I_d or D type) reactions;
substitution reaction rate:

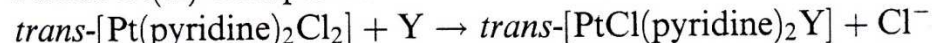


Enhancement of leaving ability:

addition of an appropriate acid

- hard H^+ for F^- , CO_3^{2-}
- soft Ag^+ for Cl^- , I^-

Rate Constants for Ligand Displacement in Some Square Planar Pt(II) Complexes^a



Y	$k_2 (M^{-1}s^{-1})$	n_{Pt}
MeOH (25 °C)	2.7×10^{-7}	0.00
MeO ⁻ (25 °C)	Very slow	<2.4
N(CN) ₂ ⁻	3.03×10^{-4}	2.87
Cl ⁻	4.5×10^{-4}	3.04
NH ₃	4.7×10^{-4}	3.07
N ₃ ⁻	1.55×10^{-3}	3.58
I ⁻	1.07×10^{-1}	5.46
(Me ₂ N) ₂ CS	0.30	5.87
(MeNH) ₂ CS	2.5	6.79
(PhNH) ₂ CS	4.13	7.01
CN ⁻ (25 °C)	4.00	7.14
PPh ₃ (25 °C)	249	8.93

Metal effect

slow reaction of the electronically stabilized ions (d^6 in OC-6; d^8 in SP-4; slower reaction rates for heavier atoms, cf. CFSE

Spectator ligand effects

A. Steric effects

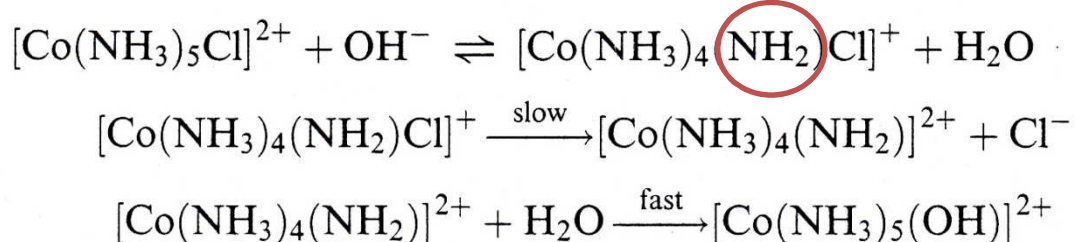
easier dissociation in the presence of large ligands; decreasing reaction rate of association

B. Electron-donor effects

better electron-donating substituents (spectator ligands) enhance the rates of dissociative reactions

C. Base-assisted hydrolysis

of ammonia and amine complexes (10^6 times faster hydrolysis of $[\text{Co}(\text{NH}_3)_5\text{Cl}]^{2+}$ in basic soln. than in acidic soln.; but no comparable effect for py or CN^- complexes)



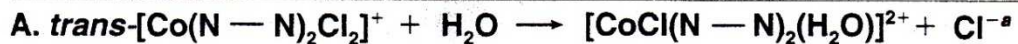
1st step:
deprotonation of the coordinated ammonia

D. Trans effect

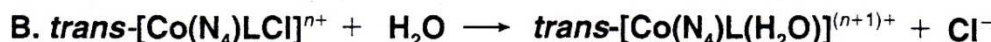
associative substitution in *SP-4* complexes

Effect of Nonleaving Ligands on Acid Hydrolysis Rates of Some Co(III) Complexes at 25 °C

A. Steric effects



$\text{N}-\text{N}$	$k (s^{-1})$
$\text{NH}_2\text{CH}_2\text{CH}_2\text{NH}_2$	3.2×10^{-5}
$\text{NH}_2\text{CH}_2\text{CHMeNH}_2$	6.2×10^{-5}
$d,l\text{-NH}_2\text{CHMeCHMeNH}_2$	1.5×10^{-4}
<i>meso</i> - $\text{NH}_2\text{CHMeCHMeNH}_2$	4.2×10^{-4}
$\text{NH}_2\text{CH}_2\text{CMe}_2\text{NH}_2$	2.2×10^{-4}
$\text{NH}_2\text{CMe}_2\text{CMe}_2\text{NH}_2$	Instantaneous
$\text{NH}_2\text{CH}_2\text{CH}_2\text{NHMe}$	1.7×10^{-5}



Complex ^{b,c}	$k (s^{-1})$
$\text{trans-}[\text{Co}(\text{cyclam})\text{Cl}_2]^+$	1.1×10^{-6}
$\text{trans-}[\text{Co}(\text{cyclam})(\text{NCS})\text{Cl}]^+$	1.1×10^{-9}
$\text{trans-}[\text{Co}(\text{cyclam})(\text{CN})\text{Cl}]^+$	4.8×10^{-7}
$\text{trans-}[\text{Co}(\text{tet-}b)\text{Cl}_2]^+$	9.3×10^{-4}
$\text{trans-}[\text{Co}(\text{tet-}b)(\text{NCS})\text{Cl}]^+$	7.0×10^{-7}
$\text{trans-}[\text{Co}(\text{tet-}b)(\text{CN})\text{Cl}]^+$	3.4×10^{-4}

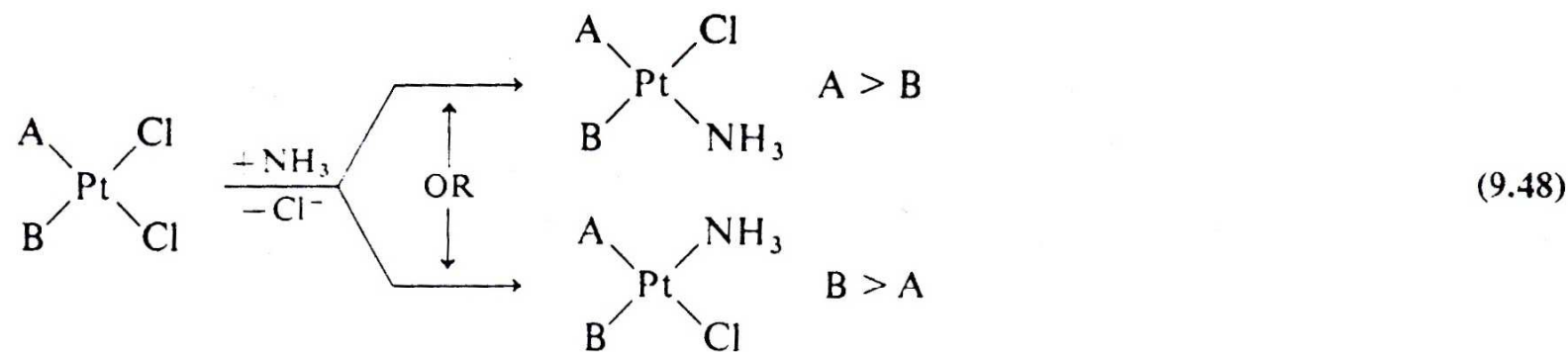
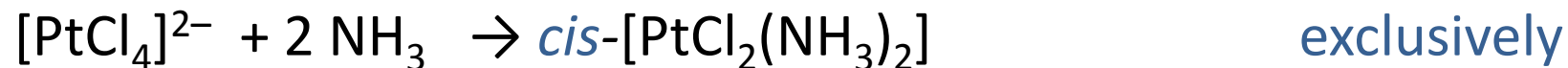
^aR. G. Pearson, C. R. Boston, and F. Basolo, *J. Am. Chem. Soc.* **75**, 3089 (1953).

^bCyclam = 1,4,8,11-Tetraazacyclotetradecane.

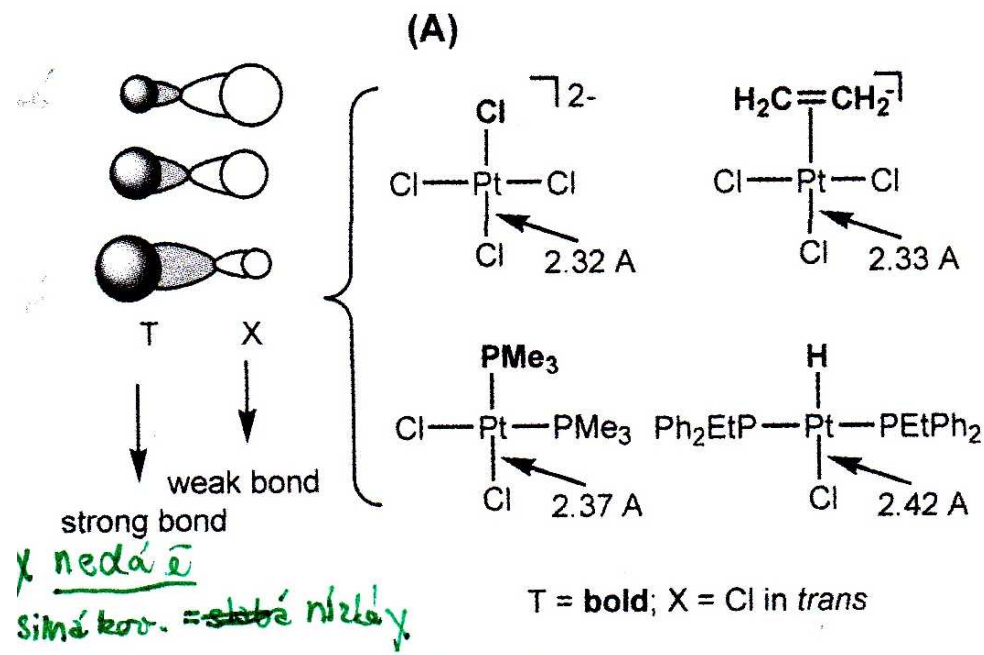
^cTet-*b* = *d,l*-1,4,8,11-Tetraaza-5,5,7,12,12,14-hexamethylcyclotetradecane.



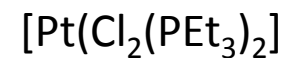
D. Trans effect, trans-series



The ordering of ligands in this series is as follows: $\text{CN}^- \sim \text{CO} \sim \text{NO} \sim \text{H}^- > \text{CH}_3^- \sim \text{SC}(\text{NH}_2)_2 \sim \text{SR}_2 \sim \text{PR}_3 > \text{SO}_3\text{H}^- > \text{NO}_2^- \sim \text{I}^- \sim \text{SCN}^- > \text{Br}^- > \text{Cl}^- > \text{py} > \text{RNH}_2 \sim \text{NH}_3 > \text{OH}^- > \text{H}_2\text{O}$.



Trans Influence – thermodynamic
different bond lengths



cis: Pt – Cl 237.6 pm

trans: Pt – Cl 229.4 pm

trans influence of $\text{PEt}_3 > \text{Cl}$

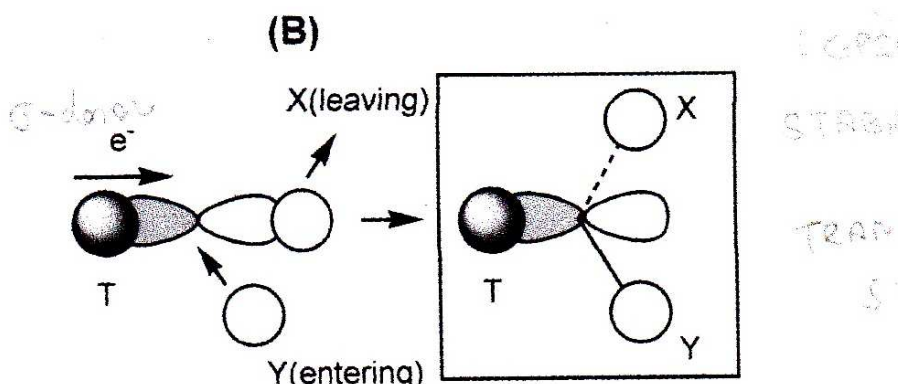


Figure 7.20 *trans*-influence, as a thermodynamic effect.

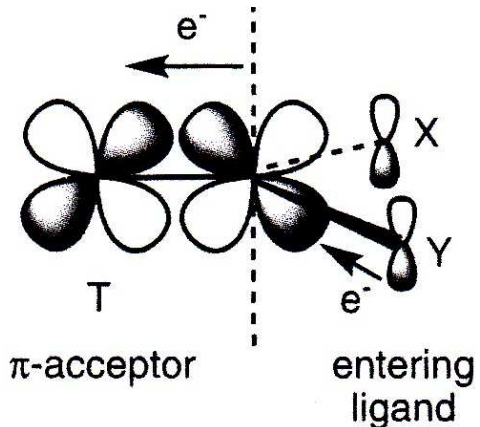


Figure 7.21 *trans*-effect due to a π -acceptor ligand.

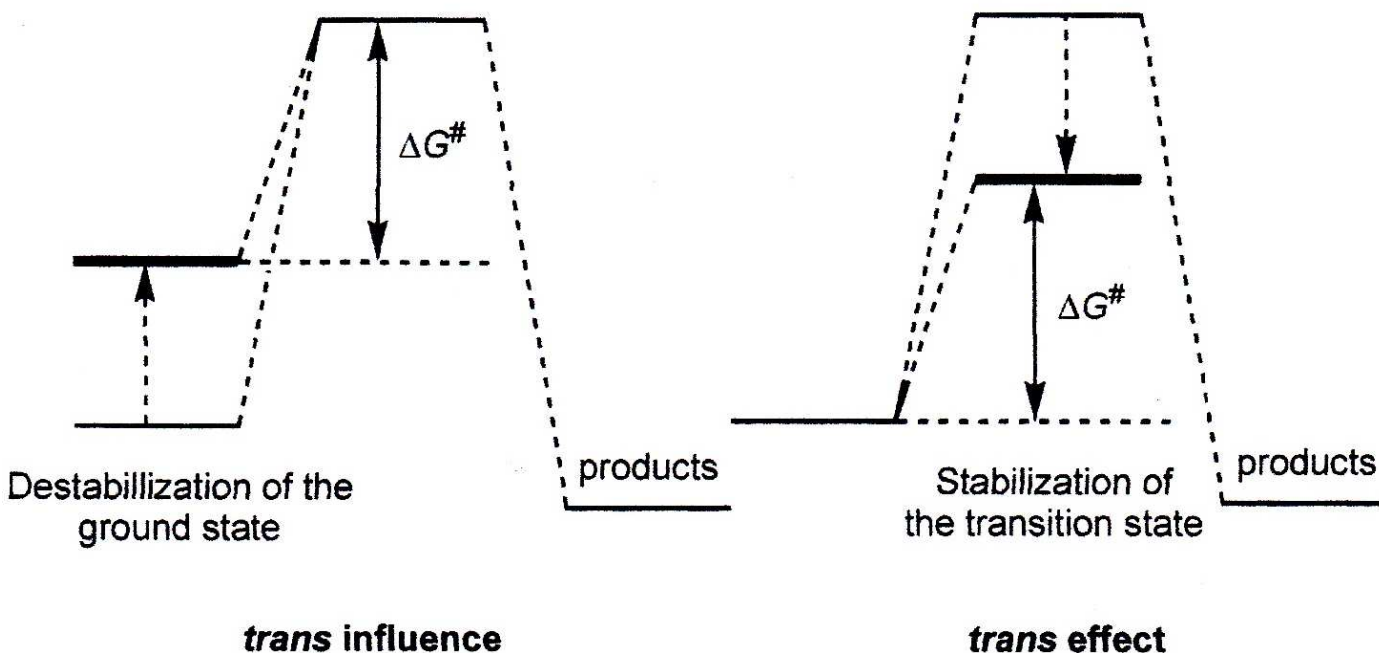


Figure 7.22 The energetic difference between *trans*-influence and *trans*-effect.

General methods of synthesis

2 common situations:

- ❖ metal salt is soluble in water, but it needs acidic media (hydrolysis)  ligand is basic
- ❖ metal salt is soluble in water  ligand is insoluble in water

Reactions in aqueous media

water behaves as a ligand

uncharged particles are poorly soluble

Reactions in non-aqueous media

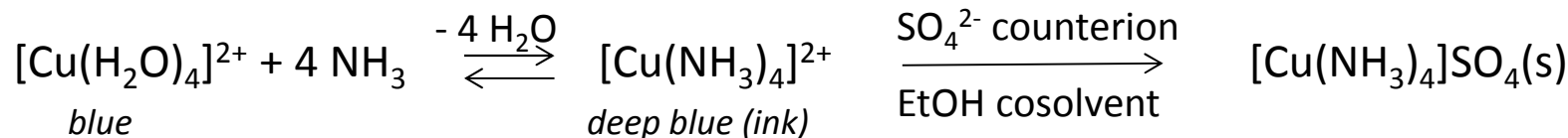
hydrated salts (e.g. CuSO₄·5H₂O) are insoluble

charged particles are poorly soluble

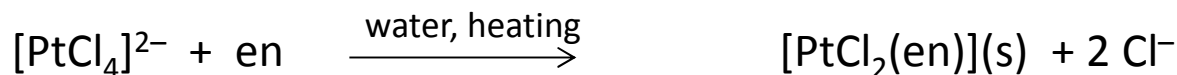
1. Substitution reactions in aqueous solutions

Excess of ligand, reaction time varies – inert vs. labile ions

Labile – quick reaction, no mixed-ligand complexes:

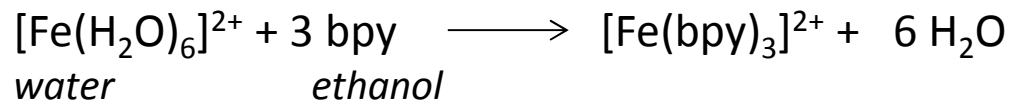


Inert – longer times, heating, mixed-ligand complexes

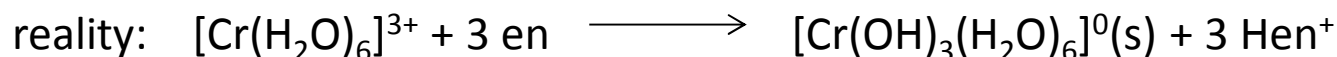
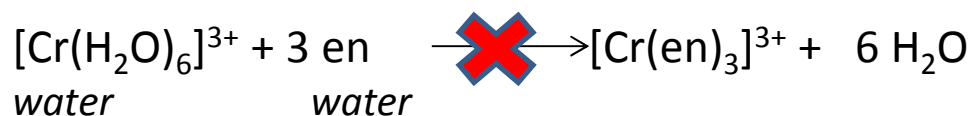


2. Substitution reactions in nonaqueous solvents

a) ligand is insoluble in water – another solvent miscible with water



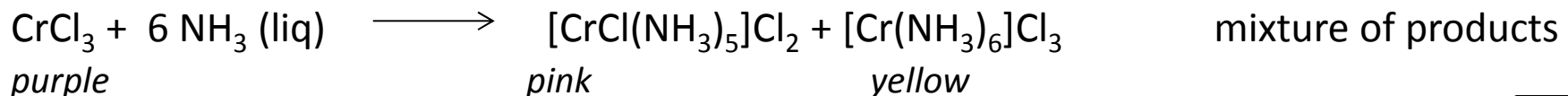
b) metal ion undergoes hydrolysis – competition between the hydrolysis and the complex formation



Solution:

anhydrous CrCl_3 in dry ether – slow, but gives the product, $[\text{Cr}(\text{en})_3]\text{Cl}_3$

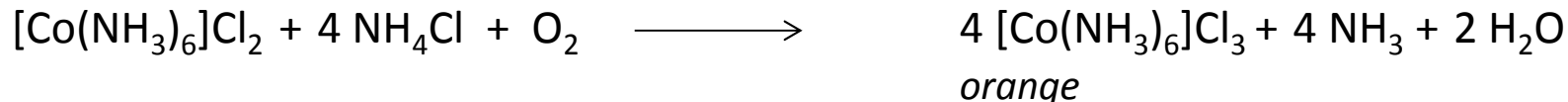
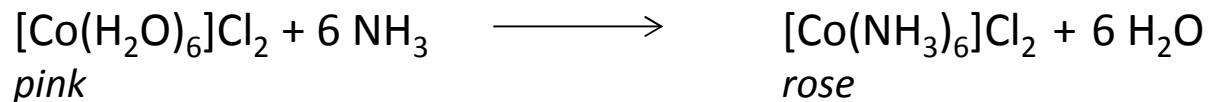
Reaction in liquid ammonia:



3. Substitution reactions on metal ions in more labile oxidation states

Cr(III), d^3 - small addition of a reducing agent (Na), Cr(II) d^4

Co(II) reacts, the product is oxidized to Co(III)



substitution of a volatile ligand

4. Substitution of weakly bound or volatile ligand

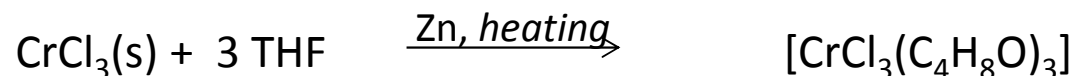
Volatile ligands: CO, NH₃, H₂O, driven off by heating, replaced



CO: labilized by irradiation



coordinating, volatile solvents (acetonitrile, tetrahydrofuran (THF), ethers) – precursors



5. Ligand construction or destruction by reaction of coordinated ligands – see the previous theme: Reactions on coordinated ligands

Uveřejněné materiály jsou určeny studentům Vysoké školy chemicko-technologické v Praze jako studijní materiál. Některá textová i obrazová data v nich obsažená jsou převzata z veřejných zdrojů. V případě nedostatečných citací nebylo cílem autorky záměrně poškodit autora/y původního díla.

S případnými výhradami se prosím obracejte na autorku tohoto výukového materiálu, aby bylo možno zjednat nápravu.



The published materials are intended for students of the University of Chemistry and Technology, Prague as a study material. Some text and image data contained therein are taken from public sources. In the case of insufficient quotations, the author's intention was not to intentionally infringe the possible author(s) rights to the original work.

If you have any reservations, please contact the author(s) of the specific teaching material in order to remedy the situation.

Mechanism of electron transfer

Redox potential and complex stability

Electron transfer:

- Outer-sphere mechanism
- Inner-sphere mechanism

Mixed-valence compounds



EUROPEAN UNION
European Structural and Investing Funds
Operational Programme Research,
Development and Education

MS
MT
MINISTRY OF EDUCATION,
YOUTH AND SPORTS

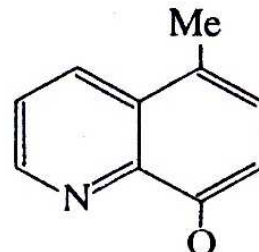


aside: Redox potential of complexes

Standard redox potential of Fe(III)/Fe(II) in selected complexes in acidic media

Fe^{III}	Fe^{II}	E°/V
$[\text{Fe}(\text{phen})_3]^{3+} + \text{e} \rightleftharpoons [\text{Fe}(\text{phen})_3]^{2+}$		1,12
$[\text{Fe}(\text{bipy})_3]^{3+} + \text{e} \rightleftharpoons [\text{Fe}(\text{bipy})_3]^{2+}$		0,96
$[\text{Fe}(\text{H}_2\text{O})_6]^{3+} + \text{e} \rightleftharpoons [\text{Fe}(\text{H}_2\text{O})_6]^{2+}$		0,77
$[\text{Fe}(\text{CN})_6]^{3-} + \text{e} \rightleftharpoons [\text{Fe}(\text{CN})_6]^{4-}$		0,36
$[\text{Fe}(\text{C}_2\text{O}_4)_3]^{3-} + \text{e} \rightleftharpoons [\text{Fe}(\text{C}_2\text{O}_4)_2]^{2-} + \text{C}_2\text{O}_4^{2-}$		0,02
$[\text{Fe}(\text{edta})]^- + \text{e} \rightleftharpoons [\text{Fe}(\text{edta})]^{2-}$		-0,12
$[\text{Fe}(\text{chin})_3] + \text{e} \rightleftharpoons [\text{Fe}(\text{chin})_2] + \text{chin}^-$ ^{a)}	Fe(II), SB	-0,30
	Fe(III), HB	

^{a)} chin = 5-methyl-8-hydroxychinolin



Modulation of redox potential by the ligand nature, enzymes

E° and stability constant of the complex

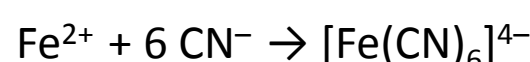
Nernst equation

$$E = E^0 - \frac{RT}{nF} \ln \frac{[red]}{[ox]}$$

Nernst-Peters equation

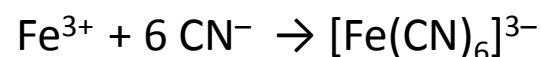
Complex: concentration of the reduced “naked” ion depends on the β of the complex

Example: ferrocyanate $[\text{Fe}(\text{CN})_6]^{4-}$ and ferricyanate $[\text{Fe}(\text{CN})_6]^{3-}$



$$\beta = 10^{43.6}$$

$$[\text{Fe}] = \frac{[\text{Fe}(\text{CN})_6]}{\beta \cdot [\text{CN}]^6}$$



$$\beta = 10^{35.4}$$

$$E = E^0 + \frac{RT}{nF} \ln \frac{\beta_{red}}{\beta_{ox}} - \frac{RT}{nF} \ln \frac{[red']}{[ox']} = E^\circ_{complex} - \frac{RT}{nF} \ln \frac{[red']}{[ox']}$$

$$E^\circ_{complex} = E^0 + \frac{RT}{nF} \ln \frac{\beta_{red}}{\beta_{ox}}$$

2 mechanisms of an electron transfer

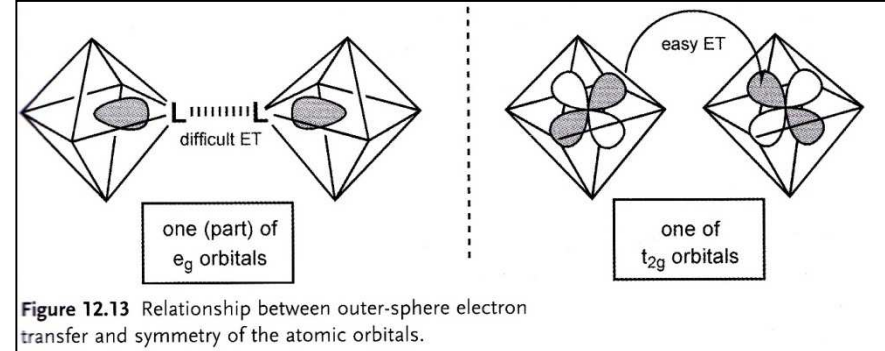
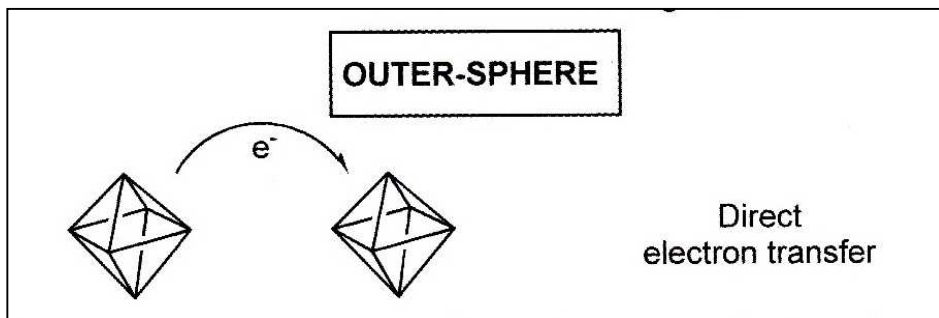


Figure 12.13 Relationship between outer-sphere electron transfer and symmetry of the atomic orbitals.

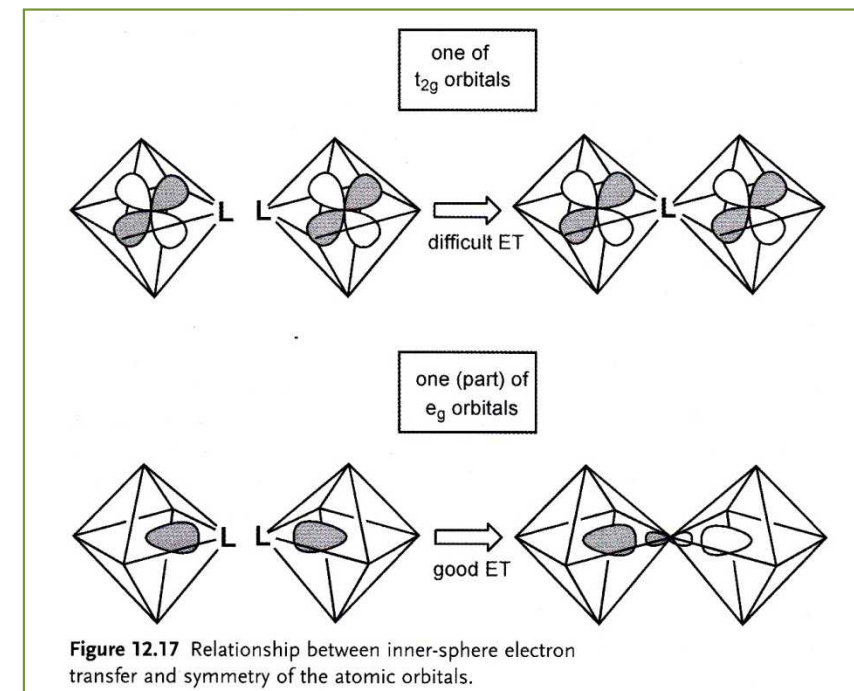
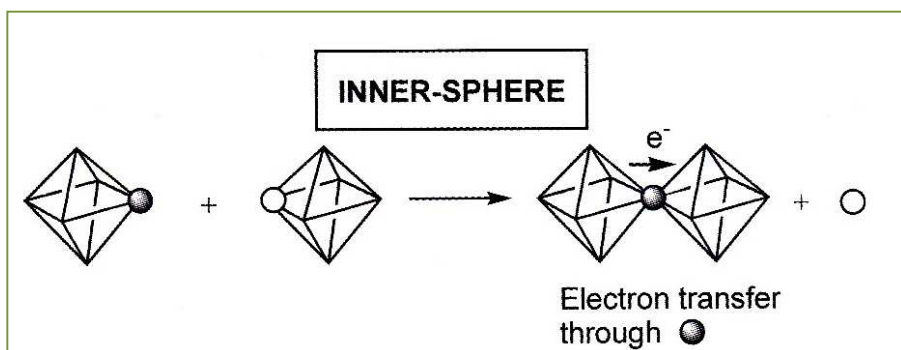


Figure 12.17 Relationship between inner-sphere electron transfer and symmetry of the atomic orbitals.

Outer-sphere mechanism - reaction rates

Table R.1 Some rate data for outer sphere redox reactions

Reacting pair	Configurations	$k_{25^\circ\text{C}}$ /dm ³ mol ⁻¹ s ⁻¹	Orbital correlation	M—L difference / pm
[Ru(bipy) ₃] ^{2+/3+}	t _{2g} ⁶ / t _{2g} ⁵	4.2×10^8	t _{2g} → t _{2g}	V. small
[Os(bipy) ₃] ^{2+/3+}	t _{2g} ⁶ / t _{2g} ⁵	2.2×10^7	t _{2g} → t _{2g}	V. small
[Fe(bipy) ₃] ^{2+/3+}	t _{2g} ⁶ / t _{2g} ⁵	3.7×10^6	t _{2g} → t _{2g}	V. small
[IrCl ₆] ^{3-/2-}	t _{2g} ⁶ / t _{2g} ⁵	2.3×10^5	t _{2g} → t _{2g}	V. small
[Ru(NH ₃) ₆] ^{2+/3+}	t _{2g} ⁶ / t _{2g} ⁵	4.0×10^3	t _{2g} → t _{2g}	4
[Ru(OH ₂) ₆] ^{2+/3+}	t _{2g} ⁶ / t _{2g} ⁵	20.0	t _{2g} → t _{2g}	9
[Fe(OH ₂) ₆] ^{2+/3+}	t _{2g} ⁴ e _g ² / t _{2g} ³ e _g ²	4.0	t _{2g} → t _{2g}	13
[Co(phen) ₃] ^{2+/3+}	t _{2g} ⁶ e _g ¹ / t _{2g} ⁶	4.4×10^{-2}	e _g → e _g	19
[Co(en) ₃] ^{2+/3+}	t _{2g} ⁵ e _g ² / t _{2g} ⁶	7.7×10^{-5}	e _g → e _g *	18
[Co(NH ₃) ₆] ^{2+/3+}	t _{2g} ⁵ e _g ² / t _{2g} ⁶	8.0×10^{-6}	e _g → e _g *	18

+ spin

* Change in spin multiplicity follows transfer

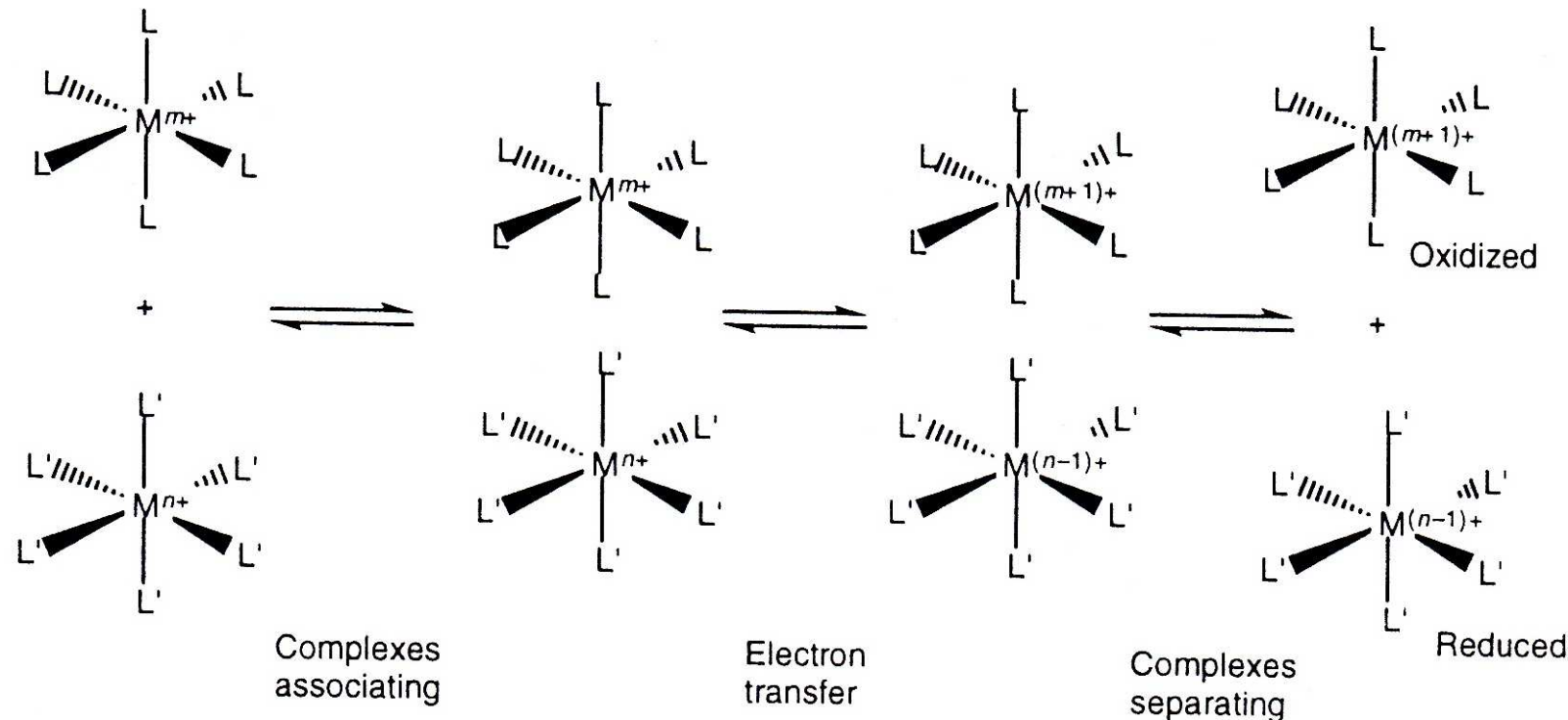
Change in M–L distance:

Franck–Condon principle; electron transfer rate is 100times faster (10^{-15} s) than atomic vibrations

Delocalizability of the ligand electrons

Outer-sphere mechanism - steps

1. Fast pre-equilibrium association
Solvent re-arrangement
2. Electron transfer



1. Fast pre-equilibrium association Solvent re-arrangement

Association – charge dependent

Table 12.1 K_{ip} values (ion pairing equilibrium constant) and k_{et} values for a range of outer-sphere redox reactions between transition metal complexes, according to z^+z^-

Reactants		K_{ip}	$k_{et} (s^{-1})$
Charge product -12			
$[\text{Co}(\text{NH}_3)_5(\text{H}_2\text{O})]^{3+}$	$[\text{Fe}(\text{CN})_6]^{4-}$	1500	0.19
$[\text{Co}(\text{NH}_3)_5(\text{py})]^{3+}$	$[\text{Fe}(\text{CN})_6]^{4-}$	2400	0.015
$[\text{Co}(\text{NH}_3)_5(3\text{-cyanopyridine})]^{3+}$	$[\text{Fe}(\text{CN})_6]^{4-}$	1300	0.346
Charge product -9			
$[\text{Co}(\text{dmso})(\text{NH}_3)_5]^{3+}$	$[\text{Fe}(\text{CN})_5(\text{imidazole})]^{3-}$	450	2.6
$[\text{Co}(\text{dmso})(\text{NH}_3)_5]^{3+}$	$[\text{Fe}(\text{CN})_5(\text{pyridine})]^{3-}$	490	0.15
$[\text{Co}(\text{NH}_3)_5(\text{pyridine})]^{3+}$	$[\text{Fe}(\text{CN})_5(\text{pyridine})]^{3-}$	860	0.0068
$[\text{Co}(\text{NH}_3)_5(\text{pyridine})]^{3+}$	$[\text{Fe}(4,4'\text{-bipyridine})(\text{CN})_5]^{3-}$	1860	0.0021
$[\text{Co}(\text{phen})_3]^{3+}$	$[\text{Co}(\text{ox})_3]^{3-}$	650	0.24
Charge products -8			
$[\text{Co}(\text{acetate})(\text{NH}_3)_5]^{2+}$	$[\text{Fe}(\text{CN})_6]^{4-}$	300	0.00037
$[\text{Co}(\text{benzoate})(\text{NH}_3)_5]^{2+}$	$[\text{Fe}(\text{CN})_6]^{4-}$	240	0.00062
$[\text{CoCl}(\text{NH}_3)_5]^{2+}$	$[\text{Fe}(\text{CN})_6]^{4-}$	38	0.027
$[\text{CoN}_3(\text{NH}_3)_5]^{2+}$	$[\text{Fe}(\text{CN})_6]^{4-}$	49	0.00062

2. Electron transfer – symmetrical systems, $\Delta G^\circ = 0$

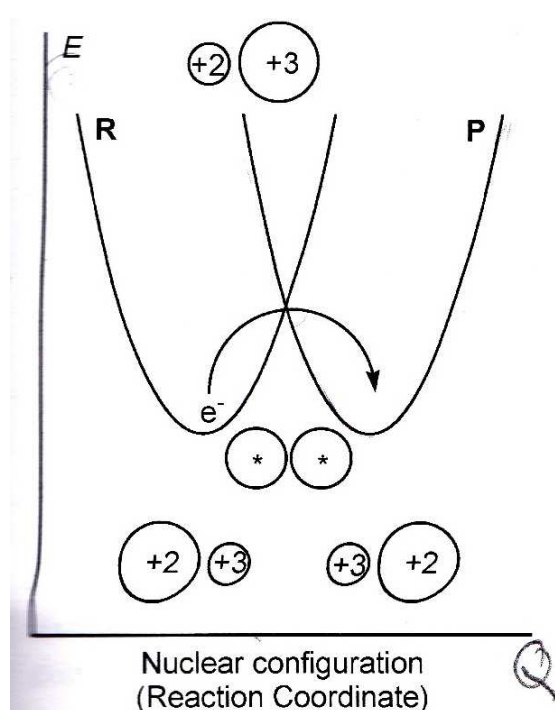
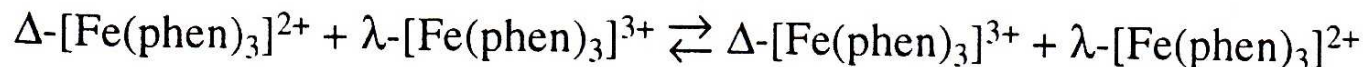
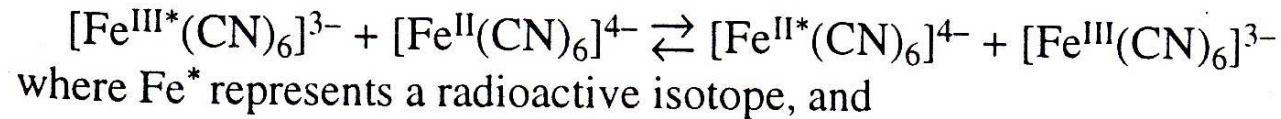
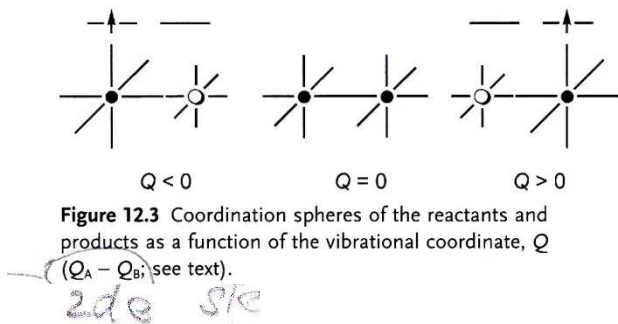


Figure 12.2 Plot of the potential energy of the reactants (R, precursor complex) and products (P, successor complex) as a function of the nuclear configuration for an electron-exchange reaction.



$$E = \lambda Q \pm f Q^2$$

Q reaction coordinate
 f reduced force constant
 λ vertical difference
 between the free energies of the reactants and products at the reactants' equilibrium configuration (when $\Delta G = 0$)

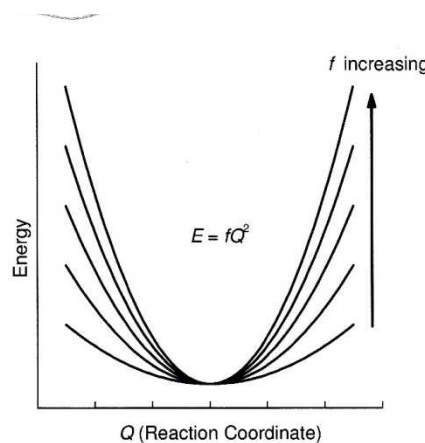


Figure 12.4 Shape of the energy surfaces as a function of the reduced force constant (f).

λ ... vertical difference between the free energies of the reactants and products at the reactants' equilibrium configuration (when $\Delta G = 0$)

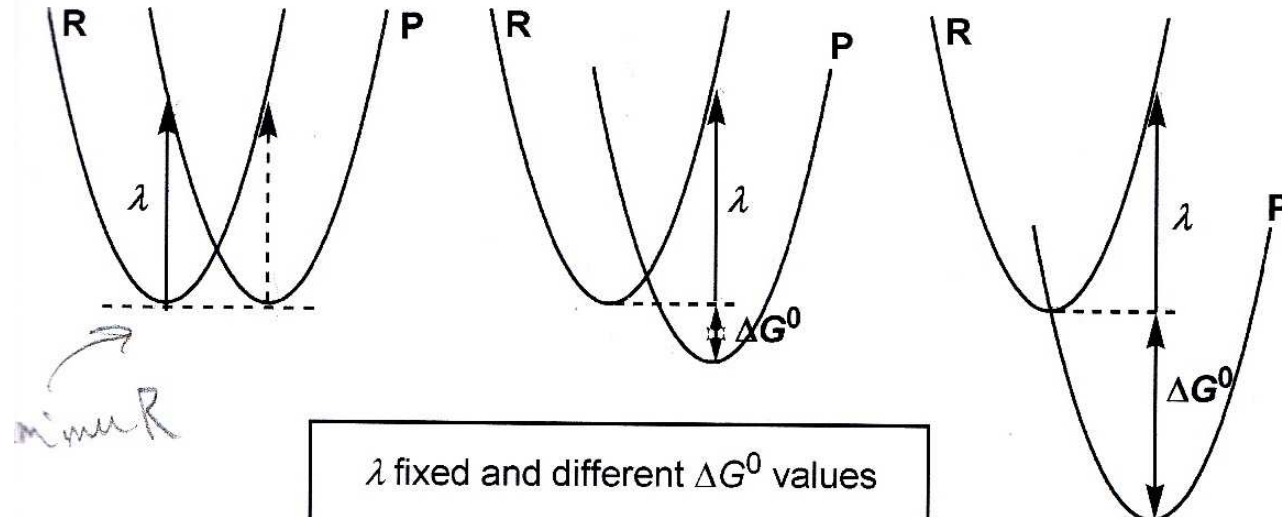


Figure 12.5 Graphical definition of λ and its comparison with ΔG^0 .

Δd ...bond length difference between the oxidised and reduced forms

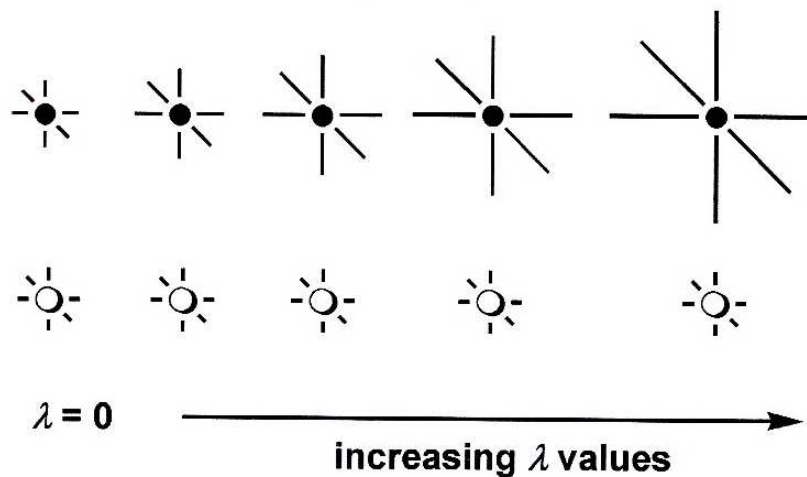


Figure 12.6 Concept of the λ parameter, as a function of Δd (oxidized and reduced form of the ion).

Examples of redox pairs with different Δd values – influence on reaction rate

Table 12.2 Relationships between Δd and k_{et} in outer-sphere redox reactions.

Reaction	Δd (\AA)	$k_{et} (M^{-1} \text{ s}^{-1})$	Reaction	Δd (\AA)	$k_{et} (M^{-1} \text{ s}^{-1})$
$[\text{Fe}(\text{CN})_6]^{3-/4-}$	0.03	2×10^4	$[\text{Fe}(\text{H}_2\text{O})_6]^{3+/2+}$	0.13	1.1
$[\text{Ru}(\text{H}_2\text{O})_6]^{3+/2+}$	0.09	20	$[\text{Cr}(\text{H}_2\text{O})_6]^{3+/2+}$	0.20	1.9×10^{-5}
$[\text{Co}(\text{bpy})_3]^{3+/2+}$	0.19	5.7	$[\text{Co}(\text{NH}_3)_6]^{3+/2+}$	0.22	2×10^{-8}

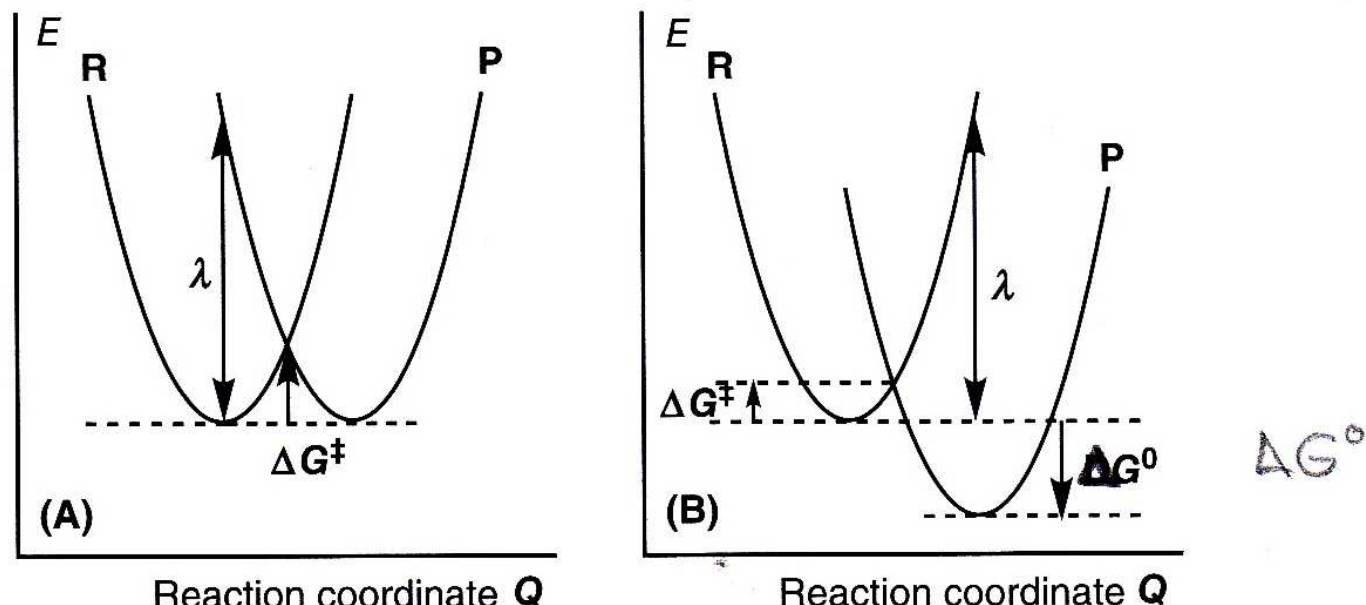
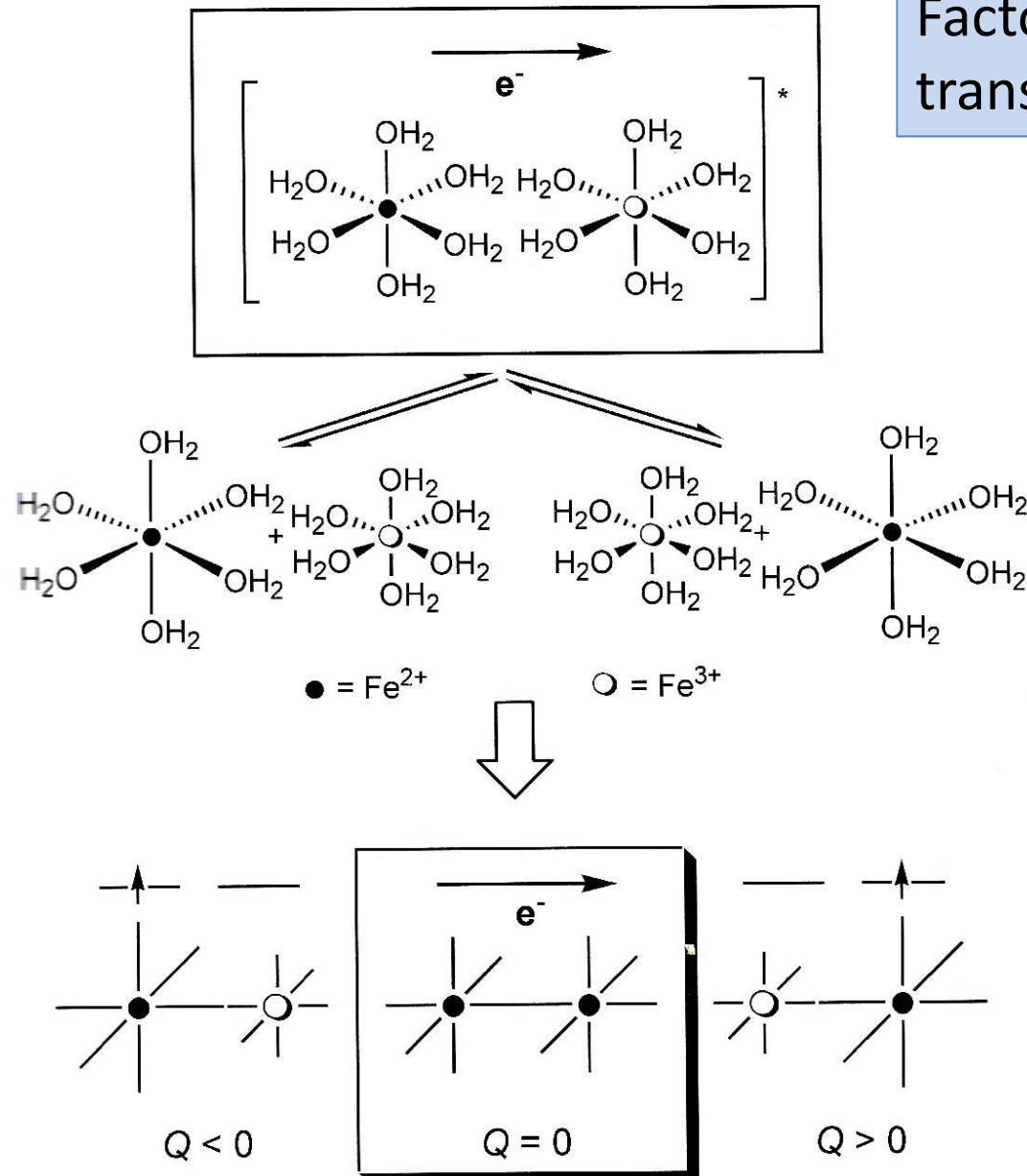


Figure 12.7 Concept of λ and ΔG^\ddagger for redox reactions with $\Delta G^\circ = 0$ (A) and $\Delta G^\circ < 0$ (B).

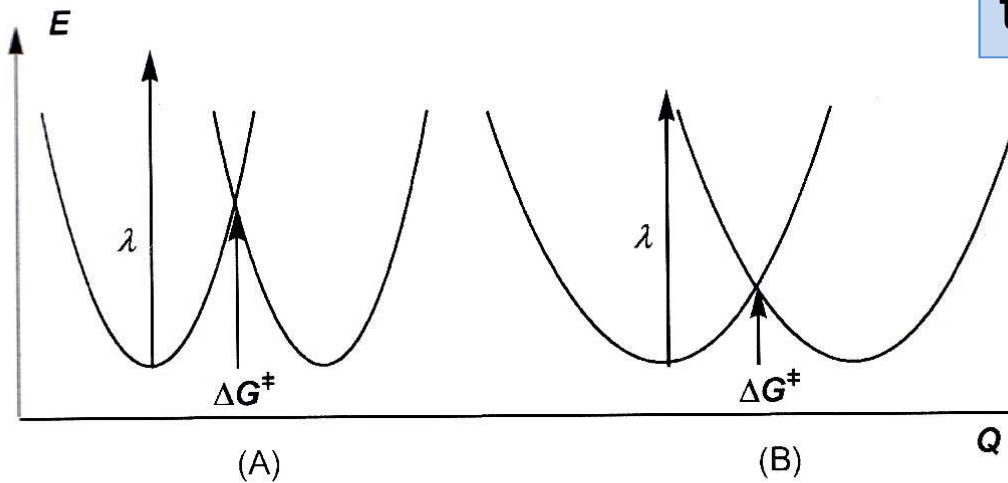


Factors that determine electron transfer, A

1. Size changes in course of vibration process
molecular rearrangement

Figure 12.8 Molecular rearrangement (vibrational) in an outer-sphere mechanism.

Factors that determine electron transfer, B



2. The shape of the energy surfaces:
different ΔG^\ddagger

Figure 12.9 Relationship between the shape of the energy surfaces (depending on f) and λ and ΔG^\ddagger (see text).

3. Large variations in
the internuclear
distances in the
equilibrium (λ)

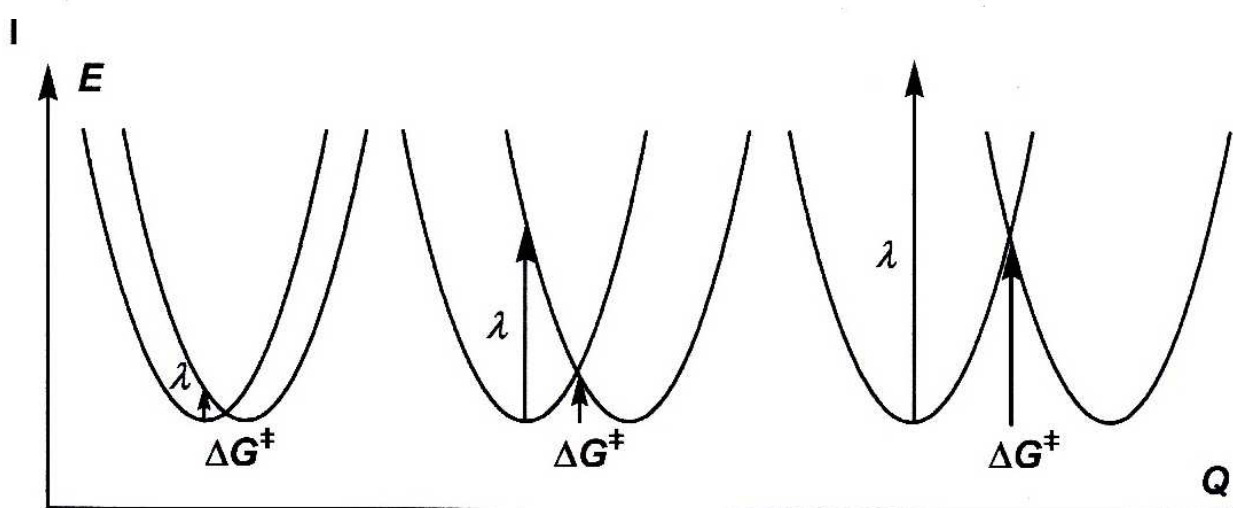


Figure 12.10 Graphical relationships between λ and ΔG^\ddagger .

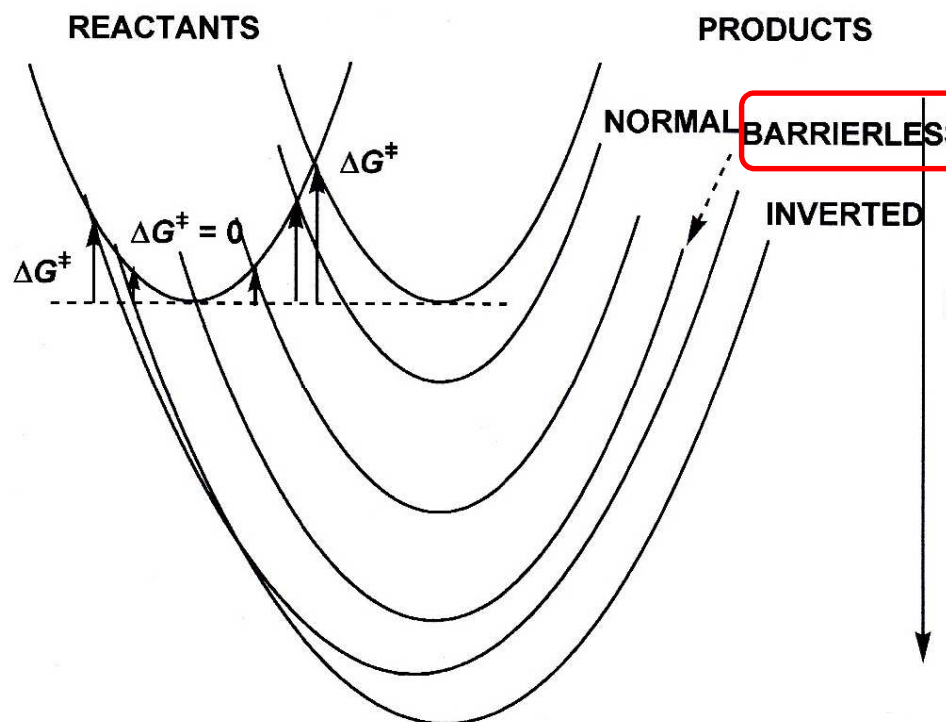


Figure 12.11 Influence of ΔG° (driving force) on the energy curves (normal, barrierless and inverted regions).

4. ΔG° of the reaction

starting from $\Delta G^\circ = 0$, 3 situations:

1. ΔG° increases, ΔG^\ddagger decreases
NORMAL REGION
2. $\Delta G^\ddagger = 0$, max. rate (k_{et} close to 10^{10-12})
BARRIERLESS REGION
3. both ΔG° and ΔG^\ddagger increase (Marcus)
INVERTED REGION

Observation:

with increasing ΔG° reaction rate (ΔG^\ddagger) increases until the barrierless point is reached.

Increasing
driving
force
(ΔG°)

rychlos
nejdlev
rosole
lze blesit

$\log k$

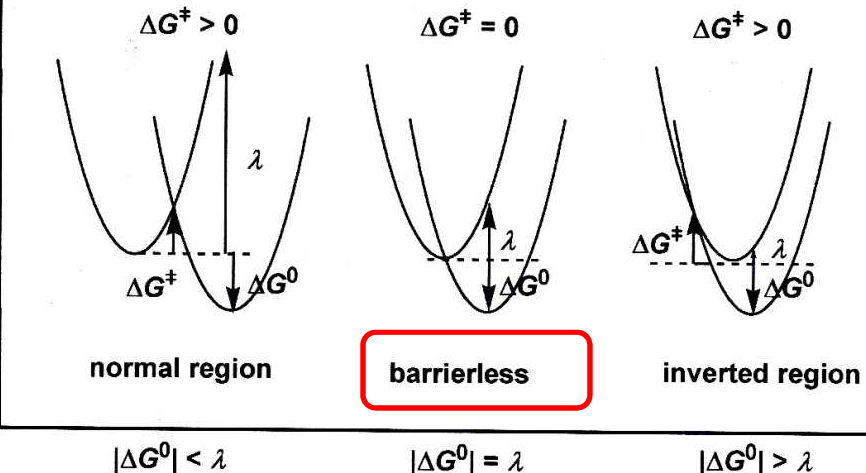


Figure 12.14 Relationships between ΔG^\ddagger , ΔG° and λ in normal, barrierless and inverted regions.

Marcus theory, Marcus law

Examples of the transition from normal to inverted region

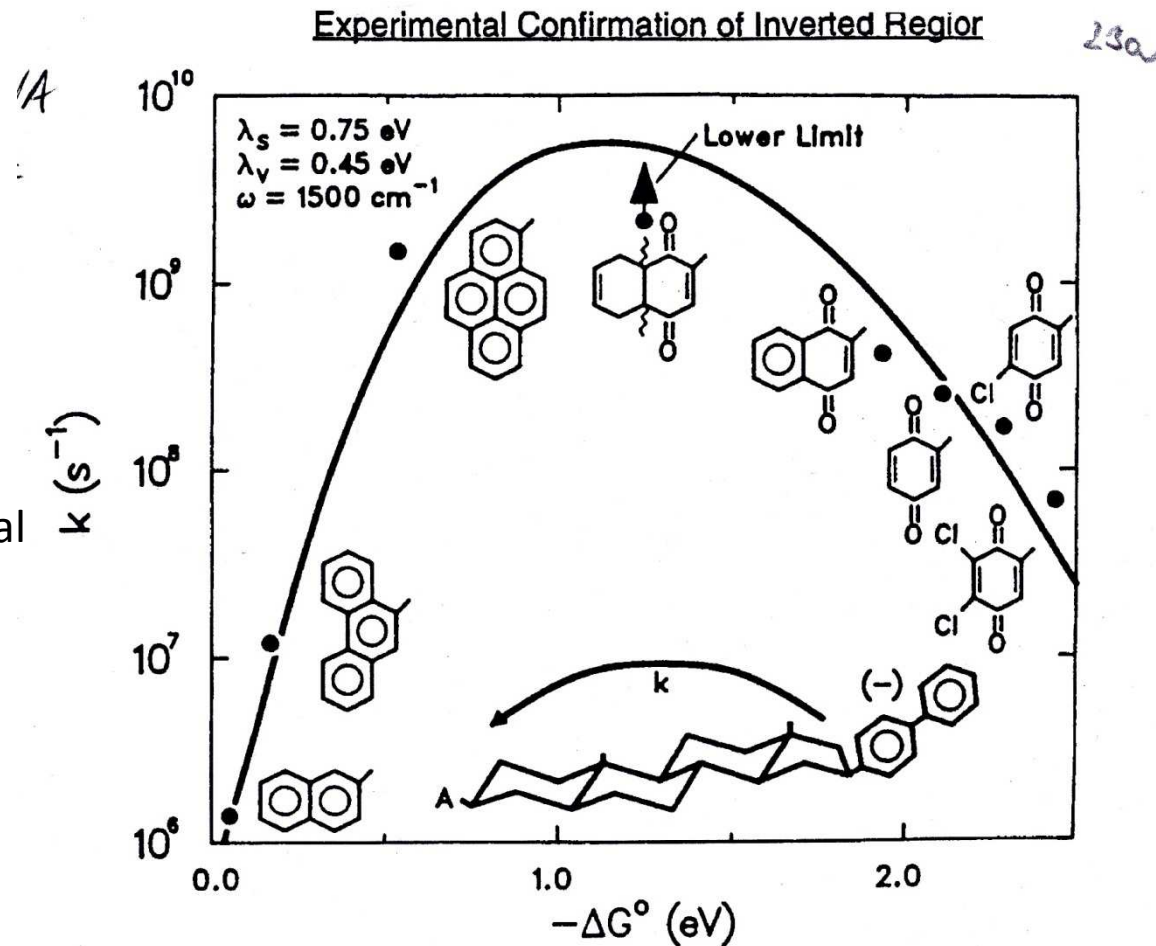
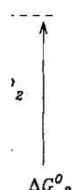


Figure 8. Inverted region effect in chemical electron transfer reactions. (Miller, et al, ref. 3).



$$\Delta G^\ddagger = \frac{\lambda}{4} \left(1 + \frac{\Delta G^\circ}{\lambda} \right)^2$$

Marcus theory, Marcus law

E of a cross-reaction derived from data of the self-exchange reactions

$$k_{12}^2 = fk_{11}k_{22}K \quad \text{or} \quad k_{12} = (k_{11}k_{22}K)^{1/2}w \quad \log K = nFE^\circ/2.303RT = nE^\circ/0.0592 \text{ (at } 25^\circ\text{C)}$$

$$\text{or} \quad 2 \ln k_{12} = \ln k_{11} + \ln k_{22} + \ln K + \ln(f)$$

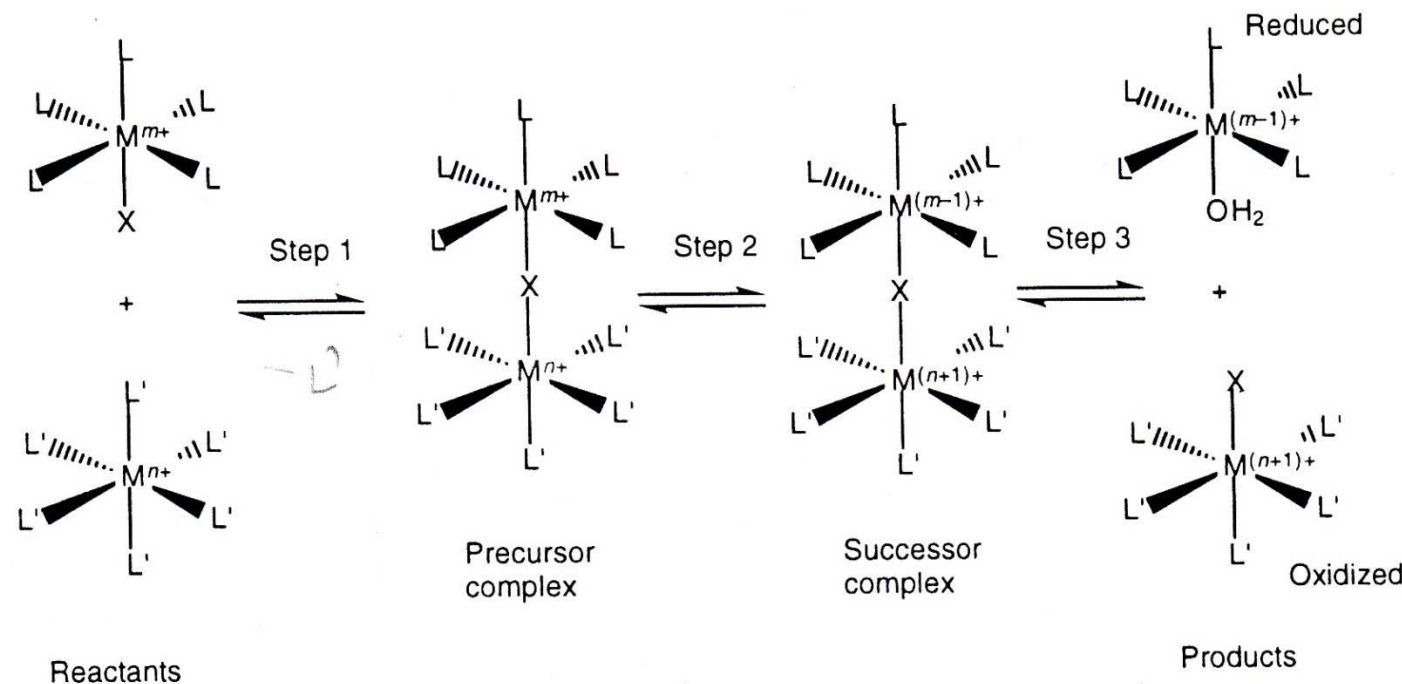
Self-Exchange Outer-Sphere Redox Rate Constants and Standard Reduction Potentials

Complex Ions	Charges	k_{11} ($\text{L mol}^{-1} \text{s}^{-1}$)	E° (V)
Ce(H ₂ O) _n	4+, 3+	4	+1.72 ^a
Cr(H ₂ O) ₆	3+, 2+	2×10^{-5}	-0.42
Mo(CN) ₈	3-, 4-	3×10^4	+0.72
W(CN) ₈	3-, 4-	7×10^4	+0.46
MnO ₄	1-, 2-	3000	+0.56
Fe(H ₂ O) ₆	3+, 2+	4	+0.77
Fe(phenanthroline) ₃	3+, 2+	3×10^7	+1.00
Fe(CN) ₆	3-, 4-	740	+0.36
Ru(H ₂ O) ₆	3+, 2+	50	+0.24
Ru(NH ₃) ₆	3+, 2+	2800	+0.10
Ru(bipyridyl) ₃	3+, 2+	4.2×10^8	+1.53
Co(NH ₃) ₆	3+, 2+	8×10^{-6}	+0.06
Co(NH ₂ CH ₂ CH ₂ NH ₂) ₃	3+, 2+	7.7×10^{-5}	-0.24
Co(bipyridyl) ₃	3+, 2+	18	
Co(terpyridyl) ₂	3+, 2+	48	
Co(phenanthroline) ₃	3+, 2+	40	+0.33
IrCl ₆	2-, 3-	2×10^5	+0.87

Inner-sphere mechanism - steps

1. Precursor bridging complex formation
2. electron transfer
3. Decomposition of the bridged complex

Rate determining step - any



Inner-sphere mechanism – role of the bridge

Second-Order Rate Constants for Selected Inner-Sphere Reactions with Variable Bridging Ligands

Oxidant	Reducant	Bridging Ligand	k ($\text{L mol}^{-1} \text{s}^{-1}$)
$[\text{Co}(\text{NH}_3)_6]^{3+}$	$[\text{Cr}(\text{OH}_2)_6]^{2+}$		8×10^{-5}
$[\text{CoF}(\text{NH}_3)_5]^{2+}$	$[\text{Cr}(\text{OH}_2)_6]^{2+}$	F^-	2.5×10^5
$[\text{CoCl}(\text{NH}_3)_5]^{2+}$	$[\text{Cr}(\text{OH}_2)_6]^{2+}$	Cl^-	6.0×10^5
$[\text{CoI}(\text{NH}_3)_5]^{2+}$	$[\text{Cr}(\text{OH}_2)_6]^{2+}$	I^-	3.0×10^6
$[\text{Co}(\text{NCS})(\text{NH}_3)_5]^{2+}$	$[\text{Cr}(\text{OH}_2)_6]^{2+}$	NCS^-	1.9×10
$[\text{Co}(\text{SCN})(\text{NH}_3)_5]^{2+}$	$[\text{Cr}(\text{OH}_2)_6]^{2+}$	SCN^-	1.9×10^5
$[\text{Co}(\text{NH}_3)_5(\text{OH}_2)]^{3+}$	$[\text{Cr}(\text{OH}_2)_6]^{2+}$	H_2O	0.1

SOURCE: From F. Basolo and R. Pearson, *Mechanisms of Inorganic Reactions*, 2nd ed., Wiley, New York; 1967.

Inner-sphere mechanism – role of the bridge

Table R.2 Rate constants for the redox reactions between a range of complexes, $[\text{Co}(\text{NH}_3)_5\text{X}]^{n+}$, with the ion $[\text{V}(\text{H}_2\text{O})_6]^{2+}$. Underlining is used to indicate ligand donor atoms

Ligand, X	$k / M^{-1} \text{ s}^{-1}$
I^-	120
Br^-	25
Cl^-	10
<u>SCN^-</u>	30
<u>NCS^-</u>	0.3
N_3^-	13
MeCO_2^-	1.2
H_2O	0.53
pyridine	4.1×10^{-3}
NH_3	8×10^{-5}

From inner- to outer-sphere mechanism – structural factors

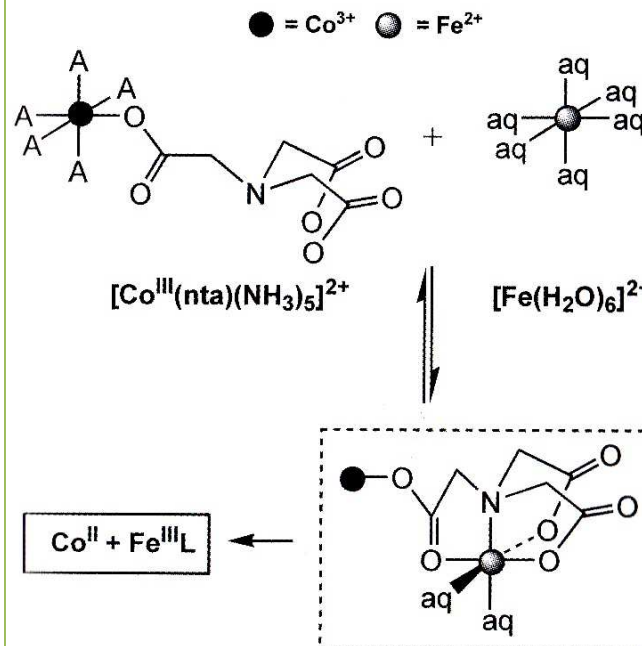


Figure 12.19 Formation of a “precursor complex” in the inner-sphere redox reaction shown in the figure (see text for explanation) (H_3nta is not necessarily fully deprotonated).

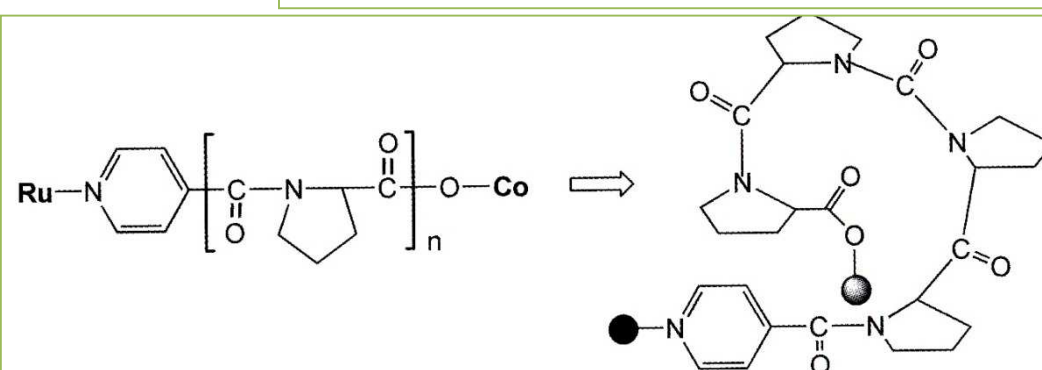


Figure 12.18 From inner-sphere to outer-sphere mechanism according to the flexibility of the bridge.

Table 12.5 The use of reactivity ratios for azido and thiocyanato complexes, in the form of complexes $[\text{CoX}(\text{NH}_3)_5]^{2+}$, in the assignment of an electron transfer mechanism [3].

Reductant	$k(X = \text{N}_3^-)/k(X = \text{NCS}^-)$	Mechanism
$[\text{TiOH}]^{2+}$ aq	400 000	inner-sphere
U^{3+} aq	40 000	inner-sphere
Cr^{2+} aq	20 000	inner-sphere
Fe^{2+} aq	3000	probably inner-sphere
Eu^{2+} aq	300	probably inner-sphere
V^{2+} aq	40	probably outer-sphere
$[\text{Cr}(\text{bpy})]^{2+}$	4	outer-sphere
$[\text{Ru}(\text{NH}_3)_6]^{2+}$	1.5	outer-sphere

Inner or Outer sphere?

- rates
- substitution in course of redox reaction
- reaction rate depends on the bridge
- Marcus law
- intermediate

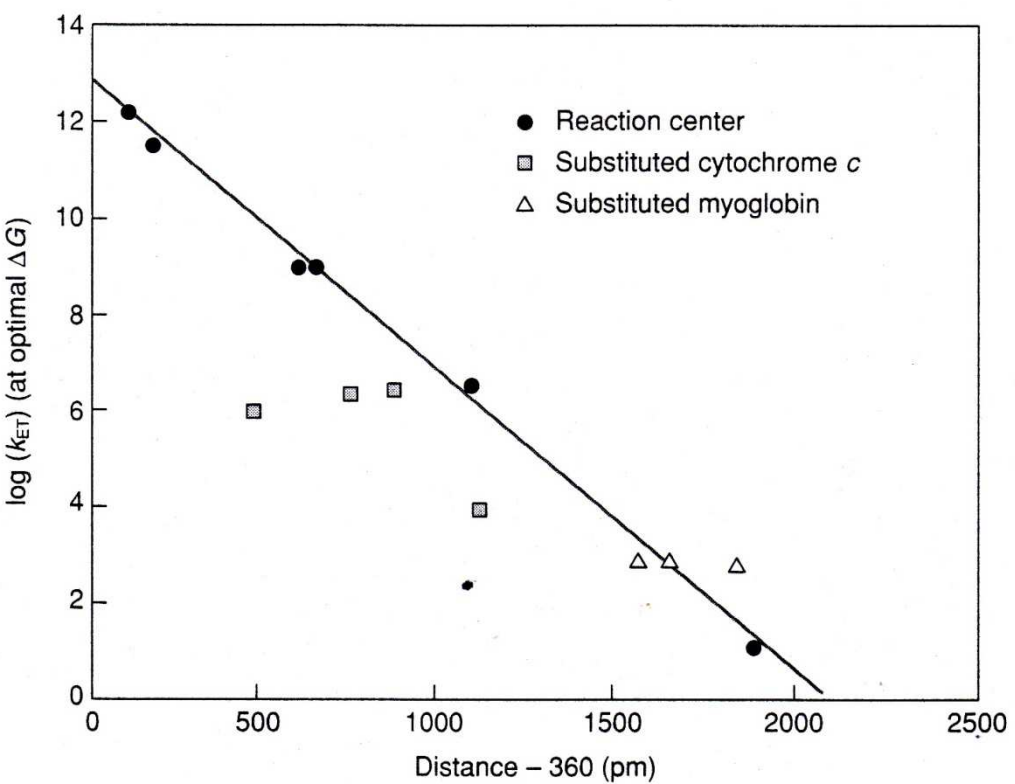
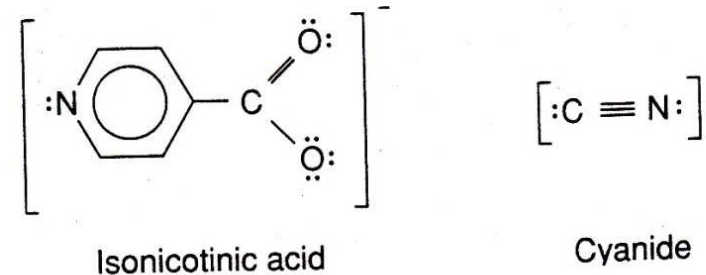
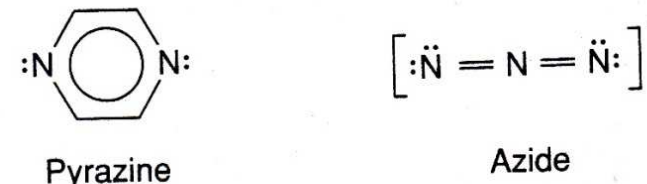
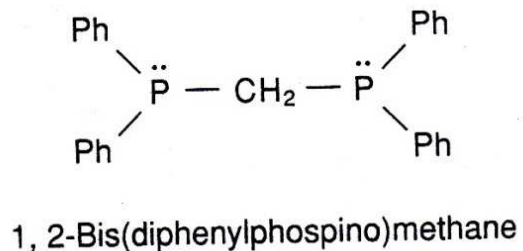
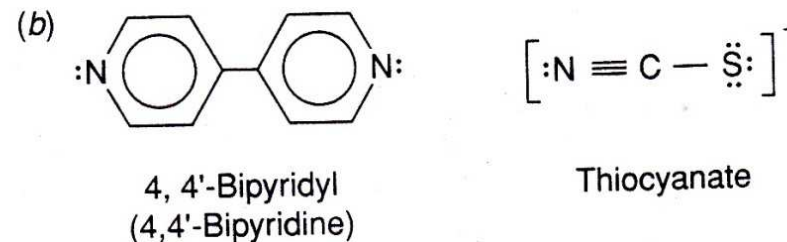
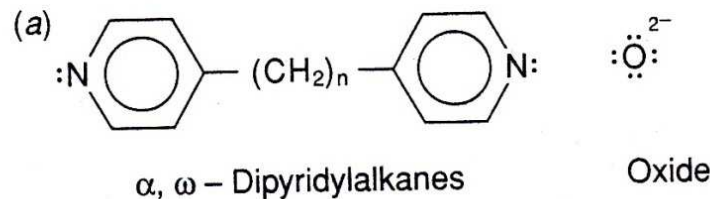


Figure 16.6

Plot showing the log of the electron-transfer rate constant, $\log k_{ET}$, as a function of metal–metal distance for several natural and ruthenium-modified proteins. [Adapted with permission from S. J. Lippard and J. M. Berg, *Principles of Bioinorganic Chemistry*, University Science Books, Sausalito, CA, 1994; p. 249.]

Examples of several common bridging ligands

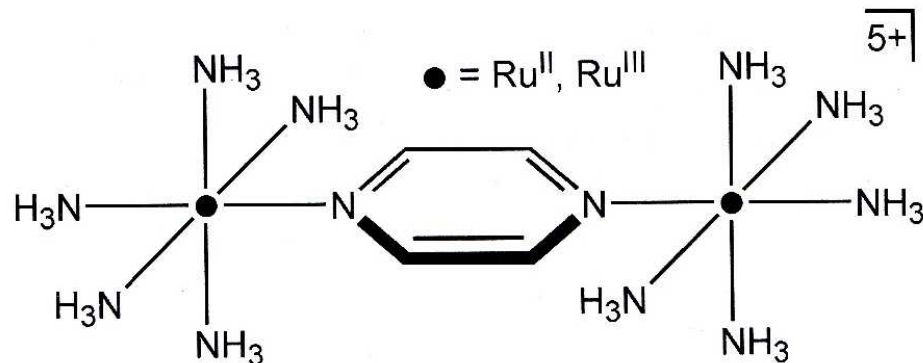


Saturated: low electronic communication between the connected metal atoms

Conjugated: enable electronic communication

Mixed – valence compounds

Creutz- Taube ion



d⁶ – d⁵ electronic configuration

Mixed-valence compound:

- presence of a bridge is not necessary
- mixed-valence complex must be stable for the two parent integer compounds
- various extent of electronic communication between the two centres – Robin and Day classification scheme

Robin – Day classification

Table 16.12
Robin and Day Classification of Mixed-Valence Compounds

Class I	Class II	Class III
Two metals in <u>very different environments</u>	Two metals in similar environments	Two metals in <u>identical environments</u>
Extra electron fully localized on one metal	Extra electron not fully localized on one metal	Extra electron fully delocalized on both metals
$d-d$ Electronic spectra of both ions seen	$d-d$ Electronic spectra of both ions modified	New electronic spectra seen
Intervalence charge-transfer bands at <u>high energy</u>	Intervalence charge-transfer bands in <u>visible or near IR</u>	Intervalence charge transfer bands <u>not seen</u>
Insulator	Semiconductor (if polymeric)	Metallic conductor (if polymeric)
Diamagnetic or paramagnetic	Ferromagnetic or antiferromagnetic at low temperatures (if polymeric)	May be ferromagnetic at high temperatures (if polymeric)

Spectroscopy

IVCT or MMCT bands: typical for Class II ,Class III

Bands characterisation:

- Class II – broad, symmetric, low-intensity, temperature dependent, solvent dependent
- Class III – intense, narrow, asymmetric, temperature and solvent independent

Robin – Day classification

Table 13.1 Characteristics of the Robin–Day classification.

	<i>Optical properties</i>	<i>Electrical properties</i>	<i>Magnetic properties</i>
Class I (Trapped electrons in ions of different symmetry)	No intervalence transfer band in the electronic spectrum. Color due to the isolated ions	Insulating	Properties of each ion
Class II (Ions of almost identical symmetry)	Intervalence transfer band in the visible or near/medium infrared. Deeper color than in isolated ions	Semiconducting (for a 1D, 2D or 3D solid)	Magnetically diluted. F or AF at low temperature
Class III (Delocalized electrons) Clusters (equivalent and indistinguishable ions)	Intervalence transfer band in the visible or near/medium infrared. Strong color.	Insulating	Magnetically diluted
Infinite Net (equivalent and indistinguishable ions)	Absorption threshold close to the IR. Opaque. Dark color. Metallic brightness	Metallic conductivity	Possible long-range ferromagnetic order at high T_c

Table 13.2 Examples of mixed-valence systems of different classes.

Class	Examples	Geometry of A	Oxid. State	Geometry of B	Oxid. State
I	[Cu(en) ₂][CuBr ₂] ₂	D _{4h}	2	linear	1
	[Co(NH ₃) ₆] ₂ [CoCl ₄] ₃	O _h	3	T _d	2
	Ga[GaCl ₄]	dodecahedral	1	T _d	3
II	[M ₃ O(carboxilato) ₆ L ₃](M = Mn, Fe, Ru)	O _h	2	O _h	3
	Fe ₄ [Fe(CN) ₆] ₃ · 4H ₂ O	O _h	2	O _h	3
	[Pt(etn) ₄][PtCl ₂ (etn) ₄]Cl ₄	D _{4h}	2	O _h	4
	(NH ₄) ₂ [SbBr ₆]	O _h	3	O _h	5
III-A (clusters)	[Nb ₆ Cl ₁₂]Cl ₂	O _h	2.33		
	[Fe ₄ S ₄ (SCH ₂ Ph) ₄] ²⁻	T _d	2.5		
	[(NH ₃) ₅ Os—N ₂ —Os(NH ₃) ₅] ⁵⁺	O _h	2.5		
	[Re ₂ Cl ₈] ³⁻	C _{4v}	2.5		
	Creutz–Taube ion	O _h	2.5		
III-B (1, 2, 3D)	K _{1.75} [Pt(CN) ₄] · 1.5H ₂ O	D _{4h} (1D)	2.25		
	K ₂ [Pt(CN) ₄]Br _{0.30} · 3H ₂ O	D _{4h} (1D)	2.30		
	Na _x TiO ₂ (0 < x < 1)	O _h (3D)	(3–4)		
	Na _x WO ₃ (0.4 < x < 0.9)	O _h (3D)	(5–6)		

Creutz–Taube ions derivatives: between Class II and Class III

Ions (+5)	λ_{\max} (nm)	ε ($M^{-1} \text{ cm}^{-1}$)
$[(\text{NH}_3)_5\text{Ru}-\text{N}(\text{C}_6\text{H}_4)-\text{Ru}(\text{NH}_3)_5]^{5+}$	1570	5000
$[(\text{NH}_3)_5\text{Ru}-\text{N}(\text{C}_6\text{H}_4-\text{C}_6\text{H}_4)-\text{Ru}(\text{NH}_3)_5]^{5+}$	1030	920
$[(\text{NH}_3)_5\text{Ru}-\text{N}(\text{C}_6\text{H}_4-\text{CH}_2-\text{C}_6\text{H}_4)-\text{Ru}(\text{NH}_3)_5]^{5+}$	960	760
$[(\text{NH}_3)_5\text{Ru}-\text{N}(\text{C}_6\text{H}_4-\text{CH}_2-\text{C}_6\text{H}_4-\text{CH}_3-\text{C}_6\text{H}_4)-\text{Ru}(\text{NH}_3)_5]^{5+}$	890	165
$[(\text{NH}_3)_5\text{Ru}-\text{N}(\text{C}_6\text{H}_4-\text{CH}_2-\text{C}_6\text{H}_4)-\text{Ru}(\text{NH}_3)_5]^{5+}$	810	30

Figure 13.14 Some Creutz–Taube ion derivatives, with the main features of their IT bands.

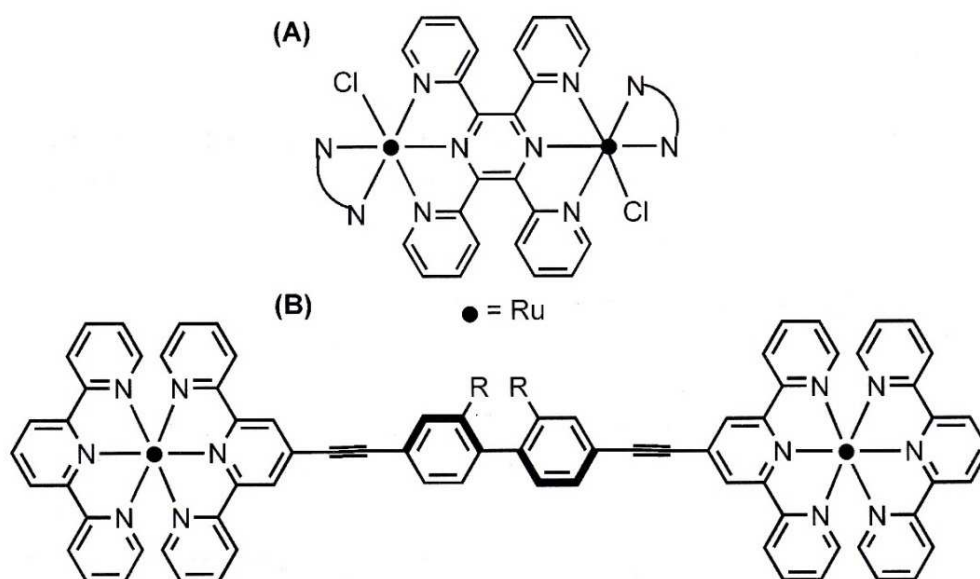


Figure 13.15 Scheme of several Creutz–Taube ion derivatives.

Class III

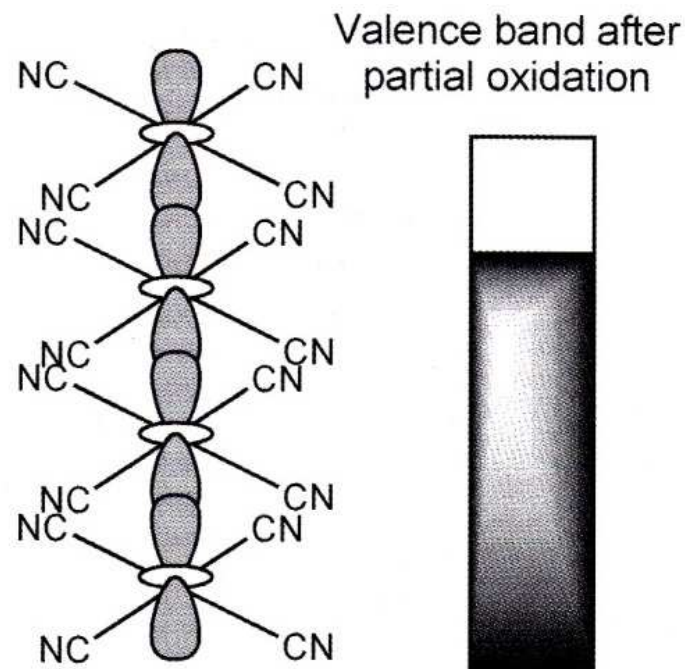


Figure 13.19 Scheme of the valence band of the partially oxidized $[\text{Pt}^{\text{II}}(\text{CN})_4]^{2-}$ compound

Molecular wires

How to tune properties of the mixed-valence compounds

- by the extent and magnitude of electronic delocalization and
- by modifying the electron transfer rate:
 1. changing ligand distortion, geometry around the metal centre - biological systems! (role of the protein)
 2. bridging ligand –ability to delocalize electrons
 3. terminal ligands – stabilization of lower oxidation states by π – acid ligands, more localized systems

Uveřejněné materiály jsou určeny studentům Vysoké školy chemicko-technologické v Praze jako studijní materiál. Některá textová i obrazová data v nich obsažená jsou převzata z veřejných zdrojů. V případě nedostatečných citací nebylo cílem autorky záměrně poškodit autora/y původního díla.

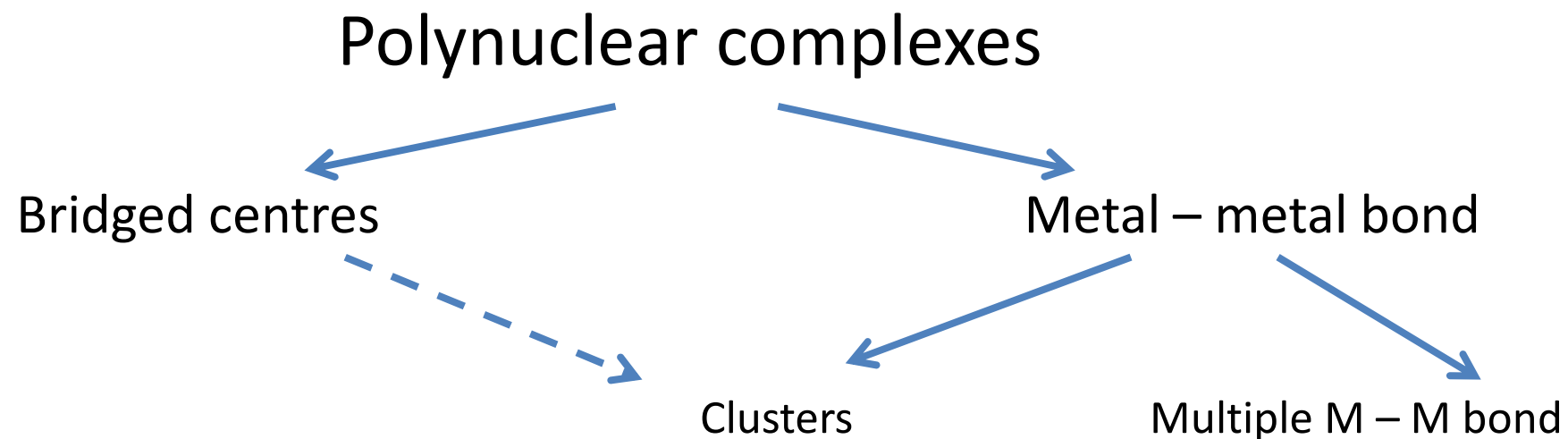
S případnými výhradami se prosím obracejte na autorku tohoto výukového materiálu, aby bylo možno zjednat nápravu.



The published materials are intended for students of the University of Chemistry and Technology, Prague as a study material. Some text and image data contained therein are taken from public sources. In the case of insufficient quotations, the author's intention was not to intentionally infringe the possible author(s) rights to the original work.

If you have any reservations, please contact the author(s) of the specific teaching material in order to remedy the situation.

Compounds containing a metal – metal bond

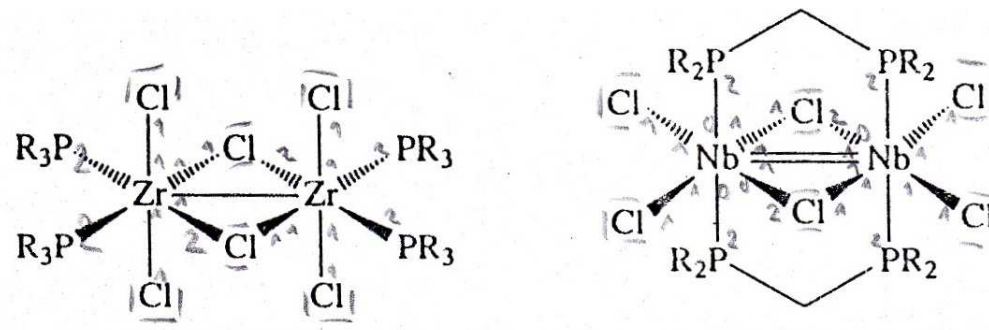


EUROPEAN UNION
European Structural and Investing Funds
Operational Programme Research,
Development and Education

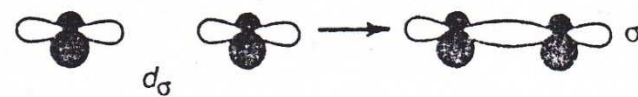


One metal – metal bond

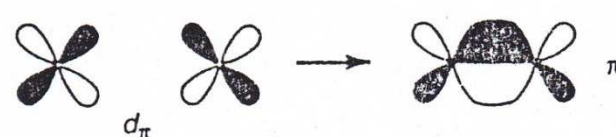
Edge-sharing bioctahedra



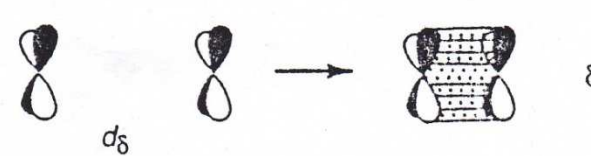
$d_{x^2-y^2}$



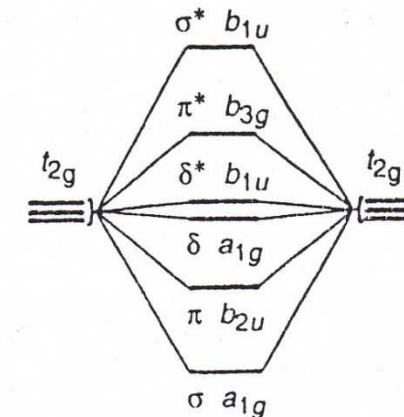
d_{yz}



d_{xz}



(a)

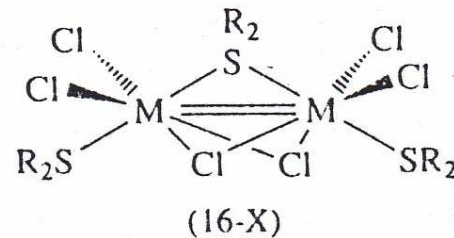
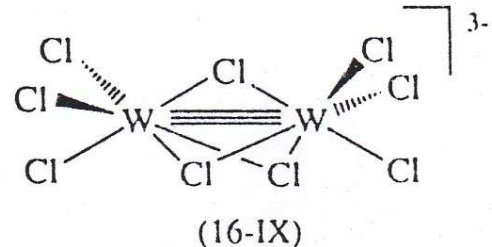


Orbital energy level diagram

(b)

Figure 16-5 (a) The three $d-d$ overlaps that can be expected in an edge-sharing bioctahedral structure. (b) The pattern of energy levels expected when only the direct overlaps are considered.

Face-sharing bioctahedra



M = Nb, Ta

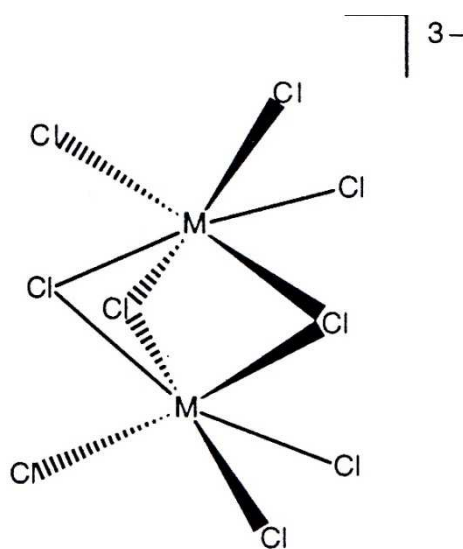


Fig. M.7 Face-sharing bi-octahedral structure of $[M_2Cl_9]^{3-}$

M = Cr, Mo, W

different properties:

W – W

242 pm, invariable, diamagnetic

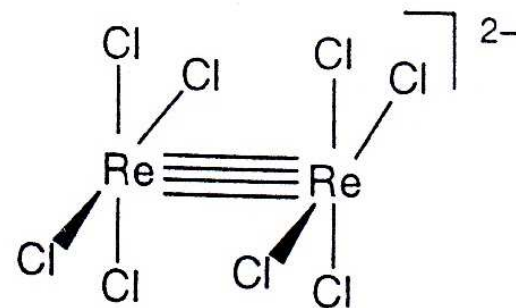
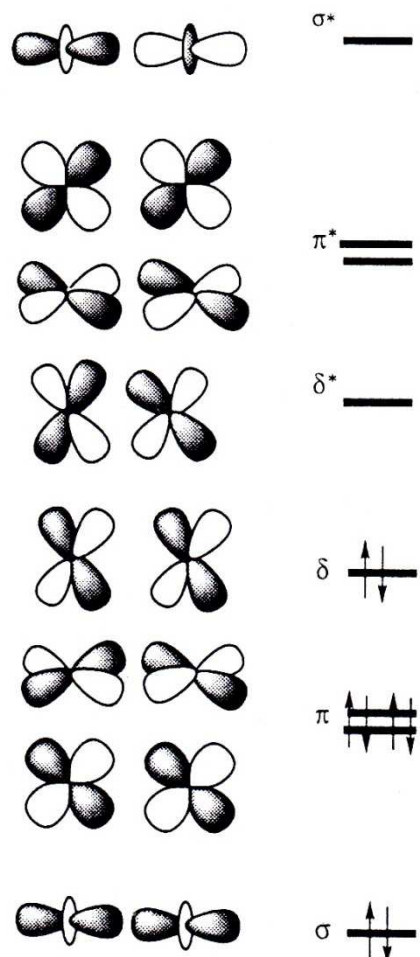
Mo–Mo

252–282 depending on the counter-cation
magnetism – two d³, AF coupling
(temperature dependence)

Cr – Cr

312 pm, no magnetic coupling

Tetragonal prismatic structure



Typical intense colours, $\delta-\delta^*$:

$[\text{Re}_2\text{Cl}_8]^{2-}$ royal blue

$[\text{Mo}_2\text{Cl}_8]^{4-}$ intense red

$[\text{Mo}_2(\text{ac})_4]^{4-}$ yellow

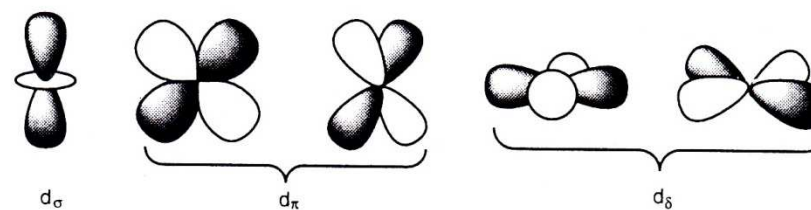


Fig. M.3 Nodal properties of d orbitals relating to the z axis

Properties of the quadruple bond

Strength: +3% of energy

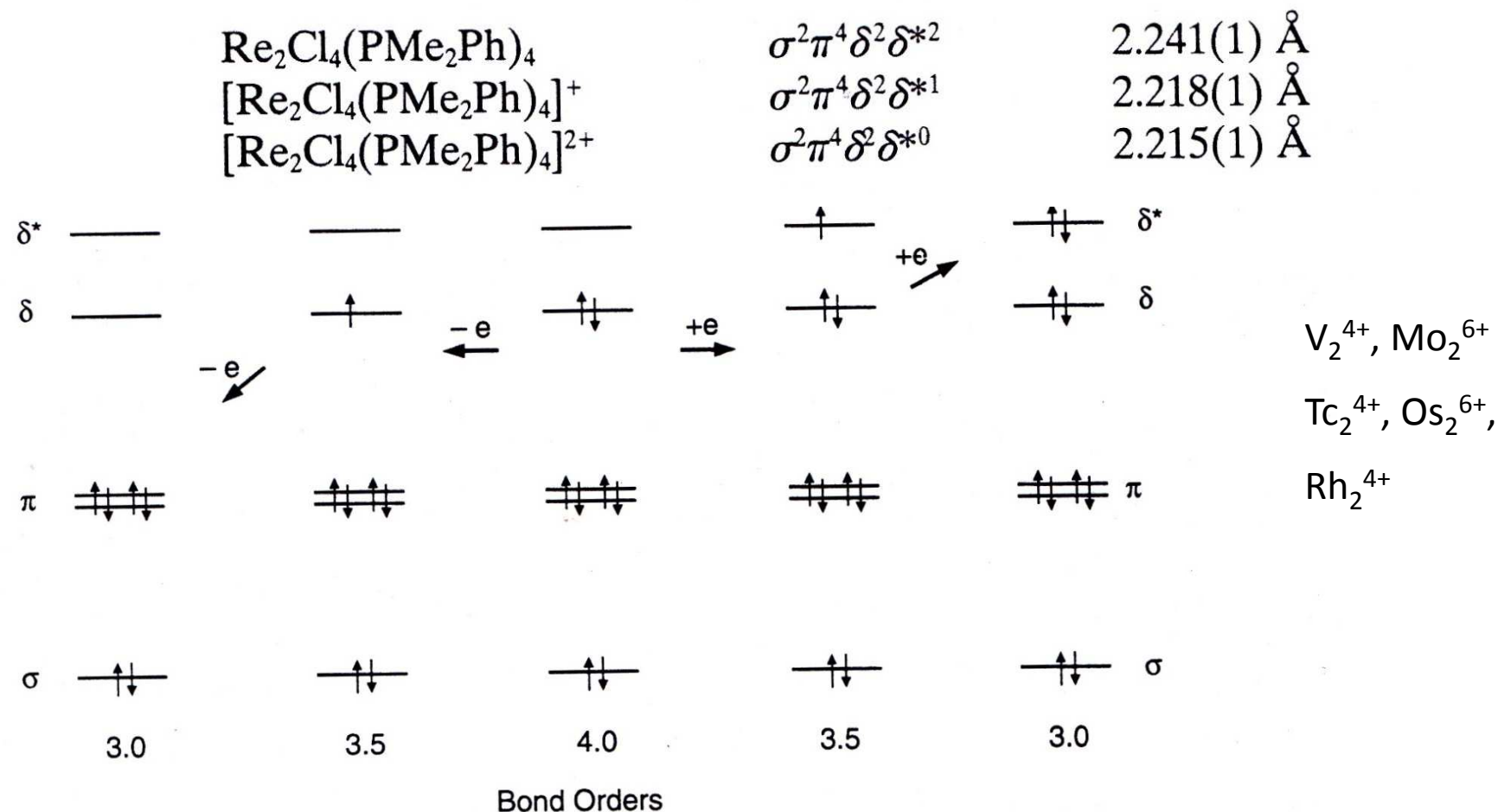


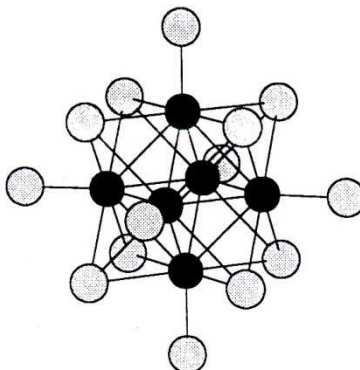
Figure 16-8 A schematic representation of how changes in the occupation of the δ and δ^* orbitals change the M–M bond order.

Presence of a M –M bond:

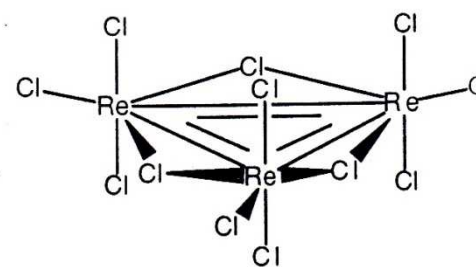
- thermochemical data (ΔH)
- bond length from X-ray data – comparison
- spectroscopy: Raman vibration of the M – M bond

Clusters

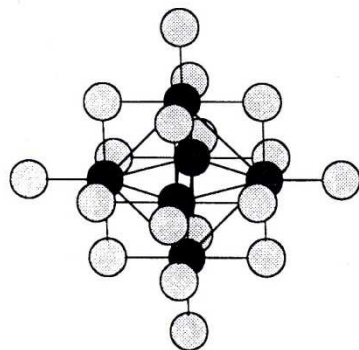
2 or more metals form a group , direct M-M bonds



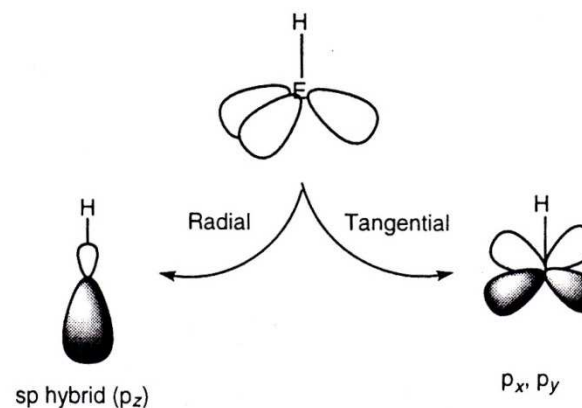
The structure of the $[Mo_6Cl_{12}Cl_6]^{2-}$ ion



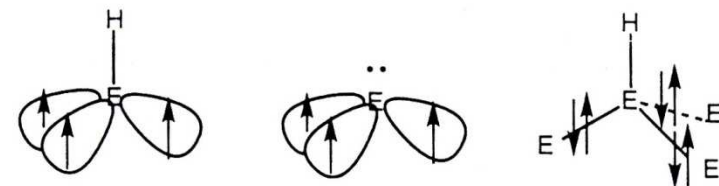
The structure of the $[Re_3Cl_{12}]^{3-}$ ion
Re-Re = 246–247 pm



The structure of the $[Ta_6Cl_{12}Cl_6]^{4-}$ ion



vertex electronic + orbital arrangement



Electron density in face centres

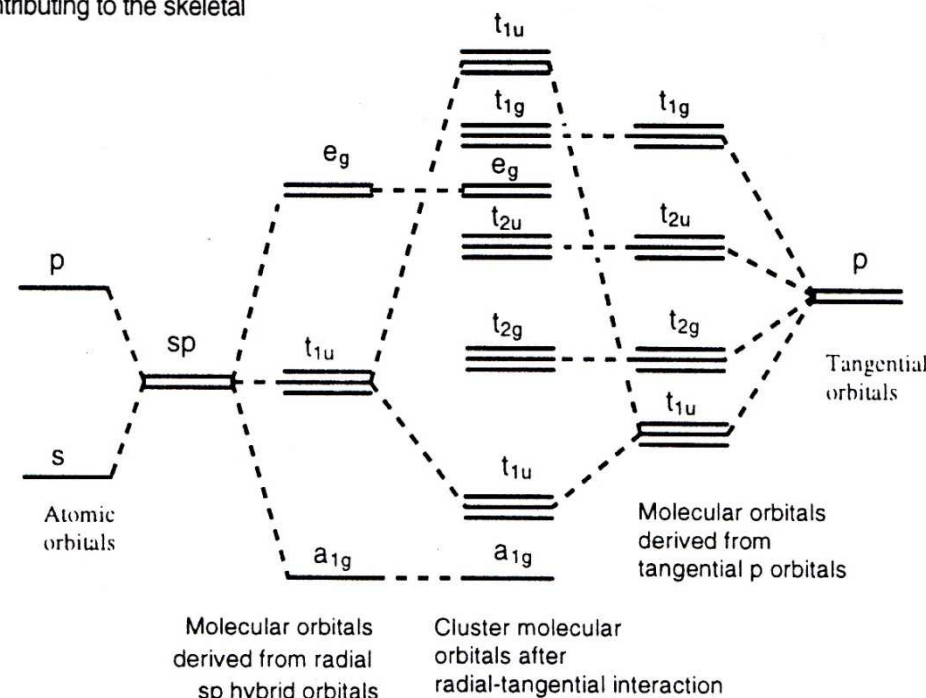
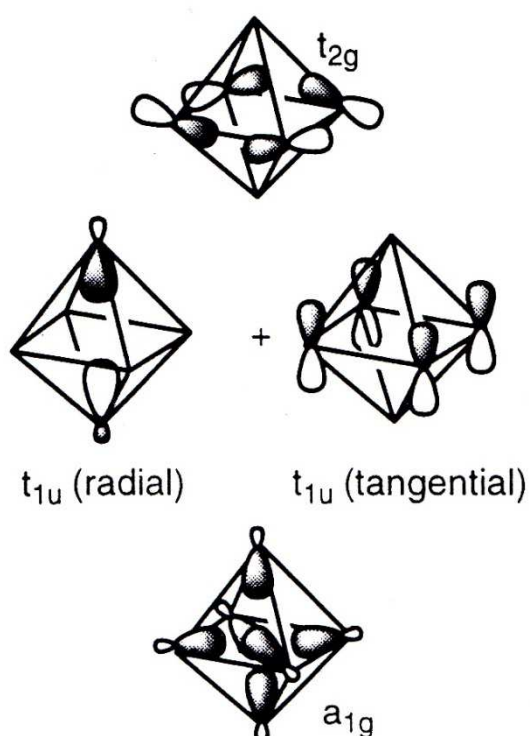


Fig. P.3 The formation of cluster molecular orbitals from the radial sp hybrids pointing into the cluster and the tangential p orbitals in octahedral $[B_6H_6]^{2-}$. The other set of sp hybrid orbitals are used to form terminal bonds between the boron atoms and the hydrogen atoms

Table P.2 Examples of deltahedral cage molecules

Geometry	Example	No. of valence electrons
Trigonal bipyramidal	$[B_5H_5]^{2-}$	22
	$C_2B_3H_5$	
	Sn_5^{2-}	
	Pb_5^{2-}	
	Tl_5^{7-}	
Octahedron	$[B_6H_6]^{2-}$	26
	$C_2B_4H_6$	
	Tl_6^{8-}	
Pentagonal bipyramid	$[B_7H_7]^{2-}$	30
	$C_2B_5H_7$	
Dodecahedron	$[B_8H_8]^{2-}$	34
	$C_2B_6H_8$	
Tricapped trigonal prism	$[B_9H_9]^{2-}$	38
	$TlSn_8^{3-}$	
	$C_2B_7H_9$	
Bicapped square-antiprism	$[B_{10}H_{10}]^{2-}$	42
	$C_2B_8H_{10}$	
	Ge_{10}^{2-}	
Octadecahedron	$[B_{11}H_{11}]^{2-}$	46
	$C_2B_9H_{11}$	
Icosahedron	$[B_{12}H_{12}]^{2-}$	50
	$C_2B_{10}H_{12}$	
	$[Al_{12}R_{12}]^{2-}$	

Deltahedral skeletons
triangular faces = bonding!

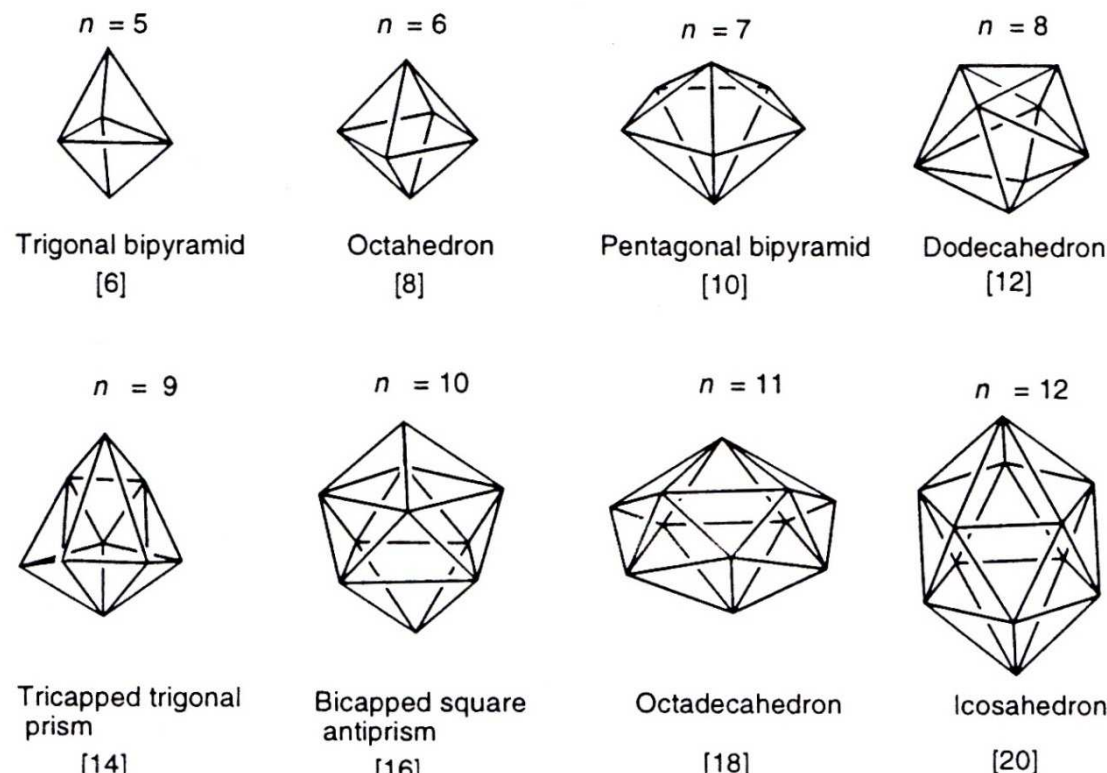


Fig. P.5 Deltahedral skeletons. The numbers in square brackets refer to the number of triangular faces

*clos*o – closed cage

nido – 1 vertex less

arachno – 2 vertices less

hypho – 3 vertices less

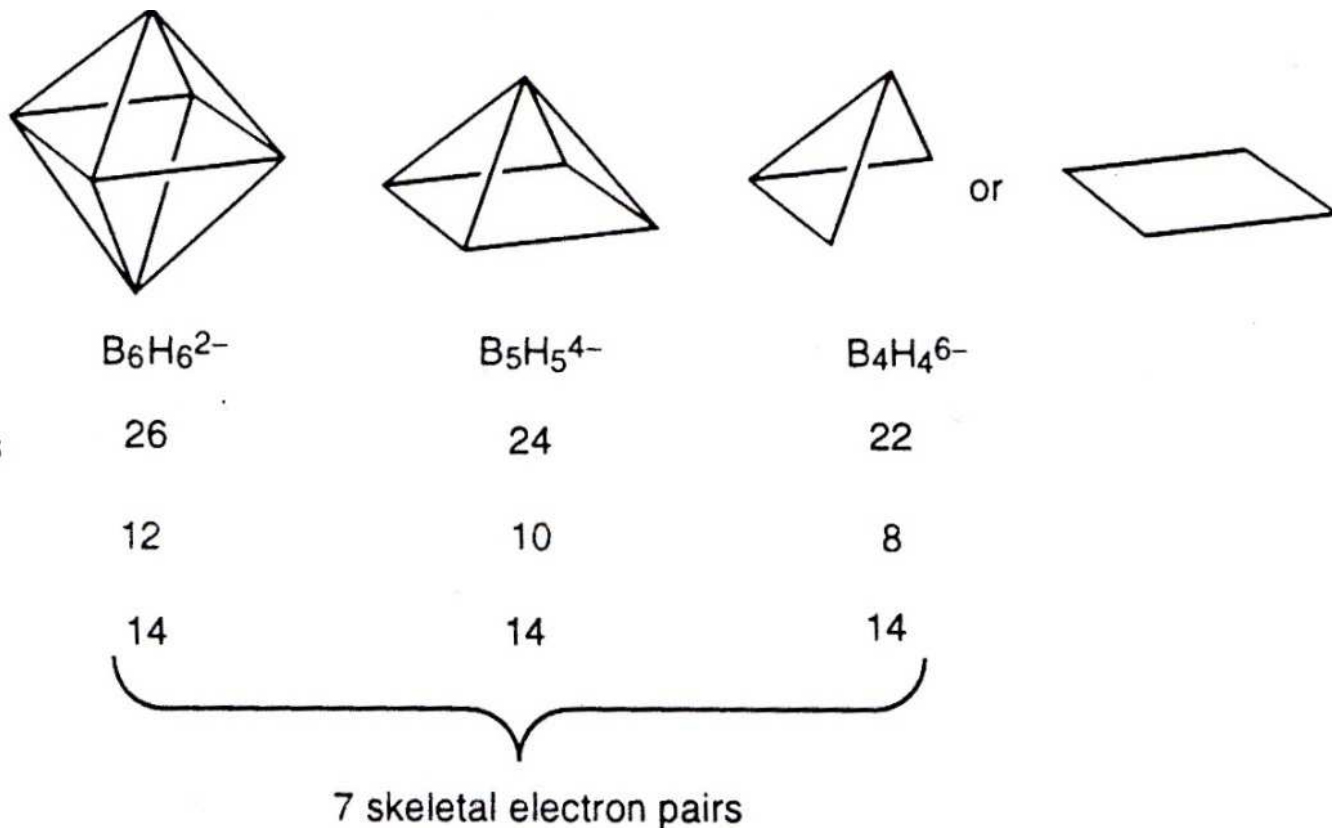


Fig. P.7 Geometric and electronic relationships on *clos*o-, *nido*-, and *arachno*-borane

PSEPT – Wade-Mingos rules

number of vertex compared with number of skeletal electrons(pairs), BH, CH

Main group element clusters

Vertices	n
Valence atomic orbitals (each vertex)	4
Skeleton atomic orbitals (each vertex)	3
SEPs for <i>clos</i> o	$n + 1$
SEPs for <i>nido</i>	$n + 2$
SEPs for <i>arachno</i>	$n + 3$
SEP for <i>hypho</i>	$n + 4$
SEP – skeleton electron pairs	

Isolobality

Isolobal groups: the same number of orbitals, similar energy

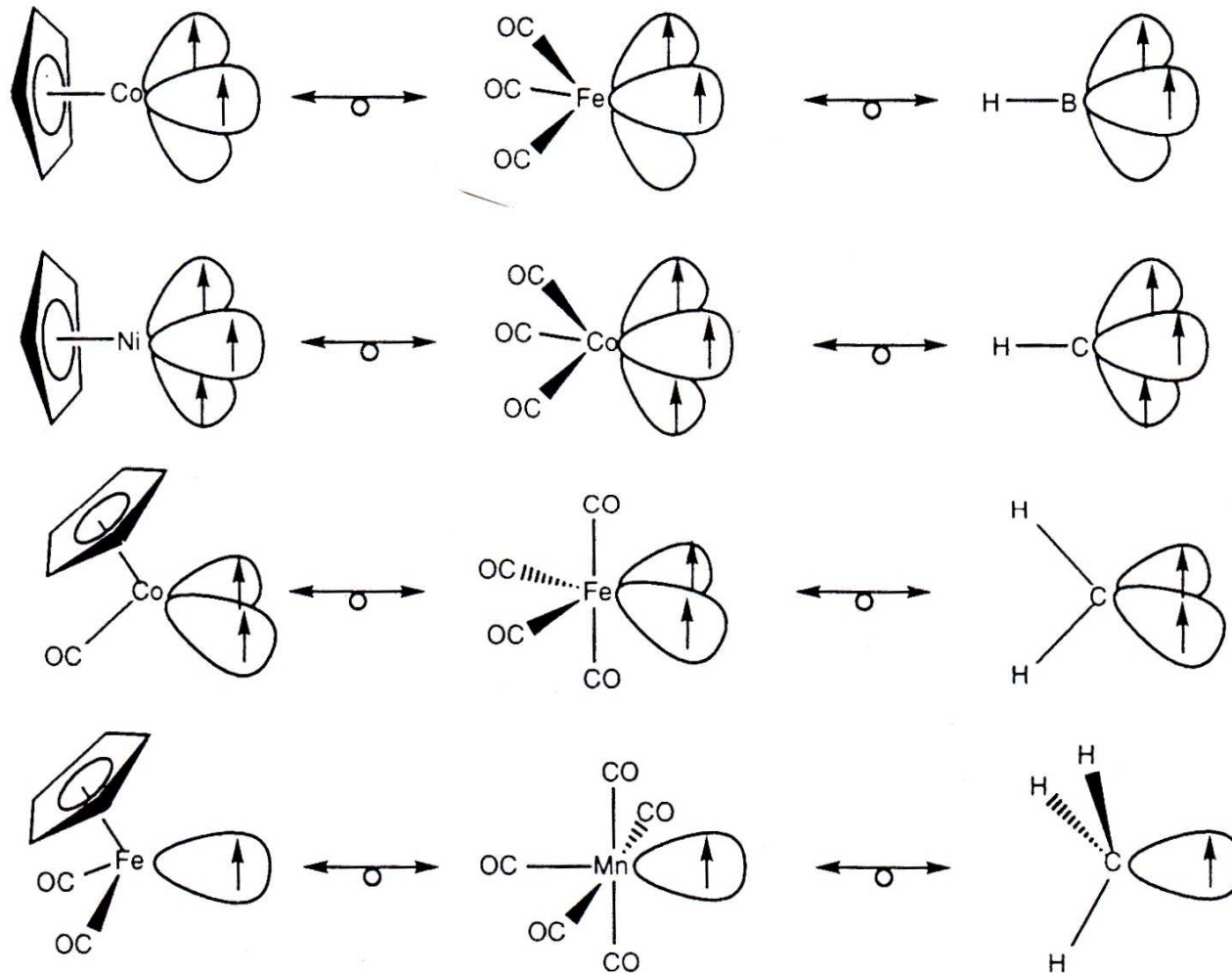


Fig. I.2 Examples of the isolobal analogy

Carboranes (carbaboranes)

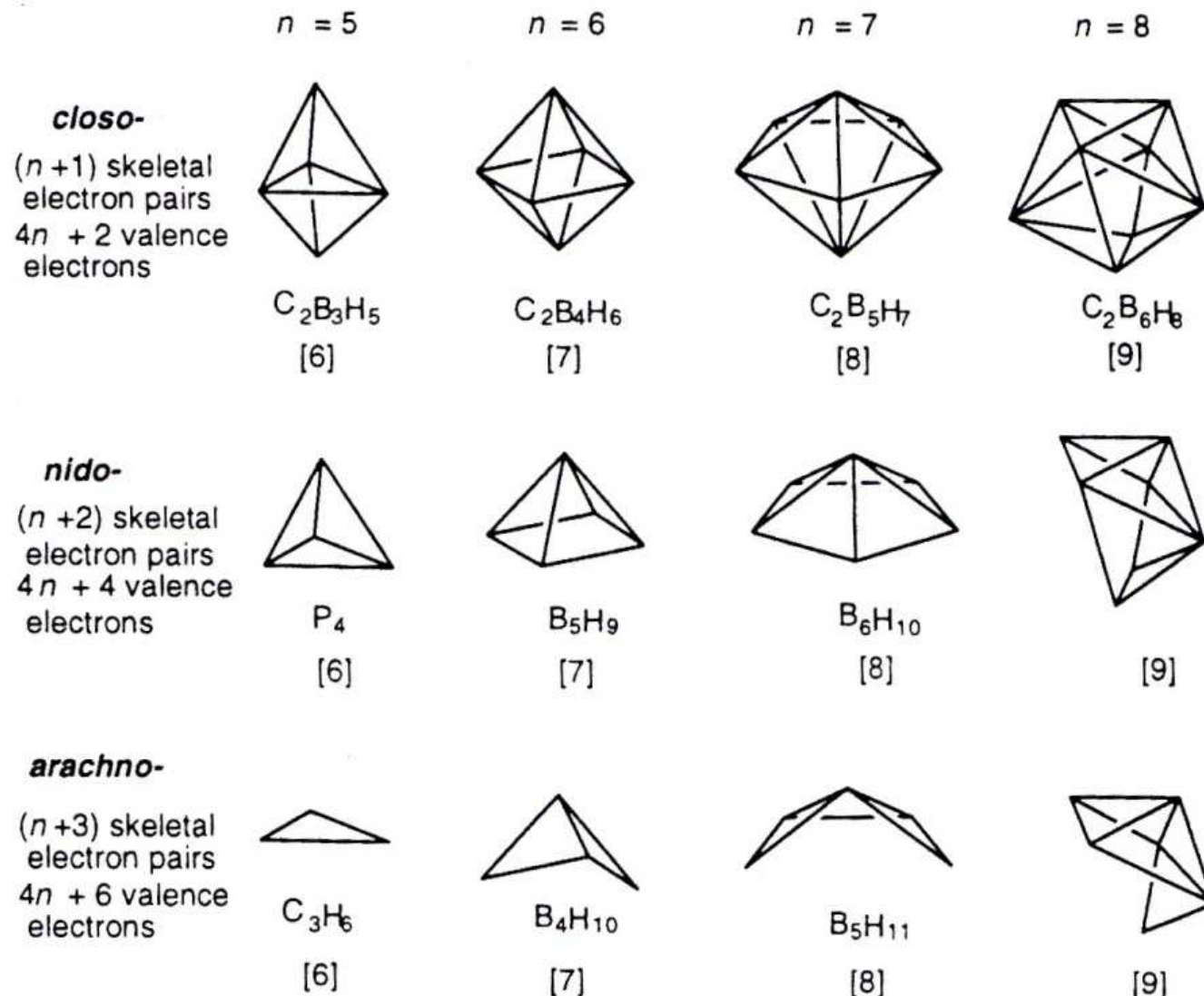


Fig. P.6 Examples of *closo*-, *nido*-, and *arachno*-polyhedral skeletons. The numbers in square brackets refer to the number of skeletal bonding electron pairs

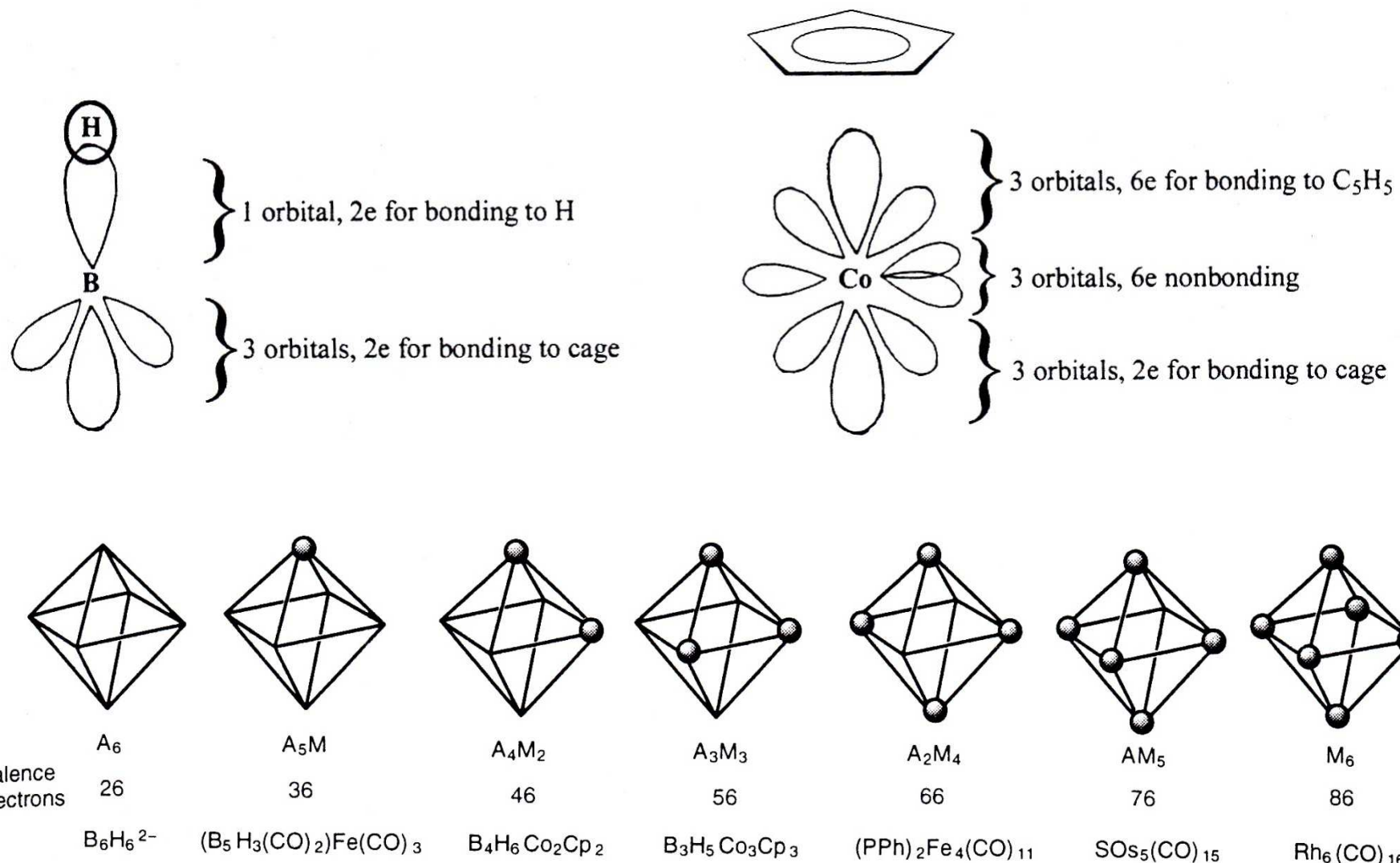


Fig. I.3 Examples of series of *closo*-octahedral cluster compounds starting with $\text{B}_6\text{H}_6^{2-}$ and ending with $\text{Rh}_6(\text{CO})_{16}$. The increment of ten valence electrons each time a metal atom is introduced into the cage is particularly noteworthy

Metal vertex, medium size clusters

Total electron count in metal clusters – PSEPT

Polyhedral Skeletal Electron Pair Theory

CVE = cluster valence electrons = metal valence electrons + electrons donated by ligands (depending on the ligand type, L gives 2, L_2X gives 5, etc.)
SE = skeletal electrons = CVE minus 12 (6 non-skeletal orbitals)

Framework Structure	Example	CVE	SEP <i>cluster</i> = $\frac{[CVE - 12n]}{2}$	Structural type	Borane equivalent
Tetrahedron	$[Ir_4(CO)_{12}]$	60	12 e = 6 pairs	<i>nido</i>	
Trigonal bipyramidal	$[Os_5(CO)_{15}]^{2-}$	72	12 e = 6 pairs	<i>clos</i>	$[B_5H_5]^{2-}$
Octahedron	$[Os_6(CO)_{18}]^{2-}$	86	14 e = 7 pairs	<i>clos</i>	$[B_6H_6]^{2-}$
Octahedron	$[Rh_6(CO)_{16}]$	86	14 e = 7 pairs	<i>clos</i>	$[B_6H_6]^{2-}$
Square pyramid	$[C \subset Ru_5(CO)_{15}]$	74	14 e = 7 pairs	<i>nido</i>	
Icosahedron	$[Sb \subset Rh_{12}(CO)_{27}]^{3-}$	170	26 e = 13 pairs	<i>clos</i>	$[B_{12}H_{12}]^{2-}$

an interstitial atom: all valence electrons belong to the skeleton (cf. the lowest MO)

More examples

Table 6.6 Selected clusters and its geometry based on the electron counting of each unit.

<i>Formula</i>	<i>Division by units</i>	<i>SEs for each unit ($v + x - 2$) or ($v + x - 12$)</i>	<i>SEPs</i>	$(n + i)$	<i>Type</i>
$[\text{Sb} \subset \text{Rh}_{12}(\text{CO})_{27}]^{3-}$	Sb 12[Rh(CO) ₂] 3CO	$5 + 12(9 + 4 - 12) + 6 +$ $\swarrow 3(\text{charge}) = 26$	13	$n + 1$	<i>closo</i>
$[\text{C}_2\text{B}_9\text{H}_{11}]^{2-}$	2(CH) 9(BH)	$(2 \times 3) + (9 \times 2) + 2$ $(\text{charge}) = 26$	13	$n + 1$	<i>closo</i>
✓ $[\text{Ge}_9]^{4-}$	9[Ge]	$(9 \times 2) + 4 (\text{charge}) = 22$	11	$n + 2$	<i>nido</i>
$[\text{Ir}_4(\text{CO})_{12}]$	4[Ir(CO) ₃]	$4(9 + 6 - 12) = 12$	6	$n + 2$	<i>nido</i>
$[\text{C} \subset \text{Fe}_4(\text{CO})_{12}]^{2-}$	C 4[Fe(CO) ₃]	$4 + 4(8 + 6 - 12) + 2$ $(\text{charge}) = 14$	7	$n + 3$	<i>arachno</i>

The capped clusters
monocapped ,



bicapped octahedra

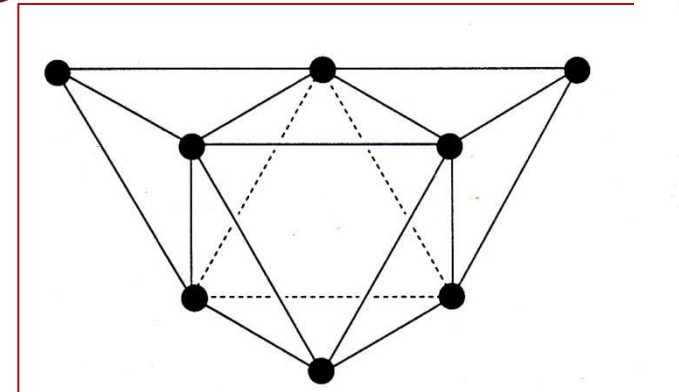


Table 6.7 Examples of the capping principle.

Cluster	CVE	14n + 2 rule for closo M_7 , M_8 and M_{10}	(14n + 2) – CVE	SEP ^a = (CVE – 12n)/2	Number of capped fragments
[Os ₇ (CO) ₂₁]	98	100	2 (1 pair)	7	1
[Os ₈ (CO) ₂₂] ²⁻	110	114	4 (2 pairs)	7	2
[Os ₁₀ C(CO) ₂₄] ²⁻	134	142	8 (4 pairs)	7	4

^a SEP = 7 pairs (14 electrons) is the characteristic number for an octahedron ($n + 1$).

Gold/nickel cluster

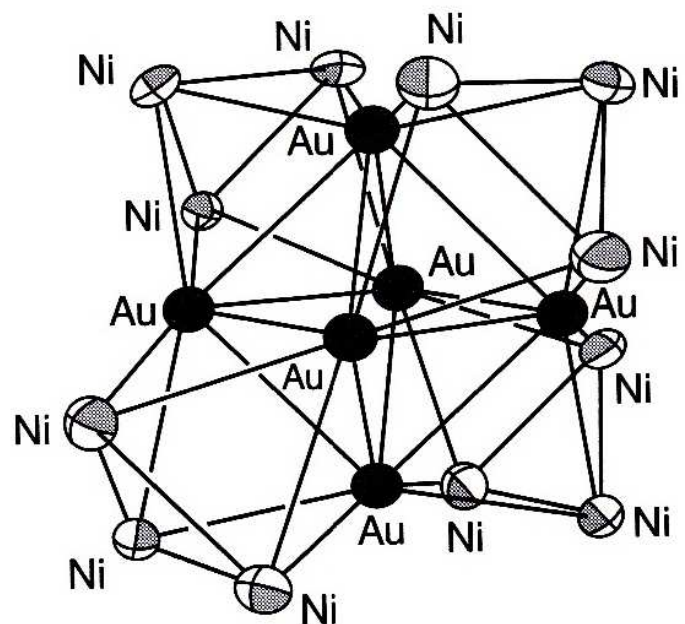
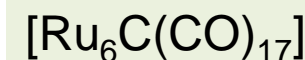
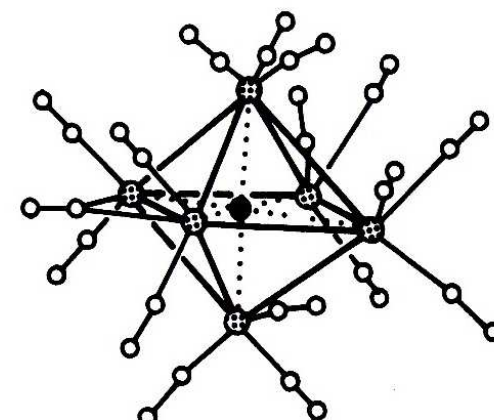
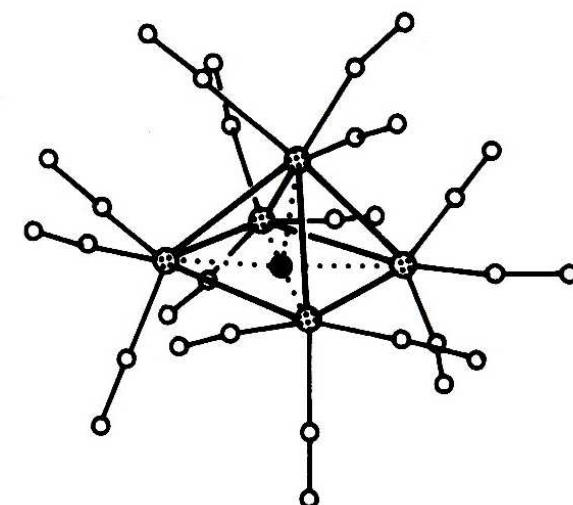


Figure 16-11 $\text{Au}_6\text{Ni}_{12}$ core of the 236-electron $[\text{Au}_6\text{Ni}_{12}(\text{CO})_{24}]^{2-}$ dianion. This 18-vertex polyhedron of cubic T_d ($43m$) symmetry may be viewed as a face-to-face condensation of four octahedral Au_3Ni_3 fragments at alternate faces of a central Au_6 octahedron (A. J. Whoolery and L. F. Dahl, *J. Am. Chem. Soc.* **1991**, *113*, 6683.)

Heteroatoms in clusters



Carboranes (carboranes) as ligands, carbollides

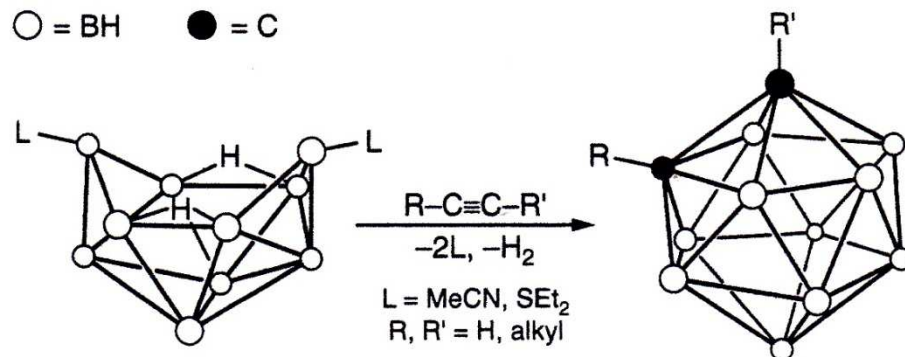


Figure 5-11 Insertion of an alkyne into the decaborane cage to form an icosahedral RR'C₂B₁₀H₁₀ carborane.

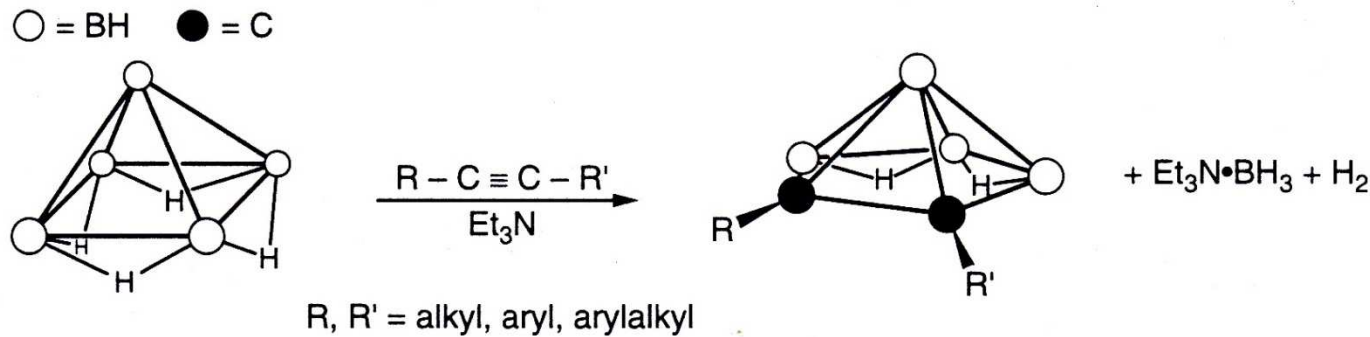
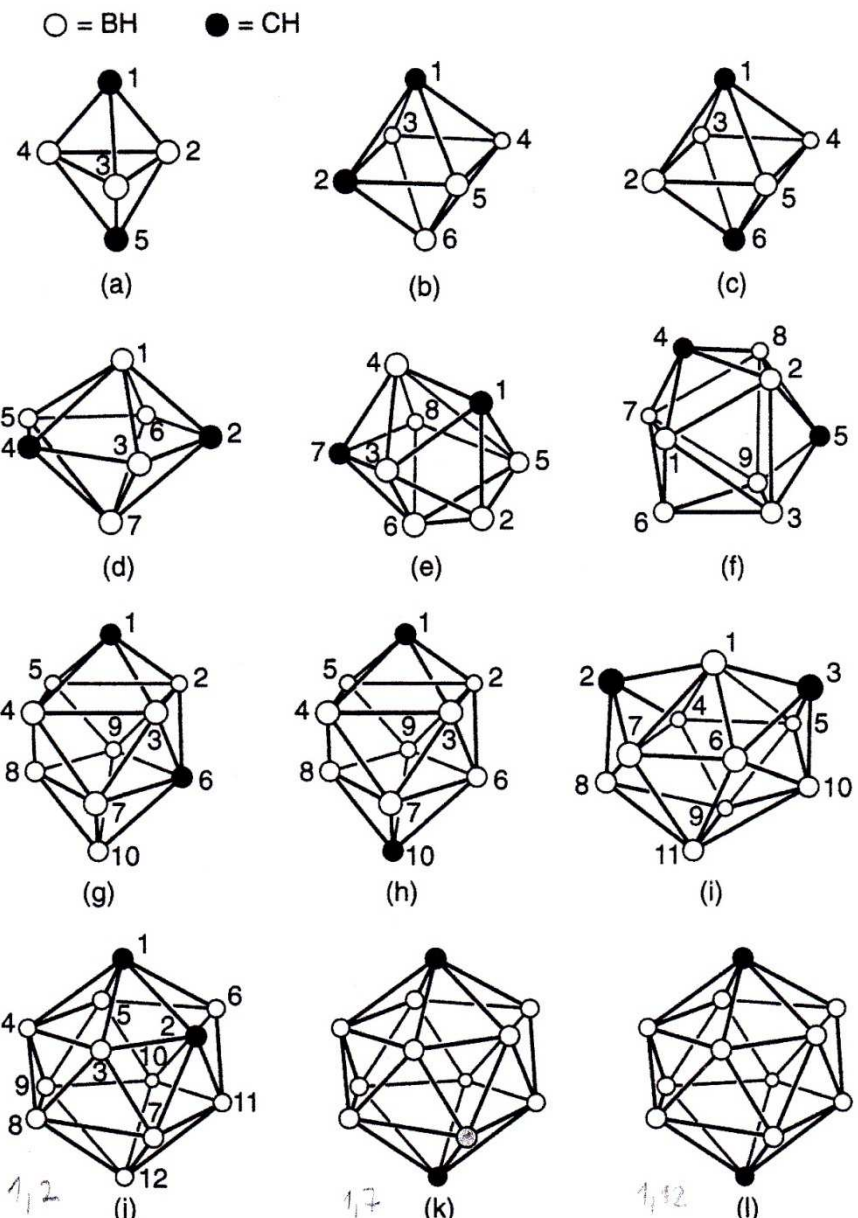


Figure 5-14 Base-promoted synthesis of *nido*-2,3-RR'C₂B₄H₆ carboranes.



3 dimensional
 aromaticity,
 “superaromatic
 molecules”, high
 thermal and oxidative
 stability

Figure 5-10 Structures of $\text{C}_2\text{B}_{n-2}\text{H}_n$ *closو-carboranes* (not all of the known isomers are shown). (a) 1,5- $\text{C}_2\text{B}_3\text{H}_5$. (b) 1,2- $\text{C}_2\text{B}_4\text{H}_6$. (c) 1,6- $\text{C}_2\text{B}_4\text{H}_6$. (d) 2,4- $\text{C}_2\text{B}_5\text{H}_7$. (e) 1,7- $\text{C}_2\text{B}_6\text{H}_8$. (f) 4,5- $\text{C}_2\text{B}_7\text{H}_9$. (g) 1,6- $\text{C}_2\text{B}_8\text{H}_{10}$. (h) 1,10- $\text{C}_2\text{B}_8\text{H}_{10}$. (i) 2,3- $\text{C}_2\text{B}_9\text{H}_{11}$. (j) 1,2- $\text{C}_2\text{B}_{10}\text{H}_{12}$. (k) 1,7- $\text{C}_2\text{B}_{10}\text{H}_{12}$. (l) 1,12- $\text{C}_2\text{B}_{10}\text{H}_{12}$.

Nido- and arachno- structures

● = BH ○ = CH ◑ = C

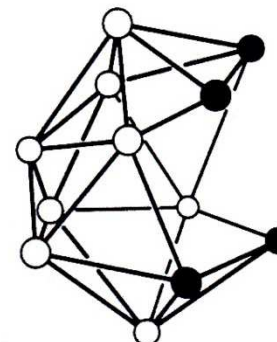
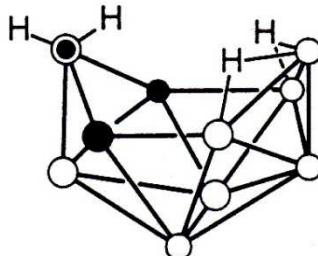
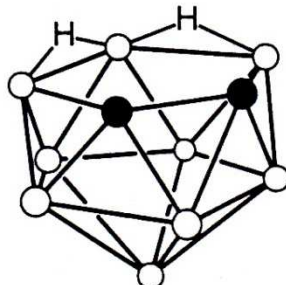
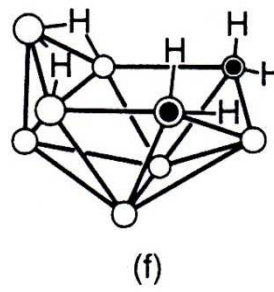
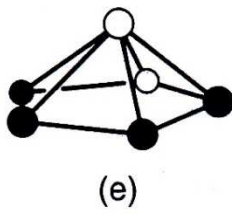
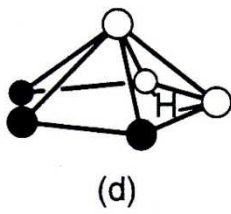
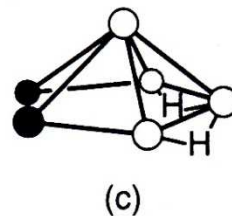
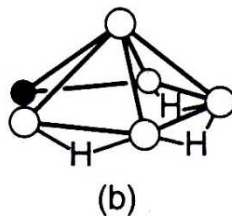
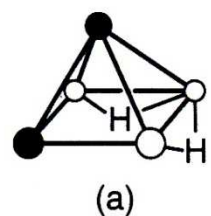
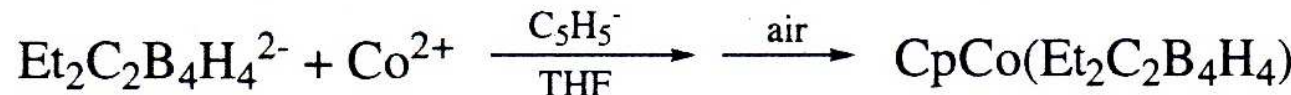
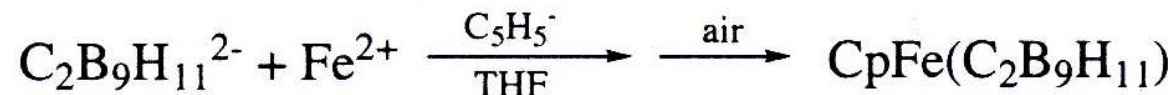
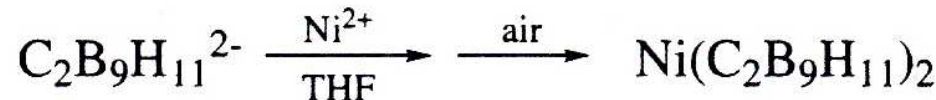


Figure 5-13 A selection of *nido*- and *arachno*-carborane structures. (a) *nido*-1,2-C₂B₃H₇. (b) *nido*-2-CB₅H₉. (c) *nido*-2,3-C₂B₄H₈. (d) *nido*-2,3,4-C₃B₃H₇. (e) *nido*-2,3,4,5-C₄B₂H₆. (f) *arachno*-C₂B₇H₁₃. (g) *nido*-C₂B₉H₁₃. (h) *arachno*-C₃B₇H₁₃. (i) *nido*-C₄B₈H₁₂. Compounds (h) and (i) are known only as C-substituted derivatives.

Metallacarboranes

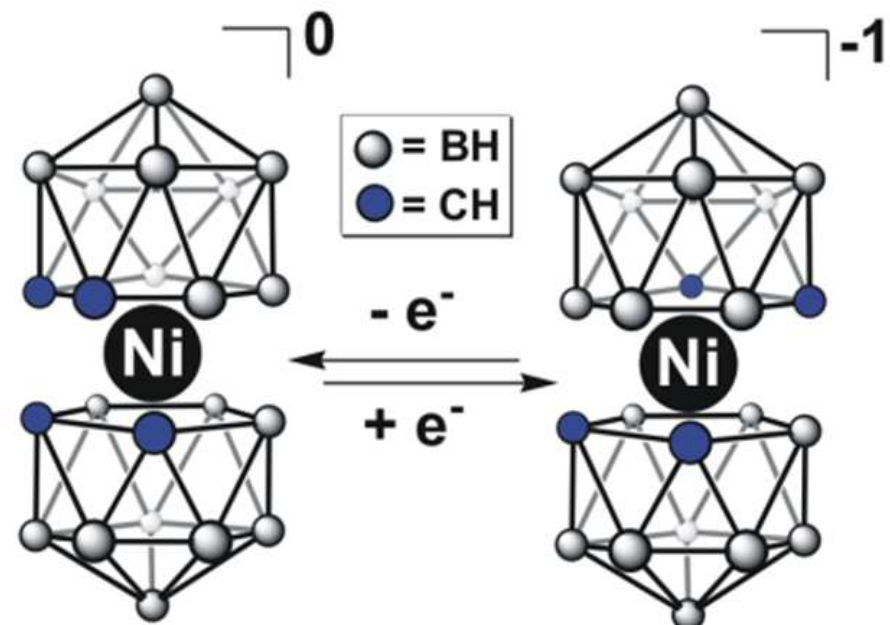


Example: nickel bis(dicarbollide)



carbollide from olla
(esp.) = pot

Various metals, stable.
Redox probes, sensors,
protease inhibitor (Co)



\circlearrowleft = BH, B ● = CH, C-alkyl, C-SiMe₃

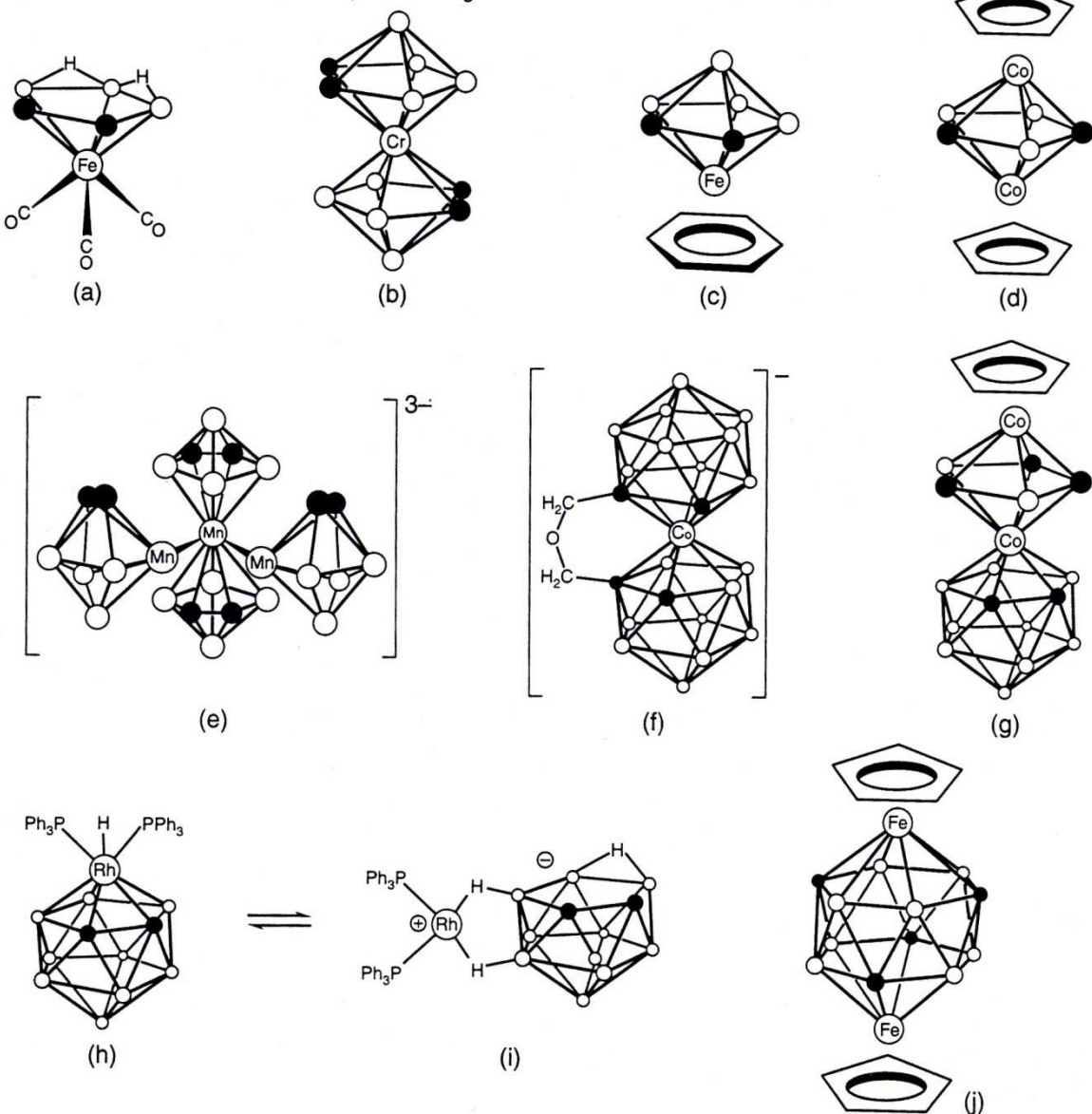


Figure 5-18 Examples of metallacarboranes. (a) *nido*-1,2,3-(CO)₃Fe(C₂B₃H₇). (b) Cr[2,3-(Me₃Si)₂C₂B₄H₄]₂. (c) 1,2,3-(C₆H₆)Fe(Et₂C₂B₄H₄). (d) 1,7,2,4-Cp₂Co₂(C₂B₃H₅). (e) Mn₃[2,3-(Me₃Si)₂C₂B₄H₄]₃⁻. (f) Co(1,2-C₂B₉H₁₀)₂-μ-O(CH₂)₂. (g) CpCo(MeEt₂C₃B₂Et₂)Co(C₂B₉H₁₁). (h) (Ph₃P)₂HRh(C₂B₉H₁₁). (i) *exo-nido*-[(Ph₃P)₂RhH₂]⁺[C₂B₉H₁₀]⁻. (j) Cp₂Fe₂(Me₄C₄B₈H₈).

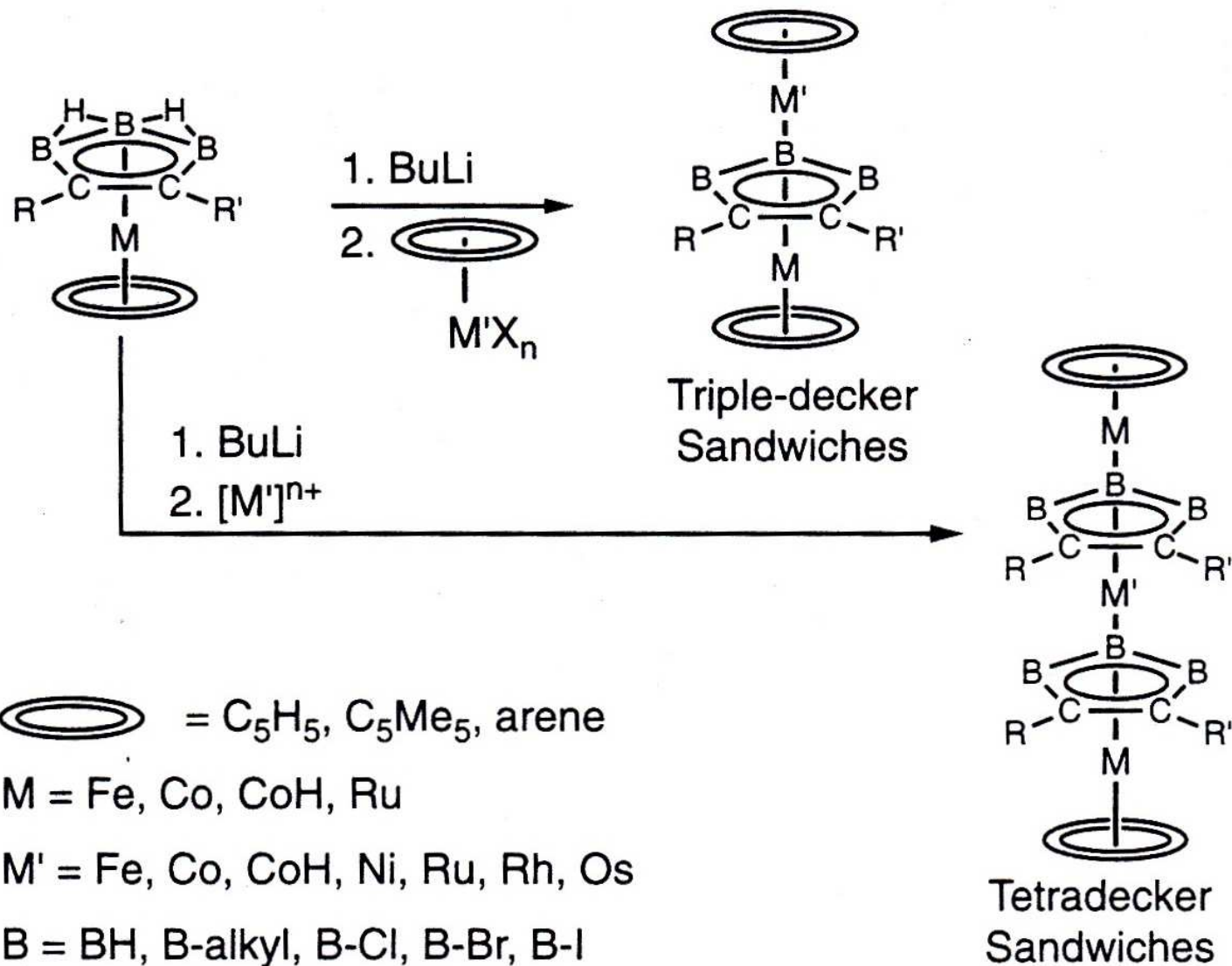


Figure 5-20 Synthesis of multidecker sandwiches *via* metal stacking reactions.

Uveřejněné materiály jsou určeny studentům Vysoké školy chemicko-technologické v Praze jako studijní materiál. Některá textová i obrazová data v nich obsažená jsou převzata z veřejných zdrojů. V případě nedostatečných citací nebylo cílem autorky záměrně poškodit autora/y původního díla.

S případnými výhradami se prosím obracejte na autorku tohoto výukového materiálu, aby bylo možno zjednat nápravu.



The published materials are intended for students of the University of Chemistry and Technology, Prague as a study material. Some text and image data contained therein are taken from public sources. In the case of insufficient quotations, the author's intention was not to intentionally infringe the possible author(s) rights to the original work.

If you have any reservations, please contact the author(s) of the specific teaching material in order to remedy the situation.

Photoreactivity

Sources: J. Ribas Gispert: Coordination Chemistry, Wiley 2008; J. Šima et al., Fotochémia, Princípy a aplikácie, STU Bratislava 2011



EUROPEAN UNION
European Structural and Investing Funds
Operational Programme Research,
Development and Education



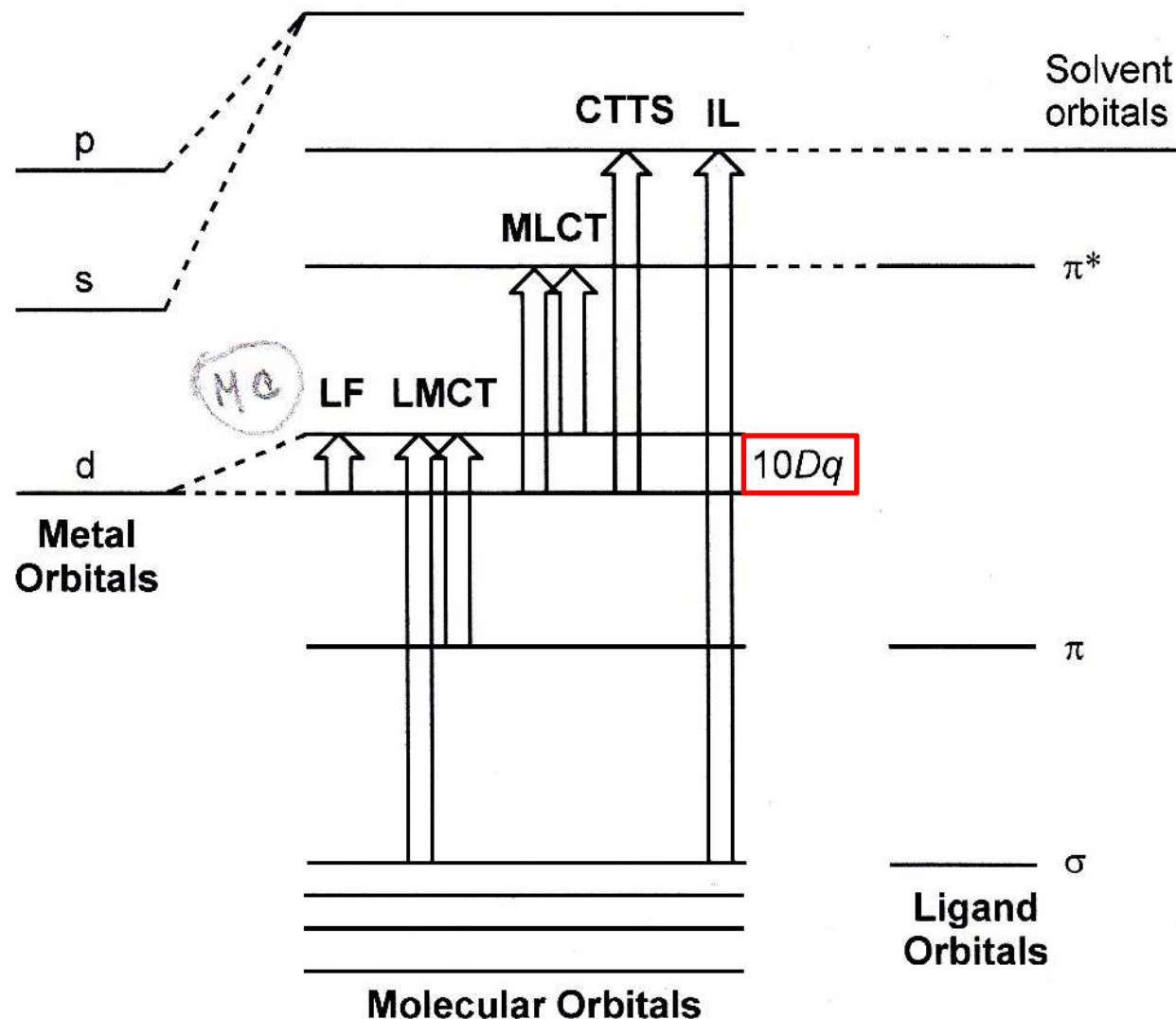


Figure 15.1 A general molecular orbital diagram for an ideal octahedral complex. The electronic transitions that may occur between the orbitals are shown

Molecular orbital diagram with possible electron transfers

Electron transfer types:

- LF – ligand field
- LMCT – ligand to metal charge transfer
- MLCT – metal to ligand charge transfer
- CTTS – charge transfer to solvent
- IL - inter

Any charge transfer band may produce charge separation followed by a photo-redox reaction.

Possible pathways:

Unimolecular processes

- d-d
- CT

Bimolecular processes

- redox (e transfer)
- energy transfer (quencher)
- collisional deactivation

Quantum yield Φ

$$\Phi = \frac{\text{number of events occurred}}{\text{number of photons absorbed}}$$

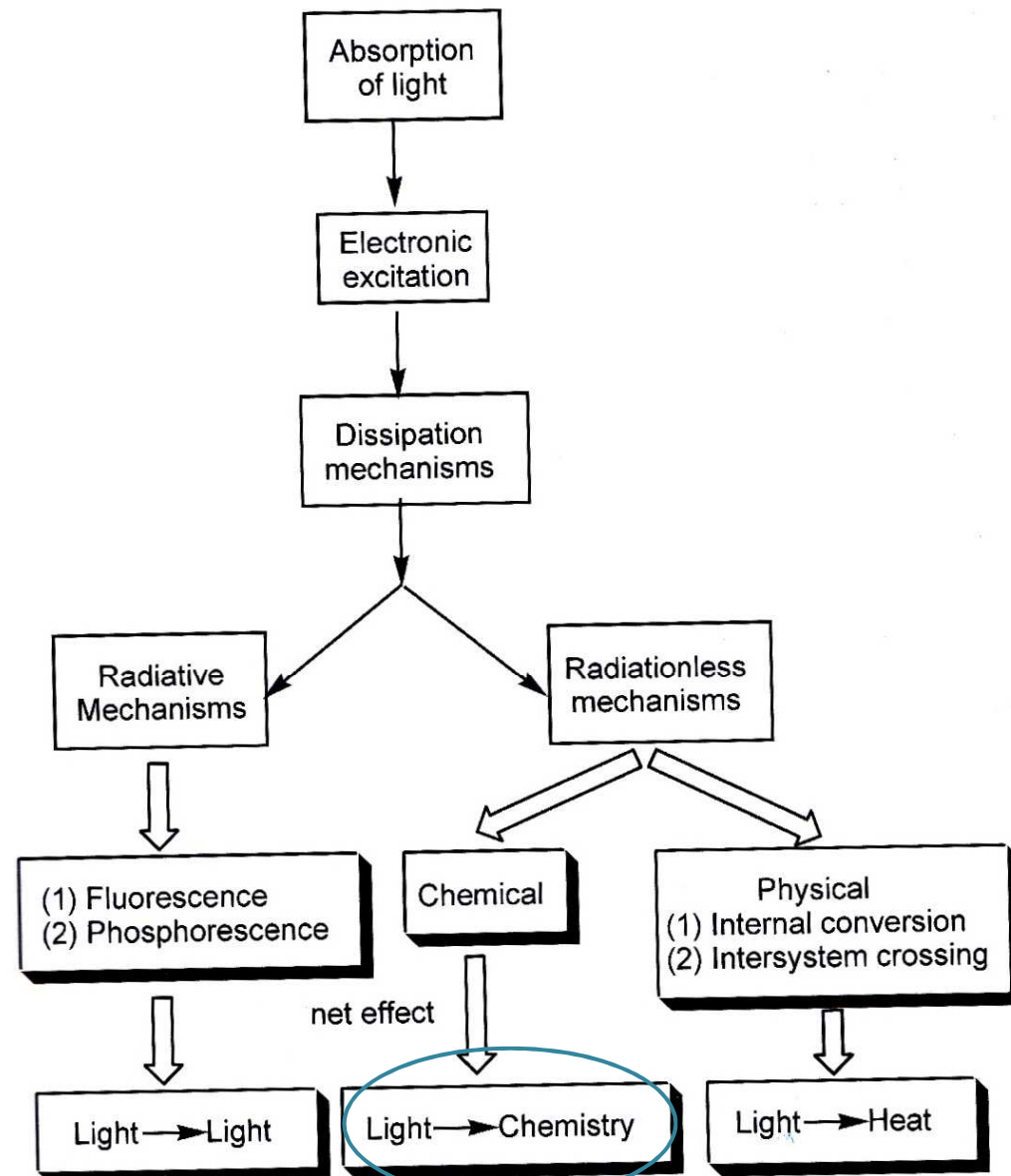
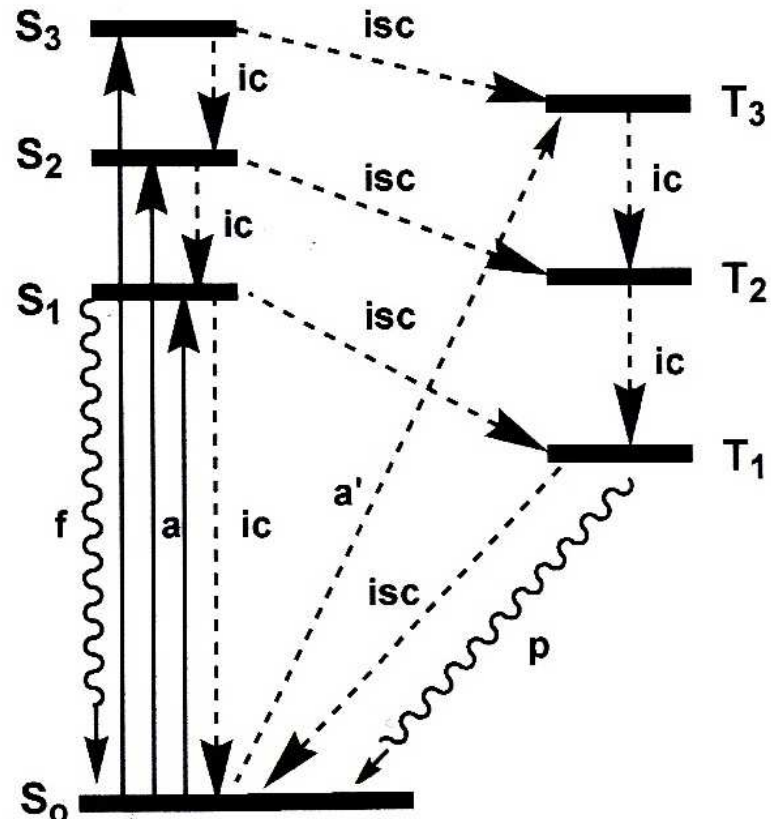


Figure 15.4 Outline of the many pathways through which the excited state can dissipate the energy gained in absorbing a photon.

General Jablonski diagram



Singlet ground state

fluorescence – from excited singlet states, fast

phosphorescence – from triplet states, delayed

Figure 15.3 A general Jablonski diagram. a and a' stand for absorption of light; f for fluorescence, p for phosphorescence; ic for internal conversion, isc for intersystem crossing. S stands for singlet and T for triplet.

Jablonski diagram, for Cr(III)

d^3 Tanabe-Sugano Diagram

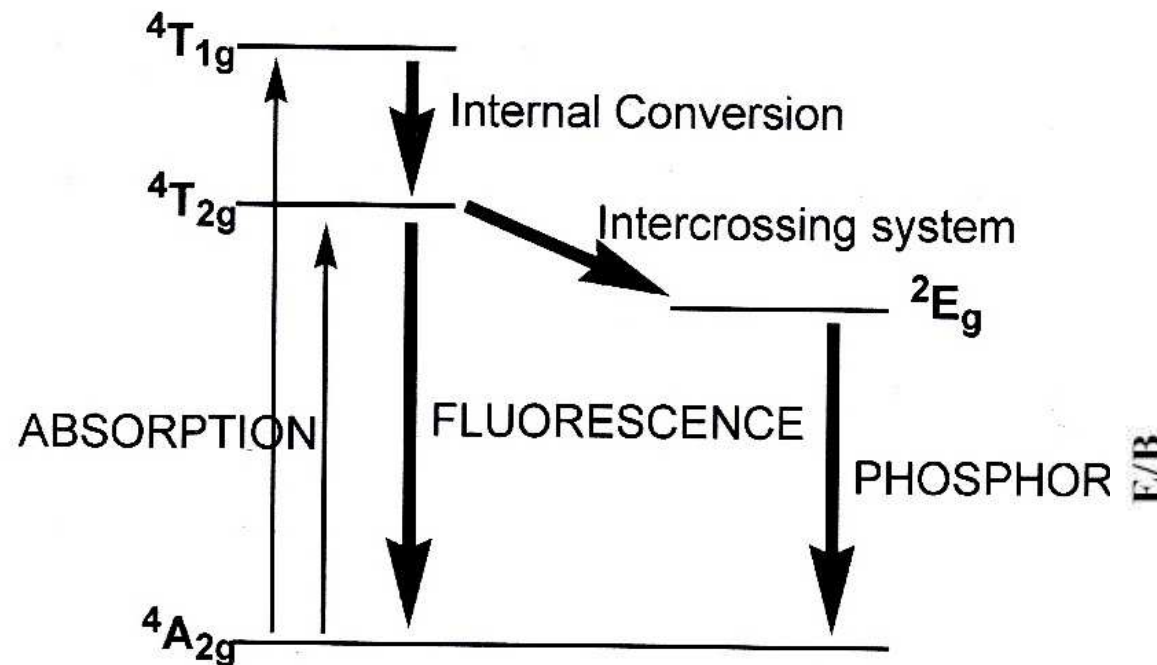
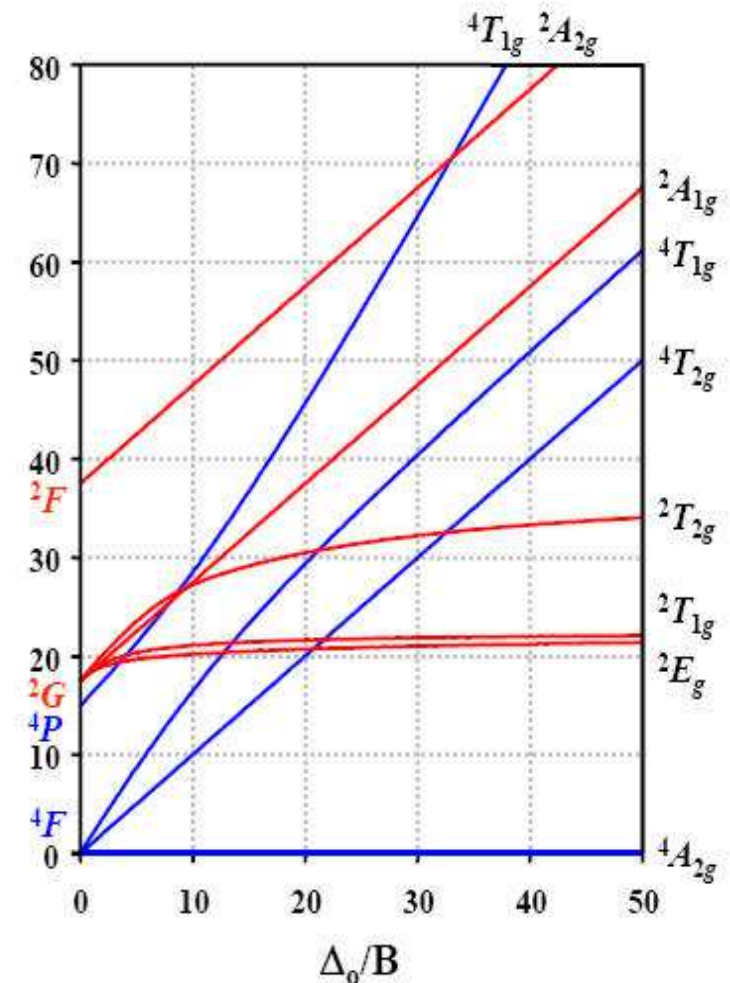
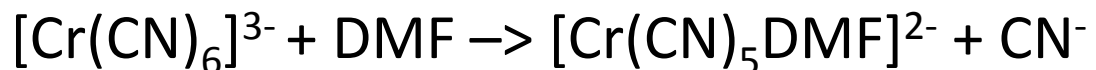


Figure 15.5 Jablonski diagram for an octahedral complex



Identification of the excited state



observed: solvation + phosphorescence

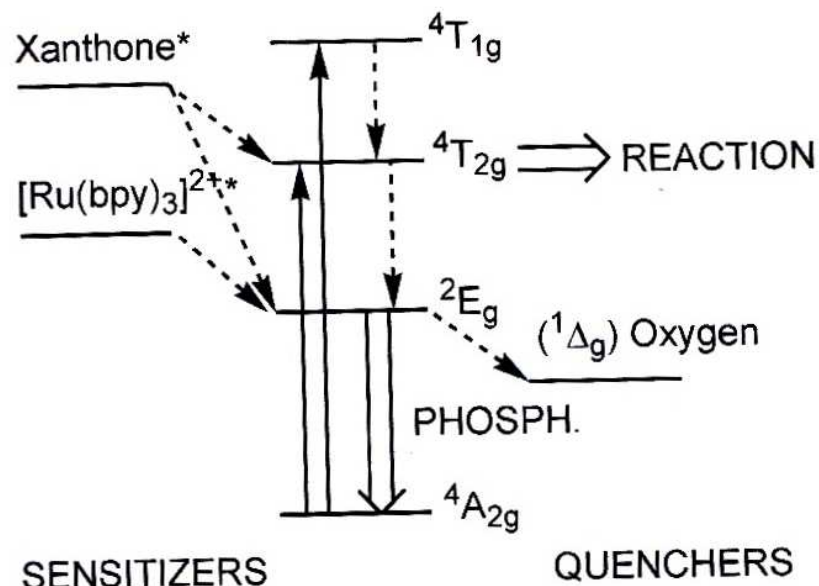


Figure 15.7 Example of identification of the excited state

EXPERIMENT

- + excited xanthone* (high energy sensitizer): population of both excited states ($^4T_{2g}$, 2E_g) -> phosphorescence + solvation observed
- + $[\text{Ru}(\text{bpy})_3]^{2+*}$ (medium energy sensitizer): only 2E_g level populated -> only phosphorescence observed
- + quencher ($^1\text{O}_2$) -> only solvation

Conclusion: phosphorescence is due to 2E_g term, solvation is due to $^4T_{2g}$ term.

Photo – redox reaction

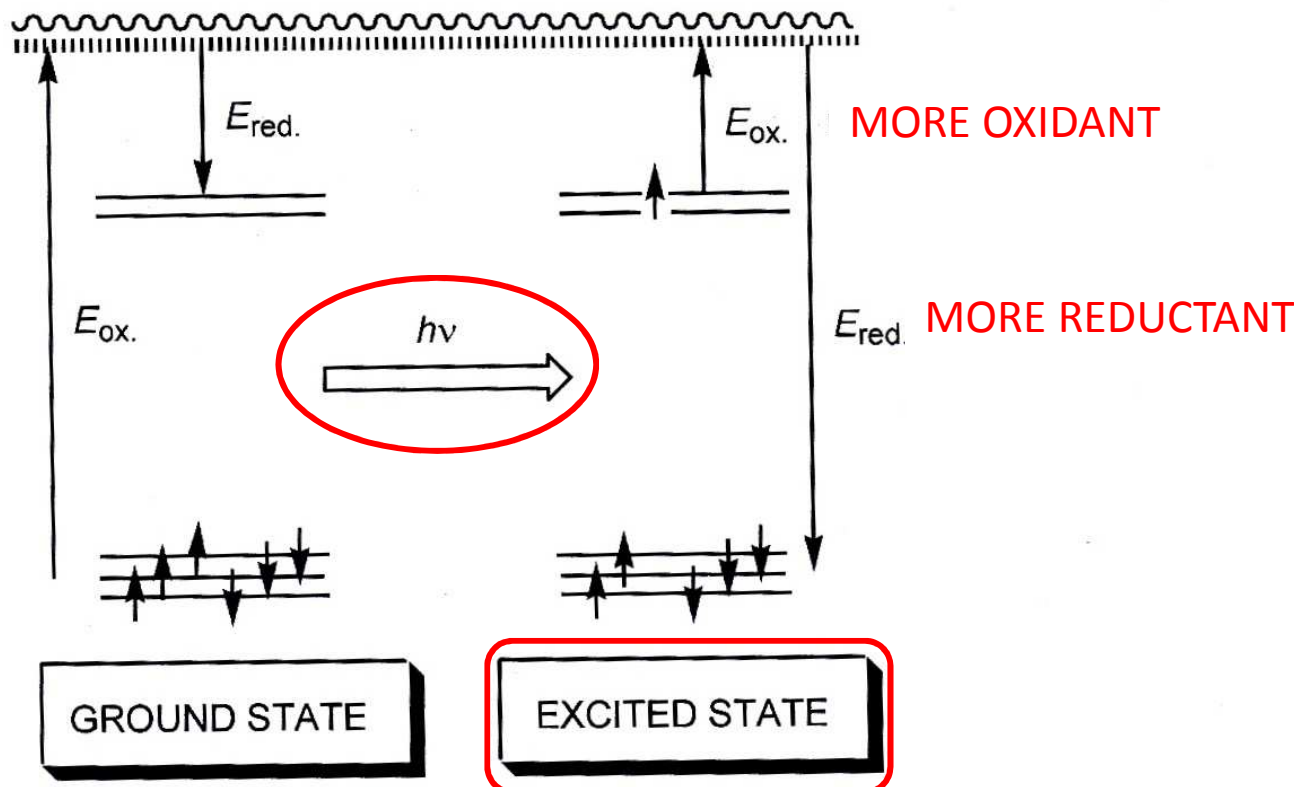
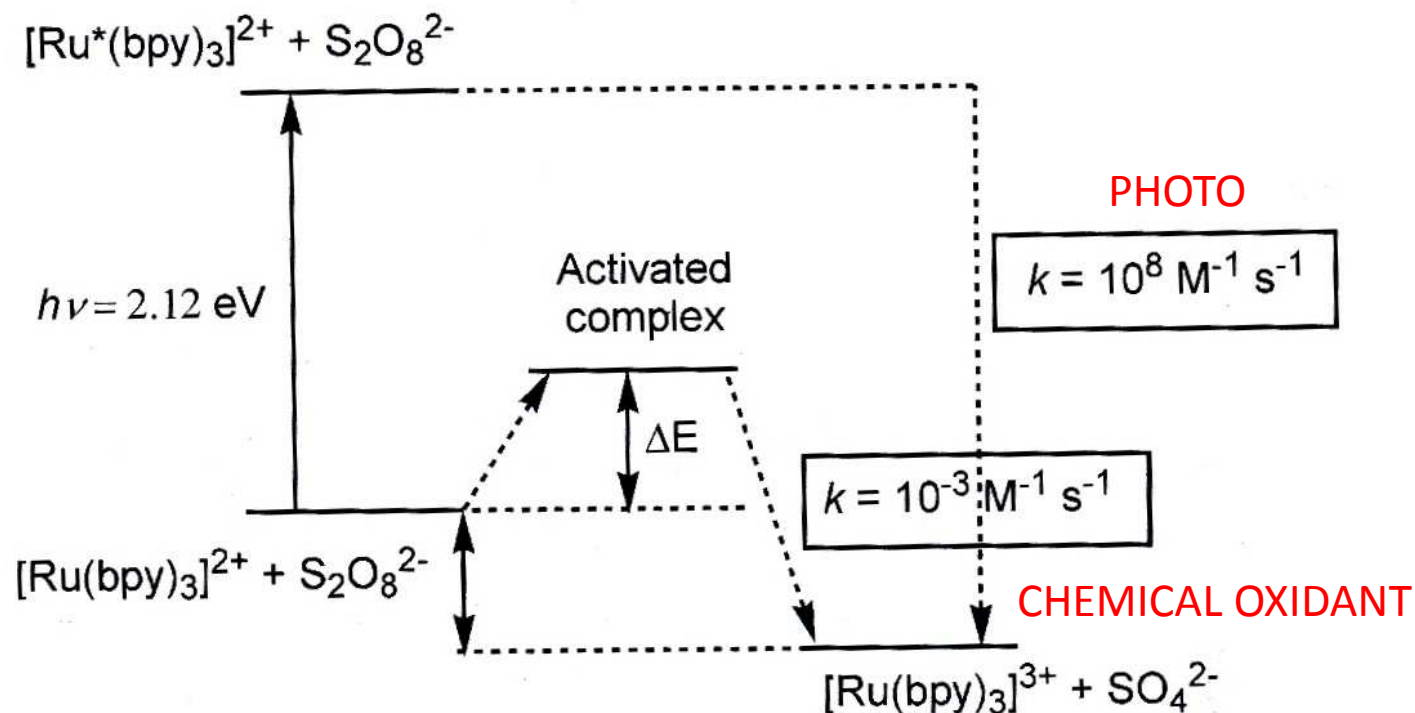


Figure 15.10 Variation of redox potentials in photochemical processes.

The photochemically excited state is more oxidizing and more reducing than the ground state from which it has been generated.

Redox processes “classical” and initiated by light - comparison

Photoredox processes – often higher reaction rate (overcoming formation of the activated complex)



[Ru(bpy)₃]²⁺ complex

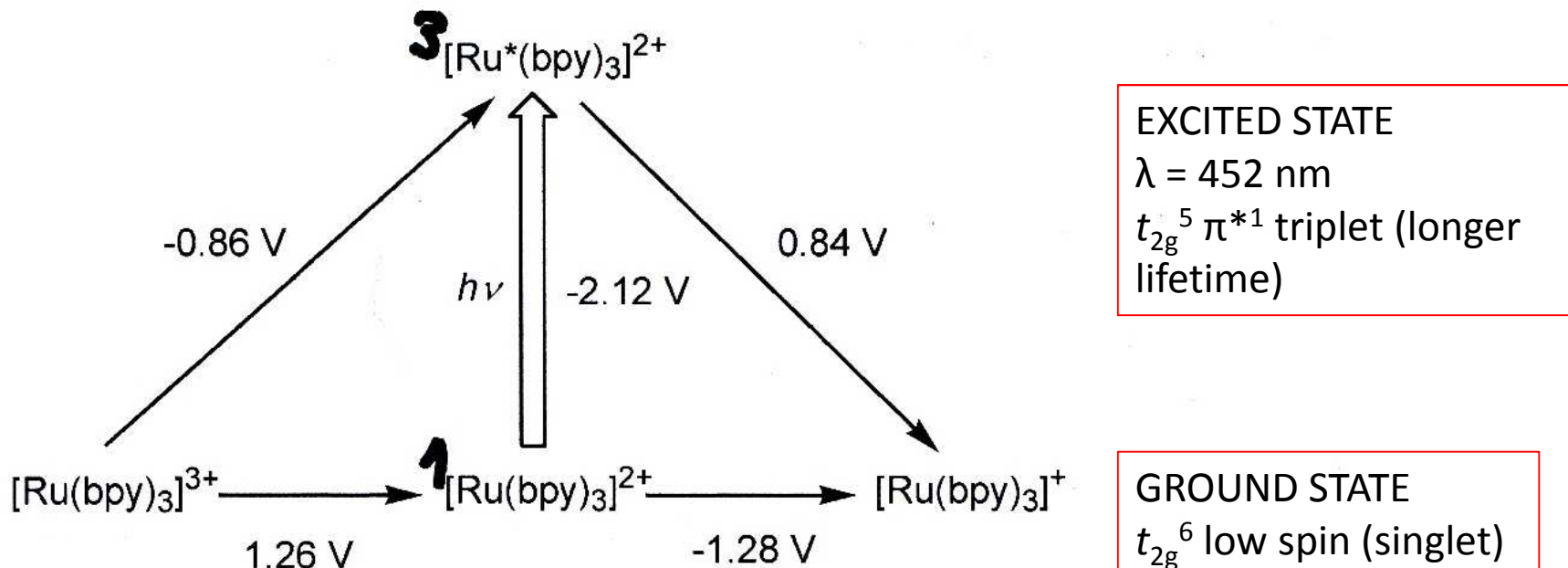


Figure 15.11 Redox potentials in the $[\text{Ru}(\text{bpy})_3]^{2+}$ system.

OXIDIZING AGENT (REDUCTION)

Ground state: $[\text{Ru}(\text{bpy})_3]^{2+} + e \rightarrow [\text{Ru}(\text{bpy})_3]^+$ $E = -1.28 \text{ V}$

Excited state: $^3[\text{Ru}^*(\text{bpy})_3]^{2+} + e \rightarrow [\text{Ru}(\text{bpy})_3]^+$ $E = +0.84 \text{ V}$ (difference -2.12 V)

REDUCING AGENT (OXIDATION)

Ground state: $[\text{Ru}(\text{bpy})_3]^{3+} + e \rightarrow [\text{Ru}(\text{bpy})_3]^{2+}$ $E = +1.26 \text{ V}$

Excited state: $[\text{Ru}(\text{bpy})_3]^{3+} + e \rightarrow ^3[\text{Ru}^*(\text{bpy})_3]^{2+}$ $E = -0.86 \text{ V}$ (difference -2.12 V)

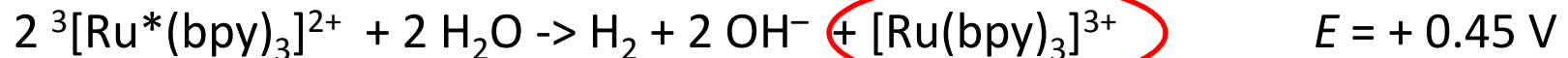
[Ru(bpy)₃]²⁺ - splitting of water upon irradiation

Theory:

reduction of water to hydrogen at pH = 7 $E = -0.41 \text{ V}$

oxidation $E = +0.82 \text{ V}$

Reaction 1 – Reduction of water by the ³[Ru*(bpy)₃]²⁺ photoexcited state:

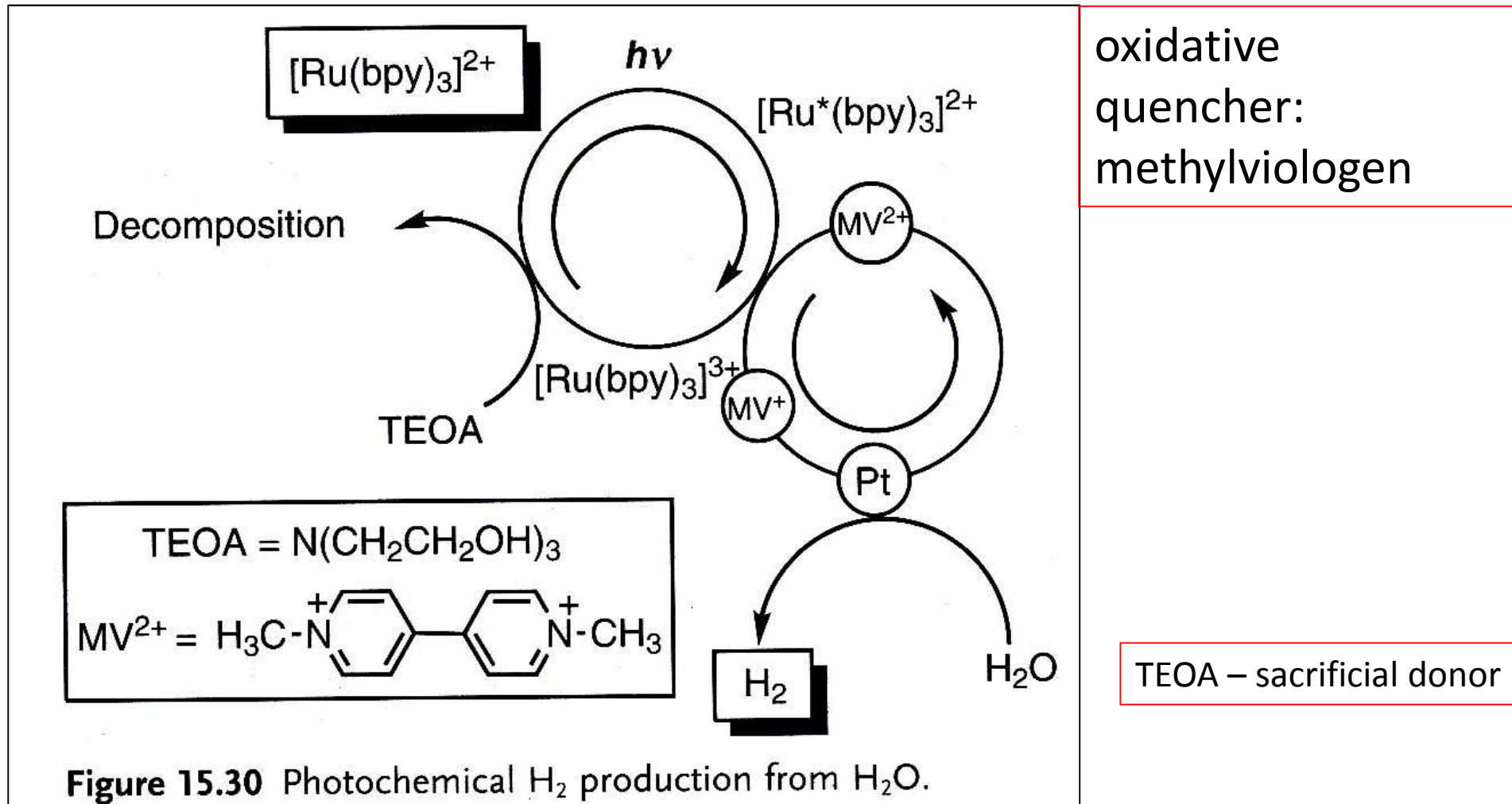


Reaction 2 – Oxidation of water by the [Ru(bpy)₃]³⁺ produced by 1

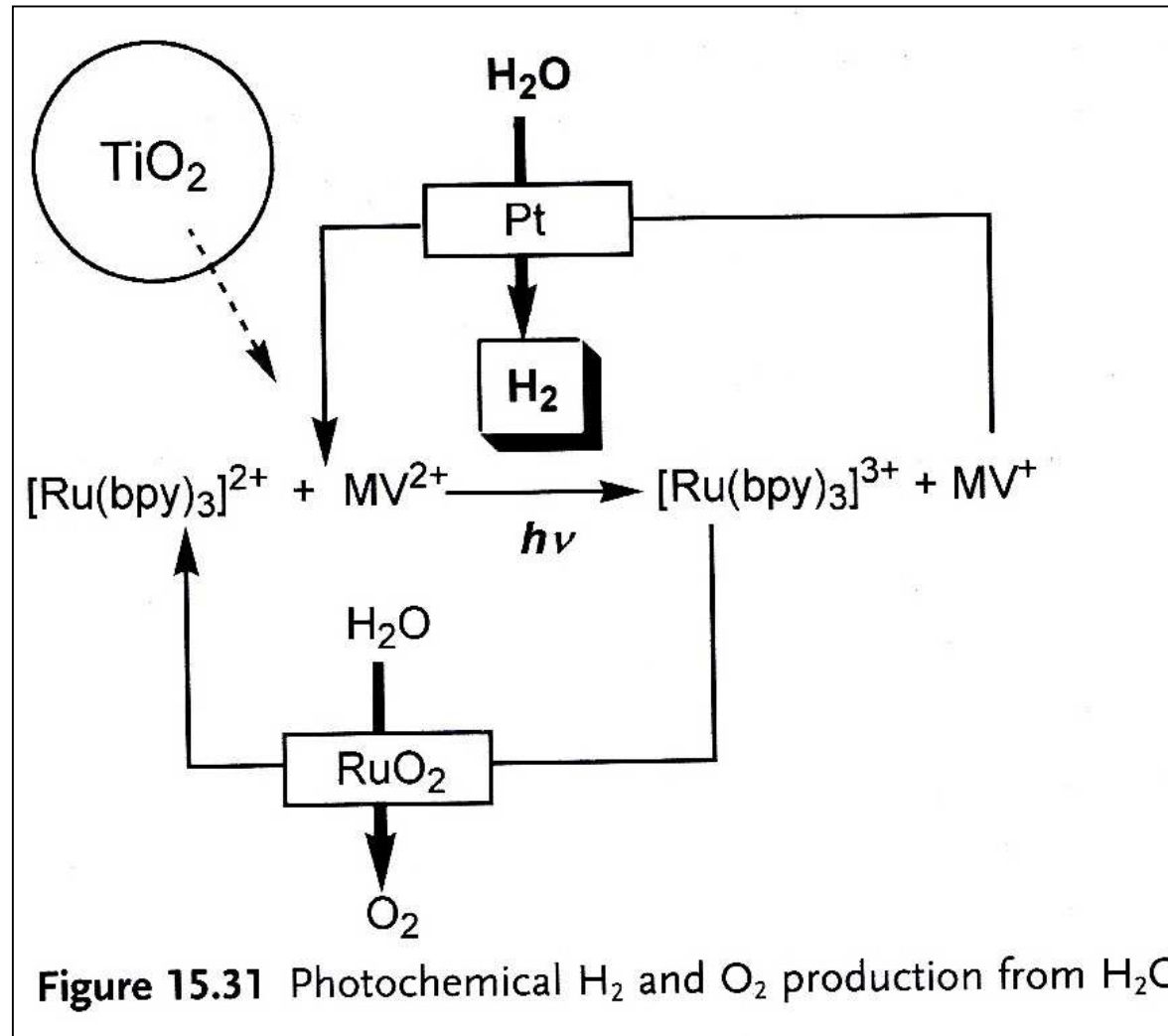


Problem: numbers of exchanged electrons are not compatible

$[\text{Ru}(\text{bpy})_3]^{2+}$: Sensitiser for hydrogen production



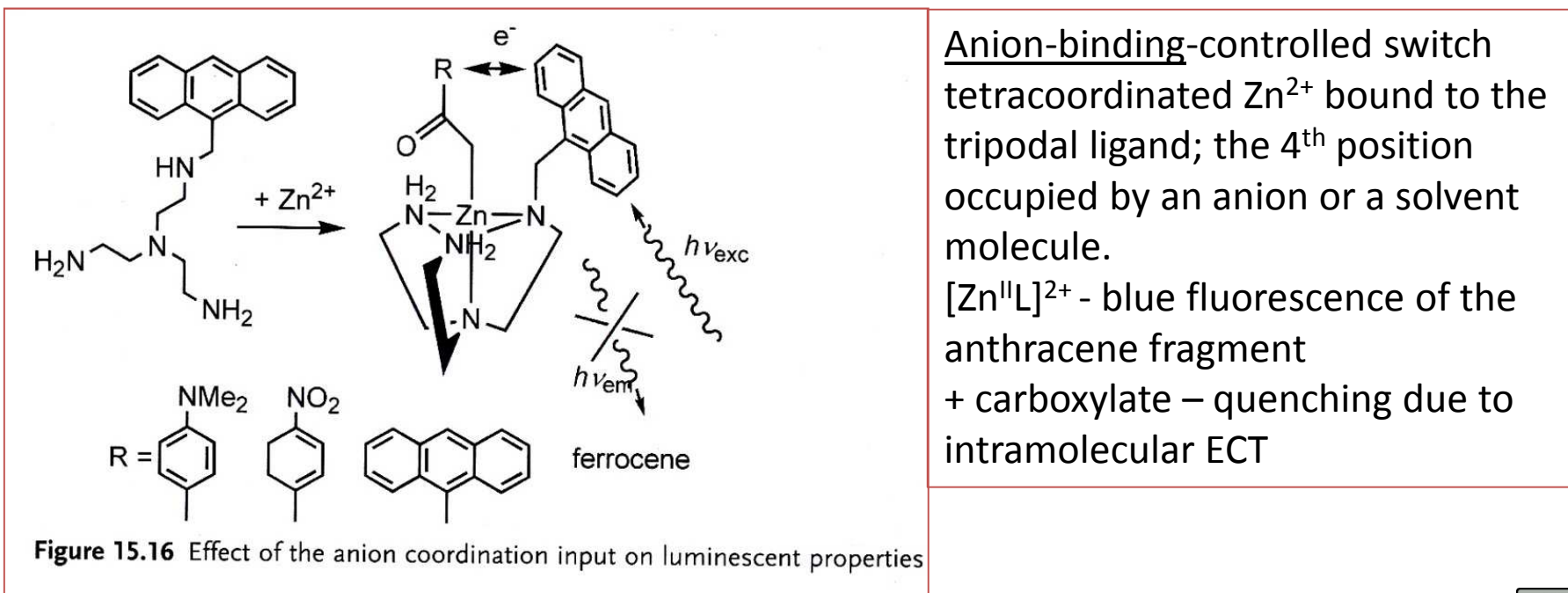
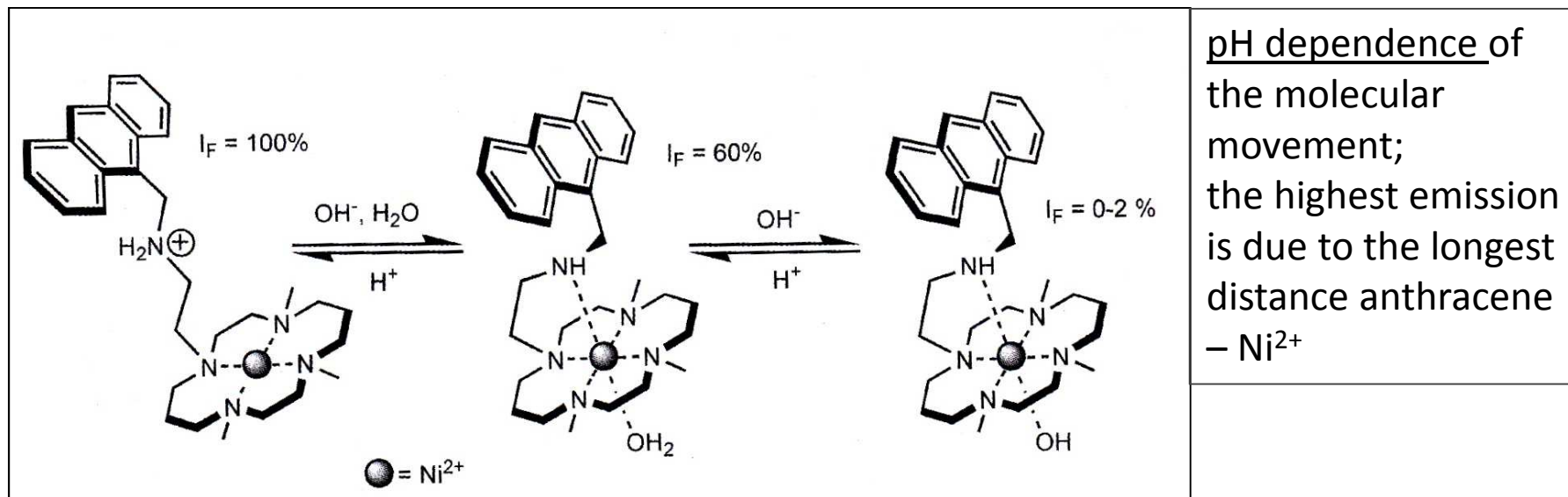
$[\text{Ru}(\text{bpy})_3]^{2+}$: simultaneous hydrogen and oxygen production



two-catalyst system
(RuO_2 , Pt)
Grätzel and co.

Figure 15.31 Photochemical H_2 and O_2 production from H_2O

Luminescence of anthracene – influence of pH and anion coordination



Antenna effect

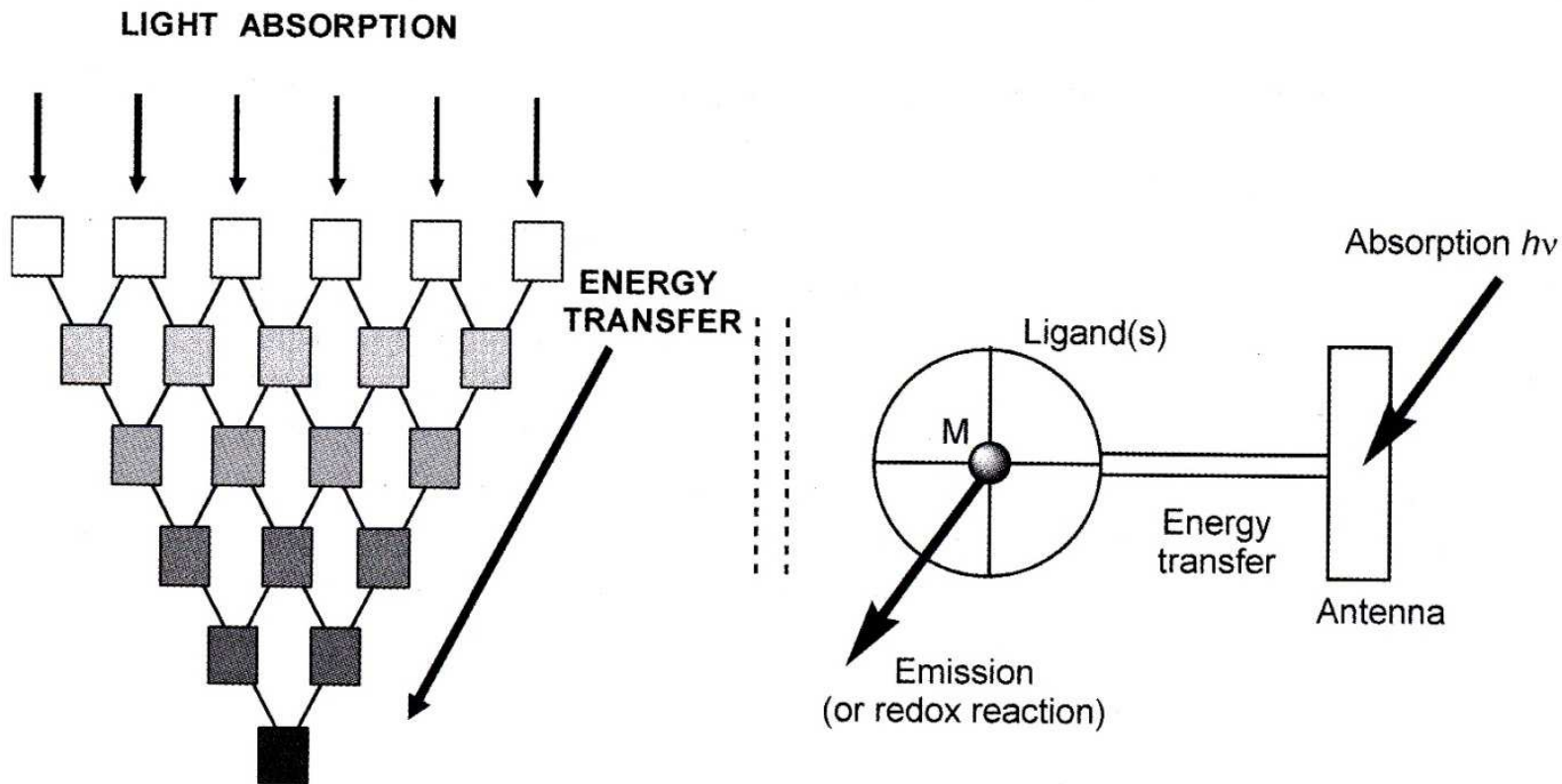


Figure 15.17 Schematic drawing of an antenna and antenna effect.

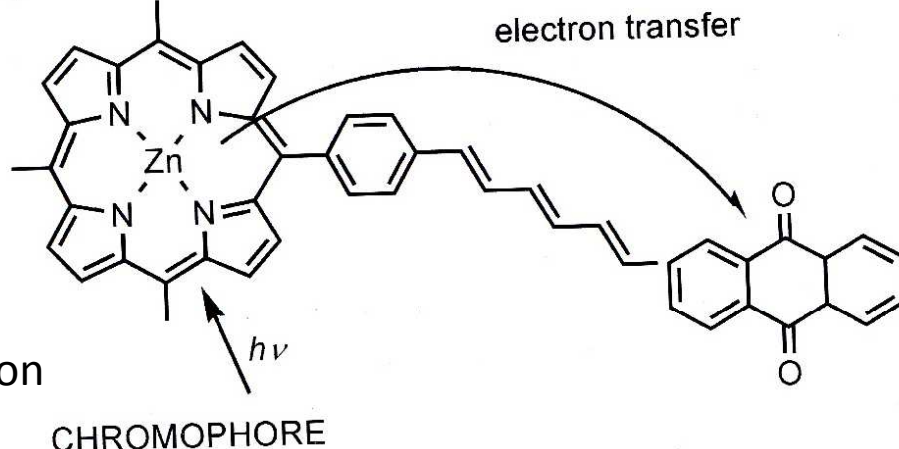
Antenna – multicomponent system:

- several chromophoric molecular species absorb the incident light
- the excited photon (different energy) is transported to a common acceptor
- higher yield of useful energy (photosynthesis!)

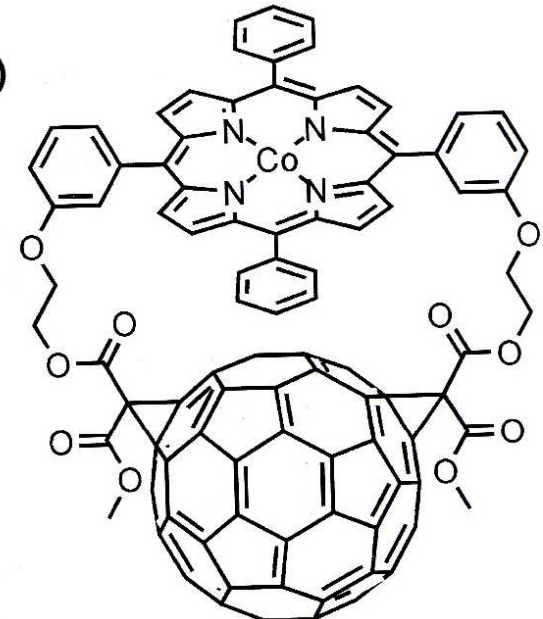
Dyads for charge separation

Charge separation
or
Charge recombination

(A)

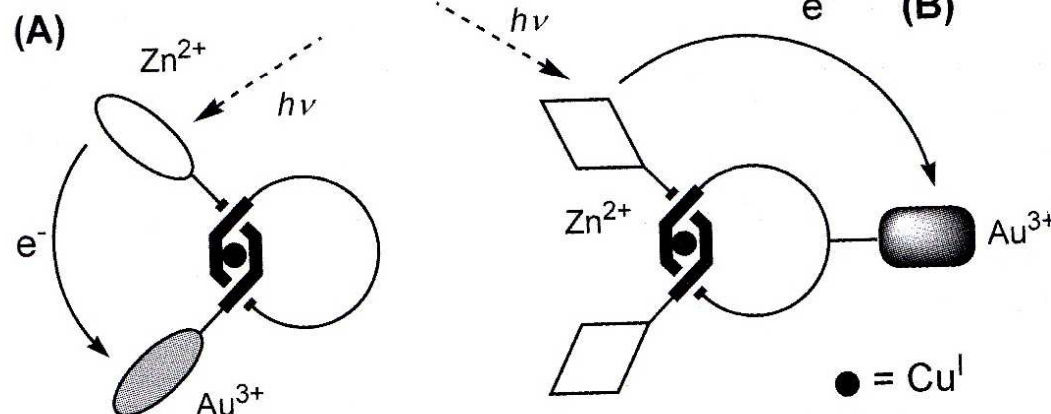


(B)



Dyads based on porphyrin chromophores

(A)



(B)

Dyads :
2-component
systems;
suitable electron
donor and
acceptor,
charge-transferring
chromophore

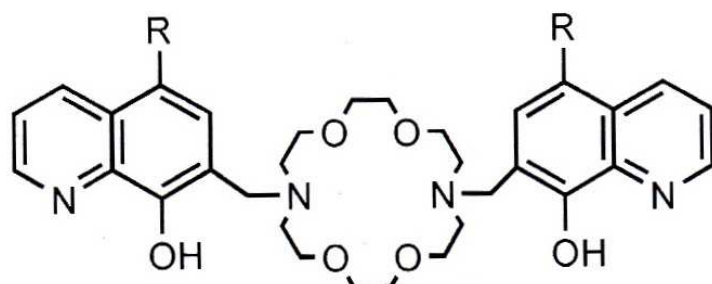
Charge separation in porphyrin-catenane derivatives

Fluorescent (or luminescent) chemosensors

are systems that modify their light emission (both enhancement or quenching) through chemical parameters: pH, complexation of metal ions, anions, molecules (O_2 , NO).

Metal-ion sensors:

- chelation enhancement of fluorescence (CHEF)
- chelation enhancement of the quenching (CHEQ)

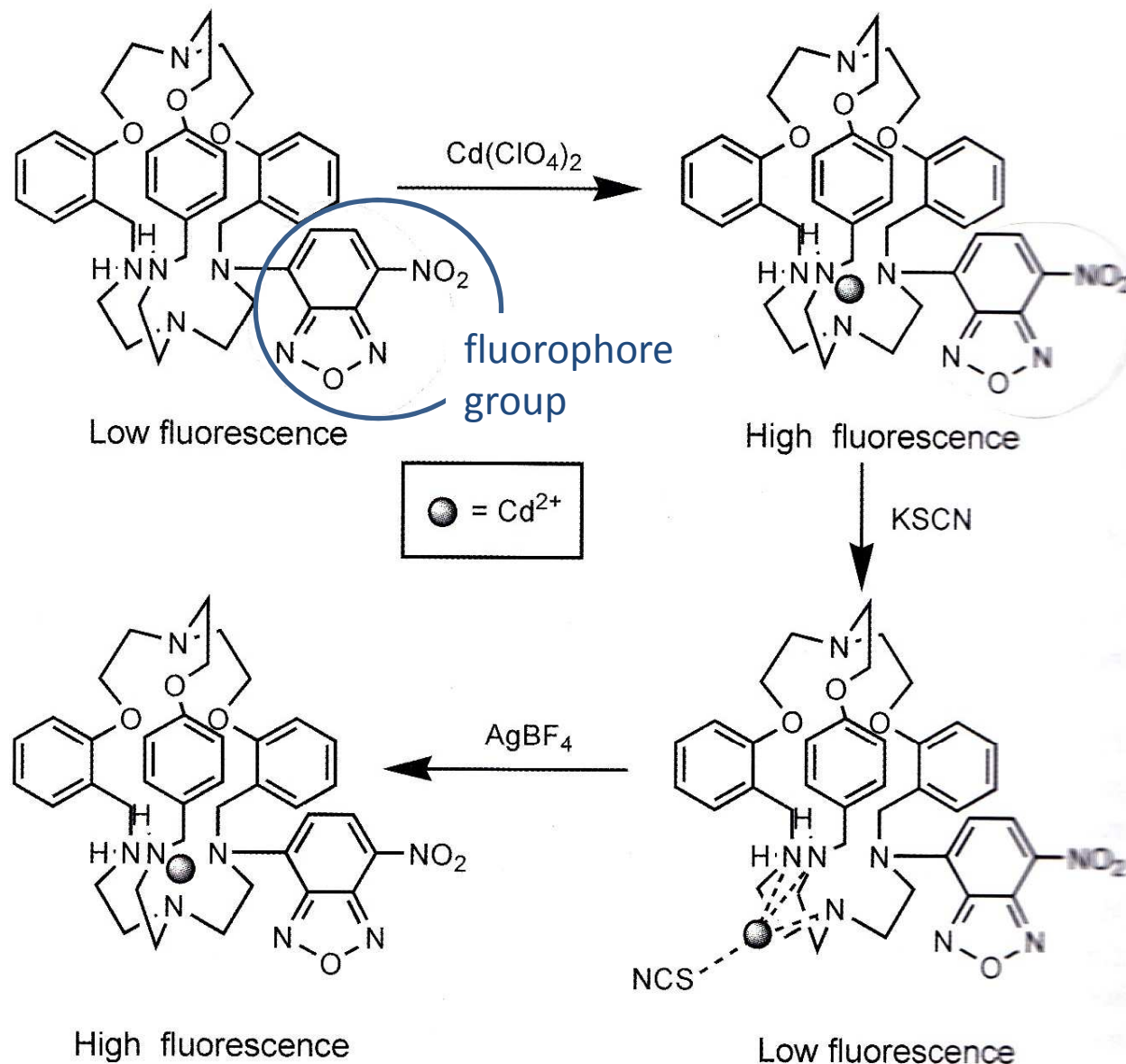


A positive fluorescent sensor for Mg(II)
in living cells – does not function with
Ca(II), non sensitive to pH changes
biological application

R = H, Cl

Figure 15.26 A fluorescent chemosensor for Mg^{2+} .

Fluorescent chemosensors



Example of a highly stable cryptand ligand sensing toxic $\text{Cd}(\text{II})$ ions (and some other divalent ions)

Without metal:
intramolecular PET takes place
(photoinduced electron transfer)
Metal in the cryptand cavity - fluorescence

Figure 15.27 Azacryptand as fluorescent chemosensor for Cd^{2+} .

General methods of synthesis of the complexes

2 common situations:

- ❖ metal salt is soluble in water, but it needs acidic media (hydrolysis)  ligand is basic
- ❖ metal salt is soluble in water  ligand is insoluble in water

Reactions in aqueous media

water behaves as a ligand

uncharged particles are poorly soluble

Reactions in non-aqueous media

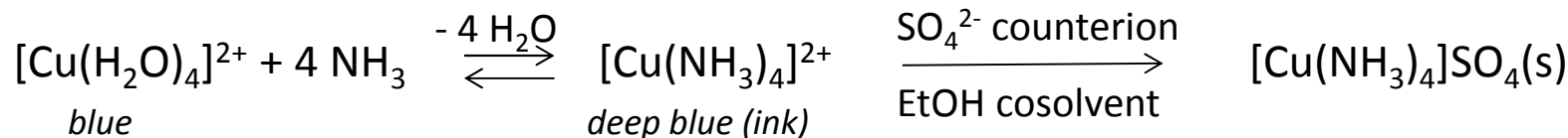
hydrated salts (e.g. $\text{CuSO}_4 \cdot 5\text{H}_2\text{O}$) are insoluble

charged particles are poorly soluble

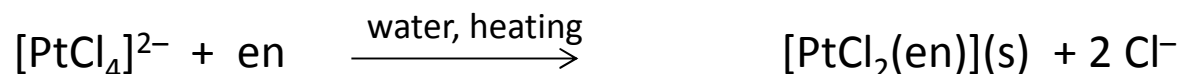
1. Substitution reactions in aqueous solutions

Excess of ligand, reaction time varies – inert vs. labile ions

Labile – quick reaction, no mixed-ligand complexes:

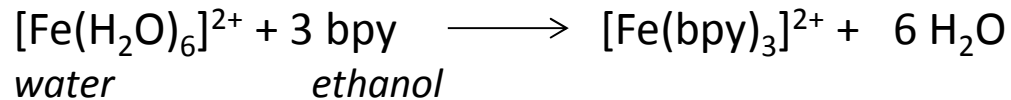


Inert – longer times, heating, mixed-ligand complexes

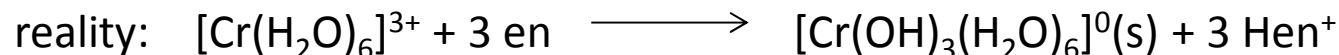
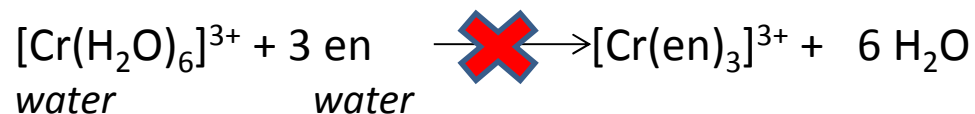


2. Substitution reactions in nonaqueous solvents

a) ligand is soluble in water – another solvent miscible with water



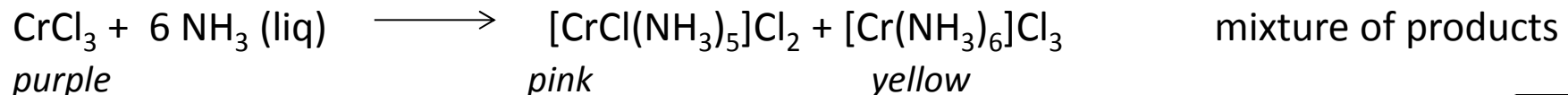
b) metal ion undergoes hydrolysis – competition between the hydrolysis and the complex formation



Solution:

anhydrous CrCl_3 in dry ether – slow, but gives the product, $[\text{Cr}(\text{en})_3]\text{Cl}_3$

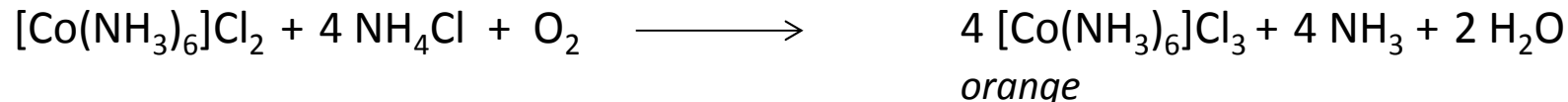
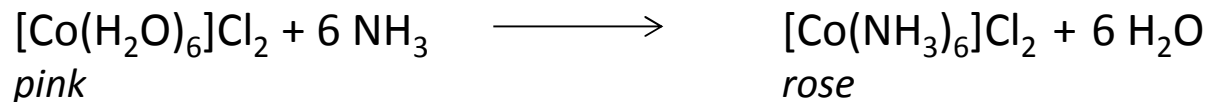
Reaction in liquid ammonia:



3. Substitution reactions on metal ions in more labile oxidation states

Cr(III), d^3 - small addition of a reducing agent (Na), Cr(II) d^4

Co(II) reacts, the product is oxidized to Co(III)



substitution of a volatile ligand

4. Substitution of weakly bound or volatile ligand

Volatile ligands: CO, NH₃, H₂O, driven off by **heating**, replaced

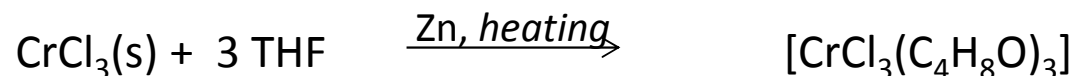


CO: stabilized by **irradiation**

“superaromatic molecules”,



coordinating, volatile solvents (acetonitrile, tetrahydrofuran (THF), ethers) – precursors



5. Ligand construction or destruction by reaction of coordinated ligands – see the chapter 9

Uveřejněné materiály jsou určeny studentům Vysoké školy chemicko-technologické v Praze jako studijní materiál. Některá textová i obrazová data v nich obsažená jsou převzata z veřejných zdrojů. V případě nedostatečných citací nebylo cílem autorky záměrně poškodit autora/y původního díla.

S případnými výhradami se prosím obracejte na autorku tohoto výukového materiálu, aby bylo možno zjednat nápravu.



The published materials are intended for students of the University of Chemistry and Technology, Prague as a study material. Some text and image data contained therein are taken from public sources. In the case of insufficient quotations, the author's intention was not to intentionally infringe the possible author(s) rights to the original work.

If you have any reservations, please contact the author(s) of the specific teaching material in order to remedy the situation.

Bioinorganic chemistry

Inorganic elements in the
chemistry of life



EUROPEAN UNION
European Structural and Investing Funds
Operational Programme Research,
Development and Education



Essential elements

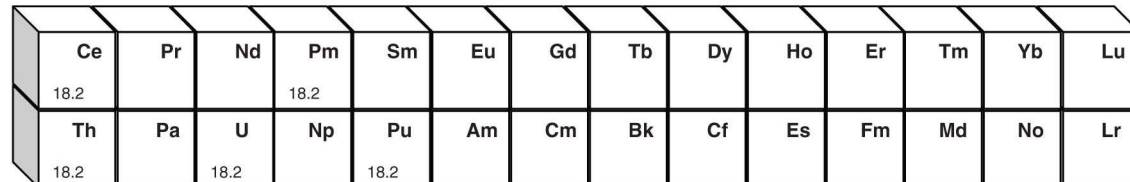
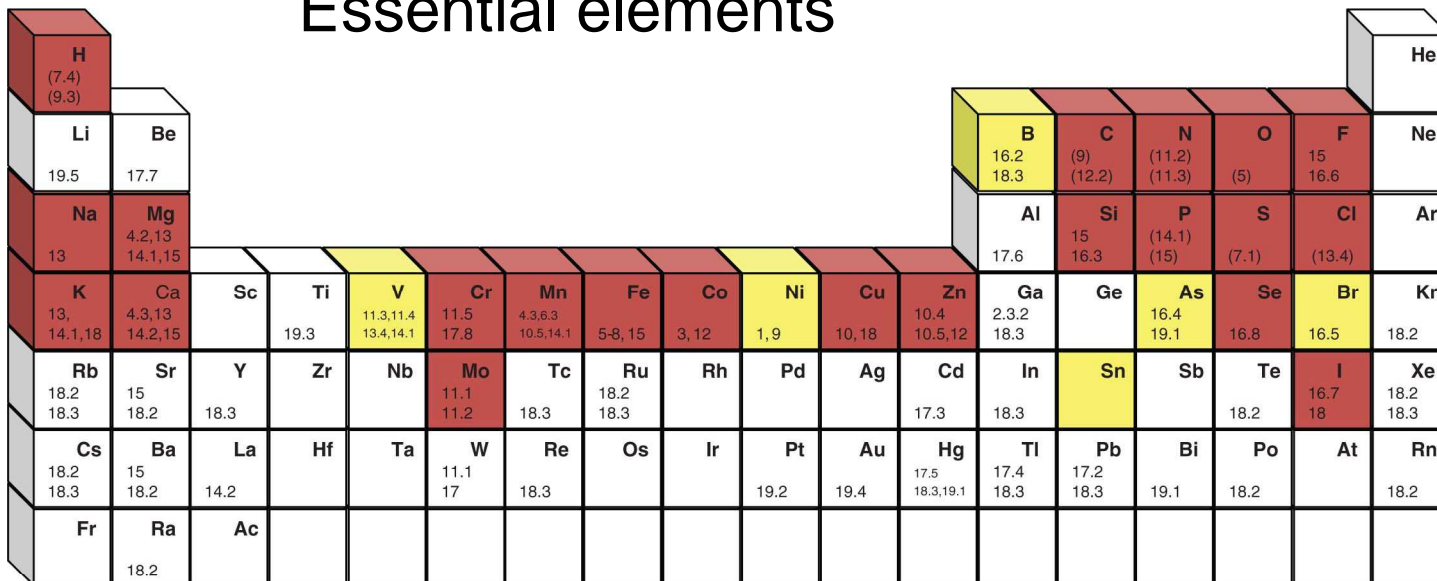


Figure 1.4

Periodic table of the elements. Indicated are the chapters and sections in which each element is discussed in this book.



presumably essential element for human beings.



essential element;

Essential: daily dose from 25 mg
Presumably essential

A human body contains also non-essential elements (Rb), contaminants (Hg)

Metals: electrolytes, structures, biomolecules

Which elements? Where?

- metalloenzymes – ca. 40% of the known enzymes, esp. oxidoreductases (**Fe**, **Cu**, **Mn**, **Mo**, **Ni**, **V**), hydrolases (**Zn**, **Mg**, **Ca**, **Fe**)
- nonenzymatic metalloproteins (haemoglobin: **Fe**)
- low-molecular-weight natural products (chlorophyll: **Mg**)
- coenzymes, vitamins (vitamin B₁₂: **Co**)
- nucleic acids (e.g. DNAⁿ⁻ (M⁺)_n: M = **Na**, **K**)
- hormones (thyroxine, triiodothyronine: **I**)
- antibiotics (e.g. ionophores: valinomycin/**K**)
- biominerals (e.g. bones, teeth, shells, coral, pearls: **Ca**, **Si** ...)

Biological function of inorganic elements

- The assembly of hard structures, endo- a exoskeletons, membrane integrity, DNA structure. **Ca, Mg, Zn; Si, P, S, O, C, F.**
- Charge carriers for fast information transfer. **Na, K, Ca, Mg**
- Formation, degradation and metabolism of organic compounds, hydrolysis. **Zn, Mg**
- Transfer of electrons (energy conversion). Stabilisation of several unusual oxidation states by bioligands. **Fe(I)/Fe(II)/ Fe(III)/Fe(IV); Cu(I)/Cu(II); Mn(II)/Mn(III)/Mn(IV); Mo(IV)/Mo(V)/Mo(VI); Co(I)/Co(II)/Co(III); Ni(I)/Ni(II)/Ni(III)**
- The redox activation of small, highly symmetrical molecules
 - hydrogen (Fe, Ni, Se)
 - oxygen (Fe, Cu uptake, Mn production)
 - nitrogen (Fe, Mo, V)
 - carbon dioxide, C1 chemistry, (Ni, Fe)
 - generation of radicals



Biological ligands for metal ions

Inorganic molecules and ions:
phosphates, carbonates, water, oxides, hydroxides, sulfides

Little is known about: lipids, carbohydrates;
 small organic molecules
 exception – ascorbate, Fe(II)/Fe(III)

flavins

The most important: **PROTEINS**
MACROCYCLIC CHELATE LIGANDS
NUCLEIC ACIDS

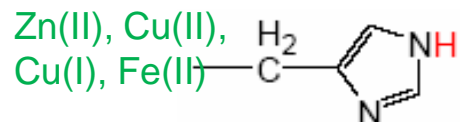
Ligands 1: PROTEINS

Donors are the functional groups in the **side chains**

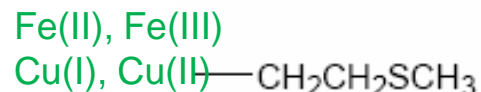
The peptidic group –C(O)–N(H)– leads to higher dielectric constant
("protein as medium")

The most important aminoacids:

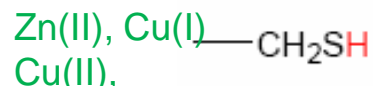
HSAB principle



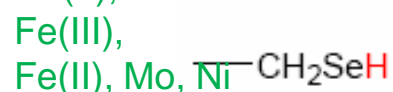
Histidine. both N, bridge, proton shuttle



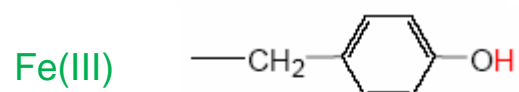
Methionine



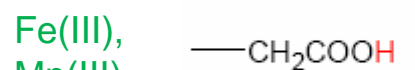
Cysteine, $pK_a \approx 8,5$; σ and π donor, bridge



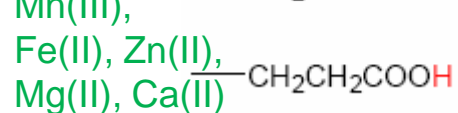
Selenocysteine, $pK_a \approx 5$;



Tyrosine, $pK_a = 10$; forms: neutral, anion, tyrosyl radical



Glutamate



$pK_a \approx 4,5$; bond η^1 *syn,anti*, η^2 , μ

Aspartate

Less frequent: **Serine** (-CH₂OH), **Threonine** (-CH(OH)CH₃), **Lysine** (-(CH₂)₄-NH₂), **Tryptophan** (indoyl group)

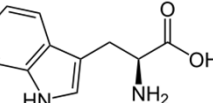
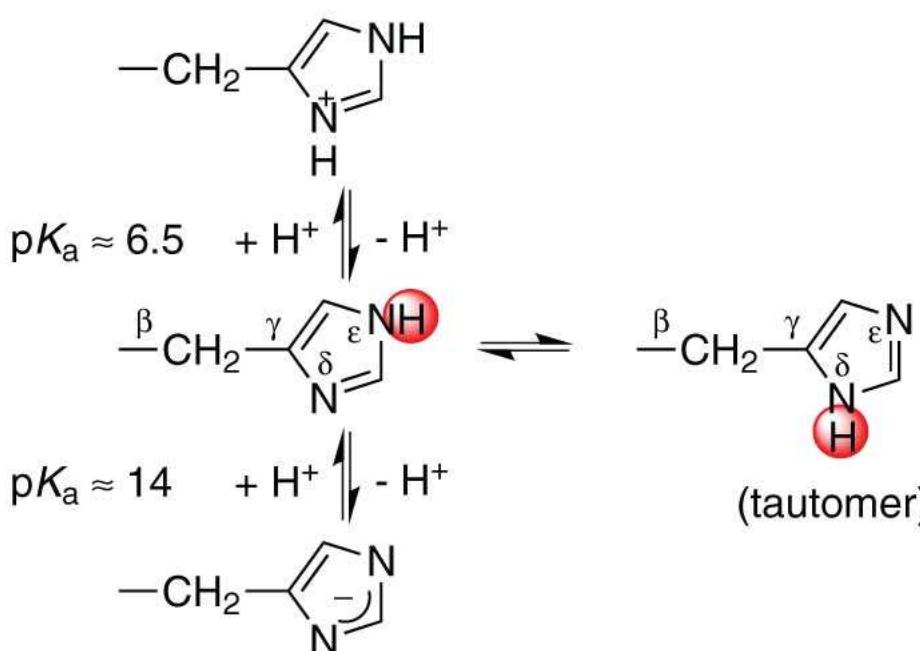
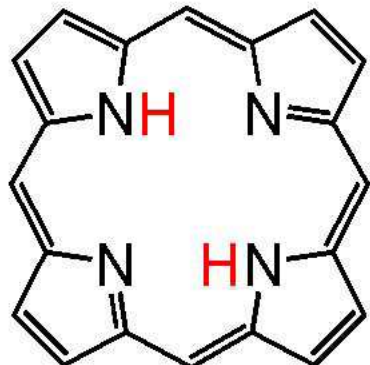


Table 2.5 The most important metal-coordinating amino acids.

α amino acid	Side chain, R $R^{\alpha}\text{CH}(\text{NH}_3^+)\text{CO}_2^-$
histidine (His)	 <p>$pK_a \approx 6.5$ $+ \text{H}^+ \rightleftharpoons - \text{H}^+$</p> <p>$pK_a \approx 14$ $+ \text{H}^+ \rightleftharpoons - \text{H}^+$</p> <p>(tautomer)</p>
methionine (Met)	$-\text{CH}_2\text{CH}_2\text{SCH}_3$
cysteine (Cys)	$-\text{CH}_2\text{SH}$
selenocysteine (SeCys)	$-\text{CH}_2\text{SeH}$
tyrosine (Tyr)	$-\text{CH}_2\text{C}_6\text{H}_4\text{OH}$
	H : acidic protons which may be substituted by a metal

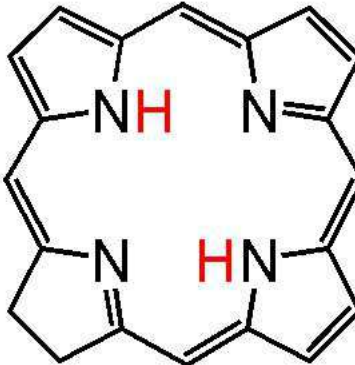
Ligands 2: Tetrapyrrolic macrocycles

Tetrapyrrolic macrocycles



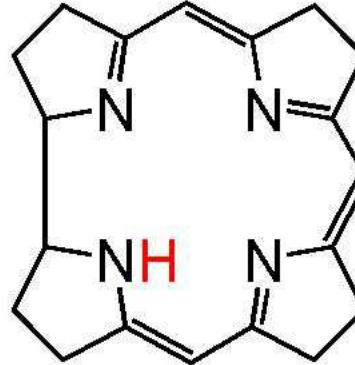
Porphyrin

Fe
hemoglobin
myoglobin
peroxidases



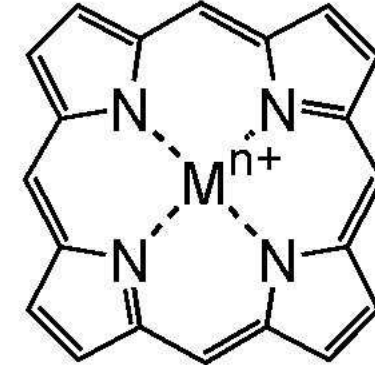
Chlorin

Mg
chlorophylls
Ni
tunichlorin



Korrin

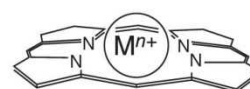
Co(II)
cobalamins



in-plane coordination
(side view)



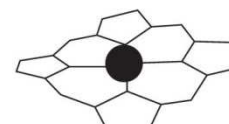
out-of-plane coordination
(side view)



"doming" of the
macrocycle



saddle-shaped
macrocycle



"ruffling" of the
macrocycle

Ni: coenzyme F₄₃₀

Figure 2.6

Typical geometrical deviations for complexes of tetrapyrrolic macrocycles (cf. [31]).

Ionophores –donor O, N

Complexing of hard cations

Lipophilic outside

valinomycin and its complex with K⁺

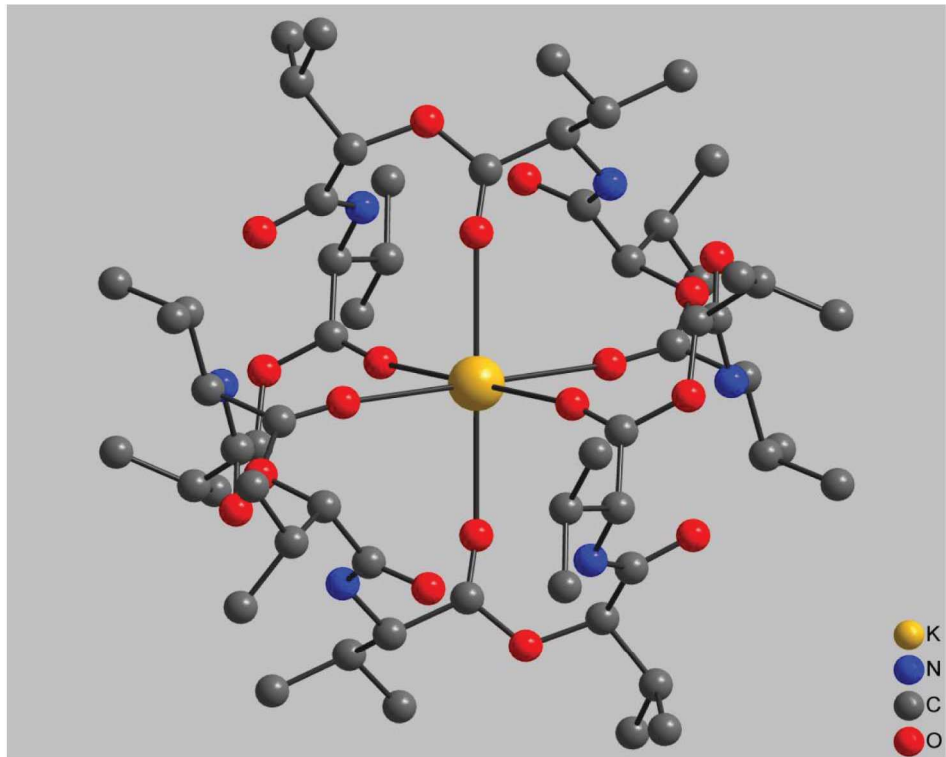
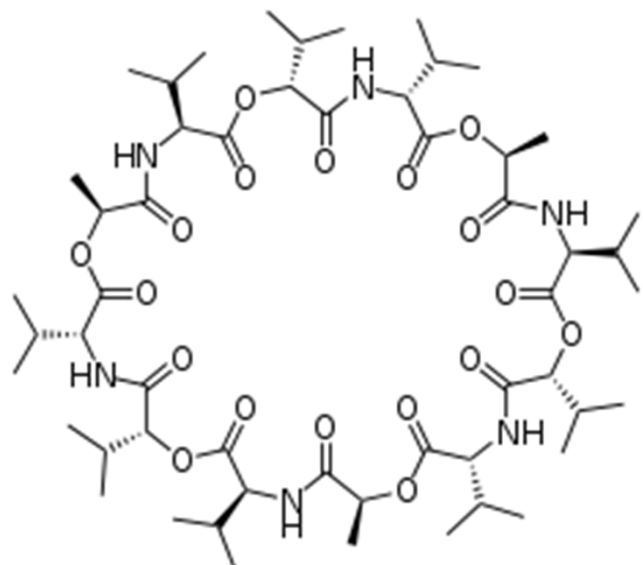


Figure 2.8

Molecular structure of the K⁺/valinomycin complex. Reprinted with permission from [35] © 1995 Bioorganicheskaya Khim/Springer.

Bioinorganic Chemistry: Inorganic Elements in the Chemistry of Life – An Introduction and Guide, Second Edition.
Written and Translated by Wolfgang Kaim, Brigitte Schwederski and Axel Klein.
© 2013 John Wiley & Sons, Ltd. Published 2013 by John Wiley & Sons, Ltd.

Nucleobases – pairing

Ligands 3: Nucleic acids

Metals influence pairing of nucleic acid polymers (H-bonding)

- Pairing of nucleobases inside DNA, complementarity of A-T and G-C
- Metal atoms: Mispairing possible (carcinogenic effect), e.g. T-G

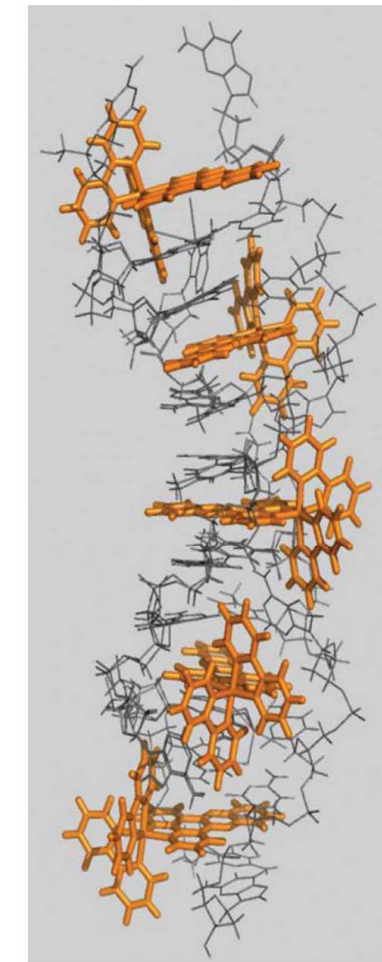
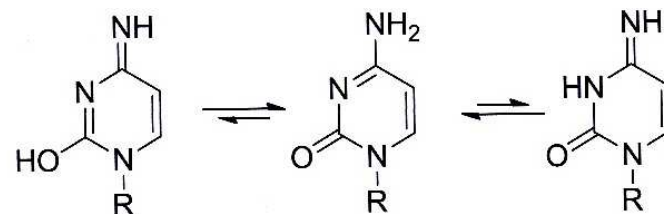
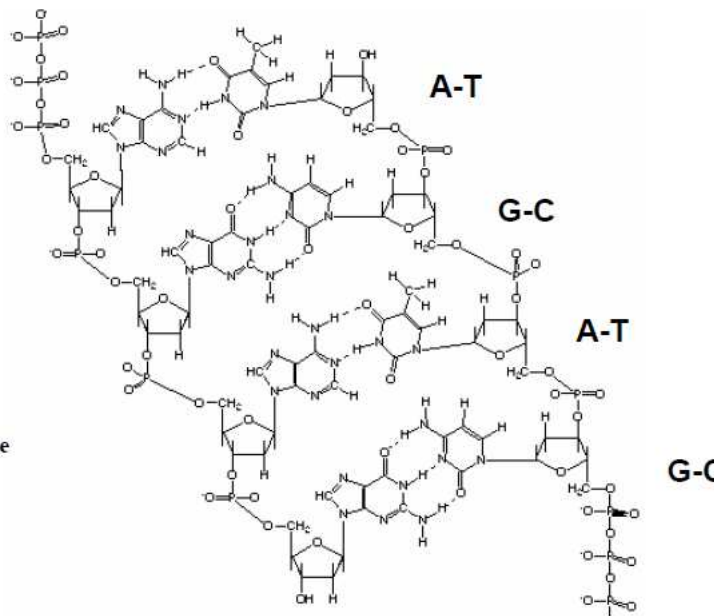
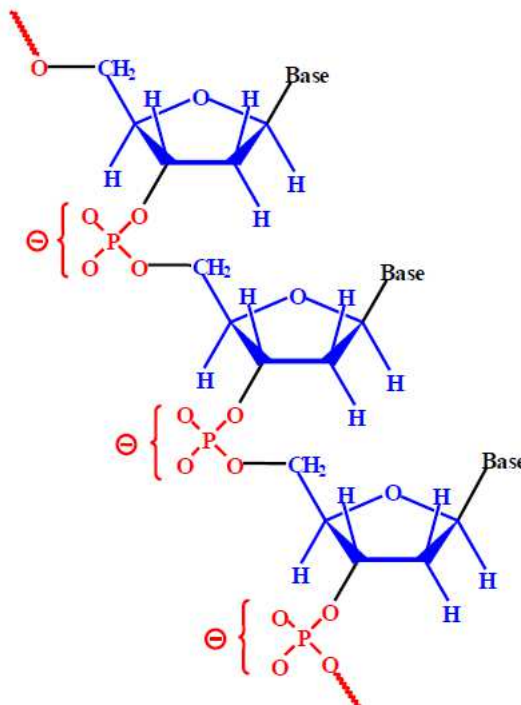
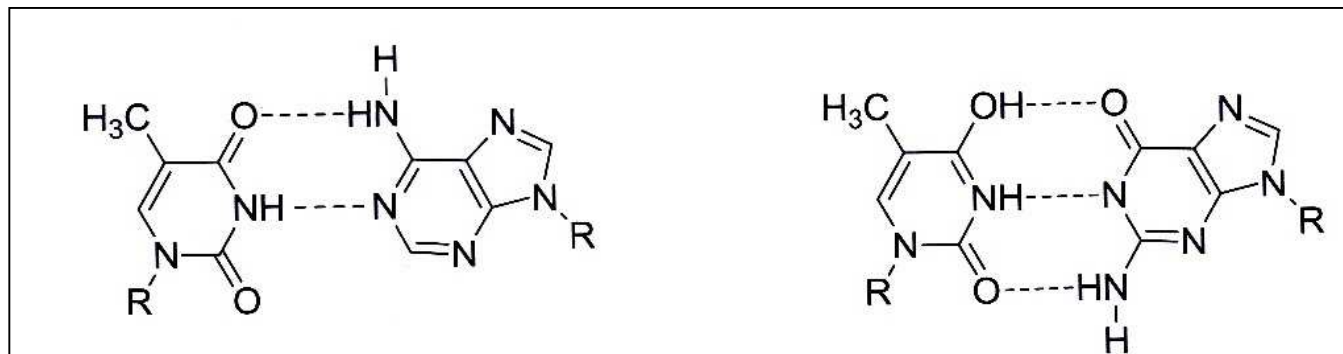
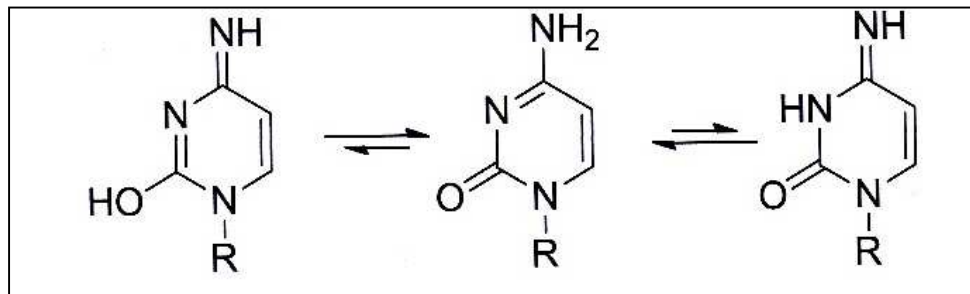


Figure 2.9

Example of a metal complex/oligonucleotide interaction (PDB

Metals: equilibrium of tautomers, cytosine



correct pairing: T – A

wrong: T – tautomeric form of G

Characteristic features of the bio-coordination compounds

1. Coordinatively unsaturated, or H_2O (not specialized electron transf.)
2. Irregular geometry, non ideal polyhedra
3. Size and shape of the substrate determined by the protein

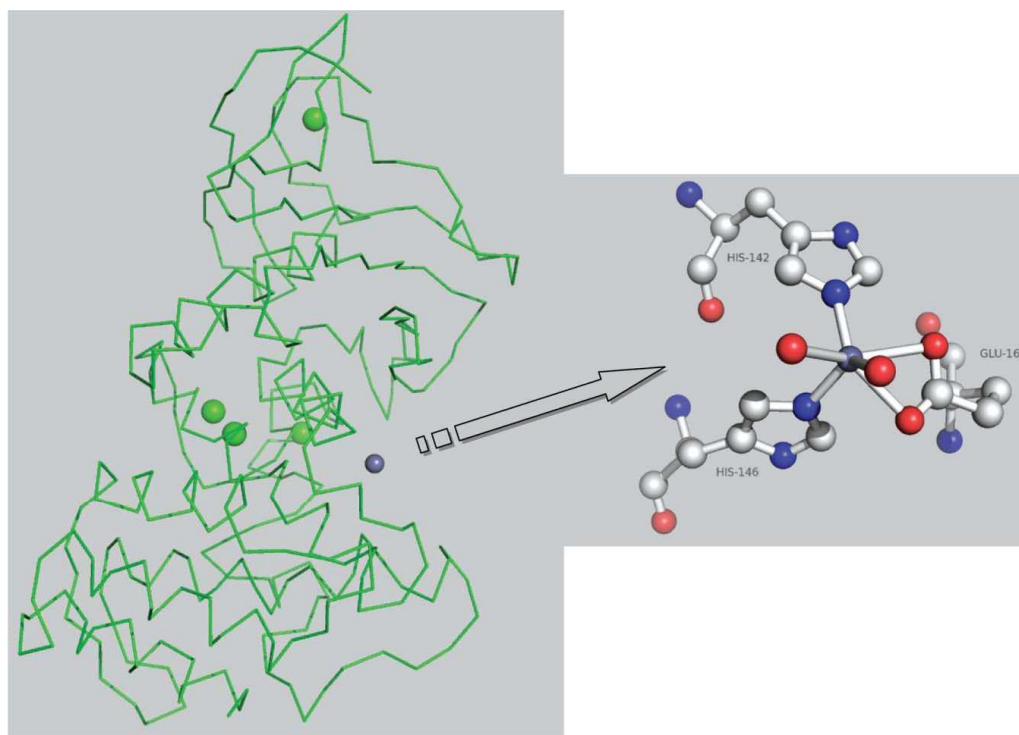


Figure 2.4

Structure of the proteolytic enzyme thermolysin (see Section 12.3) as determined by x-ray diffraction. The folding of the polypeptide chain of 316 amino acids (molecular mass 34 kDa) is shown in α carbon-backbone representation; that is, without depicting the side chains. Represented by spheres are the positions of four structure-stabilizing Ca^{2+} ions (green) and of the catalytic Zn^{2+} ion (dark grey), the detailed coordination of which (2 histidine, 1 glutamate, 2 H_2O) is shown in the insert (PDB code 1LNF) [15].

Entatic state

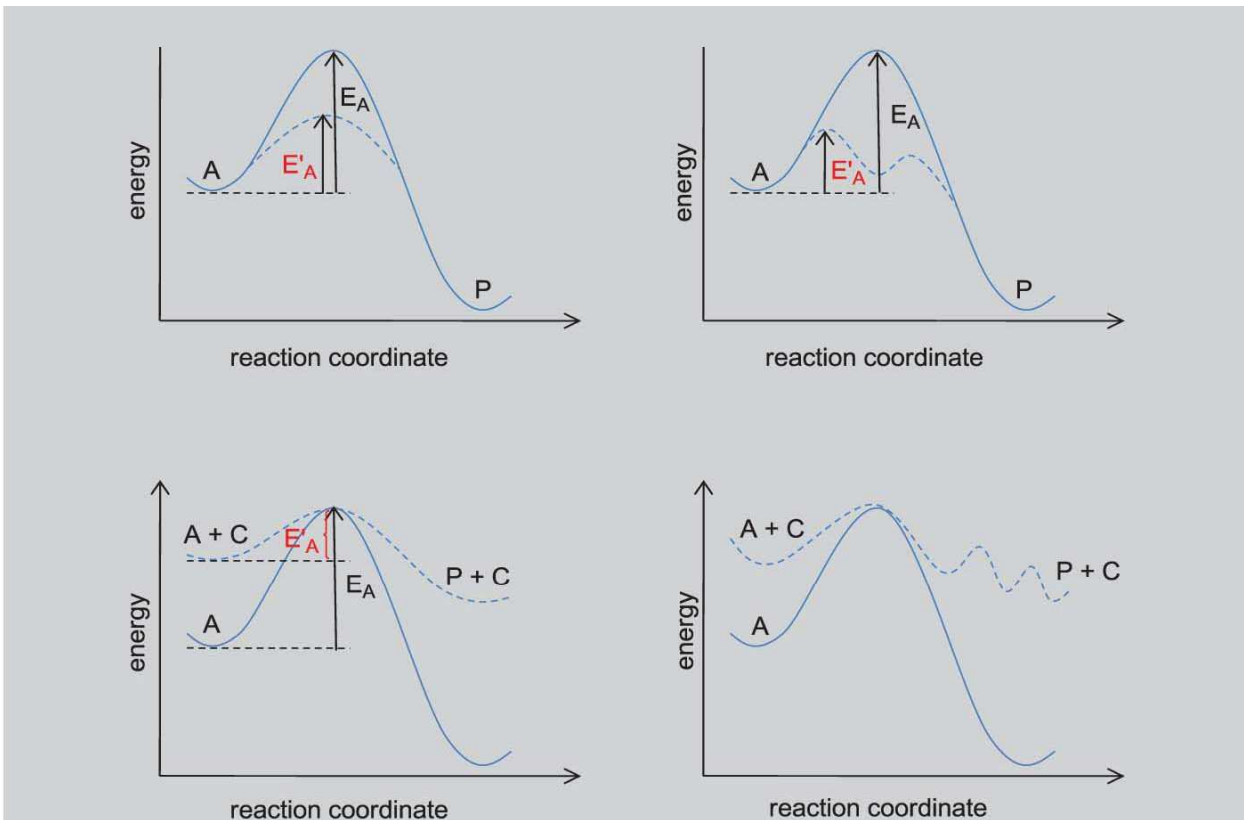
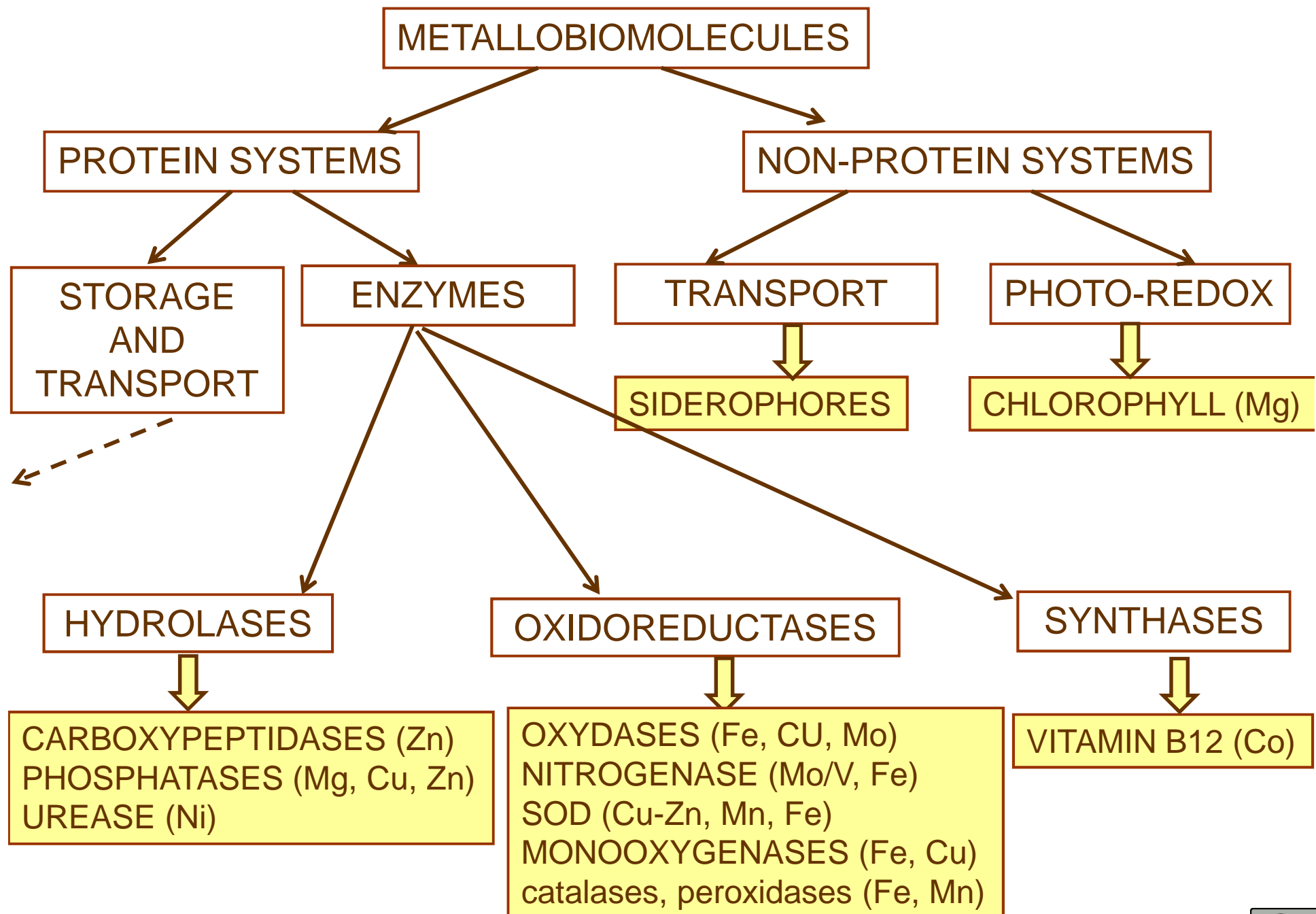


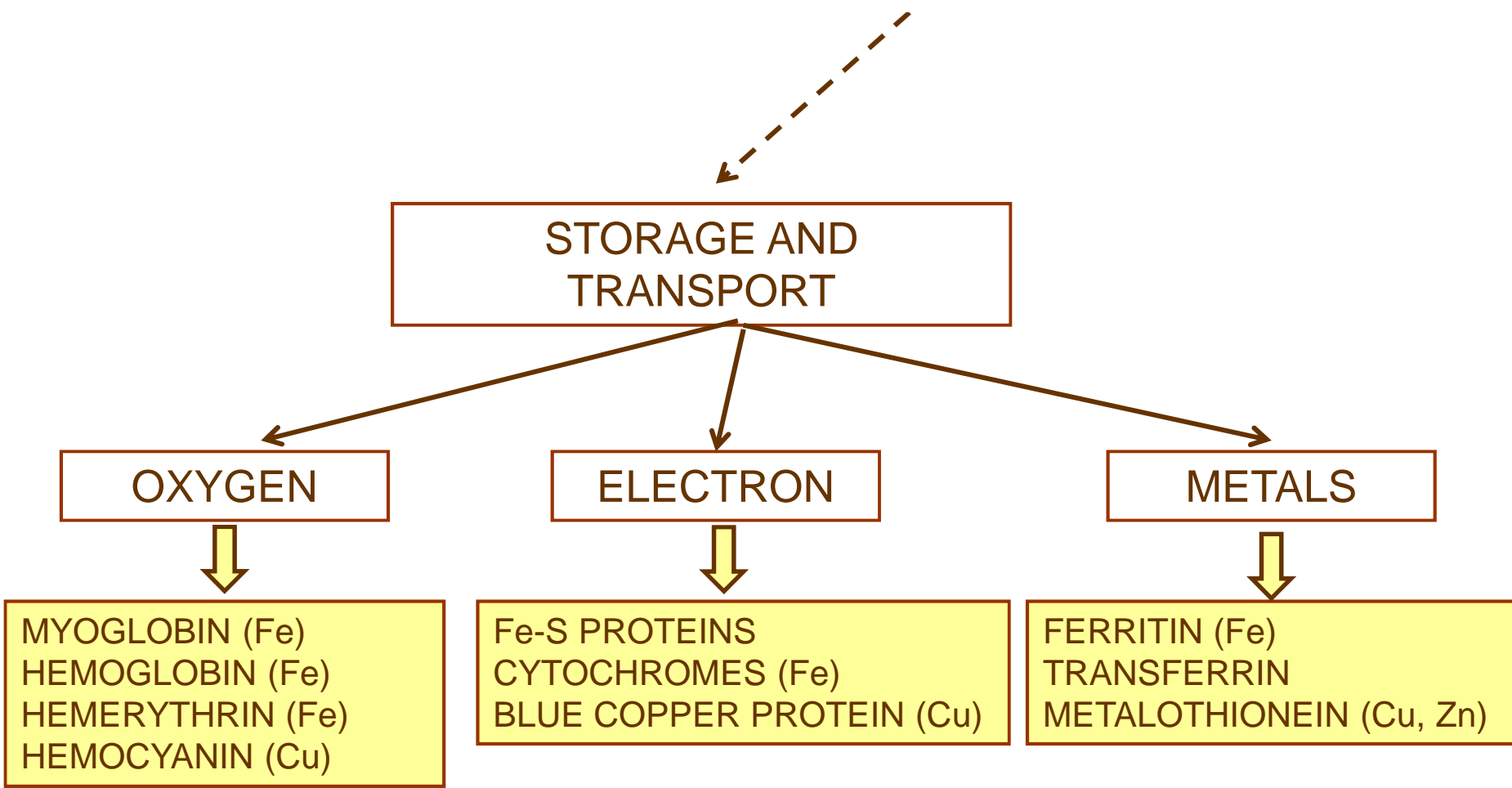
Figure 2.5

Energy profiles for catalyzed reactions at various degrees of sophistication. Upper left: conventional representation of the reduction of the activation energy $E_A \rightarrow E'_A$ upon transition from the initial state, A, to the products, P. Lower left: reduction of E_A by introduction of an “entatic” (strained, high-energy) enzymatic catalyst, C, which largely provides the preformed transition-state geometry of the substrate/catalyst complex. Upper right: realistic, multistep catalysis involving a new reaction pathway. Reprinted with permission from [19] © 1989, American Chemical Society. Lower right: realistic enzymatic catalysis.

Roles of protein:

- bond
- spatial fixation
- environment





Example 1: Chlorophyll - Mg

2 functions:

1. light harvesting, highly organized antenna – 98%
2. charge separation – 2%

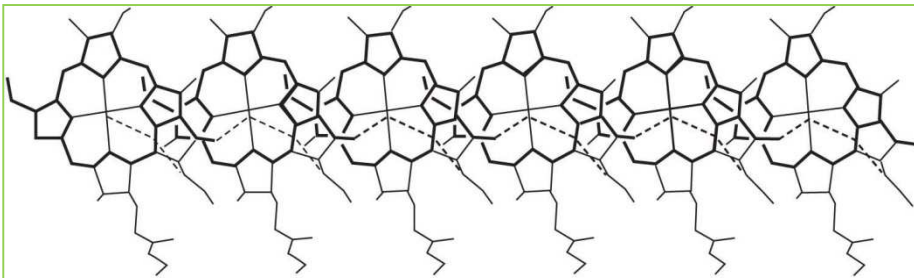


Figure 4.3

Structure of a one-dimensional aggregate occurring in crystals of ethyl chlorophyllide dihydrate. Reprinted with permission from [12] © 1975, American Chemical Society. The π electron conjugation is represented by thick lines, hydrogen bond links via water molecules by broken lines.

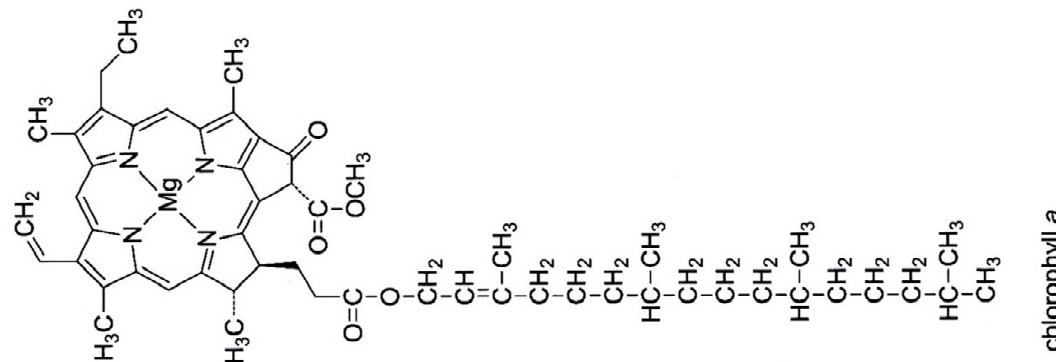
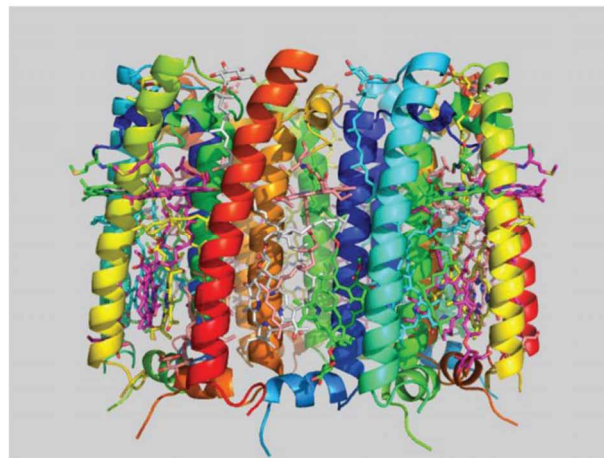
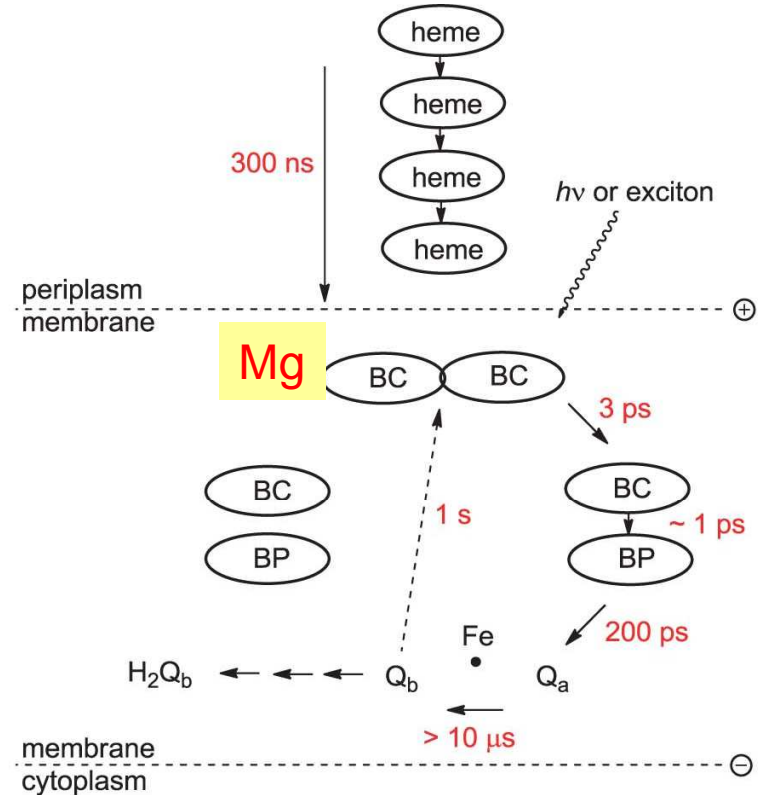
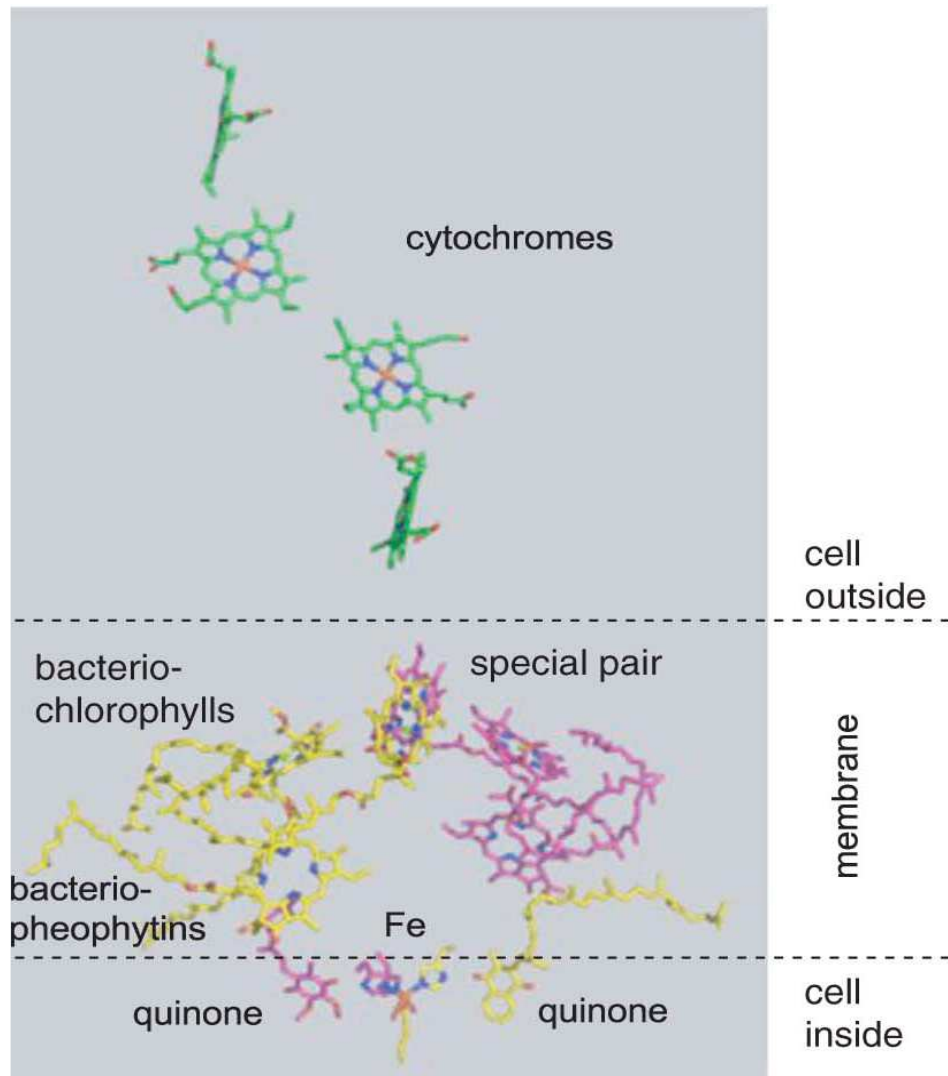


Figure 4.2

Light-harvesting architectures for *Rhodopseudomonas acidiphila*, as seen from the top (top) and the side (bottom) (PDB code 1KZU).

Charge separation

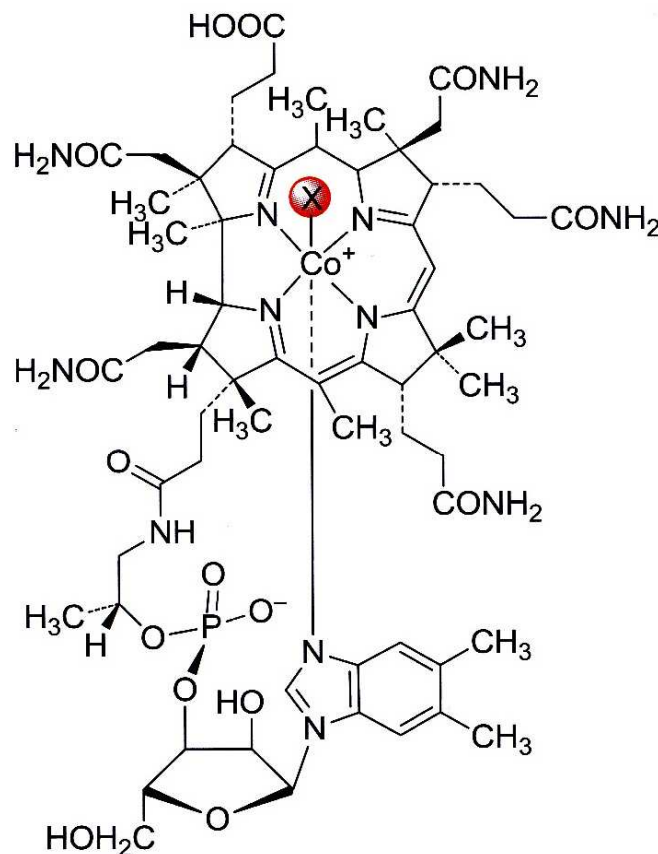


presentation of the temporal and spatial sequence of the light-induced charge separation center of bacterial photosynthesis (*Rps. viridis*, according to [4,10]).
bacteriochlorophyll; BP: bacteriopheophytin; Q_{a,b}: quinones.

Why Mg:
light (no spin-orbital coupling)
ox. state +II only
Lewis acid – structures available

Example 2: Cobalamines, Co

STRUCTURE OF COBALAMINES



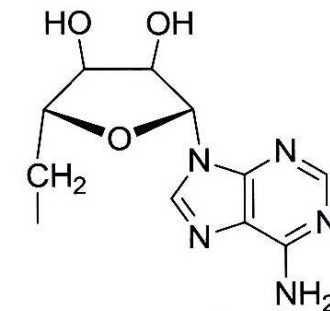
✗ = CH₃: methylcobalamin
(MeCbl or MeB₁₂)

CN: cyanocobalamin
(vitamin B₁₂)

OH: hydroxycobalamin
(vitamin B_{12a})

R: 5'-deoxyadenosyl-cobalamin
(coenzyme B₁₂ or AdoCbl)

R = 5'-deoxyadenosyl



axial ligands:

- N-donor 5,6-dimethylbenzimidazol
- C-donor CH₂R (MeCbl, AdoCbl)
- ORGANOMETALLIC MOLECULE STABLE IN WATER!

ROLE: methyl transfer

Table 3.1 Co(B₁₂)dependent enzymes and their occurrence in organisms.

Co(B ₁₂)dependent proteins	Organisms
(a) adenosylcobalamin(AdoCbl)-dependent isomerases	
methylmalonyl-CoA mutase (MCM)	archaea, bacteria, eukaryotes
isobutyryl-CoA mutase (ICM)	archaea, bacteria, eukaryotes
ethylmalonyl-CoA mutase (ECM)	archaea, bacteria, eukaryotes
glutamate mutase (GM)	archaea, bacteria
methyleneglutarate mutase (MGM)	archaea, bacteria
D-lysine 5,6-aminomutase (5,6-LAM)	bacteria
diol dehydratase (DDH)	bacteria
glycerol dehydratase (GDH)	bacteria
ethanolamine ammonia lyase (EAL)	bacteria
(b) methylcobalamin(MeCbl)-dependent methyltransferases	
methionine synthase (MetH)	bacteria, eukaryotes
methyltransferases (Mta, Mtm, Mtb, Mtt, Mts, and Mtv)	archaea, bacteria
methyltetrahydromethanopterin <i>CoM</i> methyltransferase subunit A (MtrA)	archaea
(c) B₁₂-dependent reductive dehalogenase (CprA)	bacteria

Methionin synthase

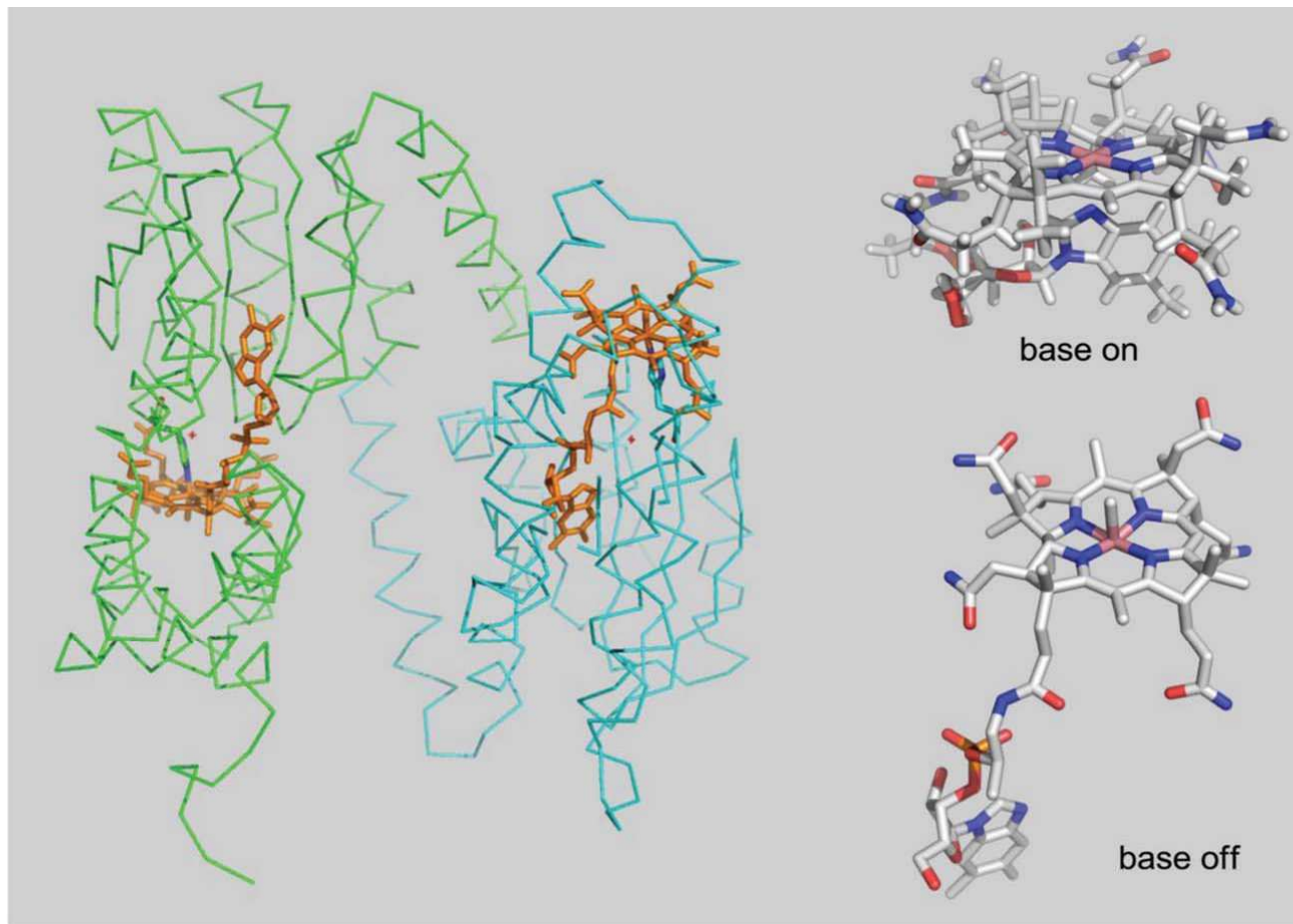
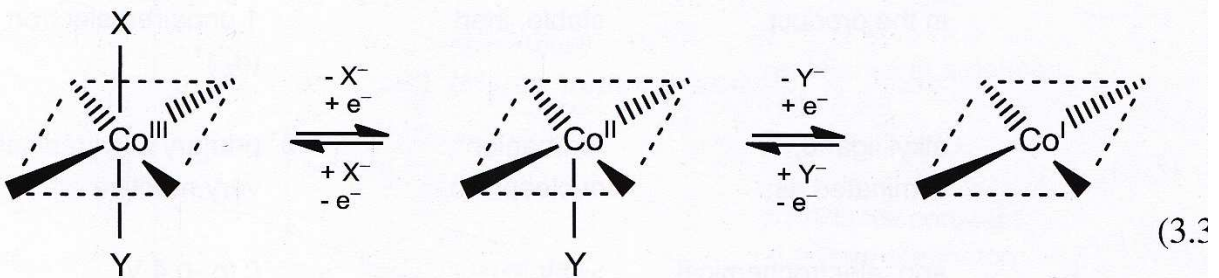


Figure 3.2

Representation of the structure of B₁₂ binding domains of methionine synthase (PDB code 1BMT) [11]; base-on/base-off configurations shown for the coenzyme.

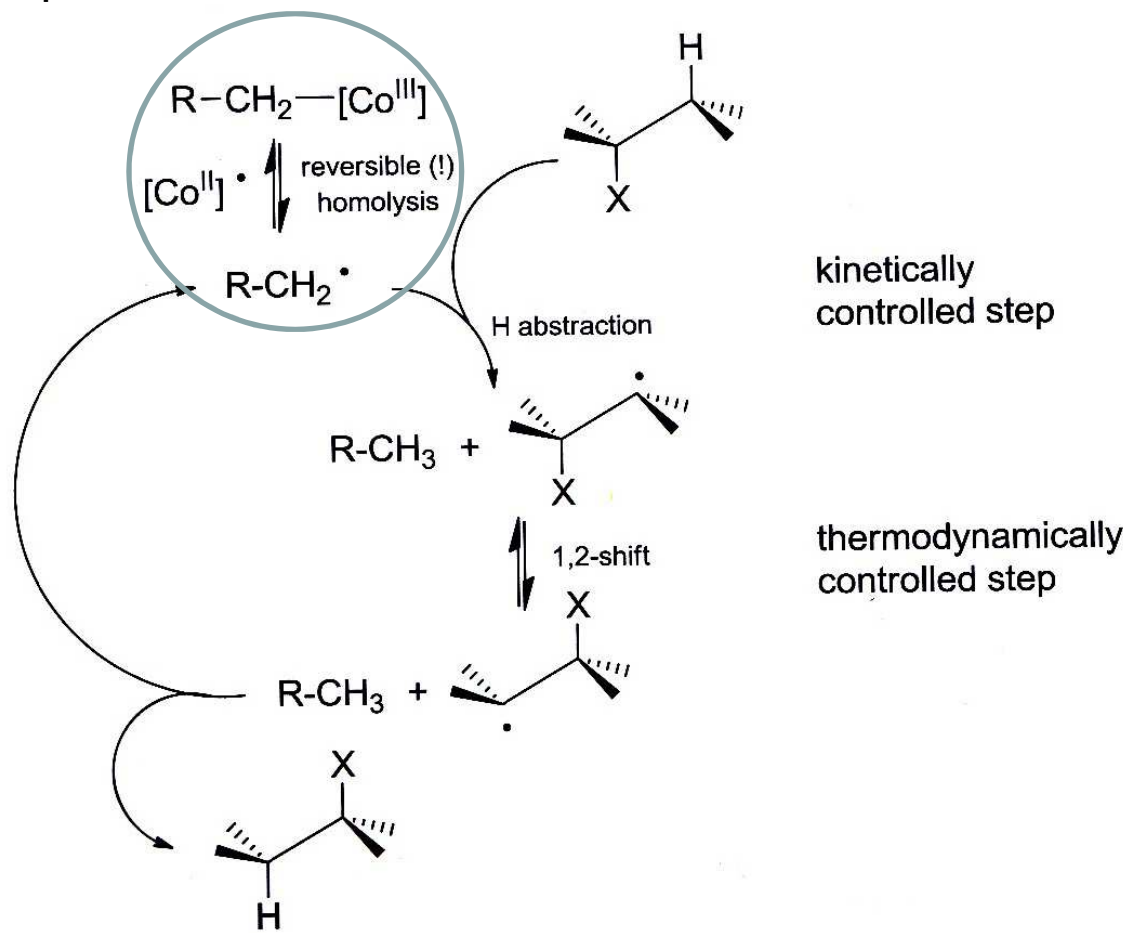
Reactivity



reductive elimination

oxidative addition

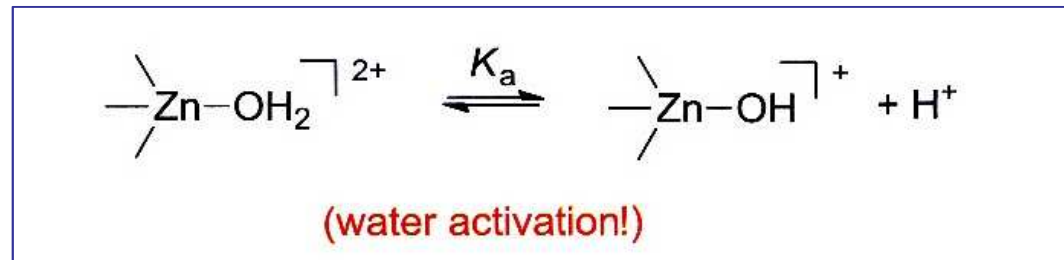
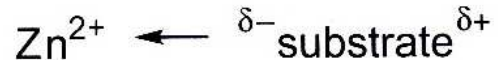
Proposed mechanism:



Why Co:
redox active, able to bond methyl reversibly
kinetic inertness of the LS Co(III)

Example 3: Hydrolases, Zn

Lewis acid, substrate polarization



Hypothetical mechanism

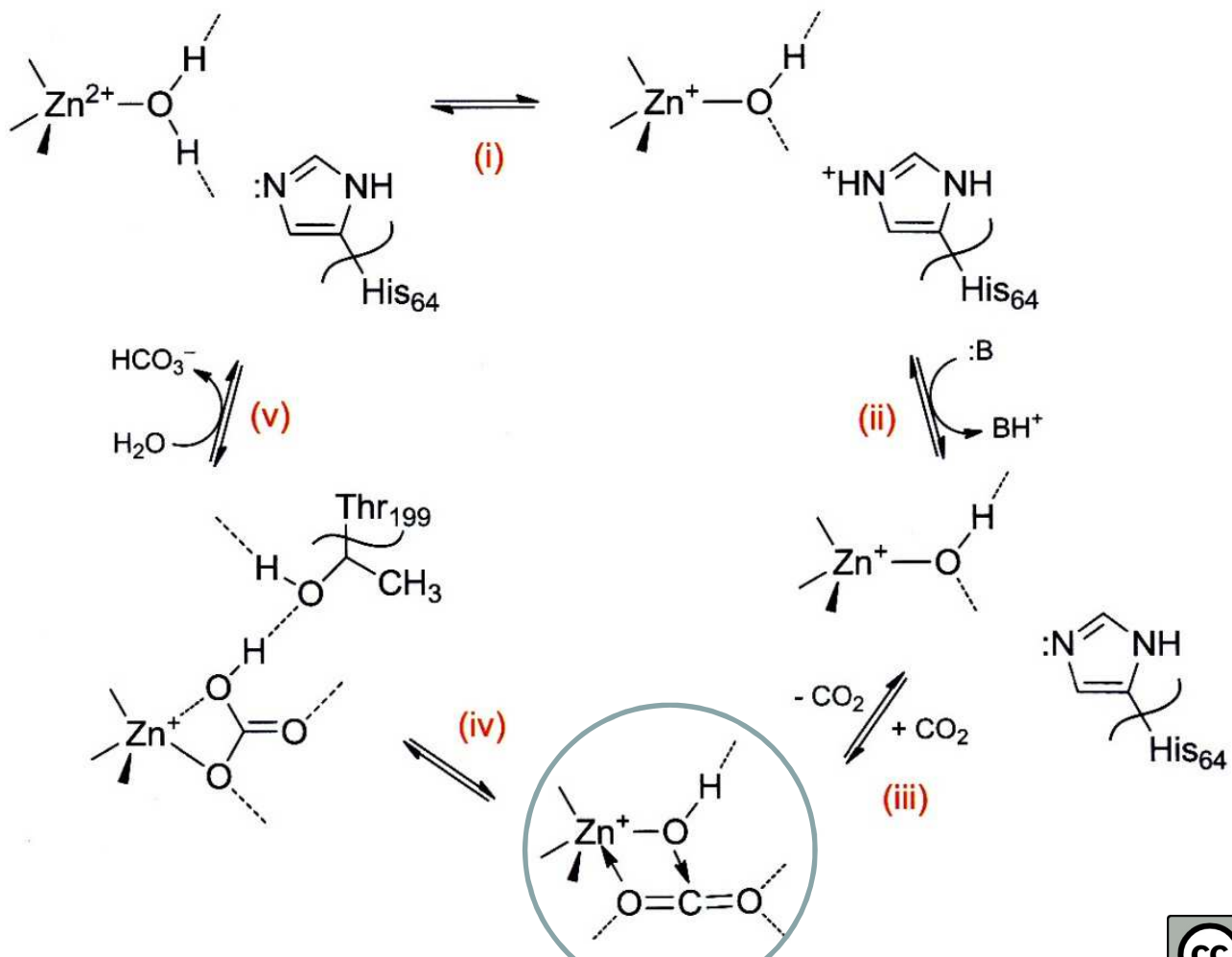


Table 12.1 Representative zinc-containing proteins.

Zinc protein	Molecular mass (kDa)	Ligands	Function
carboanhydrase (CA)	30	3 His 1 H ₂ O	hydrolysis (12.6)
carboxypeptidase (CPA)	34	2 His 1 η^2 -Glu 1 H ₂ O	hydrolysis (12.2), (12.11)
thermolysin	35	2 His 1 η^2 -Glu 1 H ₂ O	hydrolysis (12.2)
5-aminolevulinic acid dehydratase (ALAD)	8 × 35	8 × { 3 S 1 N/O	condensation (12.18)
alcohol dehydrogenase (ADH)	2 × 40	2 × { 2 Cys 1 His 1 H ₂ O	oxidation of 1° or 2° alcohols via NAD ⁺ (12.19)
glyoxalase	2 × 23	2 × { 2 His 2 × { 2 Glu? 2 H ₂ O	reduction of α -dicarbonyl compounds by glutathione (12.21)
superoxide dismutase (SOD)	2 × 16	2 × { 2 His 1 μ -His [−] 1 Asp	disproportionation of O ₂ ^{•−} (10.15)
transcription factors	TFIIIA: 40 GALA: 17	n × { 2 His 2 Cys 2 × { 4 Cys	structural function: formation of specifically folded domains
insulin hexamer	6 × 6	2 × { 3 His n L	structural function: stabilization of oligomeric storage forms
metallothionein	6	\leq 7 × 4 Cys	transport and storage protein

Carbonate dehydratase, carboanhydrase, CA



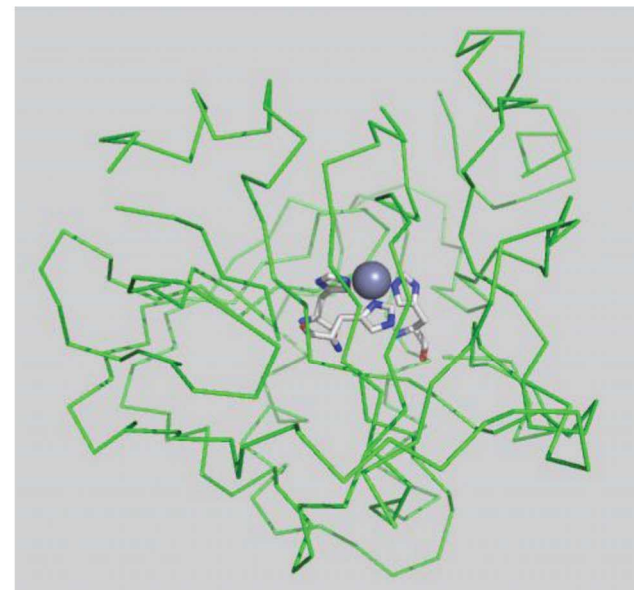
enzymatically accelerated 10^7 times, to a diffusion-controlled limit

Key reaction in :

1. photosynthesis
2. breathing
3. calcification and de calcification
4. pH regulation

in human erythrocytes, CA is the most abundant protein component after haemoglobin

Several structurally similar but differently effective and pH-dependent variants



human CA II: 3 His, H_2O , deformed tetrahedron

located at a bottom of a deep cleft

network of water molecules, the rate determining step = proton shuttle

simple CO_2 hydration – slow, half-life 20s

Figure 12.1

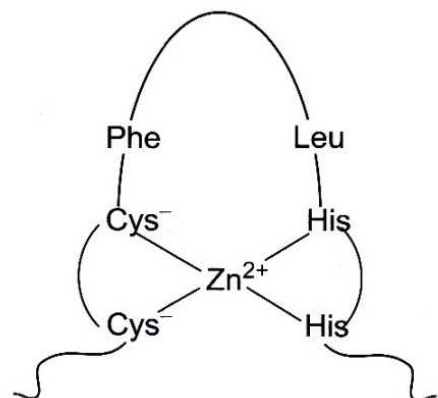
Structural representation of human CA II, showing the protein folding and the Zn^{2+} coordination to three imidazole rings of histidine side chains (PDB code 4CAC) [8].

Zinc Fingers

gene regulatory protein, loops
Zn “bridges” are stable (comp. with disulfides)

typical sequence

Cys-X_{2,4}-Cys-X₃-Phe-X₅-Leu-X₂-His-X_{3,4}-His



zinc finger modular unit from TF IIIA

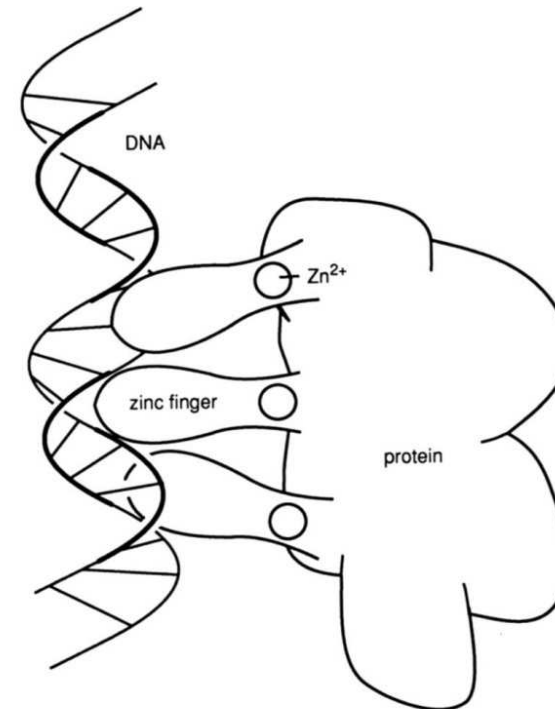
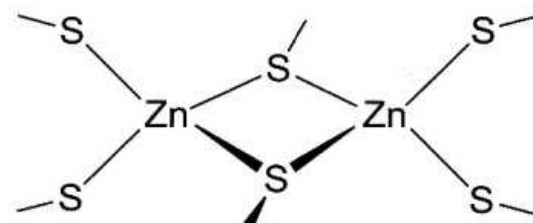


Figure 12.6

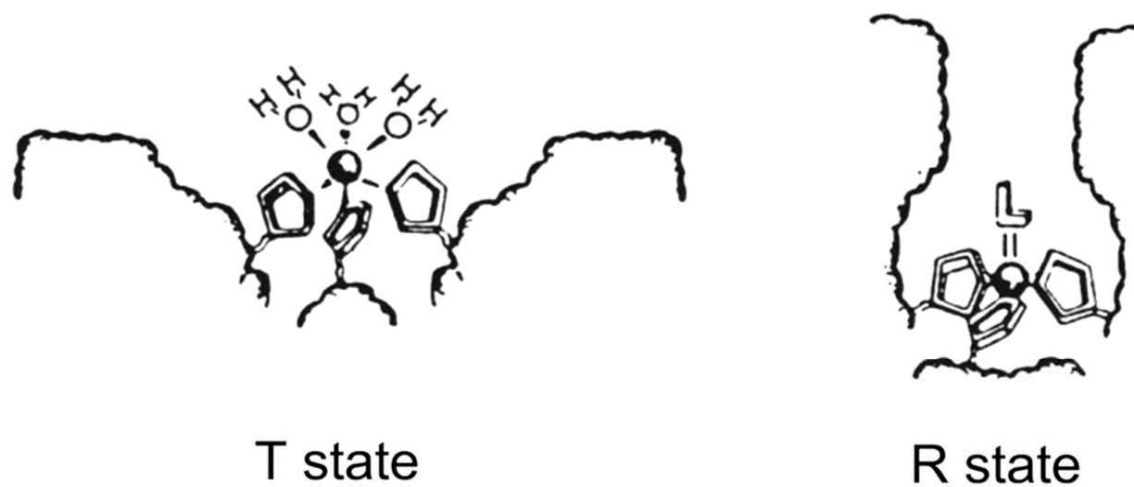
Schematic representation of the interaction between DNA and a zinc finger protein.

Yeast transcription factor:



zinc coordination by 6 Cys^- in the yeast transcription factor GAL4

Insulin



T state

R state

Figure 12.7

Arrangement of the imidazole rings of histidine ligands from three different insulin peptide around one structurally coordinating Zn^{2+} center in T- and R-states of a 2-Zn/insulin hexamer (according to [48]).

Why zinc:

- no redox activity
- easy deformation of coordination polyhedron – entatic state
- small coordination number (sterically available)

Zn containing food



Example 4: Oxygen production, Mn

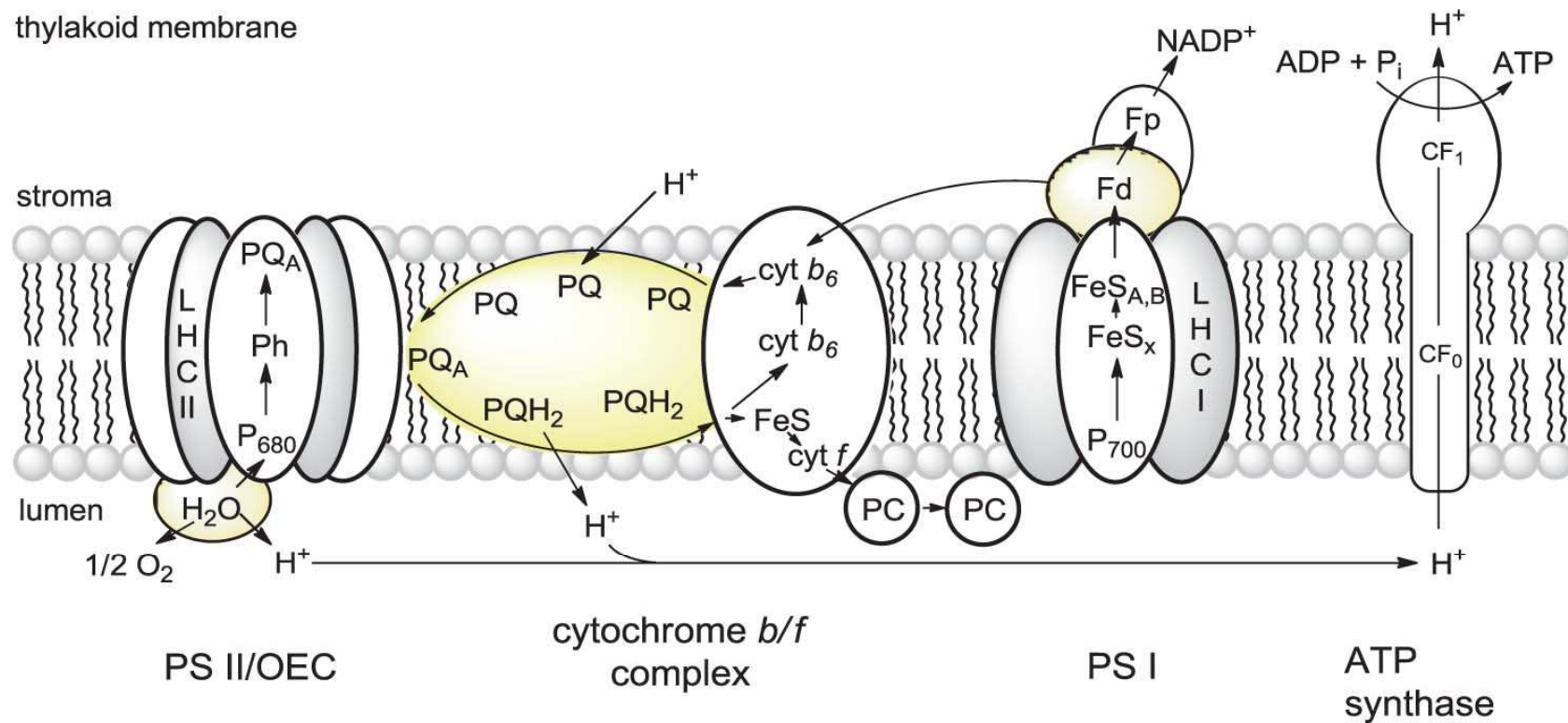


Figure 4.6

Structural organization of the lamellar thylakoid membrane of higher plants, with the following components: two photosystems (PS) and two light-harvesting complexes (LHC), an oxygen-evolving complex (OEC) at PS II (Section 4.3), a cytochrome *b/f* complex (Section 6.1), plastoquinones (PQ/PQH₂ (3.12)) and plastocyanin (PC; Section 10.1), several iron–sulfur centers (FeS; Sections 7.1–7.4), soluble ferredoxin (Fd) and the flavoprotein Fp (Ferredoxin/NADP reductase) and ATP synthase as the center of photosynthetic phosphorylation.

Active site of OEC (Oxygen Evolving Complex)

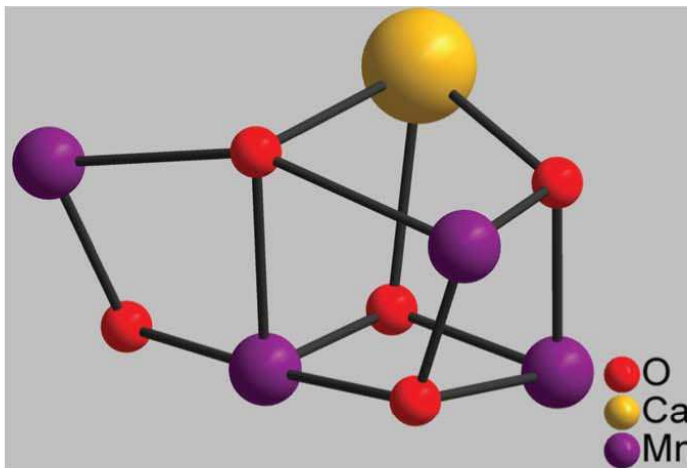
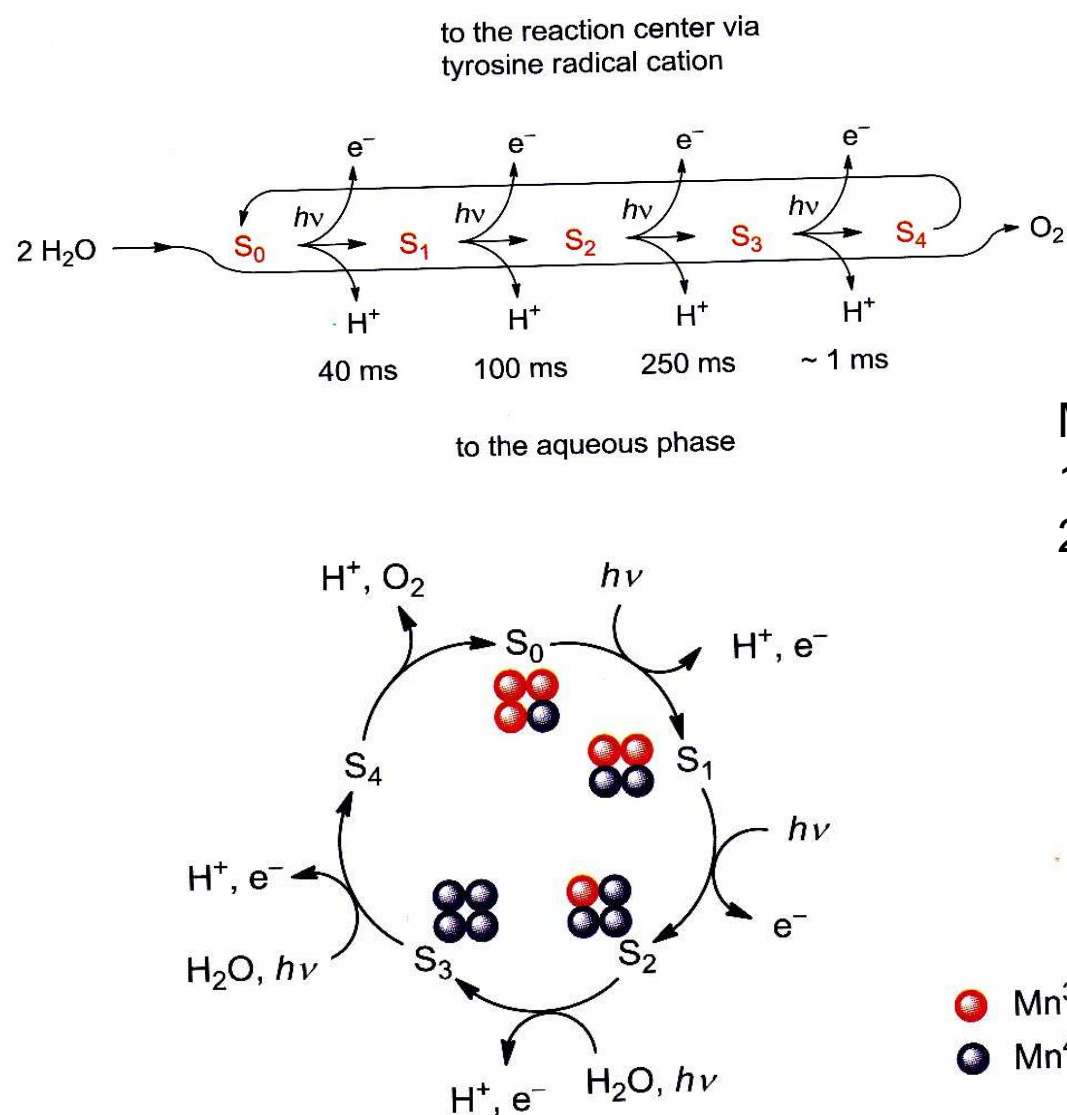


Figure 4.9

Metal coordination arrangement in the OEC from a 1.9 Å resolution x-ray crystal structure determination of PS II from the thermophilic cyanobacterium *T. vulcanus* (PDB code 3ARC) [23].

Bioinorganic Chemistry: Inorganic Elements in the Chemistry of Life – An Introduction and Guide, Second Edition.
Written and Translated by Wolfgang Kaim, Brigitte Schwederski and Axel Klein.
© 2013 John Wiley & Sons, Ltd. Published 2013 by John Wiley & Sons, Ltd.

Stepwise reduction of 4 Mn cluster, parallel electron + proton flux



5 oxidation steps, Kok cycle
flash photolysis, EPR
 S_2 : spin $\frac{1}{2}$, more Mn nuclei.
maybe $\text{Mn}^{\text{III}}\text{Mn}^{\text{IV}}_3$

Mn 4 cluster:

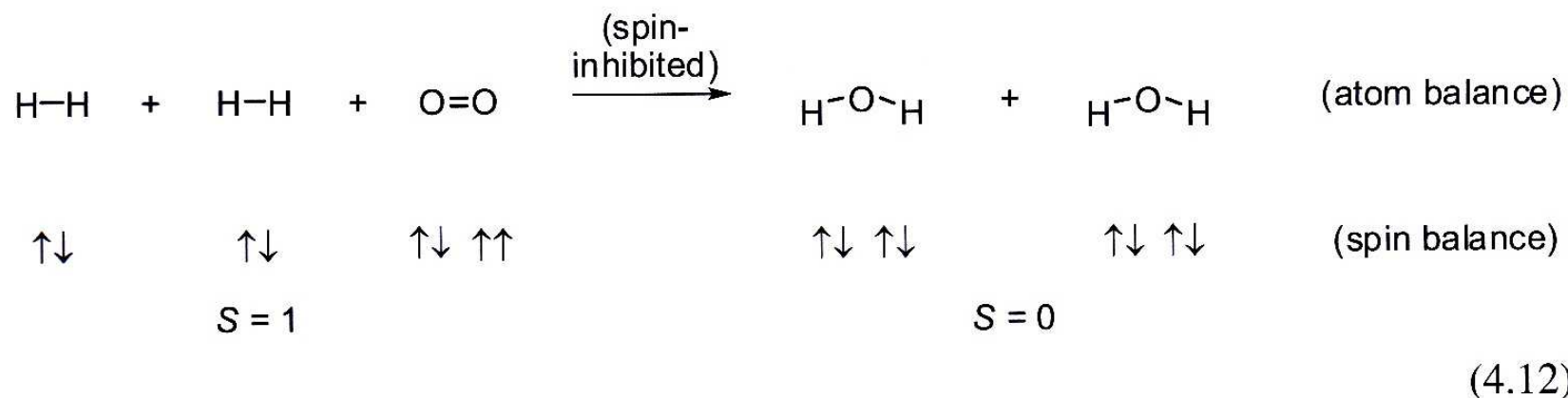
1. containment for electrons
2. non- ${}^3\text{O}_2$ retaining catalyst

Why Mn:

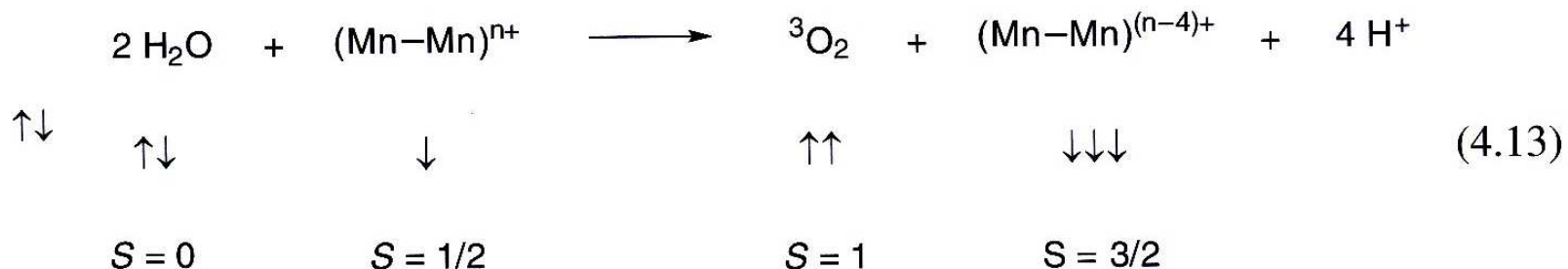
- many ox. states
- labile bonding of ligands
- remarkable stable high-spin states $-{}^3\text{O}_2$

Spin compatibility

Incompatible spins – high activation barrier, slow reaction – hydrogen + oxygen



The hypothetical spin balance (4.13) shows the possible function of catalytic metal centers with variable spin quantum numbers $S = n/2$.



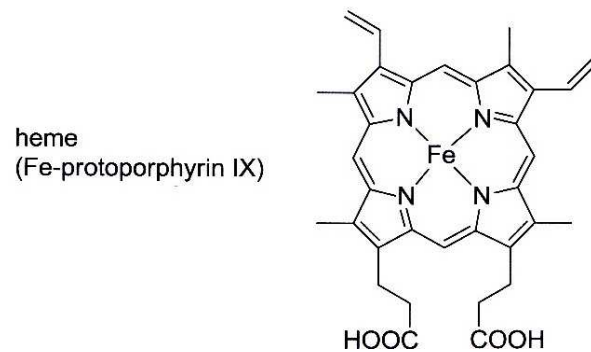
Example 4: Oxygen assimilation, Fe, Cu

Table 10.1 Correspondence of iron and copper proteins.

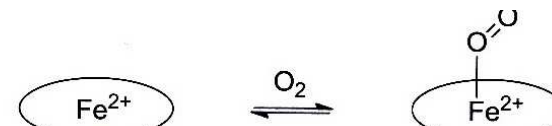
Function	Fe protein	Cu protein
O ₂ transport	hemoglobin (<i>h</i>) hemerythrin (<i>nh</i>)	hemocyanin
oxygenation	cytochrome P-450 (<i>h</i>) methane monooxygenase (<i>nh</i>) catechol dioxygenase (<i>nh</i>)	tyrosinase quercetinase (dioxygenase)
oxidase activity	peroxidases (<i>h</i>) peroxidases (<i>nh</i>)	amine oxidases laccase
electron transfer	cytochromes (<i>h</i>)	blue Cu proteins
antioxidative function	peroxidases (<i>h</i>) bacterial superoxide dismutases (<i>nh</i>)	superoxide dismutase (Cu, Zn) from erythrocytes
NO ₂ ⁻ reduction	heme-containing nitrite reductase (<i>h</i>)	Cu-containing nitrite reductase

h, heme system; *nh*, non-heme system.

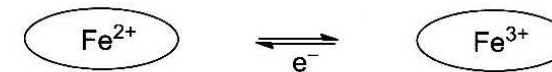
Fe complexes with tetrapyrrolic ligands – various functions



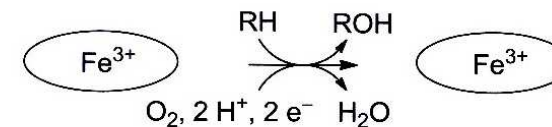
hemoglobin,
myoglobin
(section 5.2)



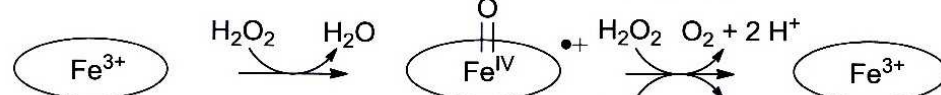
cytochromes
(section 6.1)



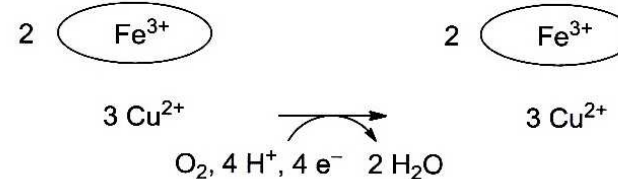
cytochrome P-450
(section 6.2)



catalase and
peroxidase
(section 6.3)



cytochrome c
oxidase
(section 10.4)

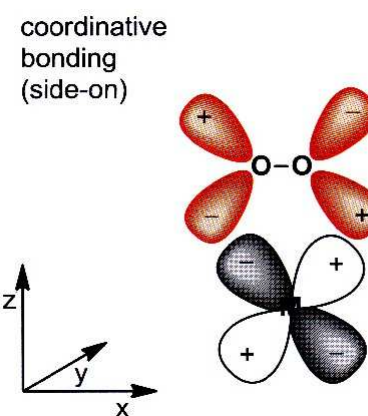
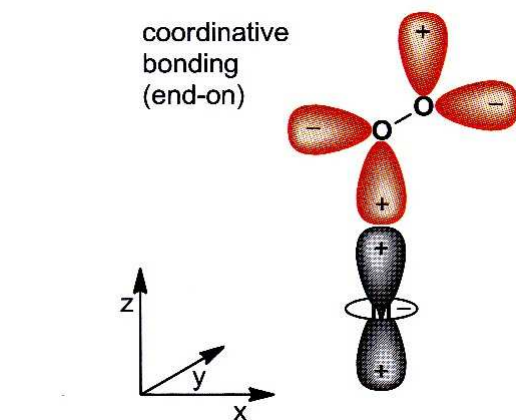


tetrapyrrolic complexes – hem proteins

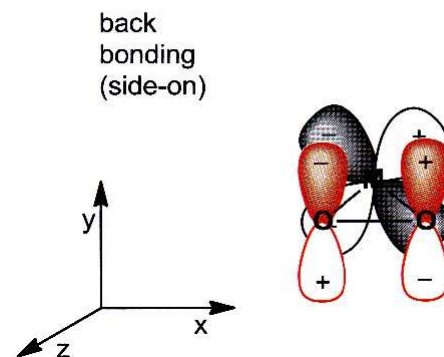
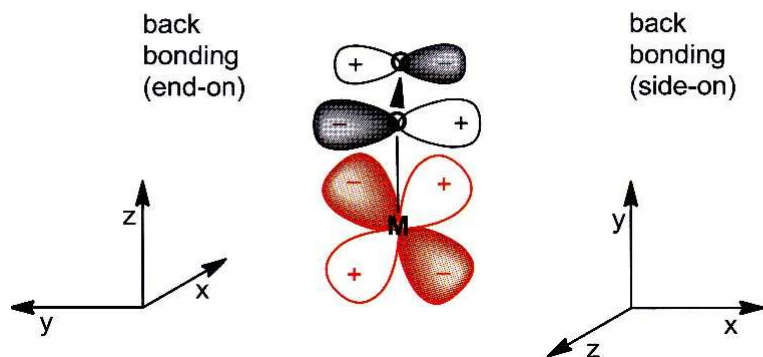
- various functions;
- modulated by the surrounding protein
- coordination number 6 – electron transfer only (cytochromes)

Coordination modes of O₂

O₂: non-innocent ligand



sigma donor



both π donor + acceptor

Hem structure

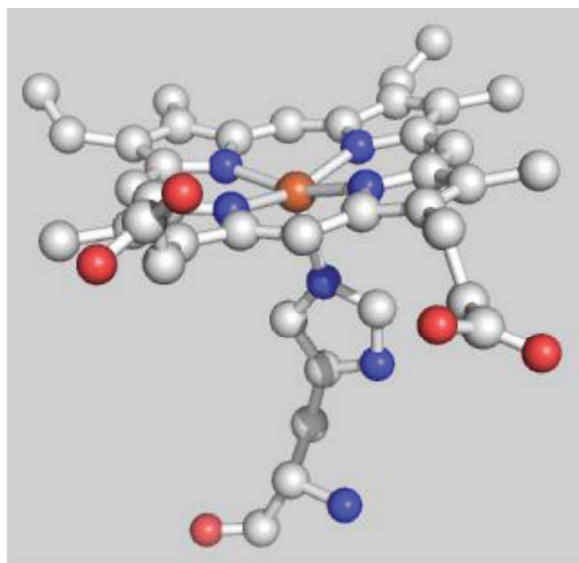


Figure 5.4

Structure of the deoxy heme unit in *Mb* and *Hb* (here shown for *Hb*, PDB code 2HHB) [13]

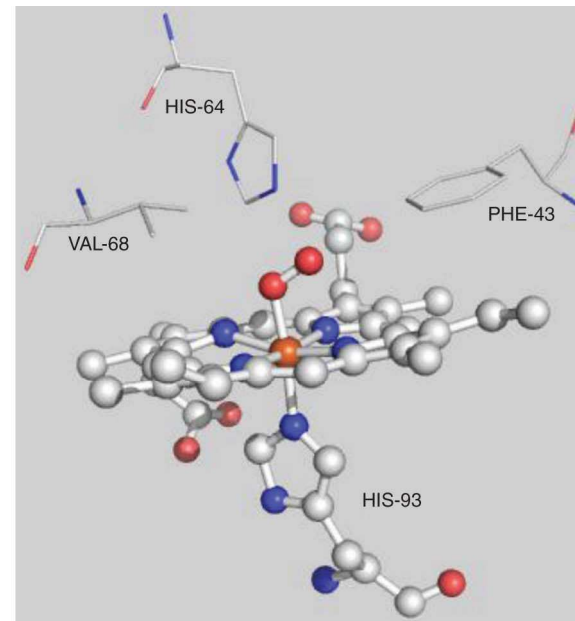


Figure 5.5

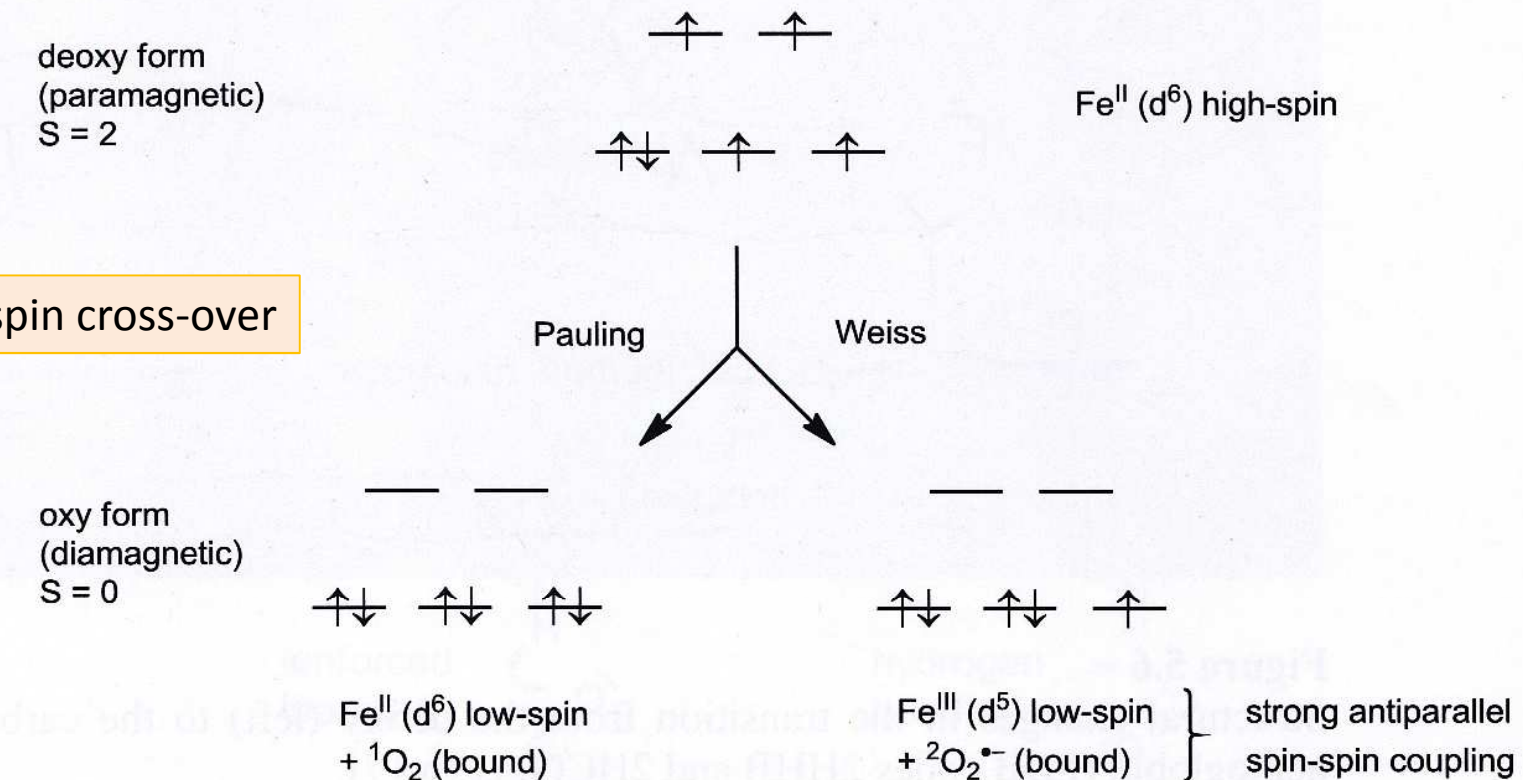
Arrangement of proximal (His_{93}) and distal (His_{64} , Val_{68} , Phe_{43}) amino acid residues with regard to oxy-myoglobin (PDB code 1MBO) [13a].

Coordination sphere: 4 N from porphyrin, N from *proximal* histidine
distal: His, Val, Phe – H bonds

Deoxy: porphyrin slightly domed; less influence to Fe(II) - **highspin**, $S=2$ – compatible with ${}^3\text{O}_2$
Oxy form – experimental data:

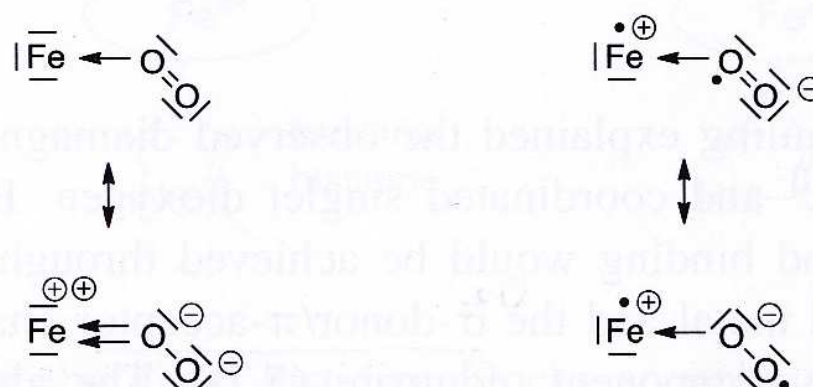
- DIAMAGNETIC
- O_2 non linear, Fe-O-O angle about 120°

Possible mechanisms, hem - O₂



Bonding:

Fe(II) σ-acceptor/π-donor
O₂ σ-donor/π-acceptor



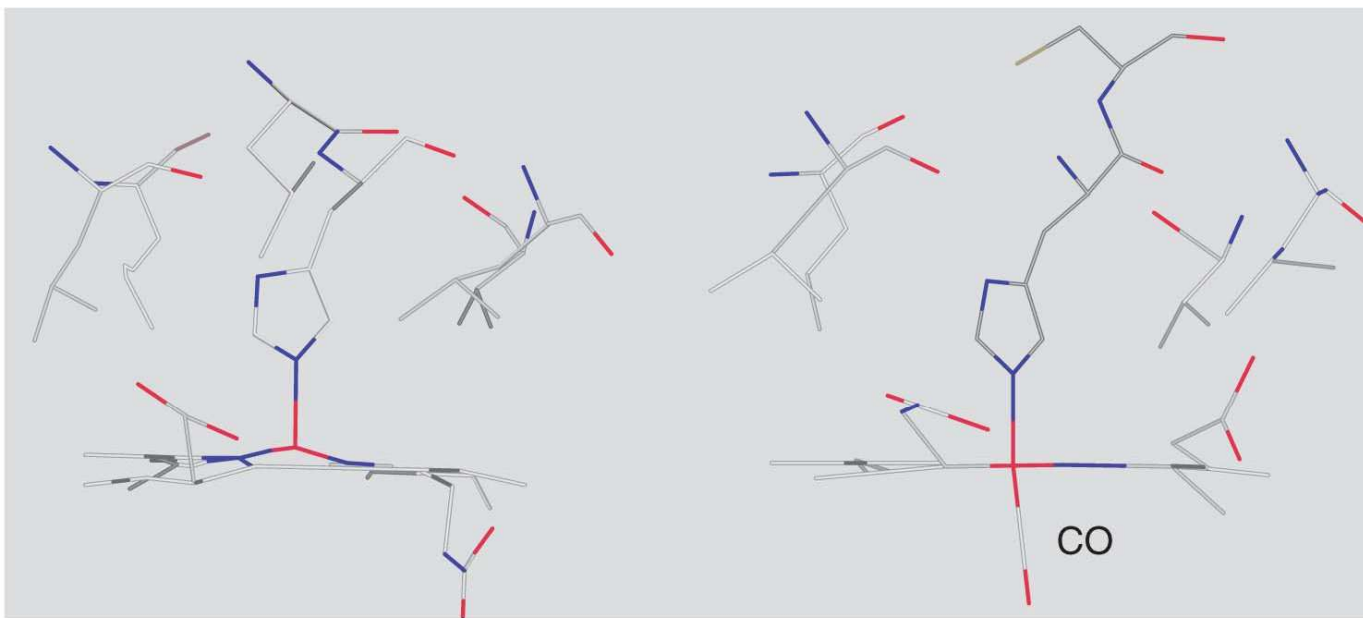
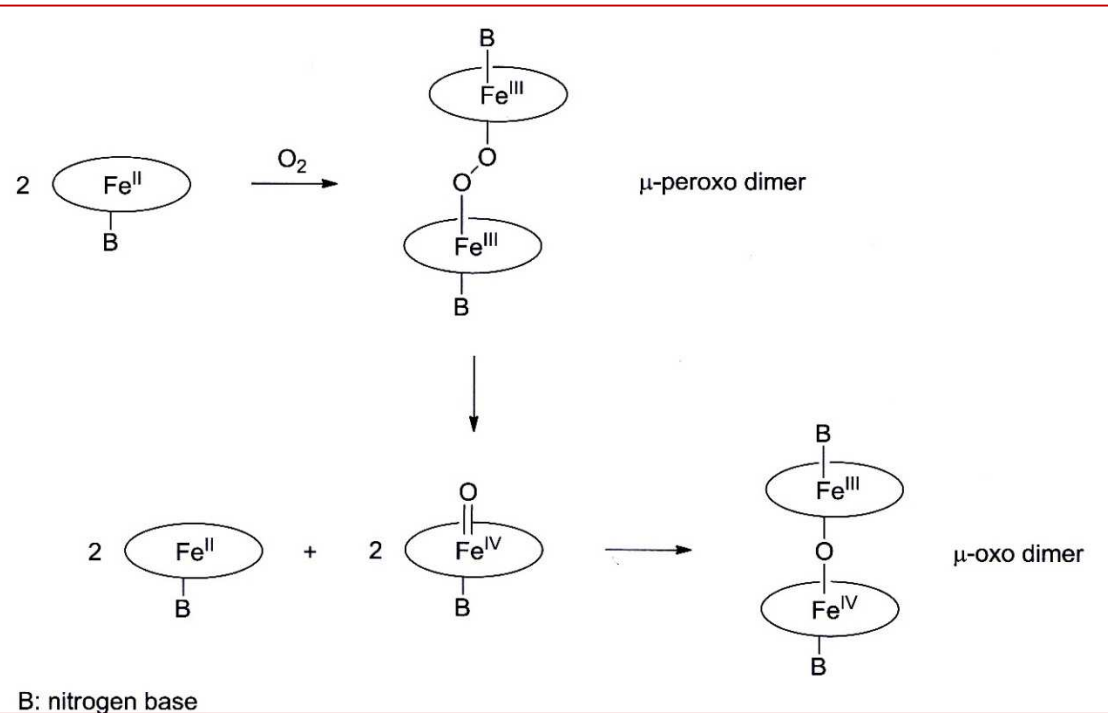


Figure 5.6

Structural changes in the transition from the deoxy (left) to the carbon monoxy form (right) of hemoglobin (PDB codes 2HHB and 2HCO) [13b,17].

Support for the Pauling model:
dioxygen can be effectively replaced by other π -acceptor ligands (CO, NO)

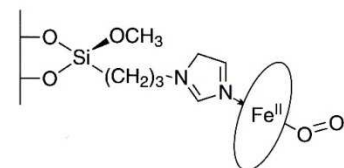
Without protein- irreversible, dimerisation



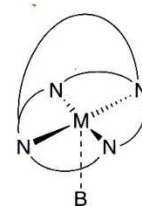
Prevention against dimerisation in model compounds:

strategies to prevent reaction (5.12):

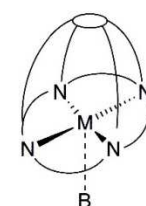
immobilization at a (polymeric) support:



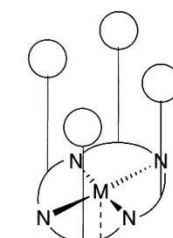
shielding in cavities:



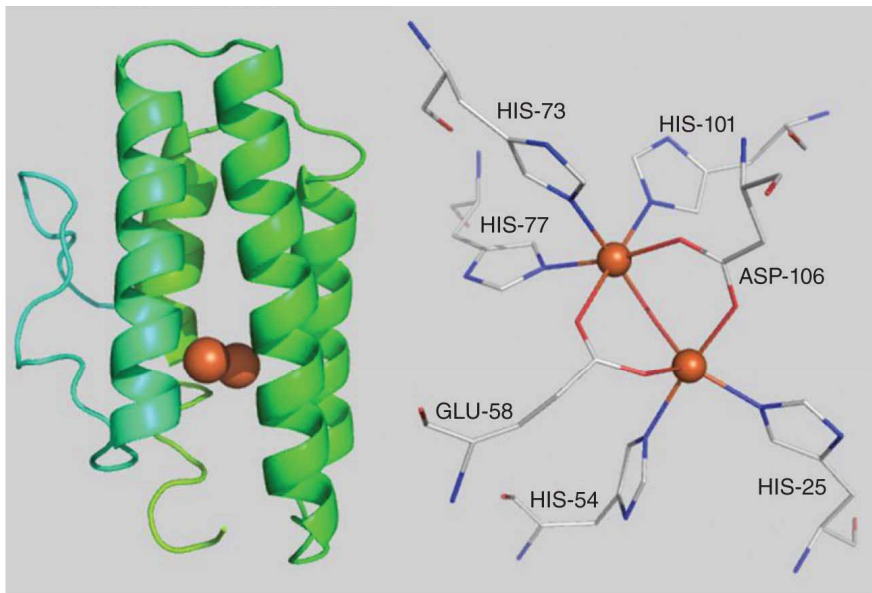
strapped



capped



picket fence

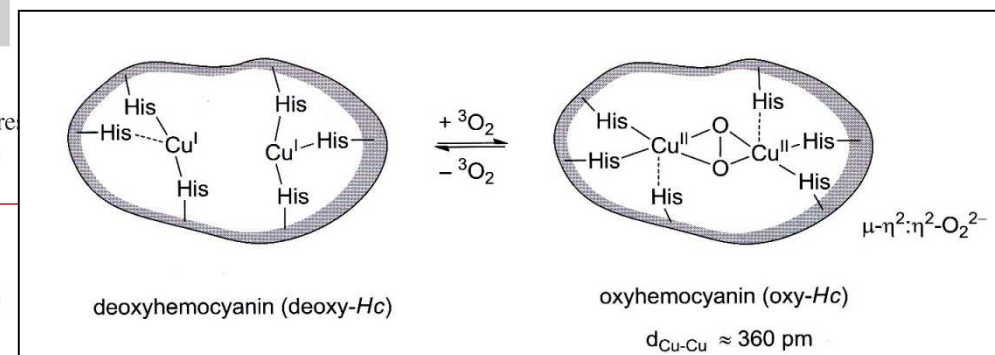
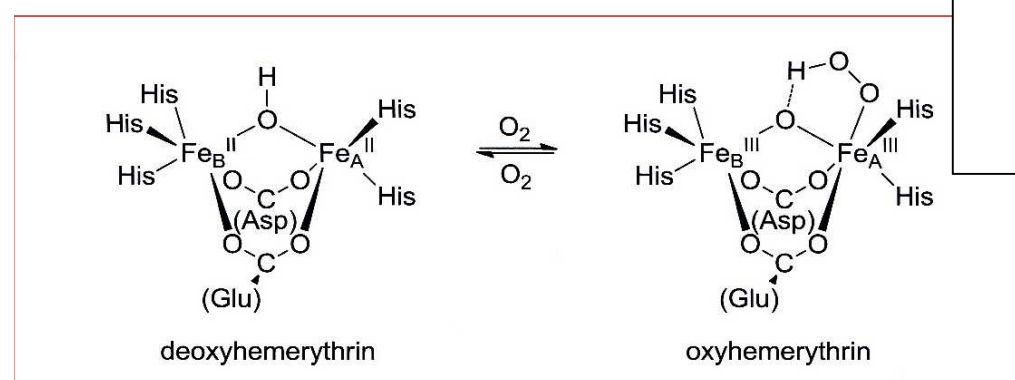


Alternative O₂ transport: hemerythrin (Fe), hemocyanin (Cu)

dimers, different binding modes

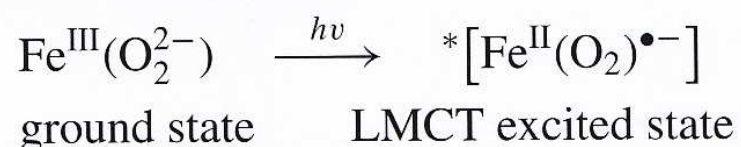
Figure 5.7

rotein folding in monomeric hemerythrin, with the positions of both iron atoms (red spheres) and the structure of the iron dimer center (right) in the deoxy form (PDB code 1HMD) [27].



deoxy: colourless
oxy: blue

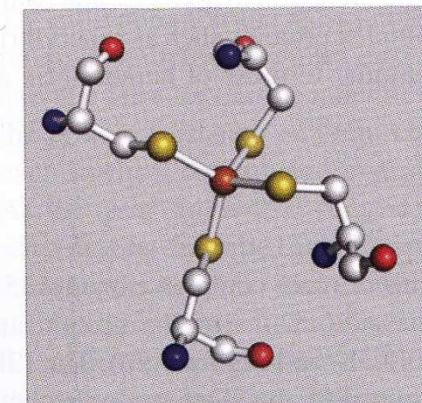
Deoxy: colourless, HS Fe(II)
Oxy: purple (CT band), 2 antiferro Fe(III), S=1/2,



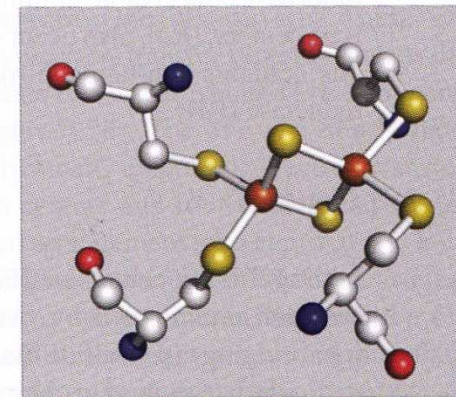
Redox Fe/S centers

Essential function in

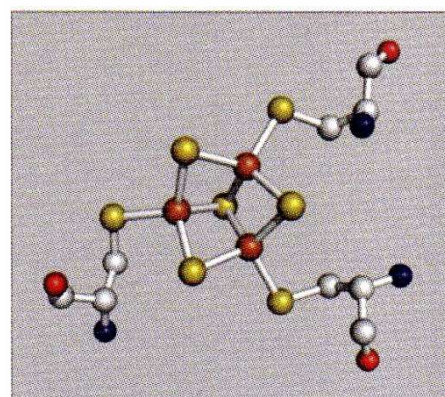
- photosynthesis
 - cell respiration
 - nitrogen fixation (plants)
- electron transfer, catalysis
various potentials



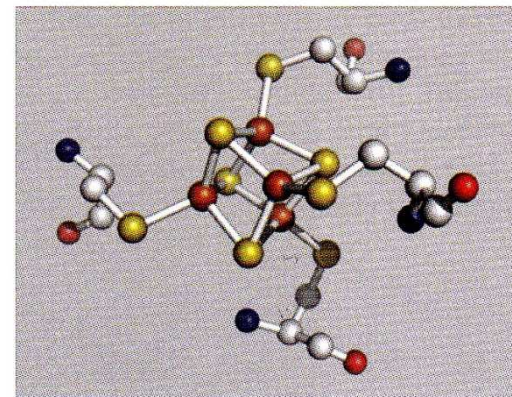
(a) $[\text{Rd}]^{3+;2+}$



(b) $[\text{2Fe-2S}]^{2+;+}$



(c) $[\text{3Fe-4S}]^{+,0}$



(d) $[\text{4Fe-4S}]^{3+;2+;+}$

Aggregation:

- 1 Fe – rubredoxin
- 2Fe-2S
- 3Fe-4S
- 4Fe-4S, cube

Fe in tetrahedron of S

Cys, sulfides

c.n. 4 – steric reason (S size)

tetrahedron => HS Fe

Uveřejněné materiály jsou určeny studentům Vysoké školy chemicko-technologické v Praze jako studijní materiál. Některá textová i obrazová data v nich obsažená jsou převzata z veřejných zdrojů. V případě nedostatečných citací nebylo cílem autorky záměrně poškodit autora/y původního díla.

S případnými výhradami se prosím obracejte na autorku tohoto výukového materiálu, aby bylo možno zjednat nápravu.



The published materials are intended for students of the University of Chemistry and Technology, Prague as a study material. Some text and image data contained therein are taken from public sources. In the case of insufficient quotations, the author's intention was not to intentionally infringe the possible author(s) rights to the original work.

If you have any reservations, please contact the author(s) of the specific teaching material in order to remedy the situation.